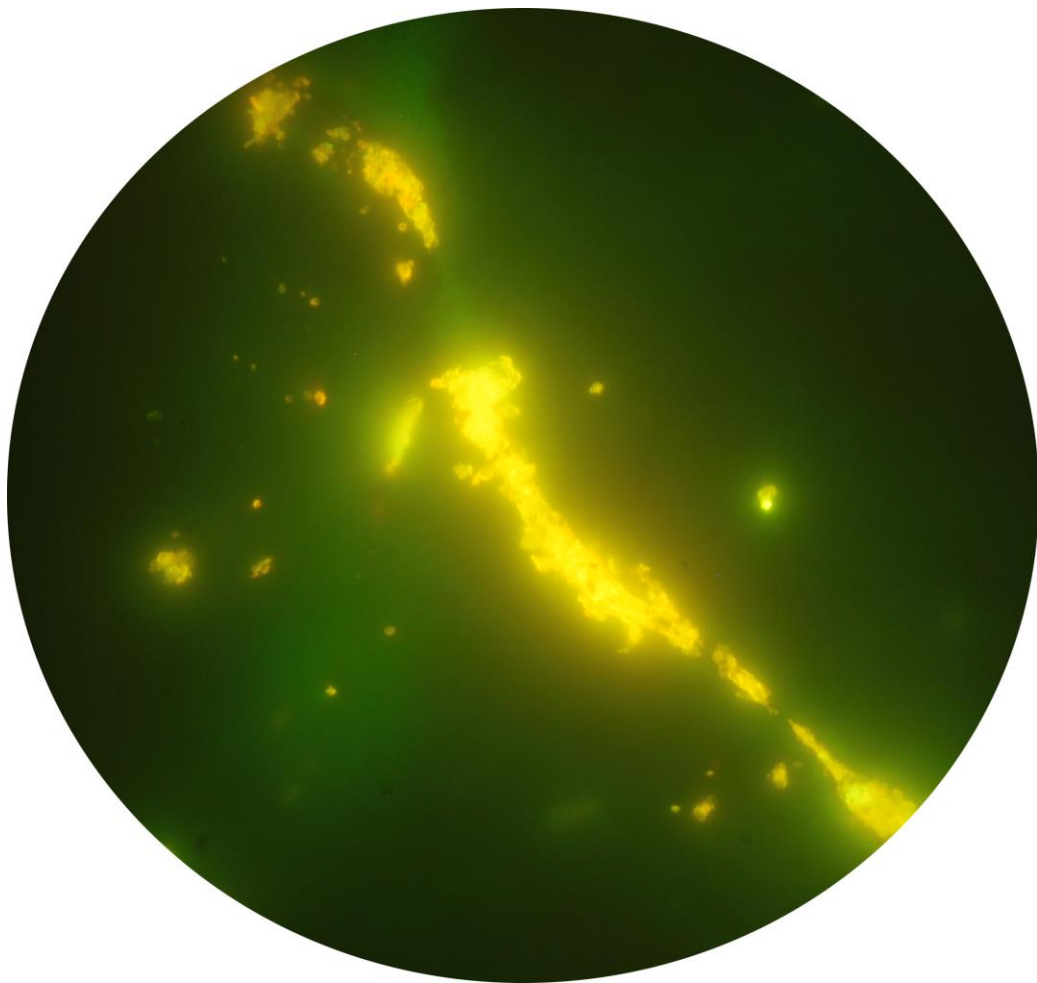


Faculty of Science
University of South Bohemia
České Budějovice

„Some like it rough“
Functioning of soil microbial communities in C and N
cycle under harsh environmental conditions

Habilitation thesis



Jiří Bárta

2019

Table of Contents

Introduction	4
Part I: “Some like it acidic” Functioning of microbial communities in C and N cycle in acid forest soils and peatlands	9
Litter quality, microbial community, and enzyme activities	9
Microorganisms involved in N cycle in acid forest soils	11
Microbial communities in peatlands and spruce swamp forests	13
Microbial communities in peatland microhabitats	14
Part II: “Some like it cold” Functioning of microbial communities in C and N cycle in Arctic Cryosols	15
Specific microbial communities in cryoturbated OM (cryOM) of Cryosols	16
The vulnerability of Cryosol C to climate change	17
Conclusions and future perspectives	19
Acknowledgment	20
References	21

Appendixes

Paper 1: Barta J, Applova M, Vanek D, Kristufkova M, Santruckova H (2010) Effect of available P and phenolics on mineral N release in acidified spruce forest: connection with lignin-degrading enzymes and bacterial and fungal communities. *BIOGEOCHEMISTRY* 97:71-87.

Paper 2: Barta J, Slajsova P, Tahovska K, Picek T, Santruckova H (2014) Different temperature sensitivity and kinetics of soil enzymes indicate seasonal shifts in C, N and P nutrient stoichiometry in acid forest soil. *BIOGEOCHEMISTRY* 117:525-537.

Paper 3: Barta J, Melichova T, Vanek D, Picek T, Santruckova H (2010) Effect of pH and dissolved organic matter on the abundance of *nirK* and *nirS* denitrifiers in spruce forest soil. *BIOGEOCHEMISTRY* 101:123-132.

Paper 4: Barta J, Tahovska K, Santruckova H, Oulehle F (2017) Microbial communities with distinct denitrification potential in spruce and beech soils differing in nitrate leaching. *SCIENTIFIC REPORTS* 7:9738.

Paper 5: Urbanova Z, Barta J (2014) Microbial community composition and in silico predicted metabolic potential reflect biogeochemical gradients between distinct peatland types. *FEMS MICROBIOLOGY ECOLOGY* 90:633-646.

Paper 6: Chronakova A, Barta J, Kastovska E, Urbanova Z, Picek T (2019) Spatial heterogeneity of belowground microbial communities linked to peatland microhabitats with different plant dominants. *FEMS MICROBIOLOGY ECOLOGY* 95:fiz130-.

Paper 7: Gittel A, Barta J, Kohoutova I, Mikutta R, Owens S, Gilbert J, Schneckner J, Wild B, Hannisdal B, Maerz J, Lashchinskiy N, Capek P, Santruckova H, Gentsch N, Shibistova O, Guggenberger G, Richter A, Torsvik VL, Schleper C, Urich T (2014) Distinct microbial communities associated with buried soils in the Siberian tundra. *ISME JOURNAL* 8:841-853.

- Paper 8:** Gittel A, **Barta J**, Kohoutova I, Schnecker J, Wild B, Capek P, Kaiser C, Torsvik VL, Richter A, Schleper C, Urich T (2014) Site- and horizon-specific patterns of microbial community structure and enzyme activities in permafrost-affected soils of Greenland. *FRONTIERS IN MICROBIOLOGY*, 5:541.
- Paper 9:** Capek P, Diakova K, Dickopp JE, **Barta J**, Wild B, Schnecker J, Alves RJE, Aiglsdorfer S, Guggenberger G, Gentsch N, Hugelius G, Lashchinsky N, Gittel A, Schleper C, Mikutta R, Palmtag J, Shibistova O, Urich T, Richter A, Santruckova H (2015) The effect of warming on the vulnerability of subducted organic carbon in arctic soils. *SOIL BIOLOGY & BIOCHEMISTRY* 90:19-29.
- Paper 10:** Wild B, Schnecker J, Alves RJE, Barsukov P, **Barta J**, Capek P, Gentsch N, Gittel A, Guggenberger G, Lashchinskiy N, Mikutta R, Rusalimova O, Santruckova H, Shibistova O, Urich T, Watzka M, Zrazhevskaya G, Richter A (2014) Input of easily available organic C and N stimulates microbial decomposition of soil organic matter in arctic permafrost soil. *SOIL BIOLOGY & BIOCHEMISTRY* 75:143-151
- Paper 11:** Gentsch N, Wild B, Mikutta R, Capek P, Diakova K, Schrumpf M, Turner S, Minnich C, Schaarschmidt F, Shibistova O, Schnecker J, Urich T, Gittel A, Santruckova H, **Barta J**, Lashchinskiy N, Fuss R, Richter A, Guggenberger G (2018) Temperature response of permafrost soil carbon is attenuated by mineral protection. *GLOBAL CHANGE BIOLOGY* 24:3401-3415.
- Paper 12:** Santruckova H, Kotas P, **Barta J**, Urich T, Capek P, Palmtag J, Alves Ricardo JE, Biasi C, Diakova K, Gentsch N, Gittel A, Guggenberger G, Hugelius G, Lashchinsky N, Martikainen PJ, Mikutta R, Schleper C, Schnecker J, Schwab C, Shibistova O, Wild B, Richter A (2018) Significance of dark CO₂ fixation in arctic soils. *SOIL BIOLOGY & BIOCHEMISTRY* 119:11-21.

Introduction

The planet Earth is ruled by the unseen majority, the microorganisms, which belong to all three domains of life – Archaea, Bacteria, and Eukaryotes. Microorganisms probably evolved more than 3.5 billion years and colonized all possible habitats due to their astonishing metabolic versatility and unique adaptive mechanisms. They outnumber macroorganisms both in cell numbers and in diversity (species richness) by orders of magnitude and are estimated to comprise up to 50% of the biomass on Earth (Whitman et al., 1998).

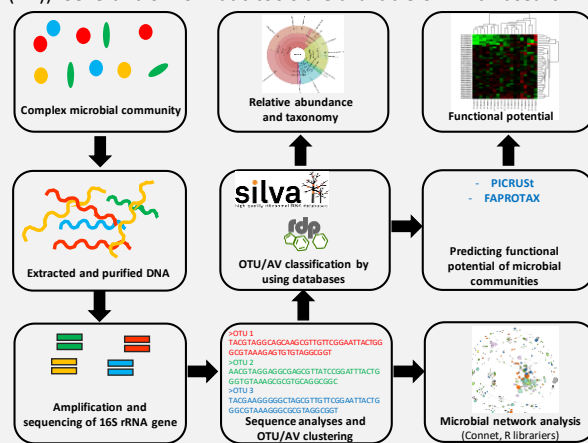
How to study microbial diversity, activity, and interactions in complex environments? Already more than 50 years ago, Robert E. Hungate defined the fundamental questions to be answered in a complete ecological analysis of natural habitat:

- *“What kinds and numbers of organisms are present?...This involves identification, classification, and enumeration.*
- *What are their activities? ... A complete determination of activities necessitates a complete knowledge of the environment.*
- *To what extent are their activities performed? ...This involves a quantitative measurement of the entire complex as well as its individual components. ...”* (Hungate, 1960).

BOX 1: Analysis of the microbial community by high-throughput targeted gene sequencing

The first next-generation sequencing (NGS) technology was introduced by Roche Life Sciences in 2005 and was able to generate approx. 10^6 reads of the length 700bp with the Titanium chemistry. Today, the most commonly used platform is Illumina technology based on sequencing by synthesis (SBS). For example, the Illumina sequencer HiSeq 4000 can produce 10^9 reads in one run, which allows scientists to analyze hundreds of samples in parallel. The procedure is as follows: After DNA or RNA extraction, the specific target genes are amplified by PCR (e.g. 16SrRNA gen for bacteria). Before sequencing, the unique sequence (usually 10-12bp long) is ligated to amplicons in each sample. These „barcodes“ allow the separation (demultiplexing) of raw reads into the original samples. Then the barcoded amplicons from different samples are pooled equimolar together. After obtaining the raw demultiplexed sequences in fastq format (the original fasta text format with included quality information they need to be quality checked. Reads with low quality (under the defined quality threshold) are discarded and only high-quality reads are sent for downstream analyses. These include forward and reverse read merging, trimming to the same length, clustering based on sequence similarity (97% similarity for operational taxonomic unit (OTU) clustering (Edgar, 2010) or 100% similarity for amplicon variants (AV)). Several bioinformatic tools are available of which usearch v11 (Edgar, 2010), dada2 (R based pipeline, (Callahan et al., 2016) and deblur (Amir et al., 2017) are commonly used because they precisely determine the species diversity in a defined (mock) community. After the OTU/AV clustering, the OTU/AV table is created by the bioinformatics algorithm, in which columns represent samples and rows relative abundances of individual OTUs/AVs in each sample. The taxonomy is assigned to each OTU/AV. There are other bioinformatic tools such as PICRUST (Douglas et al., 2018), FAPROTAX (Louca et al., 2016) or FunGene (Fish et al., 2013), which are able to translate the OTU/AV tables and generate functional tables.

OTUs/AVs can be also related with each other (e.g. using Spearman, Pearson correlations, Bray-Curtis dissimilarity, etc.) and their relationships can be visualized by network analysis (e.g. using Connet package under the Cytoscape environment (Smoot et al., 2011), or *corr* and *igraph* library under the R environment).



Before the introduction of cultivation-independent technologies, microbial ecologists were not aware of the microbial diversity "out there". Torsvik et al. (1990) showed in their study on soil microbial communities that an unexpectedly high number of microbial species was present in the DNA extracted from a grassland soil. With cultivation-independent technologies such as 16S rRNA gene (BOX 1), quantitative PCR (qPCR, BOX 2), fluorescence in situ hybridization (FISH) and metagenomics new dimensions in the characterization of complex microbial communities were reached. The large-scale sequencing approaches using DNA that was directly isolated from the natural environment allowed the discovery of many novel genes independent of cultivation efforts (Venter et al., 2004).

One of the most diverse and complex environments on Earth is soil. A single gram of soil contains billions of bacterial, archaeal and eukaryotic cells with dozens of distinct functional guilds (Torsvik and Øvreås, 2002) which have an indispensable ecological function in the global cycles of

carbon (C), nitrogen (N) and other elements. The diversity of soil microorganisms, both phylogenetic and functional, is enormous due to the immense spatial heterogeneity of soil, where steep physicochemical gradients create specific niches for distinct microbial taxa with diverse functions on micrometer scales to macroscales. Microorganisms in soil live mostly attached to soil particles and although their abundance is enormous, they colonize a very low fraction of soil surface (Young and Crawford, 2004) and they usually live in separated colonies („microbial villages“, Wilpieszski et al., 2019).

Looking from the perspective of the unicellular microorganism, the soil is a harsh and extreme environment. All imaginable factors affecting microbial life can change in very short spatiotemporal scales and microbes have to be able to get along with it or it will die. Without knowing the microbial diversity one would say that they do not have any other option. But they have. Microbes are unlike higher organisms exceptional, however, not all of them. Several microbial taxa like *Actinobacteria* have the third option which allows them to survive harsh conditions in specific dormant structures called endospores.

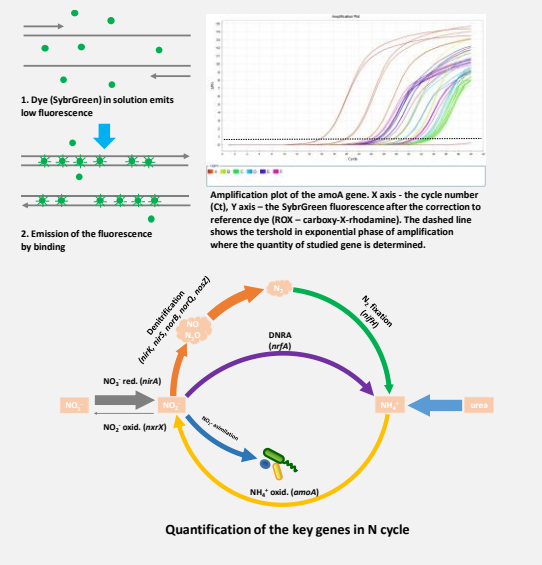
The basic and most important factors influencing the spatiotemporal changes in composition and activity of soil microorganisms are temperature, soil moisture (affecting the O₂ and nutrient availability), pH and organic matter (OM) content and composition. These factors, however, rarely act independently.

Temperature influences microbial life through the stimulation or repression of enzyme activities. Every microbe has its typical range of temperatures in which it can grow and perform metabolic transformations of the compounds from the environment. The minimum temperature defines the lowest limit where microbes can maintain the basic metabolism of the cell. The factors controlling the microbial minimum growth temperature are probably connected with the functioning of the cytoplasmic membrane which governs the transport of essential nutrients to cell enzymes. The lower limits of microbial growth and CO₂ production were -12°C and -40°C, respectively (Panikov et al., 2006). As temperatures rise, the rate of enzymatic reactions increases and growth and microbial respiration becomes faster. However, above a certain temperature, proteins and enzymes may be irreversibly damaged and microbes quickly die. For every microorganism, there is a minimum temperature below which growth is not possible, an optimum temperature at which growth is most rapid, and a maximum temperature above which growth is not possible. These three temperatures called “cardinal temperatures (CT)”, are characteristic for any given microorganism and can differ dramatically and reflect temperature optima of enzymes catalyzing essential biochemical reactions of cell metabolism. In a complex environment like soil, the changes in temperature may not always lead to expected responses based on general assumptions (Arrhenius, 1896) which may be valid for simple systems but can be hardly predictable in complex soil environment

BOX 2: Gene quantification by qPCR

The principle of quantitative polymerase reaction (real-time PCR, qPCR) is a rapid and precise determination of PCR products after each PCR cycle. The detection of the amount of PCR products is based on the measurement of the fluorescence intensity change during amplification. For this reason, either non-specific fluorescence dyes or specific probes are added to the reaction mixture during the preparation of PCR reaction. Thermocycler equipped with the fluorescence detector excites and determines the fluorescence of the dye attached to the DNA (i.e. in case of SybrGreen dye) or after the liberation from the probe (i.e. in case of the TaqMan probes). The fluorescence detection is repeated after each cycle and data are visualized in the Amplification Plot. For absolute quantification of PCR products, it is also necessary to generate the standard (calibration) curve with a known amount of gene copies of interest using genomic DNA, plasmids with an inserted gene or PCR amplicon.

The qPCR can detect even a very low number of gene copies present in the sample because their quantification is done in the exponential phase of amplification. Therefore, the qPCR is advantageously used for estimation of abundances of specific and often rare microbial functional groups involved in C and N cycles. For example, a number of gene copies of methyl coenzyme M reductase (*mcrA* gene) represent the abundance of methanogens, *nifH* gene is used for diazotrophs, *nirK* and *nirS* genes for denitrifiers.



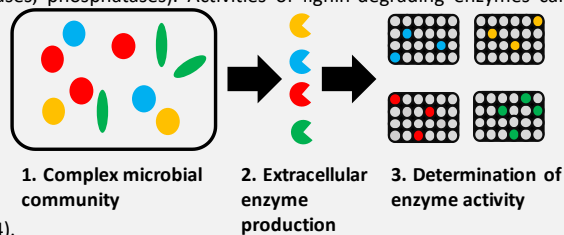
where the changes in environmental conditions often lead to the shifts in individual microbial populations with different CT values (Peleg et al., 2012).

It was also shown that the temperature responses can be significantly masked by other factors like nutrient availability (Hartley et al., 2007b), presence of plants (Hartley et al., 2007a), microbial community change (Vanhala et al., 2011), or geographical location (Karhu, 2010). The recent metastudy showed that soils from cold climatic regions and those with a high C:N ratio exhibited the strongest enhancing temperature responses (Karhu et al., 2014). It might be explained by the different temperature sensitivities of C and N processes and N availability may limit microbial activity in soils with high C:N. If the temperature sensitivities of key N-cycle processes are greater than some C-cycle processes (Billings and Ballantyne, 2013; Lehmeier et al., 2013), then it is possible that N availability may limit microbial activity following cooling, especially in soils with high C:N values. Temperature sensitivity and the response of microbial communities, therefore, significantly depends on the quality of organic matter, which is determined by the proportion of quickly recycled young and recalcitrant old C (Vanhala et al., 2011) and the amount of recalcitrant compounds, like lignin and polyphenolics (Northup et al., 1998).

BOX 3: Measuring of extracellular enzyme activities

The determination of extracellular enzyme activities can be done using chromogenic or fluorogenic substrates. The enzymatic activity is usually determined in water (water extracts) or buffered extracts at the desired pH. Fluorogenic substrates are widely preferred because they are more sensitive and can be used directly in soil extracts. Two fluorogenic substrates (4-Methylumbelliferyl, MUF, and 7-Amido-4-methylcoumarin, AMC) are attached to the defined substrate (e.g. phosphate in case of measuring phosphatase activity).

When enzyme cleaves this bond, it liberates MUF/AMC which emits fluorescence. The whole process has been parallelized using 96 well plates and detected in microplate readers. When interpreting the data, it is necessary to take into account that we do not measure the activity of a single enzyme but always a mixture of isoenzymes. The fluorogenic substrates are used to determine the activity of hydrolytic enzymes gaining C, N, and P (e.g. cellobiosidases, aminopeptidases, phosphatases). Activities of lignin-degrading enzymes can be determined only with chromogenic substrates (L-dihydroxy phenylalanine (L-DOPA) for the determination of phenoloxidase activity). It is often useful to determine the kinetic parameters of the studied enzyme (i.e. K_m and V_{max} values) which characterize the substrate affinity and maximal potential enzyme activity. However, in soils, we measure the activity not only of the single enzyme but a mixture of isoenzymes catalyzing the same reaction but produced by distinct microorganisms. The K_m and V_{max} then should be interpreted as „apparent“ values (Sinsabaugh et al., 2014).



Nutrient availability in the soil can be also influenced by different moisture and O_2 levels (Seneviratne et al., 2010). For example, upper soil layers are characterized by higher O_2 availability with the majority of aerobic microorganisms. The aerobic processes are more energetically efficient, the processes in upper soil horizons are faster which leads to higher turnover rates of OM transformations (Strakova et al., 2011), and higher activities of soil enzymes (Burns et al., 2013, **BOX 3**). Going deeper to the soil the microbial community shifts from the microaerophilic, facultatively aerobic to strictly anaerobic species. This continuum may be, however, disrupted by specific plants (e.g. *Eriophorum vaginatum* colonizing water-saturated peatlands). Organic matter in the soil is transformed in the cascade of aerobic and anaerobic metabolisms governed by distinct microbial populations. The fluctuations of moisture therefore significantly influence the composition and proportion of aerobic/anaerobic microorganisms in different soil layers and in some ecosystems like peatlands these changes may have consequences on the stability of OM and can influence the fluxes of CO_2 , CH_4 , and N_2O gasses as the main products of aerobic and anaerobic metabolism of soil microorganisms.

The soil pH strongly influences carbon, and nutrient availability (Lauber et al., 2009a), and the solubility of metals (Firestone et al., 1983; Flis et al., 1993) from which Fe and Al are probably the most important for microbial functioning. While Fe is the cofactor of oxidoreductases and its availability thus may influence the respiration efficiency of heterotrophic microbes, Al has a toxic effect on microbial cells (e.g. disruption of the cytoplasmic membrane transport at low pH (Piña and Cervantes, 1996)). There is also a strong direct pH effect on microbial metabolism. Microbial cells keep their internal pH

close to neutral. Under extremely low or high pH in the environment (e.g. in acidified soils, peatlands, saline or extremely basic soils), the energy required for maintenance of “neutral” inner pH increases. Soil microorganisms vary in their tolerance to pH extremes. Therefore, soil pH control diversity, taxonomic composition of microbial communities and their bacterial and fungal proportion ratio (Arao, 1999; Bååth and Anderson, 2003; Bardgett et al., 2001; Blagodatskaya and Anderson, 1998; Fierer and Jackson, 2006; Frostegård et al., 1993; Rousk et al., 2010a). Targeted gene sequencing (**BOX 1**) demonstrated a strong positive correlation between soil pH and microbial diversity at a continental scale (Lauber et al., 2009a), in Arctic tundra (Chu and Grogan, 2010), and across an experimental pH gradient within a single soil type (Rousk et al., 2010a).

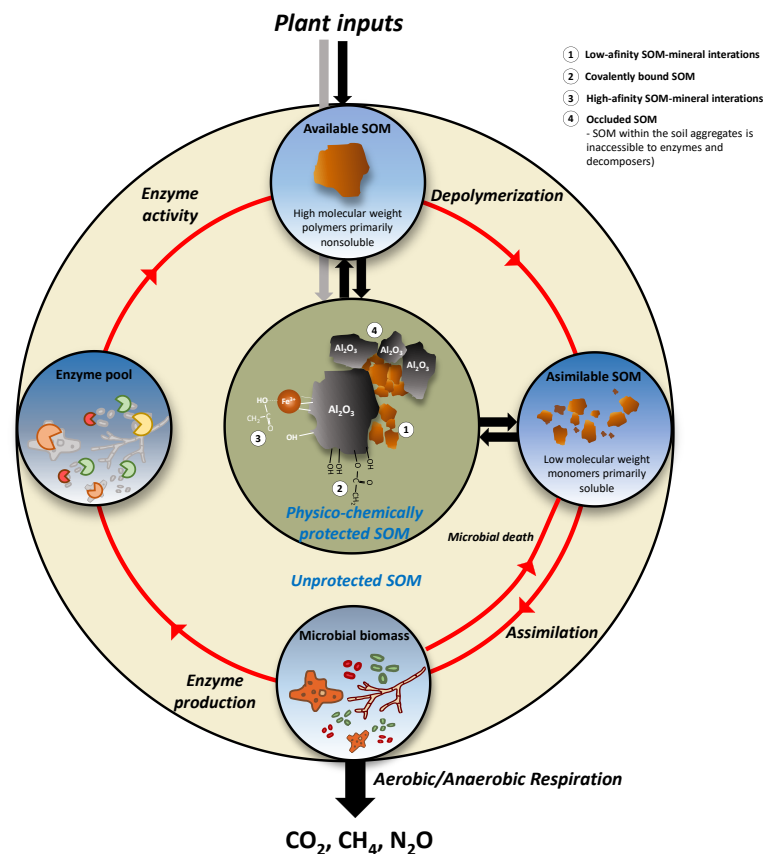


Figure 1: Conceptual model of decomposition illustrating organic matter pools and fluxes in soil (modified by Conant et al. (2011))

Organic matter represents an essential source of energy, C and macronutrients for predominantly heterotrophic soil microbial communities (**Figure 1**). The most important input of the organic matter to the soil is of plant origin. Plants support the growth of distinct soil microbial communities through the plant litter (dead leaves, stems, logs, dead belowground biomass) and diverse chemical compounds produced by living roots (rhizodeposition). The quality and quantity of plant inputs to the soil are greatly affected by both environmental conditions and biotic factors (e.g. co-occurrence of other plant species, composition of soil microbial community, herbivory (Freschet et al., 2010; Killingbeck, 1996; Stewart and Globig, 2011)). Plant litter is also qualitatively very different from rhizodeposition. Rhizodeposition is only little contributed by more complex compounds, which originate from root turnover (Jones et al., 2009). The majority of rhizodeposits are a variety of low molecular weight (LMW) compounds (e.g. organic acids, simple sugars, amino acids, soluble phenolic) with short turnover time, which are named root exudates. They represent up to 20% of net primary production (Jones et al., 2004). Root exudation is directly linked to photosynthesis and, therefore, enters the upper soil horizons more or less continuously during the whole vegetation season. They directly or indirectly affect the rhizosphere microbial community, which in turn influences SOM and

DOM contents and chemistry by its activities. For example, Giesler et al. (2007) found a direct link from tree photosynthesis through the roots and their mycorrhizal fungi to soil solution chemistry.

Litter, on the other hand, enters the soil mainly after plant senescence and thus serves as the main C and energy source during the winter. Differently from rhizodeposition, it contains only a minor proportion of LMW compounds and these are quickly consumed by soil microorganisms. The decomposition of older litter is then dependent on a slower breakdown of biopolymers (mainly, cellulose, hemicelluloses, and lignin) mediated by the action of extracellular enzymes, which are mainly produced by saprotrophic fungi and actinobacteria. Mycorrhizal fungi are also able to decay complex organic molecules but their enzymatic capacity to degrade larger molecules is lower in comparison to saprotrophs (Lindahl et al., 2007). Aboveground litter, comprising about 50 % of net primary production, accumulates on the soil surface (Bray and Gorham, 1964) and forms the litter layer, which is slowly transformed into soil organic matter in the organic horizon. Therefore, the topsoil microbial communities are directly affected by the chemical composition of the plant litter and often contain microbes capable of decomposing complex biopolymers by the activity of various extracellular enzymes.

Plant material entering the soil is decayed by microbial communities and must sooner or later pass through dissolved organic matter (DOM) in soil solution and turnover of DOM containing organic forms of C, N, and P is a major way of element cycling in soil. Microbial activity and any conditions that enhance decomposition all promote high DOM concentration (Kalbitz et al., 2000). In the field conditions hydrologic short circuit and DOM selective sorption on Fe and Al oxyhydroxides (**Figure 1**) or biofilms are other factors controlling DOM quality and quantity (Qualls and Richardson, 2000). Soil DOM originates in plant litter, roots exudation, and SOM. Root exudates and soluble organics originating in plant litter are quickly consumed by microorganisms with high portion being respired and released as CO₂ and only a portion of this new assimilated C (in a range from few to 40%) is transformed to the soil DOM (Fu et al., 2004; Hagedorn et al., 2004; Hagedorn and Schlegel, 2000; Ohno and Bro, 2006). In accordance, surface horizons directly affected by plants contain a high proportion of DOM of plant origin but moving down the profile, the proportion of microbially transformed DOM increases (Guggenberger and Kaiser, 2003). Going down to the subsoil, DOM is mineralized to CO₂ and its composition largely reflects the selective sorption on biofilms and mineral surfaces (Guggenberger and Kaiser, 2003; Qualls and Richardson, 2000).

This habilitation thesis covers my research focused on different factors affecting the community composition and activity during the transformation of soil organic matter. The distinct effects of pH, moisture, and root exudates with relation to soil physicochemical parameters and microbial community structure will be discussed. The thesis is divided into two parts. The first part summarizes my research focused on microbial communities affected by pH, moisture, and vegetation in soils of spruce forest, peatlands and spruce swamp forest. The second part summarizes the research focused on microbial communities and their activity in Arctic permafrost soils (Cryosols) with relation to increased temperature and C and N vulnerability.

Part I: “Some like it acidic” Functioning of microbial communities in C and N cycle in acid forest soils and peatlands

Plant litter decomposition is an important process in C, N and P cycles. It is microbially driven process, essential for recycling of C and nutrients. During decomposition, organic complexes are step by step enzymatically broken down into simpler compounds, nutrients bound in organics are released in forms available to plants and a part of organic C is mineralized to CO₂. Decomposition is controlled mainly by temperature, moisture, the chemical composition of the litter, and the microbial communities (Aber et al., 1990; Fassnacht and Gower, 1999; Park and Matzner, 2003; Pregitzer, 2003). The prediction and precise estimation of plant litter decomposition rates, and the amount of released mineral nutrients (i.e. NO₃⁻, NH₄⁺, and PO₄³⁺) is crucial not only for plant biomass production but also for estimating of possible nutrient leaching from soils to nearby rivers and lakes where it can directly influence the biological processes and elemental cycling.

Litter quality, microbial community, and enzyme activities

The decomposition has several stages. The initial decomposition rate and subsequent succession of the decomposing microbial community depend on the litter chemistry and the diversity of the microbial community present on the surface of the litter. The decomposition of leaves already begins when they are still connected to the plant and nutrients from senescing leaf tissues are reallocated to the living parts of the plant (Tláškal et al., 2016). The decay is initiated by the activity of microbial epiphytes and endophytes living on and inside the plant tissue (i.e. plant phyllosphere). Microorganisms associated with the surfaces and insides of leaves must be adapted to specific conditions in the phyllosphere (reviewed in Rastogi et al. (2013). The ecological role of the phyllosphere microbial community, their enzymatic activity, and their successional changes during the first months of litter decomposition are still not clear, but they are often found in the litter soil horizons (Lindahl et al., 2007; Livsey and Barklund, 1992).

Several studies confirmed that the chemical composition of the plant tissues has the main impact on the composition of phyllosphere fungal and bacterial communities and their enzymatic apparatus (Cox et al., 2001; Lucas et al., 2007), and may, therefore, have a strong impact on the initial stage of litter decomposition. From the litter quality indexes, the carbon/nitrogen (C:N) ratio has been widely used for predictions of litter decomposition rate and nutrient leaching (Carlyle et al., 1990; Müller et al., 1988). However, the C:N ratio was found to be a poor predictor when trying to estimate the amount of released mineral N (NH₄⁺ and NO₃⁻) from the highly lignified litter (Prescott, 2005). In such cases, the amount of phenolics and the phenolics:N ratio showed a much closer correlation (Berg, 1986; Berg and Ekbohm, 1991), which points to an important role of organic C composition in litter degradability. In our research, we extend the knowledge of the initial litter decomposition by the phyllosphere microbes (**Paper 1**). We linked a decomposition of the litter with different chemistry (different elemental composition and amounts of total and soluble phenolics) with activities of the key lignin-degrading enzymes, phenoloxidases, and peroxidases, and with a composition of fungal and bacterial communities present on the litter. We compared several litter types from acidic spruce forest ecosystems (soil pH below 4) – spruce needles and litter of four dominant understorey vegetation - lady fern (*Athyrium alpestre*), blueberry (*Vaccinium myrtillus*), reedgrass (*Calamagrostis villosa*) and hair grass (*Avenella flexuosa*). Our research showed that the initial litter phenolic:N and phenolic:P ratios were the best predictors of decomposition rate and mineral N release from the litters ($r \sim -0.6$). The amount of phenolics and availability of both macronutrients, N and P, are thus critical for the initial stages of litter decomposition in the strongly acidified forests. We documented that the decreasing phenolics:P ratios in the litter is connected with a higher release of available mineral and organic N. We suggest the following mechanism: activity of ligninolytic enzymes (higher on the less lignified litter) can produce low molecular phenolics with highly reactive ortho-phenolic groups (Comerford and Skinner, 1989). They can be utilized as a C-substrate by the specific taxa (e.g. *Pseudomonas* (Paca et al., 2005)) but they are also able to precipitate Fe and Al ions (Comerford and Skinner 1989), including a toxic forms of Al³⁺ occurring in the extremely acidic soils (Kopáček et al., 2002a, 2002b; Vrba et al.,

2006). Precipitation of Al and Fe can increase amounts of available P and more mineral N may be released (Northup et al., 1998). These processes likely interconnect C, N and P cycling in acidified forests.

Our molecular analyses of microbial communities inhabiting the litters were based on denaturing gradient gel analyses (DGGE). Although we were not able to evaluate deeper taxonomic information because of the DGGE limitations (Muyzer and Smalla, 1998), we showed that bacterial and fungal communities responded differently to the initial chemistry of tested litters. The differences in bacterial community composition among litters were mainly influenced by P availability, their successional changes during ongoing decomposition were also driven by the amount of available P and phenolics. Differently, the initial fungal community composition changed with the litter C:N ratio and ratios of phenolics to N and P, while successional changes were again related to the P availability. We explained the different bacterial and fungal behavior as follows. In the initial stage of litter decomposition, fungal community does the “hard job” in cleaving the litter polyphenolics with the help of their oxidative extracellular enzymes whose synthesis is highly N demanding and strongly depends on the amount of available N. Differently, bacterial community which is probably dominated by copiotrophic taxa at the initial stage of litter decomposition (Bray and Gorham, 1964; Melillo et al., 1982; Prescott, 2005; Wardle et al., 2002) use mainly the soluble organic compounds and available P for energy generation and RNA synthesis for high ribosomal activity and later may also utilize soluble LMW phenolics (Baptist et al., 2008; Elser, 2003; J. J. Elser et al., 2000; James J. Elser et al., 2000).

We found a tight correlation between microbial respiration and ligninolytic activities. We showed that the oxidative enzymes are active at temperatures around 0°C (Bremner and Zantua, 1975), which is evidence that lignin degradation and depolymerization can run in such low temperatures. We further found a stronger relationship between the activity of these enzymes and bacterial community composition at 0°C than at 10°C which indicates that microbial community composition at low temperatures are more influenced and shaped by the activity of lignin-degrading extracellular enzymes, similarly as shown by (Schnecker et al., 2014).

The lignin-degrading enzymes are, however, only a part of the huge enzyme “family” of extracellular enzymes operating in the soil, which also include a large group of hydrolytic enzymes that liberate available C, N, and P from biopolymers like cellulose, proteins, and DNA (Burns et al., 2013). Ecological studies generally determine the activities of hydrolytic enzymes that catalyze the terminal reactions of the complex cascade of biopolymer degradation (e.g. β -glucosidase produce 2 mol of glucose from 1 mol of cellobiose). The reason is obvious, these enzymes like β -glucosidase, aminopeptidases, and phosphatases produce simple sugars, amino acids or phosphates representing an “easy to take” fraction of soil dissolved organic matter (DOM, Lauber et al. (2009b)). The potential activities of these enzymes can thus be directly linked to microbial metabolism (Sinsabaugh et al., 2010), used for estimation of nutrient or energy limitation and to predict a release of available C, N and P resources from complex biopolymers.

In the following study, we focused on the effect of temperature sensitivity of enzymatic activities assessed by the coefficient Q_{10} and substrate concentration on kinetic parameters (apparent V_{max} , apparent K_m , **BOX 3**) of selected hydrolytic enzymes (**Paper 2**). It is well known that temperature and substrate availability directly influence the kinetics of soil enzymatic activity (Allison, 2006; Allison and Jastrow, 2006; Frankenberger and Tabatabai, 1991; McClaugherty and Linkins, 1990; Meentemeyer, 1978). From the saturation curve of the each isoenzyme group (**BOX 3**) in the soil, one can assess the enzymatic affinity to substrate (apparent K_m values) and the concentration of substrate at which the enzyme is fully saturated (i.e. all active centers are occupied by the substrate) and thus transforms the substrate at the maximum possible rate. Such information enables to recognize how efficient is enzymatic substrate transformation under given soil conditions and how is the present community adapted to these conditions. Evaluation of temperature sensitivity of soil enzymes involved in C, N and P acquisition can be used to model potential nutrient release throughout the season or predict a change in the system behavior under changing temperature conditions (Sinsabaugh et al., 2010; Wallenstein et al., 2009; Wallenstein and Weintraub, 2008). We again worked in the acid spruce forests ecosystems. We ran laboratory incubation experiments at different temperatures using

samples from litter and organic soil horizons. With the help of continuous *in-situ* temperature measurements, we extended our research and modeled *in-situ* enzyme activities and estimated the potential release of potentially available C, N, and P sources to litter and organic soil horizons.

Our measurements revealed that the kinetic parameters and temperature sensitivity of all measured hydrolytic enzymes differed significantly between the litter and organic soil horizons. Different substrate affinities between horizons demonstrate a very steep vertical stratification of microbial activity (Baldrian et al., 2012). Further, aminopeptidases, which liberate amino acids and short oligopeptides into the soil solution had distinct substrate affinities and temperature sensitivity than C (β -glucosidase, cellobiosidase) and P (phosphatase) acquiring enzymes. Both measured peptidases exhibited higher substrate affinities (lower apparent K_m) but lower apparent V_{max} than C-enzymes in the litter soil horizon. This indicated that peptidases in the litter horizon degraded peptides even at very low concentrations but with much lower efficiency compared to C enzymes. Moreover, both aminopeptidases showed temperature insensitivity compared to C enzyme β -glucosidase. Because of these imbalances, organic N may migrate undecomposed due to higher enzyme affinity and temperature insensitivity from the litter horizon to the lower organic soil horizon, while C compounds are decomposed and utilized faster. The distinct rates and efficiencies of enzymatic mining of C and N may point to a potential misbalance in C and N utilization (Billings and Ballantyne, 2013; Lehmeier et al., 2013). Our estimate of potential available C, N, and P release to litter and organic soil horizons based on modeling of enzymatic activities using *in-situ* measured temperatures indicated that microbial communities in the forest soil were nutrient-limited for the most of the season. It was because the N and P gaining enzymes produced by the microbial community were not able to sufficiently support the microbial community with available nutrients. These imbalances in affinities enzyme efficiencies and temperature sensitivities in C and N utilization can have consequences of available N pools in different soil horizons as proposed in other studies from the same location (Kopáček and Vrba, 2006).

We again confirmed that the presence of a high amount of phenolics is an important factor that strongly influenced the activity of enzymes. It is well known that soil enzymes create complexes with phenolic compounds and metals which commonly leads to the inhibition of their activity (Gianfreda et al., 1995b, 1995a, 1994; Violante et al., 1995). In acid soils, metals like Al^{3+} can further influence the stability of these enzyme-phenolic complexes and therefore suppress the activity of selected enzymes (Pinsonneault et al., 2016). In summary, our study demonstrated that enzymes involved in the utilization of C, N, and P which liberate easily available compounds are in imbalance and that mainly N enzymes worked at lower efficiencies than C enzymes and limit the microbial metabolism in the acid forest soil.

Microorganisms involved in N cycle in acid forest soils

Following a previous study showing the prevailing N limitation of microbial metabolism in the acid forest soils, we looked in detail on specific functional microbial guilds in N cycle and specifically on highly pH sensitive denitrification (Šimek et al., 2002). Denitrification is the main anaerobic biotic process leading to the loss of N from the soil environment. The second step in denitrification, the reduction of nitrite (NO_2^-) to nitric oxide (NO), distinguishes “true” denitrifiers from other NO_3^- -respiring bacteria (Henry et al., 2004). This reaction is catalyzed by two different types of NO_2^- reductases, either a cytochrome cd1 encoded by the *nirS* gene (*nirS* denitrifiers) or a Cu-containing enzyme encoded by the *nirK* gene (*nirK* denitrifiers). It was found that *nirS* denitrifiers are located mostly in the rhizosphere, while *nirK* denitrifiers are more abundant in bulk soil (Henry et al., 2004). Therefore, the group of *nirS* denitrifiers may contain rather fast-growing copiotrophic taxa, which can be more sensitive to available resources than *nirK* denitrifiers and change in the number and activity of *nirK* and *nirS* denitrifiers may influence the mineral N pools in acid forest soils. Moreover, in highly acidic soil, the final step of denitrification (i.e. N_2O reduction to N_2) is strongly inhibited and these soils can be important sources of N_2O as the potent greenhouse gas. To address these specific functional groups we used quantitative PCR (qPCR, **BOX 2**) which allowed us the precise determination of functional potential based on marker gene (i.e. *nirS* and *nirK* genes) quantification (Heylen et al., 2006).

We showed that the amount of denitrifiers was one order lower in acid forest soils compared to forest soil with near to neutral pH (**Paper 3**). The amount of denitrifiers and also the availability of C and N in the soil rapidly decreased at pH below 4. The low DOM availability in the acid soils is likely caused by its complexation with mobile forms of polyvalent cations like Al^{3+} and Fe^{3+} , which dominate at very low pH. The precipitated DOM is then unavailable for biological processes (**Paper 11**, Dao et al., 2018; Gentsch et al., 2015; Kaňa and Kopáček, 2006; Northup et al., 1998; Tomlinson, 2003). Low C and N availability were closely related to the abundance of *nirK* denitrifiers (close correlation of the gene abundance with available C,N, $r>0.8$) but not *nirS* denitrifiers. It was opposite to the expectations that the *nirS* denitrifiers, usually found in the rhizosphere, will respond to substrate availability. However, the *nirK* gene was significantly more abundant in our soils and it was documented that *nirK* gene is spread among more diverse microbial taxa than *nirS* gene (Heylen et al., 2006). The close relationship of C availability with *nirK* gene represents probably a response of the majority of the denitrification community. We showed that the C and N availability can limit a specific group of denitrifiers which can have consequences on potential mineral N losses via denitrification from the acidic spruce forest soils (Kopáček et al., 2006).

In our next study (**Paper 4**), we compared two adjoining systems, the spruce and beech forest, which share the bedrock, face the same climate conditions but differ in NO_3^- leaching being much lower from the spruce forest. To find an explanation of the difference in ecosystem N cycling, we linked microbial community composition and activity with soil chemistry analyses. We combined high-throughput sequencing (**BOX 1**), which allowed us a characterization of microbial communities on a fine taxonomic scale, with determining the activities of C and N gaining enzymes, microbial respiration and net N transformation processes. We found that only the bacterial but not fungal community composition differed substantially between the spruce and beech soil. This difference was mainly driven by soil pH (Fierer et al., 2007; Graham et al., 2016; Hobbie et al., 2006; Högberg et al., 2007; Lauber et al., 2009b; Reich et al., 2005), being lower in spruce than beech site, and less by C and N biogeochemistry. This implies that the bacterial community is probably responsible for the observed differences N cycling and consequent NO_3^- utilization/leaching.

Comparing the processes in C and N cycling (**Paper 1**), the first difference was found in the enzyme activities. In the spruce soil, the C acquiring enzymes were proportionally more active compared to N acquiring enzymes, which corresponded to higher DOC:DN ratio. This indicated C and energy limitation of the soil bacterial community in the spruce forest. Although the soil in a spruce forest bacteria are likely limited by low C availability connected with a low quality of plant inputs, mainly spruce needles, which are rich in waxes and polyphenolic compounds and need to be enzymatically degraded. In accordance, the spruce bacterial community had a higher proportion of families (Acidobacteriaceae subgroup 1 and Acidothermaceae) which have the enzymatic capabilities to do these transformations (Lauber et al., 2009a; Schimel and Weintraub, 2003).

We further found that the microbial community in the spruce soil uses N more efficiently than that in beech soil. There are other microbially driven processes except for microbial N immobilization (Tahovská et al., 2013), which could reduce NO_3^- concentration in the soil and thus the potential NO_3^- leaching such as denitrification and dissimilatory nitrate reduction to ammonia (DNRA). To learn about them, we translated the taxonomic information of microbial communities using the newly developed functional bioinformatics pipelines (**BOX 1**). Our data showed that denitrifiers in the spruce community were proportionally more abundant than bacteria capable of DNRA (3:1 ratio) and, at the same time, significantly more abundant compared to the beech community. The functional analysis thus revealed that very low NO_3^- concentration in the spruce soil solution may be the result of N loss through denitrification. Marked differences were mainly in the abundance of *nirK* denitrifiers, whose abundance closer correlates with the available C compared to *nirS* denitrifiers (**Paper 3**). The subsequent microbial network analyses confirmed the importance of denitrifiers and bacteria capable of DNRA in the soil community. Denitrifiers (mainly genus *Acidothermus*, and *Herminiimonas*) were among the 10 potential keystone species of the spruce bacterial community. Furthermore, microbes in the spruce community showed a higher degree of associations than the microbes in the soil of beech forest. It points to the much higher microbial interconnection, probably due to the higher substrate

complexity of litter and higher amount of phenolics (**Paper 1**), whose degradation needs to be synchronized by a variety of microbial functional guilds.

Microbial communities in peatlands and spruce swamp forests

Natural pristine peatlands and spruce swamp forests represent another “rough” environment where microbes need to cope with limited available resources and O₂. Peatlands contain a large amount of carbon in organic matter and are considered to act as a sink of atmospheric CO₂ but at the same time a significant source of CH₄ (Harriss et al., 1985), the potent greenhouse gas. Methane is produced under strictly anaerobic conditions by methanogenic Archaea and the rate of its production is driven by several interconnected factors: i) water saturation, which determines the zones of CH₄ production and oxidation (Sundh et al., 1995); ii) soil temperature (Yavitt et al., 1997); and iii) plant community composition. Some plant species can transport gases (including O₂) from atmosphere to rhizosphere supporting CH₄ oxidation (Whiting and Chanton 1992; Schimel 1995; Ström et al. 2003). Plant species further differ in exudate quality, which influences the composition of the bacterial community of primary/secondary fermenters and composition of methanogens (Basiliko et al., 2003; Galand et al., 2005) and therefore the rate of CH₄ production. The emissions of CH₄ are highly variable and differ between and also within various peatlands due to variability in vegetation composition, nutritional status, substrate availability and pH (Bubier et al., 1993; Schimel, 1995). The variability in CH₄ fluxes is not caused only by environmental factors but also by differences in methanogen communities.

The acid spruce swamp forests (SSF) are exceptional ecosystems lying between open peatlands and mineral soil forests. Like open peatlands, they accumulate peat and their ground layer is covered by *Sphagnum* mosses; however, they also resemble mineral soil forests in having a productive tree stand. They are characterized by high spatial heterogeneity and, consequently, a high diversity of biogeochemical processes (Økland et al., 2008). The internal structure and heterogeneity of SSFs are driven by dominant understory species. Trees are efficient competitors for light and water, both of which are also the dominant factors for the development of *Sphagnum* cover. Trees, together with peat mosses (*Sphagnum* sp.), are responsible for peat accumulation and associated high soil water retention. The waterlogged soil prevents tree root development and tree growth to reach its full potential. Litter of peat mosses is hardly decomposable, which is attributed to the synergistic effects of environmental factors (nutrient-poor soils with acidic and anoxic conditions) and decay resistance of the litter (Moore and Basiliko, 2006). These plants contain peculiar structural polyphenols, and polysaccharides and also excrete low molecular weight phenolics to the environment (Hájek et al., 2011) which probably hamper litter peat decomposition through their inhibitory activity on the microbial breakdown, mainly due to the inhibition of extracellular enzyme activities (Bragazza and Freeman, 2007).

Less wet habitats are usually colonized by cottongrass (*Eriophorum vaginatum*) whereas dwarf shrubs (mostly *Vaccinium myrtillus*) colonize dryer elevated habitats. The patchy co-dominants, cottongrass, and dwarf shrubs, bring internal SSF variability and may affect the functioning of the whole SSF in the way they acquire, process and invest resources (Weltzin et al., 2000). Cottongrass is non-mycorrhizal peatland vascular plant well adapted to the flooded nutrient-poor environment. It forms long-lived tussocks (>100-200 years), in which the growth of new leaves is supported almost entirely by nutrient translocation from senescing leaves (Lavoie et al., 2005). It forms a deep root system, which transports oxygen and available exudates down to anoxic organic soil layers (Chapin et al., 1993). On the other hand, blueberry and other ericaceous dwarf shrubs host mycorrhizal fungi and occupy oxic elevated “islands” in SSF. Most assimilated C transported belowground is translocated to the mycorrhiza and only a small proportion is released directly to the soil. It is, however, still unclear how this exceptional spatial heterogeneity of vegetation cover reflects the functional diversity of soil microorganisms and ongoing soil processes, which, in turn, affect SOM and DOM quality.

In the following study, we compared a composition of the methanogenic community among three peatland types (**Paper 5**). These were bogs, spruce swamp forests, and fens. The general concept is that bogs are highly acidic, nutrient-poor ecosystems with hardly degradable peat originating mainly

from peat mosses compared to fens, which are less flooded, nutrient richer, dominated by sedges and easier-decomposable sedge-formed peat. We expected that hydrogenotrophic methanogenesis would be favored in acidic bogs (Galand et al., 2005; Horn et al., 2003) and acetoclastic methanogens would prevail in richer fens (Juottonen et al., 2005). We further expected that the SSFs with its transient character would be “located” in-between on the gradient from bogs to fens. Contrary to our expectations, only the hydrogenotrophic methanogens occurred in all studied peatland types, despite their distinct vegetation composition, and CH₄ production. The *Methanomicrobiales* dominated in bogs and SSFs, whereas *Methanobacteriales* in the fens. We suggest that the absence of typical acetoclastic *Methanosarcinales*, which require relatively high acetate concentrations (Liesack et al., 2000), might be related to the competitive activity of other bacterial taxa, mainly sulfate reducers. They compete with methanogens for available substrates including acetate (Hamberger et al., 2008; Kotsyurbenko, 2005). Furthermore, acetoclastic methanogenesis appears to be severely inhibited by phenolics and other aromatic substances derived from Sphagnum mosses but also from nutrient-limited plants in general (Rooney-Varga et al., 2007).

There were also differences in the composition of overall bacterial communities among the three peatland types (**Paper 5**). The differences were driven mainly by peat decomposability and related C and N availability. The most acid bogs had a higher proportion of Acidobacteria and more unique bacterial taxa in comparison to other sites, while more bacterial taxa from Proteobacteria were detected in fens (Gupta et al., 2012; Lin et al., 2012). Acidobacteria are known to favor acidic environments (Hartman et al., 2008), **Paper 4**) and are able to grow under oligotrophic conditions (Philippot et al., 2010), while Proteobacteria are usually associated with higher availability of C (Fierer et al., 2007). The changing ratio between Proteobacteria and Acidobacteria reflected well the trophy and acidity of the sites and may be used as an indicator of these conditions in peatlands.

Due to the SSFs have a hydrological regime and microbial community composition more similar to fens than bogs, we expected that SSFs will be also functionally closer to fens. Surprisingly, the biochemical parameters of SSFs (i.e. microbial biomass and aerobic CO₂ production) were more similar to bogs. It can likely be ascribed to a low quality of SSF litter coming from the predominant spruce trees and dwarf shrubs (Strakova et al., 2011) which was also indicated by the highest C:N ratio. The results of metabolic potential (**BOX 1**) showed the highest aromatic degradation potential in the SSFs which might be the result of a higher relative abundance of Actinobacteria in SSF than in fen. Actinobacteria often participate in the decomposition of polyphenolic compounds (Peltoniemi et al., 2009), members of this phylum produce extracellular enzymes and have comparable enzymatic capabilities to fungi. They are known for their ability to degrade cellulose, lignin and other complex biopolymers in different soil habitats (Le Roes-Hill et al., 2011; McCarthy, 1987) and can, therefore, reflect higher lignin nature of the SSF environment.

Microbial communities in peatland microhabitats

We documented that the specific microhabitats, microsites dominated by the different plant species, significantly shaped the peat prokaryotic and fungal communities (**Paper 6**). Additionally, prokaryotic response to microhabitat and site was complemented by their response to gradients in soil pH and N content, factors that most strongly differentiate the plant species-defined microhabitats (Kaštovská et al., 2018). This is in agreement with previous studies reporting a strong relationship between bacteria and archaea with pH and N gradients in diverse soils (Fierer and Ladau, 2012; Rousk et al., 2010b). We specifically focused on microorganisms involved in methane cycling, on methanogens and methanotrophs. The methanogenic community was mainly shaped by pH and overall nutrient limitation and was significantly distinct in the blueberry microhabitat compared to wetter microhabitats with cottongrass and peat moss. We assume that the lower methanogenic potential in blueberry microhabitat can be attributed to the suppression of fermenters and syntrophic bacteria due to the lower water table. Methanotrophs were dominated by type II MOB (Methylocystaceae), their abundances (i.e. the quantity of *pmoA* gene) were the same regardless of the plant dominant, which is in line with previous studies in *Sphagnum* dominated peat (Kip et al., 2012). Since methanotrophs can easily be transferred by water, they are thus unlikely to be plant

species-specific (Bragina et al., 2013). Our data showed that their composition and abundance were more influenced by the pH, C:N ratio and differences in water table level.

In summary, we demonstrated that low pH influences specific activities and kinetics of soil enzymes in C and N utilization in different soil layers which may lead to imbalances in available C and N pools influencing C and N cycle and lead to potential N losses from these ecosystems. In spruce swamp forest and distinct peatlands, we found that microhabitats dominated by specific vegetation harbor different bacterial and archaeal communities with specific functional potential which can have a significant effect on CO₂ and CH₄ fluxes.

Part II: “Some like it cold” Functioning of microbial communities in C and N cycle in Arctic Cryosols

Cryosols (permafrost-affected soils) cover more than 90% of the continuous permafrost zone in the Arctic (Tarnocai and Bockheim, 2011). They represent the dominant soil in the Arctic and Subarctic regions in Canada, Alaska, Russia but also occur in the Boreal and Alpine regions.

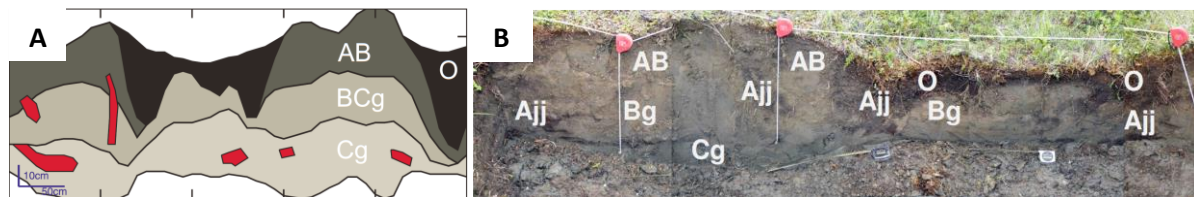


Figure 2: (A) Schematic drawings of soil profile from grass tundra (site 1, Cherskiy, east Siberia). O, Oe, Oa, OA: organic topsoil. A, AB, BCg, Cg: mineral subsoil. Ajj: buried organic-rich material (cryOM - red areas). (B) Representative picture of the excavated soil profile from grass tundra (Gittel et al., 2014)

Cryosols store more than 1300 Pg of organic carbon (C), which is about half of the global soil C and twice as much as is currently contained in the atmosphere (Tarnocai, 2009). They are, therefore, important components in the global C cycle (Schuur et al., 2008). A substantial amount of this C is stored in buried pockets of organic matter (cryOM) by the process of cryoturbation (**Figure 2**), the burial of topsoil material into deeper soil horizons by repeated freeze-thaw events. Harden (2012) estimated that across the entire northern circumpolar permafrost region, approximately 400 Pg of organic C is stored in cryOM. These C-rich pockets are distributed in the whole soil profile of the active layer as well in frozen permafrost (**Figure 2**).

Cryosols are warming rapidly, and current scenarios predict an increase of temperature up to 4.8 °C by 2100. Higher subsoil temperatures will lead to enhanced permafrost thaw, prolonged frost-free periods, increased soil active layer thickness and oxygen levels by soil drainage (Lawrence et al., 2015). It can promote the availability of large permafrost C pools including the C in cryOM for microbial decomposition. The microbial decomposition of SOM is more temperature-sensitive than primary production (Davidson and Janssens, 2006) and this may generate greenhouse gas emissions from permafrost areas and create a positive feedback to climate warming (**Figure 3**, Koven et al., 2011; Ping et al., 2015; Schuur et al., 2008; Schuur and Abbott, 2011).

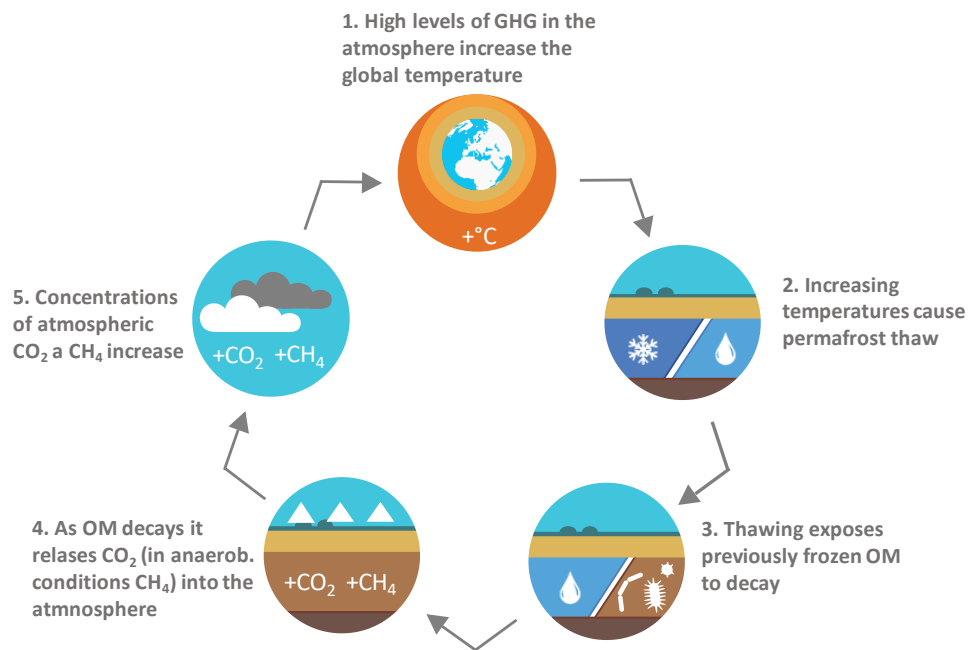


Figure 3: The positive feedback loop of permafrost melting. *Source: University of Edinburgh*

The major gap in our current understanding of the C vulnerability of cryOM is the structure and the degradation capacities of the microbial communities. Until recently, the role of microbial communities in the Arctic biogeochemical cycles has remained largely unexplored. Most of the studies have preferentially focused on microbial communities in the topsoil of cryosols active layer or specifically on the underlying permafrost (Mackelprang et al., 2017; Tveit et al., 2013; Yergeau et al., 2010) ignoring microbes in cryOM.

In our research, we wanted to fill this gap and specifically characterize microbial communities in cryOM (**Paper 7, 8**), C vulnerability affected by temperature (**Paper 9**), simulated root exudates (**Paper 10**), mineral-OM associations (**Paper 11**) and identify mechanisms of possible CO₂ attenuation (**Paper 12**).

Specific microbial communities in cryoturbated OM (cryOM) of Cryosols

To understand the vulnerability of C and N pools we need to describe in detail (**BOX 1**) the microbial communities in Cryosols and uncover their functional potential. Similarly to temperate soils, the prokaryotic communities in Cryosols are the most active at the surface soil layers, and mainly in the rhizosphere around the plant roots. Unlike the temperate soils, the soil layer influenced by plants in Cryosols is usually very thin because of the shallow rooting depth of local plant species (Iversen et al., 2015) caused by repeated freeze-thaw cycles (Schimel and Clein, 1996) which prevents the growth of roots deeper to the soil profile. This layer often contains easy available C and N sources which promote mostly copiotrophic organisms, fast-growing taxa, which recruits mainly from the Gammaproteobacteria or Bacteroidetes (Fierer et al., 2003). The available nutrients, however, rapidly decrease with depth and in deeper soil horizons oligotrophic microbes dominate because they more efficiently utilize complex and recalcitrant compounds (i.e. polyphenolic compounds) which proportionally increase with depth. In general, the abundance, diversity of prokaryotes along the soil depth profile thus follows the gradient of C and N availability and together with abiotic conditions (i.e. low to subzero temperatures, anoxia due to waterlogging) it results in distinct community patterns and less microbial biomass in deeper soil horizons (Eilers et al., 2012; Hartmann et al., 2009).

In our research (**Paper 7**) we analyzed more than 100 samples and found that specifically, cryOM does not follow the continuum of decreasing microbial abundance with depth. The cryOM harbored significantly more bacteria and archaea abundances than was found in the surrounding subsoil horizons and were similarly abundant to topsoil horizons. They reflected the higher amount of

organic matter in cryOM. Because of lower bulk density of cryOM undergo periodically increased water-logging after the active layer thaw. Anaerobic members from the Chloroflexi (Anaerolineaceae) and Firmicutes (Clostridia) and relative proportions of prokaryotic functional guilds (e.g. bacteria able to perform anaerobic respiration, fermentation, methano-/methylotrophs) were significantly enriched in cryOM (**Paper 7,8**). One of the significantly depleted anaerobic groups in cryOM were iron-reducers and methanogens. Iron-reducers respire anaerobically Fe^{III} and reduce it to Fe^{II} which can lead to destabilization of OM in organo-mineral complexes making it vulnerable to microbial decomposition (**Paper 11**). Their lower proportion in the microbial community in cryOM can contribute to lower C vulnerability. Similarly, a lower proportion of methanogens indicates a low potential for CH_4 flux from cryOM (**Paper 9**).

On the other hand, we found that Actinobacteria, and in particular the order Actinomycetales, clearly dominated in cryOM (over 50 % of assigned sequences, **Paper 7, 8**). Actinobacteria were also found as a significant part of the active prokaryotic community in the Arctic (McMahon et al., 2011). There are several reasons why Actinobacteria may benefit from an oligotrophic and anoxic environment of cryOM. Actinobacteria produce immense diversity of secondary metabolites including antibiotics, which help them outcompete other bacteria when nutrients are scarce (Van Der Heul et al., 2018). They can easier maintain metabolic activity at low and subzero temperatures because of their efficient DNA repair mechanisms (Barka et al., 2016). Their genomes contain genes encoding phenoloxidases and peroxidases (Ausec et al., 2011; Bugg et al., 2011) which predetermine them to degrade biopolymers including recalcitrant polyphenolic compounds (Lykidis et al., 2007). In cryOM, we detected unique actinobacterial anaerobic lignin degraders from family Intrasporangiaceae and class Thermoleophilia (Schellenberger et al., 2010), which comprised up to 8 % of the bacterial community (**Paper 8**). By their activities, they are able to solubilize lignin and have probably better access to available resources otherwise protected by the complex lignin matrix than other bacteria (Le Roes-Hill et al., 2011; McCarthy, 1987). Last but not least they also produce extracellular polymeric substances (EPS) which can serve as the protective cell coat against low temperatures (Zhou et al., 2016), permit the diffusion of nutrients from cells into the environment (Costa et al., 2018) and help to stabilize the OM in soil aggregates (Tisdall and Oades, 1982). All the above-mentioned factors can help Actinobacteria in getting to available resources when the amount of available C and N in cryOM is very low while lignin and polyphenolic compounds dominate (Dao et al., 2018; Gentsch et al., 2015).

Contrary to bacteria, the biomass of fungi in cryOM was very low (**Paper 7,8**) and similar to the surrounding mineral subsoil. We argue that this dramatic community shift and fungal dieback is the result of burying of OM, during which the original fungal community was not able to cope with quickly changing conditions, and was partly mixed with the subsoil community. Unlike bacteria, fungi are also more sensitive to freezing-thawing (Schostag et al., 2019). In addition, the fungal community composition was significantly different from the topsoil (**Paper 7**). Because of low abundance, the saprotrophic fungi are not able to efficiently degrade OM in cryOM. Additionally, cryOM fungi, because they lost connection with plant roots, were also depleted in mycorrhizal fungi (e.g. Russulales, Thelephorales) which may have important consequences on C vulnerability of cryOM. Mycorrhizal fungi are known for their ability to utilize organic N (Hodge et al., 2001; Talbot et al., 2008) and can, therefore, mobilize the available N to soil microbial community in highly N limited arctic soils. Together with a low abundance of saprotrophic fungi, it can limit the synthesis of extracellular C and N enzymes leading to probably low depolymerization of C- and N-rich biopolymers (Wild et al., 2013). Therefore, fungal contribution to the recalcitrant C decomposition in cryOM is probably negligible.

The vulnerability of Cryosol C to climate change

We incubated the distinct Cryosol horizons from the active layer (topsoil, subsoil, cryOM) at different temperatures ranging from 4°C to 20°C in several laboratory incubation experiments. In the first experiment, we found that C loss (determined by cumulative CO_2 and CH_4 production) was not primarily controlled by temperature and oxygen level but more strongly by microbial biomass inhabiting each horizon (**Paper 9**). The temperature did not affect microbial biomass and the cryOM

exhibited the lowest C loss from cryOM. This highlights the importance of an active microbial community already present in the specific horizon and its functional capabilities in the decomposition of present organic matter (**Paper 7, 8**). We argue that instead of producing the energetically and N demanding extracellular enzymes, the microbial community in the cryOM relies on the flux of material (e.g. enzymes and nutrients) from the topsoil organic horizons bypassing chemical-physical constraints (e.g. OM associated with soil minerals) of cryOM C decomposition. By separating the horizons for the incubation experiment we most likely interrupted the flux of nutrients from the topsoil horizon to cryOM. The enzymatic pool at the start of the incubation in the cryOM, was surprisingly high and gradually decreased during the incubation. This probably broke the links between microbial biomass (i.e. microbial community functioning) – enzymes - C and nutrient availability.

Our data, therefore, indicate that the critical driver, which limits the microbial community in Cryosols, is a long term disconnection between extracellular enzymes and microbial biomass and the occurrence of anaerobic conditions. We already described that the cryOM have different microbial communities than the topsoil. During the burying of OM, fungi almost disappeared and their role was most likely replaced by Actinobacteria with less efficient phenoloxidases and peroxidases (Godden et al., 1992) which contributes to slower C decomposition of phenolic compounds present in cryOM (Dao et al., 2018). Contrary to the topsoil horizon, enzymatic activity in cryOM depends strongly on a less active microbial community (Schnecker et al., 2015), which can lead to general deceleration of N cycling (Wild et al., 2013). A higher abundance of anaerobes (**Paper 7**) can cause a decrease of microbial biomass itself as we observed in topsoil horizons incubated under anaerobic conditions. All these factors keep the microbial community in cryOM highly N limited.

To address the possible N limitation of C decomposition in cryOM, we conducted an incubation experiment where we added simple C (glucose) and N (amino acids) compounds commonly produced during the rhizodeposition (**Paper 10**). We confirmed that the C decomposition in cryOM was highly N limited and susceptible to priming, with rates of SOM-derived respiration comparable to topsoil rates mainly after the easy available N (amino acids) addition. In systems of strong N limitation, where low N availability limits the production of extracellular enzymes, N addition can stimulate decomposition by facilitating enzyme production by fungi (Allison, 2006). Since in our study the amendment of amino acids to cryOM did not systematically increase microbial biomass or the abundance of specific microbial groups, we suggest that microorganisms invested the additional N in the production of extracellular enzymes.

Our findings are in contrast to observations of increased C storage in mineral subsoil horizons with warming (Sistla and Schimel, 2013), but supports predictions of high C losses from Cryosols if plant productivity increases (Hartley et al., 2012). These contrasting findings of the impact of higher plant productivity on soil C stocks point to a strong context-dependency of priming effects in Cryosols.

Additionally, to N limitation we found the physicochemical constraints including the associations of OM with soil minerals, which largely influence C decomposition in Cryosols (**Paper 11**). Knowledge about the distribution of C between different OM fractions would provide deeper insights into the main control mechanisms of total C mineralization. We found that 2/3 of the total C stocks within the mineral soil horizons were present in the heavy fraction (HF), which means that organic C was associated with fine silt and clay soil particles. On the other hand, the light fraction (LF) (free particulate organic matter) accounted for 1/4 and the rest was mobilized in dissolved form during the density fractionation (Gentsch et al., 2015). The OM associated with HF contributed to about 70 % of the bulk soil respiration in all the mineral soil horizons including cryOM. Consequently, the C mineralization in the HF followed the pattern of that in the bulk soil being the lowest in the cryOM which confirms our previous findings (**Paper 9, 10**). Our results thus indicate that the organic C in the HF most likely contributes largely to the CO₂ release from mineral horizons. The temperature was a strong control increasing the C mineralization during the incubation. According to the principles of kinetic theory, the temperature sensitivity of OM increases with “substrate complexity” (so-called ‘carbon-quality-temperature’ (CQT) concept, (Davidson and Janssens, 2006). We found that the HF also exhibited greater sensitivity to temperature than the faster decomposing bulk OM, however, the CQT concept fails when considering the variation in temperature sensitivity with depth. We observed

decreasing temperature sensitivity with depth regardless of the type of OM fraction. At the same time, the Q_{10} was positively correlated with the C:N ratio and $\delta^{13}\text{C}$ values. Such a pattern would suggest a greater vulnerability of OM in the lower horizons, which is not supported by the molecular structure (Dao et al., 2018). Therefore, the discrepancy between kinetic theory and the observed temperature sensitivity should be explained by reduced OC availability with increasing depth, and by mineral protection of OM (Gillabel et al., 2010). Increased metal-to-HF-OC-ratios in cryOM may also cause stronger mineral-organic binding (Kaiser and Guggenberger, 2003) which can cause lower C vulnerability in cryOM.

Because mineral-OM interactions (i.e., adsorption-desorption, coprecipitation) are strongly controlled by soil H^+ , the soil pH was also a highly significant predictor of both the OC mineralization and Q_{10} in Cryosols. Weaker binding occurs at neutral and alkaline pH, whereas desorption processes and thus the OM accessibility to decomposers are reduced at low soil pH (see the review by Kleber et al. (2015)). We observed higher C mineralization with increasing soil pH mainly in mineral horizons including cryOM.

So far, we identified two main constrains of cryOM C vulnerability and consequently CO_2 emissions: (i) N limitation and (ii) physicochemical protection of OM in deeper Cryosol horizons. We, however, found another factor that might contribute to lower CO_2 emission from deeper mineral horizons of Cryosols including cryOM (**Paper 12**). We incubated again different soil horizons and determined the dark (i.e. not affected by photosynthetic microorganisms) $^{13}\text{CO}_2$ incorporation into the soil organic matter and into microbial biomass (phospholipid fatty acids). CO_2 is the main or even the only C source for chemoautotrophs. However, a wide spectrum of heterotrophic bacteria and fungi employ carboxylases to (i) assimilate various organic substrates such as acetone, phenolics, propionate, or leucine, (ii) replenish the citric acid cycle in anaplerotic reactions and, finally, (iii) synthesize cellular compounds (Erb et al., 2011; Hesselsoe et al., 2005). We found that dark CO_2 fixation accounted on average for 0.4, 1.0, 1.1, and 16% of net CO_2 production in the organic topsoil, cryOM, mineral subsoil, and permafrost, respectively. We confirmed the data by metagenomic analyses and quantification of carboxylase genes involved in anaplerotic reactions and identified Actinobacteria (mainly the genus *Arthrobacter*) as the main group responsible for carboxylase production and probably heterotrophic CO_2 fixation. The dark CO_2 fixation may therefore partly attenuate CO_2 emission from Cryosols and particularly from deeper horizons including cryOM.

Conclusions and future perspectives

- Our research contributed to the understanding C and N cycle in soils differing in pH, oxygen availability, temperature, and nutrient availability. We applied new high throughput sequencing technologies (e.g. targeted gene sequencing and metagenomics) in characterizing the microbial communities and implemented a new bioinformatic tool that allows the prediction of main microbial functions. These detailed taxonomic and functional information we combined with quantification of microbial communities and specific genes in C and N cycle.
- We showed that the in acid soil C and N cycle is tightly linked to the activity of specific microbial taxa from Acidocateria and Actinobacteria phyla most likely through their production of specific enzymes (both oxidative and hydrolytic) which drive the critical steps in organic matter transformations. We also showed that when trying predict available C and N decomposability and link it to OM decomposition is necessary to have the information about the kinetic characteristics (apparent K_m , apparent V_{max}) to determine the enzyme-substrate affinities and possible substrate inhibitions and also determine the temperature sensitivity of studied enzymes which may largely influence the overall vulnerability of organic C and N in soil during the season.
- In highly acid forest soils with pH below 4 our research uncover that highly diverse group of *nirK* denitrifiers is the most related to the available C and N and that they are highly limited by low pH and that these may have consequences in mineral N turnover in acid forest soils when deciding if the soil will lose N or if it will stay in the system and will be recycled in microbial biomass.

- Our research on microbial communities involved in C and N within the peatland and spruce swamp forest showed that in methane cycle (mainly methanotrophs) are influenced by specific microhabitats of vegetation and that not only the oxygen level but mainly the amount of available nutrients in different vegetation habitats control the methane fluxes.
- In cold environment of the Arctic, we found that the environmental (physical-chemical) constraints of Cryosols (low temperature, low oxygen availability, low nutrient availability, and OM mineral associations) caused the selective pressure on both bacterial and fungal communities living in the Cryosols and specifically on community in cryoturbated OM (cryOM) when they were buried to the soil profile. This strong selective pressure favored probably specific taxa from the Actinobacteria phylum but on the other side almost totally suppressed the whole fungal community.
- The most important finding was that the temperature alone does not ensure that the vulnerability of OM will be higher. In Cryosol N is the most limiting factor and we proved that mainly in cryOM its increased availability may evoke a positive priming effect on OM decomposition. Last but not least we also found that Actinobacteria (mainly the genus *Arthrobacter*) are probably involved in heterotrophic CO₂ fixation, which may mitigate CO₂ emissions from Arctic Cryosols and mainly from cryOM.

We will continue to study the microbial communities in C and N cycle in different habitats, including Arctic Cryosols in the frame of the running Czech-German project “CRYOVULCAN - Vulnerability of carbon in Cryosols – substrate-microorganisms-aggregate interactions”. In our future research, we will focus in detail on microbial communities in different soil aggregates and on factors influencing the stabilization of OM.

Acknowledgment

I thank many people for helping me to achieve this milestone in my career – mainly my mentor Hana Šantrůčková for introducing me to the amazing world of soil microbiology; her and all other colleagues, collaborators, and friends for cooperation on our research projects by helping to get, discuss and publish the data and by creating friendly and inspiring working environment.

Many outstanding colleagues contributed to this habilitation during plenty of interdisciplinary collaborations. Mia Bengtsson, Hanka Bošková-Petrásková, Petr Čapek, Lenka Čapková, Keith Edwards, Norman Gentsch, Georg Guggenberger, Gustaf Hugelius, Michal Choma, Eva Kaštovská, Katka Kučerová, Peter Kuhry, Kolya Lashchinskiy, Patrick Liebmann, Jirka Mastný, Robert Mikutta, Filip Oulehle, Sebastian Petters, Tomáš Pícek, Andreas Richter, Hana Šantrůčková, Dáša Sirová, Pája Staňková, Jörg Schneckner, Christa Schleper, Olga Shibistova, Zuzka Urbanová, Daniel Vaněk, Birgit Wild, Karolina Tahovská, Jaroslav Vrba, Jana Vrbová.

My special thanks are for my family, my loves and most importantly my precious daughters Klárka and Anetka which are my sweethearts and bring everyday light to my life.

“Picture on the title page is the fluorescently labeled microbial community attached to 5000 years old organic matter in permafrost”

References

- Aber, J.D., Melillo, J.M., McLaugherty, C.A., 1990. Predicting long-term patterns of mass loss, nitrogen dynamics, and soil organic matter formation from initial fine litter chemistry in temperate forest ecosystems. *Canadian Journal of Botany* 68, 2201–2208. doi:10.1139/b90-287
- Allison, S.D., 2006. Soil minerals and humic acids alter enzyme stability: Implications for ecosystem processes. *Biogeochemistry* 81, 361–373. doi:10.1007/s10533-006-9046-2
- Allison, S.D., Jastrow, J.D., 2006. Activities of extracellular enzymes in physically isolated fractions of restored grassland soils. *Soil Biology and Biochemistry* 38, 3245–3256. doi:10.1016/j.soilbio.2006.04.011
- Amir, A., McDonald, D., Navas-Molina, J.A., Kopylova, E., Morton, J.T., Zech Xu, Z., Kightley, E.P., Thompson, L.R., Hyde, E.R., Gonzalez, A., Knight, R., 2017. Deblur Rapidly Resolves Single-Nucleotide Community Sequence Patterns. *MSystems* 2. doi:10.1128/msystems.00191-16
- Arao, T., 1999. In situ detection of changes in soil bacterial and fungal activities by measuring ¹³C incorporation into soil phospholipid fatty acids from ¹³C acetate. *Soil Biology and Biochemistry* 31, 1015–1020. doi:10.1016/S0038-0717(99)00015-2
- Arrhenius, S., 1896. in the Air upon the Temperature of Svante Arrhenius. *Philosophical Magazine and Journal of Science*.
- Ausec, L., van Elsas, J.D., Mandic-Mulec, I., 2011. Two- and three-domain bacterial laccase-like genes are present in drained peat soils. *Soil Biology and Biochemistry* 43, 975–983. doi:10.1016/j.soilbio.2011.01.013
- Bååth, E., Anderson, T.H., 2003. Comparison of soil fungal/bacterial ratios in a pH gradient using physiological and PLFA-based techniques. *Soil Biology and Biochemistry* 35, 955–963. doi:10.1016/S0038-0717(03)00154-8
- Baldrian, P., Kolářik, M., Štursová, M., Kopecký, J., Valášková, V., Větrovský, T., Žifčáková, L., Šnajdr, J., Rídl, J., Vlček, Č., Voříšková, J., 2012. Active and total microbial communities in forest soil are largely different and highly stratified during decomposition. *ISME Journal* 6, 248–258. doi:10.1038/ismej.2011.95
- Baptist, F., Zinger, L., Clement, J.C., Gallet, C., Guillemin, R., Martins, J.M.F., Sage, L., Shahnavaz, B., Choler, P., Geremia, R., 2008. Tannin impacts on microbial diversity and the functioning of alpine soils: A multidisciplinary approach. *Environmental Microbiology* 10, 799–809. doi:10.1111/j.1462-2920.2007.01504.x
- Bardgett, R.D., Jones, A.C., Jones, D.L., Kemmitt, S.J., Cook, R., Hobbs, P.J., 2001. Soil microbial community patterns related to the history and intensity of grazing in sub-montane ecosystems. *Soil Biology and Biochemistry* 33, 1653–1664. doi:10.1016/S0038-0717(01)00086-4
- Barka, E.A., Vatsa, P., Sanchez, L., Gaveau-Vaillant, N., Jacquard, C., Klenk, H.-P., Clément, C., Ouhdouch, Y., van Wezel, G.P., 2016. Taxonomy, Physiology, and Natural Products of Actinobacteria. *Microbiology and Molecular Biology Reviews* 80, 1–43. doi:10.1128/membr.00019-15
- Basiliko, N., Yavitt, J.B., Dees, P.M., Merkel, S.M., 2003. Methane biogeochemistry and methanogen communities in two Northern Peatland ecosystems, New York state. *Geomicrobiology Journal* 20, 563–577. doi:10.1080/713851165
- Berg, B., 1986. Nutrient release from litter and humus in coniferous forest soils—a mini review. *Scandinavian Journal of Forest Research* 1, 359–369. doi:10.1080/02827588609382428
- Berg, B., Ekbohm, G., 1991. Litter mass-loss rates and decomposition patterns in some needle and leaf litter types. Long-term decomposition in a Scots pine forest. VII. *Canadian Journal of Botany* 69, 1449–1456. doi:10.1139/b91-187
- Billings, S.A., Ballantyne, F., 2013. How interactions between microbial resource demands, soil organic matter stoichiometry, and substrate reactivity determine the direction and magnitude of soil respiratory responses to warming. *Global Change Biology*. doi:10.1111/gcb.12029
- Blagodatskaya, E. V., Anderson, T.H., 1998. Interactive effects of pH and substrate quality on the fungal-to-bacterial ratio and QCO₂ of microbial communities in forest soils. *Soil Biology and Biochemistry* 30, 1269–1274. doi:10.1016/S0038-0717(98)00050-9
- Bragazza, L., Freeman, C., 2007. High nitrogen availability reduces polyphenol content in Sphagnum peat. *Science of the Total Environment* 377, 439–443. doi:10.1016/j.scitotenv.2007.02.016
- Bragina, A., Berg, C., Müller, H., Moser, D., Berg, G., 2013. Insights into functional bacterial diversity and its effects on Alpine bog ecosystem functioning. *Scientific Reports* 3. doi:10.1038/srep01955
- Bray, J.R., Gorham, E., 1964. Litter Production in Forests of the World†. *Advances in Ecological Research* 2, 101–157. doi:10.1016/S0065-2504(08)60331-1
- Bremner, J.M., Zantua, M.I., 1975. Enzyme activity in soils at subzero temperatures. *Soil Biology and Biochemistry* 7, 383–387. doi:10.1016/0038-0717(75)90054-1
- Bubier, J.L., Moore, T.R., Roulet, N.T., 1993. Methane emissions from wetlands on the midboreal region of northern Ontario, Canada. *Ecology* 74, 2240–2254. doi:10.2307/1939577
- Bugg, T.D.H., Ahmad, M., Hardiman, E.M., Rahmanpour, R., 2011. Pathways for degradation of lignin in bacteria and fungi. *Natural Product Reports*. doi:10.1039/c1np00042j
- Burns, R.G., DeForest, J.L., Marxsen, J., Sinsabaugh, R.L., Stromberger, M.E., Wallenstein, M.D., Weintraub, M.N., Zoppini, A., 2013. Soil enzymes in a changing environment: Current knowledge and future directions. *Soil Biology and Biochemistry*. doi:10.1016/j.soilbio.2012.11.009
- Callahan, B.J., McMurdie, P.J., Rosen, M.J., Han, A.W., Johnson, A.J.A., Holmes, S.P., 2016. DADA2: High-resolution sample inference from Illumina amplicon data. *Nature Methods* 13, 581–583. doi:10.1038/nmeth.3869
- Čapek, P., Manzoni, S., Kaštovská, E., Wild, B., Diáková, K., Bárta, J., Schneckler, J., Biasi, C., Martikainen, P.J., Alves, R.J.E., Guggenberger, G., Gentsch, N., Hugelius, G., Palmtag, J., Mikutta, R., Shibistova, O., Ulrich, T., Schleper, C., Richter, A., Šantrůčková, H., 2018. A plant–microbe interaction framework explaining nutrient effects on primary production. *Nature Ecology and Evolution* 2, 1588–1596. doi:10.1038/s41559-018-0662-8
- Carlyle, J.C., Lowther, D.J.R., Smethurst, P.J., Nambiar, E.K.S., 1990. Influence of chemical properties on nitrogen mineralization and nitrification in podzolized sands. Implications for forest management. *Australian Journal of Soil Research* 28, 981–1000. doi:10.1071/SR9900981
- Chapin, F.S., Rincon, E., Huante, P., 1993. Environmental responses of plants and ecosystems as predictors of the impact of global change. *Journal of Biosciences* 18, 515–524. doi:10.1007/BF02703083
- Chu, H., Grogan, P., 2010. Soil microbial biomass, nutrient availability and nitrogen mineralization potential among vegetation-types in a low arctic tundra landscape. *Plant and Soil* 329, 411–420. doi:10.1007/s11104-009-0167-y
- Comerford, N.B., Skinner, M.F., 1989. Residual Phosphorus Solubility for an Acid, Clayey, Forested Soil in the Presence of Oxalate and

- Citrate. *Canadian Journal of Soil Science* 69, 111–117. doi:10.4141/cjss89-010
- Conant, R.T., Ryan, M.G., Ågren, G.I., Birge, H.E., Davidson, E.A., Eliasson, P.E., Evans, S.E., Frey, S.D., Giardina, C.P., Hopkins, F.M., Hyvönen, R., Kirschbaum, M.U.F., Lavelle, J.M., Leifeld, J., Parton, W.J., Megan Steinweg, J., Wallenstein, M.D., Martin Wetterstedt, J.Å., Bradford, M.A., 2011. Temperature and soil organic matter decomposition rates - synthesis of current knowledge and a way forward. *Global Change Biology*. doi:10.1111/j.1365-2486.2011.02496.x
- Costa, O.Y.A., Raaijmakers, J.M., Kuramae, E.E., 2018. Microbial extracellular polymeric substances: Ecological function and impact on soil aggregation. *Frontiers in Microbiology*. doi:10.3389/fmicb.2018.01636
- Cox, P., Wilkinson, S.P., Anderson, J.M., 2001. Effects of fungal inocula on the decomposition of lignin and structural polysaccharides in *Pinus sylvestris* litter. *Biology and Fertility of Soils* 33, 246–251. doi:10.1007/s003740000315
- Dao, T.T., Gentsch, N., Mikutta, R., Sauheitl, L., Shibistova, O., Wild, B., Schneckner, J., Bárta, J., Čapek, P., Gittel, A., Lashchinskiy, N., Urich, T., Šantrůčková, H., Richter, A., Guggenberger, G., 2018. Fate of carbohydrates and lignin in north-east Siberian permafrost soils. *Soil Biology and Biochemistry* 116, 311–322. doi:10.1016/j.soilbio.2017.10.032
- Davidson, E.A., Janssens, I.A., 2006. Temperature sensitivity of soil carbon decomposition and feedbacks to climate change. *Nature*. doi:10.1038/nature04514
- Douglas, G.M., Beiko, R.G., Langille, M.G.I., 2018. Predicting the Functional Potential of the Microbiome from Marker Genes Using PICRUSt, in: *Methods in Molecular Biology*. pp. 169–177. doi:10.1007/978-1-4939-8728-3_11
- Edgar, R.C., 2010. Search and clustering orders of magnitude faster than BLAST. *Bioinformatics* 26, 2460–2461. doi:10.1093/bioinformatics/btq461
- Eilers, K.G., Debenport, S., Anderson, S., Fierer, N., 2012. Digging deeper to find unique microbial communities: The strong effect of depth on the structure of bacterial and archaeal communities in soil. *Soil Biology and Biochemistry* 50, 58–65. doi:10.1016/j.soilbio.2012.03.011
- Elser, J.J., 2003. Biological stoichiometry: A theoretical framework connecting ecosystem ecology, evolution, and biochemistry for application in astrobiology. *International Journal of Astrobiology* 2, 185–193. doi:10.1017/S1473550403001563
- Elser, James J., Fagan, W.F., Denno, R.F., Dobberfuhl, D.R., Folarin, A., Huberty, A., Interlandi, S., Kilham, S.S., McCauley, E., Schulz, K.L., Siemann, E.H., Sterner, R.W., 2000. Nutritional constraints in terrestrial and freshwater food webs. *Nature* 408, 578–580. doi:10.1038/35046058
- Elser, J. J., Sterner, R.W., Gorokhova, E., Fagan, W.F., Markow, T.A., Cotner, J.B., Harrison, J.F., Hobbie, S.E., Odell, G.M., Weider, L.W., 2000. Biological stoichiometry from genes to ecosystems. *Ecology Letters*. doi:10.1046/j.1461-0248.2000.00185.x
- Erb, M., Robert, C.A.M., Turlings, T.C.J., 2011. Induction of root-resistance by leaf-herbivory follows a vertical gradient. *Journal of Plant Interactions* 6, 133–136. doi:10.1080/17429145.2010.545958
- Fassnacht, K.S., Gower, S.T., 1999. Comparison of the litterfall and forest floor organic matter and nitrogen dynamics of upland forest ecosystems in north central Wisconsin. *Biogeochemistry* 45, 265–284. doi:10.1007/bf00993003
- Fierer, N., Bradford, M.A., Jackson, R.B., 2007. Toward an ecological classification of soil bacteria. *Ecology* 88, 1354–1364. doi:10.1890/05-1839
- Fierer, N., Jackson, R.B., 2006. The diversity and biogeography of soil bacterial communities. *Proceedings of the National Academy of Sciences of the United States of America* 103, 626–631. doi:10.1073/pnas.0507535103
- Fierer, N., Ladau, J., 2012. Predicting microbial distributions in space and time. *Nature Methods*. doi:10.1038/nmeth.2041
- Fierer, N., Schimel, J.P., Holden, P.A., 2003. Variations in microbial community composition through two soil depth profiles. *Soil Biology and Biochemistry* 35, 167–176. doi:10.1016/S0038-0717(02)00251-1
- Firestone, M.K., Killham, K., McColl, J.G., 1983. Fungal toxicity of mobilized soil aluminum and manganese. *Applied and Environmental Microbiology* 46, 758–761.
- Fish, J.A., Chai, B., Wang, Q., Sun, Y., Brown, C.T., Tiedje, J.M., Cole, J.R., 2013. FunGene: The functional gene pipeline and repository. *Frontiers in Microbiology* 4. doi:10.3389/fmicb.2013.00291
- Flis, S.E., Glenn, A.R., Dilworth, M.J., 1993. The interaction between aluminium and root nodule bacteria. *Soil Biology and Biochemistry*. doi:10.1016/0038-0717(93)90066-K
- Frankenberger, W.T., Tabatabai, M.A., 1991. Factors affecting l-asparaginase activity in soils. *Biology and Fertility of Soils* 11, 1–5. doi:10.1007/BF00335825
- Freschet, G.T., Cornelissen, J.H.C., van Logtestijn, R.S.P., Aerts, R., 2010. Substantial nutrient resorption from leaves, stems and roots in a subarctic flora: What is the link with other resource economics traits? *New Phytologist* 186, 879–889. doi:10.1111/j.1469-8137.2010.03228.x
- Frostegård, Å., Bååth, E., Tunlio, A., 1993. Shifts in the structure of soil microbial communities in limed forests as revealed by phospholipid fatty acid analysis. *Soil Biology and Biochemistry* 25, 723–730. doi:10.1016/0038-0717(93)90113-P
- Fu, B.J., Liu, S.L., Chen, L.D., Lü, Y.H., Qiu, J., 2004. Soil quality regime in relation to land cover and slope position across a highly modified slope landscape, in: *Ecological Research*. pp. 111–118. doi:10.1111/j.1440-1703.2003.00614.x
- Galand, P.E., Fritze, H., Conrad, R., Yrjälä, K., 2005. Pathways for methanogenesis and diversity of methanogenic archaea in three boreal peatland ecosystems. *Applied and Environmental Microbiology* 71, 2195–2198. doi:10.1128/AEM.71.4.2195-2198.2005
- Gentsch, N., Mikutta, R., Alves, R.J.E., Bárta, J., Čapek, P., Gittel, A., Hugelius, G., Kuhry, P., Lashchinskiy, N., Palmtag, J., Richter, A., Šantrůčková, H., Schneckner, J., Shibistova, O., Urich, T., Wild, B., Guggenberger, G., 2015. Storage and transformation of organic matter fractions in cryoturbated permafrost soils across the Siberian Arctic. *Biogeosciences* 12, 4525–4542. doi:10.5194/bg-12-4525-2015
- Gianfreda, L., De Cristofaro, A., Rao, M.A., Violante, A., 1995a. Kinetic behavior of synthetic organo- and organo-mineral-urease complexes. *Soil Science Society of America Journal* 59, 811–815. doi:10.2136/sssaj1995.03615995005900030025x
- Gianfreda, L., Rao, M.A., Violante, A., 1995b. Formation and activity of urease-tannate complexes affected by aluminum, iron, and manganese. *Soil Science Society of America Journal* 59, 805–810. doi:10.2136/sssaj1995.03615995005900030024x
- Gianfreda, L., Sannino, F., Ortega, N., Nannipieri, P., 1994. Activity of free and immobilized urease in soil: Effects of pesticides. *Soil Biology and Biochemistry* 26, 777–784. doi:10.1016/0038-0717(94)90273-9
- Giesler, R., Högberg, M.N., Strobel, B.W., Richter, A., Nordgren, A., Högberg, P., 2007. Production of dissolved organic carbon and low-molecular weight organic acids in soil solution driven by recent tree photosynthate. *Biogeochemistry* 84, 1–12. doi:10.1007/s10533-007-9069-3
- Gillabel, J., Cebrian-Lopez, B., Six, J., Merckx, R., 2010. Experimental evidence for the attenuating effect of SOM protection on temperature sensitivity of SOM decomposition. *Global Change Biology* 16, 2789–2798. doi:10.1111/j.1365-2486.2009.02132.x

- Godden, B., Ball, A.S., Helvenstein, P., McCarthy, A.J., Penninckx, M.J., 1992. Towards elucidation of the lignin degradation pathway in actinomycetes. *Journal of General Microbiology* 138, 2441–2448. doi:10.1099/00221287-138-11-2441
- Graham, E.B., Knelman, J.E., Schindlbacher, A., Siciliano, S., Breulmann, M., Yannarell, A., Beman, J.M., Abell, G., Philippot, L., Prosser, J., Foulquier, A., Yuste, J.C., Glanville, H.C., Jones, D.L., Angel, R., Salminen, J., Newton, R.J., Bürgmann, H., Ingram, L.J., Hamer, U., Siljanen, H.M.P., Peltoniemi, K., Potthast, K., Bañeras, L., Hartmann, M., Banerjee, S., Yu, R.Q., Nogaró, G., Richter, A., Koranda, M., Castle, S.C., Goberna, M., Song, B., Chatterjee, A., Nunes, O.C., Lopes, A.R., Cao, Y., Kaisermann, A., Hallin, S., Strickland, M.S., García-Pausas, J., Barba, J., Kang, H., Isobe, K., Papaspyrou, S., Pastorelli, R., Lagomarsino, A., Lindström, E.S., Basiliko, N., Nemergut, D.R., 2016. Microbes as engines of ecosystem function: When does community structure enhance predictions of ecosystem processes? *Frontiers in Microbiology* 7. doi:10.3389/fmicb.2016.00214
- Guggenberger, G., Kaiser, K., 2003. Dissolved organic matter in soil: Challenging the paradigm of sorptive preservation, in: *Geoderma*. pp. 293–310. doi:10.1016/S0016-7061(02)00366-X
- Gupta, V., Smemo, K.A., Yavitt, J.B., Basiliko, N., 2012. Active Methanotrophs in Two Contrasting North American Peatland Ecosystems Revealed Using DNA-SIP. *Microbial Ecology* 63, 438–445. doi:10.1007/s00248-011-9902-z
- Hagedorn, F., Saurer, M., Blaser, P., 2004. A ¹³C tracer study to identify the origin of dissolved organic carbon in forested mineral soils. *European Journal of Soil Science* 55, 91–100. doi:10.1046/j.1365-2389.2003.00578.x
- Hagedorn, F., Schleppei, P., 2000. Determination of total dissolved nitrogen by persulfate oxidation. *Journal of Plant Nutrition and Soil Science* 163, 81–82. doi:10.1002/(sici)1522-2624(200002)163:1<81::aid-jpln81>3.3.co;2-t
- Hájek, T., Ballance, S., Limpens, J., Zijlstra, M., Verhoeven, J.T.A., 2011. Cell-wall polysaccharides play an important role in decay resistance of Sphagnum and actively depressed decomposition in vitro. *Biogeochemistry* 103, 45–57. doi:10.1007/s10533-010-9444-3
- Hamberger, A., Horn, M.A., Dumont, M.G., Murreil, J.C., Drake, H.L., 2008. Anaerobic consumers of monosaccharides in a moderately acidic fen. *Applied and Environmental Microbiology* 74, 3112–3120. doi:10.1128/AEM.00193-08
- Harden, J., 2012. The distribution and vulnerabilities of carbon in permafrost landscapes. *Quaternary International* 279–280, 188. doi:10.1016/j.quaint.2012.08.309
- Harriss, R.C., Gorham, E., Sebacher, D.I., Bartlett, K.B., Flebbe, P.A., 1985. Methane flux from northern peatlands. *Nature* 315, 652–654. doi:10.1038/315652a0
- Hartley, I.P., Garnett, M.H., Sommerkorn, M., Hopkins, D.W., Fletcher, B.J., Sloan, V.L., Phoenix, G.K., Wookey, P.A., 2012. A potential loss of carbon associated with greater plant growth in the European Arctic. *Nature Climate Change* 2, 875–879. doi:10.1038/nclimate1575
- Hartley, I.P., Heinemeyer, A., Evans, S.P., Ineson, P., 2007a. The effect of soil warming on bulk soil vs. rhizosphere respiration. *Global Change Biology* 13, 2654–2667. doi:10.1111/j.1365-2486.2007.01454.x
- Hartley, I.P., Heinemeyer, A., Ineson, P., 2007b. Effects of three years of soil warming and shading on the rate of soil respiration: Substrate availability and not thermal acclimation mediates observed response. *Global Change Biology* 13, 1761–1770. doi:10.1111/j.1365-2486.2007.01373.x
- Hartman, W.H., Richardson, C.J., Vilgalys, R., Bruland, G.L., 2008. Environmental and anthropogenic controls over bacterial communities in wetland soils. *Proceedings of the National Academy of Sciences of the United States of America* 105, 17842–17847. doi:10.1073/pnas.0808254105
- Hartmann, M., Lee, S., Hallam, S.J., Mohn, W.W., 2009. Bacterial, archaeal and eukaryal community structures throughout soil horizons of harvested and naturally disturbed forest stands. *Environmental Microbiology* 11, 3045–3062. doi:10.1111/j.1462-2920.2009.02008.x
- Henry, S., Baudoin, E., López-Gutiérrez, J.C., Martin-Laurent, F., Brauman, A., Philippot, L., 2004. Quantification of denitrifying bacteria in soils by *nirK* gene targeted real-time PCR. *Journal of Microbiological Methods* 59, 327–335. doi:10.1016/j.mimet.2004.07.002
- Hesselsoe, M., Nielsen, J.L., Roslev, P., Nielsen, P.H., 2005. Isotope labeling and microautoradiography of active heterotrophic bacteria on the basis of assimilation of ¹⁴CO₂. *Applied and Environmental Microbiology* 71, 646–655. doi:10.1128/AEM.71.2.646-655.2005
- Heylen, K., Gevers, D., Vanparys, B., Wittebolle, L., Geets, J., Boon, N., De Vos, P., 2006. The incidence of *nirS* and *nirK* and their genetic heterogeneity in cultivated denitrifiers. *Environmental Microbiology* 8, 2012–2021. doi:10.1111/j.1462-2920.2006.01081.x
- Hobbie, S.E., Reich, P.B., Oleksyn, J., Ogdahl, M., Zytkowski, R., Hale, C., Karolewski, P., 2006. Tree species effects on decomposition and forest floor dynamics in a common garden. *Ecology* 87, 2288–2297. doi:10.1890/0012-9658(2006)87[2288:TSEODA]2.0.CO;2
- Hodge, A., Campbell, C.D., Fitter, A.H., 2001. An arbuscular mycorrhizal fungus accelerates decomposition and acquires nitrogen directly from organic material. *Nature* 413, 297–299. doi:10.1038/35095041
- Högberg, M.N., Högberg, P., Myrold, D.D., 2007. Is microbial community composition in boreal forest soils determined by pH, C-to-N ratio, the trees, or all three? *Oecologia* 150, 590–601. doi:10.1007/s00442-006-0562-5
- Horn, M.A., Matthies, C., Küsel, K., Schramm, A., Drake, H.L., 2003. Hydrogenotrophic methanogenesis by moderately acid-tolerant methanogens of a methane-emitting acidic peat. *Applied and Environmental Microbiology* 69, 74–83. doi:10.1128/AEM.69.1.74-83.2003
- Hungate, R.E., 1960. Symposium: selected topics in microbial ecology. I. Microbial ecology of the rumen. *Bacteriological Reviews* 24, 353–364.
- Iversen, C.M., Sloan, V.L., Sullivan, P.F., Euskirchen, E.S., McGuire, A.D., Norby, R.J., Walker, A.P., Warren, J.M., Wullschlegel, S.D., 2015. The unseen iceberg: Plant roots in arctic tundra. *New Phytologist*. doi:10.1111/nph.13003
- Jones, D.L., Hodge, A., Kuzyakov, Y., 2004. Plant and mycorrhizal regulation of rhizodeposition. *New Phytologist*. doi:10.1111/j.1469-8137.2004.01130.x
- Jones, D.L., Nguyen, C., Finlay, R.D., 2009. Carbon flow in the rhizosphere: Carbon trading at the soil-root interface. *Plant and Soil*. doi:10.1007/s11104-009-9925-0
- Juottonen, H., Galand, P.E., Tuittila, E.S., Laine, J., Fritze, H., Yrjölä, K., 2005. Methanogen communities and Bacteria along an ecophysiological gradient in a northern raised bog complex. *Environmental Microbiology* 7, 1547–1557. doi:10.1111/j.1462-2920.2005.00838.x
- Kaiser, K., Guggenberger, G., 2003. Mineral surfaces and soil organic matter. *European Journal of Soil Science* 54, 219–236. doi:10.1046/j.1365-2389.2003.00544.x
- Kalbitz, K., Geyer, S., Geyer, W., 2000. A comparative characterization of dissolved organic matter by means of original aqueous samples and isolated humic substances. *Chemosphere* 40, 1305–1312. doi:10.1016/S0045-6535(99)00238-6
- Kaňa, J., Kopáček, J., 2006. Impact of soil sorption characteristics and bedrock composition on phosphorus concentrations in two Bohemian Forest lakes. *Water, Air, and Soil Pollution* 173, 243–259. doi:10.1007/s11270-005-9065-y

- Karhu, K., 2010. Temperature sensitivity of soil organic matter decomposition in boreal soils. *Dissertationes Forestales* 2010. doi:10.14214/df.107
- Karhu, K., Auffret, M.D., Dungait, J.A.J., Hopkins, D.W., Prosser, J.I., Singh, B.K., Subke, J.A., Wookey, P.A., Agren, G.I., Sebastià, M.T., Gouriveau, F., Bergkvist, G., Meir, P., Nottingham, A.T., Salinas, N., Hartley, I.P., 2014. Temperature sensitivity of soil respiration rates enhanced by microbial community response. *Nature* 513, 81–84. doi:10.1038/nature13604
- Kaštovská, E., Straková, P., Edwards, K., Urbanová, Z., Bárta, J., Mastný, J., Šantrůčková, H., Píček, T., 2018. Cotton-Grass and Blueberry have Opposite Effect on Peat Characteristics and Nutrient Transformation in Peatland. *Ecosystems* 21, 443–458. doi:10.1007/s10021-017-0159-3
- Killingbeck, K.T., 1996. Nutrients in senesced leaves: Keys to the search for potential resorption and resorption proficiency. *Ecology* 77, 1716–1727. doi:10.2307/2265777
- Kip, N., Fritz, C., Langelaan, E.S., Pan, Y., Bodrossy, L., Pancotto, V., Jetten, M.S.M., Smolders, A.J.P., Op Den Camp, H.J.M., 2012. Methanotrophic activity and diversity in different Sphagnum magellanicum dominated habitats in the southernmost peat bogs of Patagonia. *Biogeosciences* 9, 47–55. doi:10.5194/bg-9-47-2012
- Kleber, M., Eusterhues, K., Keiluweit, M., Mikutta, C., Mikutta, R., Nico, P.S., 2015. Mineral-Organic Associations: Formation, Properties, and Relevance in Soil Environments. *Advances in Agronomy* 130, 1–140. doi:10.1016/bs.agron.2014.10.005
- Kopáček, J., Kaňa, J., Šantrůčková, H., Porcal, P., Hejzlar, J., Píček, T., Veselý, J., 2002a. Physical, chemical and biological characteristics of soils in watersheds of the Bohemian Forest lakes: I. Plešne Lake. *Silva Gabreta* 8, 43–66.
- Kopáček, J., Stuchlík, E., Veselý, J., Schaumburg, J., Anderson, I., Fott, J., Hejzlar, J., Vrba, J., 2002b. Hysteresis in Reversal of Central European Mountain Lakes from Atmospheric Acidification. *Water, Air and Soil Pollution: Focus* 2, 91–114. doi:10.1023/A:1020190205652
- Kopáček, J., Turek, J., Hejzlar, J., Kaňa, J., Porcal, P., 2006. Element fluxes in watershed-lake ecosystems recovering from acidification: Plešně Lake, the Bohemian Forest, 2001–2005. *Biologia (Poland)* 61. doi:10.2478/s11756-007-0067-7
- Kopáček, J., Vrba, J., 2006. Integrated ecological research of catchment-lake ecosystems in the Bohemian Forest (Central Europe): A preface. *Biologia (Poland)* 61. doi:10.2478/s11756-007-0078-4
- Kotsyurbenko, O.R., 2005. Trophic interactions in the methanogenic microbial community of low-temperature terrestrial ecosystems, in: *FEMS Microbiology Ecology*. pp. 3–13. doi:10.1016/j.femsec.2004.12.009
- Koven, C.D., Ringeval, B., Friedlingstein, P., Ciais, P., Cadule, P., Khvorostyanov, D., Krinner, G., Tarnocai, C., 2011. Permafrost carbon-climate feedbacks accelerate global warming. *Proceedings of the National Academy of Sciences of the United States of America* 108, 14769–14774. doi:10.1073/pnas.1103910108
- Lauber, C.L., Hamady, M., Knight, R., Fierer, N., 2009a. Pyrosequencing-based assessment of soil pH as a predictor of soil bacterial community structure at the continental scale. *Applied and Environmental Microbiology* 75, 5111–5120. doi:10.1128/AEM.00335-09
- Lauber, C.L., Sinsabaugh, R.L., Zak, D.R., 2009b. Laccase gene composition and relative abundance in oak forest soil is not affected by short-term nitrogen fertilization. *Microbial Ecology* 57, 50–57. doi:10.1007/s00248-008-9437-0
- Lavoie, M., Paré, D., Bergeron, Y., 2005. Impact of global change and forest management on carbon sequestration in northern forested peatlands. *Environmental Reviews* 13, 199–240. doi:10.1139/a05-014
- Lawrence, D.M., Koven, C.D., Swenson, S.C., Riley, W.J., Slater, A.G., 2015. Permafrost thaw and resulting soil moisture changes regulate projected high-latitude CO₂ and CH₄ emissions. *Environmental Research Letters* 10. doi:10.1088/1748-9326/10/9/094011
- Le Roes-Hill, M., Khan, N., Burton, S.G., 2011. Actinobacterial peroxidases: An unexplored resource for biocatalysis. *Applied Biochemistry and Biotechnology* 164, 681–713. doi:10.1007/s12010-011-9167-5
- Lehmeier, C.A., Min, K., Niehues, N.D., Ballantyne, F., Billings, S.A., 2013. Temperature-mediated changes of exoenzyme-substrate reaction rates and their consequences for the carbon to nitrogen flow ratio of liberated resources. *Soil Biology and Biochemistry* 57, 374–382. doi:10.1016/j.soilbio.2012.10.030
- Liesack, W., Schnell, S., Revsbech, N.P., 2000. Microbiology of flooded rice paddies. *FEMS Microbiology Reviews*. doi:10.1016/S0168-6445(00)00050-4
- Lin, X., Green, S., Tfaily, M.M., Prakash, O., Konstantinidis, K.T., Corbett, J.E., Chanton, J.P., Cooper, W.T., Kostka, J.E., 2012. Microbial community structure and activity linked to contrasting biogeochemical gradients in bog and fen environments of the glacial lake agassiz peatland. *Applied and Environmental Microbiology* 78, 7023–7031. doi:10.1128/AEM.01750-12
- Lindahl, B.D., Ihrmark, K., Boberg, J., Trumbore, S.E., Höglberg, P., Stenlid, J., Finlay, R.D., 2007. Spatial separation of litter decomposition and mycorrhizal nitrogen uptake in a boreal forest. *New Phytologist* 173, 611–620. doi:10.1111/j.1469-8137.2006.01936.x
- Livsey, S., Barklund, P., 1992. *Lophodermium piceae* and *Rhizosphaera kalkhoffii* in fallen needles of Norway spruce (*Picea abies*). *European Journal of Forest Pathology* 22, 204–216. doi:10.1111/j.1439-0329.1992.tb00785.x
- Louca, S., Parfrey, L.W., Doebeli, M., 2016. Decoupling function and taxonomy in the global ocean microbiome. *Science* 353, 1272–1277. doi:10.1126/science.aaf4507
- Lucas, R.W., Casper, B.B., Jackson, J.K., Balsler, T.C., 2007. Soil microbial communities and extracellular enzyme activity in the New Jersey Pinelands. *Soil Biology and Biochemistry* 39, 2508–2519. doi:10.1016/j.soilbio.2007.05.008
- Lykidis, A., Mavromatis, K., Ivanova, N., Anderson, I., Land, M., DiBartolo, G., Martinez, M., Lapidus, A., Lucas, S., Copeland, A., Richardson, P., Wilson, D.B., Kyrpides, N., 2007. Genome sequence and analysis of the soil cellulolytic actinomycete *Thermobifida fusca* YX. *Journal of Bacteriology* 189, 2477–2486. doi:10.1128/JB.01899-06
- Mackelprang, R., Burkert, A., Haw, M., Mahendrarajah, T., Conaway, C.H., Douglas, T.A., Waldrop, M.P., 2017. Microbial survival strategies in ancient permafrost: Insights from metagenomics. *ISME Journal* 11, 2305–2318. doi:10.1038/ismej.2017.93
- McCarthy, A.J., 1987. Lignocellulose-degrading actinomycetes. *FEMS Microbiology Letters* 46, 145–163. doi:10.1016/0378-1097(87)90061-9
- McClagherty, C.A., Linkins, A.E., 1990. Temperature responses of enzymes in two forest soils. *Soil Biology and Biochemistry* 22, 29–33. doi:10.1016/0038-0717(90)90056-6
- McMahon, S.K., Wallenstein, M.D., Schimel, J.P., 2011. A cross-seasonal comparison of active and total bacterial community composition in Arctic tundra soil using bromodeoxyuridine labeling. *Soil Biology and Biochemistry* 43, 287–295. doi:10.1016/j.soilbio.2010.10.013
- Meentemeyer, V., 1978. Macroclimate and Lignin Control of Litter Decomposition Rates. *Ecology* 59, 465–472. doi:10.2307/1936576
- Melillo, J.M., Aber, J.D., Muratore, J.F., 1982. Nitrogen and lignin control of hardwood leaf litter decomposition dynamics. *Ecology* 63, 621–626. doi:10.2307/1936780
- Mikutta, R., Mikutta, C., Kalbitz, K., Scheel, T., Kaiser, K., Jahn, R., 2007. Biodegradation of forest floor organic matter bound to minerals via different binding mechanisms. *Geochimica et Cosmochimica Acta* 71, 2569–2590. doi:10.1016/j.gca.2007.03.002

- Moore, T., Basiliko, N., 2006. Decomposition in Boreal Peatlands, in: *Boreal Peatland Ecosystems*. pp. 125–143. doi:10.1007/978-3-540-31913-9_7
- Müller, M.M., Sundman, V., Soininvaara, O., Meriläinen, A., 1988. Effect of chemical composition on the release of nitrogen from agricultural plant materials decomposing in soil under field conditions. *Biology and Fertility of Soils* 6, 78–83. doi:10.1007/BF00257926
- Muyzer, G., Smalla, K., 1998. Application of denaturing gradient gel electrophoresis (DGGE) and temperature gradient gel electrophoresis (TGGE) in microbial ecology, in: *Antonie van Leeuwenhoek, International Journal of General and Molecular Microbiology*. pp. 127–141. doi:10.1023/A:1000669317571
- Northup, R.R., Dahlgren, R.A., McColl, J.G., 1998. Polyphenols as regulators of plant-litter-soil interactions in northern California's pygmy forest: A positive feedback?, in: *Biogeochemistry*. pp. 189–220. doi:10.1007/978-94-017-2691-7_10
- Ohno, T., Bro, R., 2006. Dissolved organic matter characterization using multiway spectral decomposition of fluorescence landscapes. *Soil Science Society of America Journal* 70, 2028–2037. doi:10.2136/sssaj2006.0005
- Økland, B., Götmark, F., Nordén, B., 2008. Oak woodland restoration: Testing the effects on biodiversity of mycetophilids in southern Sweden. *Biodiversity and Conservation* 17, 2599–2616. doi:10.1007/s10531-008-9325-4
- Paca, J., Barta, J., Bajpai, R., 2005. Comparison of dinitrotoluene degradation by a mixed culture in aqueous batch system, *Contaminated Soils, Sediments and Water*. doi:10.1007/0-387-23079-3_8
- Paca, J., Barta, J., Bajpai, R., 2005. Aerobic biodegradation of mononitrotoluenes in batch and continuous reactor systems. *Soil and Sediment Contamination* 14, 261–279. doi:10.1080/15320380590928320
- Panikov, N.S., Flanagan, P.W., Oechel, W.C., Mastepanov, M.A., Christensen, T.R., 2006. Microbial activity in soils frozen to below -39°C. *Soil Biology and Biochemistry* 38, 785–794. doi:10.1016/j.soilbio.2005.07.004
- Park, J.H., Matzner, E., 2003. Controls on the release of dissolved organic carbon and nitrogen from a deciduous forest floor investigated by manipulations of aboveground litter inputs and water flux. *Biogeochemistry* 66, 265–286. doi:10.1023/B:BIOG.0000005341.19412.7b
- Peleg, M., Normand, M.D., Corradini, M.G., 2012. The Arrhenius equation revisited. *Critical Reviews in Food Science and Nutrition*. doi:10.1080/10408398.2012.667460
- Peltoniemi, K., Fritze, H., Laiho, R., 2009. Response of fungal and actinobacterial communities to water-level drawdown in boreal peatland sites. *Soil Biology and Biochemistry* 41, 1902–1914. doi:10.1016/j.soilbio.2009.06.018
- Philippot, L., Andersson, S.G.E., Battin, T.J., Prosser, J.I., Schimel, J.P., Whitman, W.B., Hallin, S., 2010. The ecological coherence of high bacterial taxonomic ranks. *Nature Reviews Microbiology*. doi:10.1038/nrmicro2367
- Piña, R.G., Cervantes, C., 1996. Microbial interactions with aluminium. *BioMetals* 9, 311–316. doi:10.1007/BF00817932
- Ping, C.L., Jastrow, J.D., Jorgenson, M.T., Michaelson, G.J., Shur, Y.L., 2015. Permafrost soils and carbon cycling. *Soil* 1, 147–171. doi:10.5194/soil-1-147-2015
- Pinsonneault, A.J., Moore, T.R., Roulet, N.T., 2016. Temperature the dominant control on the enzyme-latch across a range of temperate peatland types. *Soil Biology and Biochemistry* 97, 121–130. doi:10.1016/j.soilbio.2016.03.006
- Pregitzer, K.S., 2003. Woody plants, carbon allocation and fine roots. *New Phytologist*. doi:10.1046/j.1469-8137.2003.00766.x
- Prescott, C.E., 2005. Do rates of litter decomposition tell us anything we really need to know? *Forest Ecology and Management* 220, 66–74. doi:10.1016/j.foreco.2005.08.005
- Qualls, R.G., Richardson, C.J., 2000. Phosphorus enrichment affects litter decomposition, immobilization, and soil microbial phosphorus in wetland mesocosms. *Soil Science Society of America Journal* 64, 799–808. doi:10.2136/sssaj2000.642799x
- Rastogi, G., Coaker, G.L., Leveau, J.H.J., 2013. New insights into the structure and function of phyllosphere microbiota through high-throughput molecular approaches. *FEMS Microbiology Letters* 348, 1–10. doi:10.1111/1574-6968.12225
- Reich, P.B., Oleksyn, J., Modrzyński, J., Mrozinski, P., Hobbie, S.E., Eissenstat, D.M., Chorover, J., Chadwick, O.A., Hale, C.M., Tjoelker, M.G., 2005. Linking litter calcium, earthworms and soil properties: A common garden test with 14 tree species. *Ecology Letters* 8, 811–818. doi:10.1111/j.1461-0248.2005.00779.x
- Rooney-Varga, J.N., Giewat, M.W., Duddleston, K.N., Chanton, J.P., Hines, M.E., 2007. Links between archaeal community structure, vegetation type and methanogenic pathway in Alaskan peatlands. *FEMS Microbiology Ecology* 60, 240–251. doi:10.1111/j.1574-6941.2007.00278.x
- Rousk, J., Bååth, E., Brookes, P.C., Lauber, C.L., Lozupone, C., Caporaso, J.G., Knight, R., Fierer, N., 2010a. Soil bacterial and fungal communities across a pH gradient in an arable soil. *ISME Journal* 4, 1340–1351. doi:10.1038/ismej.2010.58
- Rousk, J., Brookes, P.C., Bååth, E., 2010b. Investigating the mechanisms for the opposing pH relationships of fungal and bacterial growth in soil. *Soil Biology and Biochemistry* 42, 926–934. doi:10.1016/j.soilbio.2010.02.009
- Schellenberger, S., Kolb, S., Drake, H.L., 2010. Metabolic responses of novel cellulolytic and saccharolytic agricultural soil Bacteria to oxygen. *Environmental Microbiology* 12, 845–861. doi:10.1111/j.1462-2920.2009.02128.x
- Schimel, J., 1995. *Ecosystem Consequences of Microbial Diversity and Community Structure*. pp. 239–254. doi:10.1007/978-3-642-78966-3_17
- Schimel, J.P., Clein, J.S., 1996. Microbial response to freeze-thaw cycles in tundra and taiga soils. *Soil Biology and Biochemistry* 28, 1061–1066. doi:10.1016/0038-0717(96)00083-1
- Schimel, J.P., Weintraub, M.N., 2003. The implications of exoenzyme activity on microbial carbon and nitrogen limitation in soil: A theoretical model. *Soil Biology and Biochemistry* 35, 549–563. doi:10.1016/S0038-0717(03)00015-4
- Schnecker, J., Wild, B., Hofhansl, F., Alves, R.J.E., Bárta, J., Čapek, P., Fuchslueger, L., Gentsch, N., Gittel, A., Guggenberger, G., Hofer, A., Kienzl, S., Knoltsch, A., Lashchinskiy, N., Mikutta, R., Šantrůčková, H., Shibistova, O., Takriti, M., Urich, T., Weltin, G., Richter, A., 2014. Effects of soil organic matter properties and microbial community composition on enzyme activities in cryoturbated arctic soils. *PLoS ONE* 9. doi:10.1371/journal.pone.0094076
- Schnecker, J., Wild, B., Takriti, M., Eloy Alves, R.J., Gentsch, N., Gittel, A., Hofer, A., Klaus, K., Knoltsch, A., Lashchinskiy, N., Mikutta, R., Richter, A., 2015. Microbial community composition shapes enzyme patterns in topsoil and subsoil horizons along a latitudinal transect in Western Siberia. *Soil Biology and Biochemistry* 83, 106–115. doi:10.1016/j.soilbio.2015.01.016
- Schostag, M.D., Anwar, M.Z., Jacobsen, C.S., Larose, C., Vogel, T.M., Maccario, L., Jacquioid, S., Faucher, S., Priemé, A., 2019. Transcriptomic responses to warming and cooling of an Arctic tundra soil microbiome. *BioRxiv* 599233. doi:10.1101/599233
- Schuur, E.A.G., Abbott, B., 2011. Climate change: High risk of permafrost thaw. *Nature* 480, 32–33. doi:10.1038/480032a
- Schuur, E.A.G., Bockheim, J., Canadell, J.G., Euskirchen, E., Field, C.B., Goryachkin, S. V., Hagemann, S., Kuhry, P., Laflour, P.M., Lee, H., Mazhitova, G., Nelson, F.E., Rinke, A., Romanovsky, V.E., Shiklomanov, N., Tarnocai, C., Venevsky, S., Vogel, J.G., Zimov, S.A., 2008.

- Vulnerability of Permafrost Carbon to Climate Change: Implications for the Global Carbon Cycle. *BioScience* 58, 701–714. doi:10.1641/b580807
- Seneviratne, S.I., Corti, T., Davin, E.L., Hirschi, M., Jaeger, E.B., Lehner, I., Orlowsky, B., Teuling, A.J., 2010. Investigating soil moisture-climate interactions in a changing climate: A review. *Earth-Science Reviews*. doi:10.1016/j.earscirev.2010.02.004
- Šimek, M., Jiřová, L., Hopkins, D.W., 2002. What is the so-called optimum pH for denitrification in soil? *Soil Biology and Biochemistry* 34, 1227–1234. doi:10.1016/S0038-0717(02)00059-7
- Sinsabaugh, R.L., Belnap, J., Findlay, S.G., Shah, J.J.F., Hill, B.H., Kuehn, K.A., Kuske, C.R., Litvak, M.E., Martinez, N.G., Moorhead, D.L., Warnock, D.D., 2014. Extracellular enzyme kinetics scale with resource availability. *Biogeochemistry* 121, 287–304. doi:10.1007/s10533-014-0030-y
- Sinsabaugh, R.L., van Horn, D.J., Shah, J.J.F., Findlay, S., 2010. Ecoenzymatic Stoichiometry in Relation to Productivity for Freshwater Biofilm and Plankton Communities. *Microbial Ecology* 60, 885–893. doi:10.1007/s00248-010-9696-4
- Sistla, S.A., Schimel, J.P., 2013. Seasonal patterns of microbial extracellular enzyme activities in an arctic tundra soil: Identifying direct and indirect effects of long-term summer warming. *Soil Biology and Biochemistry* 66, 119–129. doi:10.1016/j.soilbio.2013.07.003
- Smoot, M.E., Ono, K., Ruschinski, J., Wang, P.L., Ideker, T., 2011. Cytoscape 2.8: New features for data integration and network visualization. *Bioinformatics* 27, 431–432. doi:10.1093/bioinformatics/btq675
- Stewart, P., Globig, S., 2011. Plant physiology, *Plant Physiology*. doi:10.2307/4109069
- Strakova, P., Niemi, R.M., Freeman, C., Peltoniemi, K., Toberman, H., Heiskanen, I., Fritze, H., Laiho, R., 2011. Litter type affects the activity of aerobic decomposers in a boreal peatland more than site nutrient and water table regimes. *Biogeosciences* 8, 2741–2755. doi:10.5194/bg-8-2741-2011
- Sundh, I., Mikkilä, C., Nilsson, M., Svensson, B.H., 1995. Potential aerobic methane oxidation in a Sphagnum-dominated peatland—Controlling factors and relation to methane emission. *Soil Biology and Biochemistry* 27, 829–837. doi:10.1016/0038-0717(94)00222-M
- Tahovská, K., Kaňa, J., Bárta, J., Oulehle, F., Richter, A., Šantrůčková, H., 2013. Microbial N immobilization is of great importance in acidified mountain spruce forest soils. *Soil Biology and Biochemistry* 59, 58–71. doi:10.1016/j.soilbio.2012.12.015
- Talbot, J.M., Allison, S.D., Treseder, K.K., 2008. Decomposers in disguise: Mycorrhizal fungi as regulators of soil C dynamics in ecosystems under global change. *Functional Ecology*. doi:10.1111/j.1365-2435.2008.01402.x
- Tarnocai, C., 2009. The impact of climate change on Canadian peatlands. *Canadian Water Resources Journal* 34, 453–466. doi:10.4296/cwrj3404453
- Tarnocai, C., Bockheim, J.G., 2011. Cryosolic soils of Canada: Genesis, distribution, and classification. *Canadian Journal of Soil Science* 91, 749–762. doi:10.4141/cjss10020
- Tisdall, J.M., Oades, J.M., 1982. Organic matter and water-stable aggregates in soils. *Journal of Soil Science* 33, 141–163. doi:10.1111/j.1365-2389.1982.tb01755.x
- Tláškal, V., Voříšková, J., Baldrian, P., 2016. Bacterial succession on decomposing leaf litter exhibits a specific occurrence pattern of cellulolytic taxa and potential decomposers of fungal mycelia. *FEMS Microbiology Ecology* 92. doi:10.1093/femsec/iw177
- Tomlinson, G.H., 2003. Acidic deposition, nutrient leaching and forest growth. *Biogeochemistry* 65, 51–81. doi:10.1023/A:1026069927380
- Torsvik, V., Goksoyr, J., Daae, F.L., 1990. High diversity in DNA of soil bacteria. *Applied and Environmental Microbiology* 56, 782–787.
- Torsvik, V., Øvreås, L., 2002. Microbial diversity and function in soil: From genes to ecosystems. *Current Opinion in Microbiology*. doi:10.1016/S1369-5274(02)00324-7
- Tveit, A., Schwacke, R., Svenning, M.M., Ulrich, T., 2013. Organic carbon transformations in high-Arctic peat soils: Key functions and microorganisms. *ISME Journal* 7, 299–311. doi:10.1038/ismej.2012.99
- Van Der Heul, H.U., Bilyk, B.L., McDowall, K.J., Seipke, R.F., Van Wezel, G.P., 2018. Regulation of antibiotic production in Actinobacteria: New perspectives from the post-genomic era. *Natural Product Reports*. doi:10.1039/c8np00012c
- Vanhala, P., Karhu, K., Tuomi, M., Björklöf, K., Fritze, H., Hyvärinen, H., Liski, J., 2011. Transplantation of organic surface horizons of boreal soils into warmer regions alters microbiology but not the temperature sensitivity of decomposition. *Global Change Biology* 17, 538–550. doi:10.1111/j.1365-2486.2009.02154.x
- Venter, J.C., Remington, K., Heidelberg, J.F., Halpern, A.L., Rusch, D., Eisen, J.A., Wu, D., Paulsen, I., Nelson, K.E., Nelson, W., Fouts, D.E., Levy, S., Knap, A.H., Lomas, M.W., Nealon, K., White, O., Peterson, J., Hoffman, J., Parsons, R., Baden-Tillson, H., Pfannkoch, C., Rogers, Y.H., Smith, H.O., 2004. Environmental Genome Shotgun Sequencing of the Sargasso Sea. *Science* 304, 66–74. doi:10.1126/science.1093857
- Violante, A., de Cristofaro, A., Rao, M.A., Gianfreda, L., 1995. Physicochemical properties of protein-smectite and protein-Al(OH) x-smectite complexes. *Clay Minerals* 30, 325–336. doi:10.1180/claymin.1995.030.4.06
- Vrba, J., Kopáček, J., Štrojsová, A., Bittl, T., Nedoma, J., Nedbalová, L., Kohout, L., Fott, J., 2006. A key role of aluminium in phosphorus availability, food web structure, and plankton dynamics in strongly acidified lakes. *Biologia (Poland)* 61. doi:10.2478/s11756-007-0077-5
- Wallenstein, M.D., McMahon, S.K., Schimel, J.P., 2009. Seasonal variation in enzyme activities and temperature sensitivities in Arctic tundra soils. *Global Change Biology* 15, 1631–1639. doi:10.1111/j.1365-2486.2008.01819.x
- Wallenstein, M.D., Weintraub, M.N., 2008. Emerging tools for measuring and modeling the in situ activity of soil extracellular enzymes. *Soil Biology and Biochemistry* 40, 2098–2106. doi:10.1016/j.soilbio.2008.01.024
- Wardle, D.A., Bonner, K.I., Barker, G.M., 2002. Linkages between plant litter decomposition, litter quality, and vegetation responses to herbivores. *Functional Ecology* 16, 585–595. doi:10.1046/j.1365-2435.2002.00659.x
- Weltzin, J.F., Pastor, J., Harth, C., Bridgman, S.D., Updegraff, K., Chapin, C.T., 2000. Response of bog and fen plant communities to warming and water-table manipulations. *Ecology* 81, 3464–3478. doi:10.1890/0012-9658(2000)081[3464:ROBAFP]2.0.CO;2
- Whitman, W.B., Coleman, D.C., Wiebe, W.J., 1998. Prokaryotes: The unseen majority. *Proceedings of the National Academy of Sciences of the United States of America*. doi:10.1073/pnas.95.12.6578
- Wild, B., Schneckler, J., Bárta, J., Čapek, P., Guggenberger, G., Hofhansl, F., Kaiser, C., Lashchinsky, N., Mikutta, R., Mooshammer, M., Šantrůčková, H., Shibistova, O., Ulrich, T., Zimov, S.A., Richter, A., 2013. Nitrogen dynamics in Turbic Cryosols from Siberia and Greenland. *Soil Biology and Biochemistry* 67, 85–93. doi:10.1016/j.soilbio.2013.08.004
- Wilpsheski, R.L., Aufrecht, J.A., Retterer, S.T., Sullivan, M.B., Graham, D.E., Pierce, E.M., Zablocki, O.D., Palumbo, A. V., Elias, D.A., 2019. Soil Aggregate Microbial Communities: Towards Understanding Microbiome Interactions at Biologically Relevant Scales. *Applied and Environmental Microbiology*. doi:10.1128/AEM.00324-19
- Yavitt, J.B., Williams, C.J., Kelman Wieder, R., 1997. Production of methane and carbon dioxide in Peatland ecosystems across north

- America: Effects of temperature, aeration, and organic chemistry of peat. *Geomicrobiology Journal* 14, 299–316.
doi:10.1080/01490459709378054
- Yergeau, E., Hogues, H., Whyte, L.G., Greer, C.W., 2010. The functional potential of high Arctic permafrost revealed by metagenomic sequencing, qPCR and microarray analyses. *ISME Journal* 4, 1206–1214. doi:10.1038/ismej.2010.41
- Young, I.M., Crawford, J.W., 2004. Interactions and self-organization in the soil-microbe complex. *Science*. doi:10.1126/science.1097394
- Zhou, L., Xing, X., Peng, B., Fang, G., 2016. Extracellular polymeric substance (EPS) characteristics and comparison of suspended and attached activated sludge at low temperatures. *Qinghua Daxue Xuebao/Journal of Tsinghua University* 56, 1009–1015.
doi:10.16511/j.cnki.qhdxxb.2016.21.051

Paper 1

Barta J, Applova M, Vanek D, Kristufkova M, Santruckova H (2010) Effect of available P and phenolics on mineral N release in acidified spruce forest: connection with lignin-degrading enzymes and bacterial and fungal communities. *BIOGEOCHEMISTRY* 97:71-87.

Effect of available P and phenolics on mineral N release in acidified spruce forest: connection with lignin-degrading enzymes and bacterial and fungal communities

Jiří Bárta · Markéta Applová · Daniel Vaněk ·
Markéta Křišťůvková · Hana Šantrůčková

Received: 2 October 2008 / Accepted: 3 August 2009 / Published online: 25 August 2009
© Springer Science+Business Media B.V. 2009

Abstract We conducted over four months a short-term laboratory incubation experiment to find the best prediction parameters (i.e. initial chemical characteristics) to explain differences in microbial respiration rates and mineral N (DIN) release in different litter in an acidified spruce forest. In addition, we wanted to find the link between the activity of key extracellular ligninolytic enzymes, phenoloxidases (PhOx) and peroxidases (Perox), microbial respiration and composition of fungal and bacterial communities. Samples of spruce needles (*Picea abies*) and litter of four dominant understorey vegetation; lady fern (*Athyrium alpestre*), blueberry (*Vaccinium myrtillus*), reedgrass (*Calamagrostis villosa*) and hair grass (*Avenella flexuosa*), were collected in 2005, 2006 and 2007 from six sites located in watersheds of two glacial lakes (Plesne Lake and Certovo Lake) in the Bohemian Forest, Czech Republic. Litter samples were incubated at 0 and 10 °C in laboratory controlled conditions for 90 days. Activities of PhOx and Perox, and C mineralization rate were measured

regularly each 14 days. Litter quality characteristics and endophytic microbial community structure, based on 16SrDNA-DGGE fingerprint of bacteria and ITS-DGGE of fungi, were determined at the beginning and end of litter incubation. Our results showed a close correlation of phenolics/P_{OX} with DIN release ($r > 0.74$, $p < 0.001$). Using multivariate analyses, P_{OX} seems to play an important role in the change of litter fungal and bacterial community composition. At 0 °C the fungal and bacterial communities of reedgrass and blueberry litter changed in relation to P_{OX} and Perox activity, while at 10 °C the fungal communities after the incubation were additionally affected by the phenolics/N_{TOT} and phenolics/P_{TOT} ratios.

Keywords Available phosphorus · DGGE · Extracellular enzyme activities · Litter decomposition · N leaching · Phenolics

Introduction

Forest plant litter decomposition is an important process in C, N and P cycles and soil formation. This process is controlled by abiotic factors, such as temperature, moisture, and chemical composition of the litter, and microbial communities (Aber et al. 1990; Couteaux et al. 1995; Fassnacht and Gower 1999; Park and Matzner 2003; Pregitzer et al. 2004).

J. Bárta (✉) · M. Applová · D. Vaněk · H. Šantrůčková
Department of Ecosystem Biology, University of South
Bohemia, Branišovská 31, 37005 České Budějovice,
Czech Republic
e-mail: bartaj03@prf.jcu.cz; barta77@seznam.cz

M. Křišťůvková
Faculty of Science, Institute for Environmental Studies,
Charles University in Prague, Benátská 2, 128 01 Prague,
Czech Republic

Chemical composition of litter influences the composition of fungal and bacterial colonizers, and their enzymatic apparatus (Cox et al. 2001; Lucas et al. 2007). The change in enzymatic activity influences the quantity of nutrients, which are released during litter decomposition, and vice versa, the release of different nutrients influences the activity of specific enzymes (Sinsabaugh et al. 2002, 2005).

Many studies have focused on trying to predict plant litter decomposition from initial litter chemical composition during short-term incubation experiments (Aber et al. 1990; Aber et al. 1998). The carbon/nitrogen (C/N) ratio was widely used for this prediction (Muller et al. 1988; Carlyle et al. 1990). However, the C/N ratio was found to be a poor predictor when trying to estimate the amount of released mineral N (DIN, NH_4^+ and NO_3^-) from highly lignified litter (Prescott 2005). A stronger correlation was found between lignin and the lignin/N ratio and mineral N release (Berg 1986; Berg and Ekbohm 1991).

Some recent studies have demonstrated that, when phenolics are included into the statistical analyses, C mineralization and DIN release rates are more closely correlated with phenolics content and phenolics/ N_{TOT} ratio, than they are with $\text{C}_{\text{TOT}}/\text{N}_{\text{TOT}}$ ratio, lignin concentration, or lignin/ N_{TOT} ratio (Fox et al. 1990; Northup et al. 1995, 1998). One of the first studies focusing on the influence of phenolics was done by Dyck et al. (1987). The authors attributed most of the variation in DIN release from *Pinus radiata* litter to differences in phenolics content. These findings showed that a high content of phenolics and low N availability can be limiting factors of DIN release from decomposing litter in acid forest soils (Kopáček et al. 2002a, b). However, acid forest soils can also be poor in P and it is very likely that low bioavailability of P is another limiting factor of litter decomposition which can affect DIN release. Even if P bioavailability and the amount of phenolics in litter could be the “driving force” in litter decomposition and DIN release in acidified spruce forests, there are still only a few studies on this topic (Šantrůčková et al. 2004, 2006).

Phenolics are the structural unit of lignin and are released during depolymerization by the activity of extracellular lignin-degrading enzymes. Fungal phenoloxidasases and peroxidases are the key enzymes involved in this process (Weintraub et al. 2007;

Fackler et al. 2006; Söderström et al. 1983; Fog 1988; Kirk and Farrell 1987; Eriksson et al. 1990; Hammel 1997; Waldrop et al. 2004; Sinsabaugh et al. 2002). Depolymerization of lignin is a crucial process because it increases the accessibility of C, N, and P for both fungal and bacterial decomposing microorganisms. Therefore, there should be a tight link between ligninolytic activity, C mineralization and fungal community composition. The depolymerization process also creates different phenolic products with high reactive hydroxyl groups, which can then play various roles in the soil. Released phenolics can react with each other forming humic substances, they can precipitate proteins, reducing the leaching of DIN (Northup et al. 1995, 1998), or predominantly precipitate toxic forms of Al^{3+} thereby increasing P bioavailability (Northup et al. 1998; Tomlinson 2003).

Temperature affects the rate of litter decomposition; its effect is closely interconnected with initial chemical composition of the litter (Meentemeyer 1978). In nutrient rich and phenolic poor litter, temperature sensitivity of litter decomposition is higher than in nutrient poor and lignin rich litter (Domisch et al. 2006). The response to temperature is stronger especially in the early stage of litter decomposition than in later phases (Jansson and Berg 1985). In addition, differential temperature sensitivity of decomposition processes can lead to an imbalance in C and N mineralization.

High DIN leaching is one of the major problems in acidified spruce forests in Central Europe. These forests have undergone great changes during the past few decades, with acid anthropogenic N depositions during the last century and bark beetle infestations being the main disturbances. The high acidity of soils led to the reduction of soil acid neutralizing capacity, increased mobility of toxic Al^{3+} ions and leaching of essential plant cations (Ca^{2+} , Mg^{2+} and K^+) and DIN from these ecosystems (Dauer et al. 2007; Tomlinson 2003; Pawłowski 1997; Kopáček et al. 2002a, b, 2006a, b; Šantrůčková et al. 2006). Soil acidity and Al mobility have been related to the physiological stress suffered by spruce trees since the 1960 s (Šantrůčková et al. 2007), there is currently a high degree of tree disturbance and defoliation. In open patches, understorey vegetation dominated by grasses, blueberries and ferns develop rapidly. Their effect on DIN leaching is still unclear (Svoboda et al. 2006; Šantrůčková et al. 2006).

The purpose of this study was to:

1. evaluate the effect of P bioavailability on litter mineralization and DIN release.
2. find the connection between phenolics/ P_{OX} ratio and litter mineralization and N release.
3. determine C mineralization, ligninolytic activity and N release at close to zero temperatures.
4. determine whether there are links between ligninolytic activity, C mineralization and dynamics of litter microbial colonizers during incubation.

Spruce needles (*Picea abies*) and the litter of four dominant understorey species (*Athyrium alpestre* (lady fern), *Vaccinium myrtillus* (blueberry), *Calamagrostis villosa* (reedgrass), and *Avenella flexuosa* (hair-grass) were incubated at 0 (average winter temperature) and 10 °C (average summer temperature) for four months. The three representative litters with different amounts of phenolics (spruce needles, blueberry and reedgrass) were analyzed for lignin-degrading enzyme (PhOx and Perox) activities and composition of fungal and bacterial communities.

Materials and methods

Study site description

Litter was collected from six different sampling sites in the watersheds of two glacial lakes: Plešné and Čertovo, which are situated at 48°47' and 49°10'N, and 13°52' and 13°11'E, respectively, at altitudes from 1030 to 1090 m a. s. l. Watershed of Plešné Lake is covered with a 160 year-old Norway spruce (*Picea abies*) forest with small areas of ash. The bedrock is composed of granites. Čertovo Lake is covered with 90–150 year-old Norway spruce forests, with sparse white fir (*Abies concolor*) and European beech (*Fagus sylvatica*); the bedrock is predominantly composed of mica-schist (muscovite gneiss) with quartzite intrusions. The understorey of both watersheds is dominated by hair grass (*Avenella flexuosa*), reedgrass (*Calamagrostis villosa*), blueberry (*Vaccinium myrtillus*), and lady fern (*Athyrium alpestre*, Svoboda et al. 2006). Soil types are mostly cambisols, podzols and litosols on steep slopes in both watersheds. Soil temperatures measured from 2001 to 2002 were close to 0 °C in winter and 10–12 °C in the summer

months. Basic physico-chemical and biochemical properties of the soils are described by Kopáček et al. (2002a, b) and Veselý (1994).

Litter collection and experimental set-up

Senescent leaves from four dominant understorey species (hair grass, reedgrass, blueberry and lady fern) and spruce needles were collected in October 2005, 2006 and 2007. Mean values of initial litter quality from the three sampling years are presented in Table 1. Fresh litter was stored in a cold room for a maximum of 24 hours. Then litter moisture was adjusted to 60% and litter was weighed (20 g) into 1,000 ml flasks in three replicates. Samples were incubated in closed flasks at 0 and 10 °C for four months; moisture was adjusted every 14 days. All results further reported in this paper are expressed on a dry weight basis (105 °C) and mean values from three replicates were used for statistical evaluations. C mineralization was determined by measuring the respiration rate, and decomposition by measuring water extractable compounds (dissolved organic C (DOC), dissolved organic N (DON) and dissolved mineral N, DIN (sum of NH_4^+ and NO_3^-) and oxalate extractable P (P_{OX}) after incubation. Oxalate extractable P (P_{OX}) is supposed to characterize biological bioavailability of P in soil (Koopmans et al. 2004; Pote et al. 1996; van der Zee et al. 1987; Schwertmann 1964). Activity of ligninolytic enzymes and composition of the microbial communities were determined on spruce needles, reedgrass and blueberry in 2007. Respired CO_2 was trapped into 1 M NaOH placed in a beaker on the surface of the litter and measurements were performed each 14 days.

Litter quality measurements

C_{TOT} , N_{TOT} , P_{OX} and phenolics were analyzed in air-dried, finely ground litter. C_{TOT} and N_{TOT} were measured using an elemental analyzer (NC Thermo-Quest, Germany). P_{OX} was determined by extraction of 0.5 g of litter with 50 ml of acid ammonium oxalate solution (0.2 M $H_2C_2O_4$ + 0.2 M $(NH_4)_2C_2O_4$ at pH 3) according to Cappo et al. (1987), but with a three-step instead of continuous extraction (Kopáček et al. 2002a). Dissolved organic carbon (DOC) and dissolved nitrogen (DN) were extracted step by step in both cold water (CW) and hot water

Table 1 Selected initial chemical properties of the litter of spruce needles and leaves of four dominant species of understorey vegetation

Litter	Initial chemical characteristics							
	C _{TOT} (mmol g ⁻¹)	C _{TOT} /N _{TOT} (molar)	C _{TOT} /P _{TOT} (molar)	P _{Ox} (μmol g ⁻¹)	Phenolics (mg g ⁻¹)	Phenolics/N _{TOT} (w/w)	Phenolics/P _{TOT} (w/w)	Phenolics/P _{Ox} (w/w)
Spruce needles	40.4 ^B (1.8)	49.2 ^B (9.9)	1179.2 ^{AB} (18.8)	1.3 ^A (0.3)	178.6 ^D (31.8)	16.0 ^C (4.3)	157.9 ^B (27.1)	9715.8 ^C (5352.1)
Lady fern	38.5 ^{AB} (1.3)	38.3 ^{AB} (12.1)	713.7 ^A (122.4)	9.5 ^C (0.31)	74.1 ^{BC} (34.9)	5.3 ^{AB} (3.8)	49.8 ^A (28.3)	244.7 ^{AB} (109.1)
Blueberry	39.0 ^{AB} (1.3)	47.8 ^{AB} (7.4)	1617.3 ^{BC} (281.7)	7.9 ^{BC} (1.2)	116.0 ^C (21.4)	10.1 ^B (1.9)	141.5 ^B (48.6)	477.8 ^B (124.1)
Reedgrass	39.3 ^{AB} (1.8)	44.2 ^{AB} (9.7)	2149.7 ^C (896.2)	5.1 ^B (2.9)	27.9 ^A (6.0)	2.7 ^A (0.8)	47.4 ^A (30.7)	236.8 ^{AB} (165.8)
Hair grass	37.1 ^A (0.4)	29.3 ^A (4.2)	784.2 ^A (95.2)	7.4 ^{BC} (1.8)	32.8 ^{AB} (5.9)	1.9 ^A (0.2)	20.3 ^A (3.2)	143.6 ^A (18.1)

The data represent averages and standard deviations shown in parenthesis ($n = 30$)

Different letters show significant differences between values within columns ($p < 0.05$)

(HW): water:litter, 10:1, v/w, 30 min at 20 °C and 16 h at 80 °C, respectively. DOC and DN in the cold and hot water extracts were determined on a TOC/TN analyzer (SKALAR FORMACS HT), and NH₄⁺ and NO₃⁻ using a flow injection analyzer (Foss Tecator 5042, Sweden). Total phenolics were determined using the method of Bärlocher and Graça (2005). Dissolved organic nitrogen (DON) was calculated by subtracting the sum of NH₄⁺ and NO₃⁻ from DN.

CO₂ trapped in 1 M NaOH was determined by volumetric titration. Values were used for calculation of cumulative respiration (mg C-CO₂ per g litter).

Analysis of Fe and Al in litter samples was done in accredited laboratory of Czech Geological Survey. In general 1 g of sample was carefully incinerated at 550 °C, than a mixture of HF, HClO₄, and H₃BO₃ was added for disruption of litter samples, and finally extracted by HCl. The resulting solution loaded to the FAAS instrument (Perkin–Elmer 3100). Acetylene-air and acetylene-N₂O for Fe and Al was used, respectively. Detection limit for Fe and Al is 0.01 mg.kg⁻¹. Oxalate extractable Al (Al_{OX}) and Fe (Fe_{OX}) were calculated by equations based on a close correlation between Al_{TOT}/Fe_{TOT} and Al_{OX}/Fe_{OX} (Kaňa, unpublished data). 289 litter samples from Plešné and Čertovo Lake watershed were analyzed for Al_{TOT}, Al_{OX}, Fe_{TOT}, Fe_{OX} amount and correlated (Eq. 1):

$$\begin{aligned} \text{Al}_{\text{OX}} &= 0.1447 \cdot \text{Al}_{\text{TOT}} + 0.6773, \quad r = 0.61, \quad p \leq 0.01 \\ \text{Fe}_{\text{OX}} &= 0.3409 \cdot \text{Fe}_{\text{TOT}} + 0.1357, \quad r = 0.83, \quad p \leq 0.001 \end{aligned} \quad (1)$$

The sorption data were fitted to the linear form of the Langmuir equation (also called Lineweaver–Burk regression) and the sorption maximum (X_{MAX}) was calculated for each litter type (Yuan and Lavkulich 1994). Calculations are based on a close correlation between the sum of Al_{OX} + Fe_{OX} and X_{MAX} (Kaňa and Kopáček 2006).

Enzyme assays

Peroxidase (Perox) and phenol oxidase (PhOx) activities were determined in three representative litters with different amounts of phenolics (spruce needles, blueberry and reedgrass) during the 2007 experiment. Activity was measured every 14 days using the methodology of Hendel et al. (2005). In general, three

replicate microtubes were used for each assay; three microtubes were used as negative substrate controls and another three microtubes served as negative sample controls. The assay tubes received 1 ml aliquots of sample suspension and 1 ml of 5 mM L-DOPA substrate in 50 mM acetate buffer. The negative sample control wells contained 1 ml aliquots of sample suspension and 1 ml of acetate buffer. The negative substrate control wells received 1 ml aliquots of acetate buffer and 1 ml substrate. For Perox assays, each well also received 100 μ l of H₂O₂ (0.3%). The microtubes were covered with aluminium foil and placed on an orbital shaker for 1 h at 20 °C. Activity was measured spectrophotometrically at 460 nm. Enzyme activity was expressed in International Enzyme Units (IEU). One unit of enzyme activity was defined as the amount of enzyme forming 1 μ mol of reaction product per hour per g of organic matter (litter). Overall ligninolytic enzyme activities were calculated as the sum of the average activities of PhOx and Perox during the incubation period.

Extraction of DNA from litter samples and PCR amplification

Composition of the microbial community (bacterial community by studying 16S rDNA and fungal community by studying the ITS regions of their genomic DNA) was determined at the beginning and then after each month of incubation during the 2007 experiment.

A portion of each litter sample (0.15 g) was taken for DNA extraction. Litters were homogenised in liquid nitrogen using a sterile mortar and pestle. Homogenised samples were transported into 1.5 ml Eppendorf microtubes and kept frozen (−70 °C) until the DNA isolation took place. For the isolation of genomic DNA from litter and soil, the DNasy[®] Plant Mini Kit (Qiagen, USA) was used according to manufacture instructions with some modifications: Bead-Beating was performed after adding the extraction buffer using a Mini Bead-Beater (BioSpec Products, Inc.) for efficient disruption of fungal spores and G⁺ bacterial cell membranes. Isolated DNA was stored in 1.5 ml Eppendorf microtubes in a freezer (−20 °C).

Fungal communities were analysed using ITS1F and ITS2 primer pairs to amplify the 300 bp fragment of the fungal ITS rDNA by PCR. The primer ITS1F

(5'-CTT GGT CAT TTA GAG GAA GTA A-3') is higher fungi ITS specific, while ITS2 (5'-GCT GCG TTC TTC ATC GAT GC-3') is a universal primer amplifying the ITS region from Eucaryotes, including both Ascomycetes and Basidiomycetes (Heuer and Smalla 1997). A 40 bp GC-clamp (5'-CGC CCG CCG CGC GCG GCG GGC GGG GCG GGG GCA CGG GGG G-3') was attached to the 5' end of the ITS2 primer to avoid a complete separation of DNA strands during denaturing electrophoresis. The reaction medium consisted of 5 μ l of PCR buffer (Sigma, 100 mM Tris-HCl, pH 8.3, 500 mM KCl, 15 mM MgCl₂), 1 μ l of dNTP (10 mM), 1 μ l of each primer (20 μ M), 1 μ l of GC-rich solution (Sigma), 2 μ l of Bovine Serum Albumin (20 mg ml⁻¹), 0.5 μ l of Taq-polymerase (5 units/ μ l, Sigma) and 2 μ l of genomic DNA brought to a final volume of 50 μ l. The amplification programme consisted of an initial cycle of denaturation at 95 °C for 3 min followed by 35 cycles of denaturation at 94 °C for 45 s, annealing at 55 °C for 45 s and extension at 72 °C for 1 min 15 s. The amplification concluded with a final elongation step at 72 °C for 8 min.

Bacterial communities were analysed using the eubacterial primer set, 968f (5'- AAC GCG AAG AAC CTT AC -3') and 1401r (5'- CGG TGT GTA CAA GAC CC -3'), to amplify by PCR a 475-bp fragment of 16S rDNA from the same DNA extract as above (Heuer and Smalla 1997). A 40-bp GC clamp was attached to the 5' end of the 968f primer. A 50 μ l PCR mixture containing 5 μ l of PCR buffer (Sigma, 100 mM Tris-HCl, pH 8.3, 500 mM KCl), 1 μ l of dNTP (10 mM), 1 μ l of each primer (100 μ M), 0.5 μ l of Taq-polymerase (Fastart, Roche Diagnostic), 2 μ l of MgCl₂, 1 μ l of GC-rich solution (Sigma), 2 μ l of BSA (3%) and 2 μ l of genomic DNA was used. The amplification regime consisted of an initial cycle of denaturation at 94 °C for 5 min, followed by 35 cycles of denaturation at 94 °C for 40 s, annealing at 56 °C for 30 s and extension at 72 °C for 1 min, concluding with an elongation step at 72 °C for 5 min.

Size of PCR amplicons was verified using 1.5% (w/v) agarose and electrophoresed with specific markers.

DGGE analyses

For DGGE analyses, 10 μ l of PCR products (approximately 150 ng) were loaded into a polyacrylamide

gel (8%) with a 40% to 70% denaturing gradient for bacteria and 38 to 50% for fungi and electrophoresed for 16 h at 60 V and 60 °C using the DCode™ Universal Mutation Detection System (BioRad, USA). The 100% denaturing stock solution consisted of 105 g urea; 100 ml deionised formamide/250 ml. Gels were stained with SYBR® Green (1:10000) and visualised under UV light.

Bands in acrylamide gels were identified and analysed using the Biorad Quantity One software v. 4.5.2. The position tolerance was set at 1% and background subtraction was applied.

Within-gel comparisons, taking into account both the presence/absence, and intensity (relative abundance of species) of bands, were performed using multivariate analyses.

Statistical evaluation

Basic statistical analyses were performed using Statistica 8.0 (StatSoft). One-way ANOVA (litter as independent variables), followed by the Tukey HSD test was used for testing differences between initial litter quality and cumulative microbial respiration of the four understorey species and spruce needles. Linear regression was used to test the correlation of NO_3^- , NH_4^+ , DOC, DN, DON, DIN, P_{OX} and cumulative mineralization rate on initial litter quality characteristics. Correlation coefficients (r) with p values were evaluated.

A unimodal type of constrained ordination, canonical analysis (CCA), was used to evaluate the relation between the litter chemical properties and extracellular enzymatic activities (explanatory variables, at the beginning and end of incubation) vs. initial and final composition of bacterial and fungal communities (response variables). The contribution of each explanatory variable was tested using forward selection and the Monte-Carlo permutation test within the CCA framework ($p < 0.05$). Only those explanatory variables that showed significant marginal and conditional effects on the microbial communities were included in the diagrams. The results were summarized using biplot diagrams. In each diagram, the percentage of explained variation between samples is shown on first and second canonical axis. The distance between the initial and final bacterial and fungal communities illustrates the magnitude of differences between the litter samples. The relative length and position of

arrows show the extent and direction of response of bacterial and fungal community structures to the litter chemical properties and extracellular enzymatic activities. The analysis was performed using CANOCO ver. 4.5 (ter Braak and Šmilauer 1998).

Results

The role of phenolics, N and P content on litter decomposition and nutrient release

Initial litter chemical characteristics differed significantly in the amounts of phenolics, and also in DOC, DON and P_{OX} , and the phenolics/ N_{TOT} , phenolics/ P_{TOT} ratios. The largest differences were between spruce needles and hair grass litter (Table 1).

There was exponential relationship between the initial amount of phenolics and P_{OX} (Fig. 1). When the amount of phenolics dropped below 0.05 mmol g^{-1} , the amount of P_{OX} dramatically increased. The amount of N_{TOT} and P_{TOT} did not correlate with the amount of phenolics (data not shown).

Initial phenolics/ P_{TOT} , phenolics/ P_{OX} and phenolics/ N_{TOT} ratios were negatively related to NO_3^- amount and positively correlated to the DOC/DN and DON/DIN ratios in water extracts after incubation (Table 2). The amount of NH_4^+ was negatively affected only by initial phenolics/ P_{TOT} and phenolics content. The phenolics/ P_{TOT} and phenolics/ P_{OX} showed in most cases higher correlation coefficients than the phenolics/ N_{TOT} ratio (Table 2).

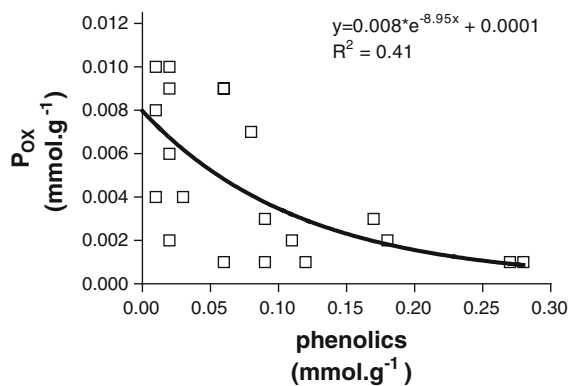


Fig. 1 Relationship between initial amount of phenolics and bioavailable P (P_{OX}). Each point represents a mean value from three replicates

Table 2 Correlation coefficients (*r*) of selected initial litter quality characteristics (phenolics, phenolics/N_{TOT}, phenolics/P_{TOT}, phenolics/P_{OX}, P_{OX}) versus the amount of NO₃⁻, NH₄⁺, DOC/DN, DON/DIN in water extracts and P_{OX} after 4 months of litter incubation at 0 and 10 °C (the first column: the sum of HW and CW extracts; the second column: CW extracts)

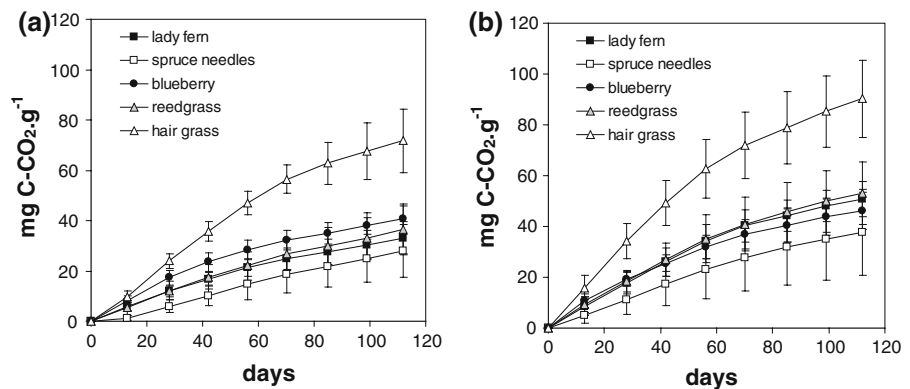
Initial litter quality	Versus	0 °C		10 °C	
		<i>r</i> (HW + CW)	<i>r</i> (CW)	<i>r</i> (HW + CW)	<i>r</i> (CW)
Phenolics/P _{TOT}	NO ₃ ⁻	-0.43*	-0.41*	-0.62***	-0.70***
	NH ₄ ⁺	-0.45*	-0.46*	-0.55**	-0.50*
	DOC/DN	0.79***	0.87***	0.68***	0.60**
	DON/DIN	0.73***	0.67***	0.45*	0.51*
	P _{OX}	-0.63**		-0.58**	
Phenolics/P _{OX}	NO ₃ ⁻	-0.61***	-0.50*	-0.75***	-0.75***
	NH ₄ ⁺	ns	ns	0.40	ns
	DOC/DN	0.67***	0.76***	0.68***	0.42*
	DON/DIN	0.75***	0.77***	0.89***	0.74***
	P _{OX}	-0.61**		-0.60**	
P _{OX}	NO ₃ ⁻	0.81***	0.66***	0.62***	0.65***
	NH ₄ ⁺	ns	ns	ns	ns
	DOC/DN	ns	ns	ns	ns
	DON/DIN	ns	ns	ns	ns
	P _{OX}	0.88***		0.96***	
Phenolics	NO ₃ ⁻	-0.48*	-0.44*	-0.65***	-0.72***
	NH ₄ ⁺	-0.40*	-0.42*	-0.52**	-0.48*
	DOC/DN	0.72***	0.80***	0.61***	0.49*
	DON/DIN	0.68***	0.62***	0.50*	0.54**
	P _{OX}	-0.61**		-0.58**	
Phenolics/N _{TOT}	NO ₃ ⁻	-0.48*	-0.43*	-0.63***	-0.66***
	NH ₄ ⁺	ns	ns	-0.49*	-0.43*
	DOC/DN	0.78***	0.84***	0.67***	0.53**
	DON/DIN	0.47*	0.70***	0.53**	0.59**
	P _{OX}	-0.58**		-0.56*	

ns not significant
 Correlation coefficients are given and their significances are marked by asterisks as follows:
 * *p* < 0.05, ** *p* < 0.01,
 *** *p* < 0.001

Cumulative microbial respiration at the end of incubation was significantly highest in hair grass litter (Tukey HSD test, *p* < 0.05) at both incubation temperatures compared to the other litter (Fig. 2a, b), which then decreased in the order: blueberry > reedgrass > lady fern > spruce needles and

reedgrass > lady fern > blueberry > spruce needles at 0 and 10 °C, respectively. However, the differences in cumulative respiration between these four litters were not statistically significant (Tukey HSD test, Fig. 2a). Cumulative microbial respiration at the end of incubation was higher at 10 °C than at 0 °C.

Fig. 2 Cumulative respiration of lady fern, spruce needles, blueberry, reedgrass and hair grass litter incubated at 0 (a) and 10 °C (b). Mean values from three independent experiments (2005, 2006, 2007) and standard deviation (*error bars*) are given



Between temperature differences were $56.6 \pm 20.8\%$ in lady fern litter, $49.0 \pm 20.2\%$ in reedgrass litter, $37.4 \pm 18.1\%$ in spruce needle litter, $27.2 \pm 17.0\%$ in hair grass litter and $24.4 \pm 10.4\%$ in blueberry litter (Fig. 2a, b).

Total cumulative respiration was negatively correlated with initial amount of phenolics, and the C_{TOT}/N_{TOT} , phenolics/ P_{TOT} , phenolics/ P_{OX} and phenolics/ N_{TOT} ratios, and positively correlated with P_{OX} (Table 3). The correlations were slightly stronger at 10 °C than at 0 °C.

Relative P saturation was the lowest for spruce needles (6.7%) and the highest for hair grass litter (22.4%, Table 4) at the beginning of litter incubation. Relative P saturation of the five incubated litters after incubation ranged from 44 to 81% at both temperatures. Relative P saturation reached approximately 44% in spruce needle litter, while it was almost 81% in hair grass litter (Table 4).

Table 3 Correlation coefficients (r) of selected initial litter quality characteristics (C_{TOT}/N_{TOT} , phenolics, phenolics/ N_{TOT} , phenolics/ P_{TOT} and P_{OX}) versus cumulative respiration after the months of litter incubation at 0 and 10 °C

Initial litter quality	Versus cumulative respiration	
	r (0 °C)	r (10 °C)
C_{TOT}/N_{TOT}	-0.45*	-0.41*
phenolics/ P_{TOT}	-0.57**	-0.63***
phenolics/ P_{OX}	-0.48*	-0.55**
phenolics/ N_{TOT}	-0.55**	-0.59**
P_{OX}	0.43*	0.46*
Phenolics	-0.57**	-0.64***

Correlation coefficients are given and their significances are marked by asterisks as follows: * $p < 0.05$, ** $p < 0.01$, *** $p < 0.001$

Table 4 Litter total P sorption capacity ($P_{OX} + X_{MAX}$) and relative P saturation ($P_{OX}/X_{MAX} + P_{OX}$) observed in five major understorey litter before incubation (initial) and after the four month of incubation at 0 and 10 °C

Litter	Initial		After 4th month at 0 °C		After 4th month at 10 °C	
	$X_{MAX} + P_{OX}$ ($\mu\text{mol g}^{-1}$)	$P_{OX}/X_{MAX} + P_{OX}$ (%)	$X_{MAX} + P_{OX}$ ($\mu\text{mol g}^{-1}$)	$P_{OX}/X_{MAX} + P_{OX}$ (%)	$X_{MAX} + P_{OX}$ ($\mu\text{mol g}^{-1}$)	$P_{OX}/X_{MAX} + P_{OX}$ (%)
Spruce needles	14.7	6.7	24.6	44.3	24.4	43.9
Lady fern	16.4	16.4	39.8	65.4	46.8	70.5
Blueberry	16.4	15.5	30.5	54.5	32.0	56.5
Reedgrass	16.2	15.1	44.5	69.3	39.5	65.3
Hair grass	17.7	22.4	73.7	81.4	65.8	79.1

Final DOC, DN, DON, NO_3^- , NH_4^+ amounts and DOC/DN at 0 and 10 °C were closely correlated (Table 5). Temperature affected final DOC, DN and NO_3^- amounts only slightly. This was indicated by the slope of the linear correlation line being close to 1. Final NH_4^+ content in water extracts and DOC/DN were lower at 10 °C than at 0 °C, while DON was higher at 10 °C.

Perox and PhOx dynamics

The activity of PhOx had similar dynamics for spruce needles and blueberry litter at 0 and 10 °C (Fig. 3a). In reedgrass litter, the activity of PhOx was higher at 0 °C than at 10 °C; it peaked at the end of the first month at $12.8 \mu\text{mol h}^{-1} \text{g}^{-1}$ (Fig. 3a). The activity of Perox showed different dynamics than PhOx at both incubation temperatures (Fig. 3b). Perox in reedgrass litter was significantly higher than in the spruce needles and blueberry litter at both temperatures. It fluctuated during incubation at 0 °C and grew at 10 °C from the beginning until the end of the second month, when it peaked at $56.5 \mu\text{mol h}^{-1} \text{g}^{-1}$ (Fig. 3b).

Average activity of PhOx over the entire incubation period was highest in reedgrass litter at 0 °C and in spruce needles and reedgrass at 10 °C (Table 6). However, the differences between spruce needles and reedgrass were not significant (Tukey HSD test, Table 6). The highest average Perox activity and overall ligninolytic activity occurred in the microbial community on reedgrass litter at both temperatures (Table 6). The differences in PhOx, Perox and overall ligninolytic activities between 0 and 10 °C were not statistically significant for all litter.

Table 5 Effect of different incubation temperatures on nutrient release, and DOC/DN and DON/DIN ratios

0 °C versus 10 °C	CW		HW + CW	
	<i>r</i>	Slope	<i>r</i>	Slope
DOC	0.88	1.02	0.84	0.83
DN	0.89	0.86	0.91	0.92
DON	0.94	1.57	0.92	1.45
NO ₃ ⁻	0.77	1.29	0.75	1.15
NH ₄ ⁺	0.70	0.50	0.72	0.48
DOC/DN	0.84	0.52	0.87	0.64
DON/DIN	ns	–	ns	–

Correlation coefficients (*r*) and slopes between released nutrients at 0 and 10 °C are shown

ns not significant

There was a close correlation between overall ligninolytic activity and respiration rate ($r = 0.77$, $p < 0.01$ and $r = 0.82$, $p < 0.01$ at 0 and 10 °C, respectively; Fig. 4). The relationship between ligninolytic enzymes and microbial respiration was similar at both temperatures, which was indicated by the similar slope of the linear regressions. The y intercept (y axis = respiration rate) was 2 times higher for 10 °C as compared to 0 °C indicating that microbial respiration was more sensitive to temperature than the activity of ligninolytic enzymes (Fig. 4).

Change of fungal and bacterial communities in relation to phenolics, N and P content

Fungal communities

The first and second canonical axes explained 50.1% of the variability of the fungal communities on spruce needles, blueberry and reedgrass at 0 °C (Fig. 5a). Variance explained by the variables selected by forward selection was 89% and decreased in order: DOC/DN (explained 26%) > P_{OX} (explained 22%) > Perox (explained 21%) > phenolics (explained 20%). During decomposition, all three communities changed their composition with relation to P_{OX}. P_{OX} influenced strongly the blueberry and reedgrass fungal communities and slightly the spruce needle community (Fig. 5a). Additionally, the fungal community of spruce needles showed a slight positive correlation with Perox activity.

At 10 °C, the first and second canonical axes explained 56.8% of the variability of the fungal communities (Fig. 5b). Variance explained by the variables selected by forward selection was 90% and decreased in order: phenolics/N_{TOT} (explained 27%) > phenolics/P_{TOT} (explained 23%) > P_{OX} (explained 21%) > PhOx (explained 19%). The fungal community of reedgrass changed composition again with relation to P_{OX}. Contrary to 0 °C, the

Fig. 3 PhOx (a) and Perox (b) activity during the decomposition of spruce needles, reedgrass and blueberry litter incubated at 0 and 10 °C. PhOx—phenoloxidase, PerOx—peroxidase

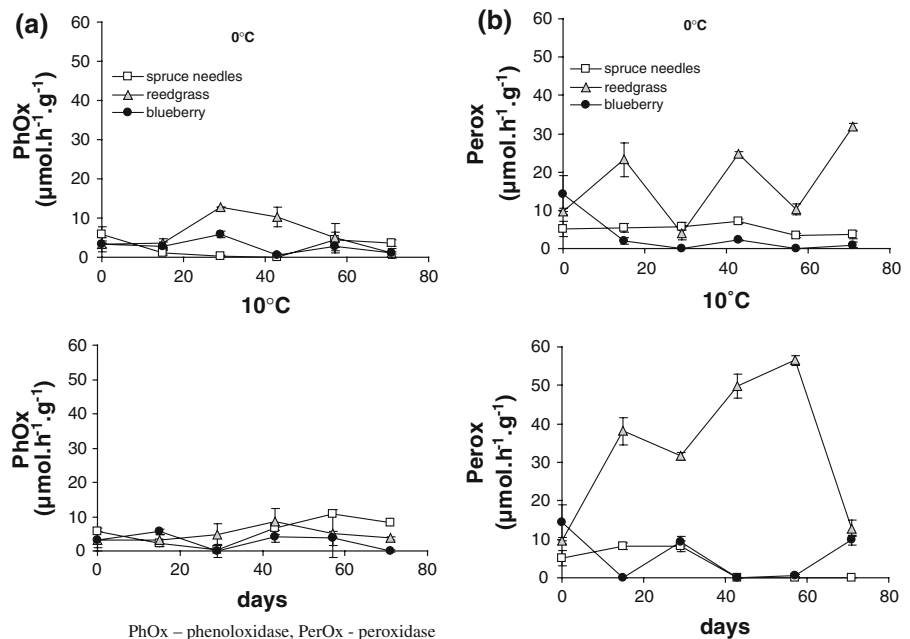
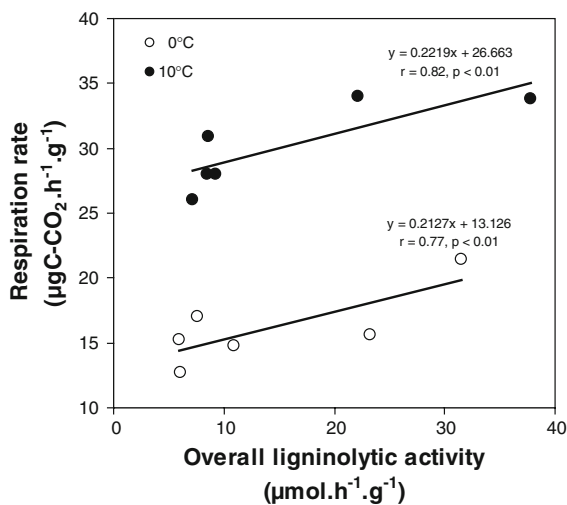


Table 6 Average activity of PhOx, Perox and overall ligninolytic activity (sum of PhOx and Perox activity) during the incubation period at 0 and 10 °C

Litter	Average enzyme activity					
	PhOx ($\mu\text{mol h}^{-1} \text{g}^{-1}$)		Perox ($\mu\text{mol h}^{-1} \text{g}^{-1}$)		Overall ligninolytic activity ($\mu\text{mol h}^{-1} \text{g}^{-1}$)	
	0 °C	10 °C	0 °C	10 °C	0 °C	10 °C
Spruce needles	2.5 ^A (2.4)	5.7 ^A (3.9)	5.0 ^A (1.4)	3.6 ^A (4.1)	7.6 ^{AB} (1.7)	9.3 ^{AB} (1.7)
Blueberry	2.7 ^A (1.9)	2.8 ^A (2.3)	3.2 ^A (5.5)	5.7 ^A (6.3)	6.0 ^A (5.9)	8.5 ^{AB} (5.1)
Reedgrass	6.0 ^A (4.6)	4.7 ^A (2.0)	17.3 ^{AB} (10.8)	33.1 ^B (19.0)	23.3 ^C (9.6)	37.8 ^C (20.3)

Standard deviations are shown in parenthesis ($n = 18$)

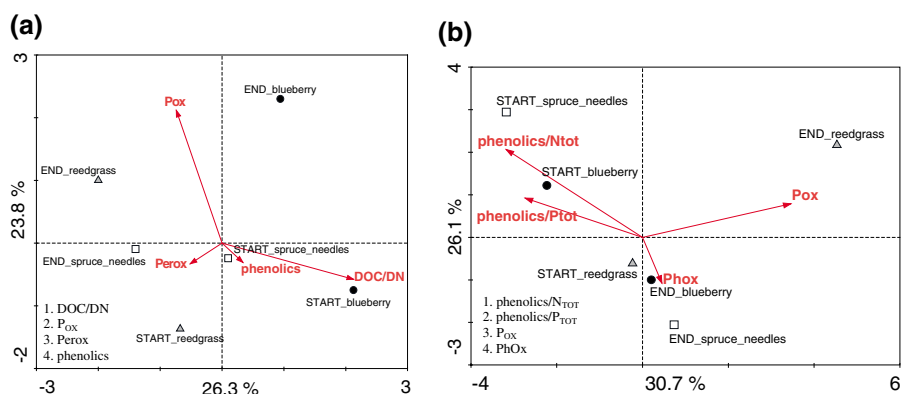
Different letters show significant differences between values within columns at 0 and 10 °C ($p < 0.05$)

**Fig. 4** Respiration rates and overall ligninolytic activities of spruce needles, blueberry and reedgrass litter at 0 and 10 °C

fungal communities of spruce needles and blueberry litter changed composition with relation to PhOx activity (Fig. 5b).

Bacterial communities

At 0 °C, the first and second canonical axes explained 50% of the variability in the bacterial communities of spruce needles, blueberry and reedgrass (Fig. 6a). Variance explained by the variables selected by forward selection was 85% and decreased in order: P_{OX} (explained 35%) > Perox (explained 22%) > phenolics (explained 17%) > phenolics/N (explained 11%). All three communities changed their composition greatly during the incubation. While the bacterial community of spruce needles changed composition under the strong influence of phenolics, P_{OX} strongly influenced the bacterial communities of

**Fig. 5** Ordination biplot of CCA displaying the effect of environmental variables (full line arrows) explaining the variance in fungal community composition (a—0 °C, b—10 °C) at the beginning and end of the incubation of spruce needle, blueberry and reedgrass litters. Monte–Carlo

permutation test was calculated and four environmental variables explaining the most variability in fungal community composition are shown. The order of explained variation by each environmental variable is displayed in *downer left corner* of ordination diagram

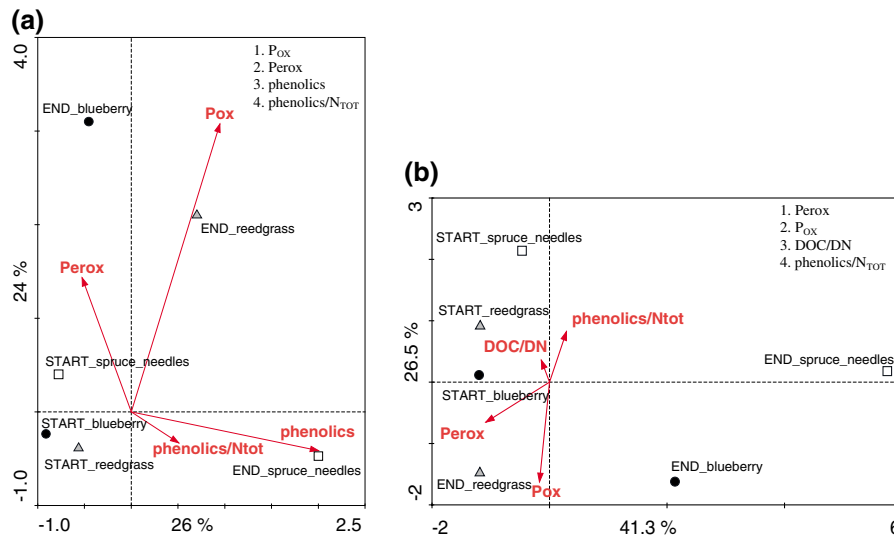


Fig. 6 Ordination biplot of CCA displaying the effect of environmental variables (*full line arrows*) explaining the variance in bacterial community composition (**a**—0 °C, **b**—10 °C) at the beginning and end of the incubation of spruce needle, blueberry and reedgrass litters. Monte–Carlo

permutation test was calculated and four environmental variables explaining the most variability of bacterial community composition are shown. The order of explained variation by each environmental variable is displayed in *upper right corner* of ordination diagram

reedgrass and blueberry litter. The bacterial community of blueberry litter was additionally affected by Perox activity.

The first and second canonical axes explained 67.8% of the variability of bacterial communities at 10 °C (Fig. 6b). Variance explained by the variables selected by forward selection was 91% and decreased in order: Perox (explained 37%) > P_{OX} (explained 25%) > DOC/DN (explained 15%) > phenolics/N_{TOT} (explained 14%). All three bacterial communities changed differently during the incubation. P_{OX} and Perox activity had similar effects on the bacterial reedgrass litter community. The blueberry litter and spruce needle communities developed according to unknown environmental variables (Fig. 6b).

Discussion

The role of phenolics, N and P in litter decomposition and nutrient release

The present study confirmed that a low amount of phenolics and low phenolics/N_{TOT} ratio in plant litter is closely related to higher DIN release during the

first four months of litter decomposition (Northup et al. 1995). In addition, we found that the phenolics/P_{OX} and phenolics/P_{TOT} ratios have similar correlation coefficients for DIN release as the phenolics/N_{TOT} ratio (Table 2).

For a better understanding of how P can influence decomposition processes, we need more information about P bioavailability (Pote et al. 1996). Greater amounts of P_{OX}, as an indicator of bioavailable P, were connected with increased NO₃⁻ release during litter decomposition in low lignified litter (i.e. reedgrass and hair grass litter, Table 2). It was also indicated by higher N mineralization and nitrification rates in reedgrass and hair grass litter (Tahovská, unpublished data). Similar results were found also *in-situ* for the litter soil horizon in the Bohemian Forest (Kaňa and Kopáček 2006; Šantrůčková et al. 2004, 2006).

Our results additionally revealed that, when phenolics were included into the statistical calculations with relation to P_{OX}, we found a close correlation with the DOC/DN and DON/DIN ratios after four months of litter incubation (Table 2). The strong relationship between phenolics and the DON/DIN ratio was first described by Northup et al. (1995).

Phenolics comprise up to 60% of plant dry weight and are well known for their protective and high reactive properties (Gallet and Lebreton 1995). In the decomposition process phenolics need to be first depolymerized from the lignin matrix by lignin degrading enzymes. The rate of carbon mineralization is a very slow in spruce needle litter as was confirmed by it having the lowest cumulative respiration of the five litters tested, as well as low ligninolytic activity (Figs. 2, 3). The amount of phenolics and P availability could be one of the reasons. Phenolics differ in their structure and complexity among plant species, which influences the quality of depolymerization products. Northup et al. (1995), explained the close relationship of DON/DIN with phenolics predominantly by the fact that high molecular weight phenolics can precipitate proteins (the major part of DON) and can therefore shift the microbial N metabolism to decrease the loss of DIN; vice versa, low molecular weight, water soluble phenolics can accelerate respiration rate and increase the release of DIN. Also, close connection between phenolics and P_{OX} can be caused by the natural properties of phenolics. Most of the low molecular weight phenolics released by depolymerization have highly reactive ortho-phenolic groups (Comerford and Skinner 1989). When released, they are able to precipitate Al and Fe ions (Northup et al. 1995, 1998; Comerford and Skinner 1989). Precipitation of Al and Fe by low molecular weight phenolics leads to higher amounts of P_{OX} and greater mineral N release from grasses. On the contrary, precipitation of proteins by high molecular weight phenolics leads to lower mineral N release and lower P_{OX} from spruce needle litter. Therefore, not only the amount of phenolics, but also the phenolics/ P_{OX} ratio seem to be important indicator of DON and DIN release (Northup et al. 1995; Gallet and Lebreton 1995; Fierer et al. 2001; Kanerva et al. 2006).

In general, there was a negative correlation between the initial amount of phenolics and P_{OX} before and after incubation in our study (Fig. 1; Table 2), which indicates that a low content of phenolics was connected with high P bioavailability. In high phenolic litter this could be caused by reduced depolymerization rates of lignin, and low molecular weight phenolics were not sufficient for precipitation of Al and Fe ions. It resulted in P being predominantly bound to recalcitrant Al and Fe

complexes (Northup et al. 1995; Comerford and Skinner 1989). In low phenolic litter (i.e. reedgrass and hair grass), the amount of P_{OX} increased during decomposition. After four months, the amount of P_{OX} almost reached the total P sorption capacity in both grasses (Table 4). Therefore, in areas dominated by reedgrass and hair grass, P_{OX} can leach to litter soil horizon from decomposing litter, because of the P saturation. Similar behavior was previously found for DIN (Šantrůčková et al. 2006; Svoboda et al. 2006; Kopáček et al. 2002a, b; 2006a, b).

Dynamics of Perox and PhOx activities and low temperature effect

The main enzymes which are responsible for lignin degradation and depolymerization are fungal and bacterial ligninolytic enzymes (Baldrian 2004; Snajdr et al. 2008), namely phenoloxidases (PhOx) and peroxidases (Perox). However, PhOx and Perox do not have the same biochemical functions. PhOx uses O_2 molecules for oxidation and is mainly responsible for degradation of more labile low molecular weight phenolics. Meanwhile, Perox uses H_2O_2 for creating unstable and highly reactive phenolic radicals and is predominantly associated with lignin depolymerization (Weintraub et al. 2007). Perox is produced by all white rot basidiomycetes, but PhOx may not be, suggesting that PhOx is not absolutely required in lignin degradation (Srinivasan et al. 1995; Dittmer et al. 1997; Rodriguez et al. 1999; Podgornik et al. 2001; Larrondo et al. 2003; Valaskova et al. 2007).

The activity of Perox increased the most on reedgrass litter at both incubation temperatures, suggesting that depolymerization in low phenolic litter is rapid from the very beginning of decomposition (Fig. 3). Therefore, there can be a sufficient amount of reactive phenolics during reedgrass litter decomposition to precipitate Al and Fe ions, which increases P bioavailability and DIN release. On the contrary, high NO_3^- concentrations are thought to inhibit ligninolytic enzymes unless they are used by the decomposing community as N source or in denitrification processes. In our experiment, NO_3^- concentrations did not reach concentrations to inhibit ligninolytic enzymes as was found by Wardlop and Zak (2006), and Waldrop et al. (2004). These authors did not find any significant decrease in PhOx and Perox activities below $10 \mu g g^{-1}$ of NO_3^- which was

the typical concentration in our experiment. However, they found significant decrease in the activity of PhOx (about 30%) and Perox (about 50%) at NO_3^- concentrations of $20 \mu\text{g g}^{-1}$.

Additionally, our experiment revealed that microbial processes were also active close to zero and that the activity was not negligible. Sometimes the activity was even higher at 0°C than at 10°C (Table 5). The activities of PhOx and Perox at 0°C were also relatively high (Di Nardo et al. 2004; Uchida et al. 2005). Our results confirmed the latest findings that microbial respiration and the activities of lignin-degrading enzymes during the winter period under snow cover are comparable to those during the summer period (Fig. 3; Table 3; Uchida et al. 2005). High Perox activity in low phenolic litter during the winter period can produce more reactive phenolics, increasing the amount of bioavailable P, which reached 69% and 82% of total P litter saturation after the four months in reedgrass and hair grass litter, respectively (Table 4).

Overall ligninolytic activity showed a close positive correlation with microbial respiration. The effect was almost identical at both incubation temperatures (Fig. 4). The differences in the factors measured at the of incubation temperature of $0\text{--}10^\circ\text{C}$ were significant ($p < 0.05$) only for respiration rate, which showed positive effect of temperature. The overall activity of ligninolytic enzymes in all three litter samples was not affected significantly by temperature (Davidson and Janssens 2006).

Dynamics of bacterial and fungal communities

There has been increasing interest in the last few years in using cultivation independent, DNA-based methods for studying bacterial and fungal communities in soil and litter (Coleman and Whitman 2005; Lynch et al. 2004; Fitter et al. 2005; Nannipieri et al. 2003; Kulhankova et al. 2006). However, many of these studies have focused on estimating the bacterial or fungal communities at a specific time of litter incubation or in a particular season and did not study changes in microbial community composition over a time period. Few of them included environmental variables, such as the chemical composition of litter, into the statistical calculations to determine the link between changes in microbial composition and bioavailability of key nutrients during litter decomposition (Fromin et al. 2002; Kulhankova et al. 2006).

Because we eliminated the direct contact of litter with soil and the long-term decomposer biota were absent, we assumed that only primary colonizers and those microorganisms already present on plant leaves (endophytes) will be responsible for litter decomposition. The ecological role of microbial primary colonizers, their enzymatic activity and their succession during the first months of litter decomposition are still not clear, but they are often found in the litter soil horizons (Lindahl et al. 2007; Livsey and Barklund 1992). Our results showed that, at a microcosm scale different nutrient availability can be closely related to composition of both bacterial and fungal communities. In general, bacterial and fungal communities compete for available nutrients when litter decomposition starts (Hoshino and Matsumoto 2007; Hoshino and Matsumoto 2004; Hurt et al. 2001). Each group has its advantages over the other. Bacteria can grow faster, but are less tolerant of acidic conditions (Fioretto et al. 2007; Killham 1994). In spruce forest ecosystems, where a lot of lignified litter is decomposed, fungi have an enzymatic advantage over bacteria. Actinomycetes are the only known representatives which are able to compete with fungi in lignin degradation (Waldrop et al. 2004; Waldrop and Zak 2006). New studies also show that Actinomycetes are leaf endophytes (Izumi et al. 2008; Li et al. 2008).

Our results revealed that composition of bacterial and fungal communities changed greatly during litter incubation (Figs. 5, 6). This change was mainly in the number and type of different bands in the DGGE gel, indicating some successional development of primary colonizers and endophytes in the microcosm during the four months (data not shown). However, only the composition of microorganisms at the beginning and end of incubation were compared together with available data on environmental variables (Figs. 5, 6).

At 0°C , the amount of phenolics was closely connected to initial composition of fungal communities in high lignified litter (i.e. spruce needles), indicating that these may be controlled by phenolics. On the contrary, phenolics were not related to the initial bacterial community on spruce needles (Fig. 6a). This seems to be in agreement with Frankland (1992), who hypothesized that the bacterial primary decomposers first utilize simple and easily available compounds and after that the more

recalcitrant ligno-cellulose complexes. Fast growing bacteria can over dominate fungi in competition for easily available nutrients in this stage of litter decomposition. Fungi, which are then in a nutrient limiting environment are obliged to depolymerize lignin and can be influenced by the amount of available phenolics (Fig. 6).

At 10 °C, fungal and bacterial communities of reedgrass at the end of the incubation responded strongly to P_{OX} (Figs. 5, 6). This is with agreement with the highest respiration rate in reedgrass litter which means that the microbial decomposers would have higher demand on P availability.

The connection of extracellular enzymes (i.e. PhOx and Perox) with the composition of microbial communities may be difficult to interpret. Is the activity of enzymes affecting microbial composition or is it the other way around? The production of extracellular enzymes is C, N and energy intensive, therefore microbes produce enzymes only when there is nutrient limitation (Koch 1985). Microbes that produce PhOx and Perox have to face several important challenges. Because these enzymes are produced and function outside the cell, products of depolymerization process (i.e. low molecular phenolics) may then diffuse away from the enzyme-producing microbes (Allison 2005). Other microbes in the system could take up these products without secreting their own enzymes. This strategy of “cheating” should arise whenever multiple organisms can benefit from the resource investment of a single organism (Velicer 2003), and could represent a competitive threat to enzyme-producing microbes. How they will succeed in “fighting” with “cheater” microbes depends also on the initial population size/density of extracellular enzyme producers (Allison 2005). Therefore, PhOx and Perox activities may affect not only the composition of ligninolytic enzymes producers, but also the composition of other microbes (i.e. fast growing bacterial communities), which lack PhOx and Perox activities.

Only Perox activity had a significant effect on bacterial community, indicating a strong dependence of bacteria on depolymerization processes. However these changes were dependent on litter type and incubation temperature (Fig. 6a, b). At 0 °C, the bacterial communities of blueberry and reedgrass litter at the end of incubation were strongly positively related to Perox activity. We did not observe a similar

pattern at 10 °C (Fig. 6b). On the contrary, the bacterial community of spruce needles changed from a positive relation to Perox at the beginning of incubation to a strongly positive relation to the amount of phenolics at the end of incubation. This could be an indication of change in bacterial community from Actinomycetes, which produced Perox at the beginning, to the “cheater” microbes, which used depolymerized phenolics at the end of the incubation. It also confirms previous findings that the competition for available nutrients play crucial role in the composition of the decomposers at the later stages of litter decomposition (Berg et al. 1993). Our results showed that this shift in microbial composition at a microcosm scale can be relatively fast, i.e. during the first four months of litter decomposition.

From the results we conclude:

- The phenolics/ P_{TOT} and phenolics/Pox ratios are good predictors of the release of DON and DIN from acid spruce forest litter.
- The higher activity of ligninolytic enzymes (i.e. Perox) in low phenolic reedgrass litter can produce highly reactive phenolics, which can either be used by the microbial community or precipitate Al and Fe ions, thereby increasing the bioavailability of P (P_{OX}) and release of DIN. This can, therefore, lead to higher DIN leaching from the areas dominated by grasses.
- Activity of lignin-degrading enzymes at 0 °C was comparable to those at 10 °C.
- There is a potential risk of bioavailable P (P_{OX}) leaching from grass dominated sites to the soil litter horizon.
- Bacterial and fungal communities of primary colonizers and endophytes change greatly during the early-stages of litter decomposition. While the change in fungal community composition of low lignified litter (i.e. reedgrass) correlates mostly with bioavailable P (P_{OX}), the change in higher lignified litter (i.e. spruce needles) correlates mostly with phenolics/ N_{TOT} , phenolics/ P_{TOT} ratios and PhOx activity (i.e. fungal community of spruce needles at 10 °C). Perox activity was responsible for the change in bacterial community composition of blueberry and reedgrass litter, while the bacterial community of spruce needle litter changed with relation to phenolics (i.e. bacterial community of spruce needles at 0 °C).

Acknowledgments This study was supported by the Czech Science Foundation, project 526/08/0751 and 206/07/1200 and the project MSM 6007665801. We acknowledge the laboratory and field assistance provided by our colleagues and students. We also thank the authorities of NP Šumava for permission to study the watershed ecosystems. We thank our American colleague Dr Keith Edwards for language correction.

References

- Aber JD, Melillo JM, McLaugherty CA (1990) Predicting long-term patterns of mass loss, nitrogen dynamics, and soil organic matter formation from initial fine litter chemistry in temperate forest ecosystems. *Can J Bot* 68:2201–2208
- Aber JD, McDowell W, Nadelhoffer K, Magill A, Berntson G, Kamakea M, McNulty S, Currie W, Rustad L, Fernandez I (1998) Nitrogen saturation in temperate forest ecosystem. *Bioscience* 48:921–934
- Allison SD (2005) Cheaters, diffusion, and nutrients constrain decomposition by microbial enzymes in spatially structured environments. *Ecol Lett* 8:626–635
- Baldrian P (2004) Increase of laccase activity during interspecific interactions of white-rot fungi. *FEMS Microbiol Ecol* 50:245–253
- Bärlocher F, Graça MAS (2005) Total Phenolics. In: Graça MAS, Bärlocher F, Gessner MO (eds) *Methods to study litter decomposition: a practical guide*. Springer, Netherlands, pp 97–100
- Berg B (1986) Nutrient release from litter and humus in coniferous forest soils—a mini review. *Scand J For Res* 1(3):359–369
- Berg B, Ekbohm G (1991) Litter mass-loss rates and decomposition patterns in some needle and leaf litter types—long-term decomposition in Scots pine forest.7. *Can J Bot* 69:1449–1456
- Berg B, McLaugherty CA, Johansson MB (1993) Litter mass-loss rates in late stages of decomposition at some climatically and nutritionally different pine sites. Long-term decomposition in a Scots pine forest.8. *Can J Bot* 71:680–692
- Cappo KA, Blume LJ, Raab GA, Bartz JK, Engels JL (1987) Analytical methods manual for the direct/delayed response project soil survey. US EPA, Las Vegas, USA, Sections 8–11
- Carlyle J, Lowther J, Smethurst P, Nambiar E (1990) Influence of chemical properties on nitrogen mineralization and nitrification in podzolized sands. Implications for forest management. *Aust J Soil Res* 28:981–1000
- Coleman DC, Whitman WB (2005) Linking species richness, biodiversity and ecosystem function in soil systems. *Pedobiologia (Jena)* 49:479–497
- Comerford NB, Skinner F (1989) Residual phosphorus solubility for an acid, clayey, forested soil in the presence of oxalate and citrate. *Can J Soil Sci* 69:111–117
- Couteaux MM, Bottner P, Berg B (1995) Litter decomposition, climate and litter quality. *Trends Ecol Evol* 10:63–66
- Cox P, Wilkinson SP, Anderson JM (2001) Effects of fungal inocula on the decomposition of lignin and structural polysaccharides in *Pinus sylvestris* litter. *Biol Fertil Soils* 33:246–251
- Dauer JM, Chorover J, Chadwick OA, Oleksyn J, Tjoelker MG, Hobbie SE, Reich PB, Eissenstat DM (2007) Controls over leaf and litter calcium concentrations among temperate trees. *Biogeochemistry* 86:175–187
- Davidson EA, Janssens IA (2006) Temperature sensitivity of soil carbon decomposition and feedbacks to climate change. *Nature* 440:165–173
- Di Nardo C, Cinquegrana A, Papa S, Fuggi A, Fioretto A (2004) Laccase and peroxidase isoenzymes during leaf litter decomposition of *Quercus ilex* in a Mediterranean ecosystems. *Soil Biol Biochem* 36:1539–1544
- Dittmer JK, Patel NJ, Dhawale SW, Dhawale SS (1997) Production of multiple laccase isoforms by *Phanerochaete chrysosporium* grown under nutrient sufficiency. *FEMS Microbiol Lett* 149:65–70
- Domisch T, Finér L, Laine J, Laiho R (2006) Decomposition and nitrogen dynamics of litter in peat soils from two climatic regions under different temperature regimes. *Eur J Soil Biol* 42:74–81
- Dyck W, Mees C, Hodgkiss P (1987) Nitrogen availability and comparison to uptake in two New Zealand *Pinus radiata* forests. *N Z J For Sci* 17:338–352
- Eriksson KEL, Blanchette RA, Ander P (1990) Microbial and enzymatic degradation of wood components. Springer, Berlin
- Fackler K, Gradinger C, Hinterstoisser B, Messner K, Schwanninger M (2006) Lignin degradation by white rot fungi on spruce wood shavings during short-time solid-state fermentations monitored by near infrared spectroscopy. *Enzyme Microb Technol* 39:1476–1483
- Fassnacht KS, Gower ST (1999) Comparison of the litterfall and forest floor organic matter and nitrogen dynamics of upland forest ecosystems in north central Wisconsin. *Biogeochemistry* 45:265–284
- Fierer N, Schimel JP, Cates RG, Zou J (2001) Influence of balsam poplar tannin fractions on carbon and nitrogen dynamics in Alaskan taiga floodplain soils. *Soil Biol Biochem* 33:1827–1839
- Fioretto A, Papa S, Pellegrino A, Fuggi A (2007) Decomposition dynamics of *Myrtus communis* and *Quercus ilex* leaf litter: mass loss, microbial activity and quality change. *App Soil Ecol* 36:32–40
- Fitter AH, Gilligan CA, Hollingworth K, Kleczkowski A, Twyman RM, Pitchford JW (2005) Biodiversity and ecosystem function in soil. *Funct Ecol* 19:369–377
- Fog K (1988) The effect of added nitrogen on the rate of decomposition of organic matter. *Biol Rev* 63:433–462
- Fox RH, Myers RJK, Vallis I (1990) The nitrogen mineralization rate of legume residues in soil as influenced by their polyphenol, lignin, and nitrogen contents. *Plant Soil* 129:251–259
- Frankland JC (1992) Mechanisms in fungal succession. In: Carroll GC, Wicklow DT (eds) *The fungal community*. Dekker, New York, pp 383–390
- Fromin N, Hamelin J, Tarnawski S, Roesti D, Jourdain-Miserez K, Forestier N, Teyssier-Cuvellé S, Gillet F, Aragno M, Rossi P (2002) Statistical analysis of denaturing gel electrophoresis (DGE) fingerprinting patterns. *Environ Microbiol* 4:634–643

- Gallet C, Lebreton P (1995) Evolution of phenolic patterns in plants and associated litters and humus of a mountain forest ecosystem. *Soil Biol Biochem* 27:157–165
- Hammel KE (1997) Fungal degradation of lignin. In: Cadisch G, Giller KE (eds) *Driven by nature: plant litter quality and decomposition*. CAB International, Wallingford, pp 33–46
- Hendel B, Sinsabaugh RL, Marxsen J (2005) Lignin-degrading enzymes: phenoloxidase and peroxidase. In: Graça MAS, Bärlocher F, Gessner MO (eds) *Methods to study litter decomposition: a practical guide*. Springer, Netherlands, pp 273–278
- Heuer H, Smalla K (1997) Application of denaturing gradient gel electrophoresis and temperature gradient gel electrophoresis for studying soil microbial communities. In: van Elsas JD, Wellington EMH, Trevors JT (eds) *Modern soil microbiology*. Marcel Dekker, Inc., New York, pp 353–373
- Hoshino YT, Matsumoto N (2004) An improved DNA extraction method using skim milk from soils that strongly adsorb DNA. *Microbes Environ* 19:13–19
- Hoshino YT, Matsumoto N (2007) DNA- versus RNA-based denaturing gradient gel electrophoresis profiles of a bacterial community during replenishment after soil fumigation. *Soil Biol Biochem* 39:434–444
- Hurt RA, Qiu X, Wu L, Roh Y, Palumbo AV, Tiedje JM, Zhou J (2001) Simultaneous recovery of RNA and DNA from soils and sediments. *Appl Environ Microbiol* 67:4495–4503
- Izumi H, Anderson IC, Killham K, Moore ERB (2008) Diversity of predominant endophytic bacteria in European deciduous and coniferous trees. *Can J Microbiol* 54:173–179
- Jansson PE, Berg B (1985) Temporal variation of litter decomposition in relation to simulated soil climate. Long-term decomposition in a Scots pine forest. *Can J Bot* 63:1008–1016
- Kaňa J, Kopáček J (2006) Impact of soil sorption characteristics and bedrock composition on phosphorus concentrations in two Bohemian Forest Lakes. *Water Air Soil Pollut* 173:243–259
- Kanerva S, Kitunen V, Kiikkilä O, Loponen J, Smolander A (2006) Response of soil C and N transformations to tannin fractions originating from Scots pine and Norway spruce needles. *Soil Biol Biochem* 38:1364–1374
- Killham K (1994) *Soil ecology*. Cambridge University Press, Cambridge
- Kirk TK, Farrell RL (1987) Enzymatic ‘combustion’: the microbial degradation of lignin. *Annu Rev Microbiol* 41:465–505
- Koch AL (1985) The macroeconomics of bacterial growth. In: Fletcher M, Floodgate GD (eds) *Bacteria in their natural environments*. Academic Press, London, pp 1–42
- Koopmans GF, Chardon WJ, de Willigen P, van Riemsdijk WH (2004) Phosphorus desorption dynamics in soil and the link to a dynamic concept of bioavailability. *J Environ Qual* 33:1393–1402
- Kopáček J, Kaňa J, Šantrůčková H, Porcal P, Hejzlar J, Píček T, Veselý J (2002a) Physical, chemical, and biochemical characteristics of soils in watersheds of the Bohemian Forest Lakes: I. Plešné Lake. *Silva Gabreta* 8:43–62
- Kopáček J, Kaňa J, Šantrůčková H, Porcal P, Hejzlar J, Píček T, Šimek M, Veselý J (2002b) Physical, chemical, and biochemical characteristics of soils in watersheds of the Bohemian Forest Lakes: II. Čertovo and Černé Lakes. *Silva Gabreta* 8:63–93
- Kopáček J, Turek J, Hejzlar J, Kaňa J, Porcal P (2006a) Element fluxes in watershed-lake ecosystems recovering from acidification: Plešné Lake, the Bohemian Forest, 2001–2005. *Biologia (Bratisl)* 61:S427–S440
- Kopáček J, Turek J, Hejzlar J, Kaňa J, Porcal P (2006b) Element fluxes in watershed-lake ecosystems recovering from acidification: Čertovo Lake, the Bohemian Forest, 2001–2005. *Biologia (Bratisl)* 61:S413–S426
- Kulhankova A, Beguiristain T, Moukoui M, Berthelin J, Ranger J (2006) Spatial and temporal diversity of wood decomposer communities in different forest stands, determined by ITS rDNA targeted TGGE. *Ann For Sci* 63:547–556
- Larrondo LF, Salas L, Melo F, Vicuña R, Cullen D (2003) A novel extracellular multicopper oxidase from *Phanerochaete chrysosporium* with ferroxidase activity. *Appl Environ Microbiol* 69:6257–6263
- Li J, Zhao GZ, Chen HH, Qin S, Xu LH, Jiang CL, Li WJ (2008) *Rhodococcus cercidiphylli* sp. nov., a new endophytic actinobacterium isolated from a *Cercidiphyllum japonicum* leaf. *Syst Appl Microbiol* 31:108–113
- Lindahl BD, Ihrmark K, Boberg J, Trumbore SE, Höglberg P, Stenlid J, Finlay RD (2007) Spatial separation of litter decomposition and mycorrhizal nitrogen uptake in a boreal forest. *New Phytol* 173:611–620
- Livsey S, Barklund P (1992) Lophodermium piceae and *Rhizosphaera kalkhoffii* in fallen needles of Norway spruce (*Picea abies*). *Eur J For Pathol* 22:204–216
- Lucas RW, Casper BB, Jackson JK, Balsler TC (2007) Soil microbial communities and extracellular enzyme activity in the New Jersey Pinelands. *Soil Biol Biochem* 39:2508–2519
- Lynch JM, Benedetti A, Insan H, Nuti MP, Smalla K, Torsvik V, Nannipieri P (2004) Microbial diversity in soil: ecological theories, the contribution of molecular techniques and the impact of transgenic plants and transgenic microorganisms. *Biol Fertil Soils* 40:363–385
- Meentemeyer V (1978) Macroclimate and lignin control of litter decomposition rates. *Ecology* 59:465–472
- Muller M, Sundman V, Soininvaara O, Meriläinen A (1988) Effect of chemical composition on the release of nitrogen from agricultural plant materials decomposing in soil under field conditions. *Biol Fertil Soils* 6:78–83
- Nannipieri P, Ascher J, Ceccherini MT, Landi L, Pietramellara G, Renella G (2003) Microbial diversity and soil functions. *Eur J Soil Sci* 54:655–670
- Northup RR, Yu Z, Dahlgren RA, Vogt KA (1995) Polyphenol control of nitrogen release from pine litter. *Nature* 377:227–229
- Northup RR, Dahlgren RA, McColl JG (1998) Polyphenols as regulators of plant-litter-soil interactions in northern California pygmy forest: a positive feedback? *Biogeochemistry* 42:189–220
- Park JH, Matzner E (2003) Controls on the release of dissolved organic carbon and nitrogen from a deciduous forest floor

- investigated by manipulations of aboveground litter inputs and water flux. *Biogeochemistry* 66:265–286
- Pawłowski L (1997) Acidification: its impact on the environment and mitigation strategies. *Ecol Eng* 8:271–288
- Podgornik H, Stegu M, Zibert E, Perdih A (2001) Laccase production by *Phanerochaete chrysosporium*—an artifact caused by Mn(III)? *Lett Appl Microbiol* 32:407–411
- Pote DH, Daniel TC, Sharpley AN, Moore PA, Edwards DR, Nichols DJ (1996) Relating extractable soil phosphorus to phosphorus losses in runoff. *Soil Sci Am J* 60:855–859
- Pregitzer KS, Zak DR, Burton AJ, Ashby JA, Macdonald NW (2004) Chronic nitrate additions dramatically increase the export of carbon and nitrogen from northern hardwood ecosystems. *Biogeochemistry* 68:179–197
- Prescott CE (2005) Do rates of litter decomposition tell us anything we really need to know? *For Ecol Manag* 220:66–74
- Rodriguez S, Longo MA, Cameselle C, Sanroman A (1999) Production of manganese peroxidase and laccase in laboratory-scale bioreactors by *Phanerochaete chrysosporium*. *Bioproc Eng* 20:531–535
- Šantrůčková H, Vrba J, Pícek T, Kopáček J (2004) Soil biochemical activity and phosphorus transformations and losses from acidified forest soils. *Soil Biol Biochem* 36:1569–1576
- Šantrůčková H, Křišťůvková M, Vaněk D (2006) Decomposition rate and nutrient release from plant litter of Norway spruce forest in the Bohemian Forest. *Biologia (Bratisl)* 61:S499–S508
- Šantrůčková H, Šantrůček J, Setlik J, Svoboda M, Kopáček J (2007) Carbon isotopes in tree rings of Norway spruce exposed to atmospheric pollution. *Environ Sci Technol* 41:5778–5782
- Schwertmann U (1964) Differenzierung der Eisenoxiden des Bodens durch extraction mit Ammoniumoxalatlösung. *Z Pflanzenerähr Düng Bodenkd* 105:194–202
- Sinsabaugh RL, Carreiro MM, Repert DA (2002) Allocation of extracellular enzymatic activity in relation to litter composition, N deposition, and mass loss. *Biogeochemistry* 60:1–24
- Sinsabaugh RL, Gallo ME, Lauber C, Waldrop MP, Zak DR (2005) Extracellular enzyme activities and soil organic matter dynamics for northern hardwood forests receiving simulated nitrogen deposition. *Biogeochemistry* 75:201–215
- Snajdr J, Valaskova V, Merhautova V, Herinkova J, Cajthaml T, Baldrian P (2008) Spatial variability of enzyme activities and microbial biomass in the upper layers of *Quercus petraea* forest soil. *Soil Biol Biochem* 40:2068–2075
- Söderström B, Bååth E, Lundgren B (1983) Decrease in soil microbial activity and biomasses owing to nitrogen amendments. *Can J Microbiol* 29:1500–1506
- Srinivasan C, D'Souza T, Boominathan K, Reddy CA (1995) Demonstration of laccase in the white rot basidiomycete *Phanerochaete chrysosporium* BKM-F1767. *Appl Environ Microbiol* 61:4274–4277
- Svoboda M, Matějka K, Kopáček J (2006) Biomass and element pools of understory vegetation in the catchments of Čertovo Lake and Plešné Lake in the Bohemian Forest. *Biologia(Bratisl)* 61:S509–S521
- ter Braak CJF, Šmilauer P (1998) CANOCO Reference manual and user's guide to Canoco for Windows. Microcomputer Power, Ithaca, 351 pp
- Tomlinson GH (2003) Acid deposition, nutrient leaching and forest growth. *Biogeochemistry* 65:51–81
- Uchida M, Mo W, Nakatsubo T, Tsuchiya Y, Horikoshi T, Koizumi H (2005) Microbial activity and litter decomposition under snow cover in cool-temperate broadleaved deciduous forest. *Agric For Meteorol* 134:102–109
- Valaskova V, Snajdr J, Bittner B, Cajthaml T, Merhautova V, Hoffichter M, Baldrian P (2007) Production of lignocellulose-degrading enzymes and degradation of leaf litter by saprotrophic basidiomycetes isolated from a *Quercus petraea* forest. *Soil Biol Biochem* 39:2651–2660
- van der Zee SEATM, Fokkink LGJ, van Riemsdijk WH (1987) A new technique for assessment of reversibly adsorbed phosphate. *Soil Sci Am J* 51:599–604
- Velicer GJ (2003) Social strife in the microbial world. *Trends Microbiol* 11:330–336
- Veselý J (1994) Investigation of the nature of the Šumava lakes: a review. *J Natl Mus (Prague) Nat Hist Ser* 163: 103–120
- Waldrop MP, Zak DR (2006) Response of oxidative enzyme activities to nitrogen deposition affects soil concentrations of dissolved organic carbon. *Ecosystems* 9:921–933
- Waldrop MP, Zak DR, Sinsabaugh RL (2004) Microbial community response to nitrogen deposition in northern forest ecosystems. *Soil Biol Biochem* 36:1443–1451
- Weintraub MN, Scott-Denton LE, Schmidt SK, Monson RK (2007) The effects of tree rhizodeposition on soil exoenzyme activity, dissolved organic carbon, and nutrient availability in a subalpine forest ecosystem. *Oecologia* 154:327–338
- Yuan G, Lavkulich LM (1994) Phosphate sorption in relation to extractable iron and aluminium in spodosols. *Soil Sci Soc Am J* 58:343–346

Paper 2

Barta J, Slajsova P, Tahovska K, Picek T, Santruckova H (2014) Different temperature sensitivity and kinetics of soil enzymes indicate seasonal shifts in C, N and P nutrient stoichiometry in acid forest soil. *BIOGEOCHEMISTRY* 117:525-537.

Different temperature sensitivity and kinetics of soil enzymes indicate seasonal shifts in C, N and P nutrient stoichiometry in acid forest soil

Jiří Bárta · Petra Šlajsová · Karolina Tahovská ·
Tomáš Pícek · Hana Šantrůčková

Received: 26 October 2012 / Accepted: 25 July 2013 / Published online: 10 August 2013
© Springer Science+Business Media Dordrecht 2013

Abstract Acid forest soils in the Bohemian Forest in Central Europe are biogeochemically imbalanced in organic C, N and P processing. We hypothesized that these imbalances can be due to different temperature sensitivities of soil enzyme activities and their affinities to substrate in litter and organic soil horizons. We measured potential activities of five main soil enzymes (β -glucosidase, cellobiohydrolase, Leu-aminopeptidase, Ala-aminopeptidase, and phosphatase) responsible for organic carbon, nitrogen and phosphorus acquisition. We also modeled potential in situ enzyme activities and nutrient release based on continuous in situ temperature measurements. We determined basic kinetic parameters (K_m , V_{max}), enzyme efficiencies (k_{cat}) and temperature sensitivities (E_a and Q_{10}) according to Michaelis–Menten kinetic and modified Arrhenius models. Our results showed significant differences in substrate affinities between the litter and organic soil horizons. Higher aminopeptidase affinity

(lower K_m) in the litter soil horizon can lead to leaching of peptidic compounds to lower soil horizons. β -Glucosidase and phosphatase showed high temperature response following the Arrhenius model. However, both aminopeptidases showed no or even decreased activity with increasing temperature. The aminopeptidase temperature insensitivity means that peptidic compounds are degraded at the same or even lower rate in warmer and colder periods of the year in acid forest soils. This imbalance results in different release of available nutrients from plant litter and soil organic matter which may affect bacterial and fungal community composition and nutrient leaching from these ecosystems.

Keywords Acid forest soil · Enzyme kinetics · Potential enzyme activity modeling · Q_{10} · Soil enzymes · Temperature sensitivity

Responsible Editor: Frank Hagedorn.

Electronic supplementary material The online version of this article (doi:10.1007/s10533-013-9898-1) contains supplementary material, which is available to authorized users.

J. Bárta (✉) · P. Šlajsová · K. Tahovská ·
T. Pícek · H. Šantrůčková
Department of Ecosystem Biology, Faculty of Science,
University of South Bohemia, Branišovská 31,
370 05 Ceske Budejovice, Czech Republic
e-mail: barta77@seznam.cz

Introduction

Soil enzymes play crucial roles in the biogeochemical cycles of carbon (C), nitrogen (N) and phosphorus (P) (Tate 2002). By the activity of cellulolytic, proteolytic and phosphorolytic enzymes, simple organic compounds like monosaccharides, amino acids or phosphates are released to the soil environment representing an important and “easy to take” fraction of soil solution. Several classes of enzymes need to cooperate in complex biopolymer degradation.

However, ecological studies generally quantify only the activities of enzymes that catalyse the terminal reactions that produce assimilable products from the C, N and P sources (Sinsabaugh et al. 2009). The potential activities of these enzymes can be linked to biogeochemical transformations, microbial metabolism rates and even used to predict microbial nutrient demand.

There are several factors influencing soil enzyme activity of which temperature, moisture and substrate availability are the most important (Meentemeyer 1978; McLaugherty and Linkins 1990; Allison 2006; Allison and Vitousek 2005; Allison and Jastrow 2006; Sierra 2012). Many studies have focused on measuring kinetic parameters while only some have focused on temperature sensitivity of essential soil enzymes in C, N and P acquisition (Burns et al. 2002; Wallenstein et al. 2009; Stone et al. 2012). This knowledge gap is in contrast with the large number of studies focused on the temperature sensitivity of litter and soil organic matter (SOM) decomposition rates where soil enzymes play a crucial role (Sinsabaugh et al. 2008; Sinsabaugh 2010; Davidson and Janssens 2006; Kirchbaum 2006). Data from the Michaelis–Menten kinetic model and temperature sensitivity measurements can give us a better insight into the potential substrate availability by determining basic kinetic parameters of soil enzymes. Additionally, from the measuring of soil enzyme activities at different temperatures and continuous measuring of in situ soil temperatures we can model in situ potential enzyme activities and also predict nutrient release throughout the season (Sinsabaugh et al. 2009; Wallenstein and Weintraub 2008; Wallenstein et al. 2009).

The aim of this study was to estimate the kinetics of five soil enzymes involved in organic C, N and P processing and their temperature sensitivities in an acidic mountainous spruce forest soil. Spruce forest soils in central Europe were subject to high anthropogenic N depositions in the second half of the last century (Kopáček et al. 2002). This extremely high N input to these forest soils imbalanced the soil biogeochemistry (Kopáček et al. 2002; Šantrůčková et al. 2004, 2006, 2009). On the one hand, high N deposition can have a positive feedback on the overall soil enzyme production because their biosynthesis is N intensive (Koch 1985). On the other hand N deposition can lead to enormous soil acidification, decrease of base cation concentrations and the soil ability to retain

N (Majer et al. 2003; Kopáček and Vrba 2006; Bárta et al. 2010; Tahovská et al. 2013). These biogeochemical imbalances can have their origin in imbalances in the soil enzyme activities. We assume that these changes can be due to the different enzyme affinities to substrates in the litter and organic soil horizons. Also, different temperature sensitivities of soil enzymes in CNP cycling can shift the dissolved organic matter (DOM) stoichiometry in warmer and colder seasonal periods.

We expect that enzyme activities will fluctuate more with temperature in the upper litter soil horizon than in the organic soil horizon. We hypothesized that: (1) Substrate affinities increase with soil depth, which corresponds with decreasing substrate concentration/availability; (2) According to the Arrhenius model soil enzyme activities will increase exponentially with increasing temperature; and (3) the soil enzyme activities will be more temperature-sensitive in the colder period of the year than in the warmer one.

Materials and methods

Study site

Study site is located in the watershed of Plešné Lake, which is situated at 48°47'N, and 13°52'E, altitude of 1300 m asl in the Bohemian Forest (Central Europe), is covered with a 160 year-old Norway spruce (*Picea abies*) forest. The bedrock is composed of granites. The understorey of the watershed is dominated by hair grass (*Avenella flexuosa*), reedgrass (*Calamagrostis villosa*), blueberry (*Vaccinium myrtillus*), and lady fern (*Athyrium alpestre*, Svoboda et al. 2006). Soil types are mostly cambisols. Basic physico-chemical and biochemical properties of the soils were described by Kopáček et al. (2002). Soil was collected from an experimental sampling site in the watershed of glacial Plešné Lake. The experimental site is ~100 × 100 m. Three replicates (each replicate was mixed from 10 randomly taken soil cores) from the litter (0–2 cm) and organic horizons (5–10 cm) were collected in October 2010, homogenized through a 3 mm sieve and kept at 4 °C for 1 week for stabilization. Soil samples for seasonal enzyme activities were taken in late May, early August, and late October 2010. Enzyme kinetics and temperature sensitivity were measured from soil samples taken in October 2010.

Soil enzyme activity determination

We determined potential enzyme activities of five soil enzymes responsible for organic C, N and P processing (Table 1). We used standard fluorometric techniques to assess the enzyme kinetics and temperature sensitivity (Marx et al. 2001). Briefly, 1 g of soil was homogenized in 100 ml of distilled water using IKA Ultra-Turrax T 10 homogenizator (IKA®-Werke GmbH & Co. KG, Germany). The soil suspensions (200 µl) were then transferred to a 96-well microplate in four analytical replicates. Then 50 µl of 4-methylumbelliferone (MUB) or 7-amino-4-methylcoumarin (AMC) labeled substrates were added. Standard curves were measured with MUB/AMC in soil slurries for every sample separately. Concentrations of MUB/AMC for standard curves were: 0, 1, 5, 10, 25, 50, 100 and 200 µM. Microplates were incubated at 30 °C for 2 h. All fluorescence measurements were done on the microplate reader INFINITE F200 (TECAN, Germany) using the excitation wavelength of 365 nm and emission wavelength of 450 nm. Units of all enzyme activities are expressed as nmol h⁻¹ g C⁻¹.

Soil enzyme kinetic parameters

Concentrations of 0, 5, 25, 50, 100, 200, 300 and 500 µM of MUB- and AMC-substrates were used for the measurement of kinetic parameters. Enzyme activities were fitted to either a nonlinear Michaelis–Menten kinetic model (1). Enzyme efficiency (k_{cat}) was calculated by Eq. (2)

$$activity = \frac{V_{max} \cdot (S)}{K_m + (S)} \quad (1)$$

$$k_{cat} = \frac{V_{max}}{K_m}, \quad (2)$$

where V_{max} is the maximum rate of enzyme reaction and/or concentration of the limiting isoenzyme (nmol min⁻¹ g⁻¹), S is the concentration of the MUB/AMC labeled substrate (µM), K_m is Michaelis–Menten constant (µM) which reflects the enzyme affinity for a given substrate.

Temperature sensitivity determination and in situ modeling

Temperature sensitivity of each enzyme was determined by measuring enzyme activity at six different temperatures (0, 5, 10, 15, 20, 25 °C). MUB- and AMC-substrate concentrations were chosen according to the kinetic results to avoid substrate limitation or inhibition. Microplates were put into the pre-heated/cooled incubators of desired temperature for 2 h. Fluorescence was measured after 5, 65 and 125 min.

Modeled in situ enzyme activities were then calculated using Eq. (3). This equation is a modification of the equation, introduced by Wallenstein et al. (2009). Instead of Wallenstein equation our equation is based on measuring enzyme activities at 6 different temperatures. In-situ temperature was measured continuously from May to October 2010 using data loggers installed in the litter and organic soil horizons at the experimental site. Temperature data were collected at 2 h intervals from which day averages,

Table 1 List of soil enzyme activities measured, assay substrate used, element in biogeochemical cycling and the biopolymer, which the enzyme degrades

Soil enzyme	Assay substrate	Element	Function
β-Glucosidase, E.C. 3.2.1.21	MUB-β-D-glucopyranoside	Carbon	Cellulose degradation: hydrolyses glucose from cellobiose
Cellobiohydrolase, E.C. 3.2.1.91	MUB-β-cellobiopyranoside	Carbon	Cellulose degradation: hydrolyses cellobiose from cellulose
Leu-aminopeptidase, E.C. 3.4.11.1	AMC-L-leucine	Nitrogen	Proteolysis: hydrolyses leucine and other hydrophobic amino acids from the N terminus of polypeptides
Ala-aminopeptidase, E.C. 3.4.11.12	AMC-L-alanine	Nitrogen	Proteolysis: hydrolyses alanine and other hydrophobic amino acids from the N terminus of polypeptides
Phosphatase, E.C. 3.1.3.2	MUB-phosphate	Phosphorus	Hydrolyses phosphate from phosphosaccharides, nucleotides, and phospholipids

minimum and maximum day temperatures were calculated. Day mean temperature was then used for modeling in situ potential enzyme activities using a modified Arrhenius model.

Q_{10} values in the range of 0–25 °C were calculated using Eq. (3)

$$Q_{10} = e^{(S \cdot 10)} \quad (3)$$

$$\text{activity}_{\text{in-situ}} = A \cdot e^{(T_{\text{in-situ}} \cdot S)}, \quad (4)$$

where S is the slope of the linear regression of \ln transformed enzyme activities in the temperature range of 0–25 °C (Table S1), $A = e^a$ where a is the Y intercept of the linear regression of \ln transformed enzyme activities, $T_{\text{in-situ}}$ is day mean temperature and e is Euler's number.

Activation energy (E_a) was calculated by fitting potential enzyme activities against temperature using nonlinear Arrhenius model (v)

$$\text{activity} = Ae^{-\frac{E_a}{RT}}. \quad (5)$$

A is the collision frequency (h^{-1}), E_a is the activation energy of enzyme reaction (J mol^{-1}), R is gas constant ($8.314 \text{ J mol}^{-1} \text{ K}^{-1}$), T is the absolute temperature (K).

Soil enzyme activities were grouped according to C, N and P acquisition activity (Sinsabaugh et al. 2009). E_C was β -glucosidase potential activity and represented organic C acquisition activity, E_N was the average of aminopeptidases potential activities and represented organic N acquisition activity and E_P was the potential activity of phosphatase and represented organic P acquisition activity.

When modeling the available C, N and P nutrients released by soil C, N and P enzymes, we assumed that E_C enzymes, having a theoretical potential activity of 1 mol h^{-1} , release 1 mol h^{-1} of 6C glucose, E_N enzymes release in average 4.5C and 1 N (i.e. the average of released C and N in form of hydrophobic Ala and/or Leu amino acids), and E_P enzymes release 1P in form of phosphate. Based on these assumptions, we were able to model the potential release of available C (Eq. 6), N (Eq. 7) and P (Eq. 8)

$$C = 6 \cdot E_C + 4.5 \cdot E_N \quad (6)$$

$$N = E_N \quad (7)$$

$$P = E_P. \quad (8)$$

Soil chemical analyses

All results are expressed on a oven-dry weight basis (105 °C, 3 h) and mean values from three replicates were used for statistical evaluations. C_{TOT} and N_{TOT} were measured in finely ground soil using an elemental analyzer (NC ThermoQuest, Germany), while P_{TOT} was determined by sequential mineralization of the samples by HNO_3 and HClO_4 , and then analyzed by flow injection analyzer (Foss Tecator 5042, Sweden). Dissolved organic carbon (DOC) and dissolved nitrogen (DN) were extracted in cold water (CW) with a water:sample ratio of 10:1, v/w, 1 h shaken at 20 °C. DOC and DN in the cold water extracts were determined on a TOC/TN analyzer (SKALAR FORMACS HT), and NH_4^+ and NO_3^- using a flow injection analyzer (Foss Tecator 5042, Sweden). Dissolved organic nitrogen (DON) was calculated by subtracting the sum of NH_4^+ and NO_3^- from DN. pH in the litter and organic soil horizons was measured in the CW extracts. Cation exchange capacity (CEC) was measured and calculated according the Thomas 1982.

Statistics

Statistical analyses were performed using Statistica 9.0 (StatSoft). One-way ANOVA (soil horizon as the independent variable), followed by the Tukey HSD test, was used for testing differences between soil chemical and kinetic parameters. Differences at $P < 0.05$ were regarded as statistically significant. Kinetic parameters (V_{max} , K_m) and activation energies (E_a) were calculated from nonlinear regression models using Michaelis–Menten (1) and Arrhenius equation (5) in GraphPad Prism 4.0 software.

Results

Chemical characteristics differed significantly between the litter and organic horizons. All parameters were significantly higher in the litter horizon with the exception of P_{TOT} , pH and CEC (Table 2).

Apparent V_{max} values for the C and P enzymes (β -glucosidase, cellobiohydrolase, and phosphatase) were significantly higher in the litter horizon while the apparent V_{max} for the N enzymes (Ala- and Leu-aminopeptidase) were higher in the organic horizon (Table 3; Fig. S1). The apparent K_m decreased with soil depth for the C and P enzymes while again the opposite was true for the N enzymes. The enzyme

Table 2 Basic chemical properties of the litter (0–2 cm) and organic soil horizons (5–10 cm)

	C _{tot} (mg g ⁻¹)	N _{tot} (mg g ⁻¹)	C _{tot} /N _{tot} (molar)	P _{tot} (mg g ⁻¹)	DOC (mg g ⁻¹)	DN (mg g ⁻¹)	DON (mg g ⁻¹)	NH ₄ ⁺ (mg g ⁻¹)	NO ₃ ⁻ (mg g ⁻¹)	pH (H ₂ O)	CEC (meq 100 g ⁻¹)
Litter	446.50 ^A (26.32)	19.56 ^A (0.44)	26.62 ^A (1.12)	0.91 ^A (0.27)	19.2 ^A (2.1)	0.59 ^A (0.19)	0.07 ^A (0.01)	0.23 ^A (0.10)	0.29 ^A (0.05)	3.59 ^A (0.15)	22.1 ^A (2.4)
Organic	275.17 ^B (106.18)	13.83 ^B (4.32)	23.21 ^B (3.75)	1.12 ^A (0.44)	13.7 ^B (1.6)	0.32 ^B (0.05)	0.02 ^B (0.01)	0.09 ^B (0.01)	0.20 ^B (0.03)	3.45 ^A (0.14)	22.8 ^A (1.8)

Different letters show significant differences between values within columns ($p < 0.05$). The data represent averages and standard errors are shown in parentheses ($n = 3$)

efficiency (k_{cat}) was significantly lower in the organic horizon than in the litter horizon for all enzymes. For N enzymes we found the highest one order decrease of the enzyme efficiency (Table 3). This clearly shows the enormous distinctness of isoenzyme pools between the litter and organic horizon in acid forest soils.

Temperature sensitivity of enzyme activities as indicated by average Q_{10} between 0 and 25 °C and activation energy (E_a) did not differ significantly between the litter and organic soil horizon for the most of the enzymes (Table 4). We were able to calculate E_a only for β -glucosidase and phosphatase. The cellobiohydrolase and both aminopeptidases did not follow the Arrhenius model. Only β -glucosidase and phosphatase had average $Q_{10} > 1$. Interestingly, both aminopeptidases had average Q_{10} values lower than 1 meaning their activities decreased with temperature; cellobiohydrolase showed a similar trend (Table 4). β -glucosidase activity was more temperature sensitive in the litter soil horizon as indicated by higher Q_{10} and E_a . On the other hand, phosphatase showed higher temperature sensitivity in the organic soil horizon (Table 4). We also compared Q_{10} values at different temperature ranges (Table S2). These results showed that Q_{10} values of both aminopeptidases were approx. 1 between 0 and 5 °C and then dropped below 1 till 20 °C. Between 20 and 25 °C Q_{10} values started to increase again. Similar trend was observed for cellobiohydrolase (Table S2).

While average daily temperature was similar in the litter and organic horizons the temperature fluctuations were much higher in the litter soil horizon (Fig. 1a). On extreme days during June and July 2010, the daily maximum and minimum temperatures differed by 10 °C. On the other hand, these fluctuations were not higher than 3 °C in the organic horizon (Fig. 1b).

Modeled in situ enzyme activities showed large differences between the E_C/E_N and E_C/E_P ratios. While the E_C/E_P ratio was stable and close to global average of 0.5 during the whole season (Figs. 2, 3), the E_C/E_N ratio fluctuated between the maximum of 5 (i.e. the global average ratio between cellulases and proteases reported by Sinsabaugh et al. 2009) and minimum of 1.5 in the litter horizon and between 2 and 0.9 in the organic horizon during the season (Fig. 2). The E_C/E_N ratio also more closely reflects temperature than the E_C/E_P ratio. This was mainly caused by the high temperature sensitivity of β -glucosidase and

Table 3 Comparison of V_{\max} , K_M , and k_{cat} for soil hydrolytic enzymes in the litter (0–2 cm) and organic soil horizons (5–10 cm)

Soil horizon	V_{\max} (nmol h ⁻¹ gC ⁻¹)		K_M (μM)		Efficiency (h ⁻¹ gC ⁻¹) * 10 ⁻³	
	Litter	Organic	Litter	Organic	Litter	Organic
β-Glucosidase	597.5 ^A (73.9)	106.0 ^B (8.7)	2.5 ^A (2.3)	0.5 ^A (0.8)	239.1 ^A (28.3)	212.3 ^A (19.4)
Cellobiohydrolase	42.9 ^A (3.3)	4.2 ^B (0.1)	0.6 ^A (0.8)	0.3 ^B (0.1)	72.1 ^A (5.8)	14.0 ^B (0.1)
Ala-aminopeptidase	38.7 ^A (2.3)	73.2 ^B (7.3)	5.9 ^A (2.4)	281.5 ^B (56.4)	7.2 ^A (3.6)	0.3 ^B (0.3)
Leu-aminopeptidase	47.6 ^A (6.7)	54.5 ^A (36.7)	13.7 ^A (9.1)	549.7 ^B (59.3)	3.5 ^A (1.7)	0.1 ^B (0.2)
Phosphatase	505.5 ^A (83.0)	82.8 ^B (3.5)	27.7 ^A (15.7)	6.9 ^B (2.1)	18.2 ^A (3.4)	12.0 ^B (4.5)

Different letters show significant differences between the litter and organic soil horizons for V_{\max} , K_M and k_{cat} ($p < 0.05$). Experimental data were fitted to the nonlinear regression using equations (i) from which V_{\max} , K_M were determined. Enzyme efficiency (k_{cat}) was calculated as V_{\max}/K_M . Average values are shown with standard error in parentheses ($n = 3$)

Table 4 Temperature sensitivity of soil hydrolytic enzymes described by average Q_{10} calculated for the temperature range from 0 to 25 °C and apparent activation energy (E_a) values in the litter and organic soil horizons

Soil horizon	Q_{10}		E_a (kJ mol ⁻¹)	
	Litter	Organic	Litter	Organic
β-Glucosidase	1.67 ^A (0.09)	1.61 ^A (0.21)	45.7 ^A (2.1)	43.8 ^A (4.1)
Cellobiohydrolase	0.72 ^A (0.14)	0.69 ^A (0.18)	ND	ND
Ala-aminopeptidase	0.66 ^A (0.14)	0.64 ^A (0.13)	ND	ND
Leu-aminopeptidase	0.62 ^A (0.08)	0.51 ^B (0.15)	ND	ND
Phosphatase	1.50 ^A (0.10)	1.74 ^A (0.48)	37.9 ^A (2.5)	46.7 ^B (2.2)

Different letters show significant differences between soil horizons ($p < 0.05$). Mean values and standard errors (in parentheses) are shown ($n = 3$). Q_{10} values for specific temperature ranges are shown in Table S2

ND not determined

temperature insensitivity of both aminopeptidases (Table 4). Results also indicate large imbalance between soil horizons: enzymatic potential of cellulases dominates in litter horizon while proteases relatively increased in the organic horizon.

Between July and August the E_C/E_N ratio averaged 3.5 in the litter horizon, which means that C enzymes were much more active compared to the N enzymes in top of the season (Fig. 2). E_C/E_N peaked in the litter horizon with the maximum of 4.7 during the mid of the July. On the other hand, at the beginning and end of the season (between May and June and between September and October) the E_C/E_N ratio was not higher than 2. In the organic horizon the E_C/E_N ratio followed the similar trend as in the litter horizon. However, the E_C/E_N ratio was ~2 times lower than in the litter horizon, which means that N enzymes were more abundant relatively to C enzymes in the organic horizon (Fig. 2).

The differences in the E_C/E_N enzyme ratio are connected with the different temperature sensitivities

of C and N processing activities (Table 4). While the activity of C enzymes increased during the season, the activity of N enzymes decreased in both horizons (Fig. 3a). In the organic horizon the E_C/E_N ratio was under the threshold ratio of 3.2 during the whole season (Allen and Gillooly 2009). Under this ratio microbes switch to N limiting metabolism. Therefore, in the organic horizon microbes are limited in N supply while in the litter horizon there are cases when microbes can switch to energy flow metabolism (Fig. 3a). These results again contrast with the E_C/E_P ratio which, under a 0.5 ratio throughout the whole season in both horizons (Fig. 3b), indicates P limiting metabolism in both horizons. Modeled versus measured enzyme activities showed that the model underestimated the observed E_C/E_P ratio in the litter horizon by 24 %, and the E_C/E_N ratio by 56 % (Fig. 4).

The modeled seasonal shifts in available C/N nutrient ratio showed again higher fluctuations in the

Fig. 1 Seasonal temperature fluctuation in the litter (a) and organic soil horizons (b). Black lines show day mean temperatures, gray area shows day minimum and maximum temperatures and dashed lines annual temperature average

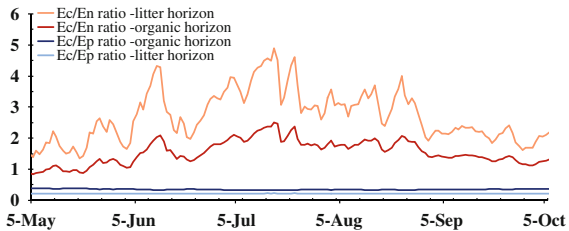
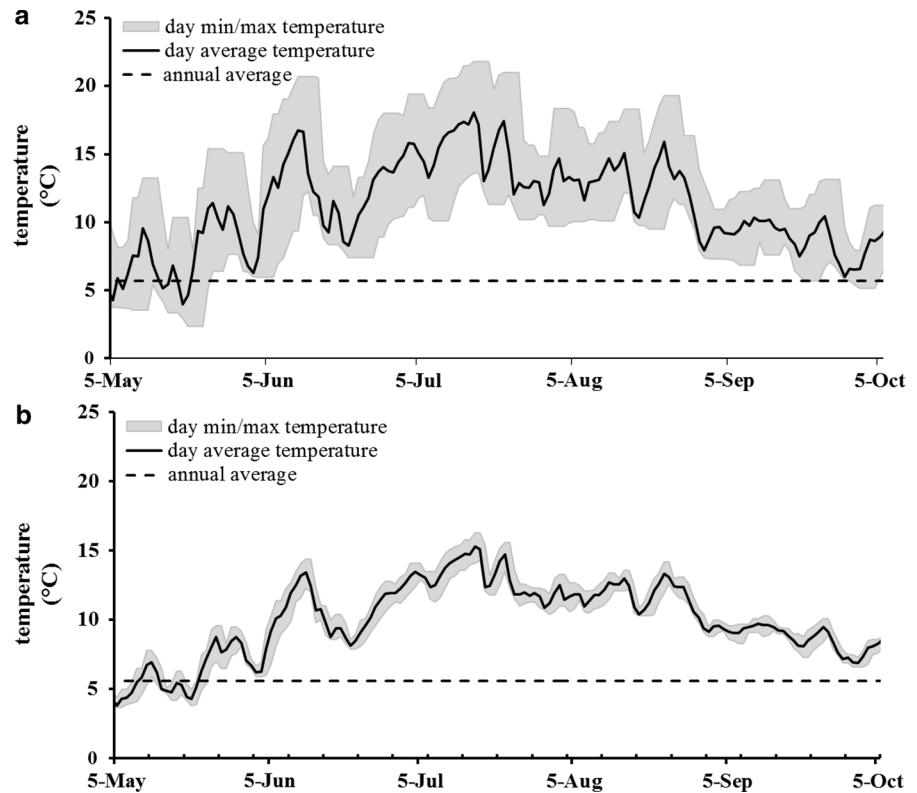


Fig. 2 Modeled in situ organic carbon (E_C), nitrogen (E_N) and phosphorus (E_P) acquisition enzyme ratios in the litter and organic soil horizons. Data represents the daily mean enzyme activities. Complete dataset for each time point in 2 h intervals is shown in Table S3

litter soil horizon (Fig. 5a). The C/N ratio ranged from a low of 12, which occurred at the beginning and end of the season, to a maximum value of 34, which was found in the litter horizon in July and August (Fig. 5a). Temperature had a greater effect on the C/N ratio than the C/P ratio (Fig. 5b). The C/N ratio increased from 12 to 34 and from 9 to 20 in the litter and organic horizons, respectively, while the C/P ratio decreased from 4 to 2.4 and from 10 to 4.5 in the litter and organic horizons, respectively.

Discussion

The five soil enzymes differed significantly in both the kinetic parameters and temperature sensitivities showing high differences between organic C, N and P processing and predicted nutrient release in acid forest soils. Different enzymatic responses were observed between the litter and organic horizons. This is likely the result of different isoenzyme pools in the litter and organic horizons reflecting differences in microbial community composition, the gene pools and expression between the litter and organic soil horizons as well as differences in phenolic compound composition affecting both the kinetics and temperature sensitivity of soil enzymes.

Differences in kinetic parameters between organic C, N and P processing enzymes

Kinetic parameters (K_m , V_{max}) are important markers of enzyme behavior giving insight into both the enzyme activity and substrate affinity, respectively. As defined by Michaelis and Menten kinetics, potential enzyme activity is a measure of the

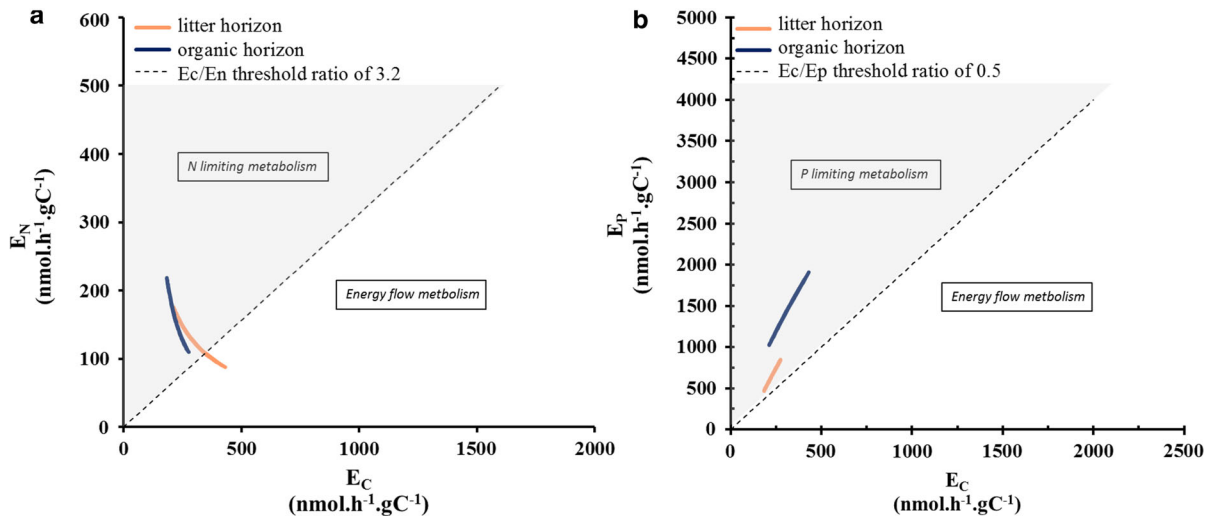


Fig. 3 Modeled fluctuations of organic C acquisition enzyme activity (E_C) in relation to organic N (E_N) and organic P (E_P) acquisition activities during the season. *Dashed lines* represents

the E_C/E_N and E_C/E_P threshold ratios for upper soil horizons (see Sinsabaugh et al. 2009)

maximum rate (V_{max}) at a defined temperature and a high nonlimiting substrate concentration (Michaelis and Menten 1913). Our study found that there can be dramatically high differences between the kinetics and efficiencies of soil enzymes in the litter and organic soil horizon (Table 3). This can be due to the fact that different microbial communities produce different isoenzymes in the litter and organic soil horizons or enzymes being complexed with clay/humus particles. Basically, both factors can simultaneously affect soil enzymes and lead to different substrate affinities to the same substrate in different soil depths (Ram et al. 2005).

Both peptidases, which are responsible for releasing amino acids from short proteins, exhibited higher enzyme efficiency and higher substrate affinity (lower K_m) in the litter than in the organic soil horizon (Table 3). This can be either due to competitive inhibition by naturally present peptidic compounds in the litter horizon, because N-rich compounds are more abundant in the litter as indicated by higher DON (Table 2) or by allosteric inhibition by phenolic compounds. Therefore, according to the lower K_m , peptidases in the litter horizon degrade peptidic compounds at lower concentrations but with higher efficiency (Table 3). Peptidases in organic horizon favor higher concentration however degrade peptidic compounds with lower efficiency. Because of this imbalance, some portion of the complex fraction of

DON moves untouched and undecomposed from the litter horizon to the lower organic soil horizon, where it is degraded by a totally different pool of peptidases. These imbalances in affinities and enzyme efficiencies in the litter and organic soil horizons can lead to the DON leaching from these soils, as proposed in other studies (Kopáček and Vrba 2006).

We found an opposite trend for phosphatase and cellulolytic enzymes, whose K_m values were significantly lower in the organic soil horizon. Simultaneously, V_{max} and enzyme efficiency decreased as well, however not as dramatically as in case of aminopeptidases. A lower K_m can be due to lower concentrations of organic C and P rich substrates in the lower soil horizon or by enzyme interaction with soil particles in the organic horizon (Nannipieri 2006). The enzyme-soil interactions with humus or clay particles can have several consequences. By this process enzymes can exhibit conformation changes (Allison and Jastrow 2006; Nannipieri 2006) which can lead to lower or no enzyme activity. Hope and Burns (1985) showed that higher CEC of soils can lead to inactivation of soil enzymes and also decrease their movement in the soil profile. In our soils, the CEC was similar in both horizons, therefore other parameters should be involved in changing the enzyme kinetics.

One of these factors can be the amount of phenolic compounds. It is well known that enzymes create very often complexes with phenolic compounds present in

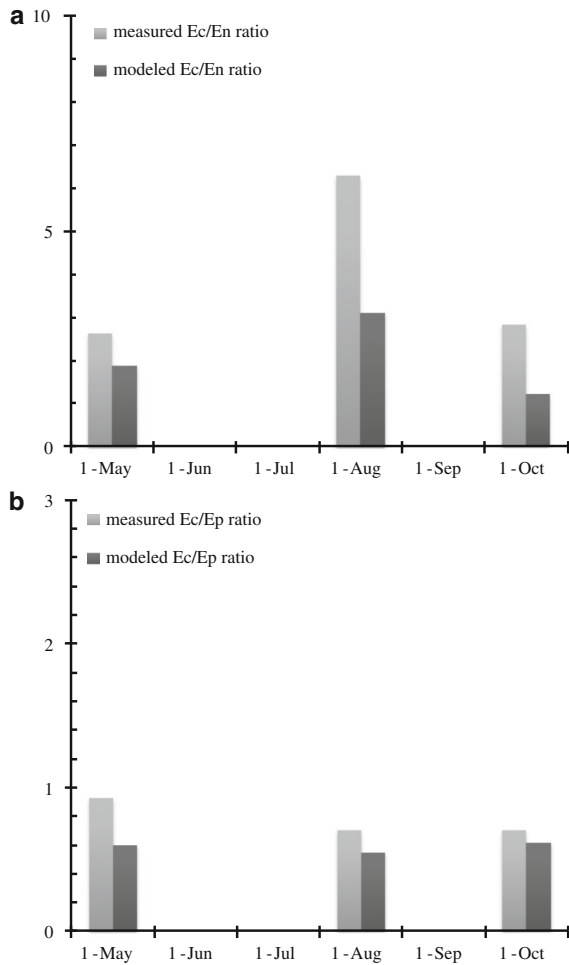


Fig. 4 Comparison of measured and modeled carbon (E_C), nitrogen (E_N) and phosphorus (E_P) acquisition enzyme ratios in the litter soil horizon. The soil samples were taken in late May, early August and late October, 2010

higher amounts in the organic soil horizon and in this case enzyme activity can be completely retarded. Our previous study showed that phenolics are present in very high concentrations in the litter horizon in our study site (Bárta et al. 2010). This high amount was the result of enormous spruce needle foliage which introduced a high amount of phenolics to the soil during the past decade. A combination of low soil pH and high amount of phenolics can strongly affect soil enzyme kinetics. Several studies reported the effect of phenolic compounds on enzyme kinetics. Gianfreda et al. (1995a, b) reported strong urease inhibition (K_I of 40 μM) by tannic acid with this inhibition increasing with increasing tannic acid concentration. These

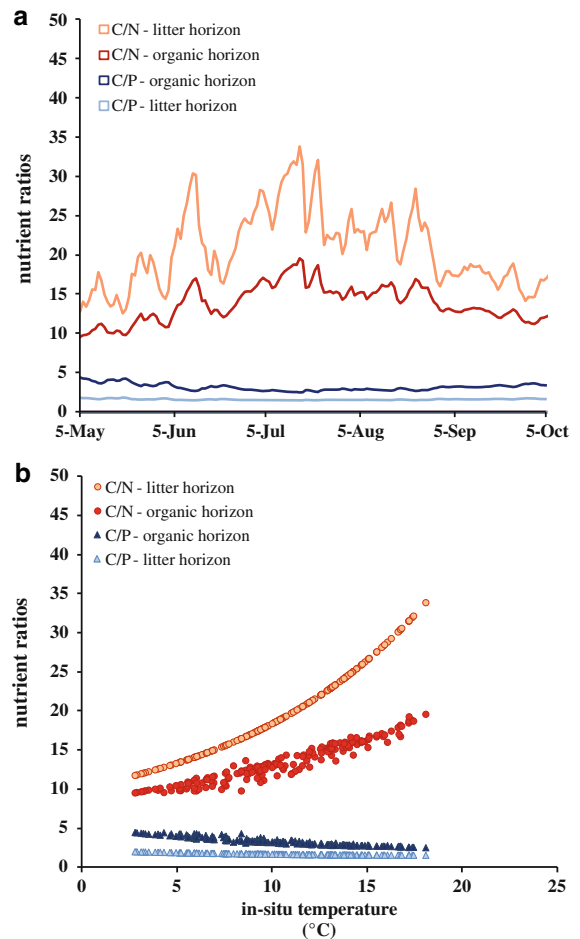


Fig. 5 Seasonal shifts in the available C/N and C/P ratio based on modeled C and N potential enzyme activities (a) and temperature dependency of these ratios during the season (b). The modeled nutrient ratios are based on the Eqs. 6, 7, and 8 (see in the “Materials and methods” section)

authors also showed that different metals can destroy or on the other hand strengthen these enzyme-phenolic complexes. While the presence of $\text{Al}(\text{OH})_3$ increased the enzyme activity, the Mn^{2+} ions create the enzyme-phenolic complex stronger which further inhibit the enzyme activity. Kandeler et al. (1996) reported that the differences observed in metal interaction with soil enzymes are connected closely with soil pH. Phenolic compounds, however, do not complex only with enzymes but also with other proteins present in soil (Northup et al. 1995, 1998). Higher amount of phenolics in our soil can therefore block other proteins from the attack of aminopeptidases which leads to their lower degradation and can increase DON leaching.

Enzyme temperature sensitivity

An exponential increase in enzyme activity with increasing temperature was found only for β -glucosidase, and phosphatase. Activation energy (E_a) of β -glucosidase was $\sim 43 \text{ kJ mol}^{-1}$ and was similar in both horizons. These values are in agreement with a recent review of Wang et al. (2012) who reported very weak response to temperature for cellobiohydrolase in mineral horizon. Authors also found that cellobiohydrolase had the lowest E_a , indicating the weakest temperature sensitivity. In our site, both cellobiohydrolase and aminopeptidases showed no or even decreased enzyme activity with increasing temperature resulting in Q_{10} values below one (Table 4). We were not able to calculate activation energies for these enzymes. This temperature insensitivity might be connected with environmental constraints in our acid soils. Our soils have extremely acidic pH around 3 (Table 1). Activation energy may change with pH by means of different binding of substrate to an active site of enzyme. Steinweg et al. (2013) reported negative effect of pH on activation energy of cellobiohydrolase. The influence of pH might be stronger than the effect of temperature which can result in no temperature sensitivity of enzyme at suboptimal pH. Our results contrasts with other recently reported studies (Wallenstein et al. 2009); however, similar results were reported by Tjoelker et al. (2001). The latter authors attributed the decline in Q_{10} to different plant species composition and therefore different litter quality input to the soil. However, no study has so far reported Q_{10} of soil enzymes below one. In our acid soil, this unusual phenomenon can be also caused by psychrophilic nature of microbial community which probably dominated in soil when it was sampled during the autumn. Psychrophilic microbes and their enzymes prefer low temperatures and denature faster at higher temperatures (Feller 2003). Another explanation may be in the high input of phenolic compounds and formation of phenolic-protein complexes. These complexes change the enzyme tertiary structure which can result in lower enzyme temperature sensitivity. Additionally, the relatively high water content in our soils decreases the diffusion of oxygen, which is needed for the efficient and complete mineralization of phenolics which can then accumulate in soil (Freeman et al. 2001; Hofrichter et al. 1999a, b; Kapich et al. 1999). All these environmental constraints (low pH

and high amount of phenolic compounds) can lead to a weak or no temperature sensitivity of soil enzymes. Ecologically, this temperature insensitivity means that organic N processing activity is imbalanced with C processing activity during the season (Figs. 2, 3).

Seasonal changes in potential enzyme activities and nutrient stoichiometry

Using the measured enzyme temperature sensitivities and with the help of continuous in situ temperature measuring we were able to model the seasonal development of organic C, N and P processing activities (Figs. 2, 3). Our model is far from ideal, because it uses only the temperature dependency without including the moisture effect (Reiners 1968; Wildung et al. 1975). Several temperature-moisture models have been published including linear, quadratic, power, exponential and modified Arrhenius models (Reinke et al. 1981; Li et al. 2000; Wang et al. 2003; Oberbauer et al. 1992). They mainly differ according to soil type and range of moisture fluctuations (Jia et al. 2006). For the present study, the moisture effect can likely be omitted since, in the studied soil, moisture content was relatively high and did not change dramatically during the season ranging from 33 to 43 % (v/v) in the litter and from 35 to 47 % (v/v) in the organic soil horizons.

Sinsabaugh et al. (2009) summarized the enzyme activities from hundreds of terrestrial and aquatic ecosystem studies. They focused on the main enzymes in organic C (E_C), N (E_N) and P (E_P) processing and found a universal $E_C:E_N:E_P$ ratio of 1:1:1 for ln-transformed activities across all ecosystems. However, if we look closer at Sinsabaugh's correlations, we find that in terrestrial ecosystems there are many cases where the enzyme E_C/E_N and E_C/E_P ratios do not follow the common 1:1 trend. Sinsabaugh pointed out that the average E_C/E_N ratio in soil is 2.8 if NAG is included as N acquiring enzyme) and 5 if only aminopeptidases are counted as N enzymes. For the E_C/E_P ratio they found general soil ratio of 0.6. Both ratios fluctuate widely in terrestrial ecosystem. These fluctuations can be caused by the extremely high temporal and spatial variability of the soil environment and differently disturbed soil ecosystems. When comparing our ratios with Sinsabaugh's it is first important to note that there are different ways to calculate E_C/E_N ratio. In our study we calculated N

acquiring enzymes as the average potential activity of both aminopeptidases. In contrast, Sinsabaugh et al. (2009) assumed *N*-acetylglucosaminidase (NAG) as solely a N acquisition enzyme and therefore summed its activity with the activity of Leu-aminopeptidase. We argue that NAG is solely a N acquiring enzyme because it liberates amino sugars which, after the cleaving of ammonia, enter the glycolysis. This makes NAG preferably a C acquiring enzyme (Caldwell 2005; Parham and Deng 2000; Pancholy and Rice 1973). Sinsabaugh's assumption was based on the results of his previous work (Sinsabaugh and Moorhead 1994) and work of Olander and Vitousek (2000) who tested the effect of N availability on NAG activity in soils. The latter authors found that NAG activity decreases as N availability increases. However, this connection may be only indirect and does not mean that NAG is the N acquiring enzyme. Additionally, Olander and Vitousek (2000) pointed out that N addition repressed NAG activity only at N limited sites. Therefore, any NAG connection to N availability may be valid only for some ecosystems. More importantly, our recent study using ^{15}N stable isotope labeling showed that microbes in acid soils prefer assimilation of amino acids compared to ammonia and nitrates (Tahovská et al. 2013). Therefore, aminopeptidases are probably the key enzymes in organic N acquisition in acid forest soils.

Other studies tried to link enzyme activities to ecological stoichiometric theory and the metabolic theory of ecology through the threshold elemental ratio (TER) concept (Allen and Gillooly 2009; Frost et al. 2006). TER is the critical elemental C:P or C:N ratio at which metabolic control of an ecological system switches from energy flow, represented by C, to limiting nutrient flow, represented by P or N (Allen and Gillooly 2009). They predicted a threshold ratio for E_C/E_P of 0.5. Our modeled and observed in situ E_C/E_P ratios are under or close to this threshold suggesting that our acid forest soils are very close to switching to P limiting metabolism during the whole season (Figs. 3b, 4). For E_C/E_N ratio and calculating with peptidases as N enzymes they predicted a threshold ratio of 3.2. The E_C/E_N ratio in our acid forest soils is different between the litter and the organic horizon (Figs. 2, 3a). The E_C/E_N ratio in the litter horizon was under the metabolic threshold of 3.2 only at the beginning and at the end of the season while the E_C/E_N in the organic horizon was under the

threshold during the whole season. In extreme, at the beginning and end of the season the E_C/E_N ratio dropped to almost 1 in the organic horizon. Moreover, the difference in E_C/E_N ratio between the litter and organic horizon was more than two times during the extreme days at the top of the season (Fig. 2). This imbalance might be connected with the close connection of the litter horizon to plant root system and their exudation. Plants produce root exudates of different quality which is closely connected with plant growth and succession. A recent study of Chaparro et al. (2013) shows that exudation of amino acids increases with plant growth therefore microbes in the litter horizon around roots are sufficiently supported by available N at the peak of the season and they do not need to invest resources and energy to degrade complex peptidic compounds. The activity of C enzymes in top of the season is therefore relatively higher compared to N enzymes which lead to higher E_C/E_N ratio (Fig. 2). This is in agreement with study of Baldrian et al. (2011) who found that the litter horizon exhibits higher proportion of expressed genes for cellulose degradation than organic horizon in acid forest soils. They also showed that cellulose decomposition is mediated by highly diverse fungal populations, largely distinct between soil horizons with Basidiomycota dominant in the litter horizon and Ascomycota in the organic horizon.

To link enzyme activity with corresponding nutrient release, we developed assumptions and from these we were able to model potential nutrient C/N and C/P ratios (see Eqs. 6–8; Fig. 5). The predicted C/N ratio in the litter horizon is very close to a recently reported observed C/N ratio of 21 in acid forest soils (Tahovská et al. 2013). However, our model again showed that the C/N ratio can fluctuate between 12 and 30 during the season being the highest in July and August. This C/N fluctuation can affect the composition of microbial community in the litter horizon and organic horizon leading to shifts in major bacterial and fungal guilds responsible for degradation of complex SOM (Baldrian et al. 2011).

Conclusions

The present study on acid forest soils produced several important findings. K_m , V_{max} differed significantly

between the litter and organic soil horizons, which suggests that different parameters control soil enzyme kinetics in the soil profile. These are (i) different isoenzymes produced by different microbial communities, and (ii) interaction of enzymes with soil particles and phenolic compounds, which can influence enzyme biophysical properties including kinetics and temperature sensitivity. Using the laboratory-determined temperature sensitivities in the range of in situ observations, we were able to model in situ enzyme activities during the vegetation season. Our modeled in situ potential enzyme activities reached in average 76 and 54 % of measured E_C/E_P and E_C/E_N enzyme ratios. Though, the observed enzyme activities may differ spatially and temporarily.

Acknowledgments This study was supported by the Czech Science Foundation, project 526/08/0751 and project GAJU 143/2010/P. We acknowledge the laboratory and field assistance provided by our colleagues and students. We also thank the authorities of the National Park Bohemian Forest for giving their permission to study the lake ecosystems. We thank Dr. Keith Edwards for language correction.

References

- Allen AP, Gillooly JF (2009) Towards an integration of ecological stoichiometry and the metabolic theory of ecology to better understand nutrient cycling. *Ecol Lett* 12:369–384
- Allison SD (2006) Soil minerals and humic acids alter enzyme stability: implications for ecosystem processes. *Biogeochemistry* 81:361–373
- Allison SD, Jastrow JD (2006) Activities of extracellular enzymes in physically isolated fractions of restored grassland soils. *Soil Biol Biochem* 38:3245–3256
- Allison SD, Vitousek PM (2005) Responses of extracellular enzymes to simple and complex nutrient inputs. *Soil Biol Biochem* 37:937–944
- Baldrian P, Kolařík M, Štursová M, Kopecký J, Valášková V, Větrovský T, Žifčáková L, Šnajdr J, Rídl J, Vlček Č, Voříšková J (2011) Active and total microbial communities in forest soil are largely different and highly stratified during decomposition. *ISME J* 6:248–258
- Bárta J, Applova M, Vanek D, Kristufkova M, Santruckova H (2010) Effect of available P and phenolics on mineral N release in acidified spruce forest: connection with lignin-degrading enzymes and bacterial and fungal communities. *Biogeochemistry* 97:71–87
- Caldwell BA (2005) Enzyme activities as a component of soil biodiversity: a review. *Pedobiologia* 49:637–644
- Chaparro JM, Badri DV, Bakker MG, Sugiyama A, Manter DK (2013) Root exudation of phytochemicals in *Arabidopsis* follows specific patterns that are developmentally programmed and correlate with soil microbial functions. *PLoS One* 8:e55731
- Davidson EA, Janssens IA (2006) Temperature sensitivity of soil carbon decomposition and feedbacks to climate change. *Nature* 440:165–173
- Feller G (2003) Molecular adaptations to cold in psychrophilic enzymes. *Cell Mol Life Sci* 60:648–662
- Freeman C, Evans D, Monteith DT, Reynolds B, Fenner N (2001) Export of organic carbon from peat soils. *Nature* 412:785
- Frost PC et al (2006) Threshold elemental ratios of carbon and phosphorus in aquatic consumers. *Ecol Lett* 9:774–779
- Gianfreda L, De Cristofaro A, Rao MA, Violante V (1995a) Kinetic behavior of synthetic organo and organo-mineral-urease complexes. *Soil Sci Soc Am J* 59:811–815
- Gianfreda L, Rao MA, Violante A (1995b) Formation and activity of urease-tannate complexes affected by aluminum, iron, and manganese. *Soil Sci Soc Am J* 59:805–810
- Hofrichter M, Vares T, Kalsi M, Galkin S, Scheibner K, Fritsche W, Hatakka A (1999a) Production of manganese peroxidase and organic acids and mineralization of 14C-labelled lignin (14C-DHP) during solid-state fermentation of wheat straw with the white rot fungus *Nematoloma frowardii*. *Appl Environ Microbiol* 65:1864–1870
- Hofrichter M, Vares T, Scheibner K, Galkin S, Sipilä J, Hatakka A (1999b) Mineralization and solubilization of synthetic lignin by manganese peroxidase *Nematoloma frowardii* and *Phlebia radiata*. *J Biotechnol* 67:217–228
- Hope CFA, Burns RG (1985) The barrier-ring plate technique for studying extracellular enzyme diffusion and microbial growth in model soil environments. *J Gen Microbiol* 131:1237–1243
- Jia B, Zhou G, Wang Y, Wang F, Wang X (2006) Effects of temperature and soil water-content on soil respiration of grazed and ungrazed *Leymus chinensis* steppes, Inner Mongolia. *J Arid Environ* 67:60–76
- Kandeler E, Kampichler C, Horak O (1996) Influence of heavy metals on the functional diversity of soil microbial communities. *Biol Fertil Soils* 23:299–306
- Kapich A, Hofrichter M, Vares T, Hatakka A (1999) Coupling of manganese peroxidase-mediated lipid peroxidation with destruction of nonphenolic lignin model compounds and 14C-labeled lignins. *Biochem Biophys Res Commun* 259:212–219
- Kirschbaum MUF (2006) The temperature dependence of organic-matter decomposition—still a topic of debate. *Soil Biol Biochem* 38:2510–2518
- Koch AL (1985) The macroeconomics of bacterial growth. In: Fletcher M, Floodgate GD (eds) *Bacteria in their natural environments*. Academic Press, London, pp 1–42
- Kopáček J, Vrba J (2006) Integrated ecological research of catchment-lake ecosystems in the Bohemian Forest (Central Europe): a preface. *Biologia* 61:363–370
- Kopáček J, Kaňka J, Šantrůčková H, Porcal P, Hejzlar J, Píček T, Veselý J (2002) Physical, chemical, and biochemical characteristics of soils in watersheds of the Bohemian Forest lakes: I. Plešné Lake. *Silva Gabreta* 8:43–62
- Li LH, Wang QB, Bai YF, Zhou GS, Xing XR (2000) Soil respiration of a *Leymus chinensis* grassland stand in the XiLin river basin as affected by over-grazing and climate. *Acta Phytocol Sin* 24:680–686

- Majer V, Cosby BJ, Kopáček J, Veselý J (2003) Modelling reversibility of Central European mountain lakes from acidification: part I—The Bohemian Forest. *Hydrol Earth Syst Sci* 7:494–509
- Marx MC, Wood M, Jarvis SC (2001) A microplate fluorimetric assay for the study of enzyme diversity in soils. *Soil Biol Biochem* 33:1633–1640
- McClaugherty CA, Linkins AE (1990) Temperature responses of enzymes in two forest soils. *Soil Biol Biochem* 22:29–33
- Meentemeyer V (1978) Macroclimate and lignin control of litter decomposition rates. *Ecology* 59:465–472
- Michaelis L, Menten ML (1913) Die kinetik der invertin wirkung. *Biochem Z* 49:334–336
- Nannipieri P (2006) Role of stabilised enzymes in microbial ecology and enzyme extraction from soil with potential applications in soil proteomics. In: Nannipieri P, Smalla K (eds) *Nucleic acids and proteins in soil*. Springer, Berlin, pp 75–94
- Northup RR, Yu Z, Dahlgren RA, Vogt KA (1995) Polyphenol control of nitrogen release from pine litter. *Nature* 377: 227–229
- Northup RR, Dahlgren RA, McColl JG (1998) Polyphenols as regulators of plant-litter-soil interactions in northern California pygmy forest: a positive feedback? *Biogeochemistry* 42:189–220
- Oberbauer SF, Gillespie CT, Cheng W, Gebauer R, Sala Serra A, Tenhunen JD (1992) Environmental effects on CO₂ efflux from riparian tundra in the northern foothills of the Brooks Range, Alaska, USA. *Oecologia* 92:568–577
- Olander LP, Vitousek PM (2000) Regulation of soil phosphatase and chitinase activity by N and P availability. *Biogeochemistry* 49:175–191
- Pancholy SK, Rice EL (1973) Soil enzymes in relation to old field succession: amylase, cellulase, invertase, dehydrogenase, and urease. *Proc Soil Sci Soc Am* 37:47–50
- Parham JA, Deng SP (2000) Detection, quantification and characterization of b-glucosaminidase activity in soil. *Soil Biol Biochem* 32:1183–1190
- Ram RJ, VerBerkmoes NC, Thelen MP, Tyson GW, Baker BJ, Blake RC, Shah M, Hettich RL, Banfield JF (2005) Community proteomics of a natural microbial biofilm. *Science* 308:1915–1920
- Reiners WA (1968) Carbon dioxide evolution from the floor of three Minnesota forests. *Ecology* 49:471–483
- Reinke JJ, Adriano DC, McLeod KW (1981) Effects of litter alteration on carbon dioxide evolution from a South Carolina pine forest floor. *Soil Sci Soc Am J* 45:620–623
- Šantrůčková H, Vrba J, Píček T, Kopáček J (2004) Soil biochemical activity and phosphorus transformations and losses from acidified forest soils. *Soil Biol Biochem* 36:1569–1576
- Šantrůčková H, Křišťůvková M, Vaněk D (2006) Decomposition rate and nutrient release from plant litter of Norway spruce forest in the Bohemian forest. *Biologia* 61:499–508
- Šantrůčková H, Tahovská K, Kopáček J (2009) Nitrogen transformations and pools in N-saturated mountain spruce forest soils. *Biol Fertil Soils* 45:395–404
- Sierra CA (2012) Temperature sensitivity of organic matter decomposition in the Arrhenius equation: some theoretical considerations. *Biogeochemistry* 108:1–15
- Sinsabaugh RL (2010) Phenol oxidase, peroxidase and organic matter dynamics of soil. *Soil Biol Biochem* 42:391–404
- Sinsabaugh RL, Moorhead DL (1994) Resource allocation to extracellular enzyme production: a model for nitrogen and phosphorus control of litter decomposition. *Soil Biol Biochem* 26:1305–1311
- Sinsabaugh RL, Lauber CL, Weintraub MN, Ahmed B, Allison SD, Crenshaw CL, Contosta AR, Cusack D, Frey S, Gallo ME, Gartner TB, Hobbie SE, Holland K, Keeler BL, Powers JS, Stursova M, Takacs-Vesbach C, Waldrop M, Wallenstein M, Zak DR, Zeglin LH (2008) Stoichiometry of soil enzyme activity at global scale. *Ecol Lett* 11: 1252–1264
- Sinsabaugh RL, Hill BH, Follstad-Shah JJ (2009) Ecoenzymatic stoichiometry of microbial organic nutrient acquisition in soil and sediment. *Nature* 462:795–799
- Steinweg JM, Jagadamma S, Frerichs J, Mayes MA (2013) Activation energy of extracellular enzymes in soils from different biomes. *PLoS One* 8:e59943
- Stone MM, Weiss MS, Goodale CL, Adams MB, Fernandez IJ, German DP, Allison SD (2012) Temperature sensitivity of soil enzyme kinetics under N-fertilization in two temperate forests. *Glob Change Biol* 18:1173–1184
- Svoboda M, Matějka K, Kopáček J (2006) Biomass and element pools of understory vegetation in the catchments of Čertovo Lake and Plešné Lake in the Bohemian Forest. *Biologia* 61:509–521
- Tahovská K, Kaňa J, Bárta J, Oulehle F, Richter A, Šantrůčková H (2013) Microbial N immobilization is of great importance in acidified mountain spruce forest soils. *Soil Biol Biochem* 59:58–71
- Tate RL (2002) Microbiology and enzymology of carbon and nitrogen cycling. In: Burns R, Dick R (eds) *Enzymes in the environment: activity, ecology and applications*. Dekker, New York, pp 227–248
- Thomas GW (1982) Exchangeable cations. In: Page AL et al (eds) *Methods of soil analysis, part 2, 2nd edn*. ASA and SSSA, Madison, pp 159–166
- Tjoelker MG, Oleksyn J, Reich PB (2001) Modelling respiration of vegetation: evidence for a general temperature dependent Q₁₀. *Glob Change Biol* 7:223–230
- Wallenstein MD, Weintraub MN (2008) Emerging tools for measuring and modeling the in situ activity of soil extracellular enzymes. *Soil Biol Biochem* 40:2098–2106
- Wallenstein MD, McMahon SK, Schimel JP (2009) Seasonal variation in enzyme activities and temperature sensitivities in Arctic tundra soils. *Glob Change Biol* 15:1631–1639
- Wang FY, Zhou GS, Jia BR, Wang YH (2003) Effects of heat and water factors on soil respiration of restoring *Leymus chinensis* Steppe in degraded land. *Acta Phytoecol Sin* 27:644–649
- Wang G, Post WM, Mayes MA, Frerichs JT, Sindhu J (2012) Parameter estimation for models of ligninolytic and cellulolytic enzyme kinetics. *Soil Biol Biochem* 48:28–38
- Wildung RE, Garland TR, Buschbom RL (1975) The interdependent effect of soil temperature and water content on soil respiration rate and plant root decomposition in arid grassland soils. *Soil Biol Biochem* 7:373–378

Paper 3

Barta J, Melichova T, Vanek D, Picek T, Santruckova H (2010) Effect of pH and dissolved organic matter on the abundance of *nirK* and *nirS* denitrifiers in spruce forest soil. *BIOGEOCHEMISTRY* 101:123-132.

Effect of pH and dissolved organic matter on the abundance of *nirK* and *nirS* denitrifiers in spruce forest soil

Jiří Bárta · Tereza Melichová · Daniel Vaněk ·
Tomáš Pícek · Hana Šantrůčková

Received: 31 October 2009 / Accepted: 11 March 2010 / Published online: 28 March 2010
© Springer Science+Business Media B.V. 2010

Abstract Acid N depositions in the Bohemian Forest during the second half of the last century caused enormous soil acidification which led to the leaching of essential nutrients including nitrates. We investigated the effect of dissolved organic matter (DOM) and pH on the abundance of 16S rDNA, *nirK* and *nirS* gene copies in four spruce forest sites. Soil samples for molecular based quantification (qPCR) were taken from the organic litter and humus layers. The amounts of dissolved organic carbon (DOC) and dissolved nitrogen (DN) were much lower in highly acidified soils. We found a strong correlation between *nirK* denitrifiers and the amount of available P ($r = 0.83$, $p < 0.001$), which suggested a higher nutrient sensitivity of this group of denitrifying bacteria. Additionally, we found that correlations between the amount of *nirK* denitrifiers and DOC and pH are exponential showing two important threshold values, being 4.8 mol kg^{-1} and 5, respectively. The amount of *nirK* denitrifiers rapidly decreased below these values. The amount of *nirK* and *nirS* denitrifiers was higher in the organic litter horizon than the organic humus horizon at all sampling sites.

Keywords Dissolved organic matter · Available phosphorus · *nirK* and *nirS* denitrifiers · Acid forest soil · N depositions · qPCR

Introduction

Spruce forest soils in Central Europe were exposed to high nitrogen (N) depositions during the second half of the last century. Atmospheric N deposition is the major anthropogenic source of N in terrestrial ecosystems of the United States, Asia and Europe (Galloway et al. 2003; Galloway and Cowling 2002; Waldrop and Zak 2006). Because of N limitation in temperate forests, additional N input can stimulate plant growth and increase aboveground carbon (C) storage (Nadelhoffer et al. 1999; Magill et al. 1997; Waldrop and Zak 2006). However, high N depositions can decrease soil pH, which leads to reduction of the soil acid neutralizing capacity and leaching of a plant's essential cations (Ca^{2+} , Mg^{2+} and K^{+}) (Dauer et al. 2007; Tomlinson 2003; Pawłowski 1997) and NO_3^- from the forest soils (Kopáček et al. 2002a, b; Šantrůčková et al. 2006). One of the reasons for higher NO_3^- leaching could be the reduction in the amount of denitrifying bacteria in the acid forest soils. However, direct evidence is missing.

Denitrification is the main anaerobic biotic process leading to losses of fixed N as well as removal of excess soluble nitrate (NO_3^-) and nitrite (NO_2^-)

J. Bárta (✉) · T. Melichová · D. Vaněk ·
T. Pícek · H. Šantrůčková
Department of Ecosystem Biology, Faculty of Science,
University of South Bohemia, Branišovská 31, 370 05
Česke Budejovice, Czech Republic
e-mail: barta77@seznam.cz

from the soil environment. The second step in denitrification, the reduction of NO_2^- to nitric oxide (NO), distinguishes “true” denitrifiers from other NO_3^- -respiring bacteria. This reaction is catalyzed by two different types of nitrite reductases, either a cytochrome cd_1 encoded by the *nirS* gene (*nirS* denitrifiers) or a Cu-containing enzyme encoded by the *nirK* gene (*nirK* denitrifiers). *NirS* denitrifiers are located mostly in the rhizosphere, while *nirK* denitrifiers are more abundant in bulk soil (Henry et al. 2004; Tiedje 1988). In this step of the denitrification process, gaseous NO can escape from the environment. Therefore, a change in the amount of *nirK* and *nirS* denitrifiers can regulate NO_3^- and NO_2^- leaching from acid forest soils.

Henry et al. (2004) found that the amount of *nirK* denitrifiers can range from 10^4 to 10^6 gene copies per gram of soil. This high difference was explained by different amounts of soil organic carbon (Kandeler et al. 2006); higher amounts of organic carbon were positively correlated with *nirK* denitrifiers but not *nirS* denitrifiers. The *nirK* denitrifiers are more taxonomically diverse than *nirS* denitrifiers, however, the latter are more abundant. They represent approximately 0.4% of total soil bacteria while the *nirK* less than 0.2% (Kandeler et al. 2006). It seems that the more taxonomically diverse group of *nirK* denitrifiers is more sensitive to environmental changes and nutrient availability than the *nirS* denitrifiers. In highly acidified spruce forest soils, the low pH affects many biological and physical processes. The most important factor is the amount of dissolved organic matter (DOM), which rapidly decreases in low pH soils (Greenland 1971; David et al. 1989). A lower amount of DOM leads to lower nutrient availability for soil bacteria and decreases their numbers. Recently, it was shown that low pH negatively affected the activity of a pure culture of *Pseudomonas mandelii* (*nirS* denitrifier) (Saleh-Lakha et al. 2009). These authors found that the expression of the *nirS* gene was significantly lower when the pH of the medium dropped below 5. However, data from in situ experiments are still missing.

The objectives of this work were to:

- (i) evaluate the effect of DOM and pH on the abundance of *nirK* and *nirS* denitrifiers;
- (ii) compare the amount of *nirK* and *nirS* denitrifiers in different soil horizons.

Materials and methods

Study site description

Soil was collected from four different sampling sites in October 2008. Two sites are located in the Bohemian Forest in South Bohemia in the watersheds of two glacial lakes (Plešné, PL and Čertovo, CT) and two sites are located in the Jizera Mountains (Černá hora (CH) and Sněžné věžičky (SV)). In each site, four random spots in three replicates were chosen. Soil was collected from the organic litter layer (0–2 cm) and organic humus layer (5–15 cm).

PL and CT are situated at $48^\circ 47'$ and $49^\circ 10'$ N, and $13^\circ 52'$ and $13^\circ 11'$ E, respectively, at altitudes from 1030 to 1090 m a.s.l. Both sites were affected by the high acid N depositions of the last century. Recently, both sites were subjected to large disturbances caused by bark beetle infestations. Watershed of PL is covered with a 160 year-old Norway spruce (*Picea abies*) forest with small areas of ash. The bedrock is composed of granites. ČL watershed is covered with 90–150 year-old Norway spruce forests, with sparse white fir (*Abies alba*) and European beech (*Fagus sylvatica*); the bedrock is predominantly composed of mica-schist (muscovite gneiss) with quartzite intrusions. The understorey of both watersheds is dominated by hair grass (*Avenella flexuosa*), reedgrass (*Calamagrostis villosa*), blueberry (*Vaccinium myrtillus*), and lady fern (*Athyrium alpestre*, Svoboda et al. 2006). Soil types are mostly cambisols, podzols and litosols on steep slopes in both watersheds. Basic physico-chemical and biochemical properties of the soils are described by Kopáček et al. (2002a, b) and Veselý (1994).

CH and SV are situated at $50^\circ 49'$ and $50^\circ 50'$ N, and $15^\circ 11'$ and $15^\circ 13'$ E, respectively, at altitudes from 1055 to 1085 m a.s.l. Both sites are covered with 90–150 year-old Norway spruce forests (*P. abies*). The bedrock is composed of granites. Soil types are mostly podzols. The understorey of both sites is dominated by hair grass (*A. flexuosa*), reedgrass (*C. villosa*), and blueberry (*V. myrtillus*).

Soil chemical analyses

Total C and N (C_{TOT} and N_{TOT} , respectively) and oxalate extractable P (P_{OX}) were analyzed in air-dried, finely ground soil. C_{TOT} and N_{TOT} were

measured using an elemental analyzer (NC ThermoQuest, Germany). Dissolved organic carbon (DOC) and dissolved nitrogen (DN) were extracted step by step in both cold water (CW) and hot water (HW): water:soil, 10:1, v/w, 30 min at 20°C and 16 h at 80°C, respectively. DOC and DN in the CW and HW extracts were determined on a TOC/TN analyzer (SKALAR FORMACS HT). P_{OX} was determined by extraction of 0.5 g of litter with 50 ml of acid ammonium oxalate solution (0.2 M $H_2C_2O_4$ + 0.2 M $(NH_4)_2 C_2O_4$ at pH 3) according to Cappo et al. (1987), but with a three-step instead of continuous extraction (Kopáček et al. 2002a). P_{OX} is supposed to characterize the biological bioavailability of P in soil (Koopmans et al. 2004; Pote et al. 1996; Schwertmann 1964; van der Zee et al. 1987). Active pH was determined in the CW extracts.

Extraction of DNA

Three replicates of each soil sample (0.25 g) were taken for DNA extraction. For the isolation of genomic DNA from soil, the Power Soil DNA Isolation kit (MoBio Laboratories Inc. Carlsbad, CA, USA) was used according to manufacturer's instructions with some modification. A Mini Bead-Beater (BioSpec Products, Inc; speed of 6 m s^{-1} for 45 s) was used for better disruption of cell walls. DNA was stored in 1.5 ml Eppendorf microtubes in a freezer (-20°C) until the next analyses.

qPCR assay

Quantitative PCR was performed with an ABI Step One (Applied Biosystems) by using SYBR green as the detection system in a reaction mixture of 20 μl containing 0.5 μM (each) primer; 10 μl of Power SYBR[®]Green PCR master mix, including AmpliTaq Gold[®] DNA Polymerase, Power SYBR[®]Green PCR buffer, deoxynucleoside triphosphate mix with dUTP, SYBR green I, ROX, and 5 mM $MgCl_2$ (Power SYBR[®]Green PCR Master Mix; Applied Biosystems, USA); and 2 μl of template DNA corresponding to 10 ng of total DNA. Bovine serum albumin (BSA, 500 ng/reaction; Fermentas, Italy) and dimethylsulfoxide (DMSO, 12.5 μmol /reaction) were used to enhance PCR efficiency. 16S rDNA gene copy numbers were determined using the eubacterial primers 341f (5-CCT ACG GGA GGC AGC AG-3) and 515r

(5-ATT CCG CGG CTG GCA-3) as described by Henry et al. (2004). The conditions for 16S rDNA real-time PCRs were 600 s at 95°C for enzyme activation (based on manufacturer recommendation) and 30 cycles of 15 s at 95°C, 30 s at 60°C and 30 s at 72°C for the denaturation, annealing and extension steps, respectively (López-Gutiérrez et al. 2004). The primers nirK876 (5'-ATY GGC GGV CAY GGC GA-3') and nirK1040 (5'-GCC TCG ATC AGR TTR TGG TT-3') were used for quantification of *nirK* denitrifiers (Henry et al. 2006). For the quantification of *nirS* denitrifiers, the primers nirSCd3aF (5'-AACGY-SAAGGARACSGG-3') and nirSR3 cd (5'-GASTTCGRTGSGTCTTSAYGAA-3') were used as described by Kandeler et al. (2006). The conditions for *nirK* and *nirS* real-time PCRs were described elsewhere (Henry et al. 2006; Kandeler et al. 2006). Fluorescence was measured after each extension step. Melting curve and agarose electrophoresis (1.5% w/v, 110 V, 45 min) was performed for quality verification of the PCR product after each qPCR. Thermal cycling, fluorescent data collection, and data analysis were carried out with ABI Step One. Two independent qPCRs were performed for each gene and soil replicate. Standard curves were obtained with serial tenfold plasmid dilutions of a known amount of plasmid DNA containing a fragment of the 16S rDNA, *nirK* and *nirS* genes, respectively.

The extracted DNA from the soil samples was also tested for the inhibitory effects of co-extracted substances (i.e. humic and fulvic acids) by determining the 16S rDNA, *nirK* and *nirS* gene copy numbers in tenfold and 100-fold dilutions of the soil DNA extract. In addition, standard plasmid DNA was quantified with and without the addition of environmental DNA, and the obtained values were included into the calculation of 16S rDNA, *nirK* and *nirS* gene copy numbers as correction factors. Also DNA extraction efficiency (ng DNA per g soil) was included into the calculation.

Using the SYBR green assay and degenerate primers for the *nirK* and *nirS* genes, it was possible to discriminate against the primer dimer fluorescence by acquiring data at a temperature of 80°C, which is above the melting point of these by-products (Henry et al. 2006). This temperature was verified by melting curve analysis (data not shown). The gene copies in the no template controls (NTCs) were 0 and less than ten copies for *nirK* and *nirS*, respectively. Less than

ten copies per assay were observed for the 16S rDNA gene. According to threshold cycles (C_T) of standards and the NTC values, a detection limit of approximately 10–100 gene copies per assay was achieved for *nirK*, *nirS* and 16S rDNA quantification, which corresponds to 10^2 – 10^3 gene copies per gram of dry soil.

Statistical evaluation

Basic statistical analyses were performed using Statistica 8.0 (StatSoft). One-way ANOVA (soil layer as independent variable), followed by the Tukey HSD test was used for testing the differences between soil quality characteristics of the four sampling sites. One-way ANOVA (site as independent variable), followed by the Tukey HSD test was used for testing the differences between the amount of *nirK*, *nirS* and 16S rDNA gene copies of the four sampling sites. Linear regression was used to test the correlation of DOC, DN, DOC_{CW} , DN_{CW} , and pH with the 16S rDNA, *nirK* and *nirS* gene copy numbers. Correlation coefficients (r) with p values were evaluated.

For pH and DOC, an exponential relationship was compared ($R_{pH}^2 = 0.802$, $R_{DOC}^2 = 0.756$), because it fitted better the experimental data values and explained more variability than the linear relationship ($R_{pH}^2 = 0.728$, $R_{DOC}^2 = 0.742$).

Results

Amount of DOM in different soil horizons and sampling sites

DOC and P_{OX} were the only compounds significantly lower in the organic humus horizons than organic litter horizons in all four sites. Amounts of C_{TOT} and N_{TOT} , as well as the amount of DN, were also lower in organic humus horizons than in organic litter horizon, but insignificantly (Table 1). pH values were not statistically different between the soil horizons in most cases, with only the organic litter horizon at CH being significantly more alkaline than the organic humus horizon from the same site (Table 1). However, pH was significantly lower at PL and CT than SV and

Table 1 Spatial variation of chemical properties of organic litter and organic humus layers in the Bohemian Forest (PL, Plešné Lake catchment; CT, Čertovo lake catchment), and The Jizera Mountains (SV, Sněžné věžičky catchment; CH, Černá hora catchment)

Site	Soil horizon	Selected soil chemical characteristics							
		C_{TOT} (mol kg ⁻¹)	N_{TOT} (mol kg ⁻¹)	DOC (mol kg ⁻¹)	DOC_{CW} (mmol kg ⁻¹)	DN (mol kg ⁻¹)	DN_{CW} (mmol kg ⁻¹)	P_{OX} (mmol kg ⁻¹)	pH (H ₂ O)
PL	Organic litter	38.58 ^B (1.72)	1.37 ^{BC} (0.21)	2.02 ^B (0.85)	124.0 ^A (7.3)	0.19 ^A (0.01)	5.3 ^{AB} (0.3)	4.95 ^B (0.79)	3.59 ^A (0.15)
	Organic humus	25.61 ^A (7.14)	1.08 ^A (0.14)	1.26 ^A (0.01)	121.8 ^A (10.0)	0.21 ^A (0.04)	5.2 ^B (0.0)	3.30 ^A (0.34)	3.45 ^A (0.13)
CT	Organic litter	40.53 ^C (2.46)	1.58 ^D (0.02)	3.24 ^C (0.87)	138.2 ^B (12.6)	0.22 ^A (0.04)	5.8 ^C (0.2)	5.61 ^C (0.03)	3.67 ^A (0.14)
	Organic humus	28.09 ^{AB} (8.57)	0.98 ^A (0.35)	2.47 ^B (0.36)	125.7 ^{AB} (15.4)	0.20 ^A (0.02)	5.4 ^{AB} (0.5)	3.38 ^A (0.75)	3.48 ^A (0.19)
SV	Organic litter	33.22 ^{AB} (19.4)	1.47 ^{BC} (0.34)	7.04 ^E (0.07)	440.0 ^E (49.1)	0.41 ^D (0.01)	5.6 ^{BC} (1.0)	9.70 ^C (3.99)	5.75 ^B (0.07)
	Organic humus	33.68 ^{AB} (9.8)	1.49 ^C (0.09)	5.45 ^D (0.12)	249.3 ^D (3.8)	0.31 ^C (0.01)	4.2 ^A (0.1)	7.78 ^C (3.48)	5.58 ^B (0.20)
CH	Organic litter	29.94 ^{AB} (3.6)	1.54 ^D (0.05)	7.20 ^E (0.71)	513.3 ^F (14.9)	0.44 ^D (0.09)	9.0 ^D (0.1)	11.71 ^D (2.88)	6.05 ^C (0.15)
	Organic humus	30.98 ^{AB} (8.8)	1.44 ^{BC} (0.27)	5.12 ^D (0.02)	184.5 ^C (28.2)	0.27 ^B (0.01)	4.2 ^{AB} (0.8)	5.81 ^{BC} (2.43)	5.28 ^B (0.14)

Different letters show significant differences between values within columns ($p < 0.05$)

Mean values of total carbon (C_{TOT}), total nitrogen (N_{TOT}), total dissolved organic carbon (DOC), dissolved organic carbon in cold water extract (DOC_{CW}), total dissolved nitrogen (DN), dissolved nitrogen in cold water extract (DN_{CW}) and pH in water extract ($n = 4$) are given with the standard deviation in brackets ($n = 4$)

CH. Comparing the highly acidic soils (PL and CT) with the more alkaline soils (SV and CH) we can see also significantly higher amounts of DOM and P_{OX} at SV and CH soils than at PL and CT soils (Table 1).

Amounts of 16S rDNA, *nirK* and *nirS* gene copy numbers in soil horizons

The total number of 16S rDNA gene copy numbers in the organic litter horizon was significantly higher at SV and CH than PL and CT (Fig. 1). A similar

pattern was observed for the *nirK* denitrifiers. On the contrary, *nirS* denitrifiers showed the opposite trend. However, the number of *nirS* denitrifiers was two orders lower than the number of *nirK* denitrifiers (Fig. 1).

The total number of bacteria at the organic humus horizon was significantly lower than the organic litter layer and significantly higher at SV and CH (Fig. 1). The amount of *nirS* denitrifiers was again two orders lower and was on the detection limit of the qPCR methodology.

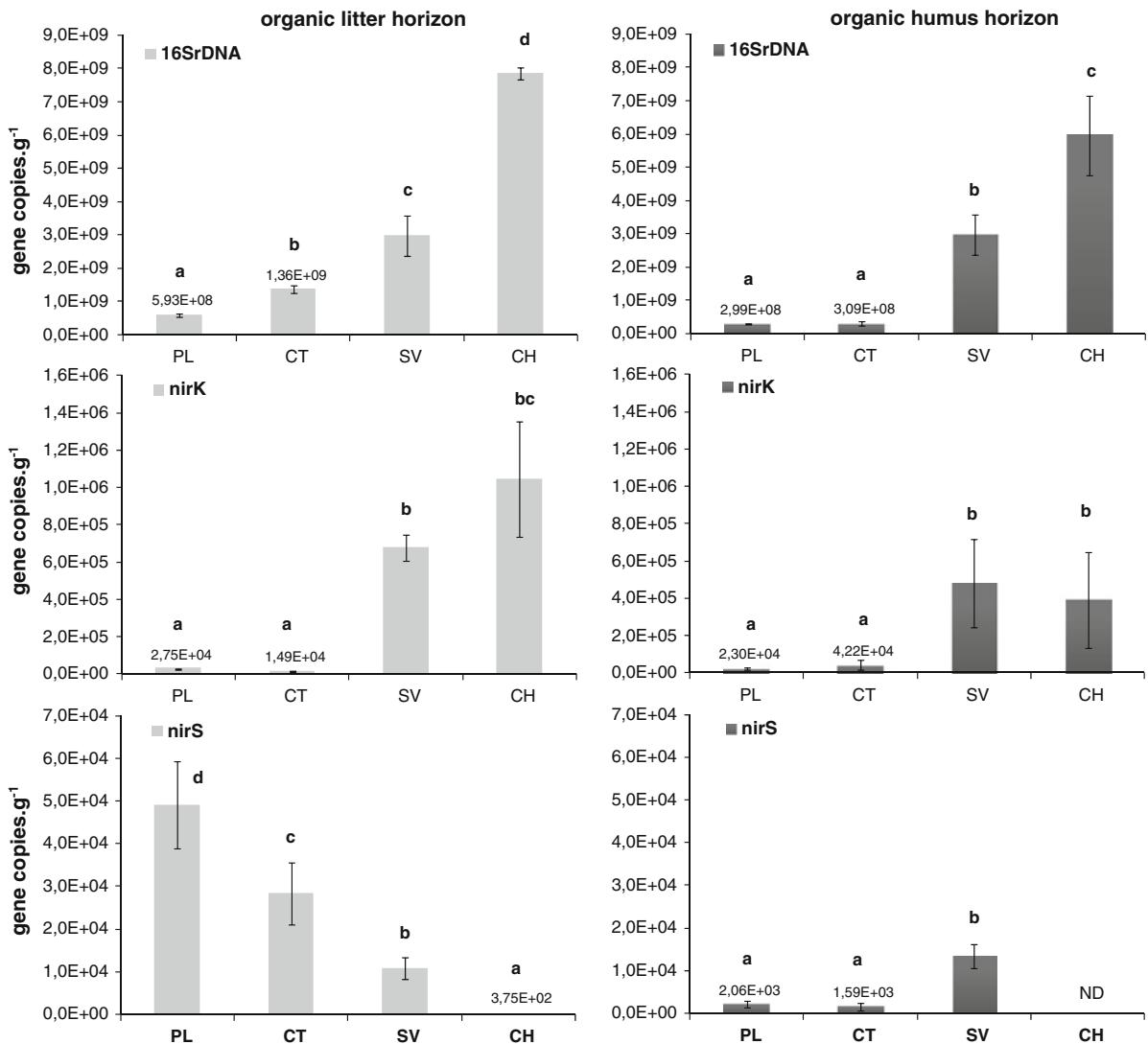


Fig. 1 Total amount of bacteria (16SrDNA gene copy numbers), and *nirK* and *nirS* denitrifiers in organic litter and organic humus horizons at PL, CT, SV and CH. ND not detected. Different letters show significant differences between sites ($n = 4$, $p < 0.05$)

Correlations between DOM, P_{OX}, pH and the 16S rDNA, *nirK* and *nirS* gene copy numbers

DOC and DN were highly positively correlated (Table 2). Also the amount of P_{OX} was highly positively correlated with pH suggesting lower P bioavailability in the PL and CT soils. A similar relationship was found between P_{OX} and DOC, and DOC and DN, showing a very close cross connection between pH and DOM.

There were also high positive correlations between DOC, DN, P_{OX} and pH, and the total amount of 16S rDNA and *nirK* gene copy numbers (Table 3). The *nirS* denitrifiers showed a positive correlation with only C_{TOT}. Interestingly, there were high positive correlations between DOC, DN and P_{OX}, and the

nirK/nirS gene ratio, showing a shift between the relative amount of these two groups depending on nutrient availability in soil (Table 3).

Closer investigation of the correlations between the number of *nirK* denitrifiers and DOC and pH revealed that these correlations had a more likely exponential relationship than linear (Fig. 2). This suggests that there should be some critical point below/above which the number of *nirK* denitrifiers rapidly decreases/increases. For DOC and pH, the critical point was approximately 4.8 mol kg⁻¹ and 5, respectively. The number of *nirK* denitrifiers rapidly decreased below these thresholds. On the contrary, DN and P_{OX} showed linear correlations with the number of *nirK* denitrifiers (Fig. 2).

Table 2 Correlation coefficients (*r*) of selected soil quality characteristics (C_{TOT}, N_{TOT}, DOC, DN, P_{OX}, and pH (H₂O)) from the organic litter and organic humus soil layers (*n* = 16)

	C _{TOT}	N _{TOT}	DOC	DN	P _{OX}	pH (H ₂ O)
C _{TOT}	–	0.78***	ns	ns	ns	ns
N _{TOT}		–	0.55*	ns	ns	ns
DOC			–	0.90***	0.77***	0.93***
DN				–	0.85***	0.84***
P _{OX}					–	0.72**
pH (H ₂ O)						–

Correlation coefficients are given and their significances are marked by asterisks as follows: * *p* < 0.05, ** *p* < 0.01, *** *p* < 0.001

ns not significant

Discussion

Quantification of 16S rDNA, *nirK* and *nirS* genes in soil environment

Quantitative real-time PCR of 16S rDNA and denitrification genes encoding NO₂⁻ reductase was used to study the ecology of denitrifiers in acidified spruce forests. 16S rDNA copy number ranged from 2.9 × 10⁸ to 7.8 × 10⁹ copies per gram of soil. These numbers are one order of magnitude lower than reported by Kandeler et al. (2006) suggesting a lower amount 16S rDNA gene copies in our experimental sites. The absolute number of 16S rDNA gene copies cannot be accurately compared to the total number of bacteria because the numbers of 16S rDNA gene

Table 3 Correlation coefficients (*r*) of selected soil quality characteristics (C_{TOT}, N_{TOT}, DOC, DOC_{CW}, DN, DN_{CW}, P_{OX}, and pH (H₂O)) versus the 16SrDNA, *nirK*, and *nirS* gene copy numbers and *nirK*/16SrDNA, *nirS*/16SrDNA, and *nirK/nirS* ratios

	16SrDNA	<i>nirK</i> denitrifiers	<i>nirS</i> denitrifiers	<i>nirK</i> /16SrDNA	<i>nirS</i> /16SrDNA	<i>nirK/nirS</i>
C _{TOT}	ns	ns	0.66**	ns	ns	ns
N _{TOT}	ns	ns	ns	ns	ns	ns
DOC	0.93***	0.86***	ns	ns	-0.51*	0.53*
DOC _{CW}	0.88***	0.90***	ns	0.50*	ns	0.66**
DN	0.87***	0.94***	ns	0.59*	-0.53*	0.69**
DN _{CW}	ns	0.60**	ns	ns	ns	0.80***
P _{OX}	0.67**	0.83***	ns	0.51*	ns	0.69**
pH (H ₂ O)	0.93***	0.85***	ns	ns	-0.54*	0.50*

Correlation coefficients are given and their significances are marked by asterisks as follows: * *p* < 0.05, ** *p* < 0.01, *** *p* < 0.001

ns not significant

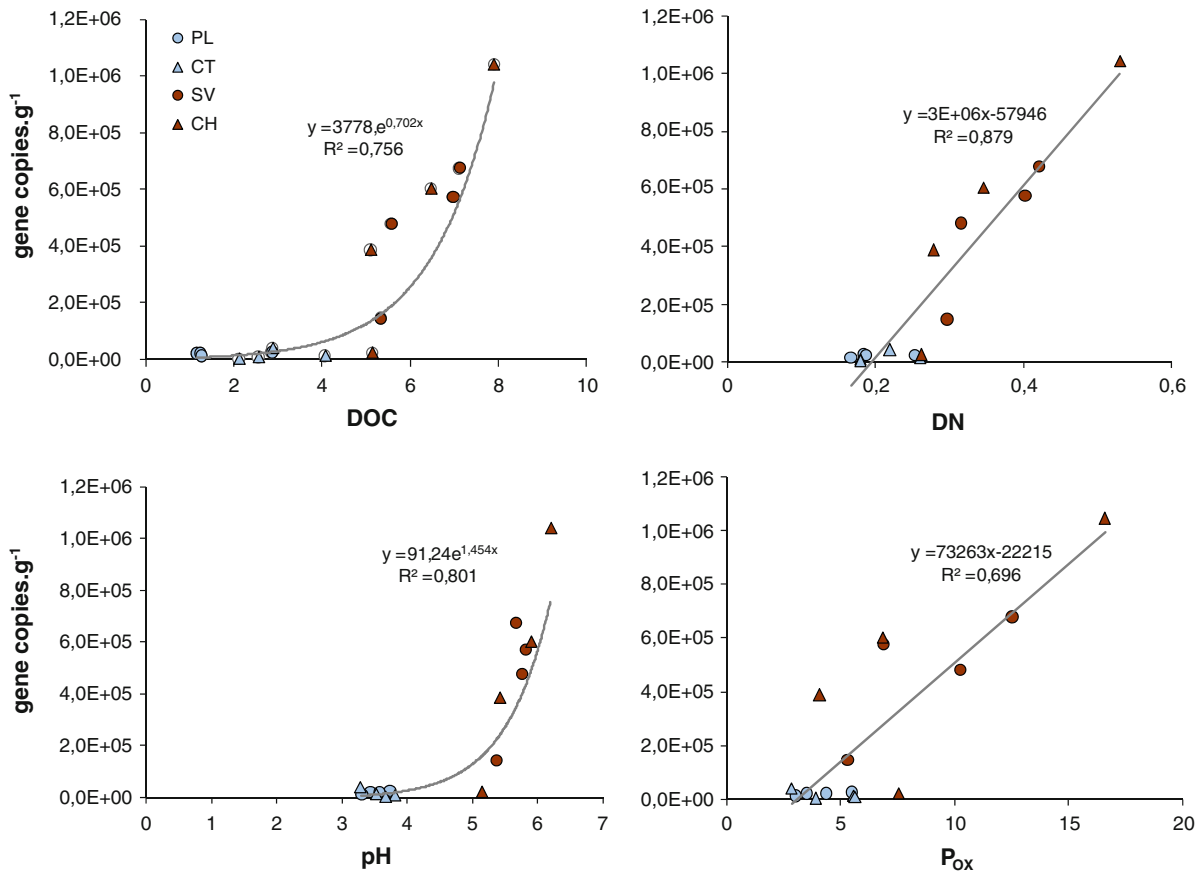


Fig. 2 Correlations of *nirK* denitrifiers with DOC, DN, pH and P_{ox}. Data are summarized for both soil horizons and sampling sites

copies per bacterial genome range from 1 to 13 copies (Chéneby et al. 2000; Fogel et al. 1999). On the contrary, *nirK* and *nirS* genes are present in only one copy per genome but also they cannot represent the absolute numbers of *nirK* and *nirS* denitrifiers because of the limitation of PCR based methods, i.e. primer specificity (Heylen et al. 2006). Our results showed that the number of *nirK* and *nirS* gene copies in forest soil is higher in the organic litter horizon (i.e. from 0 to 2 cm below ground) suggesting higher denitrification potential in higher soil horizons (Fig. 1). These results confirmed the previous study of Clément et al. (2002) who found a rapid decrease of denitrification rate with increasing soil depth.

Soil samples in our sites were taken during October 2008, which could have additional impact on denitrification. Soils are wetter at this time of year, there is a higher input of plant litter into the soil horizons, and

decomposition produces higher amounts of DOM than in drier summer periods. Together with higher decomposition goes higher O₂ consumption. This creates almost ideal conditions for denitrifiers. Clément et al. (2002) found that the seasonal variation in denitrification in the upper soil horizon is different in grassland and forest ecosystems. In grasslands, the maximum denitrification rate was reached during the autumn, while during the summer period in forests. Therefore, a vegetation shift with different DOM input can alter denitrification processes (Cabrita and Brotas 2000; van Kessel et al. 1993) and the amount and composition of *nirK* and *nirS* denitrifiers (Wertz et al. 2009). The contribution of grasses (i.e. *Calamagrostis villosa* and *A. flexuosa*) recently increased in PL and CT due to forest dieback. Therefore, the maximum denitrification rate and the amount of *nirK* and *nirS* denitrifiers can be closer to grassland ecosystems (i.e. in autumn).

Amount of DOM in acid forest soils

The amount of DOM in soil pore water plays a crucial role in the availability of nutrients for soil microorganisms. When the amount of DOM is low it becomes limiting for soil microorganisms leading to starvation and reduction of biochemical processes. The major factor influencing the amount of DOM is pH (Quails and Raines 1992; Greenland 1971; David et al. 1989). Soils at PL and CT are highly acidic, which leads to significantly lower amounts of DOC, DN and available P (P_{OX}) than at SV and CH (Table 1). Close relationships between these DOM fractions and pH were confirmed in our soils (Table 2). Three major mechanisms were proposed to explain this relation: (i) formation of insoluble compounds and subsequent flocculation of organic molecules, (ii) adsorption of organic molecules on clay material through cation bridging and (iii) complexation of organic molecules with polyvalent cations (Greenland 1971). All three processes seem to be operating. However, complexation of OM with polyvalent cations should be the most important process in our soils. In PL and CT, acidification was interconnected with higher mobility of toxic Al^{3+} forms, which can precipitate DOM making it unavailable for biological processes (Kana and Kopáček 2006; Northup et al. 1998; Tomlinson 2003). Schindler et al. (1992) described the negative effect of Al^{3+} on OM solubility in acidified lakes. These authors found that DOC may also precipitate with $Fe(OH)_3$ at $pH < 4$, which leads to an additional decrease of DOC amount. Moreover, high concentrations of Al^{3+} can damage bacterial membranes leading to higher bacterial mortality (Yaganza et al. 2004), which corresponds with our results of a one order magnitude decrease in 16S rDNA gene copies at PL and CT (Fig. 1). All of these effects could explain the exponential relationship between the number of *nirK* denitrifiers and DOC, and the rapid reduction of *nirK* denitrifiers at $pH < 4$ at these sites.

Correlation between the amount of denitrifiers and available DOM

As mentioned above, PL and CT were strongly affected by a bark beetle infestation, which has led to an enormous spruce forest dieback and high amount of spruce needles which have accumulated in the

organic litter horizon. The relatively slow decomposition of spruce needles (Bárta et al. 2010) produces a high amount of organic acids, which leads to secondary acidification of PL and CT (Šantrůčková et al. 2004, 2006, 2007).

Therefore, in these extremely acidic soils, both Al^{3+} and Fe^{3+} ions co-precipitate organic matter which leads to an enormous nutrient limitation for soil microorganisms. The *nirK* denitrifiers seem to be more sensitive to these nutrient changes than *nirS* denitrifiers. These results are in agreement with Kandeler et al. (2006). However, the *nirK* denitrifiers are still more abundant than *nirS* denitrifiers in our sites. They are more abundant in the bulk soil where selective pressure and nutrient limitation are higher than in the rhizosphere where the *nirS* denitrifiers are preferred (Henry et al. 2004). The *nirS* denitrifiers have one advantage over the *nirK* denitrifier which is that plants exude compounds which stimulate the overall growth of bacteria in the rhizosphere (Rösch et al. 2002; Livsey and Barklund 1992). Thus, the lower amount of DOM in bulk soil does not have so dramatic effect on shift of *nirS* gene abundance. Recently, some studies showed that the *nirK* gene may be more preferable for horizontal gene transfer (HRT) than the *nirS* gene. The *nirK* gene was found in highly taxonomically diverse bacterial groups. The gene was “spread” among the same habitat and does not correlate with 16S rDNA phylogeny as the *nirS* does (Heylen et al. 2006). At PL and CT, the lower amount of DOM could therefore decrease the rate of HRT between soil bacteria making them less effective in reducing higher amounts of NO_3^- and NO_2^- . These can then leach from the forest ecosystem.

In our previous work we found that P availability (P_{OX}) plays an important role in litter decomposition at PL and CT and is more important than the availability of C and N. Also the composition of bacterial and fungal communities strongly correlated with the amount of P_{OX} . The overall biodiversity and enzymatic activity of decomposing microorganisms were much higher in litter with higher amount of P_{OX} (i.e. grasses) than in litter which contained low amount of P_{OX} (i.e. spruce needles) (Bárta et al. 2010). In our current study, we found that also the amount of *nirK* denitrifiers strongly depends on P_{OX} (Table 3). Litter decomposition and nutrient availability in the upper soil horizons are closely connected. Lower microbial biodiversity on spruce

needles can lead to lower decomposition and lower amount of released nutrients into the upper soil horizons (Sinsabaugh et al. 2002, 2005). Additionally, lower ligninolytic enzymatic activity leaves a higher amount of recalcitrant polyphenolics which are not available to most soil bacteria including denitrifiers (Snajdr et al. 2008). Therefore, it seems that this is an additional process to those mentioned above, which leads to the reduction of denitrification potential in acidified spruce forests.

The *nirK/nirS* ratio

The amount of *nirS* denitrifiers did not show any correlation with DOM, however, there was a high positive correlation between DOM and the *nirK/nirS* ratio. A higher amount of DOM shifts the ratio to the *nirK* denitrifiers while in lower amounts of DOM the ratio decreases with a higher relative contribution of *nirS* denitrifiers. These results are in agreement with Winder and Levy-Booth (2009). These authors studied the effect of clear-cutting in Douglas-fir stands and found a similar reduction in the amount of denitrifiers.

In conclusion, DOM appears to strongly affect the amount of denitrifying bacteria, especially the *nirK* denitrifiers, which are highly sensitive to the amount of DOM and soil pH. This can reduce denitrification rate in the organic litter and organic humus horizons, which can lead to increased NO_3^- and NO_2^- leaching from highly acidic spruce forest soils.

Acknowledgements This study was supported by the Czech Science Foundation, project 526/08/0751 and 206/07/1200 and the project MSM 6007665801. We acknowledge the laboratory and field assistance provided by our colleagues and students. We also thank the authorities of NP Šumava and The Jizera Mountains for permission to study the spruce forest ecosystems. We thank our American colleague Dr. Keith Edwards for language correction.

References

Bárta J, Applová M, Vaněk D, Křišťůvková M, Šantrůčková H (2010) Effect of available P and phenolics on mineral N release in acidified spruce forest: connection with lignin-degrading enzymes and bacterial and fungal communities. *Biogeochemistry* 97:71–87

Cabrita MT, Brotas V (2000) Seasonal variation in denitrification and dissolved nitrogen fluxes in intertidal sediments of the Tagus estuary, Portugal. *Mar Ecol* 202: 51–65

Cappo KA, Blume LJ, Raab GA, Bartz JK, Engels JL (1987) Analytical methods manual for the direct/delayed response project soil survey. US EPA, Las Vegas (sections 8–11)

Chéneby D, Philippot L, Hartmann A, Hénault F, Germon JC (2000) 16S rRNA analysis for characterization of denitrifying bacteria isolated from three agricultural soils. *FEMS Microbiol Ecol* 34:121–128

Clément JC, Pinay G, Marmonier P (2002) Seasonal dynamics of denitrification along topohydrosequences in three different riparian wetlands. *J Environ Qual* 31:1025–1037

Dauer JM, Chorover J, Chadwick OA, Oleksyn J, Tjoelker MG, Hobbie SE, Reich PB, Eissenstat DM (2007) Controls over leaf and litter calcium concentrations among temperate trees. *Biogeochemistry* 86:175–187

David MB, Vance GF, Rissing JM, Stevenson FJ (1989) Organic carbon fractions in extracts of O and B horizons from a New England spodosol: effect of acid treatment. *J Environ Qual* 18:212–217

Fogel GB, Collins CR, Li J, Brunk CF (1999) Prokaryotic genome size and SSU rDNA copy number: estimation of microbial relative abundance from a mixed population. *Microb Ecol* 38:93–113

Galloway JN, Cowling EB (2002) Reactive nitrogen and the world: 200 years of change. *Ambio* 31:64–71

Galloway JN, Aber JD, Erisman JW, Seitzinger SP, Howarth RW, Cowling EB, Cosby BJ (2003) The nitrogen cascade. *Bioscience* 53:341–356

Greenland DJ (1971) Adsorption of humic and fulvic acids by soils. *Soil Sci* 111:34–43

Henry S, Baudion E, López-Gutiérrez JC, Martin-Laurent F, Brauman A, Philippot L (2004) Quantification of denitrifying bacteria in soils by *nirK* gene targeted real-time PCR. *J Microbiol Methods* 59:327–335

Henry S, Bru D, Stres B, Hallet S, Philippot L (2006) Quantitative detection of the *nosZ* gene, encoding nitrous oxide reductase, and comparison of the abundances of 16S rRNA, *narG*, *nirK*, and *nosZ* genes in soils. *Appl Environ Microbiol* 72:5181–5189

Heylen K, Gevers D, Vanparys B, Wittebolle L, Geets J, Boon N, De Vos P (2006) The incidence of *nirS* and *nirK* and their genetic heterogeneity in cultivated denitrifiers. *Environ Microbiol* 8:2012–2021

Kaňa J, Kopáček J (2006) Impact of soil sorption characteristics and bedrock composition on phosphorus concentrations in two Bohemian Forest Lakes. *Water Air Soil Pollut* 173:243–259

Kandeler E, Deighlmayr K, Tschirko D, Bru D, Philippot L (2006) Abundance of *narG*, *nirS*, *nirK*, and *nosZ* genes of denitrifying bacteria during primary successions of a glacier foreland. *Appl Environ Microbiol* 72:5957–5962

Koopmans GF, Chardon WJ, de Willigen P, van Riemsdijk WH (2004) Phosphorus desorption dynamics in soil and the link to a dynamic concept of bioavailability. *J Environ Qual* 33:1393–1402

Kopáček J, Kaňa J, Šantrůčková H, Porcal P, Hejzlar J, Píček T, Veselý J (2002a) Physical, chemical, and biochemical characteristics of soils in watersheds of the Bohemian Forest Lakes: I. Plešné Lake. *Silva Gabreta* 8:43–62

Kopáček J, Kaňa J, Šantrůčková H, Porcal P, Hejzlar J, Píček T, Šimek M, Veselý J (2002b) Physical, chemical, and

- biochemical characteristics of soils in watersheds of the Bohemian Forest Lakes: II. Čertovo and Černé Lakes. *Silva Gabreta* 8:63–93
- Livsey S, Barklund P (1992) *Lophodermium piceae* and *Rhizosphaera kalkhoffii* in fallen needles of Norway spruce (*Picea abies*). *Eur J For Pathol* 22:204–216
- López-Gutiérrez J, Henry S, Hallet S, Martin-Laurent F, Catroux G, Philippot L (2004) Quantification of a novel group of nitrate-reducing bacteria in the environment by real-time PCR. *J Microbiol Methods* 57:399–407
- Magill AH, Aber JD, Hendricks JJ, Bowden RD, Melillo JM, Steudler PA (1997) Biogeochemical response of forest ecosystems to simulated chronic nitrogen deposition. *Ecol Appl* 7:402–415
- Nadelhoffer KJ, Emmett BA, Gundersen P, Kjonaas OJ, Koopmans CJ, Schleppi P, Tietema A (1999) Nitrogen deposition makes a minor contribution to carbon sequestration in temperate forests. *Nature* 398:145–148
- Northrup RR, Dahlgren RA, McColl JG (1998) Polyphenols as regulators of plant-litter-soil interactions in northern Californian pygmy forest: a positive feedback? *Biogeochemistry* 42:189–220
- Pawłowski L (1997) Acidification: its impact on the environment and mitigation strategies. *Ecol Eng* 8:271–288
- Pote DH, Daniel TC, Sharpley AN, Moore PA, Edwards DR, Nichols DJ (1996) Relating extractable soil phosphorus to phosphorus losses in runoff. *Soil Sci Am J* 60:855–859
- Quails RG, Raines BL (1992) Biodegradability of dissolved organic matter in forest throughfall, soil solution, and stream water. *Soil Sci Soc Am J* 56:578–586
- Rösch C, Mergel A, Bothe H (2002) Biodiversity of denitrifying and dinitrogen-fixing bacteria in an acid forest soil. *Appl Environ Microbiol* 68:3818–3829
- Saleh-Lakha S, Shannon KE, Henderson SL, Goyer C, Trevors JT, Zebarth BJ, Buton DL (2009) Effect of pH and temperature on denitrification gene expression and activity in *Pseudomonas mandelii*. *Appl Environ Microbiol* 75:3903–3911
- Šantrůčková H, Vrba J, Pícek T, Kopáček J (2004) Soil biochemical activity and phosphorus transformations and losses from acidified forest soils. *Soil Biol Biochem* 36:1569–1576
- Šantrůčková H, Křišťůvková M, Vaněk D (2006) Decomposition rate and nutrient release from plant litter of Norway spruce forest in the Bohemian Forest. *Biologia (Bratisl)* 61:S499–S508
- Šantrůčková H, Šantrůček J, Setlík J, Svoboda M, Kopáček J (2007) Carbon isotopes in tree rings of Norway spruce exposed to atmospheric pollution. *Environ Sci Technol* 41:5778–5782
- Schindler DW, Bayley SE, Curtis PJ, Parker BR, Stainton MP, Kelly CA (1992) Natural and man-caused factors affecting the abundance and cycling of dissolved organic substances in Precambrian shield lakes. *Hydrobiologia* 229:1–21
- Schwertmann U (1964) Differenzierung der Eisenoxiden des Bodens durch Extraktion mit Ammoniumoxalat-Lösung. *Z Pflanzenernähr Düng Bodenkd* 105:194–202
- Sinsabaugh RL, Carreiro MM, Repert DA (2002) Allocation of extracellular enzymatic activity in relation to litter composition, N deposition, and mass loss. *Biogeochemistry* 60:1–24
- Sinsabaugh RL, Gallo ME, Lauber C, Waldrop MP, Zak DR (2005) Extracellular enzyme activities and soil organic matter dynamics for northern hardwood forests receiving simulated nitrogen deposition. *Biogeochemistry* 75:201–215
- Snajdr J, Valaskova V, Merhautova V, Herinkova J, Cajthaml T, Baldrian P (2008) Spatial variability of enzyme activities and microbial biomass in the upper layers of *Quercus petraea* forest soil. *Soil Biol Biochem* 40:2068–2075
- Svoboda M, Matějka K, Kopáček J (2006) Biomass and element pools of understory vegetation in the catchments of Čertovo Lake and Plešné Lake in the Bohemian Forest. *Biologia (Bratisl)* 61:S509–S521
- Tiedje JM (1988) Ecology of denitrification and dissimilatory nitrate reduction to ammonium. In: Zehnder A (ed) *Biology of anaerobic microorganisms*. Wiley, New York, pp 179–244
- Tomlinson GH (2003) Acid deposition, nutrient leaching and forest growth. *Biogeochemistry* 65:51–81
- van der Zee SEATM, Fokkink LGJ, van Riemsdijk WH (1987) A new technique for assessment of reversibly adsorbed phosphate. *Soil Sci Am J* 51:599–604
- van Kessel C, Pennock DJ, Farrell RE (1993) Seasonal variations in denitrification and nitrous oxide evolution at the landscape scale. *Soil Sci Soc Am J* 57:988–995
- Veselý J (1994) Investigation of the nature of the Šumava lakes: a review. *J Natl Mus Nat Hist Ser* 163:103–120
- Waldrop MP, Zak DR (2006) Response of oxidative enzyme activities to nitrogen deposition affects soil concentrations of dissolved organic carbon. *Ecosystems* 9:921–933
- Wertz S, Dandie CE, Goyer C, Trevors JT, Pattern CL (2009) Diversity of nirK denitrifying genes and transcripts in an agricultural soil. *Appl Environ Microbiol* 75:7365–7377
- Winder RS, Levy-Booth DJ (2009) Quantification of nitrogen cycling functional gene abundance in soil of variably-retained stands of Douglas-fir (*Pseudotsuga menziesii* ssp. *menziesii* (Mirb.) Franco). Working papers of the Finnish Forest Research Institute 128:225
- Yaganza ES, Rioux D, Simard M, Arul JI, Tweddell RJ (2004) Ultrastructural alterations of *Erwinia carotovora* subsp. *atroseptica* caused by treatment with aluminum chloride and sodium metabisulfite. *Appl Environ Microbiol* 70:6800–6808

Paper 4

Barta J, Tahovska K, Santruckova H, Oulehle F (2017) Microbial communities with distinct denitrification potential in spruce and beech soils differing in nitrate leaching. *SCIENTIFIC REPORTS* 7:9738.

SCIENTIFIC REPORTS



Correction: Author Correction

OPEN

Microbial communities with distinct denitrification potential in spruce and beech soils differing in nitrate leaching

Jiří Bárta¹, Karolina Tahovská¹, Hana Šantrůčková¹ & Filip Oulehle²

Nitrogen leaching owing to elevated acid deposition remains the main ecosystem threat worldwide. We aimed to contribute to the understanding of the highly variable nitrate losses observed in Europe after acid deposition retreat. Our study proceeded in adjacent beech and spruce forests undergoing acidification recovery and differing in nitrate leaching. We reconstructed soil microbial functional characteristics connected with nitrogen and carbon cycling based on community composition. Our results showed that in the more acidic spruce soil with high carbon content, where Acidobacteria and Actinobacteria were abundant (Proteo:Acido = 1.3), the potential for nitrate reduction and loss via denitrification was high (denitrification: dissimilative nitrogen reduction to ammonium (DNRA) = 3). In the less acidic beech stand with low carbon content, but high nitrogen availability, Proteobacteria were more abundant (Proteo:Acido = 1.6). Proportionally less nitrate could be denitrified there (denitrification:DNRA = 1), possibly increasing its availability. Among 10 potential keystone species, microbes capable of DNRA were identified in the beech soil while instead denitrifiers dominated in the spruce soil. In spite of the former acid deposition impact, distinct microbial functional guilds developed under different vegetational dominance, resulting in different N immobilization potentials, possibly influencing the ecosystem's nitrogen retention ability.

Since the industrial period, atmospheric sulphur (S) and nitrogen (N) deposition has become one of the main drivers for changing ecosystem biogeochemistry. The main consequences of long-term S and N loading lie in soil acidification and the interlinked changes in plant productivity and diversity^{1–3}, soil carbon and nutrient cycling⁴ and alteration in the soil microbial community structure⁵. Besides soil acidification, long-term N deposition can lead to an ecosystem's N saturation where the excess N may be lost in the form of nitrates⁶. Reduced depositions in the last decades started the recovery of many European ecosystems, accompanied only in some of them by reduced nitrate leaching^{7,8}.

Apart from plants, soil microbes, as essential mediators of all assimilative and dissimilative N transformation processes, play a key role in the soil mineral N balance. Nitrates accumulate in soil either under high nitrification rates and/or low nitrate reduction rates (i.e. low microbial immobilization, denitrification or dissimilative nitrate reduction to ammonium (DNRA)). Generally, it is the heterotrophic community (usually prevailing over the autotrophic), being dependent on soil carbon (C), which regulates whether N is lost or retained in the soil^{9–11}. Although we have now advanced ability to explore structures of soil microbial communities, there is still a need for studies focusing on specific links between microbial taxonomic and functional diversity and their participation in soil C and N transformation and eventually soil N retention¹².

The effect of elevated N input on soil microbial communities has been widely discussed with most studies drawing the conclusion of decreasing fungal biomass and activity, particularly mycorrhizas^{5,13–15}. Lower fungal biomass and thus lower activity of the lignin-degrading enzymes^{16,17} shift microbial utilization to easily available C and after these are quickly exhausted it may lead to overall C limitation of the microbial community^{4,18–21}. As a consequence, N mineralization and nitrate concentrations increase^{22–25}.

¹Department of Ecosystem Biology, Faculty of Science, University of South Bohemia, Branišovská 31, 370 05, České Budějovice, Czech Republic. ²Czech Geological Survey, Department of Environmental Geochemistry and Biogeochemistry, Prague, 118 21, Czech Republic. Correspondence and requests for materials should be addressed to J.B. (email: jiri.barta@prf.jcu.cz)

Elevated N loading and subsequent changes in microbial utilization of organic C can change the overall structure of a soil prokaryotic community. Particularly, copiotrophic taxa (r-strategists) namely Alpha- and Gammaproteobacteria increase at elevated N input^{26–28}. In contrast, Acidobacteria, a group which is mostly considered as oligotrophic (K-strategists), decline with increasing N loads^{27,29}. Functional metagenomic analyses showed higher relative abundances of specific gene categories associated with DNA/RNA replication, electron transport and protein metabolism after N amendments. This indicates higher growth and metabolic activity typical for copiotrophs²⁷. Such community shifts may lead to changes in substrate use efficiencies since copiotrophs are supposed to grow faster but with lower growth efficiency³⁰.

The Czech side of the central European area of the so-called “Black Triangle” located along the German-Polish-Czech border and belongs among the regions most affected by acid pollution³¹. Since the 1980s, a considerable decline in S and N deposition has occurred (more than 90% and 40% reduction, respectively) due to the restructuring of industrial and agricultural practices³¹. Here we investigated the microbial community structure using DNA sequencing in the beech and spruce soils of two adjacent forests and currently differing in their nitrate leaching⁷. We combined molecular identification data with biogeochemical soil and microbial characteristics to explore the links among microbial community composition and N transformation processes. Our primary question was whether variations in microbial community structure could help to explain observed differences in nitrate leaching between both forests. We supposed that the microbial community structure could be different between both forests due to different vegetation type per se (i.e. differences in litter composition and input, different levels of dry deposition etc.). We hypothesized that due to historically high acid deposition, the fungal abundances would be rather similar probably with a shift to saprotrophic strategy. Furthermore, the bacterial community would be dominated by Acidobacteria in both forests due to very low soil pH. However, we also recognized that copiotrophic taxa might be favoured in the beech soils that could correspond to richer N conditions there.

Materials and Methods

Sampling sites. Our experimental site, Načetín, is located on the ridge of the Ore Mountains, in the north-western part of the Czech Republic (Fig. S1). This region was exposed to extremely high acid deposition in the past³² and has currently been undergoing recovery since the 1990s³¹ (Fig. S3). The site has been intensively used for the monitoring of atmospheric deposition, soil and soil water chemistry since 1993. Two adjacent stands were studied. The spruce stand (50°35'26"N, 13°15'14"E) is located at an elevation of 784 m a.s.l. on a gentle slope oriented to the northwest and is completely dominated by Norway spruce (*Picea abies*, ~80 years old) with the understory vegetation dominated by wavy hair-grass (*Deschampsia flexuosa*), bushgrass and blueberry (Fig. S2). The beech stand (50°35'22"N, 13°16'07"E) lies at an elevation of 823 m a.s.l. and is composed of European beech (*Fagus sylvatica*, ~120 years old, spruce trees continuously died off due to the air pollution) with no understory vegetation present (only the limited presence of beech seedlings). The bedrock of both stands is gneiss, and soils are dominated by dystric cambisols. The snow cover lasts usually from November to April; the average annual temperature is 6.3 °C, and annual precipitation is ~1000 mm. Bulk N deposition averaged 11 kg N ha⁻¹ year⁻¹ and throughfall N flux was similar among stands 16 kg ha⁻¹ year⁻¹³³. In total, 16 real composite soil samples (based on two cores) were taken from 16 randomly selected plots (9 m²) in each of both forests in early May 2013. We sampled the upper organic soil layer (Of + Oh + A horizons), using a soil corer (up to 10–15 cm).

Soil solution sampling and analysis. Soil pore water samples from the forest floor were collected using Rhizon[®] suction samplers (Rhizosphere Research Products, NL), comprising 10 cm long, 2.5 mm diameter porous membranes attached to 50 ml syringes. In each forest, four to six suction lysimeters were placed in 16 randomly selected plots (9 m²). Samples were collected by applying suction overnight, and a composite sample was made in the morning to get one representative sample per plot (n = 16). The sampling was performed twice in May 2013 in all 16 plots and the averages are used. Samples were stored at 4 °C and analysed immediately after arrival in laboratory. Sulphates and nitrates were measured by ion exchange chromatography (Alltech 650, USA). Base cations and total aluminium were determined by flame atomic absorption spectrometry (AAAnalyst 200 Perkin-Elmer, USA). Ammonium was determined by indophenol blue colorimetry. Dissolved organic carbon (DOC) was measured by a nondispersive infrared detector after combustion to CO₂. Dissolved nitrogen (DN) was determined after sample combustion to NO and its reaction with O₃. For details see Oulehle *et al.*³³.

Biochemical soil properties and microbial activity. Soil pH was determined in deionized water (water:soil, 25:10, v/w) by agitating for 5 min and letting stand for 0.5 h. Dried (60 °C) and finely ground soil samples were analysed for total C (C_{tot}) and N (N_{tot}) content on an NC elemental analyser (Vario micro cube, Elementar Analysensysteme GmbH, Germany). The molar C to N ratio of the soil was calculated. Moist soil samples (10 g, 60% of water holding capacity) were placed in glass flasks sealed with perforated Parafilm and incubated for one or three weeks (10 °C). After one week incubation, the soil was either extracted (0.5 M K₂SO₄, extractant: soil, 4: 1, v/w, agitated for 45 min) or fumigated for one day with chloroform (amylene stabilized) before extraction. Then, extracts were centrifuged (4000 g, 10 min) and filtered through 0.45 µm glass fibre filter. Non-fumigated extracts were analysed for N-NH₄ and N-NO₃ using the Flow injection analyser (FIA, QuickChem 8500, Lachat Instruments, USA). Together with fumigated extracts, they were analysed for total carbon (DOC) and nitrogen (TN) content on an elemental analyser (LiqiTOC II, Elementar Analysensysteme GmbH, Germany). Microbial C (C_{mic}) and N (N_{mic}) were calculated as the difference in sulphate extractable carbon and nitrogen, respectively, between the fumigated and non-fumigated samples and corrected by the extraction efficiency factors of 0.38 for microbial C³⁴, and 0.54 for microbial N (K_{EN})³⁵. The remaining samples were after three weeks extracted in the same manner and N-NH₄ and N-NO₃ were analysed to determine net N mineralization and nitrification rate³⁶. Net N mineralization and nitrification rates were calculated as the difference between the final (21 days)

and initial (7 days) concentrations of NH_4^+ and NO_3^- , respectively, divided by the number of days³⁷. Carbon use efficiency was calculated from available substrate (soil leachate) and microbial C/N ratios³⁸. Nitrogen use efficiency was calculated as a multiple of CUE * available substrate C/N ratio (soil leachate) divided by C/N ratio of microbial biomass³⁹. All measurements were performed in two laboratory replications for each soil sample. All data were expressed on a soil dry weight basis (105 °C). Microbial respiration was measured as CO_2 production after one week's incubation of soil in hermetically closed vials in the dark (10 g, 60% of water holding capacity, 10 °C), using gas chromatography (Agilent GC HP 6850, USA). The specific respiration rate was calculated as a ratio of respiration rate and C_{mic} .

Extracellular enzyme activities. Extracellular enzyme activities were determined by microplate fluorometric assays under standard conditions. For determination of all hydrolytic enzyme activities, 1 g soil was suspended in 100 ml of distilled water and sonicated for 4 min to disrupt soil particles. 200 μL soil suspension was then added to 50 μL methylumbelliferyl (MUF) of substrate solution for β -glucosidase, exocellulase (cellobiohydrolase), phosphatase and N-acetyl-glucosaminidase determination or to 50 μL of 7-aminomethyl-4-coumarin (AMC) substrate solution for leucine-aminopeptidase determination⁴⁰. Three concentrations of each fluorogenic substrate were tested (50, 100 and 300 μM) and the one with the highest enzymatic activity where the enzyme is saturated was picked. Plates were incubated at 20 °C for 120 min. Fluorescence was quantified at an excitation wavelength 365 nm and emission wavelength 450 nm using Infinite F200 microplate reader (TECAN, Germany).

DNA extraction. Approximately 0.5 g of soil was added to a FastPrepTM Lysis Matrix E tube (MP Biomedicals, Solon, OH, USA). Hexadecyltrimethylammonium bromide (CTAB) extraction buffer, containing 5% CTAB (in 0.7 M NaCl, 120 mM potassium phosphate, pH 8.0) and 0.5 ml phenol-chloroform-isoamylalcohol (25:24:1), was added and agitated in a FastPrep Instrument (MP Biomedicals, Solon, OH, USA) at speed 5–6 for 45 s. After bead beating, the samples were extracted with chloroform and precipitated in a PEG 6000/1.6 M NaCl solution. Pellets were washed with 70% ethanol and re-suspended in molecular biology grade water. Total DNA was quantified using known concentration of genomic DNA which was used for creation of calibration curve and after addition of fluorescent dye SybrGreen the fluorescent signal was compared with unknown samples⁴¹.

Quantification of prokaryotic and eukaryotic microbial community. Quantification of bacterial, archaeal and fungal SSU rRNA genes was performed using the FastStart SybrGREEN Roche[®] Supermix and Step One system (Life Technologies, USA). Each reaction mixture (20 μl) contained 2 μl DNA template (~1–2 ng DNA), 1 μl each primer (0.5 pmol μl^{-1} each, final concentration), 6 μl dH_2O , 10 μl FastStart SybrGREEN Roche[®] Supermix (Roche, France) and 1 μl BSA (Fermentas, 20 mg μl^{-1}). Initial denaturation (3 min, 95 °C) was followed by 30 cycles of 30 s at 95 °C, 30 s at 62 °C (bacteria) and 60 °C (archaea), 15 s at 72 °C, and completed by fluorescence data acquisition at 80 °C used for target quantification. Product specificity was confirmed by melting point analysis (52 °C to 95 °C with a plate read every 0.5 °C) and amplicon size was verified with agarose gel electrophoresis. Bacterial and archaeal DNA standards consisted of a dilution series (ranging from 10^1 to 10^9 gene copies μl^{-1}) of a known amount of purified PCR product obtained from genomic *Escherichia coli* ATCC 9637 and *Pyrococcus furiosus* DSM 3639 DNA by using the SSU gene-specific primers 341F/534R and ARC78F/ARC1059R, respectively^{42,43}. R^2 values for the standard curves were >0.99. Slope values were $->3.37$ giving an estimated amplification efficiency of >93%.

The qPCR conditions for fungal quantification were as follows: initial denaturation (10 min, 95 °C) followed by 40 cycles of 1 min at 95 °C, 1 min at 56 °C, 1 min at 72 °C, and completed by fluorescence data acquisition at 72 °C used for target quantification. Fungal DNA standards consisted of a dilution series (ranging from 10^1 to 10^7 gene copies μl^{-1}) of a known amount of purified PCR product obtained from genomic *Aspergillus niger* DNA by using the SSU gene-specific primers nu-SSU-0817-5' and nu-SSU1196-3'⁴⁴. R^2 values for the fungal standard curves were >0.99. The slope was between -3.34 to -3.53 giving estimated amplification efficiency between 95 and 93%, respectively.

Detection limits for the various assays (i.e. lowest standard concentration that is significantly different from the non-template controls) were less than 100 gene copies for each of the genes per assay. Samples, standards and non-template controls were run in duplicates. To deal with potential inhibition during PCR the enhancers (BSA, DMSO) were added to the PCR mixture. Also several dilutions (10x, 20x, 50x, 100x, 1000x) for each sample were tested to see the dilution effect on Ct values.

Analyses of prokaryotic and fungal community composition. The aliquots of DNA extracts were sent to ARGONE Lab (Illinois, USA) for the preparation of a library and sequencing using MiSeq platform. The Earth Microbiome Project (EMP) protocol was used for library preparation with modified universal primers 515FB/806RB⁴⁵ and ITS1F/ITS2⁴⁶ for prokaryotic 16S rDNA and fungal ITS1 amplicons, respectively. The coverage of prokaryotic primer pair 515FB/806RB was additionally tested in-silico using ARB Silva database release 128. The primer pair 515FB/806RB covers almost uniformly all major bacterial and archaeal phyla (Table S3). Both bacterial 16SrDNA and fungal ITS1 raw pair-end reads (150 bp) were joined using ea-utils to obtain reads of approx. 250 bp length⁴⁷. Quality filtering of reads was applied as previously described⁴⁵. After quality filtering the sequences were trimmed to 250 bp. We obtained 576,133 bacterial and 806,387 fungal sequences after joining and quality trimming. Before picking the operational taxonomic units (OTU), the fungal ITS1 region was extracted from reads using ITSx algorithm⁴⁸. Both 16S and ITS1 amplicons were trimmed to equal lengths in order to avoid spurious OTU clusters⁴⁹. Bacterial reads were clustered (more than 97% similarity) to OTUs using an open-reference OTU picking protocol (QIIME 1.9.1⁴⁷, first with uclust⁴⁹ being applied to search sequences against a Greengenes version 13_05 and Silva 119 database⁵⁰. Taxonomy was assigned to each read by accepting the Greengenes or Silva119 taxonomy string of the best matching Greengenes or Silva119 sequence. Fungal reads

were clustered to OTUs using open-reference OTU picking protocol (sequence similarity 98.5%) using UNITE ver. 5.3.2015 database⁵¹. Blast algorithm (e-value ≤ 0.001) was used for taxonomic assignment. FUNguild algorithm⁵² was then used for the life style fungal assignments.

Alpha diversity metrics, Shannon diversity, Chao1 richness, and Faith's phylogenetic diversity were calculated after rarefying all samples to the same sequencing depth of 10,000 and 4,500 sequences for prokaryota and fungi, respectively. Prior to computing the Unifrac distances, singleton OTUs (i.e. OTUs with only one sequence) were filtered out, as these are likely to represent sequencing or PCR errors and/or chimeras.

Raw sequences of 16SrDNA and ITS1 amplicons were deposited in European Nucleotide Archive (ENA) under study ID PRJEB17634.

Network analyses and determination of keystone species. In microbial network analyses it is recommended to use absolute⁵³ instead of relative OTU abundances, since relative abundances can create false correlations between OTUs. Therefore, we recalculated relative abundances in each sample of the bacterial and archaeal OTU table to absolute abundances, using the data of bacterial and archaeal SSU gene copies per ng of DNA. This gave us absolute abundances of each OTU in the OTU table. We performed the recommended calculations (n_{eff} , sparsity)⁵⁴ regarding the composition of prokaryotic and fungal filtered OTU tables (i.e. removing very rare OTUs by sorting the average OTU abundances in samples from maximum to minimum and choosing only those OTUs which were presented in at least 10 samples out of 31 for prokaryotic community, and for fungal community 5 out of 22). Based on the sparsity of filtered OTU tables we chose the CoNet network algorithm as the relevant calculation method. Unstable edges were filtered out on alpha level of 0.05. We additionally increase the alpha level to 0.01 and rerun the network analyses to confirm the robustness of the network composition (Fig. S14). The resulting OTU tables, separately for beech (15 samples for prokaryota, 11 samples for fungi) and spruce (16 samples for prokaryota, 11 samples for fungi) were used for microbial network analyses. The analysis was done in Cytoscape 3.0.2 with the CoNET application^{55,56}. The parameters and settings for network analyses in CoNET application were: -parent_child_exclusion, -row_minocc 8, -correlations (Spearman, Pearson, mutual information, Bray Curtis dissimilarity and Kullback-Leibler dissimilarity). The threshold for edge selection was set to 1,000 top and bottom. During randomization, 100 iterations were calculated for edge scores. In the following bootstrap step 100 iterations were calculated and unstable edges were filtered out (p-level threshold of 0.05). We additionally increase the p-level threshold to 0.01 and rerun the network analyses (Fig. S14). The Brown method was chosen as the p-value merging method and the Benjamini-Hochberg method for multiple test correction. The resulting network for the spruce and beech prokaryotic community was visualized and analyzed (i.e. degree of nodes, betweenness centrality, closeness centrality) in Cytoscape 3.0.2 and potential keystone OTUs in the beech and spruce forests were identified⁵³.

Analyses of metabolic potential of the prokaryotic community. Two independent pipelines (PICRUSt and RDP FunGene) were used for in-silico prediction of the functional potential of the microbial community. For PICRUSt⁵⁷ analyses the rarified OTU tables to 3,900 sequences generated by Qiime 1.9.1 were used with taxonomic classification based on GreenGenes database ver. 13.05 using closed reference OTU picking method. In general, the PICRUSt pipeline first normalized each OTU abundances by SSU copy variation in bacterial genomes based on the most similar taxa. The resulting normalized table was then used for OTU functional annotation using known bacterial and archaeal genomes⁵⁷. To validate accuracy of PICRUSt metagenomics prediction the Nearest Sequenced Taxon Index (NSTI score) was calculated. The NSTI score was 0.13 ± 0.01 and 0.14 ± 0.01 for beech and spruce, respectively. According to ref.⁵⁷ these NSTI scores are typical for soil samples (NSTI approx. 0.17).

The lists of bacterial and archaeal species for each individual gene was downloaded from the FunGene database⁵⁸. Genes below without specific annotation to the gene family were manually excluded from the analyses. The condensed list of unique genera was created and used for functional annotation in an OTU table (Table S2). By combining SSU qPCR data and relative abundances of assigned bacterial genera, we were able to quantitatively identify the main N transformation pathways.

Statistics. Differences between the beech and spruce stands were examined for the biochemical soil and microbial parameters using one way ANOVA (Statistica 9.1, Statsoft, Inc.). The normality of distributions and homogeneity of variances were checked using histogram plots and Hartley-Cochran-Bartlett's tests. Correlations between selected characteristics were explored to find the most important relations.

Principal component analysis (PCA) was employed to compare microbial community composition (relative abundances) of both forests using Canoco 5.0⁵⁹. Then a constrained ordination redundancy analysis (RDA) was used to evaluate the relations between all measured biochemical parameters of soil (log transformed, except pH, explanatory variables) and the microbial community composition (log transformed relative abundance of each phyla, response variables). The contribution of each explanatory variable was tested by forward selection and the Monte-Carlo permutation test ($p < 0.05$). Only those explanatory variables that showed significant effects were included in the diagrams. The length of the gradient was tested by detrended correspondence analysis prior the selection of the appropriate ordination method. Metric (MDS) and nonmetric distance analyses (NMDS) were done on rarefied OTU tables in R-studio (R 3.4.0) using phyloseq package⁶⁰.

Results

Soil characteristics and microbial activity. The soils in both stands were highly acidic with pH ranging from 3.98 to 4.57 and from 3.92 to 4.33 in the beech and spruce soils, respectively (Table 1). Lower pH in the spruce soil was connected with lower base cations (Ca^{2+} and Mg^{2+}), and higher aluminium, and sulphate content in the soil leachate.

	Beech	Spruce	stat.
pH _{H2O}	3.98–4.57	3.92–4.33	**
Calcium (Ca ²⁺ , μmol.L ⁻¹)	15.2 (8.7)	9.0 (4.0)	*
Magnesium (Mg ²⁺ , μmol.L ⁻¹)	25.9 (10.3)	14.8 (4.9)	***
Sulphates (SO ₄ ²⁻ , μmol.L ⁻¹)	65.5 (28.3)	85.4 (36.7)	*
Total aluminium (Al _{TOT} , μmol.L ⁻¹)	23.0 (11.1)	36.3 (12.2)	**
Total carbon (C _{TOT} , mmol.g ⁻¹)	30.3 (4.8)	33.5 (1.3)	**
Total nitrogen (N _{TOT} , mmol.g ⁻¹)	1.3 (0.2)	1.3 (0.1)	ns
C _{TOT} /N _{TOT} (molar)	23.0 (1.0)	26.3 (1.7)	***
Ammonia (NH ₄ ⁺ , μmol.L ⁻¹)	2.8 (2.7)	1.0 (0.6)	ns
Nitrates (NO ₃ ⁻ , μmol.L ⁻¹)	38.2 (48.9)	4.5 (5.7)	**
Dissolved N (DN, μmol.L ⁻¹)	66.9 (61.2)	25.2 (10.2)	*
Dissolved C (DOC, μmol.L ⁻¹)	512 (242)	764 (378)	*
DOC/DN	14.0 (9.0)	30.7 (8.9)	***
DOC/NO ₃ ⁻	35.8 (39.5)	290.0 (217.8)	ns

Table 1. Chemical properties of soil and soil solution (n = 16) and spruce (n = 16) soils. Statistical significances are marked by asterisks as follows: *p < 0.05, **p < 0.01, ***p < 0.001, ns – not significant.

The spruce soils contained more soil carbon (C_{TOT}) than the beech soils, but had the same amount of nitrogen (N_{TOT}), resulting in higher spruce total C/N ratio (Table 1). Similarly, the relative proportion of available C to N (DOC/DN) in the spruce soil was roughly double the quantity found (31) in the beech soils (14). The most pronounced difference between both soils was revealed by the proportion of DOC to NO₃⁻, which was eight times higher (290) in the spruce soil (36), mainly due to very low NO₃⁻ concentration in the soil solution.

Moreover, the spruce soil displayed a greater rate of net N mineralization (ammonification + nitrification) (Table 2). However, this was mainly due to an elevated net ammonification rate that was twice as high in the spruce when compared with the beech soil. Net nitrification was generally very low in both soils with no difference due to high data variability of both forests. Interestingly, the N mineralization pattern was not in accordance with N availability. There was more mineral N (NH₄⁺ + NO₃⁻, Table 1) available in beech soils with eight times higher concentration of NO₃⁻ in the soil solution; however, N mineralization potential was two times lower.

Both soils had similar rates of basal respiration, but spruce soil had a lower microbial biomass (C_{mic}, N_{mic}), resulting in higher specific respiration of ~12 nmol C.g C_{mic}⁻¹.d⁻¹ rather than ~9 nmol C.g C_{mic}⁻¹.d⁻¹ in the beech soil (Table 2). The amount of N in microbial biomass (N_{mic}) was proportionally lower compared to microbial carbon (C_{mic}) in the spruce soil, increasing the C_{mic}/N_{mic} ratio and pointing to the higher abundance of fungi in said soil. This was supported by qPCR data, which confirmed the higher fungal SSU gene copy numbers here (Table 3).

The ratios of microbial carbon (C_{mic}) to the dissolved and total C (C_{mic}/DOC, C_{mic}/C_{TOT}, Table 2) were lower in the spruce soil, which was in line with the lower C use efficiency (CUE) of the spruce microbial community (Table 2). It also corresponded with the 38% higher spruce specific respiration. Conversely, nitrogen use efficiency (NUE) was ~30% greater in the spruce soil compared with the beech (Table 2).

The spruce soil, furthermore, displayed a more substantial difference between biomass C_{mic}/N_{mic} and available resource DOC/DN (20 vs. 6, for spruce and beech, respectively), which means that microbes in the spruce soil must cope with much larger stoichiometric difference when utilizing the C and N resources.

Total enzymatic activity was lower in the spruce soil (Table 2). The pronounced differences were mainly in N and P acquiring enzymes that significantly influenced C/N and C/P enzyme ratios. C/N and C/P enzyme ratios were much higher in the spruce soil (Table 2), suggesting proportionally higher C to N mining from complex resources.

Most of the measured processes of microbial activity in the beech soil correlated with chemical properties, while in the spruce surprisingly, the only important relationship found was for C_{mic} and soil pH (Table S1). Basal respiration in beech soil correlated positively with the available C and N (C_{TOT}, N_{TOT}, DOC and NH₄⁺), microbial C (C_{mic}), and net ammonification. Similarly, C_{mic} and N_{mic} in the beech soil were both positively affected by soil C and N availability, mainly C_{TOT}, N_{TOT}, DOC, net ammonification and NH₄⁺ (Table S1). In the spruce, microbial C was related only to available NH₄⁺. A strong correlation with soil pH and microbial C and N was found also for BG, PME and NAG activity in the beech soil (data not shown). These results suggest that the beech soil exhibited a much closer connection between soil properties, organic matter transformation and microbial activity.

Composition of bacterial, archaeal and fungal communities. Bacterial communities in both soils were dominated by three phyla: Acidobacteria, Actinobacteria and Proteobacteria which together represented 65% and 63% of assigned sequences in the beech and spruce soil, respectively (Fig. 1). Acidobacteria and Actinobacteria were more abundant in the spruce soil (29% and 17%) than in the beech (24% and 14%). On the other hand, the beech soil sustained larger community of Proteobacteria, Planctomycetes and Verrucomicrobia (21%, 4%, and 8% compared with 17%, 3% and 6% for the spruce soil). Except Halobacteria, all detected Archaeal classes: Thermoplasmata, Soil crenarchaeal group (SCG) and South African gold mine crenarchaeal group 1 (SAGMCG-1) were more numerous in the beech soil. The most pronounced difference showed archaeal class SCG from Thaumarchaeota phylum, which comprised 41% in the beech soil but only 4% in the spruce soils (Fig. 1).

	Beech	Spruce	stat.
Microbial carbon (C_{mic} , $\mu\text{mol.g}^{-1}$)	346.2 (68.9)	265.1 (77.3)	**
Microbial nitrogen (N_{mic} , $\mu\text{mol.g}^{-1}$)	45.5 (11.3)	25.8 (9.0)	***
C_{mic}/N_{mic}	7.9 (1.5)	11.0 (2.2)	***
C_{mic}/C_{TOT}	11.1 (2.8)	7.9 (2.3)	***
C_{mic}/DOC	6.4 (1.4)	5.1 (1.3)	*
Basal respiration ($\mu\text{mol.g}^{-1}\text{d}^{-1}$)	3.1 (1.2)	3.1 (0.7)	ns
Specific respiration ($\text{nmol C.g}^{-1}\text{C}_{mic}^{-1}\text{d}^{-1}$)	8.9 (2.7)	12.3 (3.7)	**
Carbon use efficiency (CUE) ^a	0.36 (0.16)	0.24 (0.06)	**
Nitrogen use efficiency (NUE) ^a	0.51 (0.13)	0.66 (0.12)	**
Critical C/N ratio ($C:N_{CR}$)	25.6 (11.5)	46.0 (8.3)	***
Net ammonification ($\text{nmol.g}^{-1}\text{h}^{-1}$)	130 (80)	250 (140)	**
Net nitrification ($\text{nmol.g}^{-1}\text{h}^{-1}$)	28 (12)	11(7)	ns
β -Glucosidase (BG, $\mu\text{mol.g}^{-1}\text{h}^{-1}$)	1.14 (0.41)	0.99 (0.22)	ns
Cellobiohydrolase (CEL, $\mu\text{mol.g}^{-1}\text{h}^{-1}$)	0.19 (0.07)	0.15 (0.05)	ns
N-acetyl- β -D-glucosaminidase (NAG, $\mu\text{mol.g}^{-1}\text{h}^{-1}$)	0.45 (0.31)	0.15 (0.05)	***
Phosphatase (PME, $\mu\text{mol.g}^{-1}\text{h}^{-1}$)	1.75 (0.57)	1.27 (0.28)	**
Leucine-aminopeptidase (LEU, $\mu\text{mol.g}^{-1}\text{h}^{-1}$)	0.03 (0.01)	0.01 (0.01)	***
BG/PME	0.66 (0.10)	0.80 (0.13)	**
BG/NAG	3.3 (1.6)	7.3 (2.5)	**
BG/LEU	40.9 (13.4)	85.2 (33.3)	***

Table 2. Biochemical properties of beech (n = 16) and spruce (n = 16) soils. Statistical significances are marked by asterisks as follows: *p < 0.05, **p < 0.01, ***p < 0.001, ns – not significant, nc – not calculated; ^aCUE and NUE were calculated from ^aavailable C (DOC) and N ($\text{NO}_3^- + \text{NH}_4^+$).

	Beech	Spruce	
Chao1 index (prokaryota)	3028 (370)	2255 (469)	***
Chao1 index (fungi)	100 (53)	139 (92)	ns
Observed species (prokaryota)	1977 (127)	1553 (182)	***
Observed species (fungi)	64 (26)	77 (34)	ns
Bacterial abundance (SSU gene copies.ngDNA ⁻¹)	6.7×10^4 (2.6×10^4)	11.7×10^4 (4.9×10^4)	**
Archaeal abundance (SSU gene copies.ngDNA ⁻¹)	2.0×10^3 (1.1×10^3)	0.9×10^3 (1.0×10^3)	**
Fungal abundance (SSU gene copies.ngDNA ⁻¹)	0.3×10^4 (0.4×10^4)	0.9×10^4 (0.7×10^4)	*
F/B ratio	0.05 (0.06)	0.08 (0.05)	ns
Proteo/Acido ratio	1.6 (0.4)	1.3 (0.3)	**

Table 3. Microbial community properties of beech (n = 16) and spruce (n = 16) soils. Statistical significances are marked by asterisks as follows: *p < 0.05, **p < 0.01, ***p < 0.001, ns – not significant.

Using Bray-Curtis distances and the Ward linkage between OTUs, 4 large OTU clusters showed distinct abundance patterns between the spruce and beech prokaryotic communities (Fig. S8). The cluster I and cluster II represented the most abundant OTUs assigned mainly to Acidobacteriaceae (Subgroup 1), showing significantly higher abundances in the spruce community. In contrast, other families of Xanthobacteraceae (Alphaproteobacteria), Bradyrhizobiaceae (Alphaproteobacteria), Opitutaceae (Verrucomicrobia) and Acidobacteria (Subgroup 3) formed larger proportions in the beech community. Deeper taxonomical analyses revealed that the 10 most abundant bacterial genera represented on average 43% and 36% in the spruce and beech prokaryotic communities, respectively (Fig. S9). Uncultured Acidobacteriaceae (Subgroup 1) bacterium, Acidothermus, Acidobacterium and Rhodanobacter figured more prominently in the spruce community. On the other hand, uncultured bacterium from Verrucomicrobia phylum, uncultured bacterium from Acidobacteria subgroup 2 and uncultured Xanthobacteriaceae bacterium were more abundant in the beech prokaryotic community.

The beech and spruce soils also differed in their alpha diversity of prokaryotic and fungal communities. The former possessed greater prokaryotic richness as indicated by Chao1 index (beech soil – 1881; spruce soil – 1389). However, the opposite was true for the fungal community, though the difference was not significant (Table 3).

The beech and spruce prokaryotic communities were clearly separated by the first RDA axis, explaining 43% of the variability in prokaryotic communities (Fig. 2). Soil pH, DOC:NO_3^- ratio and base cations ($\text{Mg}^{2+} + \text{Ca}^{2+}$) were the three environmental explanatory variables with significant effects. The relative abundance of Acidobacteria and Actinobacteria correlated positively with the higher DOC:NO_3^- ratio and with the lower

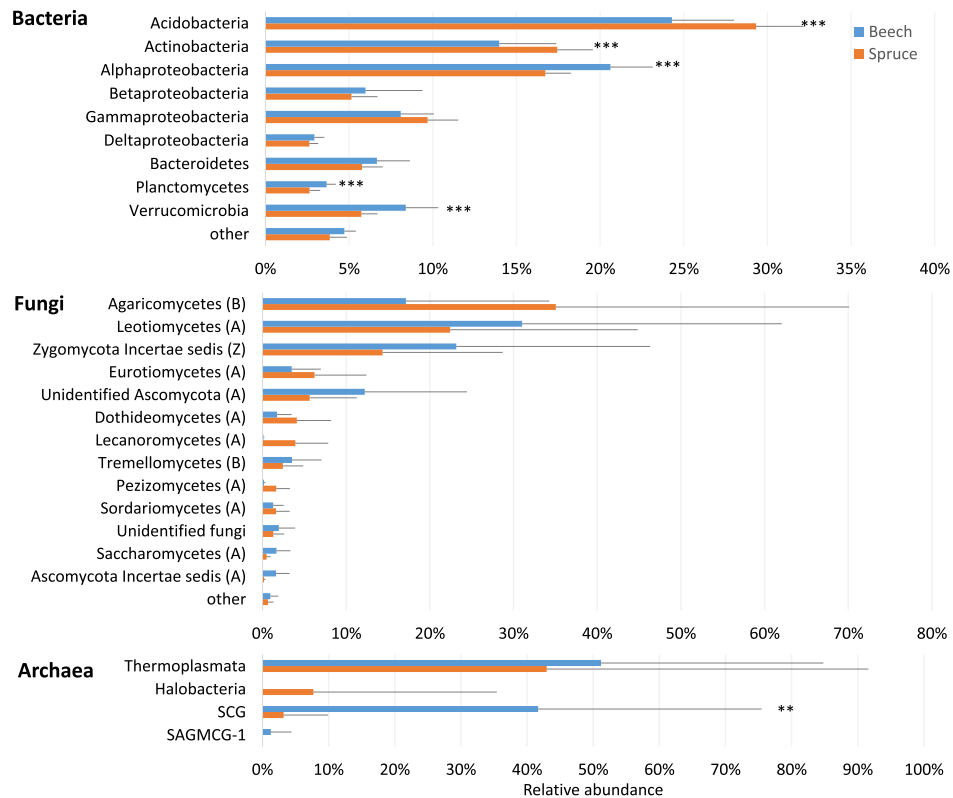


Figure 1. Differences in the composition of bacterial, fungal and archaeal communities between the beech ($n = 16$) and spruce ($n = 16$) soils. Only those phyla and classes with more than 1% of relative abundance are shown. Statistical significances are marked by asterisks as follows: * $p < 0.05$, ** $p < 0.01$, *** $p < 0.001$.

pH, while the less acidic, NO_3^- rich beech soil (Fig. 2, Table 1) supported greater numbers of Proteobacteria, Planctomycetes and Verrucomicrobia. These five most abundant phyla were the main phyla separating the beech from the spruce soil (Fig. 2). The separation of spruce and beech communities was additionally confirmed by metric and nonmetric multidimensional scaling (MDS, NMDS) analysis using Bray-Curtis distances. The MDS and NMDS analyses (Figs S10 and S12) using Bray-Curtis distances, which were done on OTU level, showed similar separation as RDA analyses using Euclidean distances (Figs 2 and S11).

Due to the very high variability among the samples, differences of major fungal phyla were not statistically significant (Fig. 1, Figs S11 and S12a,b). The spruce soil levels of Agaricomycetes (Basidiomycota) were higher (35%) than those for the beech soil (17%) while opposite was true for Leotiomycetes (Ascomycota) (beech soil – 32%; spruce soil – 25%). Analyses of fungal life strategies showed that saprotrophic fungi were more abundant in the beech soil (37%) than in the spruce soil (24%), while the opposite was true for ectomycorrhizal fungi, which amounted to 16% in the spruce and 9% in the beech soil, respectively (Fig. S6).

Both soils differed in prokaryotic functional potential calculated by PICRUSt⁵⁷ algorithms. Principal component analysis of functional potential separated the beech and spruce microbial communities along the first PCA axis, showing differences in functional potential in the beech and spruce microbial communities, however with more functionally similar samples than the taxonomic differences (Figs 1 and S5). PICRUSt functional analysis showed that the beech and spruce microbial communities differed mainly in abundance of transporting systems, N metabolism and peptidases (Fig. S4). It supported measured differences in N enzymatic activity and showed more copiotrophic nature of the beech community (i.e. more transporting systems and more processes connected with membrane like respiration).

For the OTUs, which were classified at the genus level, it was also possible to assign functional genes based on RDP FunGene database (Table S2). By combining SSU qPCR data and relative abundances of assigned bacterial genera, we were able to quantitatively identify the main N transformation pathways (Fig. 3). It allows us to reconstruct and identify differences in the N cycle in the beech and spruce microbial communities (Figs 3 and S7). Microorganisms capable of nitrate reduction (napA, narG genes), denitrification (nirK, nirS, norB, nosZ genes), N_2 fixation (nifH gene) and NH_4^+ oxidation (amoA) were more abundant in the spruce than in the beech community. The abundance of microorganisms capable of dissimilative nitrate reduction to ammonium (DNRA, nrfA gene), however, did not differ between the beech and spruce community. Therefore, in the spruce soil, the higher proportion of NO_3^- can be potentially lost via denitrification (denitrification to DNRA ratio is 3) while in the beech soil, the higher proportion of NO_3^- can be recycled in the soil system and the microbial community most likely via DNRA (denitrification to DNRA ratio is 1.4).

In the next step, network analysis was performed to describe relationships between distinct OTUs in the beech and spruce prokaryotic communities and identify the most important OTUs (i.e. keystone OTUs). We found

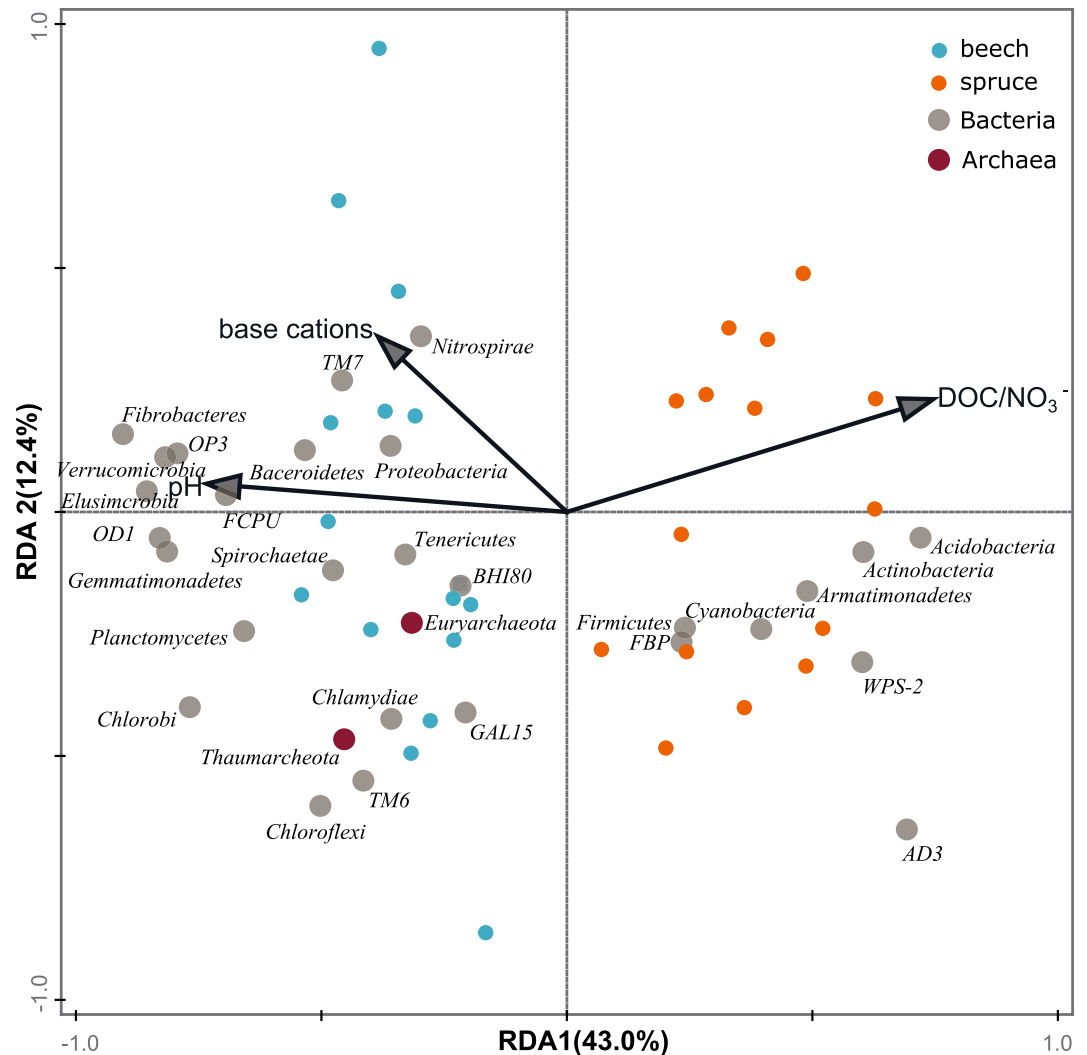


Figure 2. Redundancy analyses (RDA) of prokaryotic community. RDA of relative OTU abundances of prokaryotic phyla in the beech ($n = 16$) and spruce ($n = 16$) soils. The relation of the environmental variables to the prokaryotic community composition is shown. Each point represents an individual soil sample used in the analysis. The direction and length of arrows show the correlational strength between the abundance of each prokaryotic phylum and environmental variable. RDA1 axis explained 43.0% and RDA2 explained 12.4% of variability in prokaryotic community composition.

dramatic differences between the beech and spruce prokaryotic networks (Fig. 4a,b, Table 4, Fig. S14). While in the beech prokaryotic network the number of relationships was low and infrequent (more separate groups of interacting OTUs with only 51 significantly interacting OTUs), the opposite was true for the spruce network (103 significantly interacting OTUs with dense interacting network). The network analyses with the support of 100 instances of bootstrapping revealed 145 significant interactions (edges) in the spruce prokaryotic community while in the beech community only 45 showed very intense interconnection of prokaryotes (Fig. 4b). Interestingly, all interactions in the beech and spruce prokaryotic communities were positive (co-presence). We specifically identified 7 potential keystone OTUs in both communities (Table S2). The spruce potential keystones were mainly from the phylum Acidobacteria (4 out of 7 keystones) while the beech keystones recruited from Proteobacteria (3 out of 7 keystones). In the beech soil, microorganisms capable of DNRA (*Acidothermus*, *Planctomyces*, *Opitutus*) were among the potential keystone OTUs, but in the spruce community nitrate reducing (*Acidobacterium*) and denitrifying microorganisms (*Acidothermus*, *Herminiimonas*) dominated (Table 4).

The microbial networks of the beech and spruce fungal community showed similar trends as prokaryotic ones (Fig. S13a,b). The spruce fungal network had more interacting species (n . of nodes = 117) and also more connections (n . of edges = 498) than beech community which had 51 nodes and 246 edges, respectively. Species of *Mortierella* (Zygomycota) and *Cryptococcus* (Basidiomycota) were the most interacting in beech and spruce community, respectively.

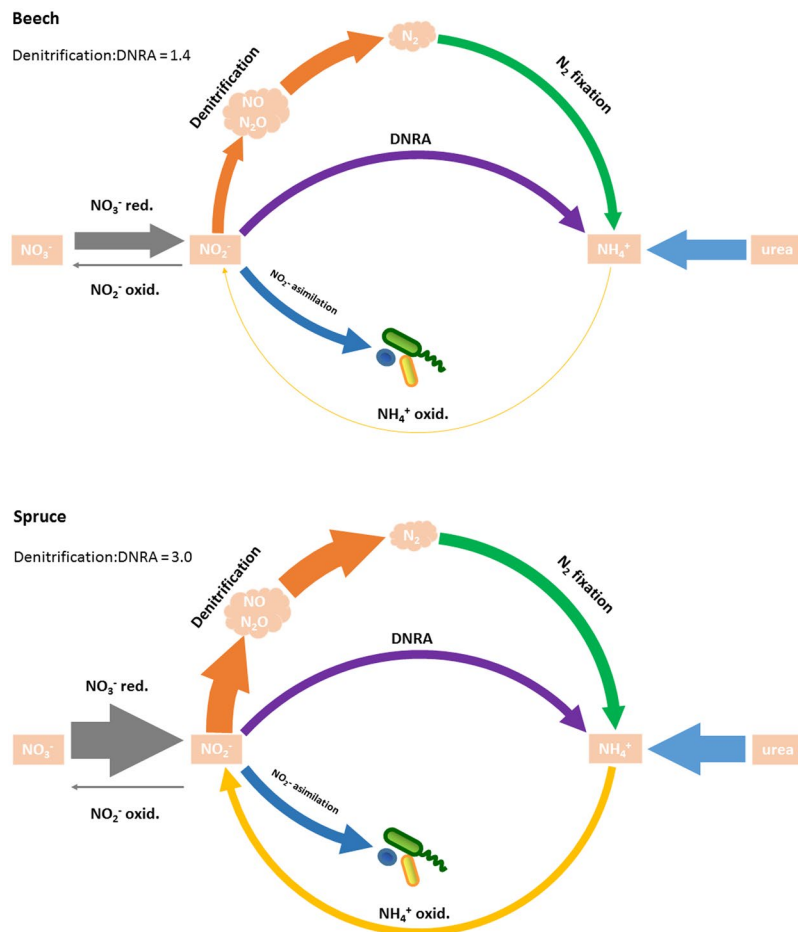


Figure 3. Conceptual scheme of main N cycle pathways in the spruce and beech soils. Nitrogen transformation processes are depicted with different colors. Pathways are based on functional assignment (RDP FunGene database, Table S2). Thickness of the arrows corresponds to absolute abundances of assigned bacterial functional guilds recalculated by qPCR.

Discussion

Our study makes use of the comparison of two closely located forests (1 km of each other) which are situated on the same acid bedrock, have similar climate and deposition history but differ in tree dominants. In the spruce forest the nitrates in the soil leachate have almost diminished since the 1990s⁷, while in the beech forest the nitrate leaching still continues. Soil solution chemistry revealed less acidic conditions in the beech compared to the spruce forest, which was surely the effect of litter type and long-term lower dry deposition⁶¹. Soil prokaryotic communities, not fungi, differed in their composition substantially between the spruce and beech, and their structures were to a certain extent linked to different soil C and N biogeochemistry.

The main difference between the spruce and beech microbial community was found in the structure of prokaryotes (Fig. 2). The spruce prokaryotic community had lower species diversity but more abundant than the beech community (Table 3), which corresponds to the published data of similar biomes⁶². It comprised three main bacterial phyla: Acidobacteria, Proteobacteria and Actinobacteria (Fig. 1). Although Archaea formed only a minor population compared to bacteria, especially in the spruce forest (Table 3), a considerable difference was found for the Soil Crenarchaeotic Group (SCG) from the phylum Thaumarchaeota that comprises over 40% of relative abundance in the beech soil compared to only a negligible part of the spruce archaeal community (Fig. 1).

The beech and spruce fungal communities were not separated (Fig. S11) and did not differ significantly even in relative abundances (Fig. 1). One reason could be that our sampling strategy, in which we wanted to pinpoint the most pronounced functional differences in the microbial community⁶³ and thus sampled the most active forest floor layer as a mixture (Of + Oh + A), diminished the differences between the beech and spruce fungal communities, usually showing the depth stratification. Despite this, we found prevailing saprotrophic strategy over the mycorrhizal in both fungal communities (Fig. S6), which is most probably the effect of former N deposition⁶⁴. The fungal community composition comprised of Ascomycota, Basidiomycota and Zygomycota (Fig. 1), which is in line with globally described patterns of temperate forests⁶⁵.

Despite only a narrow pH range and little difference between both forests (~0.2 pH units), pH and base cation concentration still explained most of the differences between the spruce and beech prokaryotic community (Fig. 2). Since soil base saturation is related to soil pH through the exchange of H⁺ between organo-mineral complexes and soil solution, it is reasonable to assume that both parameters shaped the composition of the

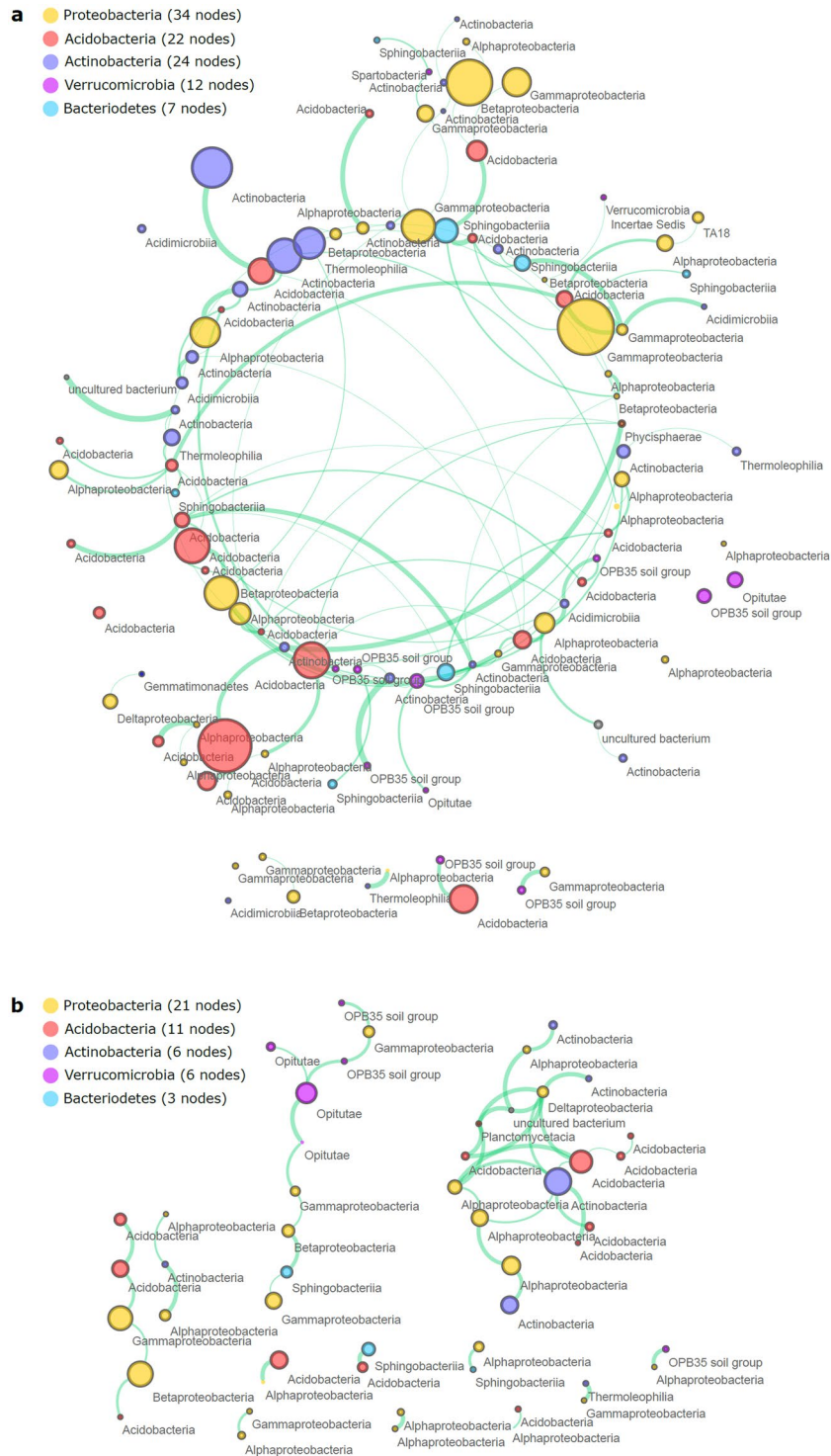


Figure 4. OTU network analyses of the beech (a) and spruce (b) prokaryotic communities. Each OTU (node) is colored by the phylum it belongs to. Labels of nodes shows respective bacterial or archaeal classes. The size of node corresponds to the average abundance of each OTU. Green color of edges shows positive relationship (i.e. co-presence of OTUs) and red edge color shows negative relationship (i.e. mutual exclusion of OTUs).

prokaryotic community simultaneously. Our results conform with the general actuality that soil pH is one of the strongest predictors of microbial community composition^{12,66–70} and that Acidobacteria often predominate in acidic soils⁷¹.

In our study, lower pH was always connected with a higher proportion of Acidobacteria and Actinobacteria (Fig. 2), representing together ~47% and ~37% of the spruce and beech bacteria, respectively (Fig. 1). This was within a range of other forest studies^{62,72}. In both forests, the subgroup 1 was the most abundant Acidobacteria

Phylum	Genus	Degree	Betweenness Centrality	Closeness Centrality	Function in N cycle
Potential keystone species in beech prokaryotic community					
Proteobacteria	<i>uncultured bacterium</i>	6	0,413	0,516	—
Actinobacteria	<i>Acidothermus</i>	6	0,385	0,516	denitrifier
Planctomycetes	<i>Planctomyces</i>	4	0,101	0,432	DNRA, nitrate reducer
Acidobacteria	<i>uncultured bacterium</i>	4	0,239	0,471	—
Proteobacteria	<i>uncultured bacterium</i>	4	0,138	0,471	—
Proteobacteria	<i>uncultured</i>	3	0,233	0,400	—
Verrucomicrobia	<i>Opitutus</i>	3	0,639	0,409	DNRA, nitrate reducer
Potential keystone species spruce prokaryotic community					
Acidobacteria	<i>Acidobacterium</i>	10	0,163	0,290	nitrate reducer
Actinobacteria	<i>uncultured Actinomycetales</i>	9	0,270	0,321	—
Acidobacteria	<i>Candidatus Solibacter</i>	7	0,133	0,271	—
Acidobacteria	<i>Candidatus Solibacter</i>	7	0,224	0,311	—
Actinobacteria	<i>Acidothermus</i>	7	0,118	0,294	denitrifier
Proteobacteria	<i>Hermiimonas</i>	6	0,099	0,295	denitrifier
Acidobacteria	<i>Candidatus Koribacter</i>	6	0,095	0,281	—

Table 4. Keystone OTUs in beech and spruce prokaryotic community. Basic properties of keystone species (degree, betweenness centrality, closeness centrality) are shown. Taxonomic classification is based on Silva 119 database. Annotated function of known bacterial genera in N cycle are shown in the last column.

group represented mostly by genera *Acidobacterium* (4% and 3% for spruce and beech, respectively), *Granulicella* (3% and 2% for spruce and beech, respectively) and *Candidatus Koribacter* (1% in both soils). *Acidobacterium* and *Granulicella* were in the top 10 most abundant genera. Jones *et al.*⁷³ showed that the abundance of Subgroup 1 strongly increased with decreasing soil pH. The high abundance of Subgroup 1 is most probably the reason why soil pH was the main important predictor of prokaryotic community composition.

In the beech community, the members of the phylum Proteobacteria were more abundant than in the spruce prokaryotic community. Within the Proteobacteria, the uncultured bacterium from the family Xanthobacteriaceae (Alphaproteobacteria) dominated. Bacteria from this family are moderately acidophilic. They are usually isolated from decaying organic material⁷⁴ as well as from nutrient rich rhizosphere⁷⁵. The next higher abundance of Verrucomicrobia and Planctomycetes in the beech community could be related, in addition to the less pronounced acidity effect⁶⁷, to high soil N availability (Table 1). Buckley *et al.*⁷⁶ (2006) showed that species richness of Planctomycetes correlated highly with NO_3^- spatial distribution in soil, and Navarrete *et al.*⁷² concurrently found that a community of Verrucomicrobia exhibited higher abundances in soils of higher fertility.

It has been suggested that soil bacteria can be classified into copiotrophic and oligotrophic categories (corresponding to the r- and K-selected strategies)^{27,68}. Although this concept can be viewed as a simplification, its application to compositional genomic data allows us to describe the ecological requirements of the soil microbial community. We expected that both forests could generally create habitats more suitable for fast-growing copiotrophs as both were exposed to high N deposition. Our data showed that the beech soil was relatively richer in available N yet at the same time much poorer in C compared to the spruce soil (Table 1). Moreover, the second most significant factor that separated the spruce and beech prokaryotic communities was the DOC/NO_3^- ratio (Fig. 2). This inverse relation of both elements has been recognized as a primary predictor of soil N retention ability^{10,11}. At the same time, we found a higher proportion of Proteobacteria to Acidobacteria in the beech than in the spruce microbial community (1.6 vs. 1.3, Table 3).

According to Fierer *et al.*⁶⁸, the phylum Proteobacteria generally comprises copiotrophic taxa. They preferentially consume labile and readily available organic C, have high nutritional requirements and exhibit high growth rates when resources are abundant^{68,77}. On the other hand, Acidobacteria can be considered as oligotrophs, which are slow-growing and exploit environments with lower nutrients, lower C availability or substrates of lower quality⁶⁸. They are, therefore, able to outcompete copiotrophs in these conditions due to their higher substrate affinities and more efficient enzymatic apparatus for utilizing complex biopolymers⁷⁸. Recent studies argue that, despite being oligotrophic, some subgroups of Acidobacteria show high relative abundances also in C rich conditions^{73,80}, indicating that additional factors other than C availability drive the metabolism of various Acidobacterial subgroups. Several studies also showed that Acidobacteria decrease under elevated N conditions while Proteobacteria increase^{20,27,79,80}. Our results suggest that the ratio of abundances of these large bacterial phyla may be connected with (i) soil N availability and (ii) the quality of C substrate rather than only C concentration^{81,82}.

Organic matter decomposition is driven by the availability of labile C and N⁸³. The DOC and DN in the soil leachate determined in our study represent a measure of labile resources, which control organic matter decomposition, including the activities of soil extracellular enzymes. Because these enzymes release low molecular weight compounds from complex biomolecules (e.g. cellulose, proteins), they also directly influence the proportions of dissolved C and N²⁵. In the spruce soil, C acquiring enzymes (Table 2) were proportionally higher compared to N acquiring enzymes, which is in accordance with the measured higher DOC:DN ratio (Table 1) and

suggests the decomposition of rather complex organic matter in the spruce soils. This corresponds with higher fungal abundance and also higher abundance of bacteria from the families Acidobacteriaceae subgroup 1 and Acidothermaceae, which are able to decompose complex substrates such as polyphenols and chitin and whose distribution in soils is connected with the quality of soil organic C⁸⁴.

The ability of soil to immobilize nitrogen is closely connected with its C-to-N stoichiometry^{9,10,85,86}. Although both soils showed similar net nitrification rates, nitrate concentrations were high only in the beech soil solution. It has been shown that during decomposition all organic N can be used for building microbial biomass when C is in excess³⁹. Microbes can then immobilize additional mineral N from the soil solution to meet their demands^{9,87}, or they can start to use nitrates in reduction processes of microbial energy metabolism (denitrification and/or dissimilative nitrate reduction to ammonia (DNRA)⁴. It might be that in C rich spruce soil with high C acquiring enzyme activity and net N mineralization, immobilization of mineral N could be more significant than in the beech soil. Concurrently, we found low C while high N use efficiencies and high specific respiration in the spruce soil supporting our assumption of possible C oversupply of spruce microbes (Table 2).

We examined the hypothesis of high nitrate immobilization in the spruce soil from the perspective of microbial community composition. Linking taxonomic classification with functional potential allowed us to identify bacterial functional guilds (e.g. N₂ fixators, nitrifiers, denitrifiers and bacteria capable of DNRA) responsible for key transformations of mineral N. In the spruce community, the occurrence of NO₃⁻ to NO₂⁻ reducers was twice as high as in the beech community. However, NO₂⁻ is a very labile compound and is immediately reduced to N gases through denitrification or via DNRA to NH₄⁺. Our data showed that denitrifiers in the spruce community were proportionally more abundant than bacteria capable of DNRA (3:1 ratio, Fig. 3) compared to the beech community. Marked differences were mainly in the abundance of nirK denitrifiers, whose abundance correlates closer with the available C compared to nirS denitrifiers⁸⁸. In contrast, the beech microbial community had a lower denitrification-to-DNRA ratio (1.4:1, Fig. 3), allowing more N to be recycled back to NH₄⁺ and possibly to NO₃⁻ via nitrification.

The functional analyses revealed that low NO₃⁻ concentration in the spruce soil solution may be the result of N losses through denitrification. This supports the generally observed fact that DOC/NO₃⁻ stoichiometry regulates ecosystem NO₃⁻ retention^{11,89}. Under the high DOC/NO₃⁻ ratio (higher than 150⁸⁹), which supplies sufficient organic C to microorganisms, denitrification predominates over DNRA and N can be lost from the soil to the atmosphere. Under low DOC/NO₃⁻¹¹, DNRA is higher or equal to denitrification and N can be recycled in the soil via NH₄⁺.

Microbial network analyses supported the importance of denitrifiers and bacteria capable of DNRA in the soil community. Both groups were among the 10 potential keystone species of both communities (Fig. 4, Table S4). Microbes capable of DNRA (*Planctomyces*, *Opitutus*) were identified as keystone in the beech soil, while denitrifiers (*Acidothermus*, *Herminiimonas*) were instead significant players in the spruce soil. Furthermore, microbes in the spruce community showed a much higher degree of associations than the beech microbes. It points to the much higher microbial interconnection in the C rich environment, probably due to the higher substrate complexity, whose degradation needs to be synchronized by a variety of microbial functional guilds. Higher interconnection may also be an indirect result of the higher abundance of fungi, which interconnects by hyphal growth spatially distant microbes⁹⁰. In contrast, microbes in the beech community were associated very rarely, partly because of, perhaps, their rather copiotrophic nature (quickly growing, quickly dying), and do not have, therefore, the reason and time to create more dense and interconnected microbial network.

Here we presented that the DNA sequencing approach in combination with in-silico functional analysis of microbial community structure can be a useful tool in predicting soil N biogeochemistry. Both forest soil microbial communities differed in their taxonomic diversity and functional diversity of the N cycle resulting in different potentials of soil N immobilization. We demonstrated that nitrates may be lost through denitrification in N saturated soils under recovery when organic matter decomposition is restored and the carbon availability increases⁷. Our study represents a basis for future testing of the nitrate reduction as potentially more important N immobilization process than was previously thought in acid forest soils.

References

- Clark, C. M. *et al.* Environmental and plant community determinants of species loss following nitrogen enrichment. *Ecol Lett* **10**, 596–607, doi:10.1111/j.1461-0248.2007.01053.x (2007).
- Cleland, E. E. & Harpole, W. S. Nitrogen enrichment and plant communities. *Year in Ecology and Conservation Biology 2010* **1195**, 46–61, doi:10.1111/j.1749-6632.2010.05458.x (2010).
- LeBauer, D. S. & Treseder, K. K. Nitrogen limitation of net primary productivity in terrestrial ecosystems is globally distributed. *Ecology* **89**, 371–379, doi:10.1890/06-2057.1 (2008).
- Kopacek, J. *et al.* Nitrogen, organic carbon and sulphur cycling in terrestrial ecosystems: linking nitrogen saturation to carbon limitation of soil microbial processes. *Biogeochemistry* **115**, 33–51, doi:10.1007/s10533-013-9892-7 (2013).
- Treseder, K. K. Nitrogen additions and microbial biomass: a meta-analysis of ecosystem studies. *Ecology Letters* **11**, 1111–1120, doi:10.1111/j.1461-0248.2008.01230.x (2008).
- Aber, J. *et al.* Nitrogen saturation in temperate forest ecosystems - Hypotheses revisited. *Bioscience* **48**, 921–934, doi:10.2307/1313296 (1998).
- Oulehle, F. *et al.* Major changes in forest carbon and nitrogen cycling caused by declining sulphur deposition. *Global Change Biology* **17**, 3115–3129, doi:10.1111/j.1365-2486.2011.02468.x (2011).
- Evans, C. D. *et al.* Recovery from acidification in European surface waters. *Hydrol Earth Syst Sc* **5**, 283–297 (2001).
- Tahovska, K. *et al.* Microbial N immobilization is of great importance in acidified mountain spruce forest soils. *Soil Biol Biochem* **59**, 58–71, doi:10.1016/j.soilbio.2012.12.015 (2013).
- Evans, C. D. *et al.* Evidence that soil carbon pool determines susceptibility of semi-natural ecosystems to elevated nitrogen leaching. *Ecosystems* **9**, 453–462, doi:10.1007/s10021-006-0051-z (2006).
- Taylor, P. G. & Townsend, A. R. Stoichiometric control of organic carbon-nitrate relationships from soils to the sea. *Nature* **464**, 1178–1181, doi:10.1038/nature08985 (2010).

12. Graham, E. B. *et al.* Microbes as Engines of Ecosystem Function: When Does Community Structure Enhance Predictions of Ecosystem Processes? *Front Microbiol* **7**, doi:10.3389/fmicb.2016.00214 (2016).
13. Demoling, F., Nilsson, L. O. & Baath, E. Bacterial and fungal response to nitrogen fertilization in three coniferous forest soils. *Soil Biology & Biochemistry* **40**, 370–379, doi:10.1016/j.soilbio.2007.08.019 (2008).
14. Hogberg, M. N., Baath, E., Nordgren, A., Arnebrant, K. & Hogberg, P. Contrasting effects of nitrogen availability on plant carbon supply to mycorrhizal fungi and saprotrophs - a hypothesis based on field observations in boreal forest. *New Phytologist* **160**, 225–238, doi:10.1046/j.1469-8137.2003.00867.x (2003).
15. Boot, C. M., Hall, E. K., Deneff, K. & Baron, J. S. Long-term reactive nitrogen loading alters soil carbon and microbial community properties in a subalpine forest ecosystem. *Soil Biol Biochem* **92**, 211–220, doi:10.1016/j.soilbio.2015.10.002 (2016).
16. Frey, S. D., Knorr, M., Parrent, J. L. & Simpson, R. T. Chronic nitrogen enrichment affects the structure and function of the soil microbial community in temperate hardwood and pine forests. *Forest Ecology and Management* **196**, 159–171, doi:10.1016/j.foreco.2004.03.018 (2004).
17. Waldrop, M. P., Zak, D. R., Sinsabaugh, R. L., Gallo, M. & Lauber, C. Nitrogen deposition modifies soil carbon storage through changes in microbial enzymatic activity. *Ecological Applications* **14**, 1172–1177, doi:10.1890/03-5120 (2004).
18. Knorr, M., Frey, S. D. & Curtis, P. S. Nitrogen additions and litter decomposition: a meta-analysis (vol 86, pg 3252, 2005). *Ecology* **89**, 888–888 (2008).
19. Janssens, I. A. *et al.* Reduction of forest soil respiration in response to nitrogen deposition. *Nat Geosci* **3**, 315–322, doi:10.1038/ngeo844 (2010).
20. Ramirez, K. S., Craine, J. M. & Fierer, N. Consistent effects of nitrogen amendments on soil microbial communities and processes across biomes. *Global Change Biol* **18**, 1918–1927, doi:10.1111/j.1365-2486.2012.02639.x (2012).
21. Hagedorn, F., Spinnler, D. & Siegwolf, R. Increased N deposition retards mineralization of old soil organic matter. *Soil Biol Biochem* **35**, 1683–1692, doi:10.1016/j.soilbio.2003.08.015 (2003).
22. Boberg, J. B., Finlay, R. D., Stenlid, J. & Lindahl, B. D. Fungal C translocation restricts N-mineralization in heterogeneous environments. *Functional Ecology* **24**, 454–459, doi:10.1111/j.1365-2435.2009.01616.x (2010).
23. Boberg, J. B., Finlay, R. D., Stenlid, J., Ekblad, A. & Lindahl, B. D. Nitrogen and Carbon Reallocation in Fungal Mycelia during Decomposition of Boreal Forest Litter. *Plos One* **9**, doi:10.1371/journal.pone.0092897 (2014).
24. de Vries, F. T., Hoffland, E., van Eekeren, N., Brussaard, L. & Bloem, J. Fungal/bacterial ratios in grasslands with contrasting nitrogen management. *Soil Biol Biochem* **38**, 2092–2103, doi:10.1016/j.soilbio.2006.01.008 (2006).
25. Schimel, J. P. & Bennett, J. Nitrogen mineralization: Challenges of a changing paradigm. *Ecology* **85**, 591–602, doi:10.1890/03-8002 (2004).
26. Ramirez, K. S., Lauber, C. L., Knight, R., Bradford, M. A. & Fierer, N. Consistent effects of nitrogen fertilization on soil bacterial communities in contrasting systems. *Ecology* **91**, 3463–3470, doi:10.1890/10-0426.1 (2010).
27. Fierer, N. *et al.* Comparative metagenomic, phylogenetic and physiological analyses of soil microbial communities across nitrogen gradients. *Isme J* **6**, 1007–1017, doi:10.1038/ismej.2011.159 (2012).
28. Campbell, B. J., Polson, S. W., Hanson, T. E., Mack, M. C. & Schuur, E. A. G. The effect of nutrient deposition on bacterial communities in Arctic tundra soil. *Environ Microbiol* **12**, 1842–1854, doi:10.1111/j.1462-2920.2010.02189.x (2010).
29. Davis, K. E. R., Sangwan, P. & Janssen, P. H. Acidobacteria, Rubrobacteridae and Chloroflexi are abundant among very slow-growing and mini-colony-forming soil bacteria. *Environ Microbiol* **13**, 798–805, doi:10.1111/j.1462-2920.2010.02384.x (2011).
30. Roller, B. R. K. & Schmidt, T. M. The physiology and ecological implications of efficient growth. *Isme J* **9**, 1481–1487, doi:10.1038/ismej.2014.235 (2015).
31. Oulehle, F., Hofmeister, J., Cudlin, P. & Hruska, J. The effect of reduced atmospheric deposition on soil and soil solution chemistry at a site subjected to long-term acidification, Nacetin, Czech Republic. *Sci Total Environ* **370**, 532–544, doi:10.1016/j.scitotenv.2006.07.031 (2006).
32. Berge, D., Fjeld, E., Hindar, A. & Kaste, O. Nitrogen retention in two Norwegian watercourses of different trophic status. *Ambio* **26**, 282–288 (1997).
33. Oulehle, F., Růžek, M., Tahovská, K., Bárta, J. & Mýška, O. Carbon and Nitrogen Pools and Fluxes in Adjacent Mature Norway Spruce and European Beech Forests. *Forests* **7** (2016).
34. Vance, E. D., Brookes, P. C. & Jenkinson, D. S. An Extraction Method for Measuring Soil Microbial Biomass-C. *Soil Biol Biochem* **19**, 703–707, doi:10.1016/0038-0717(87)90052-6 (1987).
35. Brookes, P. C. Microbial Biomass and Activity Measurements in Soil. *J Sci Food Agr* **36**, 269–270 (1985).
36. Ste-Marie, C. & Pare, D. Soil, pH and N availability effects on net nitrification in the forest floors of a range of boreal forest stands. *Soil Biol Biochem* **31**, 1579–1589, doi:10.1016/S0038-0717(99)00086-3 (1999).
37. Santruckova, H., Tahovska, K. & Kopacek, J. Nitrogen transformations and pools in N-saturated mountain spruce forest soils. *Biology and Fertility of Soils* **45**, 395–404, doi:10.1007/s00374-008-0349-4 (2009).
38. Manzoni, S., Jackson, R. B., Trofymow, J. A. & Porporato, A. The global stoichiometry of litter nitrogen mineralization. *Science* **321**, 684–686, doi:10.1126/science.1159792 (2008).
39. Mooshammer, M., Wanek, W., Zechmeister-Boltenstern, S. & Richter, A. Stoichiometric imbalances between terrestrial decomposer communities and their resources: mechanisms and implications of microbial adaptations to their resources. *Front Microbiol* **5**, doi:10.3389/Fmicb.2014.00022 (2014).
40. Bárta, J., Slajsova, P., Tahovska, K., Picek, T. & Santruckova, H. Different temperature sensitivity and kinetics of soil enzymes indicate seasonal shifts in C, N and P nutrient stoichiometry in acid forest soil. *Biogeochemistry* **117**, 525–537, doi:10.1007/s10533-013-9898-1 (2014).
41. Leininger, S. *et al.* Archaea predominate among ammonia-oxidizing prokaryotes in soils. *Nature* **442**, 806–809, doi:10.1038/Nature04983 (2006).
42. Muyzer, G., Dewaal, E. C. & Uitterlinden, A. G. Profiling of Complex Microbial-Populations by Denaturing Gradient Gel-Electrophoresis Analysis of Polymerase Chain Reaction-Amplified Genes-Coding for 16S Ribosomal-Rna. *Appl Environ Microb* **59**, 695–700 (1993).
43. Yu, Y., Lee, C., Kim, J. & Hwang, S. Group-specific primer and probe sets to detect methanogenic communities using quantitative real-time polymerase chain reaction. *Biotechnology and Bioengineering* **89**, 670–679, doi:10.1002/bit.20347 (2005).
44. Borneman, J. & Hartin, R. J. PCR primers that amplify fungal rRNA genes from environmental samples. *Appl Environ Microbiol* **66**, 4356–4360, doi:10.1128/aem.66.10.4356-4360.2000 (2000).
45. Caporaso, J. G. *et al.* Global patterns of 16S rRNA diversity at a depth of millions of sequences per sample. *P Natl Acad Sci USA* **108**, 4516–4522, doi:10.1073/pnas.1000080107 (2011).
46. Gardes, M. & Bruns, T. D. Its Primers with Enhanced Specificity for Basidiomycetes - Application to the Identification of Mycorrhizae and Rusts. *Mol Ecol* **2**, 113–118, doi:10.1111/j.1365-294X.1993.tb00005.x (1993).
47. Caporaso, J. G. *et al.* QIIME allows analysis of high-throughput community sequencing data. *Nat Methods* **7**, 335–336, doi:10.1038/nmeth.f.303 (2010).
48. Bengtsson-Palme, J. *et al.* Improved software detection and extraction of ITS1 and ITS2 from ribosomal ITS sequences of fungi and other eukaryotes for analysis of environmental sequencing data. *Methods Ecol Evol* **4**, 914–919, doi:10.1111/2041-210X.12073 (2013).

49. Edgar, R. C. UPARSE: highly accurate OTU sequences from microbial amplicon reads. *Nat Methods* **10**, 996–+, doi:10.1038/Nmeth.2604 (2013).
50. Quast, C. *et al.* The SILVA ribosomal RNA gene database project: improved data processing and web-based tools. *Nucleic Acids Res* **41**, D590–D596, doi:10.1093/nar/gks1219 (2013).
51. Koljalg, U. *et al.* Towards a unified paradigm for sequence-based identification of fungi. *Mol Ecol* **22**, 5271–5277, doi:10.1111/mec.12481 (2013).
52. Nguyen, N. H. *et al.* FUNGuild: An open annotation tool for parsing fungal community datasets by ecological guild. *Fungal Ecol* **20**, 241–248, doi:10.1016/j.funeco.2015.06.006 (2016).
53. Berry, D. & Widder, S. Deciphering microbial interactions and detecting keystone species with co-occurrence networks. *Front Microbiol* **5**, doi:10.3389/fmicb.2014.00219 (2014).
54. Weiss, S. *et al.* Correlation detection strategies in microbial data sets vary widely in sensitivity and precision. *ISME J* **10**, 1669–1681, doi:10.1038/ismej.2015.235 (2016).
55. Shannon, P. *et al.* Cytoscape: A software environment for integrated models of biomolecular interaction networks. *Genome Research* **13**, 2498–2504, doi:10.1101/gr.1239303 (2003).
56. Faust, K. *et al.* Microbial Co-occurrence Relationships in the Human Microbiome. *Plos Comput Biol* **8**, doi:10.1371/journal.pcbi.1002606 (2012).
57. Langille, M. G. I. *et al.* Predictive functional profiling of microbial communities using 16S rRNA marker gene sequences. *Nat Biotechnol* **31**, 814–+, doi:10.1038/nbt.2676 (2013).
58. Fish, J. A. *et al.* FunGene: the functional gene pipeline and repository. *Front Microbiol* **4**, doi:10.3389/fmicb.2013.00291 (2013).
59. Braak, C. J. F. t. & Smlauer, P. (2012).
60. McMurdie, P. J. & Holmes, S. phyloseq: An R Package for Reproducible Interactive Analysis and Graphics of Microbiome Census Data. *Plos One* **8**, doi:10.1371/journal.pone.0061217 (2013).
61. Oulehle, F. & Hruska, J. Tree species (*Picea abies* and *Fagus sylvatica*) effects on soil water acidification and aluminium chemistry at sites subjected to long-term acidification in the Ore Mts., Czech Republic. *J Inorg Biochem* **99**, 1822–1829, doi:10.1016/j.jinorgbio.2005.06.008 (2005).
62. Nacke, H. *et al.* Pyrosequencing-Based Assessment of Bacterial Community Structure Along Different Management Types in German Forest and Grassland Soils. *Plos One* **6**, doi:10.1371/journal.pone.0017000 (2011).
63. Prescott, C. E. & Grayston, S. J. Tree species influence on microbial communities in litter and soil: Current knowledge and research needs. *Forest Ecol Manag* **309**, 19–27, doi:10.1016/j.foreco.2013.02.034 (2013).
64. Morrison, E. W. *et al.* Chronic nitrogen additions fundamentally restructure the soil fungal community in a temperate forest. *Fungal Ecol* **23**, 48–57, doi:10.1016/j.funeco.2016.05.011 (2016).
65. Tedersoo, L. *et al.* Global diversity and geography of soil fungi. *Science* **346**, 1078–+, doi:10.1126/science.1256688 (2014).
66. Hogberg, M. N., Hogberg, P. & Myrold, D. D. Is microbial community composition in boreal forest soils determined by pH, C-to-N ratio, the trees, or all three? *Oecologia* **150**, 590–601, doi:10.1007/s00442-006-0562-5 (2007).
67. Lauber, C. L., Hamady, M., Knight, R. & Fierer, N. Pyrosequencing-Based Assessment of Soil pH as a Predictor of Soil Bacterial Community Structure at the Continental Scale. *Appl Environ Microb* **75**, 5111–5120, doi:10.1128/Aem.00335-09 (2009).
68. Fierer, N., Bradford, M. A. & Jackson, R. B. Toward an ecological classification of soil bacteria. *Ecology* **88**, 1354–1364, doi:10.1890/05-1839 (2007).
69. Reich, P. B. *et al.* Linking litter calcium, earthworms and soil properties: a common garden test with 14 tree species. *Ecol Lett* **8**, 811–818, doi:10.1111/j.1461-0248.2005.00779.x (2005).
70. Hobbie, S. E. *et al.* Tree species effects on decomposition and forest floor dynamics in a common garden. *Ecology* **87**, 2288–2297, doi:10.1890/0012-9658(2006)87[2288:Tseoda]2.0.Co;2 (2006).
71. Kielak, A. M., Barreto, C. C., Kowalchuk, G. A., van Veen, J. A. & Kuramae, E. E. The Ecology of Acidobacteria: Moving beyond Genes and Genomes. *Front Microbiol* **7**, doi:10.3389/fmicb.2016.00744 (2016).
72. Navarrete, A. A. *et al.* Differential Response of Acidobacteria Subgroups to Forest-to-Pasture Conversion and Their Biogeographic Patterns in the Western Brazilian Amazon. *Frontiers in Microbiology* **6**, doi:10.3389/fmicb.2015.01443 (2015).
73. Jones, R. T. *et al.* A comprehensive survey of soil acidobacterial diversity using pyrosequencing and clone library analyses. *ISME Journal* **3**, 442–453, doi:10.1038/ismej.2008.127 (2009).
74. Padden, A. N., Rainey, F. A., Kelly, D. P. & Wood, A. P. *Xanthobacter tagetidii* sp nov, an organism associated with *Tagetes* species and able to grow on substituted thiophenes. *Int J Syst Bacteriol* **47**, 394–401 (1997).
75. Oyaizumasuchi, Y. & Komagata, K. Isolation of Free-Living Nitrogen-Fixing Bacteria from the Rhizosphere of Rice. *J Gen Appl Microbiol* **34**, 127–164, doi:10.2323/jgam.34.127 (1988).
76. Daniel H. Buckley, Varisa Huangyutham, Tyrrell A. Nelson, Angelika Rumberger, and Janice E. Diversity of Planctomycetes in Soil in Relation to Soil History and Environmental Heterogeneity. *Thies Appl. Environ. Microbiol.* **72**(7), 4522–4531, doi:10.1128/AEM.00149-06 (2006).
77. Elser, J. J., Kyle, M., Makino, W., Yoshida, T. & Urabe, J. Ecological stoichiometry in the microbial food web: a test of the light: nutrient hypothesis. *Aquat Microb Ecol* **31**, 49–65, doi:10.3354/ame031049 (2003).
78. Dedysh, S. N. *et al.* *Bryocella elongata* gen. nov., sp nov., a member of subdivision 1 of the Acidobacteria isolated from a methanotrophic enrichment culture, and emended description of *Edaphobacter aggregans* Koch *et al.* 2008. *Int J Syst Evol Micr* **62**, 654–664, doi:10.1099/ijs.0.031898-0 (2012).
79. Naether, A. *et al.* Environmental Factors Affect Acidobacterial Communities below the Subgroup Level in Grassland and Forest Soils. *Appl Environ Microb* **78**, 7398–7406, doi:10.1128/Aem.01325-12 (2012).
80. Cederlund, H. *et al.* Soil carbon quality and nitrogen fertilization structure bacterial communities with predictable responses of major bacterial phyla. *Appl Soil Ecol* **84**, 62–68, doi:10.1016/j.apsoil.2014.06.003 (2014).
81. Hartman, W. H., Richardson, C. J., Vilgalys, R. & Bruland, G. L. Environmental and anthropogenic controls over bacterial communities in wetland soils. *P Natl Acad Sci USA* **105**, 17842–17847, doi:10.1073/pnas.0808254105 (2008).
82. Sun, H. *et al.* Bacterial diversity and community structure along different peat soils in boreal forest. *Appl Soil Ecol* **74**, 37–45, doi:10.1016/j.apsoil.2013.09.010 (2014).
83. Schimel, J. P. & Weintraub, M. N. The implications of exoenzyme activity on microbial carbon and nitrogen limitation in soil: a theoretical model. *Soil Biology & Biochemistry* **35**, 549–563, doi:10.1016/s0038-0717(03)00015-4 (2003).
84. Hansel, C. M., Fendorf, S., Jardine, P. M. & Francis, C. A. Changes in bacterial and archaeal community structure and functional diversity along a geochemically variable soil profile. *Appl Environ Microb* **74**, 1620–1633, doi:10.1128/Aem.01787-07 (2008).
85. Evans, C. D., Monteith, D. T. & Cooper, D. M. Long-term increases in surface water dissolved organic carbon: Observations, possible causes and environmental impacts. *Environ Pollut* **137**, 55–71, doi:10.1016/j.envpol.2004.12.031 (2005).
86. Goodale, C. L., Aber, J. D., Vitousek, P. M. & McDowell, W. H. Long-term decreases in stream nitrate: Successional causes unlikely; Possible links to DOC? *Ecosystems* **8**, 334–337, doi:10.1007/s10021-003-0162-8 (2005).
87. Geisseler, D., Horwath, W. R., Joergensen, R. G. & Ludwig, B. Pathways of nitrogen utilization by soil microorganisms - A review. *Soil Biol Biochem* **42**, 2058–2067, doi:10.1016/j.soilbio.2010.08.021 (2010).
88. Barta, J., Melichova, T., Vanek, D., Picek, T. & Santruckova, H. Effect of pH and dissolved organic matter on the abundance of nirK and nirS denitrifiers in spruce forest soil. *Biogeochemistry* **101**, 123–132, doi:10.1007/s10533-010-9430-9 (2010).

89. Yoon, S., Cruz-Garcia, C., Sanford, R., Ritalahti, K. M. & Löffler, F. E. Denitrification versus respiratory ammonification: environmental controls of two competing dissimilatory NO₃-/NO₂- reduction pathways in *Shewanella loihica* strain PV-4. *Isme J* **9**, 1093–1104, doi:10.1038/ismej.2014.201 (2015).
90. Simon, A. *et al.* Exploiting the fungal highway: development of a novel tool for the *in situ* isolation of bacteria migrating along fungal mycelium. *Fems Microbiol Ecol* **91**, doi:10.1093/femsec/fiv116 (2015).

Acknowledgements

This study was conducted within the framework of the project supported by the Czech Science Foundation (GA14-33311S). We are grateful to Michal Růžek and Oldřich Myška for their technical help with soil sampling and analyses. We also thank Hana Bošková and Markéta Applová for laboratory assistance and Gabriela Scott Zemanová and Ryan A. Scott for their language corrections.

Author Contributions

F.O. designed the research and provided part of soil chemistry data. J.B. analysed the microbial community composition, functional potential and microbial network, K.T. analysed N related processes and microbial and chemical characteristics of the soils. All authors contributed on writing the manuscript.

Additional Information

Supplementary information accompanies this paper at doi:10.1038/s41598-017-08554-1

Competing Interests: The authors declare that they have no competing interests.

Publisher's note: Springer Nature remains neutral with regard to jurisdictional claims in published maps and institutional affiliations.



Open Access This article is licensed under a Creative Commons Attribution 4.0 International License, which permits use, sharing, adaptation, distribution and reproduction in any medium or format, as long as you give appropriate credit to the original author(s) and the source, provide a link to the Creative Commons license, and indicate if changes were made. The images or other third party material in this article are included in the article's Creative Commons license, unless indicated otherwise in a credit line to the material. If material is not included in the article's Creative Commons license and your intended use is not permitted by statutory regulation or exceeds the permitted use, you will need to obtain permission directly from the copyright holder. To view a copy of this license, visit <http://creativecommons.org/licenses/by/4.0/>.

© The Author(s) 2017

Paper 5

Urbanova Z, **Barta J** (2014) Microbial community composition and in silico predicted metabolic potential reflect biogeochemical gradients between distinct peatland types. *FEMS MICROBIOLOGY ECOLOGY* 90:633-646.

Microbial community composition and *in silico* predicted metabolic potential reflect biogeochemical gradients between distinct peatland types

Zuzana Urbanová & Jiří Bárta

Department of Ecosystem Biology, University of South Bohemia in České Budějovice, České Budějovice, Czech Republic

Correspondence: Zuzana Urbanová, Department of Ecosystem Biology, Faculty of Science, University of South Bohemia in České Budějovice, Branišovská 31, České Budějovice 370 05, Czech Republic. Tel.: +420 387 772 261; fax: +420 387 772 368; e-mail: urbanz00@prf.jcu.cz

Received 8 April 2014; revised 21 August 2014; accepted 31 August 2014. Final version published online 22 September 2014.

DOI: 10.1111/1574-6941.12422

Editor: Tillmann Lueders

Keywords

bog; fen; spruce swamp forest; microbial diversity; bacteria; *Archaea*.

Abstract

It is not well understood how the ecological status and microbial community composition of spruce swamp forests (SSF) relate to those found in bogs and fens. To clarify this, we investigated biogeochemical parameters and microbial community composition in a bog, a fen and two SSF using high throughput barcoded sequencing of the small ribosomal subunit (SSU) variable region V4. The results demonstrated that the microbial community of SSF is positioned between those of bogs and fens, and this was confirmed by *in silico* predicted metabolic potentials. This corresponds well with the position of SSF on the trophic gradient and reflects distinct responses of microbial communities to environmental variables. Species richness and microbial diversity increased significantly from bog to fen, with SSF in between, reflecting the variation in pH, nutrient availability and peat decomposability. The archaeal community, dominated by hydrogenotrophic methanogens, was more similar in SSF and the bog compared with the fen. The composition of the bacterial community of SSF was intermediate between those of bog and fen. However, the production of CO₂ (an indicator of peat decomposability) did not differ between SSF and bog, suggesting the limiting effect of low pH and poor litter quality on the functioning of the bacterial community in SSF. These results help to clarify the transitional position of SSF between bogs and fens and showed the strong effect of environmental conditions on microbial community composition and functioning.

Introduction

Peatlands represent a specific type of wetland ecosystem, where organic matter is accumulated over millennia due to the unfavourable conditions for decomposition. They act as a sink of atmospheric CO₂, but at the same time, a large amount of CH₄ is produced in the water-saturated peat profile and released into the atmosphere (Gorham, 1991). Despite the importance of peatlands in global carbon (C) cycling and other important ecosystem services, the diversity and functioning of microbial communities in different peatland types is still not fully understood.

Peatlands comprise a wide spectrum of different types, varying in their hydrology, trophic status and vegetation. The composition and function of the microbial community vary according to heterogeneous environmental

conditions in peat, such as oxic/anoxic conditions, a wide range of redox potentials, sources of C energy and nutrients (Juottonen *et al.*, 2005; Morales *et al.*, 2006), and vegetation composition (Fisk *et al.*, 2003). Consequently, the microbial community differs among peatland types in both community composition and functioning (Galand *et al.*, 2005; Juottonen *et al.*, 2005; Kim *et al.*, 2008; Lin *et al.*, 2012). Fens possess greater microbial diversity due to the additional nutrient input from groundwater, higher pH and litter of different quality, compared with nutrient-poor acidic bogs, which receive nutrients mainly from precipitation (Galand *et al.*, 2005; Kim *et al.*, 2008; Urbanová *et al.*, 2011; Gupta *et al.*, 2012; Lin *et al.*, 2012). It is uncertain where spruce swamp forests (SSF) are located on this gradient between bogs and fens. As minerotrophic peatlands, SSF combine both peatland and mineral forest

properties and are valued especially for their high spatial heterogeneity and biological diversity, in that they provide a multitude of ecological niches along a wide hydrotopographical gradient (Økland *et al.*, 2008). Therefore, the microbial community should be expected to have high species and functional diversities.

Microbial diversity has been studied in various individual peatland types, but comparative analyses of different peatland types are still rare and existing studies have focused mainly on specific functional groups of microorganisms, for example, methanogens (Juottonen *et al.*, 2005; Merilä *et al.*, 2006), methanotrophs (Dedysh, 2009; Gupta *et al.*, 2012) or sulphate reducers (Pester *et al.*, 2012). Other studies described microbial diversity mostly in bogs (Dedysh *et al.*, 2006; Morales *et al.*, 2006; Pankratov *et al.*, 2011; Serkebaeva *et al.*, 2013), while only a few studies compared both bog and fen microbial communities (Juottonen *et al.*, 2005; Kim *et al.*, 2008; Lin *et al.*, 2012). These studies found that the most frequent bacteria in peat are the representatives of *Proteobacteria* and *Acidobacteria*, which have good adaptations to acidic conditions and exhibit many different lifestyles. The other important bacterial groups typical for peatlands were *Actinobacteria*, *Verrucomicrobia*, *Planctomycetes*, *Chloroflexi*, *Firmicutes* and *Chlamydiae*. The archaeal community has been shown to be dominated by methanogens and their composition varies according to nutrient status and prevailing substrate (Galand *et al.*, 2005; Juottonen *et al.*, 2005; Metje & Frenzel, 2007). There is only one study of the microbial community composition of SSF (Sun *et al.*, 2014), which focused entirely on the surface aerobic layer. These authors did not find any significant differences in microbial community composition compared with other forested peatlands. Their conclusions may, however, be questionable, because any site effect was probably masked by the presence of litter of similar quality.

While these studies revealed some aspects of microbial community composition in peatlands, the abundance and potential functional roles of different groups of microorganisms in distinct peatland types have not been sufficiently addressed. Furthermore, the relationships between biochemical features of distinct peatlands and their microbial community composition are still not fully understood. Among peatland types, SSF have been neglected for a long time, and it is wholly uncertain if the composition and function of their microbial community is more similar to either bog or fen or different from both.

The main goal of our study was to describe the microbial community in an SSF ecosystem and clarify its ecological status in relation to bogs and fens and to identify the similarities and/or uniqueness of their microbial community. Other aims were (a) to explain the differences in

microbial community composition with biochemical properties of different peatland types and (b) to determine and compare the metabolic potential of microorganisms in different peatland types.

To address these specific goals, we used high-throughput barcoded sequencing of bacterial and archaeal SSU genes and compared these results with biochemical parameters of the different peatland types. The newly published bioinformatics pipelines (i.e. PICRUSt) allowed us to predict the functional potential of the microbial community. For a more accurate determination of microbial community composition, SSU gene abundances were normalized based on different SSU gene copies in different microbial taxa (Langille *et al.*, 2013).

Materials and methods

Study sites

The study was carried out in an ombrotrophic bog (BOG), one minerotrophic treeless poor fen (FEN) and two spruce swamp forests (SSF) located in the Šumava Mountains, south-west Czech Republic (48°59'N, 13°28'E). BOG and SSF are situated on an upland plateau at altitudes from 1100 to 1260 m a.s.l. FEN is located at an altitude of 900 m a.s.l. This mountain region is characterized by a cold and humid climate with a mean annual temperature between 3.2 and 4.0 °C and mean annual rainfall between 1000 and 1200 mm according to altitude (1961 to 1990, statistics by the Czech Hydro-Meteorological Institute).

BOG is characterized by a well-developed surface structure with hummocks dominated by *Andromeda polifolia*, *Vaccinium uliginosum* and *Eriophorum vaginatum*, hollows with *Carex limosa* and lawns covered by *Trichophorum caespitosum*. The moss layer consists of *Sphagnum rubellum*, *S. capillifolium* and *S. magellanicum* on hummocks, while the wetter hollows are covered by *S. cuspidatum*. The moss layer is absent on lawns. *Eriophorum vaginatum* is widespread in the SSF, with other sedges and grasses common in wetter microhabitats. Drier microhabitats are characterized by *Vaccinium* dwarf shrubs. The tree canopy (*Picea abies*) can vary from 40% to 100%. FEN is characterized by a homogenous surface structure with the dominant *Carex rostrata* in the field layer and *Sphagnum flexuosum* in the moss layer. *Carex nigra*, *Viola palustris*, *Epilobium palustre*, *Potentilla palustris* and *Vaccinium oxycoccos* are frequent but not abundant.

Soil sampling and analysis

The surface layer of peat (0–30 cm) was sampled in all study sites in autumn 2010, using a corer. Each sample

consisted of five subsamples mixed together. Eight samples were taken in BOG (four samples each in the wetter *Trichophorum* lawns and drier hummocks). In each SSF, six samples were collected, taking into account surface heterogeneity. In FEN, only four samples were taken because of the homogenous vegetation structure. Directly after sampling, the samples were sieved through a 5-mm mesh and stored in tightly closed plastic bags at 4 °C for 4 weeks until soil analysis. Half of the samples from each locality were used for DNA analysis, with the soil frozen at -80 °C immediately after sieving and stored until analysis. Peat samples included part of the aerobic and part of the anaerobic zones under the mean water table level (see Table 1).

The water table was measured manually during the growing season in perforated PVC tubes, whose spacing reflected the soil sampling design on each site.

The soil samples were analysed for total C and N content using a Micro-cube elemental analyser (Elementar, Germany). Total P (P_{TOT}) was determined by perchloric acid digestion (Kopáček & Hejzlar, 1993). Oxalate-extractable P (P_{OX}) was determined by extraction of 2 g of soil with 40 mL of acid ammonium oxalate solution [$H_2C_2O_4 + (NH_4)_2 C_2O_4$ at pH 3] (Cappo *et al.*, 1987). P_{OX} is supposed to characterize the biological availability of P in the soil (Koopmans *et al.*, 2004). The C (C_{mic}) and N (N_{mic}) contents of soil microbial biomass were measured using the chloroform fumigation-extraction method (Vance *et al.*, 1987) and calculated as the difference between C and N contents in fumigated and non-fumigated samples. Coefficients of 0.38 (Vance *et al.*, 1987) and 0.54 (Brookes *et al.*, 1985) were used to

correct the results for soil microbial biomass C and N, respectively. Concentrations of soluble organic carbon (SOC) and total soluble organic nitrogen (TON) in the soil solution were analysed on a LiquiTOC II (Elementar). Total soluble inorganic nitrogen (TIN) was measured with a flow injection analyser (FIA Lachat QC8500). Soil pH was measured after shaking 10 g of each sample briefly with 25 mL of distilled water and letting it stand for 2 h. Bulk density ($g\ dm^{-3}$) was measured by weighing the intact samples after drying at 70 °C.

Aerobic production potential for CO_2 and anaerobic production potential for CH_4 were measured under laboratory conditions. Ten grams of homogenized peat was placed in a glass bottle tightly closed with a rubber stopper. The aerobic samples were regularly ventilated to keep conditions aerobic. In the anaerobic bottles, 10 mL of distilled water was added, the headspace flushed with helium, and the bottles were kept tightly closed for the whole incubation period. Samples were incubated for a period of 50 days at 15 °C. Gas in the headspace was sampled each week during the experiment, and the concentrations of CO_2 and CH_4 were determined by gas chromatography. CO_2 was determined using an HP 6850 gas chromatograph (Agilent) equipped with a 0.53 mm \times 15 m HP-Plot Q column and a 0.53 mm \times 15 m HP-Plot Molecular Sieve 5A column and a thermal conductivity detector, using helium as the carrier gas. Methane (CH_4) was determined using an HP 6890 gas chromatograph (Agilent) equipped with a 0.53 mm \times 30 m GS-Alumina column and a flame ionization detector, using nitrogen as the carrier gas.

Table 1. Biochemical characteristics of peat sampled on three types of peatlands (mean \pm standard deviation). Different letters in rows indicate statistically significant differences between peatland types ($P < 0.05$)

	BOG	SSF	FEN
C (%)	47.94 \pm 1.5a	44.51 \pm 0.9b	43.45 \pm 0.2b
N (%)	1.86 \pm 0.4a	1.32 \pm 0.3b	1.72 \pm 0.1ab
C/N	26.87 \pm 5.3a	35.14 \pm 7.7b	25.45 \pm 1.8ab
WT (cm)	-8.21 \pm 4.0a	-13.55 \pm 5.2a	-8.56 \pm 1.2a
pH	4.08 \pm 0.2a	4.19 \pm 0.1a	5.10 \pm 0.2b
Bulk density ($g\ cm^{-3}$)	0.12 \pm 0.03a	0.06 \pm 0.02b	0.07 \pm 0.01b
P_{TOT} ($mg\ g^{-1}$)	0.65 \pm 0.1a	0.70 \pm 0.2a	1.17 \pm 0.1b
P_{OX} ($mg\ g^{-1}$)	0.08 \pm 0.03a	0.04 \pm 0.01b	0.17 \pm 0.04c
SOC ($mg\ g^{-1}$)	0.99 \pm 0.3a	1.64 \pm 0.5b	1.41 \pm 0.2ab
TON ($mg\ g^{-1}$)	0.08 \pm 0.01a	0.11 \pm 0.06a	0.13 \pm 0.01a
TIN ($mg\ g^{-1}$)	0.15 \pm 0.03a	0.14 \pm 0.05a	0.17 \pm 0.04a
C_{mic} ($mg\ g^{-1}$)	5.94 \pm 1.1a	2.94 \pm 1.1b	9.05 \pm 1.6c
N_{mic} ($mg\ g^{-1}$)	0.68 \pm 0.1a	0.52 \pm 0.2a	1.11 \pm 0.2b
CO_2 aerobic production rate ($\mu L\ g^{-1}\ hod^{-1}$)	8.85 \pm 3.6a	11.70 \pm 3.0a	23.19 \pm 5.8b
CH_4 anaerobic production rate ($\mu L\ g^{-1}\ hod^{-1}$)	0.11 \pm 0.2a	1.55 \pm 0.5b	3.99 \pm 0.5c
Number of samples for peat analysis	8	12	4
Number of samples for DNA analysis	4	6	2

Total DNA extraction, purification and quantification

The Power Soil DNA Isolation Kit (MoBio Laboratories Inc., Carlsbad, CA) was used for isolation of genomic DNA from soil according to the manufacturer's instructions with some modifications. A mini Bead-Beater (Bio-Spec Products, Inc.) was used at a speed of 6 ms^{-1} for 45 s for better disruption of cell walls. DNA was stored in 1.5-mL Eppendorf microtubes in a freezer ($-20 \text{ }^{\circ}\text{C}$) until analysis. The quality of the extracted DNA was verified by electrophoresis (1% w/v, 8 V cm^{-1} , 45 min). Total DNA was quantified using SybrGreen (Leininger *et al.*, 2006).

Barcoded amplicon sequencing of bacterial and archaeal SSU rRNA genes

The PCR primers (515F/806R) targeted the V4 region of the small ribosomal subunit (SSU) rRNA, previously shown to yield accurate phylogenetic information and to have only few biases against any bacterial taxa (Liu *et al.*, 2007; Bates *et al.*, 2011; Bergmann *et al.*, 2011). The PCR samples contained 13 μL MO BIO PCR-grade water, 10 μL 5 PRIME HotMasterMix, 0.5 μL each of the forward and reverse primers (0.2 μM final concentration), and 1 μL of genomic DNA. Samples were kept at $94 \text{ }^{\circ}\text{C}$ for 3 min to denature the DNA, with amplification proceeding for 35 cycles at $94 \text{ }^{\circ}\text{C}$ for 45 s, $50 \text{ }^{\circ}\text{C}$ for 60 s, and $72 \text{ }^{\circ}\text{C}$ for 90 s; a final extension of 10 min at $72 \text{ }^{\circ}\text{C}$ was added to ensure complete amplification. The reverse primer contained a 12-base error-correcting Golay barcode to facilitate multiplexing. Each sample was amplified in triplicate, combined, quantified using Invitrogen PicoGreen and a plate reader, and equal amounts of DNA from each amplicon were pooled into a single 1.5-mL microcentrifuge tube. Cleaned amplicons were quantified using Picogreen[®] dsDNA reagent in 10 mM Tris buffer (pH 8.0). A composite sample for sequencing was created by combining equimolar ratios of amplicons from the individual samples and cleaned using the Ultra Clean[®] htp 96 well PCR clean up kit (MO BIO Laboratories). Purity and concentration of the samples were estimated by spectrophotometry. Amplicons of 250 bp were sequenced paired (150 \times 150 cycles) on the IlluminaMiSeq platform (ARGONE Lab, IL).

Analyses of microbial community composition

Raw paired reads (150 bp) were joined using ea-utils to obtain reads of *c.* 250 bp length (Aronesty, 2013). Quality filtering of reads was applied as described previously

(Caporaso *et al.*, 2011). Reads were truncated at a phred quality threshold of 20. Reads which contained ambiguities and reads whose barcode did not match an expected barcode were discarded. We obtained 646 676 sequences after joining and quality trimming. Reads were assigned to operational taxonomic units (OTUs) using a closed-reference OTU picking protocol using QIIME 1.8.0 (Caporaso *et al.*, 2010), first with uclust (Edgar, 2010) being applied to search sequences against a subset of the Greengenes database, version 13_05 (DeSantis *et al.*, 2006) filtered at 97% sequence identity. Taxonomy was assigned to each read by accepting the Greengenes taxonomy string of the best matching Greengenes sequence. Because the number of SSU rRNA genes varies from 1 to 15 copies per genome in different bacterial species, normalization of sequence abundance based on SSU gene copies of assigned taxa was performed before further analysis (Langille *et al.*, 2013). Alpha diversity metrics, Shannon diversity, Chao1 richness and Faith's phylogenetic diversity were calculated after rarefying all samples to the same sequencing depth of 11 000 sequences. Community relatedness was visualized using principal coordinates analysis (PCoA) from weighted Unifrac distances. Prior to computing the Unifrac distances, singleton OTUs (i.e. OTUs with only one sequence) were filtered out as these are likely to represent sequencing or PCR errors and/or chimeras.

Analysis of metabolic potential

In addition to the evaluation of microbial diversity, we implemented the newly developed bioinformatic pipeline PICRUSt (Langille *et al.*, 2013) to address the functional potential in different peatland sites. For this purpose, the closed-reference OTU picking protocol using QIIME 1.8.0 (Caporaso *et al.*, 2010) was used. Sequences were searched against the Greengenes database, version 13_05, and taxonomically assigned using uclust with default parameters (Edgar, 2010). The OTU table was created after rarefying samples to 15 000 sequences and further analysed using the PICRUSt pipeline on the Galaxy server. The PICRUSt pipeline scans three main functional databases, KEGG, COG and Rfam, and uses the OTU table of assigned taxa and their relative distribution in different samples to generate the relative abundance of functional categories. In the case of the KEGG database, it is possible to group functions into three level subgroups based on different KEGG functional gene ontology affiliation (i.e. metabolism, cellular processes, environmental processing). Data produced by the PICRUSt pipeline were statistically evaluated with the STAMP bioinformatics package (Parks & Beiko, 2010).

Statistics

One-way ANOVA, followed by *post hoc* Tukey's HSD test, was used to determine significant differences in biogeochemical parameters between the peatland types. Similarly, differences in the microbial community (relative sequence abundance of bacterial and archaeal phyla) between the three peatland types were investigated by one-way ANOVA followed by Tukey's HSD test. Differences were considered significant at P values < 0.05 . Pearson's correlation coefficient (r) was used to assess relations between the relative sequence abundance of bacterial phyla or archaeal classes and environmental variables (STATISTICA 9, Stat Soft).

Principal component analysis (PCA) was used to characterize microbial community variation according to peatland type and selected environmental variables (Canoco 4.5). Data were standardized by species and log-transformed. To test the relationships between community structure and environmental variables, Pearson's correlation coefficients (r) were determined between the first principal component (PCA1) scores of relative abundance and the environmental data.

Differences in environmental variables and relative sequence abundance of bacterial and archaeal phyla between the two SSF sites were tested using Student's t -test. As no significant differences were found between the samples from the two SSF sites, all six samples from these two sites were considered independent replicates unaffected by SSF locality.

Data deposition

The SSU rRNA gene sequence data were deposited in the Qiime sequence database <http://microbio.me/qiime/> project ID 2439.

Results

Biogeochemical characteristics of different peatland types

The major biogeochemical and environmental characteristics of the three investigated peatland types are listed in Table 1, where significant differences between the peatland types are indicated by different letters in rows. The BOG and FEN sites largely showed contrasting biochemical conditions, whereas for SSF most of the variables lay between the values for BOG and FEN (Table 1). In some cases, SSF was more similar to BOG (e.g. pH, P_{TOT} , N_{mic} , CO_2 production potential) and in others to FEN (e.g. C, N, bulk density). BOG peat was the most acidic (pH = 4.08), had the highest bulk density and contained

the highest amount of C and N. By contrast, FEN peat had the highest pH and was the richest in P_{TOT} , P_{OX} and other nutrient variables, such as TON and TIN. Also, microbial biomass (C_{mic} and N_{mic}) was significantly higher in FEN peat than in BOG and SSF peat (Table 1).

Significant differences were found for CO_2 and CH_4 production potentials, which reflect potential microbial activity and peat decomposability. Both of these characteristics were significantly higher in FEN than in BOG and SSF (Table 1). The aerobic CO_2 production rate was three times as high in FEN as in BOG and SSF, while anaerobic CH_4 production rate was more than twice as high in FEN as in SSF and 40 times higher than in BOG.

The matrix of correlations (not shown) between environmental variables and bacterial and archaeal relative abundance of OTUs indicated that pH, total C and N contents and potential CO_2 and CH_4 production were the most important environmental factors affecting microbial diversity. There were significant ($P < 0.05$) positive correlations with pH for most of the bacterial phyla except *Acidobacteria*, which had a negative correlation with pH ($r = -0.81$; $P < 0.05$). A significant negative correlation with total C content was found for *Alphaproteobacteria*, *Betaproteobacteria*, *Gammaproteobacteria*, *Actinobacteria*, *Elusimicrobia*, *Bacteroidetes*, *Verrucomicrobia*, *Chlorobi* and *Chloroflexi* ($P < 0.05$). By contrast, a significant positive correlation with total C content was found for *Acidobacteria* ($P < 0.05$). Similar links were observed with total N content, but most of these correlations were not significant at the 5% level.

Bacterial and archaeal diversity and richness

Before calculating alpha diversity indices, we checked the sequencing effort by calculating Good's coverage. In general, the coverage (in per cent) was very high for all samples and just slightly decreased in the order 98.5 ± 0.2 for BOG, 97.9 ± 0.2 for SSF and 96.2 ± 0.4 for FEN. Species richness as indicated by the Chao 1 index was significantly the lowest in BOG and the highest in FEN (Table 2). Also, both Shannon and Faith's diversity indices differed significantly. Both indices indicated significantly higher microbial diversity in the FEN site and the lowest in the BOG site, with SSF being in between. The numbers of OTUs which are unique or shared between peatland types are shown in Fig. 1. Only those OTUs whose absolute abundance after normalization was higher than 1 were included in the analyses. FEN had the highest amount of unique OTUs (582), representing 43% of all FEN OTUs (Fig. 1). By contrast, BOG had the highest proportion of shared OTUs, with the other two peatland types sharing 67% of all BOG OTUs (Fig. 1). When the relative abundance of each OTU is taken into account,

Table 2. Alpha index. Microbial diversity indicated by Chao1 richness, Shannon diversity and Faith's phylogenetic diversity (PD) in different peatland types*

Peat type	Number of samples	Sequence reads	Number of OTUs [†]	Chao1	Shannon	PD
BOG	4	48 319 (4490)	899 (111)	687.8 ^A (76.2)	5.9 ^A (0.4)	29.8 ^A (3.4)
SSF	6	60 506 (12 692)	1320 (205)	1011.8 ^B (129.3)	7.4 ^B (0.3)	41.2 ^B (4.6)
FEN	2	45 179 (17 087)	1913 (44)	1547.1 ^C (150.7)	8.4 ^C (0.1)	61.9 ^C (4.4)

Average values and standard errors (in parenthesis) are shown. Different letters show significant differences between sites (Tukey's HSD test, $P < 0.05$).

*Calculation of richness and diversity estimators was based on OTU tables rarefied to the same sequencing depth of 11 000 sequences.

[†]OTUs were defined as < 3% nucleotide sequence difference.

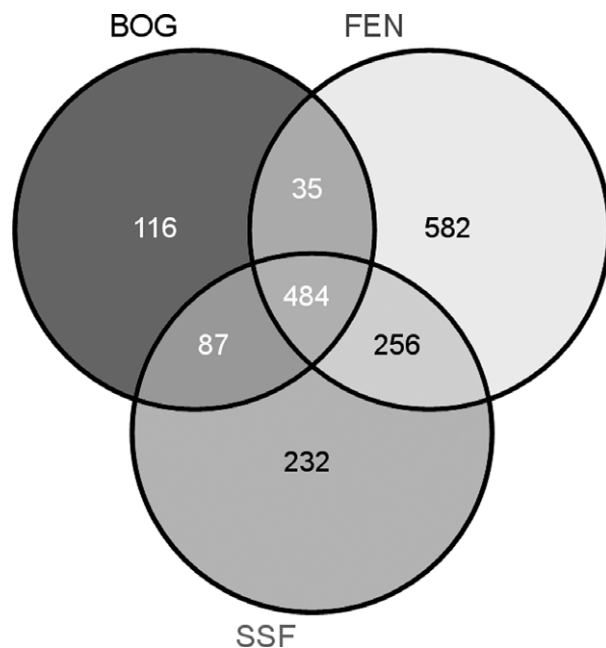


Fig. 1. OTU distribution between the three types of peatlands. The Venn diagram shows the number of OTUs unique to a single peatland type, shared by two or all three peatland types. The diagram was constructed for OTUs whose average abundance in each peatland type was > 1.

the 484 OTUs shared between all three types represent 96%, 90% and 72% of total OTU abundance for BOG, SSF and FEN, respectively, while the OTUs unique for BOG, SSF and FEN represent 1%, 3% and 13%, respectively. The SSF shared 24% of their OTUs exclusively with FEN, but only 8% with BOG. BOG and FEN shared the fewest number of common OTUs.

Microbial community composition

Altogether 38 bacterial and three archaeal phyla were identified in peat soils. The most abundant phyla, which accounted for more than 80% of all OTUs, were *Acidobacteria*, *Proteobacteria*, *Verrucomicrobia* and *Bacteroidetes* (Fig. 2). Other phyla, such as *Actinobacteria*, *Chlorobi*,

Chloroflexi, *Planctomycetes*, *Nitrospirae* and *Elusimicrobia*, were detected in all peatland types, but at lower abundances (relative OTU abundance > 1%). In addition, another 28 bacterial and archaeal phyla were identified, but considered as rare (relative OTU abundance < 1%). These rare phyla included *Archaea*, but not *Euryarchaeota*, which represented more than 1% of all OTUs in one sample each from BOG and SSF.

Microbial community composition and relative OTU abundance of the major phyla were markedly different between the BOG and FEN sites, with SSF being intermediate (Figs 2 and 3, Table 3), which reflected their distinct physical/chemical and biochemical characteristics (Table 1). Our results showed marked trends for the main bacterial phyla in BOG, SSF and FEN. All peatland types were dominated by *Acidobacteria*, but their abundance followed the trend BOG > SSF > FEN (80%, 70% and 51% of total bacterial OTUs, respectively), with the abundance in FEN being significantly lower compared with BOG and SSF ($P < 0.05$; Table 3). By contrast, relative OTU abundance of *Proteobacteria* followed the opposite trend, decreasing from FEN to BOG, with SSF in between. *Verrucomicrobia*, *Bacteroidetes*, *Actinobacteria* and *Elusimicrobia* were significantly more abundant in FEN compared with BOG (Fig. 2; Table 3). The relative OTU abundance of most bacterial phyla did not differ significantly between BOG and SSF, but the abundance of *Verrucomicrobia* and *Bacteroidetes* in SSF, for example, did differ significantly from both BOG and FEN ($P > 0.05$, Table 3).

The four most abundant classes of *Proteobacteria* (*Alpha*-, *Beta*-, *Gamma*- and *Deltaproteobacteria*) were used in further analyses because of their distinct lifestyles and metabolic capabilities (Fig. 2, Table 3). The relative OTU abundances of *Alphaproteobacteria*, *Betaproteobacteria* and *Gammaproteobacteria* decreased significantly from FEN to BOG. SSF was intermediate between the other two types, with relative OTU abundances were not significantly different from FEN (Table 3). By contrast, BOG had the highest relative OTU abundance affiliated to *Deltaproteobacteria* (7.5% of all bacterial OTUs), which were represented mostly by the order *Syntrophobacterales* (7.2%

Fig. 2. Bacterial community composition in different peatland types. Selected bacterial phyla with relative OTU abundance higher than 1%. In the case of the phylum *Proteobacteria*, phylogenetical classes (*Alpha*-, *Beta*-, *Gamma*- and *Deltaproteobacteria*) were used in the analyses. Columns represent relative OTU abundances of each peatland type error bars indicate standard deviations.

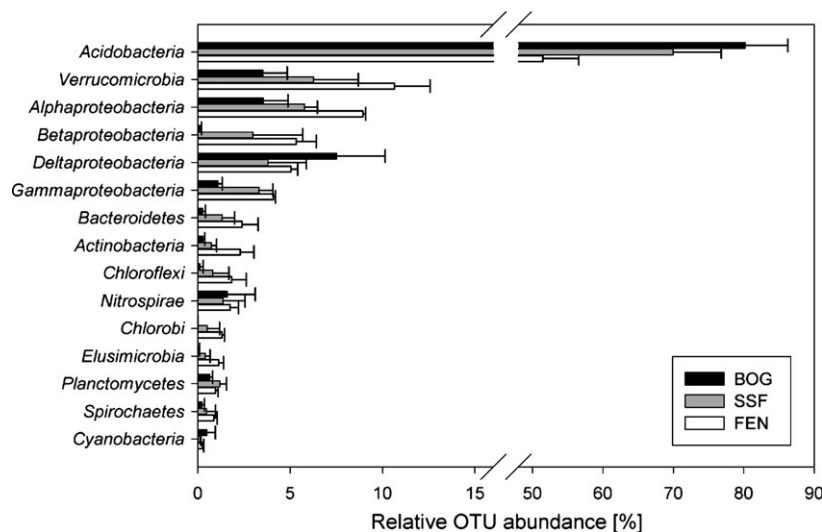
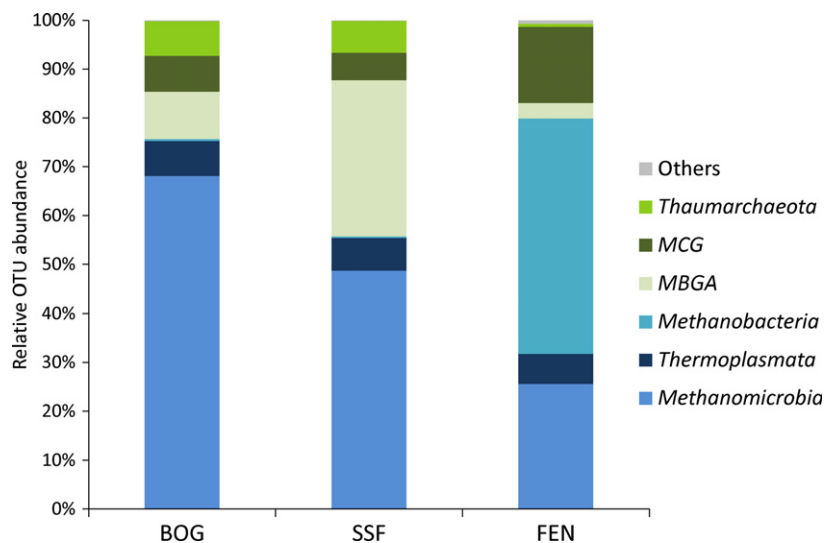


Fig. 3. Relative OTU abundance of archaeal classes based on OTUs that were detected in different peatland types based on the GreenGenes database ver. 13_05.



of all OTUs). *Syntrophobacteriales* comprised half of the OTUs affiliated to *Deltaproteobacteria* in FEN and SSF.

The archaeal community showed marked differences between the peatland types, despite the fact that relative OTU abundances of selected archaeal classes did not vary significantly between types due to high variability within sampling sites. Archaeal community composition differed between FEN and the other two peatland types (Fig. 3). The FEN archaeal community was dominated by *Methanobacteria* (48% of archaeal OTUs), which were in the minority in SSF and BOG (< 1% of archaeal OTUs). By contrast, BOG and SSF were dominated by *Methanomicrobia* (68% and 49% of archaeal OTUs, respectively). The class *Methanomicrobia* was almost entirely composed of the order *Methanomicrobiales*, representing hydrogenotrophic methanogens. OTUs affiliated to *Methanosarcinales*

were detected in all sites, but at negligible abundance (0.2–0.9% of archaeal OTUs).

Other identified archaeal classes were *Thermoplasmata*, *MBGA*, *MCG* and *Thaumarchaeota* (Fig. 3). The abundance of nitrifying *Thaumarchaeota* decreased from BOG to FEN, as was the case for *Thermoplasmata*. *Marine Benthic Group A* (*MBGA*) represented an important part of the archaeal community in SSF (31%) but only a minority of *Archaea* in BOG and FEN (Fig. 3).

Bacterial and archaeal diversity according to peatland type and environmental variables

Principal component analysis based on the relative OTU abundances of the most important bacterial and archaeal phyla (rel. OTU abundance higher than 1%) and selected

Table 3. Results of Tukey's HSD test of relative OTU abundance of particular bacterial and archaeal groups between the peatland types. Significant differences are indicated by different letters in rows ($P < 0.05$)

Bacteria	BOG	SSF	FEN
<i>Acidobacteria</i>	a	a	b
<i>Verrucomicrobia</i>	a	ab	b
<i>Alphaproteob.</i>	a	b	c
<i>Betaproteob.</i>	a	b	b
<i>Deltaproteob.</i>	a	a	a
<i>Gammaproteob.</i>	a	b	b
<i>Bacteroidetes</i>	a	ab	b
<i>Actinobacteria</i>	a	a	b
<i>Chloroflexi</i>	a	a	a
<i>Nitrospirae</i>	a	a	a
<i>Chlorobi</i>	a	a	a
<i>Elusimicrobia</i>	a	a	b
<i>Planctomycetes</i>	a	a	a
<i>Spirochaetes</i>	a	a	a
<i>Cyanobacteria</i>	a	a	a
Archaea			
<i>Methanomicrobia</i>	a	a	a
<i>MBGA</i>	a	a	a
<i>MCG</i>	a	a	a
<i>Thermoplasmata</i>	a	a	a
<i>Thaumarchaeota</i>	a	a	a
<i>Methanobacteria</i>	a	a	b

environmental variables clearly separated the three types of peatlands along the first principal coordinate axis (PCO1) (Fig. 4). PCO1 explained 60.0% of microbial

community variability. The distribution of different microbial groups along PCO1 reflected the trophic gradient from the most nutrient-poor and acidic BOG with high total C and N contents to the less acidic FEN. CO₂ and CH₄ potential productions were also positively correlated with PCO1, as was pH, indicating higher peat decomposability in FEN compared with BOG. PCO1 scores showed significant correlations ($P < 0.05$) with pH ($r = 0.64$), C ($r = -0.89$), N ($r = -0.46$), and CH₄ ($r = 0.89$) and CO₂ production ($r = 0.82$). The second axis (PCO2) explained 15.7% of total variation and separated SSF from BOG and FEN. The relative OTU abundances of bacterial phyla, such as *Deltaproteobacteria*, *Cyanobacteria*, *Euryarchaeota* and *Nitrospirae*, were negatively correlated with PCO2, while *Planctomycetes* was positively correlated with PCO2.

Principal coordinate analysis (PCoA) based on UniFrac distances showed the distinctness of microbial communities from different peatland sites (Fig. S1, Supporting Information) as reflected in the clear separation of the BOG and FEN communities. On the other hand, microbial communities from SSF showed an ambiguous pattern, with some samples being more similar to FEN and others to BOG. The SSF were additionally separated along the second (17% of explained variability) and third (9% of explained variability) PCoA axes.

The PCA analyses of functional diversity showed a pattern of sample distribution between the BOG, SSF and FEN sites (Fig. S2) similar to that of the microbial

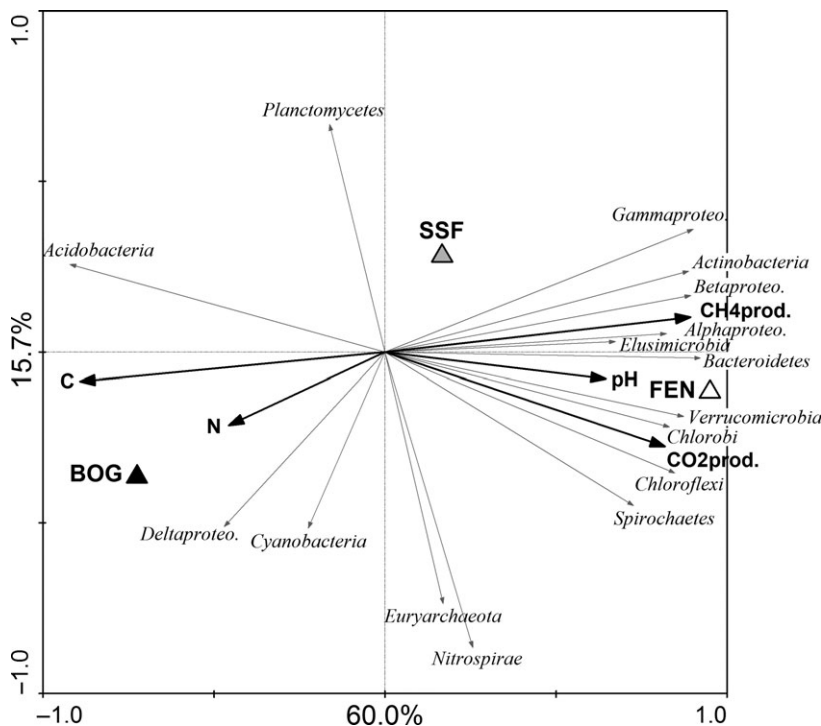


Fig. 4. Principal component analysis (PCA) of relative OTU abundances of selected phyla and environmental variables. In the case of the Proteobacteria, the phylogenetic classes (*Alpha*-, *Beta*-, *Delta*- and *Gammaproteobacteria*) were used in the analyses. The groups with relative OTU abundances $> 1\%$ were selected for the analyses. Abbreviations of environmental variables: C – total carbon content; N – total nitrogen content; CH₄prod. – potential CH₄ production measured in the laboratory; CO₂prod. – potential CO₂ production under aerobic conditions measured in the laboratory.

community composition (Figs 4 and S1). Therefore, the microbial species diversity reflects the functional diversity between our sites. Focusing on the general functional capabilities of different peatland types, we found significant differences in potential carbohydrate and amino acid metabolism and also in biosynthesis of secondary metabolites (Table S2, Supporting Information). The distribution of COG categories (clusters of orthologous groups) revealed additional specific differences in potential cellulose degradation, which was highest in BOG (Table S3b), while potential aromatic degradation (i.e. degradation of lignin and polyphenolic compounds) was highest in SSF (Table S3c).

Discussion

Bacterial community composition

In general, the bacterial community was dominated by *Acidobacteria* and *Proteobacteria* in all peatland types, followed by *Verrucomicrobia*, *Bacteroidetes*, *Actinobacteria*, *Chlorobi*, *Chloroflexi*, *Nitrospira* and *Planctomycetes*. The overall bacterial diversity and composition were comparable with those found in other peatlands (Dedysh *et al.*, 2006; Morales *et al.*, 2006; Ausec *et al.*, 2009; Pankratov *et al.*, 2011; Serkebaeva *et al.*, 2013; Sun *et al.*, 2014).

Acidobacteria are known to favour acidic environments and are able to grow under oligotrophic conditions (Philippot *et al.*, 2010), while *Proteobacteria* have been associated with higher availability of C (Fierer *et al.*, 2007). Therefore, the different relative abundances of *Proteobacteria* and *Acidobacteria* in our distinct peatland types might reflect different environmental conditions, such as pH and substrate availability. The relative abundance of *Acidobacteria* consistently increased with decreasing pH in our study sites, while the proportion of other bacterial phyla increased towards the less acidic FEN (Figs 2 and 4). The same response of *Acidobacteria* to pH was found by Hartman *et al.* (2008) in several wetland sites. Moreover, the ratio between *Proteobacteria* and *Acidobacteria* has been suggested to indicate the nutrient status of an ecosystem, with a low ratio indicating nutrient-poor conditions and vice versa (Smit *et al.*, 2001). The ratio between *Proteobacteria* and *Acidobacteria* was 0.15, 0.23 and 0.46 in BOG, SSF and FEN, respectively, indicating the most nutrient-poor conditions occurring in BOG compared with SSF and FEN. This corresponds to the general concept that bogs are very acidic ecosystems with low availability of nutrients compared with fens, while the trophic status and functioning of SSFs have been unclear. Therefore, our study fills this knowledge gap and SSFs can be placed between bogs and fens on the trophic gradient.

We expected SSF to be closer to FEN than BOG due to their similar hydrological regime and their relatively similar microbial communities. FEN offered more favourable conditions for microbes, as indicated by the significantly higher microbial biomass and aerobic potential CO₂ production in this system compared with BOG and SSF (Table 1). Contrary to our expectation, SSF was more similar to BOG in these biochemical parameters, which was probably caused by the low quality of litter from the predominant spruce trees and dwarf shrubs (Straková *et al.*, 2011), as indicated by the highest C/N ratio (Table 1). Thus, substrate quality may have prevailed over the effect of hydrology and limited the activity of microorganisms in SSFs. It has been shown previously that peatlands dominated by different plant growth forms, such as *Sphagnum*/shrubs and sedges, possessed different microbial community composition and activity (Fisk *et al.*, 2003).

Bacterial groups and their functions

By using the taxonomic affiliation of the SSU gene sequences and applying the newly developed bioinformatic pipeline PICRUSt (Langille *et al.*, 2013), we were able to evaluate the *in-silico* metabolic potential of the different peatland types. Langille *et al.* (2013) tested the predictive power of their pipeline in various ecosystems, including soil, and compared the *in silico* predicted metagenomes with real metagenomic data obtained from the same locations. They found that for the abundance of functional categories, the correlations between *in silico* predicted and metagenomically measured gene content approached 0.9 and averaged 0.8. The *in silico* prediction is based on community composition and taxonomic assignments of 16S rRNA gene sequences, which are then scanned against the whole annotated microbial genomes. Therefore, the *in silico* prediction of metabolic potential reflects to some extent species composition; however, there is no causality between species diversity and functional diversity. The same function can be performed by different species, and many microbial genes were obtained by lateral gene transfer (i.e. genes for denitrification) and therefore do not reflect the phylogenetic relationships based on 16S rRNA gene analyses (Heylen *et al.*, 2006).

According to recent studies, *Acidobacteria*, which dominated the microbial community in our sites, seem to be involved in the degradation of cellulose and aromatic compounds (Ausec *et al.*, 2009; Pankratov *et al.*, 2011). The results for metabolic potential revealed that the cellulose degradation potential was highest in BOG, where *Acidobacteria* dominated, while the aromatic degradation potential (i.e. degradation of lignin and polyphenolic compounds) was highest in SSFs (see Table S3b,c), which

might be connected with a higher input of lignin-dominated spruce foliage. Whereas the *Acidobacteria* seem to be more or less uniform with regard to their metabolism and ecological requirements, *Proteobacteria* exhibit many different lifestyles and, therefore, the relative abundance of the main proteobacterial classes also varied between the peatland types. Some members of *Proteobacteria* are known to utilize easily available substrates quickly, as well as having the ability to use different compounds as electron donors. Morales *et al.* (2006) found the *Deltaproteobacteria* to be the most frequent and probably the key group in bog ecology, because of their wide spectrum of ecological traits (e.g. sulphate reduction, iron reduction or fermentation). In our study, the majority of the sequences from *Deltaproteobacteria* were affiliated to the order *Syntrophobacterales*. Syntrophic bacteria are known as obligate anaerobic secondary fermenters with a capability for sulphate respiration. They produce H₂ as the byproduct of their metabolism, which they can provide to methanogens and/or acetogens by interspecies H₂ transfer (Schink & Stams, 2002).

High abundances of *Proteobacteria* and *Actinobacteria* were found by Sun *et al.* (2014) in an SSF; however, in our sites, *Actinobacteria* comprised only a minority of the total microbial community. This discrepancy can be explained by the different sampling design used by Sun *et al.* (2014), who sampled only the surface layer of peat, where *Actinobacteria* participate in the aerobic decomposition of litter (Peltoniemi *et al.*, 2009). Members of this phylum can produce extracellular enzymes and have enzymatic capabilities comparable with those of fungi. They are known for their ability to degrade cellulose, lignin and other complex biopolymers in different soil habitats (Mccarthy, 1987; le Roes-Hill *et al.*, 2011), which enable them to survive in environments with low C availability (Fierer *et al.*, 2003). Recently, it was found that they can dominate the bacterial community in certain arctic habitats where fungi are in the minority (Gittel *et al.*, 2014). The lower relative abundance of *Proteobacteria* in our study sites compared with previous studies (Ausec *et al.*, 2009; Serkebaeva *et al.*, 2013; Sun *et al.*, 2014) can be explained by the different approach in sequence abundance recalculation per different OTU. Our OTU abundances were based on the newly developed bioinformatics pipeline PICRUSt (Langille *et al.*, 2013), which recalculates the average number of SSU gene copies per genome, which can vary from 1 to 15 copies. This normalization helped us avoid overestimation of some groups of microorganisms. For example, without normalization the estimate of the relative abundance of *Proteobacteria* can be up to twice as high. The previous studies did not use this normalization technique.

Archaea and microorganisms involved in methane cycling

The archaeal community was mostly dominated by methanogenic *Archaea*, but members of nonmethanogenic *Euryarchaeota* and *Crenarchaeota* were also detected in all our study sites. Little attention has been paid to non-methanogenic *Archaea* in wetlands and their roles in C cycling, or metabolic pathways are still unclear. The phylum *Crenarchaeota* is a metabolically very diverse group mostly isolated from anoxic habitats, for example, acidic fen peat (Hamberger *et al.*, 2008; Tian *et al.*, 2012). In our study, two classes of *Crenarchaeota* (*MBGA*, *MCG*) were detected in all peatland types, and in SSF, they comprised almost half of all archaeal OTUs. The recently reclassified phylum *Thaumarchaeota*, composed of species with nitrifying capabilities (Herrmann *et al.*, 2012), comprised the highest proportion in the BOG.

Diversity of methanogenic community has been described to increase along the ecohydrological gradient from bogs towards fens, with CH₄ production following the same trend, production in fens being much greater than in bogs (Galand *et al.*, 2005; Juottonen *et al.*, 2005). In our study sites, potential CH₄ production also increased significantly from BOG to FEN with SSF in between. However, the sum of all OTUs assigned to methanogens did not vary much between the peatland types and did not correlate with CH₄ production. These results indicated that higher potential CH₄ production, and thus, methanogenic activity is probably driven by more suitable conditions for methanogenesis (higher substrate availability, higher pH) in FEN compared with BOG and SSFs rather than by different methanogenic community composition.

Surprisingly, the taxonomic assignment of the recovered sequences suggested that only the hydrogenotrophic methanogens occurred in all of the studied peatland types, despite their distinct vegetation composition, diverse methanogenic community and CH₄ production. The *Methanomicrobiales* were the dominant group of methanogens in BOG and SSFs, whereas *Methanobacteriales* constituted the dominant part of the methanogenic community in FEN. Both of these methanogenic groups are hydrogenotrophic methanogens reducing CO₂ and oxidizing H₂ to form CH₄. In general, hydrogenotrophic methanogenesis is favoured in acidic peatlands such as bogs and poor fens (Horn *et al.*, 2003; Galand *et al.*, 2005). Many studies detected hydrogenotrophic *Methanobacteriales* and *Methanomicrobiales* together with acetoclastic *Methanosarcinales* in bog and fen sites, where acetoclastic methanogens represented an important part of the methanogenic community and their relative abundance increased from < 10% in bogs to 40% or more in

fens (Galand *et al.*, 2005; Juottonen *et al.*, 2005; Cadillo-Quiroz *et al.*, 2006; Metje & Frenzel, 2007). Moreover, acetoclastic methanogens are assumed to prevail especially in fens with sedges (Galand *et al.*, 2005; Juottonen *et al.*, 2005; Godin *et al.*, 2012), because sedges are considered to favour acetoclastic methanogenesis in the root layer due to their provision of acetate (Strom *et al.*, 2003). Nevertheless, we detected only a negligible number of sequences affiliated to *Methanosarcinales* capable of acetate splitting in the FEN site despite its high potential CH₄ production and presence of *Carex* spp. The absence of *Methanosarcinales*, which require relatively high substrate concentrations (Liesack *et al.*, 2000), might be related to the activities of the bacterial community which provide or consume substrates for methanogens (Horn *et al.*, 2003; Kotsyurbenko, 2005; Hamberger *et al.*, 2008). Acetate can be consumed by the secondary syntrophic fermenters, which on the other hand create H₂ for hydrogenotrophic methanogens. Furthermore, acetoclastic methanogenesis appears to be severely inhibited in acidic conditions not only by the low pH or temperature (i.e. in arctic regions), but also by phenolics and other aromatic substances derived from *Sphagnum* mosses (Horn *et al.*, 2003; Kotsyurbenko *et al.*, 2007; Rooney-Varga *et al.*, 2007; Ye *et al.*, 2012). Our observations are in agreement with results obtained from Alaskan peatlands and a German bog (Horn *et al.*, 2003; Rooney-Varga *et al.*, 2007) where those authors also did not find acetoclastic methanogenesis. By contrast, Lin *et al.* (2012) and Kotsyurbenko *et al.* (2004) found the acetoclastic pathway to be dominant in Siberian and North American bogs. Apparently, specific environmental and nutritional conditions may favour different functional group of methanogens (hydrogenotrophic vs. acetoclastic) in peatlands of the same type in different geographical locations.

Methanogens provide a perfect niche for methane-oxidizing bacteria in peatlands, which represent an important functional group due to their ability to consume CH₄ and thus decrease net CH₄ emissions into the atmosphere. In our study sites, both type I and II methanotrophs were detected. Type II (*Methylocystaceae* of *Alphaproteobacteria*) were the dominant methanotrophs and accounted for 1.4%, 1.6% and 2.0% of the total bacterial community in SSF, BOG and FEN, respectively. By contrast, type I *Methylococcaceae* (*Gammaproteobacteria*) were less abundant in all peatland types and accounted for a maximum of 0.2% of the total community in FEN. These trends in methanotroph abundance are comparable with other results (Lin *et al.*, 2012; Serkebaeva *et al.*, 2013). The higher relative abundance of type II methanotrophs can be explained by their tolerance to low O₂ concentrations and ability to fix N₂ (Amaral & Knowles, 1995), which allow them to thrive in a peatland environment with a high water table and

limited N sources (e.g. high C/N ratio). Type II methanotrophs are also known for their lower affinity to CH₄; therefore, they dominate in environments with higher CH₄ concentrations (Bender & Conrad, 1995). *Methylacidiphilaceae* (phylum *Verrucomicrobia*) are the third group of microorganisms capable of methanotrophy and have been described from acidic geothermal habitats (Op den Camp *et al.*, 2009). We detected sequences affiliated to the *Methylacidiphilaceae* in all three peatland types with an average relative abundance of 0.3% of all OTUs. To the best of our knowledge, this is the first time that *Methylacidiphilaceae* have been detected in peatland ecosystems.

Our study demonstrated that the SSF microbial community is positioned between bogs and fens. This corresponds well with the position of SSF on the trophic gradient, which reflects distinct responses of microbial communities to environmental variables. From these variables, pH and peat decomposability (represented by CO₂ and CH₄ potential production) appeared to be the most important drivers structuring the microbial community. Also, *in silico* predicted metabolic potential shows that the microbial community of SSF sites oscillates between BOG and FEN, with some SSF sites being more similar to BOG and others to FEN.

This ambiguous position of SSF was confirmed by the production potentials of CO₂ and CH₄. While the compositions of the archaeal communities were relatively similar in SSF and BOG compared with FEN, their CH₄ production potentials differed significantly. By contrast, the production of CO₂ as indicator of C mineralization did not mirror the bacterial community structure of SSF, which was positioned between BOG and FEN. We explain this discrepancy with the concurrent effects of low pH and low litter quality, which both limit the functioning of distinct bacterial communities in SSF and BOG in a similar way.

The unique SSF ecosystems are intermediate between bogs and fens, and even small changes in their environmental conditions could probably influence their functioning. Future studies should address the spatial heterogeneity of SSFs with special focus on the effect of understorey vegetation and specific vegetation dominants that might influence local C fluxes in these ecosystems.

Acknowledgements

This study was supported by the Grant Agency of the Czech Republic, Project No. 13-17398S, 14-17403P and GAJU 146/2013/P. The access to computing and storage facilities owned by parties and projects contributing to the National Grid Infrastructure MetaCentrum, provided under the programme 'Projects of Large Infrastructure for Research, Development, and Innovations' (LM2010005),

is greatly acknowledged. We are grateful to the IGSG-NGS Sequencing Core at Argonne National Laboratory for preparing the SSU libraries and completing the sequencing. Dr K. Edwards and Dr G. Kerstiens revised the English in this paper.

References

- Amaral JA & Knowles R (1995) Growth of methanotrophs in methane and oxygen counter gradients. *FEMS Microbiol Lett* **126**: 215–220.
- Aronesty E (2013) Comparison of sequencing utility programs. *Open Bioinform J* **7**: 1–8.
- Ausec L, Kraigher B & Mandic-Mulec I (2009) Differences in the activity and bacterial community structure of drained grassland and forest peat soils. *Soil Biol Biochem* **41**: 1874–1881.
- Bates ST, Berg-Lyons D, Caporaso JG, Walters WA, Knight R & Fierer N (2011) Examining the global distribution of dominant archaeal populations in soil. *ISME J* **5**: 908–917.
- Bender M & Conrad R (1995) Effect of CH₄ concentrations and soil conditions on the induction of CH₄ oxidation activity. *Soil Biol Biochem* **27**: 1517–1527.
- Bergmann GT, Bates ST, Eilers KG *et al.* (2011) The under-recognized dominance of *Verrucomicrobia* in soil bacterial communities. *Soil Biol Biochem* **43**: 1450–1455.
- Brookes PC, Kragt JF, Powelson DS & Jenkinson DS (1985) Chloroform fumigation and the release of soil-nitrogen – the effects of fumigation time and temperature. *Soil Biol Biochem* **17**: 831–835.
- Cadillo-Quiroz H, Brauer S, Yashiro E, Sun C, Yavitt J & Zinder S (2006) Vertical profiles of methanogenesis and methanogens in two contrasting acidic peatlands in central New York State, USA. *Environ Microbiol* **8**: 1428–1440.
- Caporaso JG, Kuczynski J, Stombaugh J *et al.* (2010) QIIME allows analysis of high-throughput community sequencing data. *Nat Methods* **7**: 335–336.
- Caporaso JG, Lauber CL, Walters WA *et al.* (2011) Global patterns of 16S rRNA diversity at a depth of millions of sequences per sample. *P Natl Acad Sci USA* **108**: 4516–4522.
- Cappo KA, Blume LJ, Raab GA, Bartz JK & Engels JL (1987) *Analytical Methods Manual for the Direct/Delayed Response Project Soil Survey*. EPA 600/8-87/020, Las Vegas, NV, USA, pp. 8–11.
- Dedysh SN (2009) Exploring methanotroph diversity in acidic northern wetlands: molecular and cultivation-based studies. *Microbiology* **78**: 655–669.
- Dedysh SN, Pankratov TA, Belova SE, Kulichevskaya IS & Liesack W (2006) Phylogenetic analysis and *in situ* identification of Bacteria community composition in an acidic *Sphagnum* peat bog. *Appl Environ Microbiol* **72**: 2110–2117.
- DeSantis TZ, Hugenholtz P, Larsen N *et al.* (2006) Greengenes, a chimera-checked 16S rRNA gene database and workbench compatible with ARB. *Appl Environ Microbiol* **72**: 5069–5072.
- Edgar RC (2010) Search and clustering orders of magnitude faster than BLAST. *Bioinformatics* **26**: 2460–2461.
- Fierer N, Schimel JP & Holden PA (2003) Variations in microbial community composition through two soil depth profiles. *Soil Biol Biochem* **35**: 167–176.
- Fierer N, Bradford MA & Jackson RB (2007) Toward an ecological classification of soil bacteria. *Ecology* **88**: 1354–1364.
- Fisk MC, Ruether KF & Yavitt JB (2003) Microbial activity and functional composition among northern peatland ecosystems. *Soil Biol Biochem* **35**: 591–602.
- Galand PE, Fritze H, Conrad R & Yrjälä K (2005) Pathways for methanogenesis and diversity of methanogenic archaea in three boreal peatland ecosystems. *Appl Environ Microbiol* **71**: 2195–2198.
- Gittel A, Bárta J, Kohoutová I *et al.* (2014) Distinct microbial communities associated with buried soils in the Siberian tundra. *ISME J* **8**: 841–853.
- Godin A, McLaughlin JW, Webster KL, Packalen M & Basiliko N (2012) Methane and methanogen community dynamics across a boreal peatland nutrient gradient. *Soil Biol Biochem* **48**: 96–105.
- Gorham E (1991) Northern peatlands – role in the carbon-cycle and probable responses to climatic warming. *Ecol Appl* **1**: 182–195.
- Gupta V, Smemo KA, Yavitt JB & Basiliko N (2012) Active methanotrophs in two contrasting North American peatland ecosystems revealed using DNA-SIP. *Microb Ecol* **63**: 438–445.
- Hamberger A, Horn MA, Dumont MG, Murrell JC & Drake HL (2008) Anaerobic consumers of monosaccharides in a moderately acidic fen. *Appl Environ Microbiol* **74**: 3112–3120.
- Hartman WH, Richardson CJ, Vilgalys R & Bruland GL (2008) Environmental and anthropogenic controls over bacterial communities in wetland soils. *P Natl Acad Sci USA* **105**: 17842–17847.
- Herrmann M, Hadrich A & Kusel K (2012) Predominance of thaumarchaeal ammonia oxidizer abundance and transcriptional activity in an acidic fen. *Environ Microbiol* **14**: 3013–3025.
- Heylen K, Gevers D, Vanparys B, Wittebolle L, Geets J, Boon N & De Vos P (2006) The incidence of nirS and nirK and their genetic heterogeneity in cultivated denitrifiers. *Environ Microbiol* **8**: 2012–2021.
- Horn MA, Matthies C, Kusel K, Schramm A & Drake HL (2003) Hydrogenotrophic methanogenesis by moderately acid-tolerant methanogens of a methane-emitting acidic peat. *Appl Environ Microbiol* **69**: 74–83.
- Juottonen H, Galand PE, Tuittila ES, Laine J, Fritze H & Yrjälä K (2005) Methanogen communities and Bacteria along an ecohydrological gradient in a northern raised bog complex. *Environ Microbiol* **7**: 1547–1557.
- Kim SY, Lee SH, Freeman C, Fenner N & Kang H (2008) Comparative analysis of soil microbial communities and their responses to the short-term drought in bog, fen, and riparian wetlands. *Soil Biol Biochem* **40**: 2874–2880.
- Koopmans GF, Chardon WJ, Ehlert PAI, Dolfing J, Suurs RAA, Oenema O & van Riemsdijk WH (2004) Phosphorus

- availability for plant uptake in a phosphorus-enriched noncalcareous sandy soil. *J Environ Qual* **33**: 965–975.
- Kopáček J & Hejzlar J (1993) Semi-micro determination of total phosphorus in fresh-waters with perchloric-acid digestion. *Int J Environ Anal Chem* **53**: 173–183.
- Kotsyurbenko OR (2005) Trophic interactions in the methanogenic microbial community of low-temperature terrestrial ecosystems. *FEMS Microbiol Ecol* **53**: 3–13.
- Kotsyurbenko OR, Chin KJ, Glagolev MV, Stubner S, Simankova MV, Nozhevnikova AN & Conrad R (2004) Acetoclastic and hydrogenotrophic methane production and methanogenic populations in an acidic West-Siberian peat bog. *Environ Microbiol* **6**: 1159–1173.
- Kotsyurbenko OR, Friedrich MW, Simankova MV, Nozhevnikova AN, Golyshin PN, Timmis KN & Conrad R (2007) Shift from acetoclastic to H₂-dependent methanogenesis in a West Siberian peat bog at low pH values and isolation of an acidophilic *Methanobacterium* strain. *Appl Environ Microbiol* **73**: 2344–2348.
- Langille MGI, Zaneveld J, Caporaso JG *et al.* (2013) Predictive functional profiling of microbial communities using 16S rRNA marker gene sequences. *Nat Biotechnol* **31**: 814–821.
- le Roes-Hill M, Khan N & Burton SG (2011) Actinobacterial peroxidases: an unexplored resource for biocatalysis. *Appl Biochem Biotechnol* **164**: 681–713.
- Leininger S, Urich T, Schlotter M *et al.* (2006) Archaea predominate among ammonia-oxidizing prokaryotes in soils. *Nature* **442**: 806–809.
- Liesack W, Schnell S & Revsbech NP (2000) Microbiology of flooded rice paddies. *FEMS Microbiol Rev* **24**: 625–645.
- Lin X, Green S, Tfaily MM *et al.* (2012) Microbial community structure and activity linked to contrasting biogeochemical gradients in bog and fen environments of the Glacial Lake Agassiz Peatland. *Appl Environ Microbiol* **78**: 7023–7031.
- Liu ZZ, Lozupone C, Hamady M, Bushman FD & Knight R (2007) Short pyrosequencing reads suffice for accurate microbial community analysis. *Nucleic Acids Res* **35**: e120.
- Mccarthy AJ (1987) Lignocellulose-degrading actinomycetes. *FEMS Microbiol Lett* **46**: 145–163.
- Merilä P, Galand PE, Fritze H, Tuittila ES, Kukko-oja K, Laine J & Yrjälä K (2006) Methanogen communities along a primary succession transect of mire ecosystems. *FEMS Microbiol Ecol* **55**: 221–229.
- Metje M & Frenzel P (2007) Methanogenesis and methanogenic pathways in a peat from subarctic permafrost. *Environ Microbiol* **9**: 954–964.
- Morales SE, Mouser PJ, Ward N, Hudman SP, Gotelli NJ, Ross DS & Lewis TA (2006) Comparison of bacterial communities in New England *Sphagnum* bogs using terminal restriction fragment length polymorphism (T-RFLP). *Microb Ecol* **52**: 34–44.
- Økland RH, Rydgren K & Økland T (2008) Species richness in boreal swamp forests of SE Norway: the role of surface microtopography. *J Veg Sci* **19**: 67–74.
- Op den Camp HJM, Islam T, Stott MB *et al.* (2009) Environmental, genomic and taxonomic perspectives on methanotrophic *Verrucomicrobia*. *Environ Microbiol Rep* **1**: 293–306.
- Pankratov TA, Ivanova AO, Dedysh SN & Liesack W (2011) Bacterial populations and environmental factors controlling cellulose degradation in an acidic *Sphagnum* peat. *Environ Microbiol* **13**: 1800–1814.
- Parks DH & Beiko RG (2010) Identifying biologically relevant differences between metagenomic communities. *Bioinformatics* **26**: 715–721.
- Peltoniemi K, Fritze H & Laiho R (2009) Response of fungal and actinobacterial communities to water-level drawdown in boreal peatland sites. *Soil Biol Biochem* **41**: 1902–1914.
- Pester M, Knorr KH, Friedrich MW, Wagner M & Loy A (2012) Sulfate-reducing microorganisms in wetlands – fameless actors in carbon cycling and climate change. *Front Microbiol* **3**: 72.
- Philippot L, Andersson SGE, Battin TJ, Prosser JI, Schimel JP, Whitman WB & Hallin S (2010) The ecological coherence of high bacterial taxonomic ranks. *Nat Rev Microbiol* **8**: 523–529.
- Rooney-Varga JN, Giewat MW, Duddlestone KN, Chanton JP & Hines ME (2007) Links between archaeal community structure, vegetation type and methanogenic pathway in Alaskan peatlands. *FEMS Microbiol Ecol* **60**: 240–251.
- Schink B & Stams AJM (2002) Syntrophism among prokaryotes. *The Prokaryotes. An Evolving Electronic Resource for the Microbiological Community, release 3.8., Vol. 2*, (Dworkin M, Schleifer KH & Stackebrandt E, eds), pp. 309–335. Springer, New York.
- Serkebaeva YM, Kim Y, Liesack W & Dedysh SN (2013) Pyrosequencing-based assessment of the bacteria diversity in surface and subsurface peat layers of a Northern Wetland, with focus on poorly studied phyla and candidate divisions. *PLoS ONE* **8**: e63994.
- Smit E, Leeflang P, Gommans S, van den Broek J, van Mil S & Wernars K (2001) Diversity and seasonal fluctuations of the dominant members of the bacterial soil community in a wheat field as determined by cultivation and molecular methods. *Appl Environ Microbiol* **67**: 2284–2291.
- Straková P, Niemi RM, Freeman C *et al.* (2011) Litter type affects the activity of aerobic decomposers in a boreal peatland more than site nutrient and water table regimes. *Biogeosciences* **8**: 2741–2755.
- Strom L, Ekberg A, Mastepanov M & Christensen TR (2003) The effect of vascular plants on carbon turnover and methane emissions from a tundra wetland. *Glob Chang Biol* **9**: 1185–1192.
- Sun H, Terhonen E, Koskinen K, Paulin L, Kasanen R & Asiegbu FO (2014) Bacterial diversity and community structure along different peat soils in boreal forest. *Appl Soil Ecol* **74**: 37–45.
- Tian JQ, Chen H, Dong XZ & Wang YF (2012) Relationship between archaeal community structure and vegetation type in a fen on the Qinghai-Tibetan Plateau. *Biol Fertil Soils* **48**: 349–356.
- Urbanová Z, Pícek T & Bárta J (2011) Effect of peat re-wetting on carbon and nutrient fluxes, greenhouse gas production

- and diversity of methanogenic archaeal community. *Ecol Eng* **37**: 1017–1026.
- Vance ED, Brookes PC & Jenkinson DS (1987) An extraction method for measuring soil microbial biomass-C. *Soil Biol Biochem* **19**: 703–707.
- Ye RZ, Jin QS, Bohannon B, Keller JK, McAllister SA & Bridgham SD (2012) pH controls over anaerobic carbon mineralization, the efficiency of methane production, and methanogenic pathways in peatlands across an ombrotrophic-minerotrophic gradient. *Soil Biol Biochem* **54**: 36–47.

Supporting Information

Additional Supporting Information may be found in the online version of this article:

Fig. S1. UniFrac phylogenetic dissimilarity between prokaryotic communities.

Fig. S2. Principal component analysis (PCA) of functional potential distribution of BOG, SSF and FEN.

Table S1. Relative sequence abundance of all detected archaeal and bacterial classes in all samples.

Table S2. Comparison of functional potential between different peatland sites (BOG, SSF, FEN) based on KEGG mapping.

Table S3.(a) Comparison of functional potential between different peatland sites (BOG, SSF, FEN) based on clusters of orthologous groups (COG) database. (b) Potential for cellulose degradation. (c) Aromatics degradation potential constructed from biom file.

Paper 6

Chronakova A, **Barta J**, Kastovska E, Urbanova Z, Picek T (2019) Spatial heterogeneity of belowground microbial communities linked to peatland microhabitats with different plant dominants. *FEMS MICROBIOLOGY ECOLOGY* 95:fiz130-.

RESEARCH ARTICLE

Spatial heterogeneity of belowground microbial communities linked to peatland microhabitats with different plant dominants

Alica Chroňáková^{1,*}, Jiří Bárta², Eva Kaštovská², Zuzana Urbanová² and Tomáš Pícek²

¹Biology Centre, CAS, Institute of Soil Biology and SoWa RI, Na Sádkách 7, České Budějovice 370 05, Czech Republic and ²Department of Ecosystem Biology, University of South Bohemia in České Budějovice, Branišovská 1760, České Budějovice 370 05, Czech Republic

*Corresponding author: Biology Centre, Academy of Sciences of the Czech Republic, Institute of Soil Biology and SoWa RI, Na Sádkách 7, České Budějovice 370 05, Czech Republic. Tel: +420 387 775 770; Fax: +420 385 310 133; E-mail: alica.chronakova@upb.cas.cz

One sentence summary: The altered biochemical profiles of peat soils under different plant functional types, such as blueberry and cotton-grass, had a measurable and distinct impact on the soil prokaryotic and fungal communities.

Editor: Hannu Fritze

ABSTRACT

Peatland vegetation is composed mostly of mosses, graminoids and ericoid shrubs, and these have a distinct impact on peat biogeochemistry. We studied variation in soil microbial communities related to natural peatland microhabitats dominated by *Sphagnum*, cotton-grass and blueberry. We hypothesized that such microhabitats will be occupied by structurally and functionally different microbial communities, which will vary further during the vegetation season due to changes in temperature and photosynthetic activity of plant dominants. This was addressed using amplicon-based sequencing of prokaryotic and fungal rDNA and qPCR with respect to methane-cycling communities. Fungal communities were highly microhabitat-specific, while prokaryotic communities were additionally directed by soil pH and total N content. Seasonal alternations in microbial community composition were less important; however, they influenced the abundance of methane-cycling communities. Cotton-grass and blueberry bacterial communities contained relatively more α -Proteobacteria but less *Chloroflexi*, *Fibrobacteres*, *Firmicutes*, NC10, OD1 and *Spirochaetes* than in *Sphagnum*. Methanogens, syntrophic and anaerobic bacteria (i.e. *Clostridiales*, *Bacteroidales*, *Opitutae*, *Chloroflexi* and *Syntrophorhabdaceae*) were suppressed in blueberry indicating greater aeration that enhanced abundance of fungi (mainly *Archaeorhizomycetes*) and resulted in the highest fungi-to-bacteria ratio. Thus, microhabitats dominated by different vascular plants are inhabited by unique microbial communities, contributing greatly to spatial functional diversity within peatlands.

Keywords: *Sphagnum*; vascular plant; peatland; prokaryotes; fungi; soil microbial community

INTRODUCTION

Northern peatlands are highly valuable and fragile ecosystems as they store significant amount of water and C and serve as hot spots for biodiversity (Carroll et al. 2015). In temperate zones

(e.g. Central Europe, including the Czech Republic), they represent the last islands of North-Western wetland types remaining from the last ice age (Spitzer and Bufková 2012) and, as such, are protected under the Ramsar Convention as 'Wetlands of International Importance' (Subject of a Ramsar Advisory

Received: 15 January 2019; Accepted: 16 August 2019

© FEMS 2019. All rights reserved. For permissions, please e-mail: journals.permissions@oup.com

Mission since 2001). Three main peatland types may be generally defined based on water and nutrient supply: fens fed by springs and mineral and nutrient rich surface waters, bogs fed by atmospheric precipitation poor in nutrients and transitional mires fed by both. Consequently, the vegetation composition differs between fens, which are dominated by vascular plants, mostly graminoid species and *Sphagnum*-dominated bogs (Rydin and Jeglum 2006). Hydrological, soil and vegetational differences are further reflected in the differing composition of soil microbial communities between particular peatland types (Lin et al. 2012; Urbanová and Bárta 2014). In the latter study, acidotolerant oligotrophic bacteria and archaea (e.g. *Acidobacteria*, *Deltaproteobacteria* and *Methanomicrobia*) dominated in bog microbial communities, whereas fens were characterized by an increased relative abundance of *Gammaproteobacteria*, *Verrucomicrobia* and *Actinobacteria*.

Besides the differences between peatland types, a significant internal heterogeneity exists within each particular peatland system, where water table level and plant communities shape the surface into three main microform types (microhabitats): elevated and relatively dry hummocks, intermediate lawns and wet depressed hollows. These microhabitats are commonly dominated by different plant species belonging to different functional groups, with *Sphagnum* mosses in hollows, graminoids on lawns and ericoids on hummocks. Generally speaking, each plant species provides a specific niche due to the differing composition of living plant biomass, litter and compounds released to the surroundings (exudates), and this has an effect on the composition and/or activity of peatland soil microbial communities. Species within particular functional groups have similar demands as regards environmental conditions, and thus may have similar effects on their habitats through their comparable lifestyles.

Sphagnum peat is naturally resistant to microbial decay due to its organo-chemical composition, whereby phenolics and uronic acids lead to acidification, suppression of vascular plants and, together with *Sphagnum* secondary metabolites (Mellegård et al. 2009), inhibit microbial litter decomposition (Verhoeven and Toth 1995; Verhoeven and Liefveld 1997). Thus, dominance of *Sphagnum* mosses is essential for C sequestration in peatlands. Ericoid shrubs occupy aerated microhabitats (hummocks) and attract ericoid mycorrhiza, thereby significantly enhancing the fungi-to-bacteria ratio (F/B) of the soil microbial community (Bragazza et al. 2015) and facilitating microbial peat degradation and mobilization of P and N from complex soil organic matter (SOM) (Cairney and Meharg 2003). Presence of graminoids is generally connected with input of relatively nutrient-rich litter (Moore, Bubier and Bledzki 2007; Kaštovská et al. 2018; Mastný et al. 2018), significant root exudation flux into the peat (Jassey et al. 2013; Robroek et al. 2016; Edwards et al. 2018) and delivery of O₂ to the rhizosphere via root transport (Saarinen 1996). Graminoids shift the composition of the associated microbial community (Jassey et al. 2013; Robroek et al. 2015) via large exudation fluxes, including methanogenic substrates, and enhance the contribution of methanogens (Schutz, Schröder and Renzenberg 1991; Greenup et al. 2000). Similarly, as with ericoids, presence of graminoids is expected to enhance peat decomposition. However, there is large interspecies variability in water and nutritional demands (Bragazza 2006) and exudate composition among graminoids and, consequently, in their potential impact on the habitat. While true sedges (f.e. *Carex* sp.) tend to occupy nutrient-rich lawns and are associated with faster mineralization of organic matter, *Cyperaceae* (*Eriophorum* sp.) usually occupy acidic, nutrient poorer peatlands. Cotton-grass

(*Eriophorum vaginatum* L.), for example, efficiently takes up N in various forms from nearby soils and thereby stabilizes niche differences (Chapin, Moilanen and Kielland 1993; Jonasson and Shaver 1999).

It is well documented that microhabitats dominated by species of different functional types (as exist within peatlands) differ in soil microbial biomass (Bragazza et al. 2015; Kaštovská et al. 2018) and activity, such as CO₂ and CH₄ production and consumption (Bubier et al. 1993; Fisk, Ruether and Yavitt 2003; Kettunen 2003; Dorodnikov et al. 2013; Krohn et al. 2017) and extracellular enzyme activity (Parvin et al. 2018). In comparison with information on processes, there is a distinct lack of data on microbial community composition in such microhabitats. To date, only methane-cycling communities, methanogens and methanotrophs have received significant attention (Galand, Fritze and Yrjala 2003; Kotiaho et al. 2010; Kip et al. 2011; Juottonen et al. 2015; McEwing, Fisher and Zona 2015; Robroek et al. 2015), while other microbial groups, such as Actinobacteria or fungi (Peltoniemi, Fritze and Laiho 2009; Kotiaho et al. 2013), or complex microbial communities (Sundh, Nilsson and Borga 1997; Juottonen et al. 2005; Sun et al. 2014) have received far less. As vascular plants, which are commonly associated with enhanced soil microbial biomass and activity (Robroek et al. 2015), are now spreading over peatlands due to ongoing climate change (Jassey et al. 2013; Buttler et al. 2015), it is important to link the occurrence of different types of vascular plants with their associated microorganisms. An understanding of how vegetation impacts peatland microbial communities, which drive C and nutrient cycles and control greenhouse gas emissions, is critical for predicting C sequestration potential of peatlands under vegetation alteration.

We recently studied the detailed functioning of widespread but overlooked types of peatland, referred to in the literature as spruce swamp forests (Laaksonen et al. 2008; Maanaviija et al. 2014). In Central Europe and parts of Western Europe, these peatlands are located in mountainous areas comprising nutrient-poor, high-grade metamorphic rocks of the Moldanubicum zone. These are characterized by a relatively species-poor understory with a patchy distribution reflecting microsite topography. The wettest hollows are only occupied by *Sphagnum* mosses (mainly *S. fallax*), the lawns are covered by cotton-grass, a species with a highly developed tolerance to low resources (Chapin, Moilanen and Kielland 1993; Jonasson and Shaver 1999), while ericoids (i.e. blueberry (*Vaccinium myrtillus* L.) are codominant on drier hummocks. We showed that microhabitats within peatlands (i.e. hollows, lawns and hummocks) differ in peat chemical (compound and elemental) composition, reflecting biomass composition of the dominant species and differences in their nutrient acquisition efficiencies (Kaštovská et al. 2018). Their litter decomposed at significantly different rates (slowest for *Sphagnum* and roots of cotton-grass and fastest for cotton-grass shoots (Kaštovská et al. 2018)), and leached dissolved organic matter of differing quality, the composition and degradability of which mirrored that of the plant litter (Mastný et al. 2018). Plant dominants also differed in composition and flux of exudates released from roots and from the stelas of *Sphagnum*, with exudation showing further significant difference during the vegetation season (Edwards et al. 2018). All these characteristics contributed to the formation of unique environments within the peatland, which may be occupied by very different microbial communities possessing different functions. In this study, which was conducted in the same study sites (three peatlands in South Bohemia, Czech Republic), we aimed to characterize the size, composition and specificity of soil prokaryotic and fungal communities associated with

three distinct peatland microhabitats dominated by *Sphagnum*, cotton-grass and blueberry, with emphasis on the diversity and abundance of methanogens and methanotrophs. We hypothesized that:

- i) natural, long-term presence of vascular plants would increase the proportion of aerobic microbes, root-associated copiotrophs and, especially, methanotrophs in such microhabitats compared with *Sphagnum*-dominated hollows, due to root exudation of easily decomposable compounds (Edwards et al. 2018), the predominantly aerobic conditions in blueberry-dominated hummocks, and active oxygen transport to the rhizosphere by cotton-grass (Saarinen 1996).
- ii) methanogen community size would be higher in the presence of cotton-grass than with blueberry due to a greater delivery of methanogenic substrates, while the total fungal community would be greater in the latter habitat due to a lower water table and attraction to blueberry roots.
- iii) microhabitat-specific community composition would be maintained across all three peatland sites due to strong determination by natural differences in plant characteristics, while potential differences in microbial composition caused by different physico-chemical (average water level and nutritional) characteristics between sites and seasons (described before by Kaštovská et al. 2018) would be smaller.

MATERIALS AND METHODS

Sampling sites and peat sampling

Soil samples were collected in May, July and September 2013 at three study sites (Filipova, Kvilda, Tetřevská) in the Šumava Mountains, south-west Czech Republic (49° 1' 10" N, 13° 34' 47" E). All sites are situated on an upland plateau at an altitude of ~1100 m a. s. l. The area is characterized by a cold and humid climate with mean temperature ~4°C and mean annual precipitation of 1100 mm (years 1961–1990, statistics by the Czech Hydro-Meteorological Institute).

At each site, three microhabitats were selected dominated by either *Sphagnum* mosses (mainly *Sphagnum fallax*, SP), blueberry (*Vaccinium myrtillus*, L., VM, coverage 45–75%) or cotton-grass (*Eriophorum vaccinatum*, L., EV, with coverage of 25–50%). These habitats differed in their mean water table level (expressed as cm below the surface, mean ± sd of continual measurement in 2014), with the highest in SP (−5.6 ± 3.3 cm), followed by EV (−10.7 ± 4.3 cm) and the lowest in VM (−17.6 ± 4.0 cm). Based on our previous study, we knew that the selected habitats differed significantly in peat biochemistry, with SP forming the N-richest environment, EV depleting nutrients from the peat and VM stimulating decomposition processes and enhanced P availability (Kaštovská et al. 2018). In this study, selected soil and pore water chemical parameters were used to explain variability in microbial community composition (Table 1).

At each study site, four peat cores per microhabitat type were sampled (6.5 × 5.5 cm inner dimension) to a depth of 30 cm at randomly selected subsites (4 samples × 3 microhabitats × 3 sites). Due to the water table levels listed above, VM samples were half anaerobic, while SP samples were almost fully anaerobic. The soil cores were cooled throughout the field campaign and in the laboratory, where they were processed as follows. Each core was vertically dissected into equal halves and roots and other woody material were removed. The soil for molecular analysis was sampled by an ethanol-sterilized spoon along the

whole depth profile (minimum 10 g of fresh peat), homogenized by hand and immediately freeze-dried. The rest of the core was homogenized by hand and used for chemical and biochemical analysis.

DNA extraction

Total environmental DNA was extracted from 0.2 to 0.4 g of freeze-dried soils using the Griffiths method (Griffiths et al. 2000). The quality and quantity of DNA was checked by gel electrophoresis and PicoGreen® assay (Invitrogen, Waltham, MA). DNA extracts were checked for inhibition by dilution assay.

Illumina MiSeq sequencing of the 16S rRNA gene

Aliquots of DNA extracts were sent to the Argonne National Laboratory (Illinois, USA) for preparation of a library. Polymerase chain reaction (PCR) contained 13 µL PCR-grade water, 10 µL 5 PRIME HotMasterMix, 0.5 µL each of the forward 515F (Parada, Needham and Fuhrman 2016) forward (5'-GTGYCAGCMGCCGCG GTAA-3') and reverse 806R (Apprill et al. 2015) (5'-GGACTACNV GGGTWTCTAAT-3') primers (0.2 µM final concentration), and 1 µL of genomic DNA. Reactions were held at 94°C for 3 min to denature the DNA, with amplification proceeding for 35 cycles at 94°C for 45 s, 50°C for 60 s and 72°C for 90 s; a final extension of 10 min at 72°C was added to ensure complete amplification. The reverse primer contained a 12-base error-correcting Golay barcode to facilitate multiplexing. Cleaned amplicons were quantified using PicoGreen dsDNA reagent in 10 mM Tris buffer (pH 8.0, Invitrogen, Waltham, MA). A composite sample for sequencing was created by combining equimolar ratios of amplicons from the individual samples and cleaned using the Ultra Clean® htp 96-well PCR clean-up kit (MO BIO Laboratories, Carlsbad, CA). Sample purity and concentration were estimated by spectrophotometry. Amplicons were sequenced on the Illumina MiSeq platform. Forward and reverse bacterial 16S rDNA reads were joined using ea-utils to obtain reads of ~250 bp length (Caporaso et al. 2010). Quality filtering of the reads was applied as previously described (Caporaso et al. 2011). After quality filtering, the sequences were trimmed to 250 bp. We obtained 2.5 million bacterial sequences after joining and quality trimming. Both 16S and ITS1 amplicons were trimmed to equal lengths in order to avoid false positive operational taxonomic unit (OTU) clusters (Edgar 2013). Bacterial reads were clustered (>97% similarity) to OTUs using an open-reference OTU picking protocol including chimera removal (QIIME 1.9.1, (Caporaso et al. 2010)), first with uclust (Edgar 2013) being applied to compare the sequences against the Silva 119 database (Quast et al. 2013). Taxonomy was assigned to each read by accepting the Silva119 taxonomy string of the best matching Silva119 sequence. The number of sequences was rarefied to 4000 seqs per sample.

Pyrosequencing of the fungal ITS region

The barcoded PCR primers ITS1F/ITS2R (Gardes and Bruns 1993), which target the ITS region, were used to construct the fungal libraries. Fusion primers were designed according to the guidelines of Roche (www.my454.com). The PCR reaction contained 1 × Fast Start High Fidelity PCR System (Roche, Penzberg, Germany), 1 mM BSA, 25 ng of template DNA and 5 pmol of each primer. The PCR reaction conditions were as follows: 94°C for 5 min; 20 and 26 cycles (for the first round of PCR without barcodes, for the second round with barcodes, respectively) of denaturation at 94°C for 45s, annealing at 55°C

Table 1. Peat chemistry in studied microhabitats. Average levels of water table (cm), soil pH, concentrations of C and N (%), dissolved organic C (DOC; mg l⁻¹) and concentrations of mineral N forms (N-NH₄, N-NO₃; mg l⁻¹) of the peat formed in microhabitats covered only by *Sphagnum* or affected by the presence of cotton-grass or blueberry (sampled from four independent soil pits per site) in three sampling sites (Tetřevská, Filipova, Kvilda). Peat cores were sampled in May, June and September 2013 (mean, standard deviation of mean SEM, n = 36). Results of generalized linear model (GLM) on the effect of microhabitats are shown with site and time as covariates. Lower case letters show differences among peat characteristics formed in the presence of different plant dominants (P < 0.05). Abbreviations: EV—cotton-grass, SP—*Sphagnum*, VM—blueberry.

	EV	SP	VM	Microhabitat	Site	Time
Water table	-10.7 ^b ± 4.3	-5.6 ^a ± 3.3	-17.6 ^c ± 4.0	***		*
pH	4.01 ^a ± 0.03	4.31 ^a ± 0.04	3.94 ^b ± 0.02	***	***	**
Ctot	45.1 ^a ± 0.2	43.8 ^a ± 0.9	46.8 ^a ± 0.3	n.s.	***	n.s.
Ntot	1.12 ^a ± 0.05	1.63 ^b ± 0.05	1.59 ^b ± 0.03	***	**	n.s.
DOC	72.9 ^a ± 5.2	66.5 ^a ± 5.5	92.3 ^b ± 6.8	**	**	***
NH ₄	0.15 ^a ± 0.01	0.59 ^c ± 0.06	0.26 ^b ± 0.03	***	***	***
NO ₃	0.10 ^a ± 0.01	0.09 ^a ± 0.01	0.17 ^b ± 0.03	**	n.s.	*

n.s. nonsignificant.

*P < 0.05.

**P < 0.01.

***P < 0.001.

for 45s and extension at 72°C for 60s, followed by a final elongation at 72°C for 10 min. All samples were amplified in triplicates, pooled, and purified by the QIAquick PCR Purification kit (Qiagen, Hilden, Germany). The quality of the amplicons was checked by agarose (2%) gel electrophoresis and quantified using a Quant-iT dsDNA BR assay kit (Invitrogen, CA, USA). Amplicons were pooled equimolar to create two forward-oriented libraries. Subsequently, two single-stranded libraries were purified with Agencourt AMPure beads (Agencourt Bioscience Corporation, Beverly, MA, USA; Beckman Coulter) and their quality was evaluated using DNA 1000 LabChip software with a Bioanalyzer 2100 (Agilent Technologies, Waldbronn, Germany). Sequencing of the ITS region was performed on a 454 Genome Sequencer Junior system (Roche), following the manufacturer's protocol for amplicon sequencing. An initial signal processing and quality filtering of the pyrosequencing reads sequences was performed using the automatic amplicon pipeline of the GS Run Processor (Roche) to remove failed and low-quality reads from the raw data. Before picking the OTUs, the fungal ITS1 region was extracted from reads using the ITSx algorithm (Bengtsson-Palme et al. 2013). Fungal reads were clustered to OTUs using an open-reference OTU picking protocol (sequence similarity 98.5%) using uclust, which includes chimera removal (Edgar 2013), in conjunction with the UNITE ver. 5.3.2015 database (Koljalg et al. 2013). The Blast algorithm (e-value ≤ 0.001) was used for taxonomic assignment. The FUNGuild algorithm (Nguyen et al. 2016) was used for life style fungal assignments. The number of sequences was rarefied to 350 seqs per sample.

Diversity measures

The alpha diversity metrics, Shannon diversity, Chao1 richness and Faith's phylogenetic diversity (prokaryota only), were calculated after rarefying the prokaryotic and fungal samples to the same sequencing depth of 4000 and 350 sequences, respectively. Prior to computing the UniFrac distances, singleton OTUs (i.e. OTUs with only one sequence) were filtered out as these are likely to represent sequencing or PCR errors and/or chimeras (Edgar 2013).

qPCR analyses

Real-time quantitative PCR (qPCR) was used to quantify genes encoding bacterial 16S rRNA and fungal 18S rRNA to assess

bacterial and fungal abundances and Fungi:Bacteria (F/B) ratios of the communities, and the α-subunit of methyl-coenzyme M reductase (*mcrA*) and the α-subunit of methane monooxygenase (*pmoA*) to quantify the abundances of methanogens and methanotrophs, respectively. Information on selected genes, primers and conditions is summarized in Table S1 (Supporting Information). The qPCR amplifications were performed with a reaction mix consisting of 10 μL FastStart Universal SYBR Green Master (ROX) (Roche, Penzberg, Germany), the gene-specific primers and 5 μL template DNA, brought to a total volume of 20 μL with sterile water. Amplification was performed on the StepOnePlus Real-Time PCR system (Applied Biosystems, Foster City, CA). Template DNA was checked for the presence of PCR inhibitors in a serial dilution series (20x, 40x, 80x, 160x, 320x diluted DNA samples). Standard curves were constructed using 10-fold serial dilutions of plasmids containing a partial sequence of the 16S rRNA gene of a soil isolate (*Variovorax paradoxus*), the 18S rRNA gene of a soil isolate (*Fusarium sp.*), the *Methanosarcina mazei mcrA* gene (Radl et al. 2007) and an environmental clone sequence of the *pmoA* gene. Samples, standards and nontemplate controls were run in triplicates. The specificity of the qPCR reactions was checked by: (i) melting curve analysis and (ii) analyzing amplicon product sizes on a 2% agarose gel.

Statistical analysis

A GLM with sampling time and site as covariates, followed by Tukey HSD testing, was used to assess the effect of microhabitat types on soil and pore water chemistry and gene abundance. Similarly, differences between the microbial communities (relative abundance of prokaryotic and fungal taxa) associated with the three microhabitats were analyzed using the Kruskal–Wallis test followed by the post-hoc Dunn's test (Dunn 1964). Data were log- or sqrt-transformed to meet requirements for normality and homogeneity of variance. Differences were considered significant at P < 0.05, after Bonferroni correction. All statistical tests were conducted in R Studio version 3.3.2, using the dunn.test, FSA, stats and vegan packages (Dinno 2016; Oksanen et al. 2016; Ogle 2017).

Differences in the microbial communities associated with each microhabitat or season were tested by 3-way crossed permutational MANOVA (PerMANOVA) followed by pairwise t-tests. All multivariate tests were performed on sqrt transformed OTU count data under a reduced model with a restricted

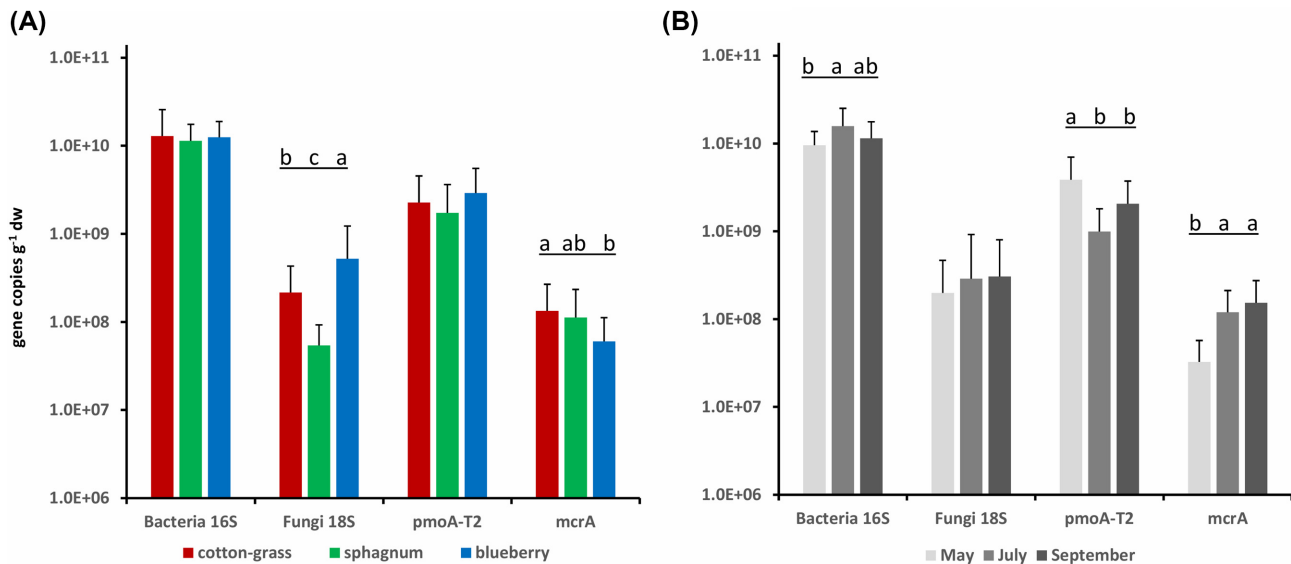


Figure 1. Gene copy numbers in peat soils across microhabitats (A) and across seasons (B). Absolute abundance of bacterial 16S rRNA (Bacteria 16S), fungal 18S rRNA (Fungi 18S), type II methanotrophic *pmoA* (*pmoA*-T2) and methanogenic *mcrA* genes from all three studied sites (Tetřevská, Filipova, Kvilda) are shown (means and standard error bars are shown, $n = 36$). Different superscripts denote significant differences among microhabitats and seasons (results of GLM with microhabitat (A) and time (B) as categorical predictors are shown). Note the logarithmic scale on the y-axis.

number of permutations ($n = 999$). Distances were calculated after Bray–Curtis and the analysis was conducted using PRIMER v6 (PERMANOVA+; Clarke and Gorley 2006). Distance-based Redundancy Analysis (db-RDA; Legendre and Anderson 1999) with iterative forward selection was further used to select environmental parameters with the strongest predictive power (Canoco v5; ter Braak and Šmilauer 2012).

Dissimilarities between community composition of different microhabitats and identification of OTUs predominantly contributing to these differences were identified by Similarity Percentage analysis (SIMPER; Clarke 1993). The Student's *t*-test (*t*) was performed on the OTUs identified in order to determine statistically over- or under-represented ($P < 0.05$) OTUs between the two microhabitat groups.

Data deposition

Sequence files were submitted to the European Nucleotide Archive (ENA), project ID PRJEB20098.

RESULTS

Abundance of bacteria, fungi and methane-cycling communities

Both the bacterial and fungal community sizes inferred from 16S rRNA and 18S rRNA gene abundances, respectively, differed between sites ($P < 0.05$), though this effect was weaker than the effects of microhabitat or time (GLM models; Table S2, Supporting Information). Bacterial abundance was similar across microhabitats (Fig. 1A), but changed significantly over time ($P < 0.01$), with a peak in July (Fig. 1B). On the other hand, while fungal community size was temporally stable it was highly microhabitat-specific ($P < 0.001$), being lowest in SP and highest in VM, with EV in between (Fig. 1A). The type of microhabitat also influenced the Fungi:Bacteria ratio (F/B), which was generally very low (from 0.08 to 0.19) and increased in the order $SP \leq EV < VM$ (Table S2, Supporting Information).

Methane-cycling microorganisms were important contributors to the prokaryotic communities, with methanotrophs forming on average 15–23% of the community and methanogens <1% (inferred from gene copy numbers; Table S2, Supporting Information). While methanotrophs were similarly abundant in different microhabitats, the methanogenic community size was significantly higher in EV than in VM, with SP in between (Fig. 1A). Both methanotroph and methanogen abundances changed significantly over time. While the size of the methanotrophic community was greatest in May and later decreased, the abundance of methanogens showed the opposite trend, with the lowest value in May and greater abundances in July and September (Fig. 1B). Methanogen, but not methanotroph, abundance differed weakly across sites ($P < 0.05$), being higher on Tetřevská than on Filipova ($P = 0.009$).

Microbial α -diversity patterns across microhabitats

After quality filtering, a total of 2.5 and 0.15 million prokaryotic and fungal sequences, respectively, were obtained from the samples analyzed. Further, both datasets were rarefied to obtain 4000 or 350 sequences per sample, representing 5284 and 505 prokaryotic and fungal OTUs, respectively. Good's coverage (Esty 1986) ranged from 72.4% to 99.3% for prokaryotes and from 92.3% to 99.7% for fungi. The α -diversity of the prokaryotic and fungal communities was generally stable across microhabitats, seasons and sites, with the exception of a significant microhabitat effect on fungal richness that decreased from VM through SP to EV (GLM models, $P < 0.05$, Table 2).

Drivers of soil microbial community composition

Microhabitat was the most significant predictor of prokaryotic and fungal community composition ($P = 0.001$ and $P = 0.002$, respectively), followed by site ($P = 0.014$ and $P = 0.01$, respectively), while the time effect was nonsignificant (tested by PERMANOVA with microhabitat and time as fixed effects and site as a random effect; Table 3). EV contained a significantly differ-

Table 2. Variation of diversity indices of prokaryotic and fungal peat communities in microhabitats: EV—cotton-grass, SP—*Sphagnum*, VM—blueberry (mean \pm standard deviations). Data were collected from all three studied sites (Tetřevská, Filipova, Kvilda). Results of GLM on the effect of microhabitat, time and site on diversity indices of respective microbial communities are shown. Different letters indicate significant difference in diversity parameters between microhabitats ($P < 0.05$).

	EV	SP	VM	Microhabitat	Time	Site
Prokaryotes						
Phylogenetic diversity	75.4 \pm 12.9	79.5 \pm 16.2	75.5 \pm 12.2	n. s.	n. s.	n. s.
chao1	2693.8 \pm 593.9	2703.7 \pm 794.0	2730.1 \pm 672.0	n. s.	n. s.	n. s.
Species (OTU) observed	997.3 \pm 192.1	1033.4 \pm 239.3	1035.5 \pm 196.3	n. s.	n. s.	n. s.
Shannon diversity (<i>H'</i>)	7.8 \pm 1.1	8.1 \pm 0.9	7.9 \pm 1.1	n. s.	n. s.	n. s.
Fungi						
chao1	59.0 \pm 21.5 ^b	66.3 \pm 35.8 ^{a,b}	91.8 \pm 31.6 ^a	*	n. s.	n. s.
Species (OTU) observed	45.5 \pm 15.3 ^b	56.7 \pm 32.6 ^{a,b}	70.7 \pm 22.7 ^a	*	n. s.	n. s.
Shannon diversity (<i>H'</i>)	2.1 \pm 1.2	2.5 \pm 0.9	2.9 \pm 0.5	n. s.	n. s.	n. s.

Table 3. Microhabitat, site and time effects on composition of soil prokaryotic and fungal communities. Results of perMANOVA based on Bray-Curtis dissimilarities of the relative abundance of OTUs (with microhabitat and time as fixed factors and site as random factor). Significant differences using Monte Carlo simulations are shown in bold ($P(\text{MC})$). Data were collected from all three studied sites (Tetřevská, Filipova, Kvilda).

source	Prokaryotes			Fungi		
	df	Pseudo-F (F.model)	P (MC)	df	Pseudo-F (F.model)	P (MC)
Microhabitat	2	2.4519	0.001	2	2.8991	0.002
Time	2	1.3014	0.147	1	1.8631	0.092
Site	2	1.5347	0.014	2	2.3097	0.010
Microhabitat \times Time	4	1.0224	0.458	2	1.1935	0.309
Microhabitat \times Site	3	1.1548	0.254	4	1.6574	0.013
Time \times Site	3	1.0120	0.463	2	0.9568	0.502
Microhabitat \times Time \times Site	5	1.0578	0.320	4	0.8064	0.812

ent prokaryotic community than the other two microhabitats on all three sites ($P < 0.05$), while differences in fungal community composition between microhabitats was site-dependent (Table S3, Supporting Information). In particular, fungal community structures in VM differed from those in EV at Kvilda and Tetřevská, but differed from SP at Filipova ($P < 0.05$ for all comparisons). Within sampling sites, Tetřevská differed significantly from Filipova in the case of prokaryotic community composition ($P < 0.05$) and from both the other sites in fungal community composition ($P < 0.05$).

Prokaryotic community composition in different microhabitats

Significant differences in soil prokaryotic communities between microhabitats and sites were corroborated by db-RDA (Fig. 2A). The explanatory variables (including abiotic factors) accounted for 33.8% of total variability in prokaryotic community composition. In addition to the effects of microhabitat and site, there was a significant effect of soil pH (iterative forward selection, Pseudo-F = 4.5, $P_{\text{adj}} = 0.04$), total N content (TN, Pseudo-F = 4.1, $P_{\text{adj}} = 0.04$) and concentration of nitrates (Pseudo-F = 1.9, $P_{\text{adj}} = 0.04$). In particular, the prokaryotic community in SP was associated with the highest soil pH, while that in EV was related to the lowest TN content (Table 1).

A test of significance was performed (SIMPER, Student's *t*-test; Table S4, Supporting Information) in order to identify differences in the relative abundance of OTUs with the largest impact on the differences across microhabitats (with contribution $>0.1\%$). The results showed that OTU15 and OTU35 (both

Rhodoplanes sp.) are specifically associated with VM, OTU78 (*C. Methanoregula*), OTU46 (*Desulfomonile* sp.), and various *Opiritales*-related OTUs are associated with EV, and *Methylocystaceae*-OTUs, especially *Methylosinus* (OTU1), with both VM and EV. On the contrary, SP had an over-representation of *Clostridiales*-, *Dehalococcoidales*- and *Myxococcales*-OTUs, indicating enlarged anaerobic microbial consortia.

In general, the prokaryotes in the peat soils across microhabitats were dominated by *Proteobacteria* and *Acidobacteria*, followed by *Verrucomicrobia*, *Firmicutes*, *Actinobacteria* and *Planctomycetes* (Fig. 3A). Nine phyla differed significantly in abundance among microhabitats (Kruskal-Wallis test, $P < 0.05$, Table 4). *Euryarchaeota*, *Fibrobacteres*, *Firmicutes* and *Chloroflexi* were more abundant in SP than in the other two microhabitats. Many of these phyla have members preferring anaerobic metabolism (e.g. methanogens, fermenters). On the contrary, the VM and EV microhabitats possessed significantly higher proportions of *Proteobacteria*, including α -*Proteobacteria*, when compared to SP. The majority of *Proteobacterial* sequences were assigned to the α - and δ -classes, contributing 21.6–31.4% and 3.9–5.6% to the total sequences in the prokaryotic community, respectively. The relative abundances of *Methylocystaceae* (α -*Proteobacteria*), which contribute to aerobic methanotrophy, were significantly higher in the VM and EV microhabitats in comparison to SP (relative abundance 20.8%, 21.1% and 14.2%, respectively). *Deltaproteobacteria* were mostly represented by various syntrophs, anaerobes and *S*-respiring bacteria. The sum of the relative abundance of potential syntrophic microbes (families: *Syntrophaceae*, *Syntrophobacteraceae*, *Syntrophomonadaceae*, *Syntrophorhabdaceae*, *Dehalococcoidaceae*, *Desulfarculaceae*, *Desulfobulbaceae* and *Desulfovibrionaceae*) was higher in SP and EV in comparison to VM

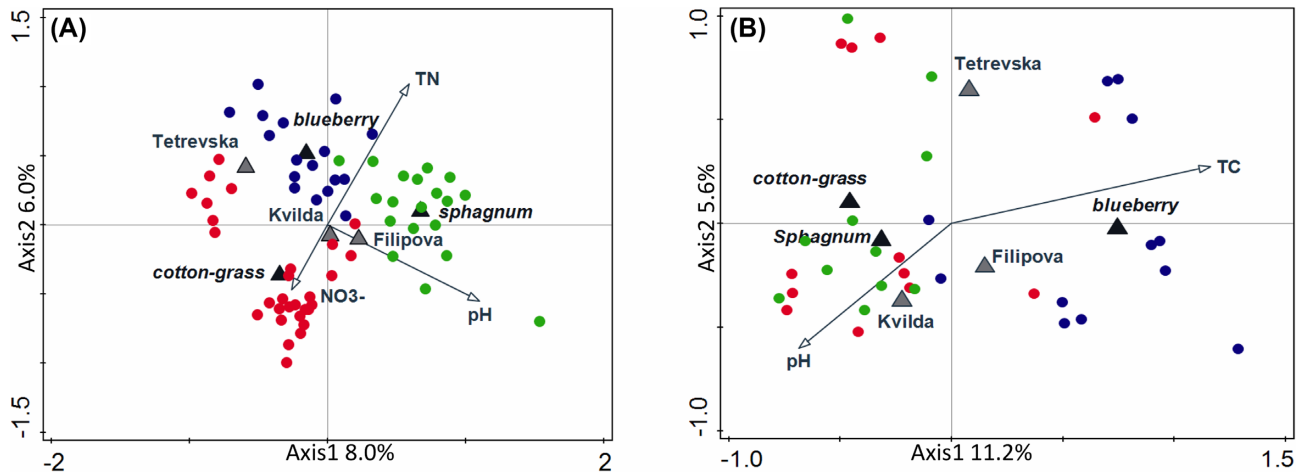


Figure 2. Soil prokaryotic (A) and fungal communities (B) separated by db-RDA analysis according to three microhabitats (cotton-grass (red dots), blueberry (blue dots) and *Sphagnum* (green dots)) and three studied sites (Tetřevská, Filipova, Kvilda). Gray arrows indicate soil physicochemical properties with significant explanatory effect.

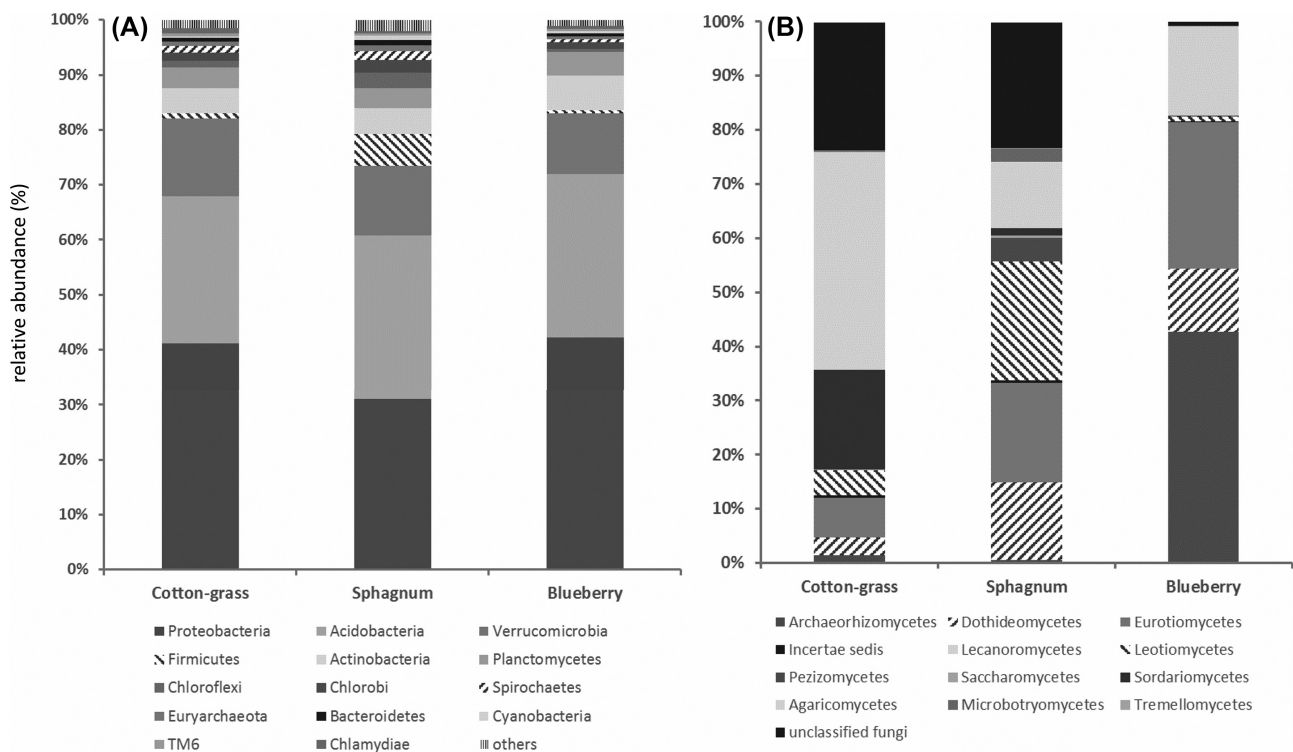


Figure 3. Changes in community composition of prokaryotes and fungi based on relative OTU abundance in peat soils across microhabitats. Data were collected from all three studied sites (Tetřevská, Filipova, Kvilda). Prokaryotic community structure (A) was performed on phylum level, while fungal community structure (B) was assessed on class level. Taxa with relative abundance higher than 1% at least at one sample type are shown.

(relative abundance 5.4%, 5.1% and 3.3%, respectively). Similarly, the relative abundance of anaerobic bacteria potentially involved in anaerobic degradation of organic matter and fermenters (sum of *Clostridia*, *Bacteroidia*, *Pedospirae*, *Opiritae* and δ -*Proteobacteria*) was higher in the SP and EV microhabitats (20.1 and 19.6%, respectively) than in VM (14.8%).

Archaea sequences were dominated by methanogenic *Euryarchaeota*. Their proportion was the lowest in VM (Table 4), which is in congruence with the methanogen abundance measured by qPCR (Fig. 1; Table S2, Supporting Information). Methanogenic lineages were represented mainly by

Methanomicrobia, *Methanobacteria* and *Thermoplasmatales*. These represented 0.8%, 0.3% and 0.1%, respectively, of the total prokaryotic community in SP, while their relative proportions in EV and VM were significantly lower ($P < 0.05$). *Methanosarcinaceae* and *Methanosaetaceae* were also detected; however, they were negligible in all habitats (relative abundance $< 0.15\%$).

Among the most abundant genera (overall relative abundance $> 0.5\%$), nine of them significantly differed among habitats (Table 4). When compared to SP, there were significantly higher abundances of *Candidatus* (*C.*) *Methanoregula* and *Opiritus* in EV and *Rhodoplanes* in VM. *Methylosinus*, belonging to the

Table 4. The relative proportion of microbial taxa (% , mean + standard deviation), which responded significantly to the differences among microhabitats (EV—cotton-grass, SP—sphagnum, VM—blueberry). Results of Kruskal–Wallis test (χ^2 test) and respective *post hoc* test (Tukey HSD test) for pairwise comparisons are shown. Data were collected from all three studied sites (Tetřevská, Filipova, Kvilda). Different letters in rows indicate statistically significant differences in relative abundance of taxa between microhabitats ($P < 0.05$). Abbreviations: C. refers to *Candidatus*.

taxon	EV	SP	VM
Prokaryotes			
Euryarchaeota	0.84 ± 0.57 ^{a,b}	1.19 ± 2.02 ^a	0.41 ± 0.39 ^b
Fibrobacteres	0.1 ± 0.13 ^a	0.21 ± 0.23 ^b	0.07 ± 0.1 ^a
Firmicutes	0.99 ± 0.64 ^a	5.75 ± 12.61 ^b	0.59 ± 0.46 ^a
Chlamydiae	0.86 ± 0.45 ^a	0.37 ± 0.28 ^b	0.53 ± 0.28 ^b
Chloroflexi	1.17 ± 1.07 ^a	2.79 ± 3.25 ^b	0.51 ± 0.6 ^c
Nitrospirae	0.37 ± 0.33 ^a	0.24 ± 0.3 ^{a,b}	0.09 ± 0.1 ^b
Proteobacteria	41.17 ± 16.29 ^a	31.04 ± 7.01 ^b	42.26 ± 13.65 ^a
Spirochaetes	1.22 ± 0.88 ^a	1.55 ± 1.13 ^a	0.55 ± 0.48 ^b
TM6	0.64 ± 0.27 ^a	0.48 ± 0.27 ^b	0.41 ± 0.17 ^b
α -Proteobacteria	27.68 ± 10.22 ^a	21.57 ± 7.66 ^b	31.35 ± 7.58 ^a
C. Koribacter	1.0 ^a	1.8 ^b	1.5 ^b
C. Methanoregula	0.6 ^a	0.2 ^b	0.2 ^b
Clostridium	0.2 ^a	0.6 ^b	0.1 ^a
Desulfomonile	1.2 ^a	0.4 ^{a,b}	0.2 ^b
Gemmata	0.2 ^a	0.1 ^b	0.3 ^a
Methylosinus	12.8 ^a	8.1 ^b	13.1 ^a
Opitutus	3.5 ^a	1.6 ^b	1.3 ^b
Rhodoplanes	2.6 ^a	3.1 ^a	5.4 ^b
Thermacetogenium	0.1 ^{a,b}	0.3 ^a	0.0 ^b
Fungi			
Archaeorhizomycetes	1.4 ± 3.3 ^a	0.5 ± 0.6 ^b	42.7 ± 28.8 ^a
Leotiomycetes	4.6 ± 7.9 ^a	21.9 ± 26.2 ^b	0.9 ± 1.2 ^a
Saccharomycetes	0.2 ± 0.3 ^{a,b}	0.4 ± 1.1 ^a	0.0 ± 0.0 ^b
Microbotryomycetes	0.1 ± 0.2 ^a	2.4 ± 2.4 ^b	0.0 ± 0.0 ^a
Tremellomycetes	0.2 ± 0.3 ^a	0.1 ± 0.3 ^{a,b}	0.0 ± 0.0 ^b

Methylocystaceae family, was enriched in both VM and EV (13.1% and 12.8%, respectively) compared to SP (8.1%, $P < 0.05$). Similar trends were observed for *Gemmata* ($P < 0.05$) and *Burkholderia*, despite the fact that, for the latter, the differences were not significant due to high variability within the biological replicates. *Clostridium* showed the opposite trend, being the highest in SP ($P < 0.05$). *Bacillus*, *Candidatus Solibacter*, *Candidatus Koribacter* and *Thermoacetogenium* preferred the *Sphagnum* microhabitat; however, the differences were not significant.

Fungal community composition in different microhabitats

In db-RDA, interactive forward selection identified microhabitat (Pseudo-F = 3.8, $P_{\text{adj}} = 0.036$) as the only significant variable determining soil fungal community structure, which explained 10.3% of total variability. Site had a much lower impact (Pseudo-F = 1.8, $P_{\text{adj}} = 0.072$; Fig. 2B). Soil fungi in VM were the most dissimilar from the others, being discriminated from SP and EV on the first axis (11.6%). The second axis (5.6%) separated the SP and EV fungal communities. Approximately 40 fungal OTUs significantly contributed to the dissimilarity among microhabitats (SIMPER, Student's *t*-test; Table S5, Supporting Information). OTUs affiliated to gg. *Archaeorhizomyces*, *Tylospora*, *Cenococcum*, *Inocybe*, *Pseudeurotium*, *Rhodotorula*, *Hypochnicium* and *Elaphocordyceps* contributed most to the difference between VM and SP, in which OTUs affiliated with the first four genera were indicative for VM. Fungal OTUs affiliated to

Rozellomycota, *Pseudeurotium*, *Sporidiobolales* (g. *Rhodotorula*), *Leotiomycetes* and *Helotiales* were over-represented in SP compared to EV and VM. Differences between VM and EV were characterized by an over-representation of *Archaeorhizomyces*-, *Chaetothyriales*-, *Cenococcum*- and *Inocybe*-OTUs in VM.

The majority of fungal sequences belonged to *Ascomycetes* and *Basidiomycetes*, being equally present in the EV microhabitat (35% and 40% of sequences in the fungal community, respectively), while *Ascomycetes* dominated in the VM and SP microhabitats (82% and 61% of sequences in the fungal community, respectively). Most of identified OTUs belonged to saprophytic fungi (data not shown). The relative abundances of *Archaeorhizomyces*, *Microbotryomycetes*, *Leotiomycetes*, *Tremellomycetes* and *Saccharomycetes* differed significantly across microhabitats (Table 3). In particular, *Archaeorhizomyces* was associated mainly with VM, reaching 42.7% relative abundance of all fungal sequences. Further, *Leotiomycetes*, *Microbotryomycetes* and *Saccharomycetes* showed significantly higher abundances in SP than in the EV and/or VM microhabitats ($P < 0.01$, Table 3). *Agaricomycetes* dominated the soil fungal community in EV (40.2%), followed by *Sordariomycetes* (18.4%); however, there was no significant difference in their relative abundances between microhabitats (Fig. 3B). Similarly, *Pezizomycetes* only achieved important numbers in SP (4.4% of fungal sequences), though these did not differ from their relative abundance in EV and VM. The most homogenous community structure was detected in VM, where the fungal community consisted of representatives from four classes. Interestingly, VM harbored a lower amount of unidentified fungal sequences than EV and SP (Fig. 3B).

DISCUSSION

In the study, we aimed to characterize the complex soil microbial communities—bacteria, archaea and fungi in relatively nutrient-poor spruce swamp forests with a focus on their internal variability related to naturally well-defined peatland microhabitats. These were *Sphagnum*-dominated hollows with the highest water level and lawns and hummocks with deeper water table levels, both dominated by vascular plant species, cotton-grass and blueberry, respectively. The plant species, *S. fallax*, cotton-grass and blueberry have been found to differ significantly in litter quality and decomposability and plant nutrient management (Kaštovská et al. 2018), in the composition and biodegradability of litter leachates and their contribution to dissolved organic matter (Mastný et al. 2018), and in exudate flux and quality (Edwards et al. 2018). These plant characteristics significantly contributed to differences found in peat composition and microbial biomasses between the microhabitats (Kaštovská et al. 2018).

In this study, we documented that the type of microhabitat was the best predictor and explained most of the variation in the composition of both prokaryotic and fungal communities within the peatland. Site had a weaker effect on community composition, showing that both prokaryotes and fungi responded further to the hydrological and nutritional heterogeneity existing between the three sampling sites. Additionally, prokaryotic response to microhabitat and site was complemented by their relation to gradients in soil pH and N content, factors that most strongly differentiate the plant species-defined microhabitats and, in our case, study sites (Kaštovská et al. 2018). This is in agreement with previous studies reporting a strong relationship between bacteria and archaea with pH and N gradients in diverse soils (Rousk et al. 2010; Fierer et al. 2012; Zhalnina et al. 2015). Interestingly, temporal changes in soil microbial community structure were least important, despite plant exudate quantity and quality varying significantly during the vegetation season (Edwards et al. 2018).

Microbial communities of *Sphagnum*-dominated habitat

The community of *Sphagnum*-dominated peat had the lowest F/B ratio among the microhabitats since prevalent anoxia due to the high water table (-5.6 ± 3.3 cm) together with a lack of roots in SP handicapped fungi. The prokaryotic community was rich in *Acidobacteria*, *Proteobacteria* (α -class) and *Verrucomicrobia*, which tolerate well acidic soil conditions and are typical for *Sphagnum*-dominated peatlands (Ivanova et al. 2016). A high relative proportion of *Acidobacteria* and *Verrucomicrobia* have even been found in bare nonvegetated peat (Elliott et al. 2015); hence, this might indicate that such bacteria can thrive in harsh nutrient-poor conditions and thus prefer oligotrophic habitats. Further, the prokaryotic community was significantly enriched by *Firmicutes*, *Actinobacteria*, *Planctomycetes*, *Chloroflexi*, *Spirochaetes*, *Euryarchaeota*, *Bacteroidetes* and *Fibrobaeteres*. Of these, members of *Acidobacteria* (*Acidobacteriaceae*, *Holophagaceae*), *Firmicutes* (*Clostridiaceae*), *Bacteroidetes*, *Fibrobaeteres* and *Spirochaetes* can contribute significantly to anaerobic cellulose degradation, representing the first step in the anaerobic food web that ends in methane production (Schmidt et al. 2015). Other members of the community, the syntrophs, although usually of low abundance in peat (the highest being 5.4% of total prokaryotic sequences in *Sphagnum*; (Schmidt et al. 2016)), convert fermentation products to methanogenic substrates, mainly

hydrogen. *Clostridiales*, for example, have their highest relative abundance in *Sphagnum* and can perform syntrophic propionate oxidation in peatlands (Tveit et al. 2015). In accord, the majority of methanogens detected (*Methanoregulaceae* and *Methanobacteriaceae*) are hydrogenotrophs, while acetoclastic methanogens were rarely present, probably indicating high competition for other methanogenic substrates. Preference for hydrogenotrophy among methanogenic Archaea is probably associated with boreal peatlands (Galand et al. 2005), and acidic, nutrient-poor *Sphagnum*-dominated peatlands, as reported previously (Horn et al. 2003; Juottonen et al. 2005; Kotsyurbenko et al. 2007; Putkinen et al. 2018). Hydrogen, which is probably easily available in *Sphagnum*-rich habitats, is a preferred substrate for the methanogenic community as it is directly released by *Sphagnum* moss (Andrus 1986). Finally, our finding support previous observations from similar peatlands in the Šumava region (Urbanová and Bárta 2014).

Fungal community was dominated by Ascomycetes members, including *Leotiomycetes*, *Eurotiomycetes* and *Dothiodesomycetes*, which are probably adapted to nutrient limited peat soils (Asemajinejad, Thorn and Lindo 2017). Other present fungal groups (e.g. *Penicillium*, *Pseudeurotium*, *Agaricomycetes*) can degrade simple organic compounds as well as complex polymers and could contribute to *Sphagnum* tissue decay (Rice, Tsuneda and Currah 2006; Thormann 2006; Jassey et al. 2012).

Cotton-grass presence favors Rhizobiales, Opiritales and Basidiomycetes

The cotton-grass-dominated habitat hosted specific prokaryotic and fungal communities differing from those found in *Sphagnum*. The relative proportion of *Proteobacteria*, including *Methylocystaceae* and *Hyphomicrobiaceae*, was significantly higher than in *Sphagnum*, whereas the relative abundance of *Firmicutes* and *Actinobacteria* (class) was apparently lower. The increase in relative proportion of α -*Proteobacteria*, *Methylocystaceae* and *Methylosinus* in cotton-grass compared to *Sphagnum* was expected and can be explained by increased soil aeration due to active oxygen transport via cotton-grass roots (Saarinen 1996). The higher oxygen concentrations together with peat nutrient deprivation due to efficient resorption and immobilization of nutrients by cotton-grass (Kaštovská et al. 2018) could reduce a contribution of the copiotrophic *Actinobacteria* and *Firmicutes*, including anaerobic *Clostridiales*. Cotton-grass exudes significant amounts of carbohydrates and organic acids (Saarnio, Wittenmayer and Merbach 2004), which can be quickly metabolized to methanogenic substrates. This likely explains the increase of *Opiritaceae*, which may be responsible for this conversion (Tveit et al. 2015) and may substitute for the fermenting and syntrophic activities of retreating *Clostridiales*. *Opiritus*, *Desulfomonile*, *Gemmata* and *C. Methanoregula* were recognized as indicative genera for the cotton-grass microhabitats, which supports the importance of anaerobic processes interacting with methanogenesis. In this respect, the cotton-grass microhabitats possessed the same abundance of methanogens as *Sphagnum* ones, indicating that cotton-grass maintains a methanogenic potential similar to *Sphagnum* moss. Cotton-grass presence did not shift the methanogenic community toward a higher proportion of acetoclastic ones, which agrees with the previous finding that its occurrence did not increase but significantly reduces the nutrient content in the peat (Kaštovská et al. 2018).

Cotton-grass fungal communities differed from those of *Sphagnum* mainly by an increased abundance of *Basidiomycetes*.

Basidiomycota are significant drivers of decomposition by producing extracellular enzymes involved in biopolymer degradation, including those indigenous to *Sphagnum* peat (Thormann 2011). Despite this, exoenzymatic activity and C mineralization measured in the soils from cotton-grass microhabitats were comparable to values from *Sphagnum* hollows and thus did not indicate an enhanced decomposition (Kaštovská et al. 2018). Surprisingly, there was the highest relative frequency of mycorrhiza in cotton-grass microhabitats (34.8% of the total fungal sequences). Ectomycorrhizal fungi were represented mainly by *Tylospora*, *Cenococcum* and *Inocybe*. These may likely reach the lawns from adjacent vegetation including spruce trees.

Blueberry favors Acidobacteria, Rhizobiales and Archeorhizomyces

Blueberry significantly affected microbial community structure through a preference for specific members of Acidobacteria. These were mainly representatives of Acidobacteriaceae, Koribacteraceae, Solibacteraceae (all subdivision 1) and Holophagaceae (subdivision 6). Together with Proteobacteria, they play an integral role in peat soils, functioning mainly as effective aromatic and cellulose degraders under oligotrophic and acidic conditions (Ausec, van Elsas and Mandic-Mulec 2011; Pankratov et al. 2011). Moreover, *Solibacter* could enhance P acquisition and availability (Lin et al. 2014), the situation which has been also recognized in the soils from blueberry microhabitats (Kaštovská et al. 2018). *Methylocystaceae* (Rhizobiales, α -Proteobacteria) relative abundance was greatly increased in blueberry microhabitats due to higher aeration and rhizodeposition of well decomposable compounds (Edwards et al. 2018). Blueberry, in contrast to cotton-grass, possessed only two abundant genera with higher relative abundances than *Sphagnum*, i.e. *Methylosinus* and *Rhodoplanes* (both α -Proteobacteria). *Rhodoplanes*, which contributes to nitrogen fixation (Buckley et al. 2007), is a common inhabitant of peatlands (Schmidt et al. 2016) and its relative abundance may be increased due to a developed ectomycorrhizosphere (Uroz et al. 2012). In line with our hypothesis, the anaerobic prokaryotes, including fermenters, syntrophic bacteria and methanogens, were significantly suppressed under blueberry when compared to *Sphagnum* and cotton-grass. Thus, we may infer that methanogenic potential is inhibited by the combined effect of microtopography and blueberry presence.

As hypothesized, the fungi were favored in better aerated microhabitats with vascular plants present compared to *Sphagnum* hollows, more pronouncedly in blueberry hummocks than cotton-grass lawns. Consequently, there was a significantly increased fungi-to-bacteria ratio in blueberry, as observed in other peat soils under ericoids (Gavazov et al. 2016). The increase in fungal abundance inferred from rDNA gene copy numbers agreed with the increase in overall soil microbial biomass in blueberry, as reported previously (Kaštovská et al. 2018). Blueberry significantly attracted mainly *Archeorhizomyces* (up to 58% of total fungal sequences), while we only detected a very minor contribution of ericoid mycorrhiza members (altogether ca 0.1% of the total fungal sequences). This indicates that there could be some methodological issues (e.g. sampling, specificity of primers, taxonomy assignment) or that ericoid mycorrhiza did not contribute significantly to nutrient acquisition and decomposition processes in the soil. Root-associated *Archeorhizomyces* were described relatively recently (Rosling et al. 2011) and their ecology and importance in the fungal community is still being debated (Choma et al. 2016). As such, we can only speculate

as to the role *Archeorhizomyces* play in our ecosystem and whether they actively interact with ericoid roots in gathering nutrients. Blueberry possessed an increased abundance of saprotrophic *Penicillium* (up to 33%) and the ectomycorrhizal *Cenococcum* (ca. 12%); thus, *Penicillium* spp. may participate significantly in decomposing blueberry litter by producing peroxidase enzymes (Yang et al. 2005), which corroborates with the increased concentration of C-acquiring exoenzymes under blueberry (Kaštovská et al. 2018).

Methane-cycling communities

The presence of vascular plants did not largely affect methanogenic community structure, which was mainly shaped by pH and overall nutrient limitation (hydrogenotrophic and acidophilic members prevailing). However, methanogenic abundance strongly decreased in the presence of blueberry; thus, we may assume lower methanogenic potential owing to the suppression of fermenters and syntrophic bacteria in comparison to other microhabitats, probably due to the lower water table.

Aerobic methanotrophs were dominated by type II MOB (*Methylocystaceae*), regardless of the plant dominant, which is in line with previous studies in *Sphagnum*-dominated peat (Kip et al. 2012). These were accompanied by *Methylacidiphilae* (*Verucomicrobia*), which employ a mixotrophic strategy by combining methane consumption and hydrogen oxidation in oxygen limiting environments (Carere et al. 2017). Since methanotrophs are ubiquitous in peatlands due to a symbiotic association with *Sphagnum* (Larmola et al. 2010), they are easily transferred by water, and thus unlikely to be plant species specific (Bragina et al. 2013). Their composition and abundance are instead influenced by the low pH (Ho et al. 2013), high C:N ratio (Lin et al. 2012) and differences in water table level (Larmola et al. 2010) in the soils studied. Quantitative data (*pmoA* type II gene copy numbers) did not show significant differences across microhabitats, which may indicate that the methane consumption potential is similar regardless of the plant dominant.

Both communities showed significant temporal changes, which may be attributed likely to seasonal changes in temperature, water table level and the availability of methanogenic substrates released by plants through root exudates (Edwards et al. 2018).

CONCLUSION

In this study, we assessed diversification of soil microbial communities related to internal heterogeneity within peatland systems related to microhabitats defined by water table and dominant plant species. The knowledge about links between the occurrence of particular plant species and its specific soil microbial community would help to understand the inner variability in microbe-driven nutrient cycling and predict possible shifts in the peatland functioning when vegetation will change. Our data show that the altered biochemical profiles of peat under studied plant functional types, ericoid blueberry and graminoid cotton-grass, together with variation in topography, had a measurable and distinct impact on the soil prokaryotic and fungal communities. The fungal communities were more affected by the specific environmental conditions of the microhabitats and the presence of vascular plants in comparison to prokaryotes. While cotton-grass significantly supported the presence of both aerobic and anaerobic microorganisms, such as methanotrophs, methanogens and syntrophs, the blueberry supported only

methanotrophs and additionally, fungi. The differences in communities are likely attributed to a combination of differences in water table levels and oxygenation of the peat profile, species-specific plant exudation, litter input and nutrient acquisition strategies. Finally, our findings show that specific community members, e.g. type II methanotrophs (α -Proteobacteria, including *Methylosinus*), *Gemmata*, *Opiritutus*, *Rhodoplanes* and *Archaeorhizomycetes*, can be indicative of microbial community response to the expected spread of vascular plants in peatlands due to decrease of water level in peatlands as a result of global climate change.

SUPPLEMENTARY DATA

Supplementary data are available at [FEMSEC](#) online.

ACKNOWLEDGEMENTS

The authors thank the Administration of Šumava National Park and Protected Landscape Area for sampling permission. We thank Martina Petřílková, Petra Beníšková, Veronika Schaabová, Hana Petrásková, Kateřina Kučerová, Daniel Vaněk and Ondřej Žampach for assistance with laboratory analysis and sample collection in the field, Vilém Děd for help with R, and Keith Edwards and Kevin Roche for English revision.

FUNDING

This work was supported by the Czech Science Foundation [grant number 13-17398S], the Ministry of Education, Youth and Sports of the Czech Republic, programme "Projects of Large Infrastructure for Research, Development, and Innovations [grant number LM2015075], and European Regional Development Fund-Project "Research of key soil-water ecosystem interactions at the SoWa Research Infrastructure" [grant number EF16.013/0001782].

Conflict of interests. None declared.

REFERENCES

- Andrus R. Aspects of Sphagnum ecology. *Can J Bot* 1986;**64**:416–26.
- Apprill A, McNally S, Parsons R et al. Minor revision to V4 region SSU rRNA 806R gene primer greatly increases detection of SAR11 bacterioplankton. *Aquat Microb Ecol* 2015;**75**:129–37.
- Asemaninejad A, Thorn R, Lindo Z. Experimental climate change modifies degradative succession in boreal peatland fungal communities. *Microb Ecol* 2017;**73**:521–31.
- Ausec L, van Elsas J, Mandic-Mulec I. Two- and three-domain bacterial laccase-like genes are present in drained peat soils. *Soil Biol Biochem* 2011;**43**:975–83.
- Bengtsson-Palme J, Ryberg M, Hartmann M et al. Improved software detection and extraction of ITS1 and ITS2 from ribosomal ITS sequences of fungi and other eukaryotes for analysis of environmental sequencing data. *Methods Ecol Evol* 2013;**4**:914–9.
- Bragazza L. A decade of plant species changes on a mire in the Italian Alps: vegetation-controlled or climate-driven mechanisms? *Clim Change* 2006;**77**:415–29.
- Bragazza L, Bardgett RD, Mitchell EAD et al. Linking soil microbial communities to vascular plant abundance along a climate gradient. *New Phytol* 2015;**205**:1175–82.
- Bragina A, Berg C, Muller H et al. Insights into functional bacterial diversity and its effects on Alpine bog ecosystem functioning. *Sci Rep* 2013;**3**:1955.
- Bubier J, Costello A, Moore TR et al. Microtopography and methane flux in boreal peatlands, northern Ontario, Canada. *Can J Bot* 1993;**71**:1056–63.
- Buckley D, Huangyutitham V, Hsu S et al. Stable isotope probing with N-15(2) reveals novel noncultivated diazotrophs in soil. *Appl Environ Microbiol* 2007;**73**:3196–204.
- Buttler A, Robroek BJM, Laggoun-Defarge F et al. Experimental warming interacts with soil moisture to discriminate plant responses in an ombrotrophic peatland. *J Veg Sci* 2015;**26**:964–74.
- Cairney JWG, Meharg AA. Ericoid mycorrhiza: a partnership that exploits harsh edaphic conditions. *Eur J Soil Sci* 2003;**54**:735–40.
- Caporaso JG, Kuczynski J, Stombaugh J et al. QIIME allows analysis of high-throughput community sequencing data. *Nat Methods* 2010;**7**:335–6.
- Caporaso JG, Lauber CL, Walters WA et al. Global patterns of 16S rRNA diversity at a depth of millions of sequences per sample. *Proc Natl Acad Sci USA* 2011;**108**:4516–22.
- Carere C, Hards K, Houghton K et al. Mixotrophy drives niche expansion of verrucomicrobial methanotrophs. *ISME J* 2017;**11**:2599–610.
- Carroll MJ, Heinemeyer A, Pearce-Higgins JW et al. Hydrologically driven ecosystem processes determine the distribution and persistence of ecosystem-specialist predators under climate change. *Nat Commun* 2015;**6**:7851.
- Chapin FS, I, Moilanen L, Kielland K. Preferential use of organic nitrogen for growth by a non-mycorrhizal arctic sedge. *Nature* 1993;**361**:150.
- Choma M, Barta J, Santruckova H et al. Low abundance of Archaeorhizomycetes among fungi in soil metatranscriptomes. *Sci Rep* 2016;**6**:38455.
- Clarke K. Nonparametric multivariate analyses of changes in community structure. *Aust J Ecol* 1993;**18**:117–43.
- Clarke K, Gorley R. *PRIMER V6: User Manual/Tutorial*. Plymouth, PRIMER-E, 2006, 192.
- Dinno A. dunn.test: Dunn's test of multiple comparisons using rank sums. R package version 1.3.2., 2016.
- Dorodnikov M, Marushchak M, Biasi C et al. Effect of microtopography on isotopic composition of methane in pore water and efflux at a boreal peatland. *Boreal Environ Res* 2013;**18**:269–79.
- Dunn O. Multiple comparisons using rank sums. *Technometrics* 1964;**6**:241–52.
- Edgar RC. UPARSE: highly accurate OTU sequences from microbial amplicon reads. *Nat Methods* 2013;**10**:996–8.
- Edwards KR, Kaštovská E, Borovec J et al. Species effects and seasonal trends on plant efflux quantity and quality in a spruce swamp forest. *Plant Soil* 2018;**426**:179–96.
- Elliott D, Caporn S, Nwaishi F et al. Bacterial and fungal communities in a degraded ombrotrophic peatland undergoing natural and managed re-vegetation. *PLoS One* 2015;**10**:e0124726.
- Esty W. The efficiency of Good's nonparametric coverage estimator. *Ann Stat* 1986;**14**:1257–60.
- Fierer N, Lauber C, Ramirez K et al. Comparative metagenomic, phylogenetic and physiological analyses of soil microbial communities across nitrogen gradients. *ISME J* 2012;**6**:1007–17.
- Fisk M, Ruether K, Yavitt J. Microbial activity and functional composition among northern peatland ecosystems. *Soil Biol Biochem* 2003;**35**:591–602.

- Galand PE, Fritze H, Yrjala K. Microsite-dependent changes in methanogenic populations in a boreal oligotrophic fen. *Environ Microbiol* 2003;**5**:1133–43.
- Galand PE, Juottonen H, Fritze H et al. Methanogen communities in a drained bog: effect of ash fertilization. *Microb Ecol* 2005;**49**:209–17.
- Gardes M, Bruns T. ITS primers with enhanced specificity for basidiomycetes—application to the identification of mycorrhizae and rusts. *Mol Ecol* 1993;**2**:113–8.
- Gavazov K, Hagedorn F, Buttler A et al. Environmental drivers of carbon and nitrogen isotopic signatures in peatland vascular plants along an altitude gradient. *Oecologia* 2016;**180**:257–64.
- Greenup A, Bradford M, McNamara N et al. The role of *Eriophorum vaginatum* in CH₄ flux from an ombrotrophic peatland. *Plant Soil* 2000;**227**:265–72.
- Griffiths R, Whiteley A, O'Donnell A et al. Rapid method for coextraction of DNA and RNA from natural environments for analysis of ribosomal DNA- and rRNA-based microbial community composition. *Appl Environ Microbiol* 2000;**66**:5488–91.
- Ho A, Kerckhof F, Luke C et al. Conceptualizing functional traits and ecological characteristics of methane-oxidizing bacteria as life strategies. *Env Microbiol Rep* 2013;**5**:335–45.
- Horn M, Matthies C, Kusel K et al. Hydrogenotrophic methanogenesis by moderately acid-tolerant methanogens of a methane-emitting acidic peat. *Appl Environ Microbiol* 2003;**69**:74–83.
- Ivanova AA, Wegner CE, Kim Y et al. Identification of microbial populations driving biopolymer degradation in acidic peatlands by metatranscriptomic analysis. *Mol Ecol* 2016;**25**:4818–35.
- Jassey V, Chiapusio G, Gilbert D et al. Phenoloxidase and peroxidase activities in Sphagnum-dominated peatland in a warming climate. *Soil Biol Biochem* 2012;**46**:49–52.
- Jassey VEJ, Chiapusio G, Binet P et al. Above- and belowground linkages in Sphagnum peatland: climate warming affects plant–microbial interactions. *Glob Change Biol* 2013;**19**:811–23.
- Jonasson S, Shaver GR. Within-stand nutrient cycling in arctic and boreal wetlands. *Ecology* 1999;**80**:2139–50.
- Juottonen H, Galand PE, Tuittila ES et al. Methanogen communities and bacteria along an ecohydrological gradient in a northern raised bog complex. *Environ Microbiol* 2005;**7**:1547–57.
- Juottonen H, Kotiaho M, Robinson D et al. Microform-related community patterns of methane-cycling microbes in boreal Sphagnum bogs are site specific. *FEMS Microbiol Ecol* 2015;**91**:fiv094.
- Kaštovská E, Straková P, Edwards K et al. Cotton-grass and blueberry have opposite effect on peat characteristics and nutrient transformation in peatland. *Ecosystems* 2018;**21**:443–58.
- Kettunen A. Connecting methane fluxes to vegetation cover and water table fluctuations at microsite level: a modeling study. *Global Biogeochem Cy* 2003;**17**:1051.
- Kip N, Dutilh BE, Pan Y et al. Ultra-deep pyrosequencing of pmoA amplicons confirms the prevalence of methylomonas and methylocystis in Sphagnum mosses from a Dutch peat bog. *Environ Microbiol Rep* 2011;**3**:667–73.
- Kip N, Fritz C, Langelaan ES et al. Methanotrophic activity and diversity in different *Sphagnum magellanicum* dominated habitats in the southernmost peat bogs of patagonia. *Biogeosciences* 2012;**9**:47–55.
- Koljalg U, Nilsson R, Abarenkov K et al. Towards a unified paradigm for sequence-based identification of fungi. *Mol Ecol* 2013;**22**:5271–7.
- Kotiaho M, Fritze H, Merilä P et al. Actinobacteria community structure in the peat profile of boreal bogs follows a variation in the microtopographical gradient similar to vegetation. *Plant Soil* 2013;**369**:103–14.
- Kotiaho M, Fritze H, Merilä P et al. Methanogen activity in relation to water table level in two boreal fens. *Biol Fertil Soils* 2010;**46**:567–75.
- Kotsyurbenko OR, Friedrich MW, Simankova MV et al. Shift from acetoclastic to H₂-dependent methanogenesis in a west Siberian peat bog at low pH values and isolation of an acidophilic Methanobacterium strain. *Appl Environ Microbiol* 2007;**73**:2344–8.
- Krohn J, Lozanovska I, Kuzyakov Y et al. CH₄ and CO₂ production below two contrasting peatland micro-relief forms: an inhibitor and $\delta^{13}\text{C}$ study. *Sci Total Environ* 2017;**586**:142–51.
- Laaksonen M, Peuhu E, Varkonyi G et al. Effects of habitat quality and landscape structure on saproxylic species dwelling in boreal spruce-swamp forests. *Oikos* 2008;**117**:1098–110.
- Larmola T, Tuittila E, Tiirola M et al. The role of Sphagnum mosses in the methane cycling of a boreal mire. *Ecology* 2010;**91**:2356–65.
- Legendre P, Anderson M. Distance-based redundancy analysis: testing multispecies responses in multifactorial ecological experiments. *Ecol Monogr* 1999;**69**:1–24.
- Lin X, Green S, Tfaily M et al. Microbial community structure and activity linked to contrasting biogeochemical gradients in bog and fen environments of the Glacial Lake Agassiz Peatland. *Appl Environ Microbiol* 2012;**78**:7023–31.
- Lin X, Tfaily M, Steinweg M et al. Microbial community stratification linked to utilization of carbohydrates and phosphorus limitation in a boreal peatland at Marcell Experimental Forest, Minnesota, USA. *Appl Environ Microbiol* 2014;**80**:3518–30.
- Maanavilja L, Aapal K, Haapalehto T et al. Impact of drainage and hydrological restoration on vegetation structure in boreal spruce swamp forests. *Forest Ecol Manag* 2014;**330**:115–25.
- Mastný J, Kaštovská E, Bárta J et al. Quality of DOC produced during litter decomposition of peatland plant dominants. *Soil Biol Biochem* 2018;**121**:221–30.
- McEwing KR, Fisher JP, Zona D. Environmental and vegetation controls on the spatial variability of CH₄. *Plant Soil* 2015;**388**:37–52.
- Mellegård H, Stalheim T, Hormazabal V et al. Antibacterial activity of sphagnum acid and other phenolic compounds found in Sphagnum papillosum against food-borne bacteria. *Lett Appl Microbiol* 2009;**49**:85–90.
- Moore TR, Bubier JL, Bledzki L. Litter decomposition in temperate peatland ecosystems: the effect of substrate and site. *Ecosystems* 2007;**10**:949–63.
- Nguyen N, Song Z, Bates S et al. FUNGuild: an open annotation tool for parsing fungal community datasets by ecological guild. *Fungal Ecol* 2016;**20**:241–8.
- Ogle DH. FSA: Fisheries Stock Analysis. R package version 0.8.10., 2017.
- Oksanen J, Blanchet FG, Friendly M et al. Vegan: Community Ecology Package. R package version 2.4-1., 2016.
- Pankratov T, Ivanova A, Dedysh S et al. Bacterial populations and environmental factors controlling cellulose degradation in an acidic Sphagnum peat. *Environ Microbiol* 2011;**13**:1800–14.
- Parada AE, Needham DM, Fuhrman JA. Every base matters: assessing small subunit rRNA primers for marine microbiomes with mock communities, time series and global field samples. *Environ Microbiol* 2016;**18**:1403–14.
- Parvin S, Blagodatskaya E, Becker J et al. Depth rather than microrelief controls microbial biomass and kinetics of C-, N-,

- P- and S-cycle enzymes in peatland. *Geoderma* 2018;**324**:67–76.
- Peltoniemi K, Fritze H, Laiho R. Response of fungal and actinobacterial communities to water-level drawdown in boreal peatland sites. *Soil Biol Biochem* 2009;**41**:1902–14.
- Putkinen A, Tuittila ES, Siljanen HMP et al. Recovery of methane turnover and the associated microbial communities in restored cutover peatlands is strongly linked with increasing Sphagnum abundance. *Soil Biol Biochem* 2018;**116**:110–9.
- Quast C, Pruesse E, Yilmaz P et al. The SILVA ribosomal RNA gene database project: improved data processing and web-based tools. *Nucleic Acids Res* 2013;**41**:D590–D6.
- Radl V, Gattinger A, Chroňáková A et al. Effects of cattle husbandry on abundance and activity of methanogenic archaea in upland soils. *ISME J* 2007;**1**:443–52.
- Rice A, Tsuneda A, Currah R. In vitro decomposition of Sphagnum by some microfungi resembles white rot of wood. *FEMS Microbiol Ecol* 2006;**56**:372–82.
- Robroek B, Jassey V, Kox M et al. Peatland vascular plant functional types affect methane dynamics by altering microbial community structure. *J Ecol* 2015;**103**:925–34.
- Robroek BJM, Albrecht RJH, Hamard S et al. Peatland vascular plant functional types affect dissolved organic matter chemistry. *Plant Soil* 2016;**407**:135–43.
- Rosling A, Cox F, Cruz-Martinez K et al. Archaeorhizomycetes: unearthing an ancient class of ubiquitous soil fungi. *Science* 2011;**333**:876–9.
- Rousk J, Baath E, Brookes P et al. Soil bacterial and fungal communities across a pH gradient in an arable soil. *ISME J* 2010;**4**:1340–51.
- Rydin H, Jeglum J. *The Biology of Peatlands*, Oxford: Oxford University Press. 2006.
- Saarinen T. Biomass and production of two vascular plants in a boreal mesotrophic fen. *Can J Bot* 1996;**74**:934–8.
- Saarnio S, Wittenmayer L, Merbach W. Rhizospheric exudation of *Eriophorum vaginatum* L.—potential link to methanogenesis. *Plant Soil* 2004;**267**:343–55.
- Schmidt O, Hink L, Horn M et al. Peat: home to novel syntrophic species that feed acetate- and hydrogen-scavenging methanogens. *ISME J* 2016;**10**:1954–66.
- Schmidt O, Horn M, Kolb S et al. Temperature impacts differentially on the methanogenic food web of cellulose-supplemented peatland soil. *Environ Microbiol* 2015;**17**:720–34.
- Schutz H, Schröder P, Rennenberg H. *Role of Plants in Regulating the Methane Flux to the Atmosphere*. San Diego: Trace Gas Emission by Plants: Academic Press, 1991.
- Spitzer K, Bufková I. *Peatlands of Šumava*. Vimperk: Administration of the Šumava National Park and Protected Landscape Area, 2012.
- Sun H, Terhonen E, Koskinen K et al. Bacterial diversity and community structure along different peat soils in boreal forest. *Appl Soil Ecol* 2014;**74**:37–45.
- Sundh I, Nilsson M, Borga P. Variation in microbial community structure in two boreal peatlands as determined by analysis of phospholipid fatty acid profiles. *Appl Environ Microbiol* 1997;**63**:1476–82.
- ter Braak C, Šmilauer P. *Canoco Reference Manual and User's Guide: Software for Ordination (Version 5.0)*. Ithaca: Microcomputer Power, 2012, 496.
- Thormann M. Diversity and function of fungi in peatlands: a carbon cycling perspective. *Can J Soil Sci* 2006;**86**:281–93.
- Thormann M. In vitro decomposition of Sphagnum-derived acrotelm and mesotelm peat by indigenous and alien basidiomycetous fungi. *Mires and Peat: International Mire Conservation Group and International Peat Society*. 2011, 1–12.
- Tveit A, Urich T, Frenzel P et al. Metabolic and trophic interactions modulate methane production by Arctic peat microbiota in response to warming. *PNAS* 2015;**112**:E2507–E16.
- Urbanová Z, Bárta J. Microbial community composition and in silico predicted metabolic potential reflect biogeochemical gradients between distinct peatland types. *FEMS Microbiol Ecol* 2014;**90**:633–46.
- Uroz S, Oger P, Morin E et al. Distinct ectomycorrhizospheres share similar bacterial communities as revealed by pyrosequencing-based analysis of 16S rRNA genes. *Appl Environ Microbiol* 2012;**78**:3020–4.
- Verhoeven JTA, Liefveld WM. The ecological significance of organochemical compounds in *Sphagnum*. *Acta Bot Neerl* 1997;**46**:117–30.
- Verhoeven JTA, Toth E. Decomposition of *Carex* and *Sphagnum* litter in fens: effect of litter quality and inhibition by living tissue homogenates. *Soil Biol Biochem* 1995;**27**:271–5.
- Yang J, Yuan H, Wang H et al. Purification and characterization of lignin peroxidases from *Penicillium decumbens* P6. *World J Microb Biot* 2005;**21**:435–40.
- Zhalnina K, Dias R, de Quadros PD et al. Soil pH determines microbial diversity and composition in the park grass experiment. *Microb Ecol* 2015;**69**:395–406.

Paper 7

Gittel A, **Barta J**, Kohoutova I, Mikutta R, Owens S, Gilbert J, Schneckner J, Wild B, Hannisdal B, Maerz J, Lashchinskiy N, Capek P, Santruckova H, Gentsch N, Shibistova O, Guggenberger G, Richter A, Torsvik VL, Schleper C, Urich T (2014) Distinct microbial communities associated with buried soils in the Siberian tundra. *ISME JOURNAL* 8:841-853.

ORIGINAL ARTICLE

Distinct microbial communities associated with buried soils in the Siberian tundra

Antje Gittel^{1,2}, Jiří Bárta³, Iva Kohoutová³, Robert Mikutta⁴, Sarah Owens^{5,6}, Jack Gilbert^{5,7}, Jörg Schneckner^{2,8}, Birgit Wild^{2,8}, Bjarte Hannisdal⁹, Joeran Maerz¹⁰, Nikolay Lashchinskiy¹¹, Petr Capek³, Hana Santrůčková³, Norman Gentsch⁴, Olga Shibistova^{4,12}, Georg Guggenberger⁴, Andreas Richter^{2,8}, Vigdis L Torsvik¹, Christa Schleper^{1,2,13} and Tim Urich^{2,13}

¹Department of Biology, Centre for Geobiology, University of Bergen, Bergen, Norway; ²Austrian Polar Research Institute, Vienna, Austria; ³Department of Ecosystems Biology, University of South Bohemia, České Budějovice, Czech Republic; ⁴Institut für Bodenkunde, Leibniz Universität Hannover, Hannover, Germany; ⁵Institute of Genomics and Systems Biology, Argonne National Laboratory, Argonne, IL, USA; ⁶Computation Institute, University of Chicago, Chicago, IL, USA; ⁷Department of Ecology and Evolution, University of Chicago, Chicago, IL, USA; ⁸Division of Terrestrial Ecosystem Research, Department of Microbiology and Ecosystem Science, University of Vienna, Vienna, Austria; ⁹Department of Earth Science, Centre for Geobiology, University of Bergen, Bergen, Norway; ¹⁰Division of Ecosystem Modelling, Institute of Coastal Research, Helmholtz Zentrum Geesthacht, Geesthacht, Germany; ¹¹Central Siberian Botanical Garden, Siberian Branch of Russian Academy of Sciences, Novosibirsk, Russia; ¹²VN Sukachev Institute of Forest, Siberian Branch of Russian Academy of Sciences, Akademgorodok, Russia and ¹³Division of Archaea Biology and Ecogenomics, Department of Ecogenomics and Systems Biology, University of Vienna, Vienna, Austria

Cryoturbation, the burial of topsoil material into deeper soil horizons by repeated freeze–thaw events, is an important storage mechanism for soil organic matter (SOM) in permafrost-affected soils. Besides abiotic conditions, microbial community structure and the accessibility of SOM to the decomposer community are hypothesized to control SOM decomposition and thus have a crucial role in SOM accumulation in buried soils. We surveyed the microbial community structure in cryoturbated soils from nine soil profiles in the northeastern Siberian tundra using high-throughput sequencing and quantification of bacterial, archaeal and fungal marker genes. We found that bacterial abundances in buried topsoils were as high as in unburied topsoils. In contrast, fungal abundances decreased with depth and were significantly lower in buried than in unburied topsoils resulting in remarkably low fungal to bacterial ratios in buried topsoils. Fungal community profiling revealed an associated decrease in presumably ectomycorrhizal (ECM) fungi. The abiotic conditions (low to subzero temperatures, anoxia) and the reduced abundance of fungi likely provide a niche for bacterial, facultative anaerobic decomposers of SOM such as members of the *Actinobacteria*, which were found in significantly higher relative abundances in buried than in unburied topsoils. Our study expands the knowledge on the microbial community structure in soils of Northern latitude permafrost regions, and attributes the delayed decomposition of SOM in buried soils to specific microbial taxa, and particularly to a decrease in abundance and activity of ECM fungi, and to the extent to which bacterial decomposers are able to act as their functional substitutes.

The ISME Journal (2014) 8, 841–853; doi:10.1038/ismej.2013.219; published online 12 December 2013

Subject Category: Microbial population and community ecology

Keywords: carbon storage; climate change; cryoturbation; microbial communities; permafrost-affected soil; soil organic matter (SOM)

Introduction

Northern latitude terrestrial ecosystems are key components in the global carbon (C) cycle (McGuire *et al.*, 2009) with permafrost-affected soils storing more than twice as much C as is currently contained in the atmosphere (IPCC, 2007; Tarnocai *et al.*, 2009). Cryoturbation processes driven by repeated freeze–thaw cycles lead to the subduction of soil organic matter (SOM) from the surface into

Correspondence: A Gittel, Center for Geomicrobiology, Department of Bioscience, Ny Munkegade 114, Building 1540, 8000 Aarhus C, Denmark.

E-mail: antjegittel80@gmail.com

or T Urich, Department of Ecogenomics and Systems Biology, University of Vienna, Althanstrasse 14, 1090 Vienna, Austria.

E-mail: tim.urich@univie.ac.at

Received 9 July 2013; revised 21 October 2013; accepted 6 November 2013; published online 12 December 2013

deeper soil layers. Cryoturbated soils (Turbels, according to the Soil Classification Working Group, 1998, or Turbic Cryosols, according to the World Reference Base for Soil Resources (WRB), Deckers *et al.*, 2002) contain more than one-third of the arctic soil organic carbon (SOC) (~581 Gt C; Tarnocai *et al.*, 2009). Although buried soil horizons contain similar amounts (g^{-1} dry weight) of C and nitrogen (N) as topsoils, radiocarbon (^{14}C) dating revealed that the C pool in these soil horizons is much older than in unburied topsoil horizons, indicating that decomposition processes are strongly retarded (Kaiser *et al.*, 2007; Hugelius *et al.*, 2010). Cryoturbation therefore is an important mechanism for long-term C storage in these soils (Davidson and Janssens 2006; Bockheim 2007). Northern latitude permafrost regions are particularly vulnerable to climate change, being exposed to the globally strongest increase in mean annual surface air temperatures (4–8 °C, IPCC, 2007). Longer frost-free vegetation periods and increased active layer depths are predicted to promote the availability of large SOC pools for microbial decomposition, leading to increased greenhouse gas emissions from these soils and thereby accelerating climate change (Schuur *et al.*, 2008; Tarnocai *et al.*, 2009; Schuur and Abbott 2011).

Besides physicochemical parameters like temperature, pH, moisture, oxygen availability, soil mineral assemblage and quality of the SOM, the microbial community structure and the accessibility of SOM to the decomposer community are thought to be crucial factors in the process of SOM accumulation and storage in soils (Schmidt *et al.*, 2011; Dungait *et al.*, 2012). The main gaps in our current understanding of SOM stabilization in buried soil horizons and its vulnerability to decomposition are however the structure and the SOM degradation capacities of the microbial community. Recent studies on arctic soils focused on microbial communities in the active layer and the underlying permafrost and targeted their functional potential (Yergeau *et al.*, 2010; Tveit *et al.*, 2012), their response to permafrost thaw (Mackelprang *et al.*, 2011) and related community dynamics to the availability of SOC (Waldrop *et al.*, 2010; Coolen *et al.*, 2011). We expanded on these studies by specifically addressing the microbial communities in cryoturbated soils, and particularly the ones associated with buried topsoils. We aimed to dissect differences in community composition and associated potential functions to identify microbial indicators for the retarded decomposition of SOM in buried soil horizons. To estimate microbial abundances and assess differences along the soil depth profiles, we quantified bacterial, archaeal and fungal SSU rRNA genes from 85 soil samples that were collected from three different vegetation zones in the Siberian tundra. These samples comprised topsoil, subsoil and buried topsoil as well as

mineral soils sampled from frozen ground below the active layer (hereafter called permafrost samples). We further characterized the microbial communities in a subset of 36 samples using prokaryotic SSU rRNA gene amplicon sequencing and pyrosequencing of the fungal Internal Transcribed Spacer (ITS) region. Changes in community structure and phylogenetic variability were linked to changes in abiotic soil properties, thus allowing us to propose potential key microorganisms involved in the degradation of SOM in buried soils.

Materials and Methods

Field site description, soil sampling and sample preparation

Soils were collected in August 2010 in northeast Siberia in a transect along the upper Kolyma river (Cherskii, Republic of Sakha, Russia). The study site covered the bioclimatic subzones E and D (Walker *et al.*, 2005), also called southern and typical tundra subzone in the Russian classification, respectively. Three sampling sites were chosen with respect to their dominant vegetation, classified as shrubby grass tundra, shrubby tussock tundra and shrubby lichen tundra (Table 1). Soils were sampled from triplicate soil pits for each of the sampling sites, resulting in a total of 85 soil samples (Table 1, Supplementary Table S1). Soil pits were 5 m in length and up to 1 m deep depending on the depth of the permafrost table (Supplementary Figure S1). After soil pits were classified into soil horizons, samples were collected using alcohol-sterilized knives. To obtain a representative sample from each soil horizon, at least three samples were pooled horizon-wise along the length of each soil profile. Organic and mineral topsoil horizons (O and A) were taken from the uppermost active layer and mineral subsoil horizons (B and C) and as well as buried topsoils (O_{jj} and A_{jj}) were sampled from deeper parts of the profile. Permafrost samples were obtained by coring (1–2 cores per soil profile, length: ~30 cm), using a steel pipe pushed into the frozen ground of the soil pits (Hugelius *et al.*, 2010). Initial soil processing included removal of living roots prior to homogenizing the soil fraction of each sample. Samples for extracting soil nucleic acids were fixed in RNeasy lysis RNA Stabilization Reagent (Ambion, Life Technologies, Carlsbad, CA, USA) and kept cold until further processing. Samples for the analyses of soil context data (as summarized in Supplementary Table S1) and enzyme activity potentials (cellobiohydrolase, endochitinase, N-acetylglucosaminidase, leucine aminopeptidase, phenoloxidase and peroxidase) were stored in closed polyethylene bags at 4 °C until analyzed. For details on analytical methods and the determination of enzyme activity potentials please refer to Supplementary Material and methods.

Table 1 Overview on sampling sites, replicate soil pits and soil samples

Site	Dominant vegetation	Replicate plots	Coordinates	Active layer depth (cm)	Number of samples ^a
Shrubby grass tundra	<i>Betula exilis</i> , <i>Salix phenophylla</i> , <i>Carex lugens</i> , <i>Calamagrostis holmii</i> , <i>Aulacomnium turgidum</i>	A	69.44°N, 161.71°E	55–65	6 (2/2/2/0)
		B	69.44°N, 161.71°E	45–63	10 (3/3/2/2)
		C	69.43°N, 161.72°E	33–63	10 (3/3/3/1)
Shrubby tussock tundra	<i>Eriophorum vaginatum</i> , <i>Carex lugens</i> , <i>Betula exilis</i> , <i>Salix pulchra</i> , <i>Aulacomnium turgidum</i>	D	69.45°N, 161.75°E	48–68	9 (3/3/2/1)
		E	69.44°N, 161.75°E	38–55	8 (3/3/2/0)
		F	69.44°N, 161.76°E	43–63	11 (4/3/2/2)
Shrubby lichen tundra	<i>Betula exilis</i> , <i>Vaccinium uliginosum</i> , <i>Flavocetraria nivalis</i> , <i>Flavocetraria cucullata</i>	G	68.75°N, 161.59°E	35–63	10 (3/3/3/1)
		H	68.75°N, 161.59°E	43–68	8 (3/2/3/0)
		I	68.75°N, 161.60°E	33–58	13 (3/3/5/2)

^aTotal number of soil samples from the respective soil pit. Numbers in brackets indicate soil samples from the four different soil horizons (topsoil/subsoil/buried topsoil/permafrost).

Nucleic acid extraction, purification and quantification

Nucleic acid extractions were conducted according to a modified bead-beating protocol (Urich *et al.*, 2008, see Supplementary Material and Methods) and further purified using the CleanAll DNA/RNA Clean-up and Concentration Micro Kit (Norgen Biotek Corp., Ontario, Canada). Total DNA was quantified using SybrGreen (Applied Biosystems, Life Technologies, Carlsbad, CA, USA; Leininger *et al.*, 2006).

Quantification of bacterial, archaeal and fungal SSU rRNA genes by quantitative PCR

Bacterial and archaeal small subunit (SSU) rRNA genes were amplified with the primer set Eub338Fabc/Eub518R (Daims *et al.*, 1999; Fierer *et al.*, 2005) for *Bacteria* and Arch519F/Arch908R (Jurgens *et al.*, 1997; Teske and Sorensen 2007) for *Archaea*. Fungal SSU genes were amplified using the primers nu-SSU-0817-5' and nu-SSU1196-3' (Borneman and Hartin, 2000). Product specificity was confirmed by melting point analysis and amplicon size was verified with agarose gel electrophoresis. Detection limits for the various assays (that is, lowest standard concentration that is significantly different from the non-template controls) were <100 gene copies for each of the genes. Samples, standards and non-template controls were run in triplicates. Please refer to Supplementary Materials and methods for details. Throughout this paper, the abundance of SSU rRNA genes will be used instead of the abundance of organisms, because such a calculation is based on a theoretical average number of functional gene copies per microorganism.

Barcoded amplicon sequencing of bacterial and archaeal SSU rRNA genes on the Illumina GAIIx platform and sequence analysis

Sample preparation was performed as described by Caporaso *et al.* (2011). Each sample was amplified in triplicate, combined and cleaned using the Ultra

Clean htp 96-well PCR clean up kit (MO BIO Laboratories, Solana Beach, CA, USA). The PCR primers (515F/806R) targeted the V4 region of the SSU rRNA, previously shown to yield accurate phylogenetic information and to have only few biases against any bacterial taxa (Liu *et al.*, 2007; Bates *et al.*, 2011; Bergmann *et al.*, 2011). Amplicons were sequenced on the Illumina GAIIx platform (Illumina Inc., San Diego, CA, USA). Quality filtering of reads was applied as described previously (Caporaso *et al.*, 2011). Reads were assigned to operational taxonomic units (OTUs, cutoff 97% sequence identity) using a closed-reference OTU picking protocol using QIIME (Caporaso *et al.*, 2010). Alpha diversity metrics and community relatedness (principal coordinate analysis, from unweighted Unifrac distances) were calculated after rarifying all samples to the same sequencing depth. For further details please refer to Supplementary Materials and methods.

Pyrosequencing of fungal ITS genes and sequence analysis

The ITS region of the fungal rRNA gene was amplified in triplicates from each sample using bar-coded primers ITS1F (Gardes and Bruns 1993) and ITS2 (White 1990). ITS-amplicons (~280 base pairs) were sequenced on half a picotiter plate of the GS FLX+ system (Roche, Basel, Switzerland) using Titanium chemistry at GATC Biotech (Konstanz, Germany). Initial read quality filtering was performed using mothur 1.27 (Schloss *et al.*, 2009) and overlapping regions of 18S rDNA, 5S and ITS2 region were trimmed using the ITS1 region extractor of the UNITE online pipeline (Abarenkov *et al.*, 2010). *De novo* and database-based chimerical sequence removal, OTU-picking and taxonomic assignment were performed using the QIIME bioinformatic pipeline (Caporaso *et al.*, 2010). Details on the procedure can be found in Supplementary Materials and methods.

Statistical analyses to evaluate the linkage between variability of soil context data and microbial community structure

Principal component analysis was used to summarize the soil context data (Supplementary Table S1) and the prokaryotic community structure (relative abundance of bacterial and archaeal taxa, Supplementary Table S2). After data standardization (zero mean and unit s.d.) and centered log-ratio transformation with multiplicative zero replacement (Aitchison, 1982; Martín-Fernández *et al.*, 2003; Jørgensen *et al.*, 2012), community structure and soil context data were effectively reduced to a single variable (PC1 score). To test for relationships between community structure and soil context data, Spearman rank-order correlations (ρ) were determined between the first principal component (PC1) scores of the relative abundance and the geochemical data. To assess the correlation between variability of the community structure and soil context data, Spearman's ρ was computed between PC1 scores from the relative abundance data and the original soil context data. To further test the community–environment relationships, we applied a unimodal type of constrained ordination, canonical correspondence analysis (CCA). Soil context parameters (explanatory variables, Supplementary Table S1) were related to differences in prokaryotic and fungal community structure (that is, changes in relative OTU abundances; response variables). The contribution of each explanatory variable was tested using forward selection and the Monte-Carlo permutation test within the CCA framework (Canoco v5; Ter Braak and Šmilauer, 2012).

Further statistical analyses

To determine significant differences in gene abundances, gene abundance ratios, taxa abundances (bacterial/archaeal, phyla and OTUs) and enzyme activity potentials between soil horizons (topsoil,

subsoil, buried soil and permafrost), one-way ANOVA followed by Tukey's HSD test was performed. Differences were considered significant at P -values < 0.05 . Prior to one-way ANOVA, Shapiro–Wilk tests and Bartlett tests were used to examine whether the conditions of normality and homogeneity of variance were met and followed by log-transformation (gene abundances) or square-root transformation (taxa abundances). Pearson's product–moment correlation (R) was used to assess linkages between individual taxa, gene abundances and enzyme activities as well as between geochemical data and diversity measures. All analyses were performed in R 2.15.0 (R Development Core Team; Team RDC, 2012). The STAMP bioinformatic package (Parks and Beiko, 2010) was used to determine significant differences in the relative abundance of fungal taxa between topsoils, subsoils and buried soils (Welch's test, two-sided, P -values < 0.05).

Data deposition

The SSU rRNA gene sequence data are available from MG-RAST (project numbers 44668685.3–44668734.3). Fungal raw reads were deposited in NCBI Sequence Read Archive (SRA) under the submission ID SUB282590 and BioProject ID PRJNA209792.

Results

Soil characteristics

Major soil properties varied significantly between soil horizons (Table 2). Total organic carbon (TOC), total nitrogen (TN), carbon-to-nitrogen (C/N) ratios and water content were highest in topsoils and lowest in subsoils, whereas pH was highest in subsoils. Buried topsoils were lower in pH than in subsoils, and showed higher TOC and TN values as well as higher C/N ratios and water content (Table 2).

Table 2 Soil context data and potential enzyme activities in topsoils, buried topsoils and subsoils^a

	Topsoils	Subsoils	Buried topsoils
<i>Soil chemical data</i>			
pH	5.3 ± 0.4 (c)	6.1 ± 0.6 (a)	5.8 ± 0.4 (b)
TOC (% dry weight)	15.5 ± 11.7 (a)	1.3 ± 0.8 (c)	10.4 ± 5.7 (b)
TN (% dry weight)	0.7 ± 0.5 (a)	0.1 ± 0.0 (b)	0.6 ± 0.3 (a)
C/N ratio	20.2 ± 6.8 (a)	11.5 ± 1.8 (c)	16.2 ± 2.1 (b)
Water content (%)	49.8 ± 22.2 (a)	17.2 ± 1.3 (b)	40.8 ± 9.3 (a)
<i>Potential activities (nmol h⁻¹ g⁻¹ dry soil)</i>			
Hydrolytic enzymes ^b	1572.3 ± 867.6 (a)	85.4 ± 61.9 (c)	481.4 ± 352.2 (b)
Oxidative enzymes ^c	9894.5 ± 5548.8 (a)	5092.9 ± 3539.7 (b)	13 480.9 ± 6069.1 (a)

^aMean and standard deviations. Small letters indicate significant differences ($P < 0.05$) between soil horizons as determined by one-way ANOVA and Tukey's HSD test. Number of samples from topsoils/buried topsoil/subsoils: 27/24/25 (chemical data) and 16/22/18 (enzyme activities). Detailed information on soil chemical data is available in Supplementary Table S1.

^bSum of potential activities of all hydrolytic enzymes measured (cellobiohydrolase, endochitinase, N-acetylglucosaminidase, leucine aminopeptidase).

^cSum of potential activities of all oxidative enzymes measured (phenoloxidase, peroxidase).

Principal component analysis analysis on a comprehensive data set of soil properties (Supplementary Table S1) placed buried topsoil horizons at an intermediate position and supported the finding that buried topsoil horizons were highly variable with regard to their soil properties, resulting in a shared ordination space with unburied topsoil and subsoil horizons (Supplementary Figure S2).

High prokaryotic abundances accompanied by a reduction of fungal abundance in buried soil horizons
Quantitative PCR (qPCR) was used to estimate numbers of bacterial, archaeal and fungal SSU rRNA genes from a total of 85 samples. Figure 1 shows abundances for one representative soil profile for each vegetation zone. Detailed soil horizon profiles and quantification results for individual soil pits can be found in Supplementary Figures S3A–C. Average bacterial SSU gene abundances were

highest in topsoil samples (3.5×10^{10} genes g^{-1} soil) and decreased with depth, based on the mean of all vegetation types and biological replicates. However, abundances were much higher in buried topsoil horizons (9.4×10^9 genes g^{-1} soil) than in the surrounding subsoils (3.7×10^8 genes g^{-1} soil, one-way ANOVA, $P < 0.01$). Average fungal SSU gene copy numbers were significantly higher in topsoils (6.4×10^{10} genes g^{-1} soil) than in buried topsoils and subsoils (8.1×10^7 and 1.7×10^8 genes g^{-1} soil, respectively, one-way ANOVA, $P < 0.01$). In permafrost samples, bacterial SSU rRNA gene copies ranged from 0.1×10^6 to 3.8×10^6 genes g^{-1} dry soil. Fungal SSU genes could only be amplified from a single permafrost sample and accounted for 0.4×10^6 genes g^{-1} dry soil. The mean ratio between fungal and bacterial SSU rRNA gene copies (fungal:bacterial ratios, FB) was lowest in buried topsoils (FB = 0.03) resulting from a decrease in fungal SSU genes compared with the topsoil samples (FB = 5.5, one-way ANOVA, $P < 0.05$).

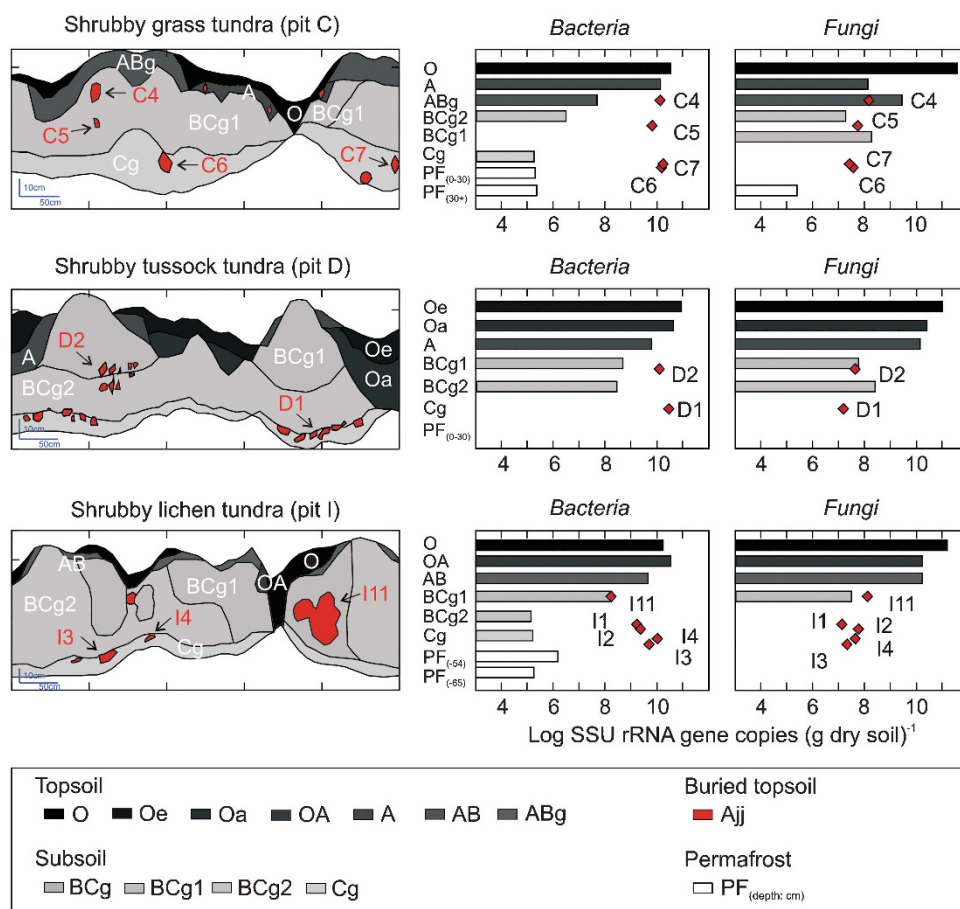


Figure 1 Schematic drawings of one representative soil pit profile for each vegetation type (shrubby grass tundra: pit C, shrubby tussock tundra: pit D and shrubby lichen tundra: pit I). O, Oe, Oa, OA, A, AB, ABg, BCg, Cg: subsoil. Ajj: buried topsoils, PF: permafrost (depth in cm below surface indicated in brackets). Location of buried topsoils (Ajj) is indicated and labeled with the corresponding sample ID. If sample IDs are missing, location of the soil sample was only reported in the soil pit description, but not included in the drawings. Bar charts show abundances of *Bacteria* and *Fungi* as bacterial and fungal SSU gene copy numbers g^{-1} dry soil (logarithmic scale). Supplementary Figures S3A–C provide information on SSU rRNA gene quantifications for all nine soil pits (three replicates per vegetation type, including the ones presented in this figure).

The observation of a significant decrease in FB ratios in buried topsoils held true for all three vegetation types (Figure 2).

Archaeal SSU rRNA genes accounted for <2% of the total number of prokaryotic SSU rRNA gene copies in buried topsoils and subsoils. On average, archaeal gene copies were one order of magnitude higher in the buried topsoils (1.2×10^8 genes g^{-1} dry soil) than in the subsoils (0.1×10^8 genes g^{-1} dry soil). Amplification of archaeal SSU rRNA genes from topsoil samples resulted in unspecific fragments (Supplementary Figure S4). Sequencing identified these fragments to be of fungal origin. Thus, the co-amplification of fungal DNA resulted in an overestimation of archaeal SSU rRNA genes in these samples (see Supplementary Figures S3A–C).

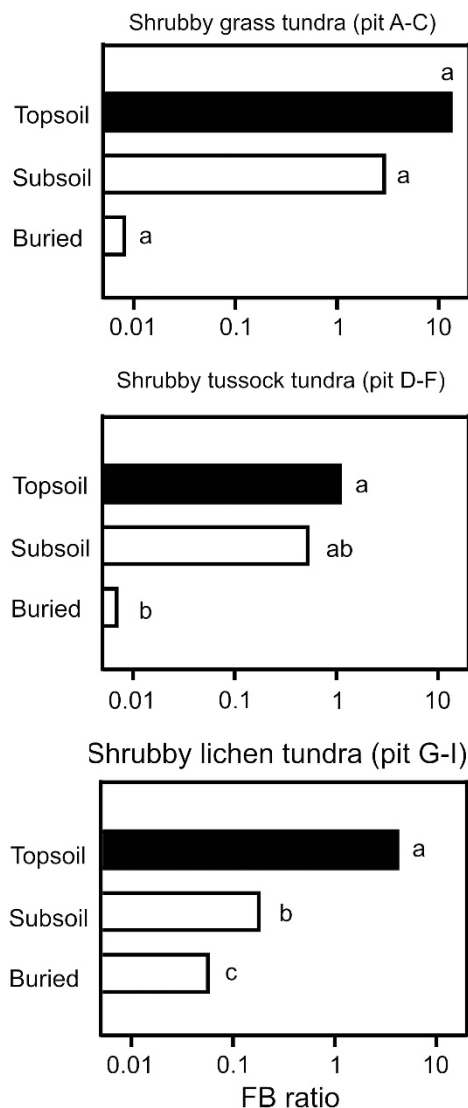


Figure 2 Fungal–bacterial (FB) ratios for the three different sampling sites as calculated from bacterial and fungal SSU rRNA gene copies g^{-1} dry soil. Small letters indicate significant differences between soil horizons as determined by one-way ANOVA and Tukey’s HSD test.

Potential hydrolytic and oxidative enzyme activities

Hydrolytic enzymes showed significantly higher potential activities (g^{-1} dry soil) in topsoils than in buried topsoils (one-way ANOVA, $P < 0.01$, Table 2). Potential oxidative enzyme activities were higher in buried topsoils than in non-buried topsoils, but this difference was not significant (Table 2). Both potential hydrolytic and oxidative enzyme activities were lowest in subsoils and significantly different from activities in buried and non-buried topsoil horizons (one-way ANOVA, $P < 0.05$). Hydrolytic and oxidative enzyme activities were positively correlated to bacterial SSU gene abundances (Pearson’s $R > 0.5$, $P < 0.01$), whereas fungal SSU gene abundances only showed significant correlations to the potential activity of hydrolytic enzymes (Pearson’s $R > 0.6$, $P < 0.01$), but not to oxidative enzyme activities ($P > 0.05$).

Sequencing statistics and distribution of microbial taxa across all horizons

Illumina tag sequencing of 36 samples (Supplementary Tables S2 and S3) yielded a total of 1.36×10^6 bacterial and archaeal SSU rRNA gene sequences and 2.81×10^5 fungal ITS sequences after extensive read-quality filtering (see Materials and methods for details). Bacterial and archaeal sequences clustered in 4580 OTUs, representing 98 classes (93 bacterial and 5 archaeal) within 38 phyla (for a detailed list of taxa and their relative abundance, see Supplementary Table S2). The dominant bacterial phyla were *Actinobacteria*, *Proteobacteria* (alpha-, beta- and gamma classes), *Verrucomicrobia*, *Acidobacteria* and *Bacteroidetes*, accounting for $\sim 84\%$ of all sequences. In addition, *Gemmatimonadetes*, *Chloroflexi*, *Deltaproteobacteria*, *Firmicutes* and *Planctomycetes* were present in all soil horizons, but at lower abundances (14% of all sequences), and 29 other rare phyla ($< 0.5\%$ each) were identified. Rare phyla included archaeal taxa that represented $< 0.1\%$ of all sequence reads. Most of them were affiliated with the *Thaumarchaeota* (order *Nitrososphaerales*) and the *Euryarchaeota* (orders *Methanomicrobiales* and *Methanobacteriales*).

Fungal ITS sequences were clustered into 3397 OTUs representing 19 classes within 6 phyla (for a detailed list of taxa and their relative abundance, see Supplementary Table S3). Across all soil horizons, the most abundant phyla were *Ascomycota* (66.8%) and *Basidiomycota* (30.1%). *Ascomycota* were dominated by *Leotiomycetes* (42.2%). Within the *Basidiomycota*, the class *Agaricomycetes* accounted for the majority of all sequences (69.9%). Other phyla (including the *Chytridiomycota*, *Glomeromycota* and *Zygomycota*) accounted for only a minor fraction of the fungal community across all horizons ($\sim 3\%$).

Major differences in prokaryotic community composition and diversity among soil horizons and linkage to environmental context data

Bacterial community composition in unburied topsoils and buried topsoils showed significant differences on the phylum level (Figure 3a), including higher relative abundances of *Actinobacteria* and *Gemmatimonadetes* (one-way ANOVA, $P < 0.05$) and a decrease of *Acidobacteria*, *Proteobacteria* (alpha-, gamma- and delta-subclasses) and *Planctomycetes* (one-way ANOVA, $P < 0.01$) in the buried horizons. The only significant difference between subsoils and buried topsoils was a lower relative abundance of *Deltaproteobacteria* in the latter (one-way ANOVA, $P < 0.05$). Community composition of individual buried topsoil horizons was highly variable, in particular with regard to the relative abundance of members of the phyla *Chloroflexi* and *Verrucomicrobia* (Supplementary Figure S5, Supplementary Table S2). A major fraction of OTUs from buried topsoils was shared either with topsoils or subsoils alone or with both topsoil and subsoil horizons (1853 OTUs, 86.5% of all OTUs from buried topsoils; Supplementary Figure S6), reflecting the process of topsoil material being buried into

deeper soil and the invasion of microorganisms from the surrounding mineral horizons. A minor fraction of OTUs was exclusively detected in buried topsoils (290 OTUs, 13.5% of all OTUs from buried topsoils, Supplementary Figure S6). None of these OTUs accounted for $> 0.001\%$ of all sequences recovered from these horizons. Species richness and diversity were highest in topsoil horizons followed by buried topsoils and mineral subsoils (one-way ANOVA, $P < 0.001$; Figure 4). Likewise, there were significant positive correlations between alpha diversity metrics (Shannon, Faith's PD) and the measured soil variables. While soil pH was the strongest predictor of alpha diversity in topsoils (Pearson's $R > 0.6$, $P < 0.001$), strongest correlations in buried topsoils were found for TOC and TN (Pearson's $R > 0.7$, $P < 0.05$ each). None of the measured soil parameters were significantly correlated with species richness and diversity in subsoils.

Principal coordinate analysis based on unweighted UniFrac distances supported the distinctness of the communities in buried and unburied soil horizons (Figure 5a), showing a separation of the topsoil communities from those of the buried topsoils and subsoils along the first principal coordinate. While topsoil communities in individual samples were highly similar to each other, communities in buried topsoils and subsoils exhibited a larger between-sample variability. Biplot analysis of unweighted UniFrac distances and the relative abundance of the eight most abundant phyla showed that *Acidobacteria*, *Bacteroidetes* and *Verrucomicrobia* were associated with topsoils, whereas the phyla *Chloroflexi*, *Gemmatimonadetes* and *Firmicutes* were associated with a cluster of subsoil and buried topsoil horizons (Figure 5b). The clustering of soil horizons was broadly congruent with principal component analysis using relative taxa abundance data (Supplementary Figure S2) and CCA of relative OTU abundances (Figure 5c), indicating that the measured soil context parameters explained most of the biological variation.

To further investigate whether the prokaryotic community structure was related to changes in soil characteristics, principal component analysis was performed independently on the soil context data (Supplementary Table S1) and the relative taxa abundance data (Supplementary Table S2). Sample scores on PC1 of the two data sets (soil context and prokaryotic community structure) showed a significant rank-order correlation at the phylum level ($\rho = 0.621$, $P < 0.001$), (Supplementary Figure S7) demonstrating that changes in the soil properties (PC1 explained 52% of the variation) co-varied with changes in the community structure (PC1 explained 22% of the variance at phylum level). PC1 scores (prokaryotic community structure) were extracted and showed significant correlations with pH ($\rho = -0.754$, $P < 0.001$), C/N ratio ($\rho = 0.649$, $P < 0.001$), TOC ($\rho = 0.505$, $P < 0.01$), moisture ($\rho = 0.436$, $P < 0.01$), $\delta^{13}\text{C}$ ($\rho = -0.605$, $P < 0.001$)

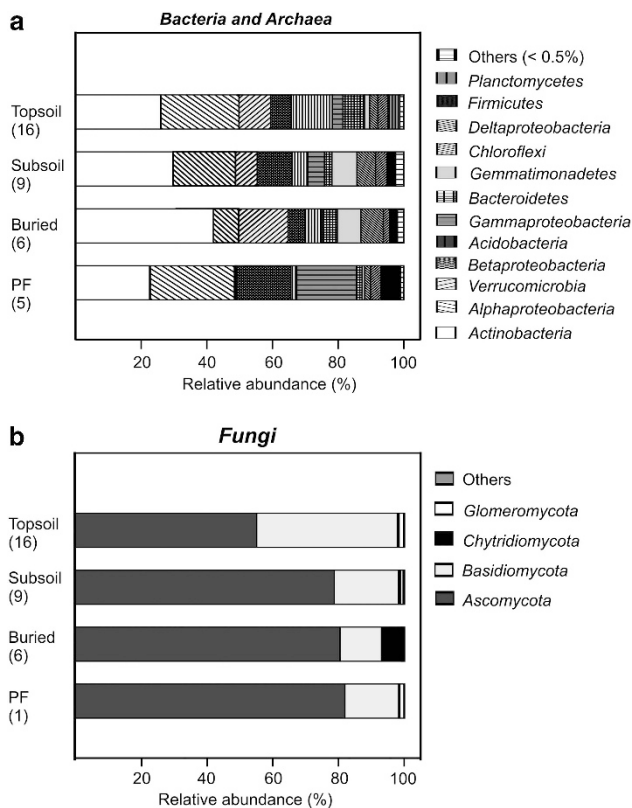


Figure 3 Prokaryotic (a) and fungal (b) community structure shown as relative abundance on phylum level and based on SSU rRNA gene Illumina tag sequencing and fungal ITS pyrosequencing, respectively. 'Others' include phyla with $< 0.5\%$ relative abundance (see Supplementary Tables S2 and S3 in the supplementary for detailed information). Number of samples analyzed given in brackets.

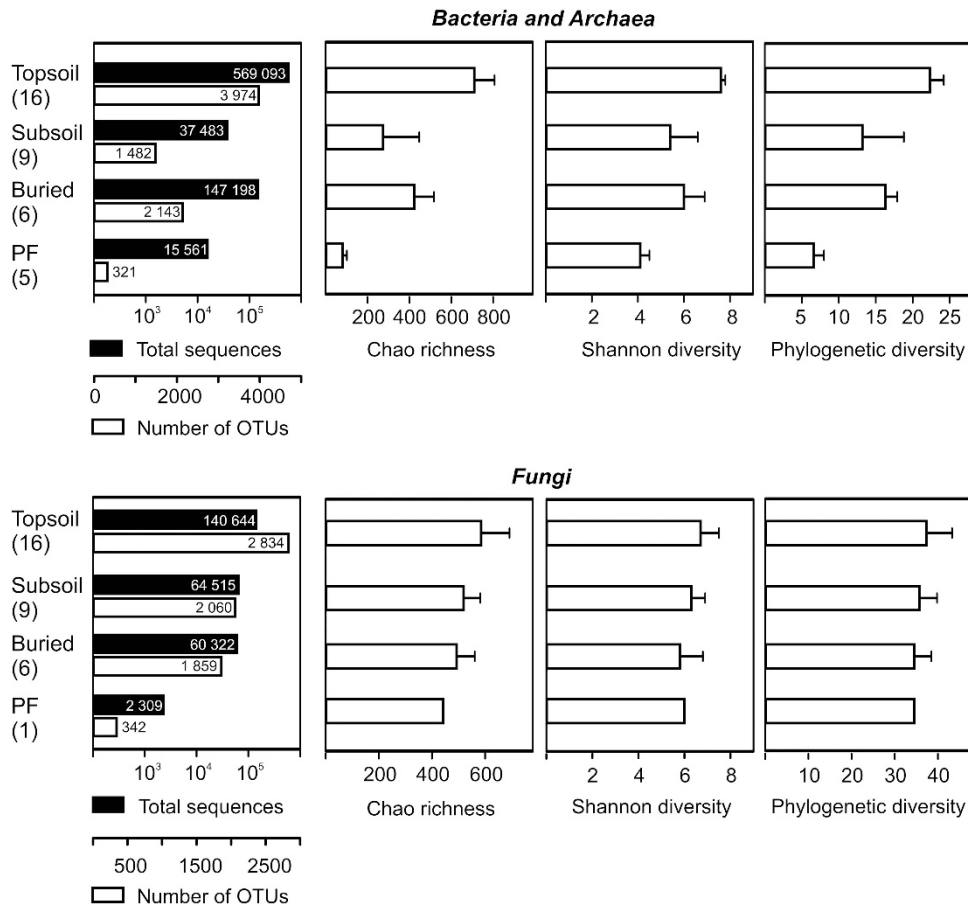


Figure 4 Overview of total sequences, number of OTUs, and microbial diversity topsoils, subsoils, buried topsoils and permafrost samples. Microbial diversity indicated by Chao1 richness, Shannon diversity and Faith's phylogenetic diversity (PD). Calculation of richness and diversity estimators was based on OTU tables rarified to the same sequencing depth (that is, the lowest one of total sequencing reads). Total sequences refer to the total number of taxonomically assigned sequences (see Material and Methods for details). OTUs were defined as <3% nucleotide sequence difference.

and $\delta^{15}\text{N}$ ($\rho = -0.543$, $P < 0.001$) (Supplementary Figures S8A–F). For buried topsoils, strongest PC1 score correlations were found for TOC ($\rho = 0.886$, $P < 0.05$) and TN ($\rho = 0.886$, $P < 0.05$) (Supplementary Figure S8G–H). These results were in agreement with the CCA that identified pH, $\delta^{13}\text{C}$ and $\delta^{15}\text{N}$ having the strongest positive influence on axis 1, while C/N ratio, TOC TN and moisture were acting most negatively (Figure 5c).

Major differences in fungal community composition and diversity among soil horizons and taxo–environment relationships

Fungal community composition was significantly different in topsoils compared with buried topsoils and subsoils (Figure 3b). The relative abundance of *Basidiomycota* was significantly higher (one-way ANOVA, Tukey's HSD test, $P < 0.05$) in topsoils (42.6%) than in buried topsoils (12.6%) and subsoils (19.5%). *Ascomycota* dominated in buried topsoils (80.4%) and subsoils (78.7%) with *Leotiomycetes* and *Sordariomycetes* being the most abundant classes. *Chytridiomycota* accounted for 6% of all

sequences from buried topsoils, resulting from an exceptionally high relative abundance in one sample (G4, Supplementary Table S3), but accounting for <1% in all other samples. In particular, the ectomycorrhizal (ECM) families *Russulales*, *Thelephorales* and *Sebacinales* showed significantly lower abundance in buried than in unburied topsoils (Welch's *t*-test, two-sided, $P < 0.05$; Supplementary Figure S9). A major fraction of fungal OTUs from buried topsoils was shared either with topsoils or subsoils alone or with both topsoil and subsoil horizons (1650 OTUs, 88.8% of all OTUs from buried topsoils; Supplementary Figure S6). A minor fraction of OTUs was exclusively detected in buried topsoils (209 OTUs, 11.2% of all OTUs from buried topsoils, Supplementary Figure S6). Species richness and diversity were slightly, but not significantly higher in topsoils than in subsoils and buried topsoils (one-way ANOVA, $P > 0.05$; Figure 4).

To examine species–environment relationships, CCA was applied to fungal OTU abundance and a set of 14 environmental variables (Figure 6). The first two CCA axes (CCA1 and CCA2) explained 72.8% of

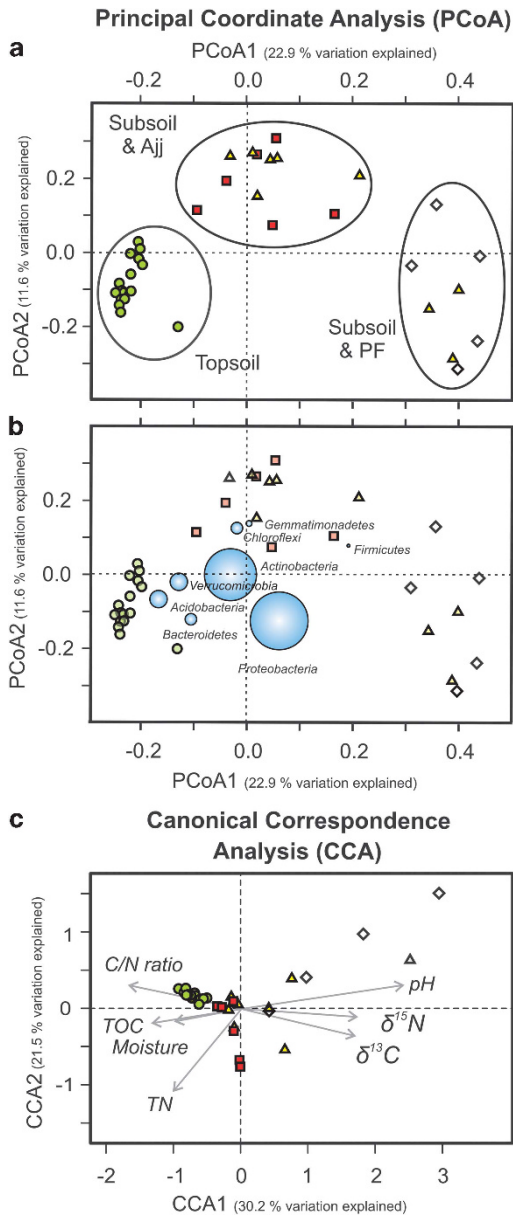


Figure 5 Phylogenetic dissimilarity between soil samples. Topsoils: green circles, subsoils: yellow triangles, buried topsoils: red squares, permafrost: white diamonds. See Supplementary Table S2 in the supplementary for detailed information on samples analyzed. (a) Principal coordinate analysis plot illustrating unweighted UniFrac distances between bacterial communities in individual samples. (b) The coordinates of the eight most abundant taxa are plotted as a weighted average of the coordinates of all samples, where the weights are the relative abundances of the taxon in the samples. The size of the sphere representing a taxon is proportional to the mean relative abundance of the taxon across all samples. (c) CCA plot for the first two dimensions to show the relationship between prokaryotic community structure (relative abundance of bacterial and archaeal OTUs) and environmental parameters. Correlations between environmental variables and CCA axes are represented by the length and angle of arrows (environmental factor vectors).

the total variance in the fungal community composition and 13.7% of the cumulative variance of the fungal species–environment relationship (Figure 6).

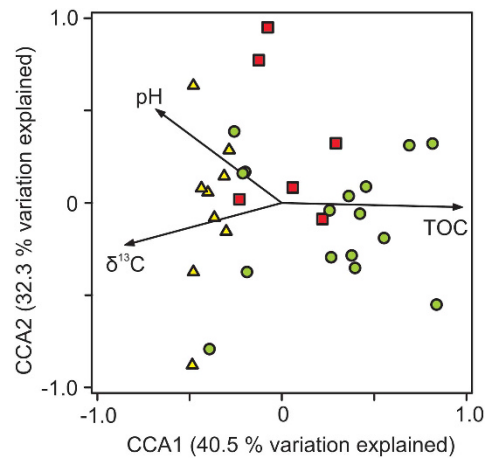


Figure 6 CCA ordination plots for the first two dimensions to show the relationship between fungal community structure (relative abundance of fungal OTUs) and environmental parameters. Topsoils: green circles, subsoils: yellow triangles, buried topsoils: red squares. See Supplementary Table S3 in the supplementary for detailed information on samples analyzed. Correlations between environmental variables and CCA axes are represented by the length and angle of arrows (environmental factor vectors).

CCA1 distinguished fungal topsoil communities from subsoil communities. Exceptions were mixed soil horizons (AB horizons) that were initially classified as topsoil horizons, but clustered with the subsoil communities in CCA analysis. Fungal communities in buried topsoils were placed at an intermediate position. CCA indicated that only TOC, pH and $\delta^{13}\text{C}$ contributed significantly to the species–environment relationship ($P < 0.05$, 1000 Monte Carlo permutations), providing 13.7% of the total CCA explanatory power. It was furthermore indicated that the spatial distribution of certain genera within the *Basidiomycota* and *Ascomycota* was related to distinct soil environmental parameters (Supplementary Figure S10). The distribution of *Ascomycota* was correlated to changes in pH and $\delta^{13}\text{C}$ values, whereas the distribution of *Basidiomycota* was related to changes in TOC content.

Discussion

The low abundance of ECM basidiomycota is a potential key factor in the reduced degradation of SOM in buried soils

Recently, evidence is building up that the stability of organic matter in soil is mainly controlled by its stabilization in soil mineral associations, its accessibility to the decomposer community, the presence and activity of extracellular enzymes, and microbial community structure, rather than being controlled by its molecular structure or chemical recalcitrance (Schmidt *et al.*, 2011; Dungait *et al.*, 2012). Stabilization mechanisms for SOC are of particular interest in Northern high latitude soils as they contain ~50% of the global SOC pool and are particularly

vulnerable to changes in abiotic conditions (for example, temperatures, moisture). Although fungi have a critical role in the transformation of SOM, fungal communities in terrestrial ecosystems of the Northern high latitudes are still poorly studied (Timling and Taylor, 2012). Fungi, and in particular saprotrophic basidiomycetes, are thought to be the dominant producers of extracellular enzymes catalyzing the breakdown of biopolymers to low-molecular weight dissolved organic matter that can then be utilized by other microorganisms (Bailey *et al.*, 2002; Baldrian 2008). We found pronounced differences in the abundance and composition of the fungal communities between unburied and buried topsoil horizons. It was indicated that lower fungal to bacterial ratios in buried than in unburied topsoil horizons resulted from a significant reduction in *Basidiomycota*, specifically of the ECM families *Russulales*, *Thelephorales* and *Sebacinales* (Supplementary Figure S9). Interestingly, there is accumulating evidence that mycorrhizal fungi, besides saprotrophs, may act as potent decomposers of SOM and have a crucial role in SOM transformation especially in arctic and boreal ecosystems (Talbot *et al.*, 2008). Although primarily considered to metabolize low-molecular weight carbon compounds, ECM fungi have been shown to produce extracellular enzymes to break down nutrient and C-rich molecules (Read and Perez-Moreno 2003; Read *et al.*, 2004; Talbot *et al.*, 2008). Recent studies however suggested that ECM fungi are responsible for degrading different C and nutrient fractions of SOM than saprotrophic communities and that the decomposition of SOM by ECM fungi is linked to their depolymerization abilities for organic N and P compounds (Rineau *et al.*, 2013; Talbot *et al.*, 2013). So far, only few ECM fungi were found to produce enzymes that break down C-rich biopolymers like cellulose, pectin or lipids in culture (Talbot and Treseder, 2010). Talbot *et al.*, 2008 suggested several mechanisms by which ECM fungi may contribute to SOM decomposition, one of them described as the 'Coincidental Decomposer' hypothesis. According to this hypothesis, SOM decomposition by ECM fungi is a consequence of exploiting the soil for nutrients. ECM fungi thereby contribute substantially to the mobilization of N-rich SOM and, consequently, to an increase in host plant C-fixation and subsequent input of C to the soil (Lindahl *et al.*, 2007; Orwin *et al.*, 2011; Hobbie *et al.*, 2013). Consequently, the low abundance of ECM fungi in buried topsoils presumably leads to less mobilization of N and results in an even higher N-limitation in arctic soils. In addition, ECM fungi in buried topsoils have lost their connection to the host plant and are therefore not 'primed' by plant-derived carbon ('Priming Effect' hypothesis, Talbot *et al.*, 2008). Thus, the synthesis of extracellular fungal enzymes is probably low and depolymerization of C- and N-rich substrates dramatically decreases. Indeed, Wild *et al.* (2013) described on average

84% reduction in protein depolymerization and 68% reduction in amino acid uptake in buried topsoils. Thus, the reduced abundance of ECM fungi, their reduced activity in the depolymerization of N-rich compounds together with unfavorable abiotic conditions such as subzero temperatures and high moisture presumably lead to a retarded decomposition and thus to the stabilization of OM in buried topsoils in Northern high latitude regions.

The distinctness of the bacterial community in buried topsoils reflects soil properties

As surface soil is rich in labile carbon and nitrogen and represents the primary location of root exudates, the presence of rapidly growing copiotrophic microorganisms is favored (Fierer *et al.*, 2007). In contrast, slow-growing oligotrophic organisms are better adapted to resource-poor locations and complex organic substrates and therefore occur in deeper soil horizons. Together with rather harsh abiotic conditions (low to subzero temperatures, high moisture, anoxia due to water logging), the distribution of microorganisms along the soil depth profile thus follows gradients of C and N availability as well as SOM composition, resulting in distinct community patterns and less microbial biomass in deeper soil horizons (Hartmann *et al.*, 2009; Eilers *et al.*, 2012). However, our analyses showed that pockets of buried topsoil horizons interrupted this continuum by being different from the subsoil in major soil parameters (for example, higher TOC, TN), and harboring a prokaryotic community with significantly higher bacterial and archaeal abundances than found in the surrounding subsoil horizons. As buried topsoils showed similarly low fungal abundances as the surrounding subsoil horizons, the remarkably low FB ratios in the buried topsoils were foremost a consequence of the high bacterial abundances therein. Prokaryotic communities in topsoil horizons were phylogenetically highly similar (Figure 5a) and relatively uniform in composition across all pits regardless of geographic position and landscape cover (Supplementary Figure S5). In contrast, communities in buried topsoils and subsoils were not only distinct from the topsoil communities, but also highly variable (Supplementary Figure S5). This variability in community composition was most likely a result of the greater variability in soil properties, namely the concentration and quality of the SOM. Abundance patterns of prokaryotic OTUs affiliated with potential representatives of distinct metabolic traits (for example, anaerobic respiration, fermentation, methano-/methylotrophy) further supported the hypothesis that community structure reflected differences in soil properties (Supplementary Table S4). The elevated abundance of OTUs assigned to fermentative members of the *Chloroflexi* (*Anaerolineae*) and the *Firmicutes* (*Clostridia*) as well as members of the anaerobic, sulfur- and

metal-reducing *Desulfuromonadales* (*Geobacteraceae*) indicated the potential for anaerobic degradation processes to occur in these deeper soil horizons.

Actinobacteria, in particular the order *Actinomycetales*, dominated the prokaryotic community in buried topsoils and were found in significantly higher relative abundance than in non-buried topsoils (Figure 3a). *Actinobacteria* were shown to maintain metabolic activity and DNA repair mechanisms at subzero temperatures (Johnson *et al.*, 2007). As buried soils experience longer freezing periods than topsoil horizons, this adaptation might select for *Actinobacteria* and disfavor the growth and/or maintenance of other taxa. This hypothesis is in line with a cross-seasonal study on arctic tundra soils that indicated that *Actinobacteria* might be persistent in the active fraction of the soil community over seasons and are thus ecologically relevant in frozen soils (McMahon *et al.*, 2011). More importantly, members of this phylum have been described to be adapted to low carbon availability (Fierer *et al.*, 2003) as well as to be metabolically versatile, including specialists that are able to solubilize and modify lignin and lignocelluloses and thereby gain access to the associated polysaccharides (McCarthy 1987; Roes-Hill *et al.*, 2011). Laccase-like genes were found in the genomes of diverse bacteria, including actinobacteria, supporting the hypothesis that the capability to modify lignin and decompose lignin derivatives is more widespread among the bacteria than previously thought (Ausec *et al.*, 2011; Bugg *et al.*, 2011). Buried soil horizons that undergo water-logging after active layer thaw might periodically turn anoxic, thereby restricting fungal growth and activity, resulting in a lower fungal abundance and creating a niche for bacterial, presumably anaerobic lignin degraders such as the actinomycetes (Boer *et al.*, 2005; DeAngelis *et al.*, 2011). Though being functionally redundant, actinobacterial activity in lignin degradation and transformation apparently does not resemble fungal activities as decomposition in buried soils is strongly retarded. This discrepancy might be due to differences in bacterial and fungal biomass, lower cell-specific enzyme activities, as well as morphological restrictions such as the absence of hyphae structures to efficiently penetrate the substrate.

Interestingly, the highest correlations between potential oxidative enzyme activities (phenoloxidase, peroxidase) and taxon abundance were found for rare bacterial taxa (for example, the candidate phylum SC3, Pearson's $R > 0.6$, $P < 0.01$), either indicating that those might contribute to the production of key enzymes involved in lignin degradation or solely act as so-called 'cheaters' participating from the products being available from exoenzymatic breakdown of polymers (Allison 2005), as suggested in an evolutionary context in the Black Queen Hypothesis (Morris *et al.*, 2012).

In summary, our study demonstrates that microbial community structure in buried topsoil horizons is distinct from that in unburied topsoil and the surrounding mineral subsoil horizons. Opposing trends in bacterial and fungal abundances were manifested in remarkably low FB ratios in buried topsoil horizons. The decrease in abundance of ECM fungi and the extent to which bacterial decomposers are able to act as functional substitutes in SOM transformations are proposed as microbial key factors in the retarded decomposition of SOM in buried soils of Northern latitude permafrost regions. The response of the fungal community to rising temperatures and concomitant changes in environmental parameters such as soil moisture and plant cover will be of particular interest in the scope of drastic changes in the arctic climate.

Conflict of Interest

The authors declare no conflict of interest.

Acknowledgements

We thank all members of the CryoCARB consortium that participated in field work in Cherskii in 2010 and their invaluable contributions to this manuscript by fruitful discussions. Sergey A Zimov is highly acknowledged for providing facilities at the Northeast Science Station (Cherskii, Russia) and access to the sampling site. Kristýna Kvardová is thanked for help with nucleic acid extractions. This work was funded by the Research Council of Norway as a part of the International Program CryoCARB (Long-term Carbon Storage in Cryoturbated Arctic Soils; NFR—200411). Jiří Bárta and Tim Urich received financial support from the EU Action program (Austria-Czech Republic, ID 60p14). Andreas Richter acknowledges the support of the Austrian Science Fund (FWF I370-B17).

References

- Abarenkov K, Henrik Nilsson R, Larsson K-H, Alexander IJ, Eberhardt U, Erland S *et al.* (2010). The UNITE database for molecular identification of fungi—recent updates and future perspectives. *New Phytol* **186**: 281–285.
- Aitchison J. (1982). The statistical analysis of compositional data. *J R Stat Soc Ser B (Methodol)* **44**: 139–177.
- Allison SD. (2005). Cheaters, diffusion and nutrients constrain decomposition by microbial enzymes in spatially structured environments. *Ecol Lett* **8**: 626–635.
- Ausec L, Zakrzewski M, Goesmann A, Schlüter A, Mandic-Mulec I. (2011). Bioinformatic analysis reveals high diversity of bacterial genes for laccase-like enzymes. *PLoS One* **6**: e25724.
- Bailey VL, Smith JL, Bolton H Jr. (2002). Fungal-to-bacterial ratios in soils investigated for enhanced C sequestration. *Soil Bio Biochem* **34**: 997–1007.
- Baldrian P. (2008). Enzymes of saprotrophic basidiomycetes. In: Boddy L, Frankland JC, West P (eds). *Ecology*

- of *Saprotrophic Basidiomycetes*. Academic Press: London, UK, pp 19–41.
- Bates ST, Berg-Lyons D, Caporaso JG, Walters WA, Knight R, Fierer N. (2011). Examining the global distribution of dominant archaeal populations in soil. *ISME J* **5**: 908–917.
- Bergmann GT, Bates ST, Eilers KG, Lauber CL, Caporaso JG, Walters WA *et al.* (2011). The under-recognized dominance of *Verrucomicrobia* in soil bacterial communities. *Soil Bio Biochem* **43**: 1450–1455.
- Bockheim JG. (2007). Importance of cryoturbation in redistributing organic carbon in permafrost-affected soils. *Soil Sci Soc Am J* **71**: 1335–1342.
- Boer Wd, Folman LB, Summerbell RC, Boddy L. (2005). Living in a fungal world: impact of fungi on soil bacterial niche development. *FEMS Microbiol Rev* **29**: 795–811.
- Borneman J, Hartin RJ. (2000). PCR primers that amplify fungal rRNA genes from environmental samples. *Appl Environ Microbiol* **66**: 4356–4360.
- Bugg TDH, Ahmad M, Hardiman EM, Singh R. (2011). The emerging role for bacteria in lignin degradation and bio-product formation. *Curr Opin Biotechnol* **22**: 394–400.
- Caporaso JG, Kuczynski J, Stombaugh J, Bittinger K, Bushman FD, Costello EK *et al.* (2010). QIIME allows analysis of high-throughput community sequencing data. *Nat Methods* **7**: 335–336.
- Caporaso JG, Lauber CL, Walters WA, Berg-Lyons D, Lozupone CA, Turnbaugh PJ *et al.* (2011). Global patterns of 16S rRNA diversity at a depth of millions of sequences per sample. *Proc Natl Acad Sci USA* **108**: 4516–4522.
- Coolen MJL, van de Giessen J, Zhu EY, Wuchter C. (2011). Bioavailability of soil organic matter and microbial community dynamics upon permafrost thaw. *Environ Microbiol* **13**: 2299–2314.
- Daims H, Brühl A, Amann R, Schleifer KH, Wagner M. (1999). The domain-specific probe EUB338 is insufficient for the detection of all bacteria: development and evaluation of a more comprehensive probe set. *Syst Appl Microbiol* **22**: 434–444.
- Davidson EA, Janssens IA. (2006). Temperature sensitivity of soil carbon decomposition and feedbacks to climate change. *Nature* **440**: 165–173.
- DeAngelis KM, Allgaier M, Chavarria Y, Fortney JL, Hugenholtz P, Simmons B *et al.* (2011). Characterization of trapped lignin-degrading microbes in tropical forest soil. *PLoS One* **6**: e19306.
- Deckers JA, Driessen PM, Nachtergaele FO, Spaargaren OC. (2002). World Reference Base for Soil Resources. In: Lal R (eds). *Encyclopedia of Soil Science*. Marcel Dekker: New York, NY, USA, pp 1446–1451.
- Dungait JAJ, Hopkins DW, Gregory AS, Whitmore AP. (2012). Soil organic matter turnover is governed by accessibility not recalcitrance. *Global Change Biol* **18**: 1781–1796.
- Eilers KG, Debenport S, Anderson S, Fierer N. (2012). Digging deeper to find unique microbial communities: the strong effect of depth on the structure of bacterial and archaeal communities in soil. *Soil Bio Biochem* **50**: 58–65.
- Fierer N, Schimel JP, Holden PA. (2003). Variations in microbial community composition through two soil depth profiles. *Soil Bio Biochem* **35**: 167–176.
- Fierer N, Jackson JA, Vilgalys R, Jackson RB. (2005). Assessment of soil microbial community structure by use of taxon-specific quantitative PCR assays. *Appl Environ Microbiol* **71**: 4117–4120.
- Fierer N, Bradford MA, Jackson RB. (2007). Toward an ecological classification of soil bacteria. *Ecology* **88**: 1354–1364.
- Gardes M, Bruns TD. (1993). ITS primers with enhanced specificity for basidiomycetes—application to the identification of mycorrhizae and rusts. *Mol Ecol* **2**: 113–118.
- Hartmann M, Lee S, Hallam SJ, Mohn WW. (2009). Bacterial, archaeal and eukaryal community structures throughout soil horizons of harvested and naturally disturbed forest stands. *Environ Microbiol* **11**: 3045–3062.
- Hobbie E, Ouimette A, Schuur EG, Kierstead D, Trappe J, Bendiksen K *et al.* (2013). Radiocarbon evidence for the mining of organic nitrogen from soil by mycorrhizal fungi. *Biogeochemistry* **114**: 381–389.
- Hugelius G, Kuhry P, Tarnocai C, Virtanen T. (2010). Soil organic carbon pools in a periglacial landscape: a case study from the central Canadian Arctic. *Permafrost Periglacial Processes* **21**: 16–29.
- Intergovernmental Panel on Climate Change (IPCC) (2007). *Climate Change 2007: The Scientific Basis*. Cambridge University Press: Cambridge, UK.
- Johnson SS, Hebsgaard MB, Christensen TR, Mastepanov M, Nielsen R, Munch K *et al.* (2007). Ancient bacteria show evidence of DNA repair. *Proc Natl Acad Sci USA* **104**: 14401–14405.
- Jurgens G, Lindström K, Saano A. (1997). Novel group within the kingdom *Crenarchaeota* from boreal forest soil. *Appl Environ Microbiol* **63**: 803–805.
- Jørgensen SL, Hannisdal B, Lanzén A, Baumberger T, Flesland K, Fonseca R *et al.* (2012). Correlating microbial community profiles with geochemical data in highly stratified sediments from the Arctic Mid-Ocean Ridge. *Proc Natl Acad Sci USA* **109**: E2846–E2855.
- Kaiser C, Meyer H, Biasi C, Rusalimova O, Barsukov P, Richter A. (2007). Conservation of soil organic matter through cryoturbation in arctic soils in Siberia. *J Geophys Res* **112**: G02017.
- Leininger S, Ulrich T, Schloter M, Schwark L, Qi J, Nicol GW *et al.* (2006). Archaea predominate among ammonia-oxidizing prokaryotes in soils. *Nature* **442**: 806–809.
- Lindahl BD, Ihrmark K, Boberg J, Trumbore SE, Höglberg P, Stenlid J *et al.* (2007). Spatial separation of litter decomposition and mycorrhizal nitrogen uptake in a boreal forest. *New Phytol* **173**: 611–620.
- Liu Z, Lozupone C, Hamady M, Bushman FD, Knight R. (2007). Short pyrosequencing reads suffice for accurate microbial community analysis. *Nucleic Acids Res* **35**: e120.
- Mackelprang R, Waldrop MP, DeAngelis KM, David MM, Chavarria KL, Blazewicz SJ *et al.* (2011). Metagenomic analysis of a permafrost microbial community reveals a rapid response to thaw. *Nature* **480**: 368–371.
- Martín-Fernández JA, Barceló-Vidal C, Pawlowsky-Glahn V. (2003). Dealing with zeros and missing values in compositional data sets using nonparametric imputation. *Math Geol* **35**: 253–278.
- McCarthy AJ. (1987). Lignocellulose-degrading actinomycetes. *FEMS Microbiol Lett* **46**: 145–163.
- McGuire AD, Anderson LG, Christensen TR, Dallimore S, Guo L, Hayes DJ *et al.* (2009). Sensitivity of the carbon cycle in the Arctic to climate change. *Ecol Monogr* **79**: 523–555.

- McMahon SK, Wallenstein MD, Schimel JP. (2011). A cross-seasonal comparison of active and total bacterial community composition in Arctic tundra soil using bromodeoxyuridine labeling. *Soil Bio Biochem* **43**: 287–295.
- Morris JJ, Lenski RE, Zinser ER. (2012). The Black Queen hypothesis: evolution of dependencies through adaptive gene loss. *mBio* **3**: pii e00036–12.
- Orwin KH, Kirschbaum MUF St, John MG, Dickie IA. (2011). Organic nutrient uptake by mycorrhizal fungi enhances ecosystem carbon storage: a model-based assessment. *Ecol Lett* **14**: 493–502.
- Parks DH, Beiko RG. (2010). Identifying biologically relevant differences between metagenomic communities. *Bioinformatics* **26**: 715–721.
- Read DJ, Perez-Moreno J. (2003). Mycorrhizas and nutrient cycling in ecosystems—a journey towards relevance? *New Phytol* **157**: 475–492.
- Read DJ, Leake JR, Perez-Moreno J. (2004). Mycorrhizal fungi as drivers of ecosystem processes in heathland and boreal forest biomes. *Canad J Bot* **82**: 1243–1263.
- Rineau F, Shah F, Smits MM, Persson P, Johansson T, Carleer R *et al*. (2013). Carbon availability triggers the decomposition of plant litter and assimilation of nitrogen by an ectomycorrhizal fungus. *ISME J* **7**: 2010–2022.
- Roes-Hill M, Khan N, Burton S. (2011). Actinobacterial peroxidases: an unexplored resource for biocatalysis. *Appl Biochem Biotechnol* **164**: 681–713.
- Schloss PD, Westcott SL, Ryabin T, Hall JR, Hartmann M, Hollister EB *et al*. (2009). Introducing mothur: open-source, platform-independent, community-supported software for describing and comparing microbial communities. *Appl Environ Microbiol* **75**: 7537–7541.
- Schmidt MWI, Torn MS, Abiven S, Dittmar T, Guggenberger G, Janssens IA *et al*. (2011). Persistence of soil organic matter as an ecosystem property. *Nature* **478**: 49–56.
- Schuur EAG, Bockheim J, Canadell JG, Euskirchen E, Field CB, Goryachkin SV *et al*. (2008). Vulnerability of permafrost carbon to climate change: implications for the global carbon cycle. *BioScience* **58**: 701–714.
- Schuur EAG, Abbott B. (2011). Climate change: High risk of permafrost thaw. *Nature* **480**: 32–33.
- Soil Classification Working Group (1998). *The Canadian System of Soil Classification*, 3rd edn NRC Research Press: Ottawa, ON, Canada.
- Talbot JM, Allison SD, Treseder KK. (2008). Decomposers in disguise: mycorrhizal fungi as regulators of soil C dynamics in ecosystems under global change. *Functional Ecol* **22**: 955–963.
- Talbot JM, Treseder KK. (2010). Controls over mycorrhizal uptake of organic nitrogen. *Pedobiologia* **53**: 169–179.
- Talbot JM, Bruns TD, Smith DP, Branco S, Glassman SI, Erlandson S *et al*. (2013). Independent roles of ectomycorrhizal and saprotrophic communities in soil organic matter decomposition. *Soil Bio Biochem* **57**: 282–291.
- Tarnocai C, Canadell JG, Schuur EAG, Kuhry P, Mazhitova G, Zimov S. (2009). Soil organic carbon pools in the northern circumpolar permafrost region. *Global Biogeochem Cycles* **23**: GB2023.
- Team RDC (2012). *R: a Language and Environment for Statistical Computing*. R Foundation for Statistical Computing: Vienna, Austria.
- Ter Braak CJF, Šmilauer P. (2012). *Canoco Reference Manual and User's Guide: software for ordination*, version 5.0.
- Teske A, Sorensen KB. (2007). Uncultured archaea in deep marine subsurface sediments: have we caught them all? *ISME J* **2**: 3–18.
- Timling I, Taylor DL. (2012). Peeking through a frosty window: molecular insights into the ecology of Arctic soil fungi. *Fung Ecol* **5**: 419–429.
- Tveit A, Schwacke R, Svenning MM, Urich T. (2012). Organic carbon transformations in high-Arctic peat soils: key functions and microorganisms. *ISME J* **7**: 299–311.
- Urich T, Lanzén A, Qi J, Huson DH, Schleper C, Schuster SC. (2008). Simultaneous assessment of soil microbial community structure and function through analysis of the meta-transcriptome. *PLoS One* **3**: e2527.
- Waldrop MP, Wickland KP, White R, Berhe AA, Harden JW, Romanovsky VE. (2010). Molecular investigations into a globally important carbon pool: permafrost-protected carbon in Alaskan soils. *Global Change Biol* **16**: 2543–2554.
- Walker DA, Raynolds MK, Daniëls FJA, Einarsson E, Elvebakk A, Gould WA *et al*. (2005). The circumpolar Arctic vegetation map. *J Veg Sci* **16**: 267–282.
- White TJ, Bruns T, Lee S, Taylor J. (1990). Amplification and direct sequencing of fungal ribosomal RNA genes for phylogenetics. In: Innis MA, Gelfand DH, Sninsky JJ, White TJ (eds). *PCR Protocols, A Guide to Methods and Applications*. Academic Press: London, UK, pp 315–322.
- Wild B, Schneckner J, Bárta J, Čapek P, Guggenberger G, Hofhansl F *et al*. (2013). Nitrogen dynamics in Turbic Cryosols from Siberia and Greenland. *Soil Bio Biochem* **67**: 85–93.
- Yergeau E, Hogues H, Whyte LG, Greer CW. (2010). The functional potential of high Arctic permafrost revealed by metagenomic sequencing, qPCR and microarray analyses. *ISME J* **4**: 1206–1214.

Supplementary Information accompanies this paper on The ISME Journal website (<http://www.nature.com/ismej>)

Paper 8

Gittel A, **Barta J**, Kohoutova I, Schnecker J, Wild B, Capek P, Kaiser C, Torsvik VL, Richter A, Schleper C, Urich T (2014) Site- and horizon-specific patterns of microbial community structure and enzyme activities in permafrost-affected soils of Greenland. *FRONTIERS IN MICROBIOLOGY*, 5:541.



Site- and horizon-specific patterns of microbial community structure and enzyme activities in permafrost-affected soils of Greenland

Antje Gittel^{1,2*}, Jiří Bárta³, Iva Kohoutová³, Jörg Schneckner^{4,5}, Birgit Wild^{4,5}, Petr Čapek³, Christina Kaiser⁴, Vigdis L. Torsvik¹, Andreas Richter^{4,5}, Christa Schleper^{1,5,6} and Tim Urich^{5,6*}

¹ Department of Biology, Centre for Geobiology, University of Bergen, Bergen, Norway

² Department of Bioscience, Center for Geomicrobiology, Aarhus University, Aarhus, Denmark

³ Department of Ecosystems Biology, University of South Bohemia, České Budějovice, Czech Republic

⁴ Division of Terrestrial Ecosystem Research, Department of Microbiology and Ecosystem Science, University of Vienna, Vienna, Austria

⁵ Austrian Polar Research Institute, Vienna, Austria

⁶ Division of Archaea Biology and Ecogenomics, Department of Ecogenomics and Systems Biology, University of Vienna, Vienna, Austria

Edited by:

Rich Boden, University of Plymouth, UK

Reviewed by:

Ulas Karaoz, Lawrence Berkeley National Laboratory, USA

Nathan Basiliko, Laurentian University, Canada

Lisa Y. Stein, University of Alberta, Canada

*Correspondence:

Antje Gittel, Department of Bioscience, Center for Geomicrobiology, Aarhus University, Ny Munkegade 114, Building 1540, 8000 Aarhus C, Denmark
e-mail: antjegittel80@gmail.com;
Tim Urich, Department of Ecogenomics and Systems Biology, University of Vienna, Althanstrasse 14, 1090 Vienna, Austria
e-mail: tim.urich@univie.ac.at

Permafrost-affected soils in the Northern latitudes store huge amounts of organic carbon (OC) that is prone to microbial degradation and subsequent release of greenhouse gasses to the atmosphere. In Greenland, the consequences of permafrost thaw have only recently been addressed, and predictions on its impact on the carbon budget are thus still highly uncertain. However, the fate of OC is not only determined by abiotic factors, but closely tied to microbial activity. We investigated eight soil profiles in northeast Greenland comprising two sites with typical tundra vegetation and one wet fen site. We assessed microbial community structure and diversity (SSU rRNA gene tag sequencing, quantification of bacteria, archaea and fungi), and measured hydrolytic and oxidative enzyme activities. Sampling site and thus abiotic factors had a significant impact on microbial community structure, diversity and activity, the wet fen site exhibiting higher potential enzyme activities and presumably being a hot spot for anaerobic degradation processes such as fermentation and methanogenesis. Lowest fungal to bacterial ratios were found in topsoils that had been relocated by cryoturbation ("buried topsoils"), resulting from a decrease in fungal abundance compared to recent ("unburied") topsoils. *Actinobacteria* (in particular *Intrasporangiaceae*) accounted for a major fraction of the microbial community in buried topsoils, but were only of minor abundance in all other soil horizons. It was indicated that the distribution pattern of *Actinobacteria* and a variety of other bacterial classes was related to the activity of phenol oxidases and peroxidases supporting the hypothesis that bacteria might resume the role of fungi in oxidative enzyme production and degradation of phenolic and other complex substrates in these soils. Our study sheds light on the highly diverse, but poorly-studied communities in permafrost-affected soils in Greenland and their role in OC degradation.

Keywords: climate change, extracellular enzyme activities, Greenland, permafrost-affected soils, microbial communities

INTRODUCTION

It has been predicted that due to the strong increase in mean annual surface air temperature (up to 8°C), 25% of the arctic permafrost could thaw until the end of this century (IPCC, 2007). Increased active layer depths and longer frost-free vegetation periods are predicted to accelerate the microbial decomposition of soil organic matter (SOM) and, together with higher nutrient availability, may generate a positive feedback to climate warming (Biasi et al., 2008; Schuur et al., 2008; Tarnocai et al., 2009; Schuur and Abbott, 2011; MacDougall et al., 2012). In addition to abiotic factors such as elevated temperatures, changes in hydrology, moisture, quantity and quality of the SOM, the extent of this feedback will greatly depend on the response of the

microbial communities as the main biotic drivers of biogeochemical processes (Singh et al., 2010; Xu et al., 2011; Graham et al., 2012).

The diversity of microbial communities in permafrost-affected soils, their functional potential and the coupling of SOM properties and microbial activity have been increasingly recognized and addressed in several studies in Siberia (Ganzert et al., 2007; Liebner et al., 2008; Gittel et al., 2014; Schneckner et al., 2014), the Canadian Arctic (Yergeau et al., 2010; Frank-Fahle et al., 2014), Alaska (Mackelprang et al., 2011; Lipson et al., 2013; Tas et al., 2014), and Svalbard (Tveit et al., 2012, 2014; Alves et al., 2013). High-arctic permafrost regions in Greenland, however, have received only little attention so far, despite the recognized

relevance of thawing permafrost and the potential decomposition of organic carbon (OC) stocks (Masson-Delmotte et al., 2012; Elberling et al., 2013; Ganzert et al., 2014). The top permafrost is thawing at present (more than 1 cm per year) and model simulations predicted an increase of active layer depth by 35 cm as a result of 6°C warming in the next 70 years (Hollesen et al., 2011; Masson-Delmotte et al., 2012). Data on the amount of OC stored in soils in the high Arctic permafrost regions of Greenland are still incomprehensive and, as recent studies suggested, the total OC pool in these regions is probably underestimated (Horwath Burnham and Sletten, 2010; Hugelius et al., 2013). Cryoturbation, the burial of topsoil material into deeper soil horizons by repeated freeze–thaw events, is an important storage mechanism for SOM (Kaiser et al., 2007). Very little information is available on OC stocks in cryoturbated soil pockets in Greenland (Palmtag, 2011), but globally they contain more than one third of the total OC stored in arctic soils (Tarnocai et al., 2009; Harden et al., 2012). We recently showed that microbial communities in cryoturbated material were not adapted to the available substrate having a potentially restraining effect on enzyme activities (Gittel et al., 2014; Schneckner et al., 2014). This decoupling of microbial community composition from SOM properties might explain the persistence of OC in buried topsoils, but also implies that a shift in community composition and enhanced microbial activity in cryoturbated soil pockets would reinforce a positive feedback to climate change.

In this study, we sampled organic and mineral topsoils, mineral subsoils, and buried topsoils from the active layer as well as frozen mineral soils (hereafter called permafrost samples) at three sites in northeastern Greenland. We aimed to (1) explore the microbial diversity and community composition, (2) determine potential activities of oxidative and hydrolytic extracellular enzymes involved in the degradation of organic matter, and (3) assess possible correlations between enzyme activities and shifts in community composition. We hypothesized that different sampling sites and/or soil horizons harbor distinct communities and that changes in community structure are reflected in the enzymatic and thus the degradation potential of these communities. We were particularly interested in the distribution patterns of both fungal and bacterial decomposers (e.g., actinobacteria) that have previously been identified as critical components in the delayed decomposition of organic matter in cryoturbated soils (Gittel et al., 2014).

MATERIALS AND METHODS

FIELD SITE DESCRIPTION AND SOIL SAMPLING

Soils were sampled in close vicinity to the Zackenberg Research Station, northeast Greenland (74°28'N, 20°32'W). The climate is characterized by a mean annual air temperature of around –10°C and an annual precipitation of about 150 mm. Minimum air temperatures are below –40°C, and sub-surface temperatures (5 cm below the surface) are below –18° for about 4 months per year (Elberling and Brandt, 2003). Samples were taken from 3 different sampling sites (Table S1, Figure S1). Sites 1 and 3 were characterized by frost boils and earth hummocks and dominated by a diverse community of typical tundra vegetation (e.g., *Salix arctica*, *Vaccinium uliginosum*). Site 2 was a wet fen dominated by mosses

and grasses (e.g., *Eriophorum angustifolium*). Two to three replicate plots that were distributed within an area of approximately 50 × 50 m were sampled at each sampling site (site 1: plots A–C, site 2: plots D–F, and site 3: plots G,H; Figure S1). For each plot, 3–5 replicate soil cores were collected close to each other (max. area: 1 × 1 m) to obtain enough material from each soil horizon. Main soil horizons were identified and pooled to obtain one replicate sample. Soil material was sampled from the active layer and the permafrost layer (PF), resulting in a total of 37 soil samples (Table S2). Soil classification follows the USDA Soil Taxonomy (Soil Survey Staff, 2010). Samples from the active layer included organic and mineral topsoil horizons (O and A), mineral subsoil horizons (B), and topsoil material that was buried into deeper soil horizons by cryoturbation (Ojj and Ajj, collectively called “J” in the following). Initial soil processing included removal of living roots prior to homogenizing the soil fraction of each sample. Samples for extracting total nucleic acids were fixed in RNAlater RNA Stabilization Reagent (Ambion Inc., Life Technologies) and kept cold until further processing. Samples for the analyses of soil properties, microbial biomass and potential enzyme activities were stored in closed polyethylene bags at 4°C until analyzed.

SOIL PROPERTIES, MICROBIAL BIOMASS AND EXTRACELLULAR ENZYME ACTIVITIES

Soil water content was estimated by drying the soil over night at 60°C and reweighing the samples. Total organic carbon (TOC) and total nitrogen (TN) contents were determined in dried (60°C) and ground samples with an EA IRMS system (EA 1110, CE Instruments, Milan, Italy, coupled to a Finnigan MAT Delta Plus IRMS, Thermo Fisher Scientific). Microbial C and N were determined using chloroform-fumigation extraction (Kaiser et al., 2010). Fumigated and non-fumigated soil samples were extracted with 0.5 M K₂SO₄ and analyzed for extracted C and N on a TOC/TN analyzer (LiquiC TOC II, Elementar, Germany). Microbial C and N were calculated as the difference in C and N concentrations between fumigated and non-fumigated samples.

Potential extracellular hydrolytic and oxidative enzyme activities involved in the degradation of organic macromolecules (namely cellulose, chitin, peptides, lignin) were measured according to Kaiser et al. (2010) using microplate fluorometric and photometric assays. The enzymes under study, their acronyms, function and substrates are listed in **Table 1**. One gram of sieved soil was suspended in 100 ml sodium acetate buffer (100 mM, pH 5.5) and ultra-sonicated at low-energy. Potential activities of 1,4-β-cellobiohydrolase (CBH), 1,4-β-poly-N-acetylglucosaminidase (chitotriosidase, CHT), β-N-acetylglucosaminidase (NAG), and leucine aminopeptidase (LAP) were measured fluorometrically using 4-methylumbelliferyl- (MUF) and aminomethylcoumarin- (AMC) substrates (Marx et al., 2001; Kaiser et al., 2010). 200 μL of the soil suspension and 50 μL substrate (MUF-β-D-cellobioside, MUF-N-acetyl-β-D-glucosaminide, MUF-β-D-N,N',N''-triacetylchitotrioside, and L-leucine-7-amido-4-methyl coumarin, respectively) were pipetted into black microtiter plates in 5 analytical replicates. For each sample, a standard curve with methylumbelliferyl was used for calibration of cellobiosidase, N-acetylglucosaminidase and chitotriosidase, whereas aminomethylcoumarin was used for calibration of

Table 1 | Hydrolytic and oxidative extracellular enzymes assayed.

Enzyme	Acronym	Type/Function	Substrate	EC number
1,4- β -cellobiohydrolase	CBH	Hydrolytic, C-acquiring	Cellulose	3.2.1.91
1,4- β -poly-N-acetylglucosaminidase (chitotriosidase) ^a	CHT	Hydrolytic, N-acquiring (also liberates C)	Chitin, peptidoglycan	3.2.1.14
β -N-acetylglucosaminidase (exochitinase) ^a	NAG	Hydrolytic, N-acquiring (also liberates C)	Chitin, peptidoglycan	3.2.1.52
Leucine aminopeptidase	LAP	Hydrolytic, N-acquiring	Peptides	3.4.11.1
Phenoloxidase	POX	Oxidative, C- and N-acquiring	Lignin, phenolic and other complex compounds	1.10.3.2
Peroxidase	PER	Oxidative, C- and N-acquiring	Lignin, phenolic and other complex compounds	1.11.1.7

^aChitotriosidase activity is defined as the random cleavage at internal points in the chitin or peptidoglycan chain. Exochitinase activity is defined as the progressive action starting at the non-reducing end of chitin or peptidoglycan with the release of chitobiose or N-acetyl-glucosamine units.

leucine amino-peptidase. Plates were incubated for 140 min in the dark and fluorescence was measured at 450 nm emission at an excitation of 365 nm (Tecan Infinite M200 fluorimeter). Potential phenol oxidase (POX) and peroxidase (PER) activities were measured photometrically using the L-3,4-dihydroxyphenylalanine (L-DOPA) assay (Sinsabaugh et al., 1999; Kaiser et al., 2010). Subsamples were taken from the soil suspension (see above) and mixed with a 20 mM L-DOPA solution (1:1). Samples were shaken for 10 min, centrifuged and aliquotes were pipetted into microtiter plates (6 analytical replicates per sample). Half of the wells additionally received 10 μ L of a 0.3% H₂O₂ solution for measurement of peroxidase. Absorption was measured at 450 nm at the starting time point and after 20 h. Enzyme activity was calculated from the difference in absorption between the two time points.

NUCLEIC ACID PREPARATION FOR QUANTITATIVE PCR

Nucleic acid extractions were conducted according to a modified bead-beating protocol (Urich et al., 2008). Soil samples were washed with DEPC-PBS (Diethylpyrocarbonate, 0.1%; 1 \times phosphate-buffered saline) to remove the RNAse. Approximately 0.5 g of soil was added to a FastPrep™ Lysis Matrix E tube (MP Biomedicals, Solon, OH, USA). Hexadecyltrimethylammonium bromide (CTAB) extraction buffer containing 5% CTAB (in 0.7 M NaCl, 120 mM potassium phosphate, pH 8.0) and 0.5 mL phenol-chloroform-isoamylalcohol (25:24:1) was added and shaken in a FastPrep Instrument (MP Biomedicals, Solon, OH, USA) at speed 5–6 for 45 s. After bead beating, the samples were extracted with chloroform and precipitated in a PEG 6000/1.6 M NaCl solution. Pellets were washed with 70% ethanol and re-suspended in molecular biology grade water. Nucleic acids were further purified using the CleanAll DNA/RNA Clean-up and Concentration Micro Kit (Norgen Biotek Corp., Ontario, Canada). Total DNA was quantified using SybrGreen (Leininger et al., 2006).

QUANTIFICATION OF SSU rRNA GENES BY QUANTITATIVE PCR

Bacterial, archaeal and fungal SSU rRNA genes were amplified as described previously (Gittel et al., 2014). Briefly, bacterial and archaeal SSU rRNA genes were amplified with the primer set Eub338Fbc/Eub518R (Daims et al., 1999; Fierer et al.,

2005) for *Bacteria* and Arch519F/Arch908R (Jurgens et al., 1997; Teske and Sorensen, 2007) for *Archaea*. Fungal SSU genes were amplified using the primers nu-SSU-0817-5' and nu-SSU1196-3' (Borneman and Hartin, 2000). Product specificity was confirmed by melting point analysis and amplicon size was verified with agarose gel electrophoresis. Bacterial and archaeal DNA standards consisted of a dilution series (ranging from 10⁰ to 10⁸ gene copies μ L⁻¹) of a known amount of purified PCR product obtained from genomic *Escherichia coli* DNA and *Natrialba magadii* DNA by using the SSU gene-specific primers 8F/1492R and 21F/1492R, respectively (DeLong, 1992; Loy et al., 2002). Fungal DNA standards consisted of a dilution series (ranging from 10⁰ to 10⁷ gene copies μ L⁻¹) of a known amount of purified PCR product obtained from genomic *Fusarium oxysporum* DNA by using the SSU gene-specific primers nu-SSU-0817-5' and nu-SSU1196-3' (Borneman and Hartin, 2000). Samples, standards and non-template controls were run in triplicates. Detection limits for the assays (i.e., lowest standard concentration that is significantly different from the non-template controls) were less than 100 gene copies for each of the genes. For statistical analyses (calculation of means and deviations per site, One-Way ANOVA), samples below the detection limit have been assigned a value of half the detection limit of the respective assay.

NUCLEIC ACID PREPARATION AND BARCODED AMPLICON SEQUENCING

Nucleic acid extraction and bacterial and archaeal SSU rRNA amplification were performed according to standardized protocols of the Earth Microbiome Project (www.earthmicrobiome.org/emp-standard-protocols). Amplicons were sequenced on the Illumina MiSeq platform (Caporaso et al., 2011, 2012). Sequence data along with MiMARKs compliant metadata are available from the Qiime database (<http://www.microbio.me/emp/>, study no. 1034).

SEQUENCE ANALYSIS

Quality filtering of reads was applied as described previously (Caporaso et al., 2011). Reads were truncated at their first low-quality base (defined by an "A" or "B" quality score). Reads shorter than 75 bases were discarded, as were reads whose barcode did not match an expected barcode. Reads were assigned to operational

taxonomic units (OTUs) using closed-reference OTU picking protocol in QIIME version 1.7.0 (Caporaso et al., 2010), with uclust (Edgar, 2010) being applied to search sequences against a subset of the Greengenes database version 13_5 (DeSantis et al., 2006) with reference sequences clustered at 97% sequence identity. Reads were assigned to OTUs based on their best hit to this database at greater than or equal to 97% sequence identity. Reads without a hit were discarded. A major advantage of this procedure is that the OTUs are defined by trusted reference sequences. It furthermore serves as a quality control filter: erroneous reads will likely be discarded as not hitting the reference data set. The primary disadvantage is that sequences that are not already known (i.e., represented in the reference data set) will be excluded. Taxonomy was assigned by accepting the Greengenes taxonomy string of the best matching Greengenes sequence. Alpha and beta diversity analyses were performed on data rarefied to 17,000 sequences per sample. Principal coordinates analysis (PCoA) was used to visualize differences between sampling sites and soil horizons using unweighed Unifrac distances, a distance measure between communities using phylogenetic information (Lozupone and Knight, 2005). To assess differences in community structure between sites, soil horizons and replicate pits, a matrix of Bray-Curtis distances of square-root transformed relative abundances of each OTU was used for permutational ANOVA (PERMANOVA). Alpha diversity measures (richness, Shannon and inverse Simpson indices and evenness) were calculated in R 2.15.0 (R Development Core Team, 2012) using the packages vegan (Oksanen et al., 2007) and fossil (Vavrek, 2011). To test for the presence of a core prokaryotic community and distinct phylotypes in buried topsoils, we acquired the core OTUs being present in all buried topsoil samples on the non-rarefied data set using the `compute_core_microbiome` function in Qiime.

FURTHER STATISTICAL ANALYSES

All analyses were performed in R 2.15.0 (R Development Core Team, 2012) using the packages vegan (Oksanen et al., 2007),

FactoMineR (Husson et al., 2013), and missMDA (Josse and Husson, 2013). Prior to One-Way ANOVA, Shapiro-Wilk tests and Bartlett tests were used to examine whether the conditions of normality and homogeneity of variance were met by non-transformed data sets as well as transformed data sets (log transformation: soil properties, biomass and gene abundance variables, square-root transformation: OTU abundance data). One-Way ANOVA was followed by Tukey's HSD test to determine significant differences between soil horizon (O/A, B, J, and PF) for each site. Differences were considered significant at $P < 0.05$.

Principle component analysis (PCA) was used to summarize data on soil properties and microbial biomass. Data were standardized (zero mean and unit standard deviation), and the number of dimensions were estimated by cross-validation and missing values were imputed using the package missMDA (Josse and Husson, 2013). Canonical correspondence analysis (CCA) was applied to relate microbial activity (potential enzyme activities) to differences in community structure (i.e., changes in relative OTU abundances). Potential enzyme activities were standardized to zero mean and unit standard deviation. Pearson's product-moment correlation (R) was used to assess linkages between individual OTUs, soil properties and enzyme activities.

RESULTS

SOIL PROPERTIES AND MICROBIAL BIOMASS

Soil samples were collected from three different sites in north-east Greenland including two sites with typical tundra vegetation (site 1, $n = 15$ and site 3, $n = 9$), and a wet fen site (site 2, $n = 13$), and from four different soil horizons at each of these sites: organic and mineral topsoil (O and A, $n = 10$), mineral subsoil (B, $n = 8$), buried topsoil (J, $n = 12$), and the permafrost layer (PF, $n = 7$). Topsoil horizons exhibited a higher moisture, TOC and TN content, as well as higher microbial biomass (Cmic, Nmic) compared to buried topsoils, mineral subsoils and permafrost samples (Table 2). Buried topsoils were characterized by higher moisture, TOC, TN, Cmic, and Nmic than the mineral

Table 2 | Soil properties and microbial biomass^a.

Site	Soil group*	Number of samples	Moisture (%)	TOC (% dw)	TN (% dw)	CN ratio	Cmic ($\mu\text{mol g}^{-1}\text{ dw}$)	Nmic ($\mu\text{mol g}^{-1}\text{ dw}$)
1	A	5	45.5 ± 8.8 (a)	12.4 ± 4.2 (a)	0.8 ± 0.2 (a)	14.6 ± 1.1 (a)	161.5 ± 76.2 (a)	15.1 ± 8.7 (a)
	B	3	21.2 ± 4.5 (b)	2.0 ± 0.8 (bc)	0.1 ± 0.1 (bc)	13.6 ± 0.2 (a)	38.3 ± 13.2 (b)	1.8 ± 0.9 (a)
	J	4	36.8 ± 7.1 (ab)	7.6 ± 2.5 (ab)	0.5 ± 0.1 (ab)	14.6 ± 1.9 (a)	59.1 ± 32.1 (ab)	3.1 ± 2.6 (a)
	PF	3	24.8 ± 6.9 (b)	0.7 ± 0.2 (c)	0.04 ± 0.03 (c)	18.8 ± 9.2 (a)	33.1 ± 7.4 (ab)	1.0
2	O	3	77.2 ± 4.2 (a)	29.0 ± 2.4 (a)	1.4 ± 0.1 (a)	20.3 ± 1.4 (a)	175.5 (a)	24.6 ± 20.4 (a)
	B	3	29.2 ± 5.3 (b)	4.5 ± 2.5 (b)	0.3 ± 0.2 (b)	15.6 ± 0.5 (a)	22.6 ± 9.2 (b)	2.0 ± 1.3 (a)
	J	5	70.1 ± 13.0 (a)	17.8 ± 5.4 (c)	1.1 ± 0.5 (a)	18.2 ± 4.3 (a)	62.0 ± 26.2 (b)	3.0 ± 1.3 (a)
	PF	2	33.1 ± 11.9 (b)	2.4 ± 2.3 (b)	0.2 ± 0.1 (b)	13.7 ± 2.6 (a)	10.6 ± 2.8 (b)	3.9
3	O	2	42.9 ± 1.8 (a)	17.5 ± 0.2 (a)	0.8 ± 0.0 (a)	21.3 ± 0.3 (a)	316.0 ± 10.4 (a)	29.6 ± 6.3 (a)
	B	2	20.1 ± 3.1 (b)	2.3 ± 0.8 (b)	0.2 ± 0.1 (b)	14.8 ± 0.3 (b)	33.5 ± 22.2 (b)	1.9 ± 0.7 (b)
	J	3	35.0 ± 5.8 (a)	8.5 ± 2.1 (c)	0.5 ± 0.1 (c)	16.8 ± 1.3 (b)	69.5 ± 63.7 (b)	6.5 ± 7.2 (b)
	PF	2	91.2 ± 0.5 (c)	2.4 ± 0.5 (b)	0.2 ± 0.0 (b)	14.6 ± 1.0 (b)	143.2 ± 118.5 (ab)	10.8 (ab)

^aMeans and standard deviations were calculated from soil samples classified into each soil group. Small letters in brackets indicate significant differences as determined by One-Way ANOVA and Tukey's HSD test.

*Soil samples were grouped according to their total organic carbon (TOC). For details see Table S2 (Supplementary Material).

TOC, total organic carbon; TN, total nitrogen; CN ratio, carbon-to-nitrogen ratio; Cmic, microbial carbon; Nmic, microbial nitrogen.

subsoils they were embedded in, although these differences were not significant in all of the sampling sites (Table 2). Moisture, TOC, and TN in topsoil and buried topsoil samples from site 2 were higher than in the corresponding samples from sites 1 and 3. PCA analysis separated O and A horizons along the first principal component and placed J horizons at an intermediate position (Figure S2). B horizons and PF samples were positioned closer to each other, thus representing higher between-sample similarity than O, A and J horizons.

ABUNDANCES OF BACTERIA, ARCHAEA AND FUNGI

On average, bacterial SSU rRNA gene abundances per gram dry soil were highest in topsoil samples and buried topsoils and were two to four orders of magnitude lower in mineral subsoils and permafrost samples (Figure 1). In contrast, average fungal SSU rRNA gene copy numbers were one to two orders of magnitude higher in topsoils than in buried topsoils. Mineral subsoils did not show any significant differences in fungal SSU rRNA gene abundances when compared to buried topsoils, while permafrost

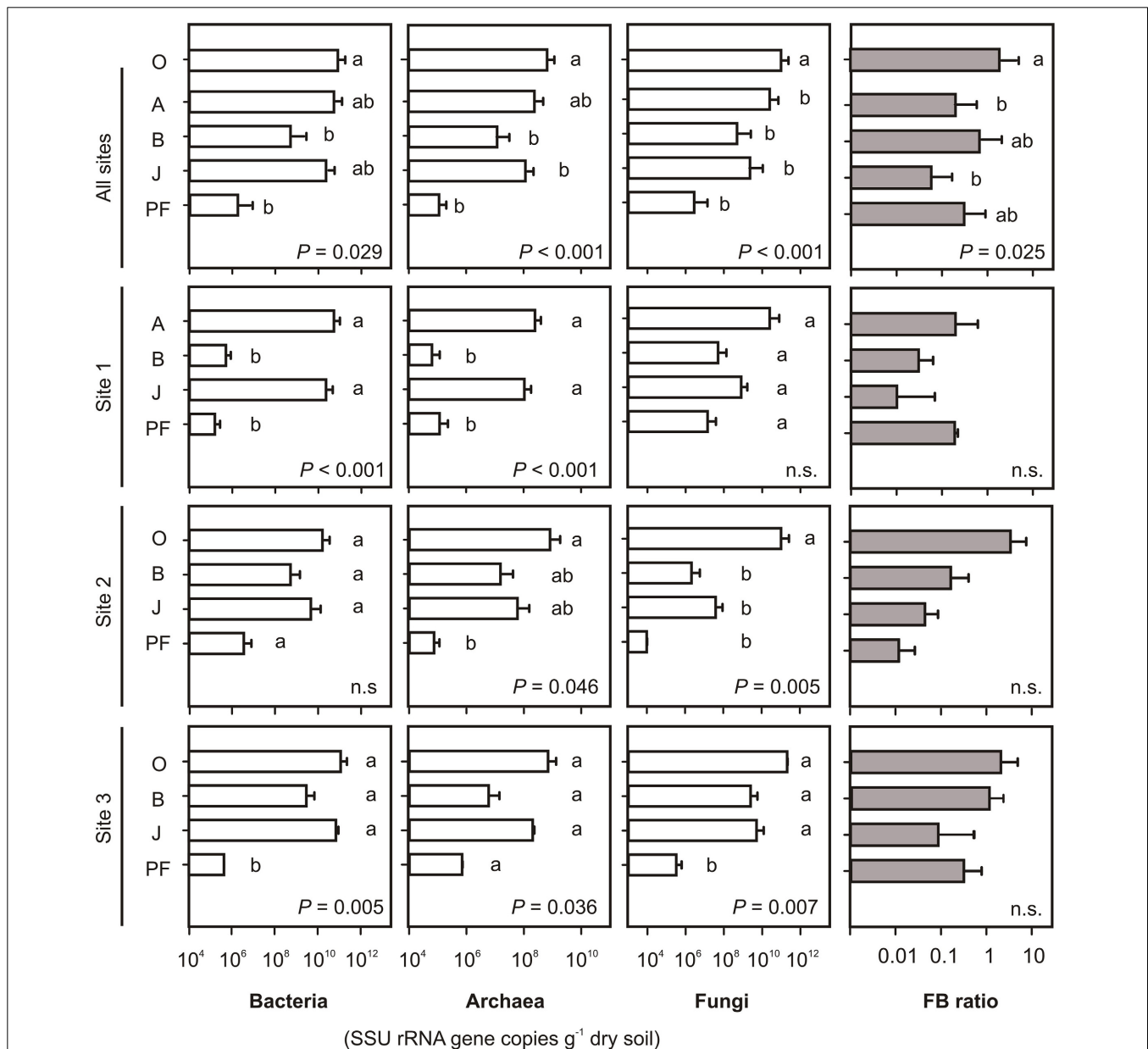


FIGURE 1 | Abundances of Bacteria, Archaea and Fungi shown as bacterial, archaeal and fungal SSU rRNA gene copy numbers per gram dry soil and fungal-bacterial (FB) ratios. Note the difference in scaling of bacterial and fungal vs. archaeal abundances. Error bars for individual sites represent SD from 2 to

5 samples per soil type. Small letters indicate significant differences between soil horizons as determined by One-Way ANOVA and Tukey's HSD test. *P*-values indicate overall significant differences. O, organic topsoil; A, mineral topsoil; B, mineral subsoil; J, buried topsoil; PF, permafrost layer.

samples exhibited the lowest fungal abundances. Thus, the disproportion in bacterial and fungal abundances in topsoils and buried topsoils led to highest fungal-bacterial (FB) ratios in O horizons ($FB = 3.23$, **Figure 1**), and lowest in J horizons ($FB = 0.05$). Significant differences in FB ratio were found between O and A topsoil horizons as well as between O and J horizons (One-Way ANOVA, $P < 0.05$). Archaeal gene copies followed the bacterial distribution pattern and were highest in topsoil horizons and buried topsoils. They were two to three orders of magnitude lower in mineral subsoils and permafrost samples. The fraction of archaeal SSU rRNA genes proportionally increased with depth being lowest in O and A horizons (0.01% of the total number of prokaryotic SSU rRNA gene copies) and highest in permafrost samples (0.4%).

General observations as described above were also apparent for the individual sampling sites, including highest bacterial, archaeal and fungal abundances in topsoils and buried topsoils, and lower abundances in subsoils and permafrost samples (**Figure 1**). While differences in bacterial and archaeal SSU rRNA gene abundances were significant at sites 1 and 3, differences at site 2 were only minor or not significant (**Figure 1**). Fungal SSU rRNA abundances at site 2 were significantly higher in topsoils than in any other horizon. At site 3, fungal abundance was significantly lower in permafrost samples than in topsoil and subsoil horizons as well as buried topsoils. Differences in FB ratios between horizons were not significant (**Figure 1**).

Similar patterns in bacterial, archaeal and fungal SSU rRNA gene distributions were found when soil organic carbon (OC) was taken into account (Figure S3). However, differences in gene abundances per gram OC between soil horizons were less pronounced when compared to calculations on the dry weight basis (represented by lower P -values or insignificant differences, Figure S3).

DIFFERENCES IN PROKARYOTIC COMMUNITY COMPOSITION AND DIVERSITY BETWEEN SITES AND HORIZONS

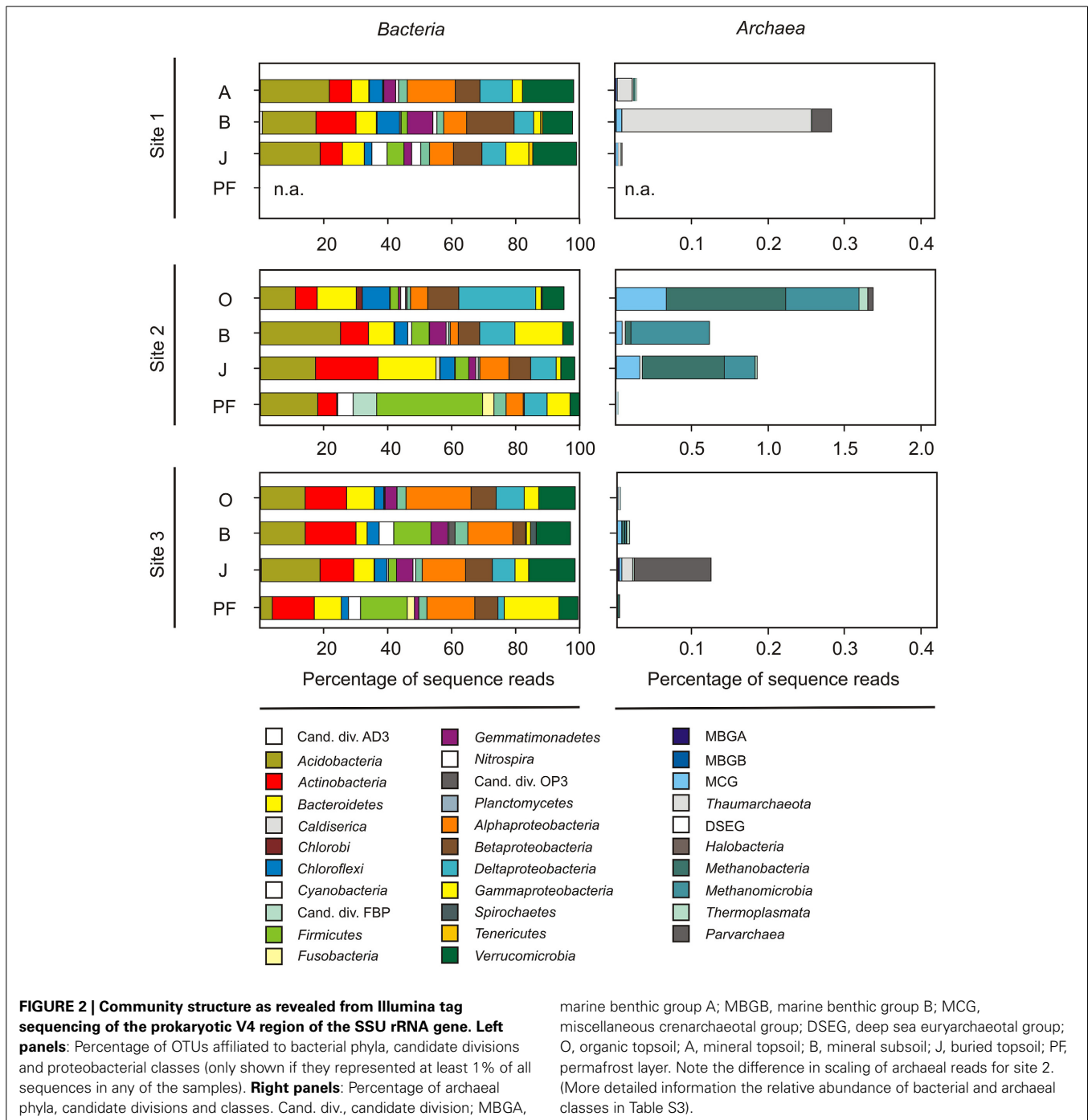
Twenty-seven samples covering the four different soil horizons (O and A, B, J, and PF) were subjected to Illumina tag sequencing of the V4 SSU rRNA gene region (sequence and metadata available from <http://www.microbio.me/emp/>, study no. 1034). Sequencing was successful for 20 of these samples (**Table 3**, Table S3) and yielded a total of 1,975,888 bacterial and archaeal SSU rRNA gene sequences after extensive read-quality filtering (see Materials and Methods for details) with 86% being taxonomically classified using closed-reference OTU picking. Bacterial and archaeal sequences clustered in 10,309 OTUs, representing 157 classes (147 bacterial and 10 archaeal) within 55 phyla (including 30 candidate phyla). The dominant phyla were *Proteobacteria* (α , β , δ , and γ), *Acidobacteria*, *Actinobacteria*, *Verrucomicrobia*, *Bacteroidetes*, and *Firmicutes* accounting for ~84% of all sequences (**Figure 2**). In addition, *Chloroflexi*, *Gemmatimonadetes*, *Planctomycetes*, *Cyanobacteria*, and *Nitrospirae* were present in all soil horizons, but at lower abundances (~12% of all sequences), and 38 other rare phyla (<0.5% each) were identified. Rare phyla included archaeal taxa that represented 0.3% of all sequence reads. The majority of archaeal reads was assigned to the classes *Methanomicrobia* and *Methanobacteria* within the *Euryarchaeota* comprising 39.8% of all archaeal reads. For site 2, sequence reads assigned to archaeal taxa comprised 0.9% of all reads obtained from site 2 samples, whereas they only accounted for 0.05 and 0.01% at sites 1 and 3, respectively (**Figure 2**). This finding was in line with lower archaeal SSU rRNA gene abundances at sites 1 and 3 than at site 2 (as determined by qPCR). Furthermore, the majority of sequences retrieved from site 2 was affiliated with methanogenic taxa of the families *Methanosarcinaceae*, *Methanobacteriaceae*, and *Methanosaetaceae* in the phylum *Euryarchaeota*, whereas

Table 3 | Sequencing statistics, diversity and evenness estimates^a.

Site	Soil group	Number of samples	Number of sequences	Classified (%)	Number of OTUs	Chao1	Shannon	Inverse Simpson	Pielou's evenness
1	A	3	297648	85.0	3262 ± 231 (a)	4209 ± 291 (a)	6.36 ± 0.11 (a)	175.4 ± 41.2 (a)	0.79 ± 0.01 (a)
	B	2	113553	87.1	1402 ± 469 (a)	2095 ± 392 (a)	5.78 ± 0.19 (a)	129.4 ± 11.8 (a)	0.80 ± 0.02 (a)
	J	2	477139	85.6	2591 ± 3335 (a)	3394 ± 4035 (a)	4.93 ± 1.98 (a)	89.5 ± 91.6 (a)	0.70 ± 0.07 (a)
	PF	0	ns	ns	ns	ns	ns	ns	ns
2	O	1	113205	80.3	3126 (a)	4133 (a)	6.18 (a)	138.4 (a)	0.77 (a)
	B	2	185477	87.9	851 ± 336 (b)	1422 ± 233 (b)	4.12 ± 0.45 (ab)	20.4 ± 11.2 (b)	0.61 ± 0.03 (a)
	J	3	272337	86.7	1131 ± 282 (b)	1780 ± 479 (b)	4.62 ± 0.33 (ab)	35.0 ± 13.0 (b)	0.66 ± 0.07 (a)
	PF	1	35414	91.1	274 (b)	530 (b)	3.49 (b)	22.6 (b)	0.62 (a)
3	O	2	207447	85.3	3803 ± 240 (a)	4928 ± 321 (a)	6.64 ± 0.03 (a)	250.0 ± 16.8 (a)	0.81 ± 0.01 (a)
	B	1	59861	88.3	483 (a)	877 (a)	4.38 (a)	51.8 (a)	0.71 (b)
	J	2	169150	85.0	2391 ± 1755 (a)	3300 ± 2004 (a)	6.10 ± 0.57 (a)	166.4 ± 69.2 (a)	0.80 ± 0.01 (a)
	PF	1	44657	89.6	619 (a)	1203 (a)	4.48 (a)	36.1 (a)	0.70 (b)

^aMeans and standard deviations were calculated from replicate soil samples classified into the respective soil group at the respective site. Detailed data for each soil sample can be found in Table S3 (Supplementary Material). Small letters in brackets indicate significant differences as determined by One-Way ANOVA and Tukey's HSD test.

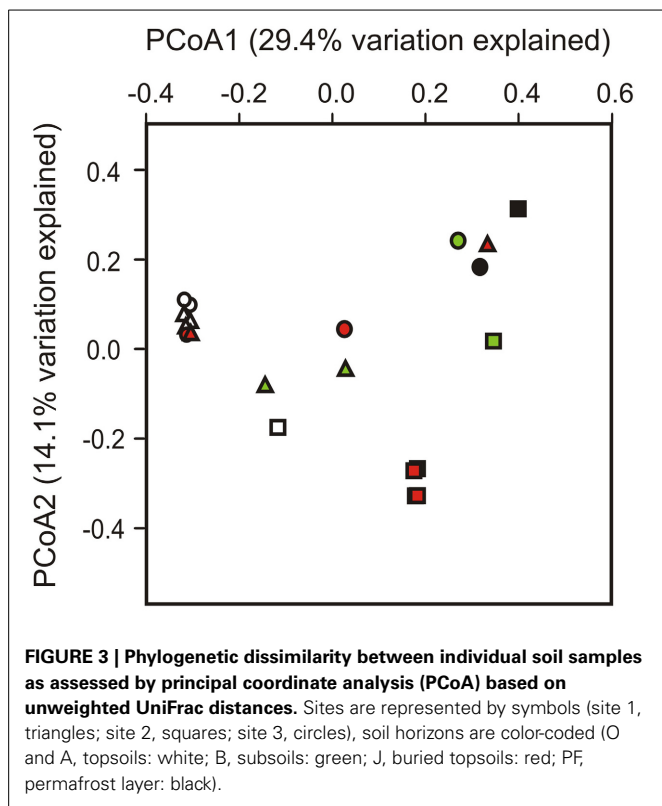
Ns, sequencing not successful.



members of the *Thaumarchaeota* and several other non-methanogenic archaea dominated at sites 1 and 3 (Figure 2).

To test whether different sites and/or soil horizons harbor distinct communities, we applied PERMANOVA and PCoA. A Bray-Curtis distance matrix of square-root transformed, relative OTU abundances was analyzed by PERMANOVA in a three-factor design to test for differences between sampling sites, soil horizons and replicate soil pits. Significant differences were returned for sampling site (Pseudo- $F = 10.27$, $p(\text{perm}) = 0.001$) and soil horizon (Pseudo- $F = 6.12$, $p(\text{perm}) = 0.007$), but not for the

soil pit factor (Pseudo- $F = 2.42$, $p(\text{perm}) = 0.097$). No interactions between factors (site, horizon, pit) were apparent ($P > 0.05$ in all instances). PCoA based on unweighted UniFrac distances was used to visualize clusters of similar communities according to sampling site, soil horizon and soil pit (Figure 3). Most significant differences were found between sampling sites (Pseudo- $F = 29.96$, $p(\text{perm}) = 0.001$), followed by soil horizons (Pseudo- $F = 22.03$, $p(\text{perm}) = 0.002$), and soil pits (Pseudo- $F = 5.93$, $p(\text{perm}) = 0.025$). Topsoil samples from sites 1 and 3 formed a distinct cluster that also included two out of four of the buried soil



samples from these sites (samples A4 and G4), but excluded topsoil and buried topsoil samples from site 2 (Figure 3). In contrast, buried topsoils from site 2 formed a distinct cluster and were thus separated from the corresponding topsoil sample as well as from samples from sites 1 and 3 (Figure 3). Subsoil and permafrost samples did not show consistent clusters according to sampling site and/or soil horizon.

Species richness and diversity were generally higher in topsoils than in buried topsoils, mineral subsoil horizons and the underlying permafrost (Table 3). However, this difference was only significant at site 2 (One-Way ANOVA, $P < 0.05$). Samples from buried topsoils at sites 1 and 3 were highly variable in species richness and diversity resulting in statistically insignificant differences between horizons (Table 3).

POTENTIAL ENZYME ACTIVITIES AND CORRELATIONS WITH MICROBIAL COMMUNITY STRUCTURE

Potential hydrolytic enzyme activities (per gram dry soil) were highest in topsoil samples (O and/or A), followed by buried topsoils, mineral subsoils and permafrost samples (Figure 4). This difference was significant for CBH, CHT, LAP, and to some extent for NAG (One-Way ANOVA, $P < 0.05$). Potential NAG activity was similarly high in topsoil and buried topsoil samples and significantly lower in mineral subsoils and permafrost samples. Potential oxidative enzyme activities were highest in samples from topsoils (O) and buried topsoils (Figure 4). However, due to the high variability between sampling sites, differences in POX and PER activities in topsoils, mineral subsoils and permafrost samples were not significant (One-Way ANOVA, $P > 0.05$). Potential POX and PER activities were significantly higher in active layer

samples from site 2 compared to the corresponding soil samples from sites 1 and 3 (One-Way ANOVA, $P > 0.05$, Figure 4, Table S4). In contrast, only few significant differences were found for the potential hydrolytic enzyme activities in samples from the same soil horizon at the different sites (Figure 4, Table S4).

When potential enzyme activities were calculated per gram organic carbon (OC), differences between horizons became smaller and less significant for hydrolytic enzymes (Figure S4). For oxidative enzymes, the pattern changed to mineral subsoils (and permafrost samples) exhibiting a higher potential activity on a per gram OC basis than topsoils and buried topsoils. Differences for same soil horizons at the different sites got less pronounced for oxidative enzyme activities and did not show a clear pattern for hydrolytic enzymes (Table S5).

CCA was used to examine whether potential enzyme activities were correlated to changes in community structure (Figure 5). The first three axes of the model explained 77% of the total variation within the OTU abundance data in relation to the six enzyme activities measured. Samples from site 2 were separated from samples from sites 1 and 3 along the first axis (CC1). POX and PER activities exerted the strongest positive influence on axis 1. It was furthermore indicated that the spatial distribution of several classes within the *Actinobacteria* (e.g., class *Actinobacteria*) and the *Bacteroidetes* (e.g., class *Bacteroidia*), as well as putatively anaerobic members of the *Firmicutes* (*Clostridia*), the *Chloroflexi* (*Anaerolinea*, *Dehalococcoidetes*), and methanogenic *Euryarchaeota* (*Methanomicrobia*) were positively correlated with potential POX and PER activities (Figure S5).

DISTRIBUTION OF SELECTED TAXA ASSOCIATED WITH KNOWN FUNCTIONS

Sequences matching putative anaerobic taxa (e.g., fermenters, sulfate reducers, metal reducers, methanogens) were highly abundant in the wet fen site accounting for up to 38% of all sequences in the O horizon (Figure 6). While the relative contribution of these taxa to the total community was similarly high in all horizons at site 2 (except for the permafrost sample), their proportion increased with depth at sites 1 and 3 (Figure 6). Here, there relative abundance increased from 2.32% in the O horizons to 9.8% in the permafrost (averaged over all samples from the respective horizons at these sites). Methanogenic archaea were particularly abundant at the wet fen site (0.5–1.3% in the active layer horizons). A high diversity of aerobic methane-oxidizing bacteria (MOB) was found at all sites and in all horizons and included MOB of type I (*Methylococcaceae*) and type II (*Methylobacteriaceae*, *Methylocystaceae*, *Beijerinckaceae*), and the recently described *Methylacidiphilae* within the phylum *Verrucomicrobia* (Table S3). Type I MOB were more abundant than type II MOB in mineral soil horizons in the active layer (38 vs. 18% of all MOB, respectively). Type II MOB predominated in topsoils and buried topsoils (38 and 46% of all MOB, respectively) together with a large fraction of putative methanotrophic *Verrucomicrobia* (52 and 40% of all MOB, respectively).

DISCUSSION

The top permafrost in northeastern Greenland is thawing at present, making stored carbon prone to microbial decomposition and potentially leading to an increased future release of CO₂

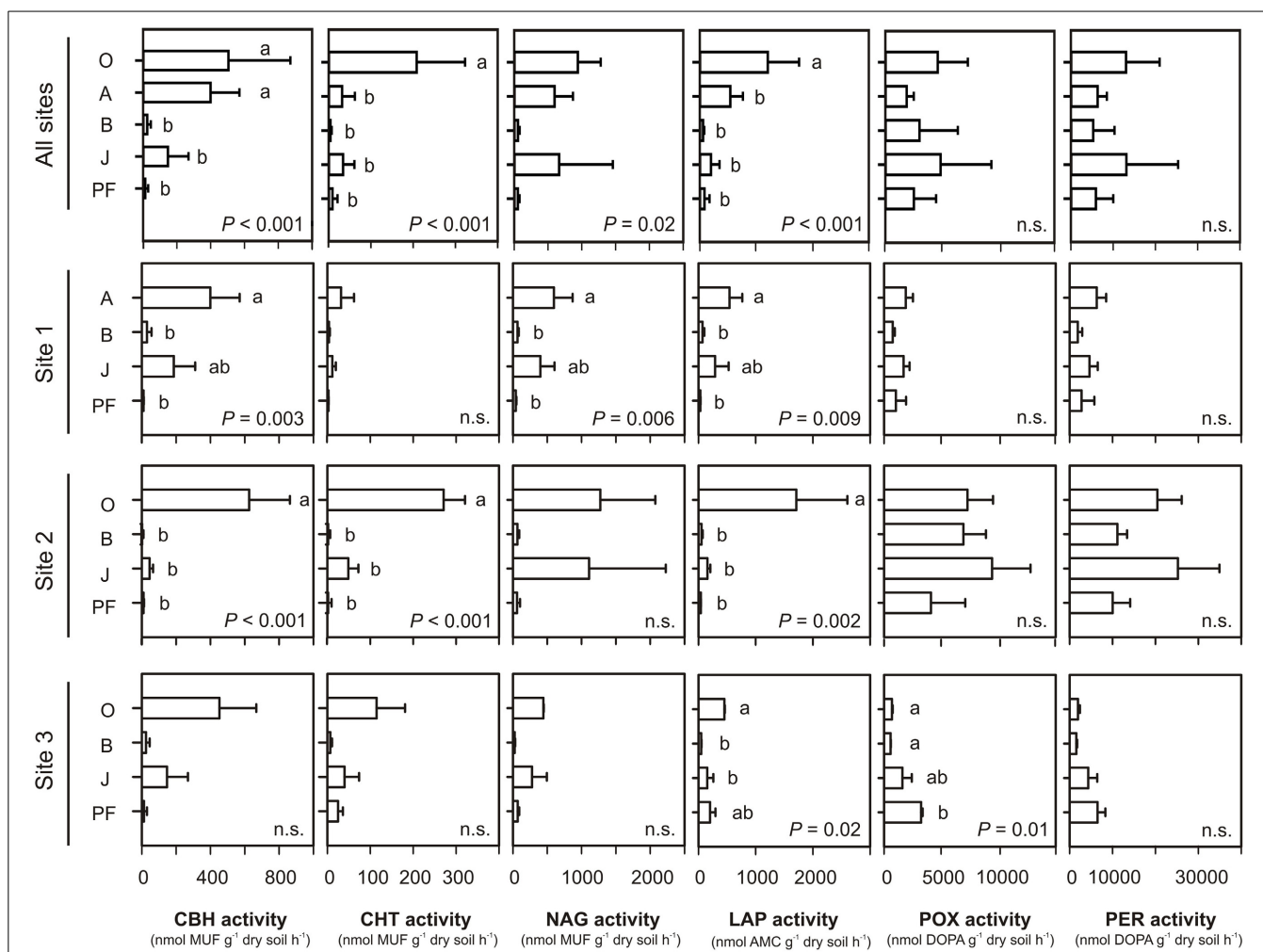


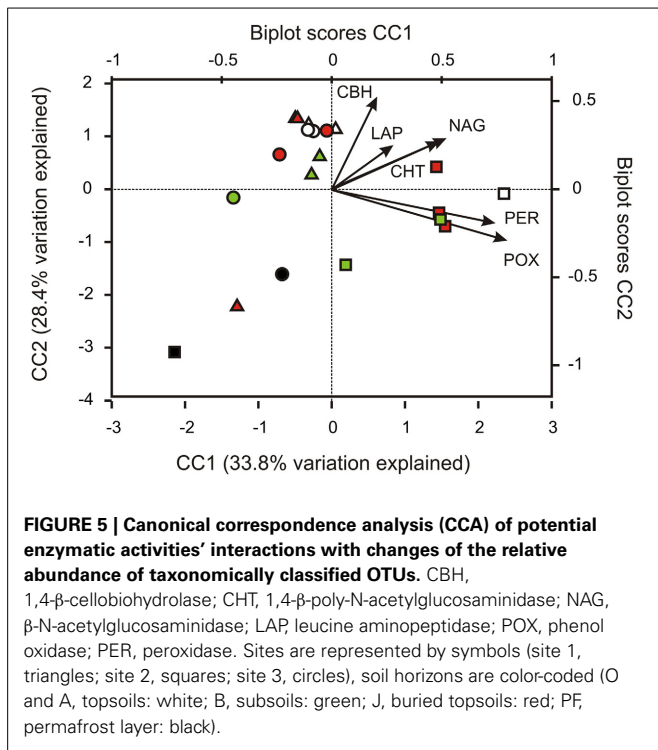
FIGURE 4 | Potential extracellular enzymes activities calculated per gram dry soil. Means and standard deviations were calculated from soil samples classified into each soil group. Small letters indicate significant differences between soil horizons as determined by One-Way ANOVA and Tukey's HSD test. CBH, 1,4-β-cellobiohydrolase; CHT, 1,4-β-poly-N-acetylglucosaminidase; NAG, β-N-acetylglucosaminidase; LAP, leucine aminopeptidase; POX, phenol

oxidase; PER, peroxidase; MUF, 4-methylumbelliferyl; AMC, aminomethylcoumarin; DOPA, L-3,4-dihydroxyphenylalanin; O, organic topsoil; A, mineral topsoil; B, mineral subsoil; J, buried topsoil; PF, permafrost layer. For NAG activity, an overall significant P-values was obtained, but no significant pairwise-differences between horizons were found (lowest pairwise P-values for O vs. B: 0.058, and O vs. PF: 0.067).

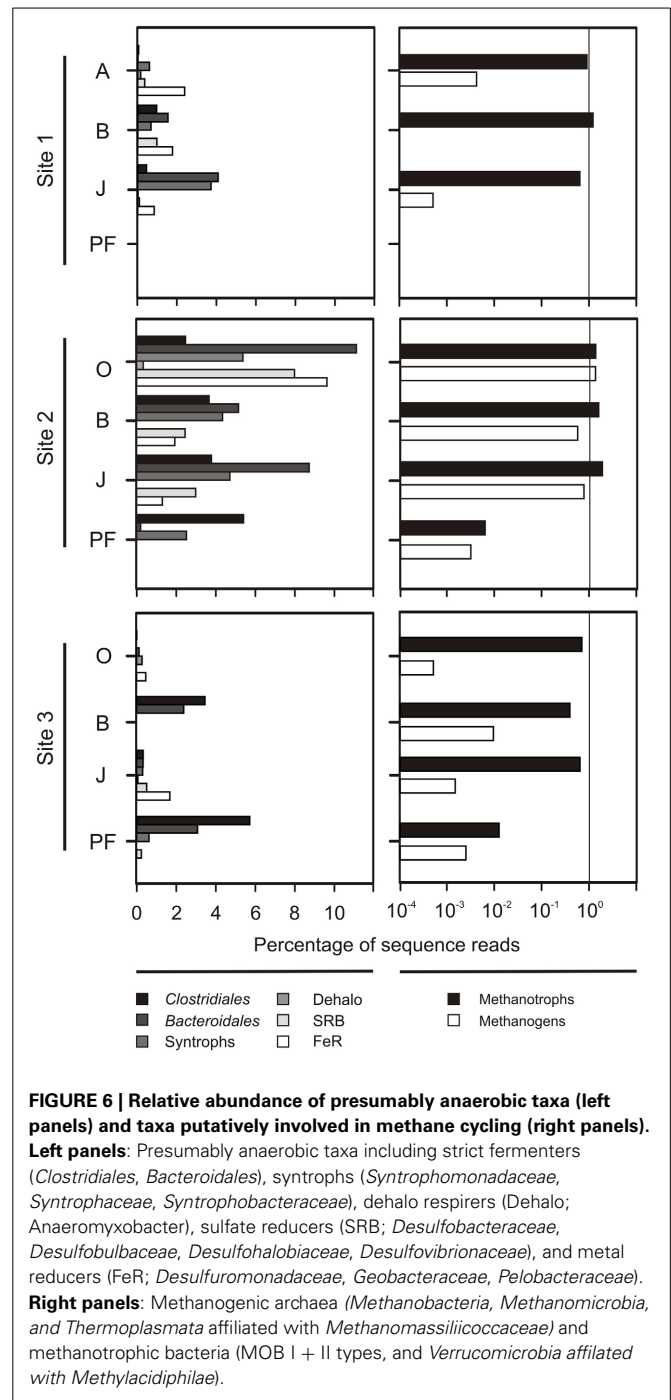
and CH₄ (Elberling et al., 2013). However, the knowledge on microbial communities in permafrost-affected soils in Greenland is rather scarce, restricted to only few sampling sites (Ganzert et al., 2014) and limited to certain physiological or functional guilds (such as methanotrophs) (Bárcena et al., 2011). Thus, our study provides valuable information on the structure, diversity and SOM degradation potential of microbial communities in permafrost-affected soils, and thereby contributes to the understanding of the impact of climate warming on microorganisms and *vice versa* (Graham et al., 2012; Jansson and Tas, 2014).

Our findings support recent studies in the Siberian Arctic that described microbial communities in topsoils buried by cryoturbation as distinct from unburied topsoil communities (Gittel et al., 2014; Schnecker et al., 2014). Fungal-bacterial ratios differed significantly between organic (O) and mineral (A) topsoil horizons as well as between topsoils (O) and buried topsoils (J), being

lowest in the latter. This corroborated the hypothesis that fungi play a critical role in the delayed decomposition of SOM in buried topsoils (Gittel et al., 2014; Schnecker et al., 2014). However, in contrast to the strong effect of soil horizon on the beta diversity in permafrost-affected soils from Siberia (Gittel et al., 2014), buried topsoils from Greenland were more heterogeneous both in diversity, abundance and enzymatic activities. For instance, the bacterial core community (OTUs present in all buried topsoil samples) consisted of only twenty-one OTUs comprising members of the phyla *Acidobacteria*, *Actinobacteria*, *Bacteroidetes*, *Chloroflexi*, *Firmicutes*, and the α-, β-, δ-*Proteobacteria*. This core community accounted for 4.5, 15.0, and 3.4% of the total community at sites 1, 2, and 3, respectively. The most abundant OTU (Greengenes OTU ID 637267) in buried topsoils was affiliated with the family *Intrasporangiaceae* (*Actinobacteria*). Its abundance was particularly high in buried topsoils from site 2 (8.3% of the



total community). Although this OTU was also present in 90% of all other soil samples, it only accounted for an average of 1.7% to the total community in non-buried topsoils, mineral subsoils and permafrost samples. Members of the *Intrasporangiaceae* also constituted a major fraction of the prokaryotic community in mineral subsoils and buried topsoils from the Siberian Arctic, where they accounted for up to 30 and 47% of the total community, respectively (Gittel et al., 2014). It has been hypothesized that members of this family have adapted to the low availability of carbon and energy sources and the harsh abiotic conditions in permafrost-affected soils and cryoenvironments explaining their ubiquitous distribution in these habitats (Hansen et al., 2007; Steven et al., 2008; Yergeau et al., 2010; Yang et al., 2012). Recent studies suggested that they are able to degrade cellulose, cellobiose (which is a product of enzymatic cellulose hydrolysis), and lignin in agricultural soils (Schellenberger et al., 2010; Giongo et al., 2013). Indeed, CCA analysis indicated a linkage between the distribution of the class *Actinobacteria* and the potential activity of peroxidases and phenol oxidases (Figure S5). This supports the hypothesis that *Actinobacteria* might significantly contribute to lignin degradation and transformation in periodically anoxic environments (e.g., water-logged soil horizons), where fungal degradation activities are restricted (Boer et al., 2005; DeAngelis et al., 2011; Gittel et al., 2014). Growing molecular evidence furthermore points to the ecological importance of bacterial laccases, the probably largest class of phenol oxidases, as they were found to be highly diverse and present in a wide range of bacterial phyla, amongst others including *Actinobacteria*, *Acidobacteria*, *Bacteroidetes*, *Firmicutes*, *Proteobacteria*, and *Verrucomicrobia*, as well as in archaea (Nakamura et al., 2003; Ausec et al., 2011a,b; Freedman and Zak, 2014). It has been argued that bacterial laccase



expression might be more efficient compared to fungal laccases due to the lack of introns and posttranslational modifications (Ausec et al., 2011b) and that both their diversity and activity in soils might be much greater than that of their fungal equivalent (Kellner et al., 2008). Potential oxidative enzyme activities (per gram dry soil) did not show significant differences between soil horizons and thus did not follow the change in community composition, and the decrease in fungal and bacterial abundances and total microbial biomass with depth (Figure 4). This might either suggest that the abundance, and by extension the activity,

of fungi producing these enzymes did not change with depth, and that the decrease in total fungal abundance resulted from a decreased abundance of saprotrophic fungi. The latter have previously been shown to be correlated to the activity of hydrolytic enzymes and thus linked to soil properties such as C, N, and moisture (Talbot et al., 2013). It might however also indicate that bacteria of the above mentioned phyla resume and more efficiently express oxidative enzyme activities, while ectomycorrhizal fungi decreased with depth as a result of lacking plant support, e.g., root exudates (Talbot et al., 2008; Gittel et al., 2014). Furthermore and in contrast to hydrolytic enzymes, both phenol oxidases and peroxidase unspecifically catalyze reactions that do not necessarily lead to the acquisition of carbon and nutrients, e.g., mitigation of toxicity of phenols and metals, or antimicrobial defense (Sinsabaugh, 2010). Thus, soil chemistry (i.e., organic matter content) had less of an effect on their activity resulting in insignificant differences between soil horizons (Figure 4).

We found a pronounced effect of the sampling site and concomitant abiotic factors on community composition (Figures 2, 3, Figure S2), with the wet fen site (site 2) being a putative hot spot for anaerobic degradation processes such as methanogenesis and fermentation (Figure 6). A large variety of presumably anaerobic taxa including strict fermenters, syntrophs, sulfate reducers, and metal reducers showed particularly high relative abundances in the active layer of the wet fen site presumably favored by high moisture and low oxygen levels (Figure 6). In accordance with a recent metagenomic study on arctic peat soil (Lipson et al., 2013), putative members of these functional guilds were also detected in permafrost samples suggesting that the respective processes occur both in the active layer and the underlying permafrost. With increasing temperatures in the Northern Latitudes and deepening of the active layer, higher soil moisture and lower oxygen levels will become more prevalent leading to shifts in microbial community composition and functionality toward anaerobic degradation processes (Allan et al., 2014; Frank-Fahle et al., 2014).

Net methane release from arctic soils is regulated by the balance between methane production by anaerobic methanogenic archaea and its conversion to CO₂ by primarily aerobic methane-oxidizing bacteria (Liebner et al., 2009; Graef et al., 2011; Allan et al., 2014). Both activities are affected by a variety of environmental factors such as temperature, water table depth, substrate availability and redox potential, and their balance will eventually determine whether arctic soils act as a source or a sink for methane. Both hydrogenotrophic and acetoclastic methanogens were found in the active layer of all our sampling sites, but were particularly abundant at the wet fen site (Figure 6). Significantly higher moisture and thus lower oxygen levels in the active layer of site 2 probably provided more favorable conditions for methanogens than at sites 1 and 3. Members of the *Methanobacteriales* and the *Methanomicrobiales* (using H₂/CO₂ for methanogenesis) dominated in the topsoil horizons, whereas *Methanosarcinales* dominated in mineral subsoils. The latter are able to generate methane from a broad range of substrates including acetate, H₂/CO₂ and methylated compounds (e.g., methanol). This depth-related succession from a hydrogenotrophic to a metabolically more flexible methanogenic community has been found in other permafrost environments, such as arctic wetlands

and peat soils, and has been attributed to advantages in the competition for substrates and their independence from syntrophic interactions (Høj et al., 2005; Tveit et al., 2012; Lipson et al., 2013; Frank-Fahle et al., 2014).

In line with previous reports from various cold environments (Liebner et al., 2009; Yergeau et al., 2010; Tveit et al., 2012), type I MOB outnumbered type II MOB in mineral soil horizons in the active layer, while type II MOB predominated in topsoils and buried topsoils together with a large fraction of putative methanotrophic *Verrucomicrobia* (52 and 40% of all MOB, respectively). Together with few other studies (Barbier et al., 2012; Martineau et al., 2014), our results thus indicated that MOB diversity was much larger than expected and—depending on the soil horizon and its properties—is clearly not restricted to type I MOB. However, the environmental factors (pH, CH₄ partial pressure, soil temperature) determining the dominance of one or the other MOB type, the balance between methane oxidation and methanogenesis and the ecological implications for arctic environments need further research.

The collective results presented here shed light on the highly diverse microbial communities in permafrost-affected soils in Northeast Greenland, their enzymatic degradation potential and the distribution of functional guilds involved in the anaerobic degradation of SOM (fermentation, methanogenesis). Site-specific differences were apparent between the typical tundra sites and the wet fen site, the latter being a potential hot spot for degradation activities. In addition, shifts in community composition between unburied and buried topsoils (decrease in fungal abundance and a predominance of *Actinobacteria* and other potential bacterial laccase producers) and stable oxidative enzyme activities with depth supported the hypothesis that bacteria might resume the role of fungi in the degradation of phenolic compounds such as lignin.

AUTHOR CONTRIBUTIONS

Antje Gittel, Jiří Bárta, Tim Urich and Andreas Richter designed the research presented in this manuscript. Antje Gittel directed and performed the molecular work and sequence data analyses on prokaryotic communities. Jiří Bárta and Iva Kohoutová performed the quantification of fungal communities. Petr Čapek contributed with data on microbial biomass. Jörg Schneckner and Birgit Wild determined enzyme activity potentials and soil geochemical properties. Samples were collected by Christina Kaiser and Andreas Richter. Antje Gittel performed all statistical analyses. Antje Gittel, Jiří Bárta and Tim Urich wrote the manuscript with input from Christina Kaiser, Jörg Schneckner, Birgit Wild, Vidis L. Torsvik, and Andreas Richter.

ACKNOWLEDGMENTS

This work was part of the International Program CryoCARB (Long-term Carbon Storage in Cryoturbated Arctic Soils) and funded by the Research Council of Norway (NFR—200411), the Austrian Science Fund (FWF I370-B17) and the Grant Agency of South Bohemia University (GAJU project no. 146/2014/P). Jiří Bárta and Tim Urich received additional financial support from the EU Action program (Austria-Czech Republic, ID 60p14). Christa Schleper acknowledges additional financial support from

the Austrian Science Fund (FWF P25369-B22). Sample processing, sequencing and core amplicon data analysis were performed by the Earth Microbiome Project (www.earthmicrobiome.org/) and all amplicon and meta data has been made public through the data portal (www.microbio.me/emp). We thank all members of the CryoCarb project for support and discussion. Nathalia Khilkevich and Kristýna Kvardova are thanked for help with nucleic acid extractions.

SUPPLEMENTARY MATERIAL

The Supplementary Material for this article can be found online at: <http://www.frontiersin.org/journal/10.3389/fmicb.2014.00541/abstract>

REFERENCES

- Allan, J., Ronholm, J., Mykytczuk, N. C. S., Greer, C. W., Onstott, T. C., and Whyte, L. G. (2014). Methanogen community composition and rates of methane consumption in Canadian High Arctic permafrost soils. *Environ. Microbiol. Rep.* 6, 136–144. doi: 10.1111/1758-2229.12139
- Alves, R. J. E., Wanek, W., Zappe, A., Richter, A., Svenning, M. M., Schleper, C., et al. (2013). Nitrification rates in Arctic soils are associated with functionally distinct populations of ammonia-oxidizing archaea. *ISME J.* 7, 1620–1631. doi: 10.1038/ismej.2013.35
- Ausec, L., van Elsas, J. D., and Mandic-Mulec, I. (2011a). Two- and three-domain bacterial laccase-like genes are present in drained peat soils. *Soil Biol. Biochem.* 43, 975–983. doi: 10.1016/j.soilbio.2011.01.013
- Ausec, L., Zakrzewski, M., Goesmann, A., Schlüter, A., and Mandic-Mulec, I. (2011b). Bioinformatic analysis reveals high diversity of bacterial genes for laccase-like enzymes. *PLoS ONE* 6:e25724. doi: 10.1371/journal.pone.0025724
- Barbier, B. A., Dziduch, I., Liebner, S., Ganzert, L., Lantuit, H., Pollard, W., et al. (2012). Methane-cycling communities in a permafrost-affected soil on Herschel Island, Western Canadian Arctic: active layer profiling of mcrA and pmoA genes. *FEMS Microbiol. Ecol.* 82, 287–302. doi: 10.1111/j.1574-6941.2012.01332.x
- Bárcena, T. G., Finster, K. W., and Yde, J. C. (2011). Spatial patterns of soil development, methane oxidation, and methanotrophic diversity along a receding glacier forefield, Southeast Greenland. *Arct. Antarct. Alp. Res.* 43, 178–188. doi: 10.1657/1938-4246-43.2.178
- Biasi, C., Meyer, H., Rusalimova, O., Hämmerle, R., Kaiser, C., Baranyi, C., et al. (2008). Initial effects of experimental warming on carbon exchange rates, plant growth and microbial dynamics of a lichen-rich dwarf shrub tundra in Siberia. *Plant Soil* 307, 191–205. doi: 10.1007/s11104-008-9596-2
- Boer, W., de Folman, L. B., Summerbell, R. C., and Boddy, L. (2005). Living in a fungal world: impact of fungi on soil bacterial niche development. *FEMS Microbiol. Rev.* 29, 795–811. doi: 10.1016/j.femsre.2004.11.005
- Borneman, J., and Hartin, R. J. (2000). PCR primers that amplify fungal rRNA genes from environmental samples. *Appl. Environ. Microbiol.* 66, 4356–4360. doi: 10.1128/AEM.66.10.4356-4360.2000
- Caporaso, J. G., Kuczynski, J., Stombaugh, J., Bittinger, K., Bushman, F. D., Costello, E. K., et al. (2010). QIIME allows analysis of high-throughput community sequencing data. *Nat. Methods* 7, 335–336. doi: 10.1038/nmeth.f.303
- Caporaso, J. G., Lauber, C. L., Walters, W. A., Berg-Lyons, D., Huntley, J., Fierer, N., et al. (2012). Ultra-high-throughput microbial community analysis on the Illumina HiSeq and MiSeq platforms. *ISME J.* 6, 1621–1624. doi: 10.1038/ismej.2012.8
- Caporaso, J. G., Lauber, C. L., Walters, W. A., Berg-Lyons, D., Lozupone, C. A., Turnbaugh, P. J., et al. (2011). Global patterns of 16S rRNA diversity at a depth of millions of sequences per sample. *Proc. Natl. Acad. Sci. U.S.A.* 108, 4516–4522. doi: 10.1073/pnas.1000080107
- Daims, H., Brühl, A., Amann, R., Schleifer, K. H., and Wagner, M. (1999). The domain-specific probe EUB338 is insufficient for the detection of all Bacteria: development and evaluation of a more comprehensive probe set. *Syst. Appl. Microbiol.* 22, 434–444. doi: 10.1016/S0723-2020(99)80053-8
- DeAngelis, K. M., Allgaier, M., Chavarria, Y., Fortney, J. L., Hugenholtz, P., Simmons, B., et al. (2011). Characterization of trapped lignin-degrading microbes in tropical forest soil. *PLoS ONE* 6:e19306. doi: 10.1371/journal.pone.0019306
- DeLong, E. F. (1992). Archaea in coastal marine environments. *Proc. Natl. Acad. Sci. U.S.A.* 89, 5685–5689. doi: 10.1073/pnas.89.12.5685
- DeSantis, T. Z., Hugenholtz, P., Larsen, N., Rojas, M., Brodie, E. L., Keller, K., et al. (2006). Greengenes, a chimera-checked 16S rRNA gene database and workbench compatible with ARB. *Appl. Environ. Microbiol.* 72, 5069–5072. doi: 10.1128/AEM.03006-05
- Edgar, R. C. (2010). Search and clustering orders of magnitude faster than BLAST. *Bioinformatics* 26, 2460–2461. doi: 10.1093/bioinformatics/btq461
- Elberling, B., and Brandt, K. K. (2003). Uncoupling of microbial CO₂ production and release in frozen soil and its implications for field studies of arctic C cycling. *Soil Biol. Biochem.* 35, 263–272. doi: 10.1016/S0038-0717(02)00258-4
- Elberling, B., Michelsen, A., Schadel, C., Schuur, E. A. G., Christiansen, H. H., Berg, L., et al. (2013). Long-term CO₂ production following permafrost thaw. *Nat. Clim. Change* 3, 890–894. doi: 10.1038/nclimate1955
- Fierer, N., Jackson, J. A., Vilgalys, R., and Jackson, R. B. (2005). Assessment of soil microbial community structure by use of taxon-specific quantitative PCR assays. *Appl. Environ. Microbiol.* 71, 4117–4120. doi: 10.1128/AEM.71.7.4117-4120.2005
- Frank-Fahle, B. A., Yergeau, É., Greer, C. W., Lantuit, H., and Wagner, D. (2014). Microbial functional potential and community composition in permafrost-affected soils of the NW Canadian Arctic. *PLoS ONE* 9:e84761. doi: 10.1371/journal.pone.0084761
- Freedman, Z., and Zak, D. R. (2014). Atmospheric N deposition increases bacterial laccase-like multicopper oxidases: implications for organic matter decay. *Appl. Environ. Microbiol.* 80, 4460–4468. doi: 10.1128/AEM.01224-14
- Ganzert, L., Bajerski, F., and Wagner, D. (2014). Bacterial community composition and diversity of five different permafrost-affected soils of North East Greenland. *FEMS Microbiol. Ecol.* 89, 426–441. doi: 10.1111/1574-6941.12352
- Ganzert, L., Jurgens, G., Münster, U., and Wagner, D. (2007). Methanogenic communities in permafrost-affected soils of the Laptev Sea coast, Siberian Arctic, characterized by 16S rRNA gene fingerprints. *FEMS Microbiol. Ecol.* 59, 476–488. doi: 10.1111/j.1574-6941.2006.00205.x
- Giongo, A., Favet, J., Lapanje, A., Gano, K., Kennedy, S., Davis-Richardson, A., et al. (2013). Microbial hitchhikers on intercontinental dust: high-throughput sequencing to catalogue microbes in small sand samples. *Aerobiologia (Bologna)* 29, 71–84. doi: 10.1007/s10453-012-9264-0
- Gittel, A., Bárta, J., Kohoutová, I., Mikutta, R., Owens, S., Gilbert, J., et al. (2014). Distinct microbial communities associated with buried soils in the Siberian tundra. *ISME J.* 8, 841–853. doi: 10.1038/ismej.2013.219
- Graef, C., Hestnes, A. G., Svenning, M. M., and Frenzel, P. (2011). The active methanotrophic community in a wetland from the High Arctic. *Environ. Microbiol. Rep.* 3, 466–472. doi: 10.1111/j.1758-2229.2010.00237.x
- Graham, D. E., Wallenstein, M. D., Vishnivetskaya, T. A., Waldrop, M. P., Phelps, T. J., Pfiffner, S. M., et al. (2012). Microbes in thawing permafrost: the unknown variable in the climate change equation. *ISME J.* 6, 709–712. doi: 10.1038/ismej.2011.163
- Hansen, A. A., Herbert, R. A., Mikkelsen, K., Jensen, L. L., Kristoffersen, T., Tiedje, J. M., et al. (2007). Viability, diversity and composition of the bacterial community in a high Arctic permafrost soil from Spitsbergen, Northern Norway. *Environ. Microbiol.* 9, 2870–2884. doi: 10.1111/j.1462-2920.2007.01403.x
- Harden, J. W., Koven, C. D., Ping, C.-L., Hugelius, G., David McGuire, A., Camill, P., et al. (2012). Field information links permafrost carbon to physical vulnerabilities of thawing. *Geophys. Res. Lett.* 39, L15704. doi: 10.1029/2012GL051958
- Høj, L., Olsen, R. A., and Torsvik, V. L. (2005). Archaeal communities in High Arctic wetlands at Spitsbergen, Norway (78°N) as characterized by 16S rRNA gene fingerprinting. *FEMS Microbiol. Ecol.* 53, 89–101. doi: 10.1016/j.femsec.2005.01.004
- Hollesen, J., Elberling, B., and Jansson, P. E. (2011). Future active layer dynamics and carbon dioxide production from thawing permafrost layers in Northeast Greenland. *Glob. Chang. Biol.* 17, 911–926. doi: 10.1111/j.1365-2486.2010.02256.x
- Horwath Burnham, J., and Sletten, R. S. (2010). Spatial distribution of soil organic carbon in northwest Greenland and underestimates of high Arctic carbon stores. *Glob. Biogeochem. Cycles* 24, GB3012. doi: 10.1029/2009GB003660

- Hugelius, G., Bockheim, J. G., Camill, P., Elberling, B., Grosse, G., Harden, J. W., et al. (2013). A new data set for estimating organic carbon storage to 3 m depth in soils of the northern circumpolar permafrost region. *Earth Syst. Sci. Data* 5, 393–402. doi: 10.5194/essd-5-393-2013
- Husson, F., Josse, J., Le, S., and Mazet, J. (2013). *FactoMineR: Multivariate Exploratory Data Analysis and Data Mining with R*. R Package version 1.25 2013. Available online at: <http://cran.r-project.org/package=FactoMineR>
- IPCC. (2007). *Intergovernmental Panel on Climate Change (IPCC), Climate Change 2007: The Scientific Basis*. Cambridge: Cambridge University Press.
- Jansson, J. K., and Tas, N. (2014). The microbial ecology of permafrost. *Nat. Rev. Microbiol.* 12, 414–425. doi: 10.1038/nrmicro3262
- Josse, J., and Husson, F. (2013). Handling missing values in exploratory multivariate data analysis methods. *J. Soc. Fr. Stat.* 153, 79–99. Available online at: <http://publications-sfds.fr/ojs/index.php/J-SFds/article/view/122/112>
- Jurgens, G., Lindström, K., and Saano, A. (1997). Novel group within the kingdom Crenarchaeota from boreal forest soil. *Appl. Environ. Microbiol.* 63, 803–805.
- Kaiser, C., Koranda, M., Kitzler, B., Fuchsluger, L., Schnecker, J., Schweiger, P., et al. (2010). Belowground carbon allocation by trees drives seasonal patterns of extracellular enzyme activities by altering microbial community composition in a beech forest soil. *New Phytol.* 187, 843–858. doi: 10.1111/j.1469-8137.2010.03321.x
- Kaiser, C., Meyer, H., Biasi, C., Rusalimova, O., Barsukov, P., and Richter, A. (2007). Conservation of soil organic matter through cryoturbation in arctic soils in Siberia. *J. Geophys. Res.* 112, G02017. doi: 10.1029/2006JG000258
- Kellner, H., Luis, P., Zimdars, B., Kiesel, B., and Buscot, F. (2008). Diversity of bacterial laccase-like multicopper oxidase genes in forest and grassland Cambisol soil samples. *Soil Biol. Biochem.* 40, 638–648. doi: 10.1016/j.soilbio.2007.09.013
- Leininger, S., Urich, T., Schloter, M., Schwark, L., Qi, J., Nicol, G. W., et al. (2006). Archaea predominate among ammonia-oxidizing prokaryotes in soils. *Nature* 442, 806–809. doi: 10.1038/nature04983
- Liebner, S., Harder, J., and Wagner, D. (2008). Bacterial diversity and community structure in polygonal tundra soils from Samoylov Island, Lena Delta, Siberia. *Int. Microbiol.* 11, 195–202. doi: 10.2436/20.1501.01.60
- Liebner, S., Rublack, K., Stuehrmann, T., and Wagner, D. (2009). Diversity of aerobic methanotrophic bacteria in a permafrost active layer soil of the Lena Delta, Siberia. *Microb. Ecol.* 57, 25–35. doi: 10.1007/s00248-008-9411-x
- Lipson, D. A., Haggerty, J. M., Srinivas, A., Raab, T. K., Sathe, S., and Dinsdale, E. A. (2013). Metagenomic insights into anaerobic metabolism along an Arctic Peat soil profile. *PLoS ONE* 8:e64659. doi: 10.1371/journal.pone.0064659
- Loy, A., Lehner, A., Lee, N., Adamczyk, J., Meier, H., Ernst, J., et al. (2002). Oligonucleotide microarray for 16S rRNA gene-based detection of all recognized lineages of sulfate-reducing prokaryotes in the environment. *Appl. Environ. Microbiol.* 68, 5064–5081. doi: 10.1128/AEM.68.10.5064-5081.2002
- Lozupone, C., and Knight, R. (2005). UniFrac: a new phylogenetic method for comparing microbial communities. *Appl. Environ. Microbiol.* 71, 8228–8235. doi: 10.1128/AEM.71.12.8228-8235.2005
- MacDougall, A. H., Avis, C. A., and Weaver, A. J. (2012). Significant contribution to climate warming from the permafrost carbon feedback. *Nat. Geosci.* 5, 719–721. doi: 10.1038/ngeo1573
- Mackelprang, R., Waldrop, M. P., DeAngelis, K. M., David, M. M., Chavarria, K. L., Blazewicz, S. J., et al. (2011). Metagenomic analysis of a permafrost microbial community reveals a rapid response to thaw. *Nature* 480, 368–371. doi: 10.1038/nature10576
- Martineau, C., Pan, Y., Bodrossy, L., Yergeau, E., Whyte, L. G., and Greer, C. W. (2014). Atmospheric methane oxidizers are present and active in Canadian high Arctic soils. *FEMS Microbiol. Ecol.* 89, 257–269. doi: 10.1111/1574-6941.12287
- Marx, M.-C., Wood, M., and Jarvis, S. C. (2001). A microplate fluorimetric assay for the study of enzyme diversity in soils. *Soil Biol. Biochem.* 33, 1633–1640. doi: 10.1016/S0038-0717(01)00079-7
- Masson-Delmotte, V., Swingedouw, D., Landais, A., Seidenkrantz, M.-S., Gauthier, E., Bichet, V., et al. (2012). Greenland climate change: from the past to the future. *Wiley Interdiscip. Rev. Clim. Chang.* 3, 427–449. doi: 10.1002/wcc.186
- Nakamura, K., Kawabata, T., Yura, K., and Go, N. (2003). Novel types of two-domain multi-copper oxidases: possible missing links in the evolution. *FEBS Lett.* 553, 239–244. doi: 10.1016/S0014-5793(03)01000-7
- Oksanen, J., Kindt, R., Legendre, P., O'Hara, B., Stevens, M. H. H., Oksanen, M. J., et al. (2007). *The Vegan Package—Community Ecology Package*. R package version 2.0-9. Available online at: <http://CRAN.R-project.org/package=vegan>
- Palmtag, J. (2011). *Soil Organic Carbon Storage in Continuous Permafrost Terrain with an Emphasis on Cryoturbation—Two Case Studies from NE Greenland and NE Siberia*. Master thesis, Department of Physical Geography and Quaternary Geology, Stockholm University, Stockholm, 73.
- R Development Core Team. (2012). *R: A Language and Environment for Statistical Computing*. Vienna: R Foundation for Statistical Computing. ISBN 3-900051-07-0. Available online at: <http://www.R-project.org/>
- Schellenberger, S., Kolb, S., and Drake, H. L. (2010). Metabolic responses of novel cellulolytic and saccharolytic agricultural soil Bacteria to oxygen. *Environ. Microbiol.* 12, 845–861. doi: 10.1111/j.1462-2920.2009.02128.x
- Schnecker, J., Wild, B., Hofhansl, F., Alves, R. J. E., Bárta, J., Capek, P., et al. (2014). Effects of soil organic matter properties and microbial community composition on enzyme activities in cryoturbated arctic soils. *PLoS ONE* 9:e94076. doi: 10.1371/journal.pone.0094076
- Schuur, E. A. G., and Abbott, B. (2011). Climate change: high risk of permafrost thaw. *Nature* 480, 32–33. doi: 10.1038/480032a
- Schuur, E. A. G., Bockheim, J., Canadell, J. G., Euskirchen, E., Field, C. B., Goryachkin, S. V., et al. (2008). Vulnerability of permafrost carbon to climate change: implications for the global carbon cycle. *Bioscience* 58, 701–714. doi: 10.1641/B580807
- Singh, B. K., Bardgett, R. D., Smith, P., and Reay, D. S. (2010). Microorganisms and climate change: terrestrial feedbacks and mitigation options. *Nat. Rev. Microbiol.* 8, 779–790. doi: 10.1038/nrmicro2439
- Sinsabaugh, R. L. (2010). Phenol oxidase, peroxidase and organic matter dynamics of soil. *Soil Biol. Biochem.* 42, 391–404. doi: 10.1016/j.soilbio.2009.10.014
- Sinsabaugh, R. L., Klug, M. J., Collins, H. P., Yeager, P. E., and Petersen, S. O. (1999). “Characterizing soil microbial communities,” in *Standard Soil Methods for Long-term Ecological Research*, eds. G. P. Robertson, D. C. Coleman, C. S. Bledsoe, and P. Sollins (New York, NY: Oxford University Press), 318–348.
- Soil Survey Staff. (2010). *Keys to Soil Taxonomy*. 11th Edn. Washington, DC: USDA, U.S. Department of Agriculture-Natural Resources Conservation Service.
- Steven, B., Pollard, W. H., Greer, C. W., and Whyte, L. G. (2008). Microbial diversity and activity through a permafrost/ground ice core profile from the Canadian high Arctic. *Environ. Microbiol.* 10, 3388–3403. doi: 10.1111/j.1462-2920.2008.01746.x
- Talbot, J. M., Allison, S. D., and Treseder, K. K. (2008). Decomposers in disguise: mycorrhizal fungi as regulators of soil C dynamics in ecosystems under global change. *Funct. Ecol.* 22, 955–963. doi: 10.1111/j.1365-2435.2008.01402.x
- Talbot, J. M., Bruns, T. D., Smith, D. P., Branco, S., Glassman, S. I., Erlandson, S., et al. (2013). Independent roles of ectomycorrhizal and saprotrophic communities in soil organic matter decomposition. *Soil Biol. Biochem.* 57, 282–291. doi: 10.1016/j.soilbio.2012.10.004
- Tarnocai, C., Canadell, J. G., Schuur, E. A. G., Kuhry, P., Mazhitova, G., and Zimov, S. (2009). Soil organic carbon pools in the northern circumpolar permafrost region. *Glob. Biogeochem. Cycles* 23, GB2023. doi: 10.1029/2008GB003327
- Tas, N., Prestat, E., McFarland, J. W., Wickland, K. P., Knight, R., Berhe, A. A., et al. (2014). Impact of fire on active layer and permafrost microbial communities and metagenomes in an upland Alaskan boreal forest. *ISME J.* 8, 1904–1919. doi: 10.1038/ismej.2014.36
- Teske, A., and Sorensen, K. B. (2007). Uncultured archaea in deep marine subsurface sediments: have we caught them all? *ISME J.* 2, 3–18. doi: 10.1038/ismej.2007.90
- Tveit, A., Schwacke, R., Svenning, M. M., and Urich, T. (2012). Organic carbon transformations in high-Arctic peat soils: key functions and microorganisms. *ISME J.* 7, 299–311. doi: 10.1038/ismej.2012.9
- Tveit, A., Urich, T., and Svenning, M. M. (2014). Metatranscriptomic analysis of Arctic peat soil microbiota. *Appl. Environ. Microbiol.* 80, 5761–5772. doi: 10.1128/AEM.01030-14
- Urich, T., Lanzén, A., Qi, J., Huson, D. H., Schleper, C., and Schuster, S. C. (2008). Simultaneous assessment of soil microbial community structure and function through analysis of the meta-transcriptome. *PLoS ONE* 3:e2527. doi: 10.1371/journal.pone.0002527
- Vavrek, M. J. (2011). fossil: palaeoecological and palaeogeographical analysis tools. *Palaeontol. Electron.* 14, 16. Available online at: http://www.uv.es/pardomv/pe/2011_1/238/238.pdf
- Xu, C., Liang, C., Wullschlegel, S., Wilson, C., and McDowell, N. (2011). Importance of feedback loops between soil inorganic nitrogen and microbial communities in the heterotrophic soil respiration response to global warming. *Nat. Rev. Microbiol.* 9, 222. doi: 10.1038/nrmicro2439-c1
- Yang, S., Wen, X., Jin, H., and Wu, Q. (2012). Pyrosequencing investigation into the bacterial community in Permafrost Soils along the China-Russia crude oil pipeline (CRCOP). *PLoS ONE* 7:e52730. doi: 10.1371/journal.pone.0052730

Yergeau, E., Hogues, H., Whyte, L. G., and Greer, C. W. (2010). The functional potential of high Arctic permafrost revealed by metagenomic sequencing, qPCR and microarray analyses. *ISME J.* 4, 1206–1214. doi: 10.1038/ismej.2010.41

Conflict of Interest Statement: The authors declare that the research was conducted in the absence of any commercial or financial relationships that could be construed as a potential conflict of interest.

Received: 05 August 2014; accepted: 29 September 2014; published online: 16 October 2014.

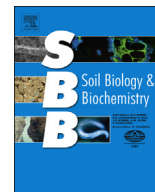
Citation: Gittel A, Bárta J, Kohoutová I, Schneckner J, Wild B, Čapek P, Kaiser C, Torsvik VL, Richter A, Schleper C and Urich T (2014) Site- and horizon-specific

patterns of microbial community structure and enzyme activities in permafrost-affected soils of Greenland. Front. Microbiol. 5:541. doi: 10.3389/fmicb.2014.00541
This article was submitted to *Terrestrial Microbiology*, a section of the journal *Frontiers in Microbiology*.

Copyright © 2014 Gittel, Bárta, Kohoutová, Schneckner, Wild, Čapek, Kaiser, Torsvik, Richter, Schleper and Urich. This is an open-access article distributed under the terms of the Creative Commons Attribution License (CC BY). The use, distribution or reproduction in other forums is permitted, provided the original author(s) or licensor are credited and that the original publication in this journal is cited, in accordance with accepted academic practice. No use, distribution or reproduction is permitted which does not comply with these terms.

Paper 9

Capek P, Diakova K, Dickopp JE, **Barta J**, Wild B, Schneckner J, Alves RJE, Aiglsdorfer S, Guggenberger G, Gentsch N, Hugelius G, Lashchinsky N, Gittel A, Schleper C, Mikutta R, Palmtag J, Shibistova O, Urich T, Richter A, Santruckova H (2015) The effect of warming on the vulnerability of subducted organic carbon in arctic soils. *SOIL BIOLOGY & BIOCHEMISTRY* 90:19-29.



The effect of warming on the vulnerability of subducted organic carbon in arctic soils



Petr Čapek^{a,*}, Kateřina Diáková^a, Jan-Erik Dickopp^b, Jiří Bárta^a, Birgit Wild^{c,d,e}, Jörg Schnecker^{c,d,f}, Ricardo Jorge Eloy Alves^{d,g}, Stefanie Aiglsdorfer^g, Georg Guggenberger^h, Norman Gentsch^h, Gustaf Hugelius^j, Nikolaj Lashchinsky^k, Antje Gittel^{l,m}, Christa Schleper^{d,g,k}, Robert Mikutta^{h,i}, Juri Palmtag^j, Olga Shibistova^{h,n}, Tim Urich^{d,g,o}, Andreas Richter^{c,d}, Hana Šantrůčková^{a,**}

^a University of South Bohemia, Department of Ecosystems Biology, Branišovská 31, České Budějovice, Czech Republic

^b Institute of Systematic Botany and Ecology, University of Ulm, Albert-Einstein-Allee 11, D-89081 Ulm, Germany

^c University of Vienna, Department of Microbiology and Ecosystem Research, Division of Terrestrial Ecosystem Research, Althanstrasse 14, 1090 Vienna, Austria

^d Austrian Polar Research Institute, Althanstrasse 14, 1090 Vienna, Austria

^e University of Gothenburg, Department of Earth Sciences, Guldhedsgatan 5A, 40530 Gothenburg, Sweden

^f University of New Hampshire, Department of Natural Resources & the Environment, Durham, NH 03824, USA

^g University of Vienna, Department of Ecogenomics and Systems Biology, Division of Archaea Biology and Ecogenomics, Vienna, Austria

^h Leibniz Universität Hannover, Institute of Soil Science, Herrenhäuser Strasse 2, 30419 Hannover, Germany

ⁱ Martin-Luther-University Halle-Wittenberg, Soil Sciences, 06120 Halle, Germany

^j University of Stockholm, Department of Physical Geography, 10691 Stockholm, Sweden

^k Central Siberian Botanical Garden, Siberian Branch of the Russian Academy of Sciences, St. Zolotodolinskaya 101, 630090 Novosibirsk, Russian Federation

^l University of Bergen, Department of Biology, Centre for Geobiology, Thormøhlensgate 53B, 5020 Bergen, Norway

^m Center for Geomicrobiology, Department of Bioscience, Ny Munkegade 114, 8000 Aarhus C, Denmark

ⁿ VN Sukachev, Institute of Forest, Siberian Branch of the Russian Academy of Sciences, Akademgorodok, 660036 Krasnoyarsk, Russian Federation

^o University of Greifswald, Institute for Microbiology, 17489 Greifswald, Germany

ARTICLE INFO

Article history:

Received 24 April 2015

Received in revised form

10 July 2015

Accepted 13 July 2015

Available online 4 August 2015

Keywords:

Subducted organic horizon

Soil carbon loss

Incubation

Temperature

Microbial biomass

Enzymes

ABSTRACT

Arctic permafrost soils contain large stocks of organic carbon (OC). Extensive cryogenic processes in these soils cause subduction of a significant part of OC-rich topsoil down into mineral soil through the process of cryoturbation. Currently, one-fourth of total permafrost OC is stored in subducted organic horizons. Predicted climate change is believed to reduce the amount of OC in permafrost soils as rising temperatures will increase decomposition of OC by soil microorganisms. To estimate the sensitivity of OC decomposition to soil temperature and oxygen levels we performed a 4-month incubation experiment in which we manipulated temperature (4–20 °C) and oxygen level of topsoil organic, subducted organic and mineral soil horizons. Carbon loss (C_{LOSS}) was monitored and its potential biotic and abiotic drivers, including concentrations of available nutrients, microbial activity, biomass and stoichiometry, and extracellular oxidative and hydrolytic enzyme pools, were measured. We found that independently of the incubation temperature, C_{LOSS} from subducted organic and mineral soil horizons was one to two orders of magnitude lower than in the organic topsoil horizon, both under aerobic and anaerobic conditions. This corresponds to the microbial biomass being lower by one to two orders of magnitude. We argue that enzymatic degradation of autochthonous subducted OC does not provide sufficient amounts of carbon and nutrients to sustain greater microbial biomass. The resident microbial biomass relies on allochthonous fluxes of nutrients, enzymes and carbon from the OC-rich topsoil. This results in a “negative priming effect”, which protects autochthonous subducted OC from decomposition at present. The vulnerability of subducted organic carbon in cryoturbated arctic soils under future climate conditions will largely depend on the amount of allochthonous carbon and nutrient fluxes from the topsoil.

© 2015 Elsevier Ltd. All rights reserved.

* Corresponding author. Tel.: +420 387772347; fax: +420 387 772 368.

** Corresponding author. Tel.: +420 387772361; fax: +420 387 772 368.

E-mail addresses: petacapek@gmail.com (P. Čapek), hana.santruckova@prf.jcu.cz (H. Šantrůčková).

1. Introduction

Soils in permafrost areas contain an estimated $\sim 1300 \pm 200$ Pg of organic carbon (OC), of which ~ 500 Pg resides in non-permafrost soils or in deeper taliks or is seasonally thawed (i.e. in the “active layer”), while ~ 800 Pg is perennially frozen (Hugelius et al., 2014). Much of this OC is predicted to be vulnerable to extensive decomposition under warming climate conditions of the northern circumpolar region (Davidson and Janssens, 2006; Zimov et al., 2006; Schuur et al., 2008, 2009). Several studies in the arctic have already shown increasing carbon loss from upper top and permanently frozen soil horizons under higher temperatures (Oechel et al., 1993; Schuur et al., 2009; Schädel et al., 2014). As well as rising temperatures, recent model scenarios predict an increase of precipitation and the occurrence of more numerous anaerobic sites, which can lead to methane production and release of additional carbon from permafrost-affected soils (Olefeldt et al., 2013). Therefore, both aerobic and anaerobic carbon transformation processes need to be included in predictions of OC vulnerability to decomposition.

Permafrost soils are extensively affected by cryogenic processes (repeated freeze and thaw cycles of the active layer), which result in subduction of carbon rich topsoil organic horizons deeper into the soil profile (Bockheim and Tarnocai, 1998). The amount of OC in subducted organic horizons can make up 90% of total OC in the first meter of soil (Bockheim, 2007), and in total it represents approximately one-fourth of all OC currently stored in permafrost soils (Harden et al., 2012). Recent data indicates lower OC quality and distinctly different microbial community composition and enzyme activities of subducted organic horizons in comparison with topsoil organic horizons (Harden et al., 2012; Gittel et al., 2014; Schneckler et al., 2014; Gentsch et al., 2015a, 2015b), which presumably is the cause of the retarded decomposition of subducted OC previously observed (Kaiser et al., 2007; Wild et al., 2014). As a result, the age of organic C in cryoturbated organic pockets could reach several thousand years (Bockheim, 2007; Kaiser et al., 2007; Hugelius et al., 2014; Palmtag et al., 2015). Although the effects of temperature and oxygen level on the rate of OC decomposition are generally well studied and many investigations have documented significant positive effects of both, specific studies on subducted OC are still scarce (Schädel et al., 2014).

Without a direct manipulation study, the vulnerability of subducted OC decomposition to warming is currently impossible to predict from these findings. The effect of temperature on OC decomposition is not uniform across published studies because it is confounded by other factors such as oxygen level, OC quality, nutrients, microbial physiology and enzymatic performance (e.g. Giardina and Ryan, 2000; Brown et al., 2004; Hyvonen et al., 2005; Conant et al., 2008; Allen and Gillooly, 2009; Allison et al., 2010; Davidson et al., 2012; Steinweg et al., 2013). Because of such multifactorial control, no general mechanism of the temperature effect on OC decomposition has become widely accepted (Reichstein et al., 2005; Agren and Wetterstedt, 2007; Allison et al., 2010; Sierra, 2012). According to kinetic theory, the temperature sensitivity of OC decomposition is a function of OC quality (Knorr et al., 2005; Davidson and Janssens, 2006; Conant et al., 2008). The lower the OC quality, the higher is the temperature sensitivity as the decomposition of low quality OC requires more energy. According to metabolic theory, the temperature sensitivity of OC decomposition is determined by the temperature sensitivity of heterotrophic microbial metabolism and thus is independent of OC quality per se (Allen et al., 2005; Yvon-Durocher et al., 2012). Variability in temperature sensitivity of OC decomposition depends entirely on changes in the amount and physiology of microbial biomass, which might be induced by a multitude of different factors

(for example, OC quality change). When estimating the effects of temperature and other abiotic or biotic factors on OC decomposition, it is necessary to include not only the effect of OC quality but also effects on microbial activity.

The main objective of the present study was to estimate the temperature sensitivity of OC decomposition in a subducted organic horizon under aerobic and anaerobic conditions and identify key factors determining this sensitivity. We hypothesize that the observed distinctly different composition of microbial communities, low OC quality and inadequate enzymatic activities in the subducted organic horizon pose the barrier for OC utilization by microbial biomass. We expect the increase of OC depolymerization by extracellular enzymes leading to an increase of carbon and nutrient supply to microbial biomass and its increase at higher temperatures. This will result in higher temperature sensitivity of OC decomposition in comparison with regular soil horizons. We further expect slower decomposition of subducted OC and lower temperature sensitivity under anaerobic conditions. To test these hypotheses we set up a 4-month incubation experiment, in which we manipulated the temperature and oxygen level of subducted organic, upper organic and lower mineral horizons. We determined soil carbon loss and the potential biotic and abiotic drivers of OC decomposition, including concentrations of available nutrients, microbial activity and its biomass and stoichiometry, and extracellular oxidative and hydrolytic enzyme pools.

2. Materials and methods

2.1. Soil sampling and preparation

Soil samples for the incubation experiment were collected from a shrubby moss tundra site on the Taymir peninsula, Russia ($72^{\circ}29.57'N$, $101^{\circ}38.62'E$). This area is within a continuous permafrost zone. Active layer depth at the sampling site reached 65–90 cm in August 2011. Vegetation was dominated by *Cassiope tetragona*, *Carex arctisibirica* and *Aulacomnium turgidum*. The soil was classified as fine loamy to coarse loamy Typic Aquiturbel according to the US Soil Taxonomy (Soil Survey Staff, 1999) or as Turbic Cryosol according to the World Reference Base for Soil Resources (IUSS Working Group WRB, 2007). Bulk samples from three different horizons within the active layer were collected: topsoil organic material from an OA horizon at the surface (further referred to as O horizon), subducted organic material from an Ajj horizon, and mineral subsoil material from the BCg horizon, the latter two from a depth of 50–70 cm. The mineral subsoil material sampled did not include cryoturbated organic material. Living roots were removed from bulk samples after sampling and soil material was kept at 4 °C until processing. Bulk soil material was homogenized before the start of the laboratory incubation and assessed for basic chemical, physical and microbial characteristics (Table 1).

2.2. Incubation setup

A 19 week-long incubation experiment was performed for each soil horizon (O, Ajj and BCg) at three different temperatures (4, 12 and 20 °C) and three moisture levels (50, 80 and 100% of water holding capacity; WHC) in four replicates. The two lower moisture treatments (50 and 80% WHC) used aerobic conditions, whereas the 100% WHC treatment used anaerobic conditions. Aerobic treatments were regularly flushed with moist air to maintain the oxygen concentration at the atmospheric level and to avoid oxygen limitation. For the anaerobic treatment, the headspaces of the incubation bottles were maintained anoxic by filling them with a He/CO₂ mixture (5% CO₂, 95% He). A CO₂ concentration of 5% was chosen to correspond with CO₂ concentrations commonly detected

Table 1

Basic physical (BD – bulk density, CEC – cation exchange capacity, $\delta^{13}\text{C}$ – soil carbon isotopic signature), chemical ($\text{pH}_{\text{H}_2\text{O}}$ – pH in water, pH_{KCl} – exchangeable pH, OC – total soil organic carbon, N_{TOT} – total soil nitrogen, C_{EX} – K_2SO_4 extractable organic carbon, DON – K_2SO_4 extractable organic nitrogen, NH_4^+ – K_2SO_4 extractable ammonium, NO_3^- – K_2SO_4 extractable nitrates, P_{EX} – NaHCO_3 extractable phosphorus) and microbial (C_{MB} – microbial carbon, N_{MB} – microbial nitrogen, P_{MB} – microbial phosphorus) characteristics as well as stoichiometric parameters (C: N_{TOT} – total soil organic carbon to total soil nitrogen ratio, C: N_{MB} – microbial carbon to nitrogen ratio, C: P_{MB} – microbial carbon to phosphorus ratio) for organic (O), subducted organic (Ajj) and mineral (BCg) horizons. Numbers listed in the table are means with standard deviations in italic ($n = 3$). The label u.d. indicates a value below the detection limit of the method. The values where no standard deviations are listed were measured without replication.

Horizon	$\text{pH}_{\text{H}_2\text{O}}$	pH_{KCl}	BD g cm^{-3}	CEC meq kg^{-1}	OC %	N_{TOT} %	$\delta^{13}\text{C}$ [‰] vs. PDB	C_{EX} $\mu\text{mol g}^{-1}$	C_{MB}
O	6.2	5.8	1.2	276.8	11.58	0.57	-27.62	28.18	174.07
		<i>0.1</i>		<i>17.4</i>	<i>0.23</i>	<i>0.01</i>	<i>0.17</i>	<i>2.36</i>	<i>3.19</i>
Ajj	6.3	6.3	1.4	150.5	3.97	0.15	-27.56	3.76	10.57
		<i>0.2</i>		<i>0.8</i>	<i>0.07</i>	<i>0.00</i>	<i>0.17</i>	<i>0.76</i>	<i>0.50</i>
BCg	6.7	6.6	1.8	105.2	0.58	0.03	-26.84	1.22	2.21
		<i>0.3</i>		<i>4.4</i>	<i>0.01</i>	<i>0.00</i>	<i>0.25</i>	<i>0.73</i>	<i>0.36</i>
Horizon	DON $\mu\text{mol g}^{-1}$	NH_4^+	NO_3^-	N_{MB}	P_{EX}	P_{MB}	C: N_{TOT} mol mol^{-1}	C: N_{MB}	C: P_{MB}
O	7.25	1.99	0.09	9.33	0.21	2.82	20.42	18.66	61.69
	<i>0.09</i>	<i>0.00</i>	<i>0.00</i>	<i>0.09</i>	<i>0.01</i>	<i>0.07</i>	<i>0.21</i>	<i>0.47</i>	<i>2.43</i>
Ajj	u.d.	0.29	0.16	0.65	0.24	0.15	26.18	16.42	73.97
		<i>0.00</i>	<i>0.00</i>	<i>0.06</i>	<i>0.01</i>	<i>0.04</i>	<i>0.32</i>	<i>1.98</i>	<i>16.92</i>
BCg	u.d.	0.29	0.03	0.20	0.06	0.01	18.67	11.72	160.70
		<i>0.00</i>	<i>0.00</i>	<i>0.07</i>	<i>0.00</i>	<i>0.01</i>	<i>0.67</i>	<i>4.28</i>	<i>49.23</i>

in anaerobic soils (Nobel and Palta, 1989). As a control, one bottle per temperature and oxygen treatment was incubated without soil. A more detailed description of the incubation setup is given in [Supplementary Material and methods](#).

2.3. Gas analyses

Incubation bottles were kept closed during the whole incubation. CO_2 and CH_4 accumulation and O_2 consumption were measured weekly for the first 3 weeks and then bi-weekly during the rest of the incubation period (11 times in total). After determination of accumulated CO_2 and CH_4 and consumed O_2 , bottles were flushed with ambient air (aerobic bottles) or with 100% He amended with 5% CO_2 (anaerobic bottles). All three gases were measured again approx. 1 h after flushing to acquire starting concentrations for the calculation of CO_2 and CH_4 production rates and O_2 consumption rate during the next interval.

During the measurements the headspace of incubation vessels was mixed, using a gas-tight membrane pump (KNF Laboport Mini Diaphragm Vacuum Pump, KNF Neuberger, INC., Trenton, USA) in order to remove any stratification of gas layers. The closed loop connecting incubation vessel and membrane pump was equipped with a sampling unit (SwageLok, Solon, USA) from which gas samples (0.2 ml) were taken with 1 ml syringes for immediate gas analysis. CO_2 and CH_4 were analyzed using a gas chromatograph (Agilent 7820A GC, Agilent Technologies, Santa Clara, USA) with a flow rate of 10 ml/min and an oven temperature of 40 °C and equipped with flame ionization and thermal conductivity detectors. Oxygen concentration was measured with an optical method using non-invasive optical oxygen sensors (PST3, PreSens, Regensburg, Germany).

2.4. Chemical soil parameters

Soil pH was measured in extracts of 1 part soil to 5 parts water. The effective cation exchange capacity (CEC) was determined as the sum of exchangeable base cations ($\text{BC}_{\text{ex}} = \text{sum of Ca}^{2+}, \text{Mg}^{2+}, \text{Na}^+, \text{K}^+$) and exchangeable acidity (the sum of $\text{Al}^{3+}_{\text{ex}}$ and H^+_{ex}), each multiplied by the respective number of charges per ion, according to Thomas (1982). The amounts of total soil organic carbon (OC) and of total soil nitrogen (N_{TOT}) were measured using an NC 2100 soil analyzer (Thermo Quest Italia S.p.A., Rodano, MI). For $\delta^{13}\text{C}$

determination, an elemental analyzer (Vario micro cube, Elementar Analysen System GmbH, Germany) coupled to an isotope ratio mass spectrometer (IR-MS DELTA plus XL, Finnigan, Germany) was used. Concentrations of available carbon, nitrogen and phosphorus were measured according to Vance et al. (1987), Brookes et al. (1985, 1982), respectively. Soil samples were free of inorganic carbon (Gentsch et al., 2015a). Details of the analytical procedures used are given in [Supplementary Material and methods](#).

2.5. Microbial biomass and enzyme activities

Microbial carbon, nitrogen and phosphorus concentrations ($\text{C}_{\text{MB}}, \text{N}_{\text{MB}}, \text{P}_{\text{MB}}$) were estimated by chloroform-fumigation extraction (Brookes et al., 1982, 1985; Vance et al., 1987). Details are given in [Supplementary Material and methods](#).

Potential extracellular enzyme activities were determined for seven soil enzymes responsible for organic carbon, nitrogen and phosphorus processing. Because the activities of extracellular enzymes were determined under standardized conditions (unbuffered water extracts at 20 °C) they should be considered as proxies of the enzyme pools. For details on the determination of enzyme activities please refer to [Supplementary Material and methods](#).

The sum of all measured potential enzymatic activities describes the total enzymatic pool in the soil (E_{CNP}). Within this pool there are different classes of enzymes, which we divided into categories according to their product formation with respect to microbial nutrient acquisition. The sum of β -glucosidases and cellobiosidases defines the inherent category of carbon acquisition enzymes (E_{C}). The sum of leucine and alanine aminopeptidases defines the inherent category of nitrogen acquisition enzymes (E_{N}), and the sum of phosphatases and phosphodiesterases defines the category of phosphorus acquisition enzymes (E_{P}). Phenoloxidases are a special case of oxidative enzymes, which can degrade lignin-like compounds and by doing so may serve carbon and nitrogen acquisition (Godbold et al., 2006; Fontaine et al., 2007; Sinsabaugh and Shah, 2012). We treat these enzymes separately as a special case within E_{CNP} .

2.6. Statistical analyses and data evaluation

There was no significant difference between the moisture treatments at 50 and 80% WHC in any of the biochemical or

chemical characteristics and gas exchange rates. Therefore, the data from these two moisture treatments was pooled for statistical analyses (further referred to as 'aerobic treatment'). By doing so, we designed a complete factorial design of the experiment with two treatments differing in oxygen status (aerobic treatment: $n = 8$, and anaerobic treatment: $n = 4$) within each horizon and temperature treatment.

Cumulative carbon loss (C_{LOSS}) from the soil, as a measure of OC decomposability, was calculated as the sum of CO_2 and CH_4 production integrated over the incubation period. A simple exponential function was used to describe C_{LOSS} as a function of temperature:

$$C_{LOSS} = R \cdot e^{a \cdot T},$$

where T is temperature and R and a are function parameters. Q_{10} as a measure of the temperature sensitivity of C_{LOSS} was calculated from the exponential function as follows:

$$Q_{10} = e^{a \cdot 10},$$

Q_{10} expresses the relative change of C_{LOSS} with a $10^\circ C$ increase. To allow direct comparison of temperature sensitivity between soil horizons, we tested the effect of soil horizon on a parameter with nonlinear mixed-effect models, using the program R (R Core Team, 2014) and package nlme (Pinheiro et al., 2013). We tested the statistical difference by comparing exponential functions having a parameter fixed for all horizons, separately estimated for each horizon or randomly varying among horizons. For the comparison we used the Akaike information criterion (AIC).

Absolute differences in C_{LOSS} between horizons, temperature and oxygen status treatments were evaluated by 3-way ANOVA. C_{LOSS} data were log-transformed and normality checked with the Shapiro–Wilk test. To evaluate the differences between the individual treatments we used the post-hoc Tukey HSD test. Since the effect of soil horizon on C_{LOSS} was (in terms of explained variability) much greater than the effects of temperature and oxygen status, the ANOVA was followed by multiple linear regression analysis to find the best predictors of C_{LOSS} across horizons. The best statistical model was chosen from all measured parameters (chemical parameters, microbial parameters and enzyme potential activities), temperature and oxygen status by applying a stepwise algorithm. Because multi-collinearity in soil chemical parameters, microbial parameters or enzyme potential activities often occurs across horizons, ridge regression was used to avoid unstable predictors. Ridge regression was carried out in R (R Core Team, 2014) using package MASS.

The relationship between temperature and oxygen consumption rate was described by a Gaussian model (Tuomi et al., 2008):

$$O_2 = R \cdot e^{a \cdot T + b \cdot T^2},$$

where O_2 is oxygen consumption rate, T is temperature in degrees Celsius and R , a and b are model parameters. This model allows calculating the temperature at which oxygen consumption rate is maximal (T_{MAX}):

$$T_{MAX} = \frac{a}{-2 \cdot b}$$

Above T_{MAX} , oxygen consumption rate decreases with temperature. The Gaussian model parameters were estimated using nonlinear mixed-effect models. The effects of chemical and biochemical variables on model parameters were tested. The best model fit was chosen based on the AIC.

For the aerobic treatments the respiration quotient (RQ) was calculated as the molar ratio of CO_2 production to O_2 consumption. An RQ value equal to 1 indicates degradation of simple organic compounds via the citric acid cycle. RQ values below 1 indicate degradation of reduced, more recalcitrant organic compounds, which need more oxygen to be oxidized (Dilly, 2003). RQ was evaluated using 3-way ANOVA with temperature, oxygen status and horizon as factors. Before the analysis, data were root-square transformed (RQ) and normality was checked with the Shapiro–Wilk test. To evaluate the differences between the individual treatments we used the post-hoc Tukey HSD test.

For the statistical evaluation of soil enzymatic classes, microbial biomass, carbon-to-nutrient ratios (C_{MB} , $C:N_{MB}$, $C:P_{MB}$) and soil nutrients (nitrates – NO_3^- , ammonium ions – NH_4^+ , dissolved organic nitrogen – DON, potassium sulfate extractable carbon – C_{EX} , sodium bicarbonate extractable phosphorus – P_{EX}), generalized linear models with gamma distribution were used. Relationships between enzyme class potential activities and soil nutrients or microbial biomass were tested by linear regression analysis.

3. Results

3.1. Aerobic incubations

3.1.1. Microbial activity and soil carbon loss

Microbial activity, expressing itself as CO_2 production and O_2 consumption rates, was constant over time in all treatments of all horizons throughout the 4-month incubation period, as shown by the constant slopes of cumulative CO_2 production and O_2 consumption (Figs. S2 and S3). The total amount of CO_2 produced during incubation denotes the cumulative carbon loss (C_{LOSS}). C_{LOSS} over the incubation period was consistently higher, at all temperatures, in the O horizon, followed by the Ajj horizon and the BCg horizon ($F = 596.1$, $df = 2$, $p < 0.001$). C_{LOSS} from the O horizon was about ten times higher than from the Ajj horizon, which in turn was ten times higher than from the BCg horizon. The difference between horizons was so large that it accounted for 87% of all explained variability. Normalized to the amount of OC in the respective horizon, C_{LOSS} was still 5 times higher in the O horizon, compared to the BCg and Ajj horizons, which were similar to each other (Fig. 1). Linear regression combined with ridge regression revealed the amounts of carbon and phosphorus in soil microbial biomass as the best and most stable predictors of C_{LOSS} across horizons ($F = 4189.0$, $df = 1$, $p < 0.001$). The control exerted by the microbial biomass over C_{LOSS} is also indicated by the strong correlation between C_{MB} or P_{MB} and C_{LOSS} (Fig. 2). No such correlation, however, was found for N_{MB} .

In all horizons, C_{LOSS} increased exponentially with temperature. Temperature sensitivity, expressed as Q_{10} , was statistically indistinguishable between horizons (Fig. S4), with an overall mean of 2.41.

A contrasting temperature sensitivity was, however, found for O_2 consumption. While oxygen consumption increased exponentially with temperature in the O horizon, in the Ajj and BCg horizons it increased only between $4^\circ C$ and $12^\circ C$ and then decreased again between $12^\circ C$ and $20^\circ C$ (Fig. 3a). This pattern was consistent during the whole incubation period (Fig. S3). T_{MAX} of O_2 consumption was estimated as $13.1^\circ C$ for the Ajj and $12.0^\circ C$ for the BCg horizon.

The respiration quotient ($RQ = CO_2/O_2$) was significantly higher in the O horizon than in the Ajj and BCg horizons (Fig. 3b). It continuously increased with temperature in the O horizon, but only in a narrow range from 0.59 to 0.74. RQ in the Ajj and BCg horizons significantly increased only between $12^\circ C$ and $20^\circ C$, from 0.2 to 0.6 in the Ajj horizon and from 0.1 to 0.3 in the BCg horizon. These

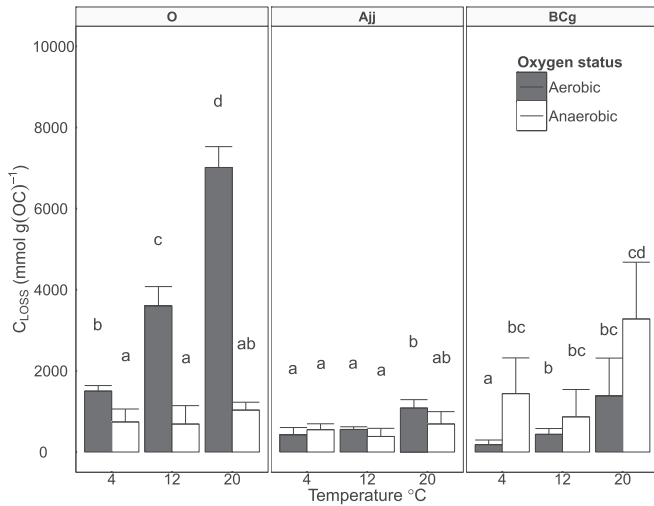


Fig. 1. Cumulative soil carbon loss (C_{LOSS}) from the organic (O), subducted organic (Ajj) and mineral (BCg) horizon, respectively, in 6 different incubation treatments (combinations of 3 temperatures and 2 oxygen levels). Filled bars represent aerobic treatments and open bars anaerobic treatments. Bar heights represent means and error bars standard deviations. Results of post-hoc comparisons of means within each horizon are indicated by letters above the bars.

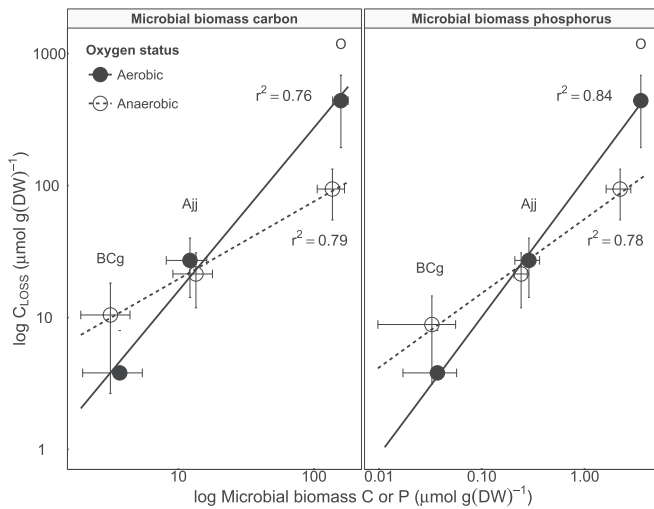


Fig. 2. Correlations between cumulative soil carbon loss (C_{LOSS}) and concentration of microbial biomass carbon and phosphorus. Open symbols show C_{LOSS} from the organic (O), subducted organic (Ajj) and mineral (BCg) horizon incubated anaerobically, averaged over 3 different temperature treatments (4, 12 and 20 °C), filled symbols show the same for aerobic incubations. Error bars express standard deviation of the mean. Coefficients of determination are given in the plot. Note that both axes use logarithmic scales.

large increases were caused by the different temperature responses of CO_2 production and O_2 consumption (Fig. 3a).

3.1.2. Microbial biomass

The microbial biomass (C_{MB}) present at the start of the incubation was highest in the O horizon, with significantly and sequentially lower values in the Ajj and BCg horizons ($F = 454.9$, $df = 2$, $p < 0.001$), reflecting the trend observed for C_{EX} and nutrient contents (Table 1). Normalized to the amount of OC, C_{MB} was 4–5 times higher in the O horizon than in the BCg and Ajj horizons (Fig. 1). During the incubation, C_{MB} decreased at 20 °C in the O horizon ($F = 12.7$, $df = 5$, $p < 0.001$; Fig. 4a) and increased at 12 °C in the Ajj horizon ($F = 3.1$, $df = 5$, $p = 0.02$; Fig. 4a). In the BCg horizon, C_{MB} increased significantly at 12 °C and 20 °C ($F = 6.9$, $df = 2$, $p < 0.001$).

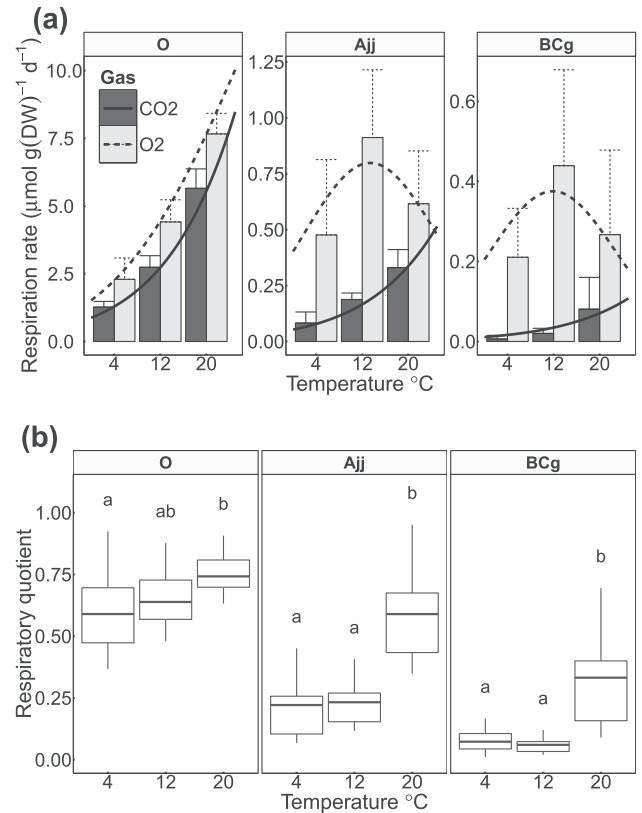


Fig. 3. (a): Respiration rate in aerobic conditions estimated from CO_2 production (gray bars) or O_2 consumption (black bars) in the organic (O), subducted organic (Ajj) and mineral (BCg) horizon in 3 different temperature treatments. Bar heights represent means and error bars standard deviations. Solid and dashed lines indicate temperature trends according to exponential (CO_2 production) and Gaussian (O_2 production) functions, respectively. (b): Box plots of the ratio of CO_2 production to O_2 consumption rates. The middle line represents median, boxes comprise second and third quartiles, and Whiskers show the lowest datum still within 1.5 IQR of the lower quartile, and the highest datum still within 1.5 IQR of the upper quartile.

Microbial biomass stoichiometry (Fig. 4b,c; $C:N_{MB}$, $C:P_{MB}$) differed between horizons, with higher initial $C:N_{MB}$ in the O horizon, and sequentially lower values in the Ajj and BCg horizons ($F = 24.4$, $df = 2$, $p < 0.001$) (Table 1). By contrast, initial $C:P_{MB}$ was highest in the BCg horizon, followed by lower values in the Ajj and then the O horizon ($F = 52.2$, $df = 2$, $p < 0.001$) (Table 1). $C:N_{MB}$ and $C:P_{MB}$ changed significantly during the incubation, with $C:P_{MB}$ decreasing in all three horizons, but significantly so only in the O horizon ($F = 176.1$, $df = 1$, $p < 0.001$). $C:N_{MB}$ showed horizon-specific responses: it decreased significantly in the O horizon ($F = 66.6$, $df = 1$, $p < 0.001$), whereas it increased in the Ajj horizon ($F = 7.0$, $df = 1$, $p = 0.011$). In the BCg horizon, $C:N_{MB}$ increased significantly over the incubation period only at 20 °C ($F = 14.3$, $df = 5$, $p < 0.001$) (Fig. 4b).

3.1.3. Soil enzymes

The total enzyme pool (E_{CNP}), per mol of microbial biomass, was highest in the BCg horizon, with sequentially lower values in the Ajj and O horizons, at the beginning of the incubation ($F = 79.6$, $df = 2$, $p < 0.001$) (Fig. S5). During the incubation, E_{CNP} decreased significantly in the Ajj and BCg horizons but not in the O horizon. Regardless of the decrease in Ajj and BCg horizons, E_{CNP} remained lowest in the O horizon ($F = 45.5$, $df = 2$, $p < 0.001$). The initial differences in E_{CNP} between Ajj and BCg horizons decreased during the incubation period, with both horizons yielding similar values at the end of the incubation (Fig. S5). E_{CNP} was not significantly

affected by temperature in the Ajj and BCg horizons, whereas in the O horizon it increased with temperature ($F = 6.4$, $df = 2$, $p = 0.007$).

Over the incubation period, individual enzymes within E_{CNP} changed in all horizons, and so did the various classes of enzymes grouped with respect to nutrient acquisition (E_C , E_N and E_P ; Fig. 5). In all horizons, the E_P and E_N pools decreased ($F = 3021.3$, $df = 5$, $p < 0.001$, and $F = 954.7$, $df = 5$, $p < 0.001$, respectively) compared to their initial values (Fig. 5). The E_C pool increased in the O horizon, but decreased in the Ajj and BCg horizons ($F = 2591.3$, $df = 5$, $p < 0.001$). The increase of the E_C pool in the O horizon reflected the increase of both the hydrolytic enzymes (cellobiosidase and β -glucosidase).

Like hydrolytic enzymes, phenoloxidases decreased in relation to their initial values in Ajj and BCg horizons (Fig. 6), whereas they increased in the O horizon ($F = 2591.3$, $df = 5$, $p < 0.001$). There was an insignificant increase of phenoloxidases with temperature in the O horizon. In BCg and Ajj horizons, phenoloxidases were highest at 12 °C.

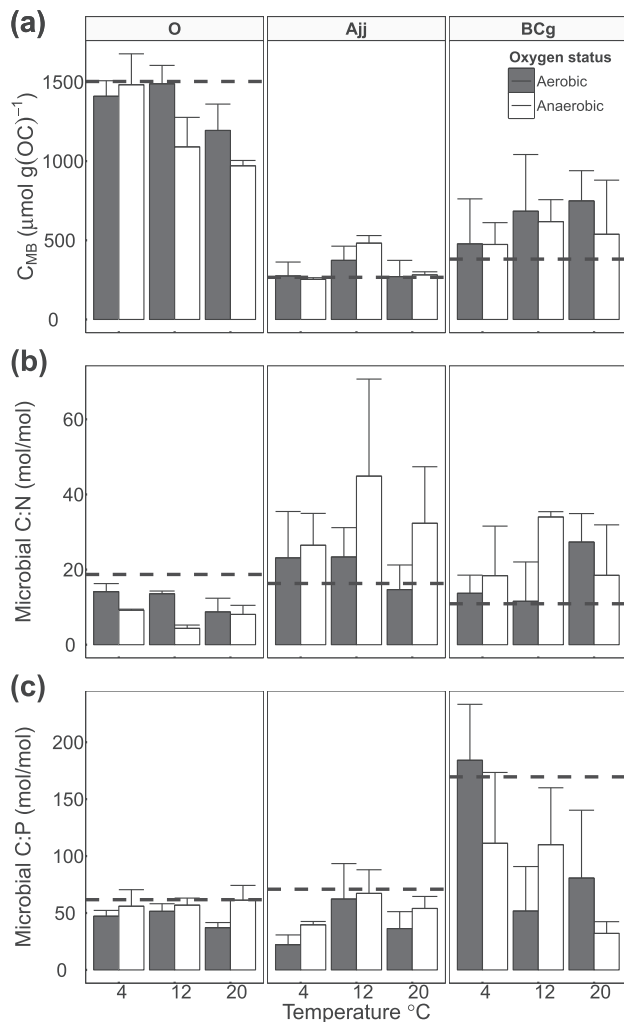


Fig. 4. Microbial biomass carbon (a), microbial biomass C:N (b) and C:P (c) in the organic (O), subducted organic (Ajj) and mineral (BCg) horizon in 6 different treatments. Filled bars represent aerobic treatments and open bars anaerobic treatments. Bar heights represent means and error bars standard deviations. Dashed horizontal lines show values at the start of the experiment.

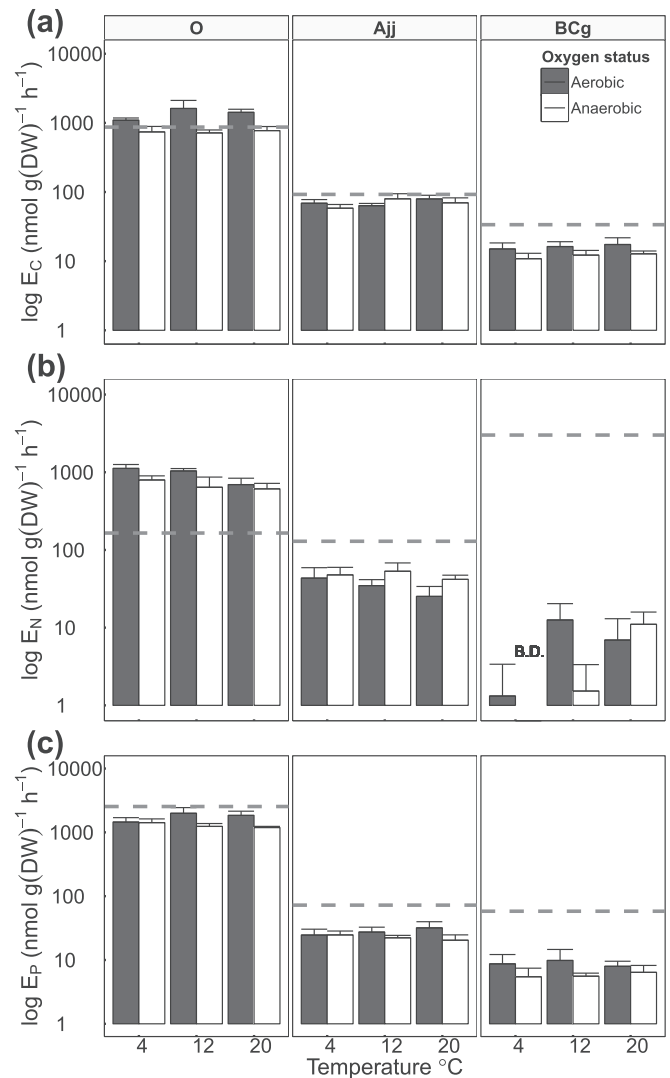


Fig. 5. E_C (a), E_N (b) and E_P (c) enzyme classes in the organic (O), subducted organic (Ajj) and mineral (BCg) horizon in 6 different treatments. Filled bars represent aerobic treatments and open bars anaerobic treatments. Bar heights represent means and error bars standard deviations. Dashed horizontal lines show values at the start of the experiment. All enzyme classes are defined as sums of two different hydrolytic enzymes ($E_C = \beta$ -glucosidase + cellobiosidase; $E_N = \text{alanin-aminopeptidase} + \text{leucine-aminopeptidase}$; $E_P = \text{phosphoesterase} + \text{phosphodiesterase}$). Note that y-axes have logarithmic scale.

3.2. Anaerobic incubations

3.2.1. Microbial activity and soil carbon loss

As was the case under aerobic conditions, CO_2 production rates under anaerobic conditions were constant throughout the incubation at all temperatures and in all horizons (Fig. S2). The total amount of CO_2 produced by microbial activity during incubation represents the cumulative C_{LOSS} from the Ajj and BCg horizons, where no methane production was detected. In the O horizon, CH_4 production occurred from the 9th week to the end of incubation and thus C_{LOSS} was given by the sum of cumulative CO_2 and CH_4 production (Fig. 1). At the end of the incubation, CH_4 production represented 12, 39 and 42% of C_{LOSS} at 4, 12 and 20 °C, respectively.

As under aerobic conditions, C_{LOSS} was higher at all temperatures in the O horizon, followed by the Ajj and then the BCg horizon ($F = 44.4$, $df = 2$, $p < 0.001$), although the differences were not as pronounced as under aerobic conditions. However, normalized to

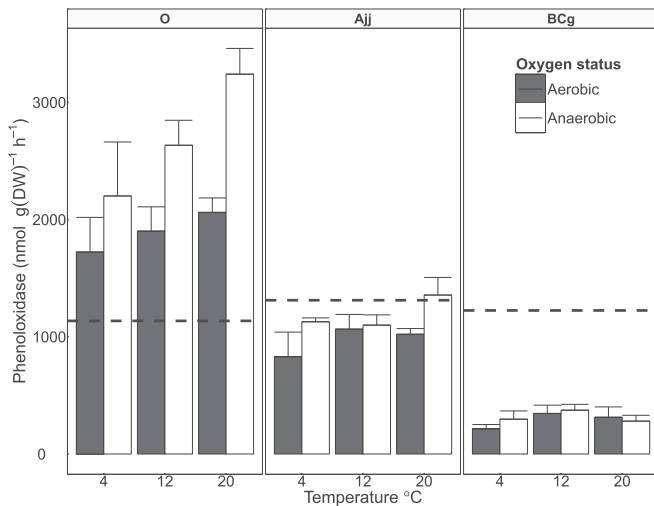


Fig. 6. Phenoloxidases in the organic (O), subducted organic (Ajj) and mineral (BCg) horizon in 6 different treatments. Filled bars represent aerobic treatments and open bars anaerobic treatments. Bar heights represent means and error bars standard deviations. Dashed horizontal lines show values at the start of the experiment.

the amount of OC, C_{LOSS} was highest in the BCg, followed by the O and then Ajj horizon (Fig. 1). C_{LOSS} again strongly correlated with C_{MB} and P_{MB} (Fig. 2), a similar response as in aerobic conditions, although it increased more slowly with both C_{MB} and P_{MB} .

The temperature sensitivity of C_{LOSS} under anaerobic conditions was generally lower than under aerobic conditions (Fig. S4). C_{LOSS} did not increase between 4 °C and 12 °C and increased only slightly between 12 °C and 20 °C (Fig. 1). Temperature sensitivity was again statistically indistinguishable between horizons, regardless of the contribution of CH_4 production to C_{LOSS} in the O horizon. The overall mean temperature sensitivity (Q_{10}) for all horizons was 1.38.

3.2.2. Microbial biomass

C_{MB} changes during the anaerobic incubation followed a similar pattern compared with the aerobic treatment (Fig. 4). C_{MB} in the O horizon decreased during incubation at 20 °C but, in contrast to the aerobic treatment, it also decreased at 12 °C ($F = 8.6$, $df = 1$, $p = 0.015$). C_{MB} in the Ajj horizon increased at 12 °C, similarly to the aerobic treatment ($F = 67.3$, $df = 2$, $p < 0.001$). C_{MB} in the BCg horizon increased at all temperatures, but this increase was not significant.

$C:N_{MB}$ (Fig. 4b,c) in the O horizon decreased ($F = 36.5$, $df = 1$, $p < 0.001$) during the incubation, similarly to the aerobic treatment but to a greater degree. $C:P_{MB}$ did not change during the incubation and thus there was no detectable temperature effect. In the Ajj horizon, $C:N_{MB}$ increased at 4 °C, but in contrast to the aerobic treatment, it decreased at higher temperatures. The $C:N_{MB}$ decrease was dependent on incubation temperature ($F = 55.9$, $df = 1$, $p < 0.001$). $C:P_{MB}$ decreased only at 4 and 20 °C, consistent with the response under aerobic conditions. In the BCg horizon, $C:N_{MB}$ increased at 4 and 12 °C, but decreased at 20 °C ($F = 28.6$, $df = 2$, $p < 0.001$). $C:P_{MB}$ decreased at all temperatures and the decrease was highest at 20 °C ($F = 12.2$, $df = 1$, $p < 0.001$).

3.2.3. Soil enzymes

Total enzyme pools (E_{CNP}), per mol C_{MB} , were nearly identical to those found under aerobic conditions (Fig. S5). The only difference was a steeper increase with temperature in the O horizon. In contrast to the aerobic treatment, all E_C ($F = 2009.2$, $df = 5$, $p < 0.001$), E_N ($F = 566.1$, $df = 5$, $p < 0.001$) and E_P ($F = 2788.8$, $df = 5$, $p < 0.001$) pools decreased during the incubation in all horizons

(Fig. 5). No temperature effect was found except for an E_N increase with temperature in the BCg horizon ($F = 11.5$, $df = 2$, $p = 0.027$).

In general, phenoloxidases showed similar trends to those under aerobic conditions in O and BCg horizons (Fig. 6). In the BCg horizon the trend was identical, but in the O horizon phenoloxidases increased more steeply with temperature and were higher than those found under aerobic conditions at all temperatures. In the Ajj horizon, phenoloxidase activities were higher compared to the aerobic treatment at 4 and 20 °C and were the same at 12 °C.

3.3. Link between microbial biomass, enzymes, C and nutrient availability

Detailed information about C and nutrient availabilities in the different horizons and their changes during incubation is given in Supplementary Results. Across the six temperature/oxygen treatments, changes of microbial biomass, hydrolytic enzymes and the main macronutrients during the incubation were well correlated with each other in the O horizon, but not in the Ajj and BCg horizons (Table 2, Figs. S7 and S8). In the O horizon, E_C , E_N and E_P pools were negatively related to available C (C_{EX}), N (ammonia + nitrates) and P (P_{EX}) concentration, respectively. Furthermore, the E_N pool was positively related to $C:N_{MB}$ and both E_C and E_P were negatively related to $C:P_{MB}$. No significant relationship was found in the BCg horizon. The only significant relationship we found in the Ajj horizon was the negative relationship between E_P and $C:P_{MB}$. In contrast to hydrolytic enzymes, phenoloxidases were negatively related to C_{MB} only in the O horizon (Fig. S9). In the Ajj and BCg horizons, we found no relationship between phenoloxidases and any microbial or soil variables.

4. Discussion

We have shown that carbon loss from OC subducted through cryogenic soil movements was lower by one order of magnitude than from organic top soil under both aerobic and anaerobic conditions in absolute terms. In relative terms, C_{LOSS} per unit OC was still approx. 5 times lower compared to organic topsoil, which was similar to or lower than in mineral subsoil. We found that the amount of microbial biomass, which is much lower in the subducted organic horizon than in the top organic horizon, is responsible for this difference. We further investigated the factors controlling the amount of microbial biomass in subducted organic horizon. We argue that microbial biomass is not controlled by the carbon and nutrient supply from degradation of subducted OC by extracellular enzymes. While microbial biomass and nutrient availability are related to extracellular enzyme pools in the organic topsoil, these variables are unrelated in the subducted organic horizon. We suggest that allochthonous material from top organic soil affects microbial biomass in subducted organic and mineral soil horizons. Temperature and oxygen level were identified as secondary controls on C_{LOSS} .

4.1. Temperature sensitivity of soil carbon loss and its link to microbial biomass

C_{LOSS} exponentially increased with temperature, with a mean Q_{10} value of 2.41 across all horizons under aerobic conditions. The 95% confidence interval (95% CI) was 2.36–2.54, so the temperature sensitivity of OC decomposition across horizons was indistinguishable from the value of 2.48, which is predicted by metabolic theory across ecosystems (Brown et al., 2004; Allen et al., 2005; Allen and Gillooly, 2009; Yvon-Durocher et al., 2012). This theory postulates that C_{LOSS} from soil results from two variables: (i) the amount of microbial biomass and (ii) its respiration rate, which is

Table 2
Results of linear regression between different microbial (C:P_{MB} – microbial biomass C:P, C:N_{MB} – microbial biomass C:N) and soil variables (C_{EX} – K₂SO₄ extractable C, N_{MIN} – sum of K₂SO₄ extractable ammonium and nitrates, P_{EX} – NaHCO₃ extractable P) and enzyme categories in respect to C (E_C), N (E_N) and P (E_P) for top organic (O), subducted organic (Ajj) and mineral (BCg) soil horizons incubated under aerobic and anaerobic conditions and 3 different temperatures (4, 12 and 20 °C). Table shows slopes, R² and p values of linear regression. Statistically significant regressions are given in bold face.

Horizon	Enzyme category	Microbial variables	Soil variables	R ²	slope		p	
O	E _C	C:P _{MB}	C _{EX}	0.56	0.39	–20.8	–19.4	<0.001
	E _N	C:N _{MB}	N _{MIN}	0.54	0.37	54.5	–32.0	<0.001
	E _P	C:P _{MB}	P _{EX}	0.31	0.20	–18.8	–0.8	<0.001
Ajj	E _C	C:P _{MB}	C _{EX}	–0.02	–0.03	–0.1	–0.1	0.504
	E _N	C:N _{MB}	N _{MIN}	0.01	–0.02	0.3	8.6	0.287
	E _P	C:P _{MB}	P _{EX}	0.16	0.06	–0.2	–0.1	0.012
BCg	E _C	C:P _{MB}	C _{EX}	–0.02	–0.02	0.0	–0.3	0.458
	E _N	C:N _{MB}	N _{MIN}	–0.01	0.02	0.1	30.5	0.389
	E _P	C:P _{MB}	P _{EX}	–0.04	0.07	0.0	–0.2	0.734

invariably affected by temperature in all heterotrophic microorganisms using oxygen as electron acceptor. In agreement with the first postulate, absolute C_{LOSS} was well correlated with microbial biomass across all horizons in our experiment. As to the second postulate, the temperature sensitivity of C_{LOSS} was uniform across horizons and we did not observe any major change of microbial biomass within any horizon. Normalized to microbial biomass, the temperature response of microbial specific respiration activity (CO₂ production rate per unit biomass in the last week of the experiment, just before microbial biomass assessment) was, in accord with the metabolic theory, almost identical in all horizons (Fig. S9c).

C_{LOSS} in anaerobic conditions occurred predominantly through CO₂ production while the contribution of methanogenesis was negligible in all horizons, indicating that fermentations and anaerobic respiration were the principal processes driving C_{LOSS}. The temperature sensitivity of C_{LOSS} (Q₁₀ = 1.38, 95% CI = 1.06–1.58) was close to 1.41, the mean value for data obtained from a range of arctic soils (Treat et al., 2015). However, our Q₁₀ is still within the range of 0.67–4.10 reported by Treat et al. (2015).

C_{LOSS} showed lower temperature sensitivity than under aerobic conditions, but again it was the same in all soil horizons. In contrast to aerobic conditions, we found a significant decrease of microbial biomass in the O horizon at 12 and 20 °C, which might affect C_{LOSS} from the O horizon at higher temperatures. Normalized to microbial biomass, specific respiration activity at the end of the incubation experiment showed different temperature sensitivities for different horizons, being higher in the Ajj and BCg horizons than in the O horizon (Fig. S9c). We suggest that temperature sensitivity of C_{LOSS} under anaerobic conditions reflects the temperature sensitivities of different pathways of anaerobic metabolism. In anaerobic conditions inorganic and organic electron acceptors are used and metabolic rate as well as specific respiration activity depends on e[–] acceptors, which could be expected to differ between horizons. If inorganic e[–] acceptors prevail, specific respiration activity is higher than when predominantly organic e[–] acceptors are used. It is very likely that organic e[–] acceptors prevailed in the O horizon, which lacks inorganic e[–] acceptors, and that the role of inorganic e[–] acceptors would be greater in Ajj and BCg horizons. Gentsch et al. (2015b) found high concentrations of oxalate-extractable Fe, which goes into solution at the initial stage of dissimilatory Fe (III) reduction in the BCg and Ajj horizons at our study site. In Ajj and

BCg horizons, Fe (III) could be an important e[–] acceptor, to which microorganisms are able to transfer electrons directly or via humic substances (Lovley et al., 1996), which are especially abundant in the Ajj horizon (Gentsch et al., 2015b).

The effects of temperature and oxygen availability on C_{LOSS} were relatively small compared to the effect of microbial biomass, which explained most of the variability in the data. The proportion of C_{MB} in OC decreased in the order O > BCg > Ajj. The Ajj horizon had the lowest proportion of C_{MB} in OC, and accordingly, the C_{LOSS} per OC observed here was similar or even lower than in the mineral BCg horizon. Similar results were also shown by Wild et al. (2014) and Kaiser et al. (2007) in arctic soils. The low proportion of C_{MB} in OC in the Ajj horizon suggests that the subducted organic horizon contains a large amount of organic carbon that is barely accessible to the microbial community. This could be connected to lower OC quality (Gentsch et al., 2015b) and inefficient enzymatic OC depolymerization (Gittel et al., 2014; Schneckner et al., 2014). Independently of temperature, low quality OC degradation in subducted organic horizons does not provide a sufficient supply of carbon and nutrients to maintain greater microbial biomass. Microbial biomass in the Ajj horizon remained approximately the same at all temperatures (Fig. 4a).

4.2. Broken link between microbial biomass, enzymes, C and nutrient availability

Lower OC quality in subducted organic or mineral soil horizons is the result of a greater degree of OC processing compared with topsoil horizons (Gentsch et al., 2015b). In mineral horizons, most of the OC is associated with clay-sized minerals, and in subducted organic matter as coprecipitates with hydrolyzable Fe and Al as well. Thus, the microbial community has to overcome more constraints to decompose OC in Ajj and BCg horizons than in the O horizon. It explains why C_{MB} relative to OC is lower in Ajj and BCg horizons than in the O horizon (Fig. 4a).

To overcome chemical–physical constraints the microbial community produces extracellular enzymes. First oxidative enzymes cleave aromatic ring structures and break C–C bonds in phenolic and aliphatic compounds, then hydrolytic enzymes can utilize liberated C and N chains, which become available to microbes (Kouno et al., 2002; Sinsabaugh, 2010; Sinsabaugh and Shah, 2012). The reaction of oxidative enzymes with their substrate is

considered to be the rate limiting step of low quality OC decomposition (Schimel and Weintraub, 2003; Allison, 2006; Herman et al., 2008). This step requires more energy than the reaction of hydrolytic enzymes with their substrate and is connected with higher activation energy and thus higher temperature sensitivity (Conant et al., 2011). Decomposition of low quality OC is therefore considered to be more temperature sensitive than decomposition of high quality OC (Conant et al., 2008). Based upon that assumption we expected an increase of C and nutrient supply from enzymatic decomposition of low quality OC at higher temperatures (Agren and Wetterstedt, 2007) in the Ajj horizon, followed by microbial biomass increase, which would effectively increase the temperature sensitivity of C_{LOSS} . But microbial biomass remained almost unchanged at all temperatures and we did not observe any difference in temperature sensitivity of C_{LOSS} between horizons, which naturally differ in OC quality. We argue that instead of relying on the energetically demanding production of extracellular enzymes, the microbial community in the Ajj and BCg horizons relies on the flux of allochthonous material from the topsoil organic horizon bypassing chemical–physical constraints (Fig. 7). Nutrient and enzyme pools consist largely of allochthonous nutrients and enzymes in both horizons. By separating the horizons for the experiment we interrupted the flux of enzymes and nutrients from the topsoil horizon. Allochthonous enzymes and nutrients, which were present at the start of the incubation in the Ajj and BCg horizons, were gradually degraded, and autochthonous production was minor, resulting in decreasing nutrient and enzyme pools. This broke the links between microbial biomass and enzymes, C and nutrient availability, respectively (Figs. S6 and S7 and Table 2). We see three lines of evidence for that interpretation:

- (i) Enzyme pools in the Ajj and BCg horizons were surprisingly high at the start of the incubation, which is unlikely to be the product of microbial activity in those horizons. There is some uncertainty regarding phenoloxidase assessment in Ajj and BCg horizons. These horizons contain more reactive Fe than the O horizon (Gentsch et al., 2015b). Reactive Fe was shown to be able to oxidize the substrate L-DOPA and cause overestimation of phenoloxidase activity (Hall and Silver, 2013). However, not only phenoloxidases but also all six hydrolytic enzymes showed high potential activities in Ajj and BCg horizons, especially at the start of the incubation. When enzyme pools were calculated per mol of microbial biomass, they were greater by one order of magnitude than in the O horizon, and 3 to 4 times higher than at the end of the

incubation (Fig. S5). Such huge enzymatic pools are unlikely to be composed solely of autochthonous enzymes released by microbes in these horizons. Enzyme production is an energy-demanding process, and due to its negative energy balance, decomposition of low quality OC cannot serve as a sufficient energy source for the required production of enzymes (Fontaine and Barot, 2005; Moorhead and Sinsabaugh, 2006; Fontaine et al., 2007; Allison, 2012). Thus enzyme pools in Ajj and BCg horizons were composed mainly of allochthonous enzymes, which degraded spontaneously during incubation and did not specifically target OC in this horizon.

- (ii) Spontaneity of decrease of both oxidative and hydrolytic enzymes is supported by the fact that enzyme pools decreased without any link to microbial biomass stoichiometry and nutrient availability (Figs. S6 and S7). Hydrolytic enzymes (especially E_N and E_P) decreased even though nutrient concentration decreased (NH_4^+ , NO_3^- and $P-PO_4$, Table S1). By contrast, the total enzyme pool slightly increased in the O horizon. Enzymes were negatively related to carbon and nutrient availability in this horizon. The greater nutrient availability was, the smaller was the enzyme pool, as microbes were provided with sufficient amounts of nutrients and enzyme production was not needed (Figs. S6 and S7). The enzyme pool was also related to microbial stoichiometry, indicating a direct link between microbes and enzyme activity. This was not seen in Ajj and BCg horizons.
- (iii) Low specificity of enzymes was indicated by a significantly higher ratio of phenoloxidases to hydrolases in the Ajj (7.9) and BCg (12.1) horizons than in the O horizon (0.7), which indicates disruption of the enzyme cascade that is needed for efficient low quality OC degradation and effective supply of C and nutrients to microbial biomass. Unspecific high phenoloxidase activity in the Ajj and BCg horizons led to an increase of DOC and DON and disrupted the ratio between CO_2 production and O_2 consumption (RQ; Fig. 3b). The RQ values below 0.6 reported here (down to 0.1 and 0.2 in the BCg and Ajj horizons, respectively) have not previously been observed in soil incubation studies (Dilly, 2003), suggesting an additional O_2 -consuming process such as oxidative processes mediated by phenoloxidases. The amounts of CO_2 produced and O_2 consumed during microbial metabolism should be proportional. For carbohydrates, which are believed to be the most common carbon source in soils, the RQ is exactly 1. Under natural conditions, the vast majority of studies have shown RQ values ranging from 0.7 to 1.2 in aquatic ecosystems (Berggren et al., 2012), and from 0.6 to 1 in soils (Li et al., 2014). Taking into account the CO_2 production rates in Ajj and BCg horizons and the lowest RQ value found in the literature, we estimated that the potential amount of O_2 used by phenoloxidases could account for up to an average of 75, 70 and 23% of the microbial oxygen demand in the Ajj horizon and 96, 93 and 58% of it in the BCg horizon at 4, 12 and 20 °C, respectively.

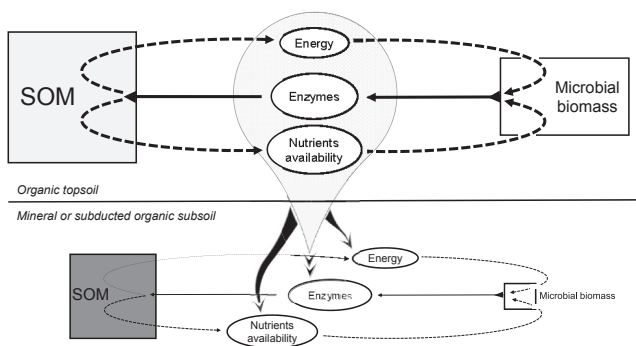


Fig. 7. Diagram of connections between microbial biomass, soil OC, enzymatic production and nutrient availability within and between soil horizons. The energy availability for enzymatic production within each soil horizon is critical; the low quality soil OC of subsoil horizons provides no energy and thus enzymatic production in subsoil horizons is directly dependent on fresh carbon flow from the topsoil organic horizon. Together with fresh carbon, extracellular enzymes and nutrients are transported down the soil profile, affecting enzymatic pools and nutrient availability of subsoil horizons.

4.3. Subducted organic carbon under climate change

We found that C_{LOSS} from cryoturbated arctic soils is primarily driven by microbial biomass and that the temperature and oxygen level has a secondary effect on the metabolic rate of microorganisms. The subducted organic horizon turned out to contain little microbial biomass and therefore its C_{LOSS} was low under both aerobic and anaerobic conditions over the whole range of temperatures investigated. The proportion of microbial biomass to OC

in the subducted organic horizon was the lowest of all horizons studied. All lines of evidence suggest that this pattern was caused by chemical–physical characteristics of subducted OC (Gentsch et al., 2015a) whose decomposition does not provide the microbial community with a sufficient supply of C and nutrients. In field conditions, the microbial community in subducted organic horizons relies on the allochthonous influx of fresh carbon and nutrients from the topsoil, while decomposition of autochthonous, physically and chemically protected OC lags behind (Fig. 7). It suppresses the effect of autochthonous OC quality on temperature sensitivity of carbon loss and stabilizes subducted OC (Kaiser et al., 2007). This can be perceived as a negative priming effect (Kuzyakov et al., 2000). We believe that this is a common mechanism which “protects” subducted OC from decomposition in cryoturbated arctic soils. Patterns of vertical carbon fluxes in cryoturbated arctic soils were also observed by Gentsch et al. (2015b) and Xu et al. (2009).

Organic carbon supply by the organic topsoil is critical for subducted OC decomposition, as has already been suggested by Wild et al. (2014). If the flux of carbon and nutrients is small, autochthonous subducted OC may be protected from decomposition, and microbes utilize mainly allochthonous C and nutrients from influx (negative priming effect; Kuzyakov et al., 2000). If the flux of C and nutrients is high (e.g. after uplift of subducted OC and root ingrowth), microbial activity is stimulated to a degree that autochthonous subducted OC is decomposed as well (positive priming effect; Kuzyakov et al., 2000; Wild et al., 2014). The positive priming effect, destabilizing subducted OC, may result from input of exudates. Under future climate change the priming may even be enhanced by an expected shift in the composition of the plant community, producing litter of higher quality (Cable et al., 2009; DeMarco et al., 2014). Under this scenario, a substantial loss from subducted OC, which is protected at present, may occur.

Acknowledgments

This study was supported by the International Program CryoCARB (MSM 7E10073 - CryoCARB) and GAJU project no. 146/2013P. We thank two anonymous reviewers for their constructive comments, which helped us to improve the manuscript.

Appendix A. Supplementary data

Supplementary data related to this article can be found at <http://dx.doi.org/10.1016/j.soilbio.2015.07.013>.

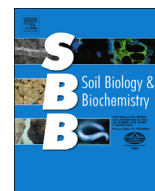
References

- Agren, G.I., Wetterstedt, J.A.M., 2007. What determines the temperature response of soil organic matter decomposition? *Soil Biology & Biochemistry* 39, 1794–1798.
- Allen, A.P., Gillooly, J.F., 2009. Towards an integration of ecological stoichiometry and the metabolic theory of ecology to better understand nutrient cycling. *Ecology Letters* 12, 369–384.
- Allen, A.P., Gillooly, J.F., Brown, J.H., 2005. Linking the global carbon cycle to individual metabolism. *Functional Ecology* 19, 202–213.
- Allison, S.D., 2006. Brown ground: a soil carbon analogue for the green world hypothesis? *American Naturalist* 167, 619–627.
- Allison, S.D., 2012. A trait-based approach for modelling microbial litter decomposition. *Ecology Letters* 15, 1058–1070.
- Allison, S.D., Wallenstein, M.D., Bradford, M.A., 2010. Soil-carbon response to warming dependent on microbial physiology. *Nature Geoscience* 3, 336–340.
- Berggren, M., Lapiere, J.-F., del Giorgio, P.A., 2012. Magnitude and regulation of bacterioplankton respiratory quotient across freshwater environmental gradients. *Isme Journal* 6, 984–993.
- Bockheim, J.G., 2007. Importance of cryoturbation in redistributing organic carbon in permafrost-affected soils. *Soil Science Society of America Journal* 71, 1335.
- Bockheim, J.G., Tarnocai, C., 1998. Recognition of cryoturbation for classifying permafrost-affected soils. *Geoderma* 81, 281–293.
- Brookes, P.C., Landman, A., Pruden, G., Jenkinson, D.S., 1985. Chloroform fumigation and the release of soil-nitrogen - a rapid direct extraction method to measure microbial biomass nitrogen in soil. *Soil Biology & Biochemistry* 17, 837–842.
- Brookes, P.C., Powlson, D.S., Jenkinson, D.S., 1982. Measurement of microbial biomass phosphorus in soil. *Soil Biology & Biochemistry* 14, 319–329.
- Brown, J.H., Gillooly, J.F., Allen, A.P., Savage, V.M., West, G.B., 2004. Toward a metabolic theory of ecology. *Ecology* 85, 1771–1789.
- Cable, J.M., Ogle, K., Tyler, A.P., Pavao-Zuckerman, M.A., Huxman, T.E., 2009. Woody plant encroachment impacts on soil carbon and microbial processes: results from a hierarchical Bayesian analysis of soil incubation data. *Plant and Soil* 320, 153–167.
- Conant, R.T., Drijber, R.A., Haddix, M.L., Parton, W.J., Paul, E.A., Plante, A.F., Six, J., Steinweg, J.M., 2008. Sensitivity of organic matter decomposition to warming varies with its quality. *Global Change Biology* 14, 868–877.
- Conant, R.T., Ryan, M.G., Agren, G.I., Birge, H.E., Davidson, E.A., Eliasson, P.E., Evans, S.E., Frey, S.D., Giardina, C.P., Hopkins, F.M., Hyvonen, R., Kirschbaum, M.U.F., Lavelle, J.M., Leifeld, J., Parton, W.J., Steinweg, J.M., Wallenstein, M.D., Wetterstedt, J.A.M., Bradford, M.A., 2011. Temperature and soil organic matter decomposition rates - synthesis of current knowledge and a way forward. *Global Change Biology* 17, 3392–3404.
- Davidson, E.A., Janssens, I.A., 2006. Temperature sensitivity of soil carbon decomposition and feedbacks to climate change. *Nature* 440, 165–173.
- Davidson, E.A., Samanta, S., Caramori, S.S., Savage, K., 2012. The Dual Arrhenius and Michaelis-Menten kinetics model for decomposition of soil organic matter at hourly to seasonal time scales. *Global Change Biology* 18, 371–384.
- DeMarco, J., Mack, M.C., Bret-Harte, M.S., 2014. Effects of arctic shrub expansion on biophysical vs. biogeochemical drivers of litter decomposition. *Ecology* 95, 1861–1875.
- Dilly, O., 2003. Regulation of the respiratory quotient of soil microbiota by availability of nutrients. *FEMS Microbiology Ecology* 43, 375–381.
- Fontaine, S., Barot, S., 2005. Size and functional diversity of microbe populations control plant persistence and long-term soil carbon accumulation. *Ecology Letters* 8, 1075–1087.
- Fontaine, S., Barot, S., Barre, P., Bdioui, N., Mary, B., Rumpel, C., 2007. Stability of organic carbon in deep soil layers controlled by fresh carbon supply. *Nature* 450, 277–U210.
- Gentsch, N., Mikutta, R., Alves, R.J.E., Bárta, J., Čapek, P., Gittel, A., Hugelius, G., Kuhry, P., Lashchinskiy, N., Palmtag, J., Richter, A., Santrůčková, H., Schneckler, J., Shibistova, O., Urich, T., Wild, B., Guggenberger, G., 2015a. Storage and transformation of organic matter fractions in cryoturbated permafrost soils across the Siberian Arctic. *Biogeosciences Discuss* 12, 2697–2743.
- Gentsch, N., Mikutta, R., Shibistova, O., Wild, B., Schneckler, J., Richter, A., Urich, T., Gittel, A., Santrůčková, H., Bárta, J., Lashchinskiy, N., Mueller, C.W., Fuß, R., Guggenberger, G., 2015b. Properties and bioavailability of particulate and mineral-associated organic matter in Arctic permafrost soils, Lower Kolyma Region, Russia. *European Journal of Soil Science* 66, 722–734.
- Giardina, C.P., Ryan, M.G., 2000. Evidence that decomposition rates of organic carbon in mineral soil do not vary with temperature. *Nature* 404, 858–861.
- Gittel, A., Bárta, J., Kohoutova, I., Mikutta, R., Owens, S., Gilbert, J., Schneckler, J., Wild, B., Hannisdal, B., Maerz, J., Lashchinskiy, N., Čapek, P., Santrůčková, H., Gentsch, N., Shibistova, O., Guggenberger, G., Richter, A., Torsvik, V.L., Schleper, C., Urich, T., 2014. Distinct microbial communities associated with buried soils in the Siberian tundra. *Isme Journal* 8, 841–853.
- Godbold, D.L., Hoosbeek, M.R., Lukac, M., Cotrufo, M.F., Janssens, I.A., Ceulemans, R., Polle, A., Velthorst, E.J., Scarascia-Mugnozza, G., De Angelis, P., Miglietta, F., Peressotti, A., 2006. Mycorrhizal hyphal turnover as a dominant process for carbon input into soil organic matter. *Plant and Soil* 281, 15–24.
- Hall, S.J., Silver, W.L., 2013. Iron oxidation stimulates organic matter decomposition in humid tropical forest soils. *Global Change Biology* 19, 2804–2813.
- Harden, J.W., Koven, C.D., Ping, C.L., Hugelius, G., McGuire, A.D., Camill, P., Jorgenson, T., Kuhry, P., Michaelson, G.J., O'Donnell, J.A., Schuur, E.A.G., Tarnocai, C., Johnson, K., Grosse, G., 2012. Field information links permafrost carbon to physical vulnerabilities of thawing. *Geophysical Research Letters* 39.
- Herman, J., Moorhead, D., Berg, B., 2008. The relationship between rates of lignin and cellulose decay in aboveground forest litter. *Soil Biology & Biochemistry* 40, 2620–2626.
- Hugelius, G., Strauss, J., Zubrzycki, S., Harden, J.W., Schuur, E.A.G., Ping, C.L., Schirmer, L., Grosse, G., Michaelson, G.J., Koven, C.D., O'Donnell, J.A., Elberling, B., Mishra, U., Camill, P., Yu, Z., Palmtag, J., Kuhry, P., 2014. Estimated stocks of circumpolar permafrost carbon with quantified uncertainty ranges and identified data gaps. *Biogeosciences* 11, 6573–6593.
- Hyvonen, R., Agren, G.I., Dalias, P., 2005. Analysing temperature response of decomposition of organic matter. *Global Change Biology* 11, 770–778.
- IUSS Working Group WRB, 2007. World Reference Base for Soil Resources 2006. First Update 2007. Rome.
- Kaiser, K., Meyer, H., Biasi, C., Rusalimova, O., Barsukov, P., Richter, A., 2007. Conservation of soil organic matter through cryoturbation in arctic soils in Siberia. *Journal of Geophysical Research-Biogeosciences* 112.
- Knorr, W., Prentice, I.C., House, J.I., Holland, E.A., 2005. Long-term sensitivity of soil carbon turnover to warming. *Nature* 433, 298–301.
- Kouno, K., Wu, J., Brookes, P.C., 2002. Turnover of biomass C and P in soil following incorporation of glucose or ryegrass. *Soil Biology & Biochemistry* 34, 617–622.
- Kuzyakov, Y., Friedel, J.K., Stahr, K., 2000. Review of mechanisms and quantification of priming effects. *Soil Biology & Biochemistry* 32, 1485–1498.
- Li, X.Z., Rui, J.P., Xiong, J.B., Li, J.B., He, Z.L., Zhou, J.Z., Yannarell, A.C., Mackie, R.I., 2014. Functional potential of soil microbial communities in the maize rhizosphere. *Plos One* 9.

- Lovley, D.R., Coates, J.D., Blunt-Harris, E.L., Phillips, E.J.P., Woodward, J.C., 1996. Humic substances as electron acceptors for microbial respiration. *Nature* 382, 445–448.
- Moorhead, D.L., Sinsabaugh, R.L., 2006. A theoretical model of litter decay and microbial interaction. *Ecological Monographs* 76, 151–174.
- Nobel, P.S., Palta, J.A., 1989. Soil O₂ and CO₂ effects on root respiration of cacti. *Plant and Soil* 120, 263–271.
- Oechel, W.C., Hastings, S.J., Vourlitis, G., Jenkins, M., Riechers, G., Grulke, N., 1993. Recent change of arctic tundra ecosystems from a net carbon-dioxide sink to a source. *Nature* 361, 520–523.
- Olefeldt, D., Turetsky, M.R., Crill, P.M., McGuire, A.D., 2013. Environmental and physical controls on northern terrestrial methane emissions across permafrost zones. *Global Change Biology* 19, 589–603.
- Palmtag, J., Hugelius, G., Lashchinskiy, N., Tamstorf, M.P., Richter, A., Elberling, B., Kuhry, P., 2015. Storage, landscape distribution, and burial history of soil organic matter in contrasting areas of continuous permafrost. *Arctic Antarctic and Alpine Research* 47, 71–88.
- Pinhero, J., Bates, D., DebRoy, S., Sarkar, D., R Development Core Team, 2013. nlme: Linear and Nonlinear Mixed Effects Models. R package version 3, pp. 1–113.
- R Core Team, 2014. R: a Language and Environment for Statistical Computing. R Foundation for Statistical Computing, Vienna, Austria. URL: <http://www.R-project.org/>.
- Reichstein, M., Katterer, T., Andren, O., Ciais, P., Schulze, E.D., Cramer, W., Papale, D., Valentini, R., 2005. Temperature sensitivity of decomposition in relation to soil organic matter pools: critique and outlook. *Biogeosciences* 2, 317–321.
- Schädel, C., Schuur, E.A.G., Bracho, R., Elberling, B., Knoblauch, C., Lee, H., Luo, Y., Shaver, G.R., Turetsky, M.R., 2014. Circumpolar assessment of permafrost C quality and its vulnerability over time using long-term incubation data. *Global Change Biology* 20, 641–652.
- Schimel, J.P., Weintraub, M.N., 2003. The implications of exoenzyme activity on microbial carbon and nitrogen limitation in soil: a theoretical model. *Soil Biology & Biochemistry* 35, 549–563.
- Schnecker, J., Wild, B., Hofhansl, F., Alves, R.J.E., Barta, J., Čapek, P., Fuchslueger, L., Gentsch, N., Gittel, A., Guggenberger, G., Hofer, A., Kienzl, S., Knoltsch, A., Lashchinskiy, N., Mikutta, R., Santrúcková, H., Shibistova, O., Takriti, M., Urich, T., Weltin, G., Richter, A., 2014. Effects of soil organic matter properties and microbial community composition on enzyme activities in cryoturbated arctic soils. *Plos One* 9.
- Schuur, E.A.G., Bockheim, J., Canadell, J.G., Euskirchen, E., Field, C.B., Goryachkin, S.V., Hagemann, S., Kuhry, P., Lafleur, P.M., Lee, H., Mazhitova, G., Nelson, F.E., Rinke, A., Romanovsky, V.E., Shiklomanov, N., Tarnocai, C., Venevsky, S., Vogel, J.G., Zimov, S.A., 2008. Vulnerability of permafrost carbon to climate change: implications for the global carbon cycle. *Bioscience* 58, 701–714.
- Schuur, E.A.G., Vogel, J.G., Crummer, K.G., Lee, H., Sickman, J.O., Osterkamp, T.E., 2009. The effect of permafrost thaw on old carbon release and net carbon exchange from tundra. *Nature* 459, 556–559.
- Sierra, C.A., 2012. Temperature sensitivity of organic matter decomposition in the Arrhenius equation: some theoretical considerations. *Biogeochemistry* 108, 1–15.
- Sinsabaugh, R.L., 2010. Phenol oxidase, peroxidase and organic matter dynamics of soil. *Soil Biology & Biochemistry* 42, 391–404.
- Sinsabaugh, R.L., Shah, J.J.F., 2012. Ecoenzymatic stoichiometry and ecological theory. *Annual Review of Ecology, Evolution, and Systematics* 43, 313–343.
- Soil Survey Staff, 1999. Soil Taxonomy: a Basic System of Soil Classification for Making and Interpreting Soil Surveys. U.S. Department of Agriculture, Natural Resources Conservation Service.
- Steinweg, J.M., Dukes, J.S., Paul, E.A., Wallenstein, M.D., 2013. Microbial responses to multi-factor climate change: effects on soil enzymes. *Frontiers in Microbiology* 4.
- Thomas, G., 1982. Exchangeable cations. In: Page, A.L. (Ed.), *Methods of Soil Analysis, Part 2: Chemical and Microbiological Properties, Part 2*. American Society of Agronomy, Madison, Wisconsin, pp. 159–166.
- Treat, C.C., Natali, S.M., Ernakovich, J., Iversen, C.M., Lupascu, M., McGuire, A.D., Norby, R.J., Roy Chowdhury, T., Richter, A., Santrúcková, H., Schädel, C., Schuur, E.A.G., Sloan, V.L., Turetsky, M.R., Waldrop, M.P., 2015. A pan-Arctic synthesis of CH₄ and CO₂ production from anoxic soil incubations. *Global Change Biology* 21, 2787–2803.
- Tuomi, M., Vanhala, P., Karhu, K., Fritze, H., Liski, J., 2008. Heterotrophic soil respiration - comparison of different models describing its temperature dependence. *Ecological Modelling* 211, 182–190.
- Vance, E.D., Brookes, P.C., Jenkinson, D.S., 1987. An extraction method for measuring soil microbial biomass-C. *Soil Biology & Biochemistry* 19, 703–707.
- Wild, B., Schnecker, J., Alves, R.J.E., Barsukov, P., Barta, J., Čapek, P., Gentsch, N., Gittel, A., Guggenberger, G., Lashchinskiy, N., Mikutta, R., Rusalimova, O., Santrúcková, H., Shibistova, O., Urich, T., Watzka, M., Zrazhevskaya, G., Richter, A., 2014. Input of easily available organic C and N stimulates microbial decomposition of soil organic matter in arctic permafrost soil. *Soil Biology and Biochemistry* 75, 143–151.
- Xu, C., Guo, L., Ping, C.-L., White, D.M., 2009. Chemical and isotopic characterization of size-fractionated organic matter from cryoturbated tundra soils, northern Alaska. *Journal of Geophysical Research* 114.
- Yvon-Durocher, G., Caffrey, J.M., Cescatti, A., Dossena, M., del Giorgio, P., Gasol, J.M., Montoya, J.M., Pumpanen, J., Staehr, P.A., Trimmer, M., Woodward, G., Allen, A.P., 2012. Reconciling the temperature dependence of respiration across timescales and ecosystem types. *Nature* 487, 472–476.
- Zimov, S.A., Schuur, E.A.G., Chapin, F.S., 2006. Permafrost and the global carbon budget. *Science* 312, 1612–1613.

Paper 10

Wild B, Schnecker J, Alves RJE, Barsukov P, **Barta J**, Capek P, Gentsch N, Gittel A, Guggenberger G, Lashchinskiy N, Mikutta R, Rusalimova O, Santruckova H, Shibistova O, Urich T, Watzka M, Zrazhevskaya G, Richter A (2014) Input of easily available organic C and N stimulates microbial decomposition of soil organic matter in arctic permafrost soil. *SOIL BIOLOGY & BIOCHEMISTRY* 75:143-151.



Input of easily available organic C and N stimulates microbial decomposition of soil organic matter in arctic permafrost soil



Birgit Wild^{a,b,*}, Jörg Schnecker^{a,b}, Ricardo J. Eloy Alves^{b,c}, Pavel Barsukov^d, Jiří Bárta^e, Petr Čapek^e, Norman Gentsch^f, Antje Gittel^{b,g}, Georg Guggenberger^f, Nikolay Lashchinskiy^h, Robert Mikutta^f, Olga Rusalimova^d, Hana Šantrůčková^e, Olga Shibistova^{f,i}, Tim Urich^{b,c}, Margarete Watzka^a, Galina Zrazhevskayaⁱ, Andreas Richter^{a,b,**}

^a University of Vienna, Department of Microbiology and Ecosystem Science, Division of Terrestrial Ecosystem Research, Vienna, Austria

^b Austrian Polar Research Institute, Vienna, Austria

^c University of Vienna, Department of Ecogenomics and Systems Biology, Division of Archaea Biology and Ecogenomics, Vienna, Austria

^d Siberian Branch of the Russian Academy of Sciences, Institute of Soil Science and Agrochemistry, Novosibirsk, Russia

^e University of South Bohemia, Department of Ecosystems Biology, České Budějovice, Czech Republic

^f Leibniz University Hannover, Institute of Soil Science, Hannover, Germany

^g University of Bergen, Centre for Geobiology, Department of Biology, Bergen, Norway

^h Siberian Branch of Russian Academy of Sciences, Central Siberian Botanical Garden, Novosibirsk, Russia

ⁱ Siberian Branch of Russian Academy of Sciences, VN Sukachev Institute of Forest, Krasnoyarsk, Russia

ARTICLE INFO

Article history:

Received 17 January 2014

Received in revised form

1 April 2014

Accepted 6 April 2014

Available online 22 April 2014

Keywords:

Priming

Organic matter decomposition

Phospholipid fatty acid (PLFA)

Tundra

Permafrost

ABSTRACT

Rising temperatures in the Arctic can affect soil organic matter (SOM) decomposition directly and indirectly, by increasing plant primary production and thus the allocation of plant-derived organic compounds into the soil. Such compounds, for example root exudates or decaying fine roots, are easily available for microorganisms, and can alter the decomposition of older SOM (“priming effect”). We here report on a SOM priming experiment in the active layer of a permafrost soil from the central Siberian Arctic, comparing responses of organic topsoil, mineral subsoil, and cryoturbated subsoil material (i.e., poorly decomposed topsoil material subducted into the subsoil by freeze–thaw processes) to additions of ¹³C-labeled glucose, cellulose, a mixture of amino acids, and protein (added at levels corresponding to approximately 1% of soil organic carbon). SOM decomposition in the topsoil was barely affected by higher availability of organic compounds, whereas SOM decomposition in both subsoil horizons responded strongly. In the mineral subsoil, SOM decomposition increased by a factor of two to three after any substrate addition (glucose, cellulose, amino acids, protein), suggesting that the microbial decomposer community was limited in energy to break down more complex components of SOM. In the cryoturbated horizon, SOM decomposition increased by a factor of two after addition of amino acids or protein, but was not significantly affected by glucose or cellulose, indicating nitrogen rather than energy limitation. Since the stimulation of SOM decomposition in cryoturbated material was not connected to microbial growth or to a change in microbial community composition, the additional nitrogen was likely invested in the production of extracellular enzymes required for SOM decomposition. Our findings provide a first mechanistic understanding of priming in permafrost soils and suggest that an increase in the availability of organic carbon or nitrogen, e.g., by increased plant productivity, can change the decomposition of SOM stored in deeper layers of permafrost soils, with possible repercussions on the global climate.

© 2014 The Authors. Published by Elsevier Ltd. This is an open access article under the CC BY license (<http://creativecommons.org/licenses/by/3.0/>).

* Corresponding author. University of Vienna, Department of Microbiology and Ecosystem Science, Division of Terrestrial Ecosystem Research, Vienna, Austria. Tel.: +43 1 4277 76666.

** Corresponding author. University of Vienna, Department of Microbiology and Ecosystem Science, Division of Terrestrial Ecosystem Research, Vienna, Austria. Tel.: +43 1 4277 76660.

E-mail addresses: birgit.wild@univie.ac.at (B. Wild), andreas.richter@univie.ac.at (A. Richter).

1. Introduction

Soil organic matter (SOM) decomposition rates in permafrost soils are expected to increase with rising temperatures in the Arctic (Hartley et al., 2008; Conant et al., 2011). In addition to the direct temperature effect, warming might also indirectly affect SOM decomposition, mediated by an increase in plant net primary production. Higher plant productivity is accompanied by an increased input of plant-derived C into the soil (as root litter or root exudates), and can thus increase soil C stocks, as observed for a mineral subsoil in the Alaskan tundra (Sistla et al., 2013). In contrast, higher productivity was found to reduce soil C stocks in a sub-arctic system, offsetting the increase in above- and belowground plant biomass, and, consequently, leading to a net loss of C from the ecosystem (Hartley et al., 2012).

Plants supply the soil microbial community with a range of organic compounds that can be either immediately taken up by microorganisms (e.g., sugars, amino acids and organic acids from root exudation), or that can be easily decomposed (e.g., cellulose and protein from root litter). These organic compounds can stimulate the soil microbial community to decompose more SOM (“priming effect”; Bingeman et al., 1953), (i) by promoting microbial groups that target complex compounds of SOM (Fontaine et al., 2003), (ii) by providing the energy to break down these compounds (Blagodatskaya and Kuzyakov, 2008), or (iii) by providing C for microbial growth, thus increasing microbial N demand and facilitating N mining, i.e., the microbial breakdown of SOM to get access to N (Craine et al., 2007; Dijkstra et al., 2013).

The latter two mechanisms might be of particular importance in arctic soils. Microbial activity in arctic soils is considered N limited (Sistla et al., 2012), suggesting that an increased allocation of plant C to the soil might strongly stimulate N mining. Additionally, microbial activity in subsoil horizons in general is considered energy limited (Fontaine et al., 2007), as the subsoil is poorly rooted, and supply of plant-derived compounds from root exudation and root litter is scarce. With 80% of arctic SOM located below 30 cm (Tarnocai et al., 2009), a large amount of SOM might be protected from decomposition by energy limitation of microbial decomposers, and might thus be particularly susceptible to an increased input of plant-derived compounds. So far, it is unknown how SOM decomposition in different horizons of arctic permafrost soils will respond to an increased input of plant-derived organic compounds, and what mechanisms might be involved.

We here report on the susceptibility of different soil horizons from a tundra ecosystem in the central Siberian Arctic to an increased availability of organic compounds. In a priming experiment, we compared organic topsoil and mineral subsoil material, as well as cryoturbated material, i.e., topsoil material that was buried in the subsoil by freeze–thaw processes (Bockheim, 2007; Tarnocai et al., 2009). Cryoturbated organic matter is common in arctic soils, accounting for approximately 400 Gt of C (Harden et al., 2012). Although it is chemically similar to topsoil organic matter (Xu et al., 2009), it shows retarded decomposition as indicated by low respiration rates (Kaiser et al., 2007) and relatively old radiocarbon ages (Kaiser et al., 2007; Xu et al., 2009; Hugelius et al., 2010). We hypothesized that an increased availability of organic compounds would stimulate SOM decomposition in the subsoil (i.e., in mineral subsoil and cryoturbated horizons) by providing energy for microbial decomposers, but less so in the topsoil, where energy is not limiting. Additionally, we tested if priming of SOM decomposition was connected to N mining, by comparing the effect of organic substrates with and without N. We expected that N-containing substrates would result in a weaker priming effect than substrates without N, by reducing the dependence of the microbial

community on SOM as an N source. Finally, we investigated if priming of SOM decomposition was connected to a shift in microbial community composition.

To that end, we analyzed SOM-derived respiration and microbial community composition in soil samples amended with ^{13}C -labeled glucose, cellulose, amino acids, or protein, in comparison with unamended controls. We thus compared substrates containing N to substrates without N, as well as monomeric substrates to polymeric substrates. Since monomeric substrates are immediately available for microorganisms, whereas polymeric substrates need to be broken down by extracellular enzymes before microbial uptake, they might differ in their effect on microbial community composition and function, and thus on SOM decomposition (Fontaine et al., 2003).

2. Material & methods

2.1. Soil sampling

Soils were sampled on the Taymyr peninsula in the central Siberian Arctic ($72^{\circ} 29.57' \text{ N}$, $101^{\circ} 38.62' \text{ E}$), from a shrubby moss tundra (bioclimatic subzone D; CAVM Team, 2003) dominated by *Cassiope tetragona*, *Carex arctisibirica*, *Tomentypnum nitens* and *Aulacomnium turgidum*. The soil was described as a Turbic Cryosol according to the World Reference Base for Soil Resources (IUSS Working Group WRB, 2007) or Typic Aquiturbel according to the US Soil Taxonomy (Soil Survey Staff, 1999), with fine to coarse loamy texture and an active layer depth of around 80 cm at the time of sampling in August 2011. We took samples from three soil horizons in the active layer: We sampled the OA horizon (topsoil material), as well as a buried Ajj (cryoturbated material) and the adjacent BCg horizon (mineral subsoil material), the latter two from a depth of 50–70 cm. Soils were sampled in a 2 m-wide soil profile by pooling samples taken horizontally with a metal soil corer within each horizon. We took care that the mineral subsoil material sampled did not include buried organic material and vice versa. Living roots were carefully removed and samples homogenized by hand directly after sampling. Carbon and nitrogen contents of the individual horizons were 9.4% C and 0.5% N for topsoil material, 4.3% C and 0.2% N for cryoturbated material, and 0.6% C, 0.1% N for mineral subsoil material (determined with a Perkin Elmer 2400 Series II CHNS/O analyzer).

2.2. Incubation experiment

To investigate the effect of increased C availability on SOM decomposition, we amended the soils with ^{13}C -labeled glucose, amino acids, cellulose, or protein. ^{13}C -labeled glucose was purchased from Sigma–Aldrich (U- ^{13}C , 99 at%), ^{13}C -labeled amino acids from Cambridge Isotope Laboratories (algal amino acid mixture, U- ^{13}C , 97–99 at%), ^{13}C -labeled cellulose from Isolife (low degree of polymerization *Cichorium intybus*, U- ^{13}C , >97 at%), and ^{13}C -labeled protein from Sigma–Aldrich (algal crude protein extract, U- ^{13}C , 98 at%). All substrates were mixed with the respective unlabeled compounds to 10 at% ^{13}C before application, and all substrates were applied in dry form.

Aliquots of fresh soil were amended with glucose, amino acids, cellulose or protein of 10 at% ^{13}C , in five replicates of 25 g per treatment, or left unamended as controls (three sets of five 25 g replicates). We adjusted the amount of substrate to the approximate C content of each horizon by adding $554 \mu\text{g C g}^{-1}$ to topsoil material, $138 \mu\text{g C g}^{-1}$ to cryoturbated material and $55 \mu\text{g C g}^{-1}$ to mineral subsoil material. One set of controls was immediately harvested to determine the initial state before the start of the incubation; the remaining samples were filled into microcosms

(50 ml polypropylene tubes with aeration holes in the bottom, for a detailed description see [Inselsbacher et al., 2009](#)) that were then loosely plugged with synthetic wool, and incubated at 10 °C. Since we expected a faster response to monomeric (glucose, amino acids) than to polymeric substrates (cellulose, protein), we incubated samples for either six days (glucose, amino acids, and one set of controls) or ten days (cellulose, protein, and one set of controls).

2.3. Respiration

Respiration rates were determined in four replicate microcosms on days 0, 1, 2, 3, 4, 6 (glucose and amino acids, plus controls), or 0, 2, 4, 6, 8, 10 (cellulose and protein, plus controls) after the start of the incubation, with the first sampling immediately after substrate amendment. For respiration measurements, we removed the synthetic wool from the microcosms, attached polypropylene tubes to the microcosms (resulting in an overall headspace of 133–141 ml) and tightened the systems with rubber seals as described elsewhere ([Inselsbacher et al., 2009](#)). We incubated microcosms at 10 °C, took samples of 15 ml from the headspace after 10, 25 and 40 min (5, 10, 20 and 30 min for the glucose treatment), and injected the gas samples into pre-evacuated gas vials. After each sampling, we replaced the removed gas volume with air from a gas bag, filled with ambient air of known CO₂ concentration and isotopic composition (CO₂ concentrations of 473–632 ppm depending on the sampling date, 1.09 atom% ¹³C). Concentration and isotopic composition of CO₂ were measured with a GasBench II system coupled to a Delta V Advantage IRMS (Thermo Scientific), and corrected for the replaced gas volume. We then calculated the contribution of SOM-derived C to respiration using the equation:

$$R_{\text{SOM}} = R_{\text{total}} \cdot (\text{at}\%_{R_{\text{total}}} - \text{at}\%_{\text{sub}}) / (\text{at}\%_{\text{SOM}} - \text{at}\%_{\text{sub}}), \quad (1)$$

where R_{total} and R_{SOM} are total and SOM-derived respiration, and $\text{at}\%_{R_{\text{total}}}$, $\text{at}\%_{\text{SOM}}$, and $\text{at}\%_{\text{sub}}$ are C isotope compositions (in atom% ¹³C) of total respiration, SOM and the added substrate, respectively.

2.4. Microbial biomass and community composition

We estimated microbial biomass as concentration of phospholipid fatty acids (PLFAs), described microbial community composition using PLFAs as biomarkers for different microbial groups, and assessed microbial substrate preferences by tracing C derived from the added substrates into individual PLFAs. Aliquots of 1 g fresh soil were stored in RNAlater ([Schnecker et al., 2012](#)), and processed following [Frostegård et al. \(1991\)](#), with the modifications described by [Kaiser et al. \(2010b\)](#). Briefly, PLFAs were extracted from the samples with chloroform/methanol/citric acid buffer, purified on silica columns (LC-Si SPE, Supelco) with chloroform, acetone, and methanol, amended with methyl-nonadecanoate as internal standard, and converted to fatty acid methyl esters (FAMES) by alkaline methanolysis. We determined concentration and isotopic composition of individual FAMES on a GC-IRMS system consisting of a Trace GC coupled to a Delta V Advantage IRMS over a GC Isolink interface (Thermo Scientific). Samples were injected in splitless mode at 300 °C, and individual FAMES were separated on a DB-23 column (Agilent; GC-method: 70 °C for 1.5 min, ramp of 30 °C min⁻¹ to 150 °C, 150 °C for 1 min, ramp of 4 °C min⁻¹ to 230 °C, 230 °C for 20 min) with 1.5 ml helium min⁻¹ as carrier gas. We used qualitative standard mixes (37 Comp. FAME Mix and Bacterial Acid Methyl Esters CP Mix, Sigma–Aldrich) for peak

identification, and the internal standard methyl-nonadecanoate for quantification. Concentration and isotopic composition of each PLFA were corrected for C added during derivatization. We further considered only PLFAs that were detectable in all horizons, using i15:0, a15:0, i16:0, i17:0 and a17:0 as markers for Gram-positive bacteria, 16:1ω7, 18:1ω7 and cy17:0(9/10) as markers for Gram-negative bacteria, 18:1ω9 and 18:2ω6 as markers for fungi, and 16:0, 17:0, 18:0, 20:0, 16:1ω5, 16:1ω11 and 19:1ω8 as non-specific PLFAs ([Kaiser et al., 2010a, 2010b](#)). We expressed all PLFA values on the basis of C in PLFAs: Total concentrations are presented as total C in all PLFAs, the relative contributions of individual PLFAs as percentages thereof.

To compare the microbial utilization of different substrates across soil horizons, we calculated substrate use efficiency by comparing the amounts of substrate-derived C respired and incorporated into PLFAs, using the equations

$$CR_{\text{sub}} = CR_{\text{total}} \cdot (\text{at}\%_{CR_{\text{total}}} - \text{at}\%_{\text{SOM}}) / (\text{at}\%_{\text{sub}} - \text{at}\%_{\text{SOM}}), \quad (2)$$

$$PLFA_{\text{sub}} = PLFA_{\text{total}} \cdot (\text{at}\%_{PLFA_{\text{total}}} - \text{at}\%_{\text{SOM}}) / (\text{at}\%_{\text{sub}} - \text{at}\%_{\text{SOM}}), \quad (3)$$

and

$$\text{Substrate use efficiency} = (PLFA_{\text{sub}}) / (PLFA_{\text{sub}} + CR_{\text{sub}}). \quad (4)$$

CR_{total} and CR_{sub} represent total and substrate-derived C in cumulative respiration, $PLFA_{\text{total}}$ and $PLFA_{\text{sub}}$ total and substrate-derived C in PLFAs, and $\text{at}\%_{CR_{\text{total}}}$, $\text{at}\%_{PLFA_{\text{total}}}$, $\text{at}\%_{\text{SOM}}$, and $\text{at}\%_{\text{sub}}$ are C isotope compositions (in atom% ¹³C) of total cumulative respiration, total PLFAs, SOM and the added substrate, respectively. Substrate use efficiency values thus reflect the partitioning of C between respiration and microbial growth (incorporation into PLFAs). Since we did not apply correction factors to convert PLFA concentrations into total microbial C, substrate use efficiency values should only be used for comparison between horizons and treatments.

We additionally determined microbial biomass using chloroform-fumigation-extraction ([Kaiser et al., 2011](#)). Samples fumigated with chloroform, as well as unfumigated samples, were extracted with 0.5 M K₂SO₄ and analyzed for C concentration with an HPLC-IRMS system in direct injection mode against sucrose standards (for description of the system see [Wild et al., 2010](#)). Microbial C was calculated as the difference between fumigated and non-fumigated samples.

2.5. Statistical analyses

All statistics were performed with R 2.15.0 ([R Development Core Team, 2012](#)), with packages [vegan](#) ([Oksanen et al., 2012](#)) and [ecodist](#) ([Goslee and Urban, 2007](#)). We preferentially used parametric methods, and log-transformed data, if necessary, to meet conditions of normal distribution and homoscedasticity. If conditions could not be met, we applied non-parametric methods.

We performed one-way ANOVAs with Tukey's HSD tests between treatments and controls for each soil horizon to test for effects of substrate addition on cumulative SOM-derived respiration, and two-way ANOVA to test for differences in substrate use efficiency across all horizons and substrates. Since PLFA data did not meet the conditions for parametric methods, we applied Mann–Whitney-U tests to assess differences in absolute amounts

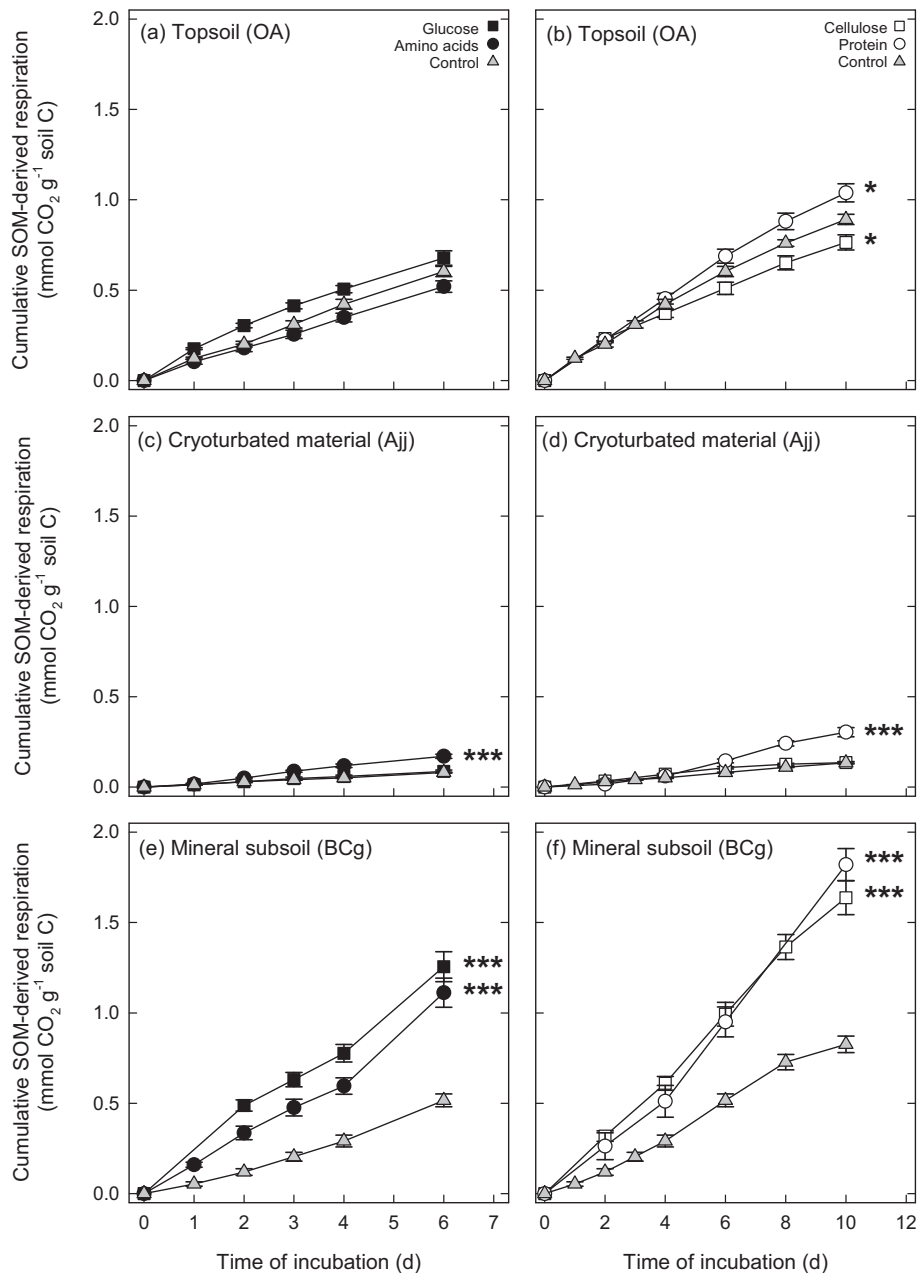


Fig. 1. Cumulative SOM-derived respiration of topsoil, cryoturbated, and mineral subsoil horizons from a tundra ecosystem in the central Siberian Arctic. Samples were amended with glucose, amino acids, cellulose or protein (added at levels corresponding to approximately 1% of soil organic C), or left unamended as controls. Points represent means \pm standard errors of four replicates. Significant differences between amended samples and controls at the end of the incubation are indicated (*, $p < 0.05$; **, $p < 0.01$; ***, $p < 0.001$).

of total and substrate-derived C, and the relative contributions of individual PLFAs to both. We further performed non-metric multidimensional scaling (NMDS) to describe the effects of substrate addition on microbial community composition (% of total C in PLFAs; scaled data), and to describe the distribution of substrate-derived C across the community (% of total substrate-derived C in PLFAs; scaled data). Differences in PLFA patterns were assessed using cluster analysis (Ward hierarchical clustering) and analysis of similarities (ANOSIM). Throughout this text, we use the term “significant” only when referring to statistical results (with differences considered significant at $p < 0.05$).

3. Results

3.1. Basal respiration and priming effect

Respiration rates of unamended control samples differed between soil horizons by more than one order of magnitude, with higher rates in topsoil ($0.379 \pm 0.030 \mu\text{mol CO}_2 \text{ g}^{-1} \text{ dry soil h}^{-1}$, mean \pm standard error) than in cryoturbated and mineral subsoil horizons (0.024 ± 0.002 and $0.019 \pm 0.002 \mu\text{mol CO}_2 \text{ g}^{-1} \text{ dry soil h}^{-1}$, respectively). Considering the differences in C content between soil horizons, respiration rates were in the same range for topsoil and mineral subsoil (4.050 ± 0.317 and

$3.227 \pm 0.351 \mu\text{mol CO}_2 \text{ g}^{-1} \text{ soil C h}^{-1}$), but accounted for only 14% of the topsoil rates in the cryoturbated horizon ($0.547 \pm 0.043 \mu\text{mol CO}_2 \text{ g}^{-1} \text{ soil C h}^{-1}$), indicating a slower decomposition of cryoturbated organic matter (Fig. 1, Supplementary Table 1).

The addition of organic compounds significantly affected SOM-derived respiration in all horizons. The response of SOM-derived respiration in the topsoil was weak, and significant differences were only observed for cellulose (−14%) and protein treatments (+17%; Fig. 2). In the mineral subsoil, however, all amendments (glucose, amino acids, cellulose, and protein) increased SOM-derived respiration two- to threefold (Fig. 2), demonstrating a strong priming of SOM decomposition by all substrates, which ultimately lead to a higher cumulative respiration than in the topsoil (per soil C; Fig. 1). For cryoturbated material, additions of amino acids and protein doubled SOM-derived respiration, whereas additions of glucose and cellulose had no significant effect (Fig. 2). This suggests that N availability was a major control on SOM decomposition in the cryoturbated horizon.

The addition of organic substrates can increase the turnover of microbial C, resulting in higher respiration rates without changing SOM decomposition (“apparent priming”, Blagodatskaya and Kuzyakov, 2008). In our study, the priming effect in both mineral subsoil (all substrates) and cryoturbated material (amino acids and protein) was in all cases much larger than the initial microbial biomass (Supplementary Table 2), eliminating apparent priming as an explanation for the observed increase in SOM-derived respiration.

3.2. Microbial communities

We found different microbial communities in topsoil, cryoturbated, and mineral subsoil horizons, with the latter two harboring the most similar communities. Communities in cryoturbated and mineral subsoil horizons were distinguished from topsoil communities by lower abundances of fungi (18:1 ω 9, 18:2 ω 6) and Gram-negative bacteria (18:1 ω 7, cy17:0), and higher abundances of the non-specific PLFAs 16:0, 18:0 and 20:0 (Supplementary Fig. 1, Supplementary Table 3).

The addition of monomeric substrates (glucose, amino acids) caused a significant increase in the total amount of PLFAs in topsoil and cryoturbated horizons, and a decrease in the mineral subsoil (significant only for glucose; Supplementary Table 3). Microbial community composition in the topsoil was hardly affected by substrate additions, whereas microbial community composition in cryoturbated and mineral subsoil material changed significantly after addition of monomeric substrates (Fig. 3). Specifically, relative

abundances of the non-specific PLFAs 18:0 and 20:0 decreased, and abundances of fungi (18:1 ω 9) and Gram-negative bacteria (cy17:0, 16:1 ω 7, 18:1 ω 7) increased (Supplementary Table 3). The addition of monomeric substrates to cryoturbated and mineral subsoil material thus shifted the microbial community composition closer to the topsoil. In contrast, the addition of polymeric substrates (cellulose, protein) had little effect on microbial community composition (Fig. 3, Supplementary Table 3). The community changes in cryoturbated and mineral subsoil material thus suggest a specific stimulation of fast-growing microbial groups by substrates that can be immediately taken up by microorganisms (i.e., glucose and amino acids).

The response of microbial biomass and microbial community composition to substrate additions, did, however, not reflect the response of SOM decomposition. Changes in biomass and community composition were connected to substrate complexity, whereas priming of SOM decomposition was unspecific (mineral subsoil) or connected to N (cryoturbated material).

3.3. Substrate use

Substrate use efficiency was significantly lower in the mineral subsoil than in topsoil and cryoturbated horizons, i.e., a higher proportion of substrate-derived C was respired and a smaller proportion incorporated into PLFAs (Fig. 4). Comparing different substrates, C from amino acids was more efficiently incorporated into PLFAs than C from glucose, cellulose, and protein.

The incorporation of C from different substrates into PLFAs suggests specific substrate preferences of different microbial groups. In cryoturbated material, the incorporation pattern of substrate-derived C depended on the presence of N in the substrate (Fig. 5; separation displayed along MDS 1), and on substrate complexity (separation along MDS 2). In particular, C from N-containing substrates was preferentially incorporated into the Gram-negative biomarkers 18:1 ω 7, cy17:0, and into the fungal biomarker 18:1 ω 9, which together contained 47% and 39% of C from amino acids and protein incorporated into PLFAs, but only 25% and 22% of C from glucose and cellulose (Supplementary Table 4). Carbon from monomeric substrates was preferentially incorporated into a15:0 (Gram-positive biomarker) and 16:1 ω 7 (Gram-negative biomarker), and C from polymeric substrates into 18:2 ω 6 (fungal biomarker), as well as the non-specific PLFAs 16:0, 17:0, 18:0 and 20:0. A separation due to substrate N content and substrate complexity was not found for other horizons. In topsoil and mineral subsoil, glucose, amino acid and protein treatments had more similar incorporation patterns, whereas cellulose was distinct due to a preferential incorporation into a set of Gram-positive

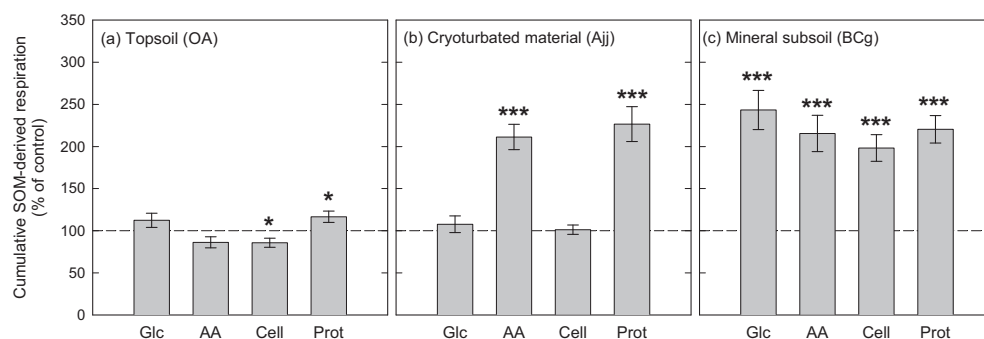


Fig. 2. Cumulative SOM-derived respiration of topsoil, cryoturbated, and mineral subsoil horizons from a tundra ecosystem in the central Siberian Arctic, after incubation with glucose (Glc), amino acids (AA), cellulose (Cell) or protein (Prot). Bars represent means \pm standard errors of four replicates, expressed as percent of unamended controls which are depicted by the dashed line. Significant differences between amended samples and controls are indicated (*, $p < 0.05$; **, $p < 0.01$; ***, $p < 0.001$).

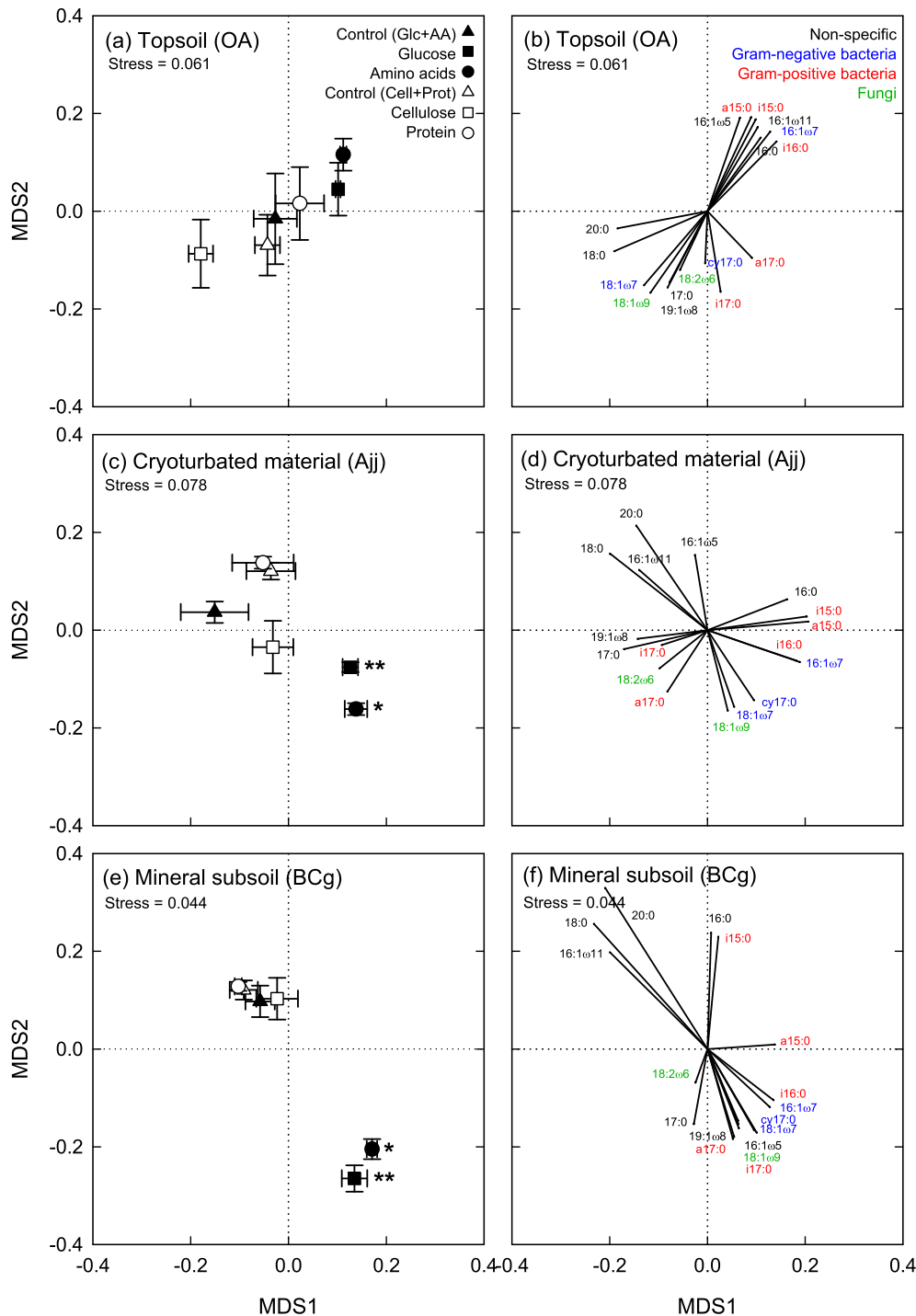


Fig. 3. Phospholipid fatty acid (PLFA) patterns in topsoil, cryoturbated, and mineral subsoil horizons from a tundra ecosystem in the central Siberian Arctic. Samples were amended with glucose, amino acids, cellulose or protein, or left unamended as controls. Patterns are displayed by non-metric multidimensional scaling (NMDS) of PLFA abundances (% of total C in PLFAs). Points represent means \pm standard errors of five replicates; significant differences to the respective controls are indicated (*, $p < 0.05$; **, $p < 0.01$; ***, $p < 0.001$). Data of PLFA abundances are presented in [Supplementary Table 3](#).

biomarkers (i17:0, a17:0) and non-specific PLFAs (16:0, 16:1 ω 5, and 16:1 ω 11) in the topsoil, and into the non-specific PLFA 16:0 in the mineral subsoil ([Supplementary Table 4](#)).

4. Discussion

Arctic permafrost soils contain large amounts of organic C, with recent estimates of approximately 400 Gt C in mineral subsoil and

cryoturbated subsoil horizons each, and 250 Gt C in organic topsoil horizons ([Harden et al., 2012](#)). This organic C might be vulnerable to priming, caused by an increasing availability of plant-derived organic compounds with rising temperatures.

We found that organic topsoil, mineral subsoil and cryoturbated horizons responded differently to an increased availability of organic compounds. Substrate additions hardly affected rates of SOM-derived respiration in the organic topsoil, whereas rates more

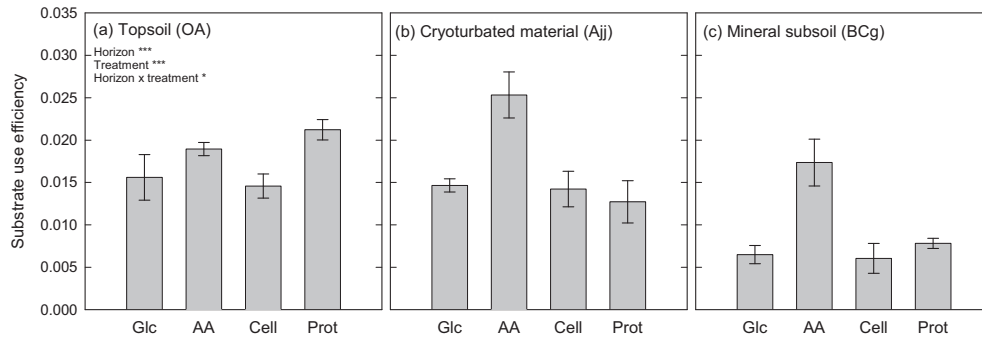


Fig. 4. Substrate use efficiency of topsoil, cryoturbated, and mineral subsoil horizons from a tundra ecosystem in the central Siberian Arctic, after incubation with ^{13}C -labeled glucose (Glc), amino acids (AA), cellulose (Cell) or protein (Prot). Substrate use efficiency was estimated as the proportion of substrate-derived C in PLFAs over substrate-derived C in both PLFAs and respiration. Bars represent means \pm standard errors of four replicates.

than doubled in the mineral subsoil, irrespective of the substrate added (Fig. 2). Substrate use efficiency (the fraction of substrate taken up invested into PLFAs) was lower in the mineral subsoil than in the other horizons (Fig. 4), indicating that a higher proportion of the available substrate was needed to generate energy. These findings thus support our hypothesis of energy limitation in the mineral subsoil in arctic permafrost soil. Energy limitation of SOM decomposition in mineral subsoil horizons has also been shown for a temperate grassland, where the addition of cellulose induced the mineralization of millennia-old soil organic C (Fontaine et al., 2007).

In our study, priming of SOM decomposition in the mineral subsoil was not connected to an increase in microbial biomass or a change in community composition, since significant community changes were only observed for glucose and amino acid amendments, but not for cellulose or protein (Fig. 3, Supplementary Table 3). Priming was also not connected to N mining of microbial decomposers, since substrates with and without N similarly stimulated SOM decomposition (Fig. 2).

In contrast to the mineral subsoil, SOM decomposition in cryoturbated material was not altered by additions of glucose and cellulose, but doubled when amino acids or protein were added (Fig. 2). This specific response to the N-containing substrates, as well as the higher substrate use efficiency than in the mineral subsoil (Fig. 4), suggest that microbial decomposers in the cryoturbated horizon were not limited in energy, but in N. Cryoturbated material is usually similar in N content and C/N ratio to organic or mineral topsoil horizons, but has lower N transformation rates (Kaiser et al., 2007; Wild et al., 2013), suggesting that N bound in cryoturbated organic material is poorly available for microorganisms (e.g., due to binding to phenolic compounds; Olk et al., 2006). In our study, the C/N ratio of cryoturbated material (21.4) even slightly exceeded the C/N ratio of the organic topsoil (18.5); this might have further promoted N limitation in cryoturbated material.

Carbon from N-containing substrates (amino acids and protein) was preferentially incorporated into fungal (18:1 ω 9) and Gram-negative bacterial biomarkers (18:1 ω 7, cy17:0; Fig. 5). Each of these markers was of significantly lower relative abundance in the cryoturbated than in the topsoil horizon, accounting for a total of 13% (cryoturbated) and 40% (topsoil) of C in PLFAs (means of controls; Supplementary Fig. 1). Differences in microbial community composition between topsoil and cryoturbated horizons have previously been suggested to contribute to the slower decomposition of cryoturbated material (Schnecker et al., 2014), in particular the lower abundance of fungi in cryoturbated horizons (Wild et al.,

2013; Gittel et al., 2014). Fungi are pivotal for the decomposition of organic material in most terrestrial systems (de Boer et al., 2005; Strickland and Rousk, 2010), and can benefit from higher N availability (Rousk and Bååth, 2007; Grman and Robinson, 2013; Koranda et al., 2014). However, although the preference of specific microbial groups for N-containing compounds is striking, this does not necessarily identify these groups as responsible for priming.

Nitrogen addition often decreases SOM decomposition rates, by reducing N mining of microbial decomposers (e.g., Craine et al., 2007). On the other hand, in systems of strong N limitation, where low N availability limits the production of SOM-degrading enzymes, N addition can stimulate decomposition by facilitating enzyme production by fungi (Allison et al., 2009). Since in our study the amendment of amino acids and protein to cryoturbated material did not systematically increase microbial biomass or the abundance of specific microbial groups (Fig. 3, Supplementary Table 3), we suggest that microorganisms invested the additional N in the production of extracellular enzymes.

Within a relatively short period, SOM decomposition in the subsoil, but not in the topsoil, was strongly stimulated by increased availability of organic C (mineral subsoil) or organic N (cryoturbated material). Rising temperatures in the Arctic (IPCC, 2007) are expected to promote soil C availability by increasing plant primary productivity (Bhatt et al., 2010; Xu et al., 2013) and thus C allocation from plants to the soil. Nitrogen availability might also benefit from higher plant productivity, if the additional input of N-containing compounds by plants (e.g., proteins) exceeds the increase in plant N uptake (Weintraub and Schimel, 2005). In addition, N availability might further increase if SOM decomposition rates increase (Nadelhoffer et al., 1991; Hobbie, 1996; Schimel et al., 2004; Schaeffer et al., 2013).

In our study, mineral subsoil material was particularly susceptible to priming, with rates of SOM-derived respiration exceeding topsoil rates (as related to soil C) after substrate addition. Our findings are thus in contrast to observations of increased C storage in mineral subsoil horizons with warming (Sistla et al., 2013), but support predictions of high C losses from arctic soils if plant productivity increases (Hartley et al., 2012). These contrasting findings on the impact of higher plant productivity on soil C stocks point to a strong context-dependency of priming effects in arctic soils. Our study provides key insights into the mechanisms behind priming effects in permafrost soils; this will allow possible feedbacks from belowground plant–microbe interactions to be incorporated into larger-scale models of arctic C balances in a future climate.

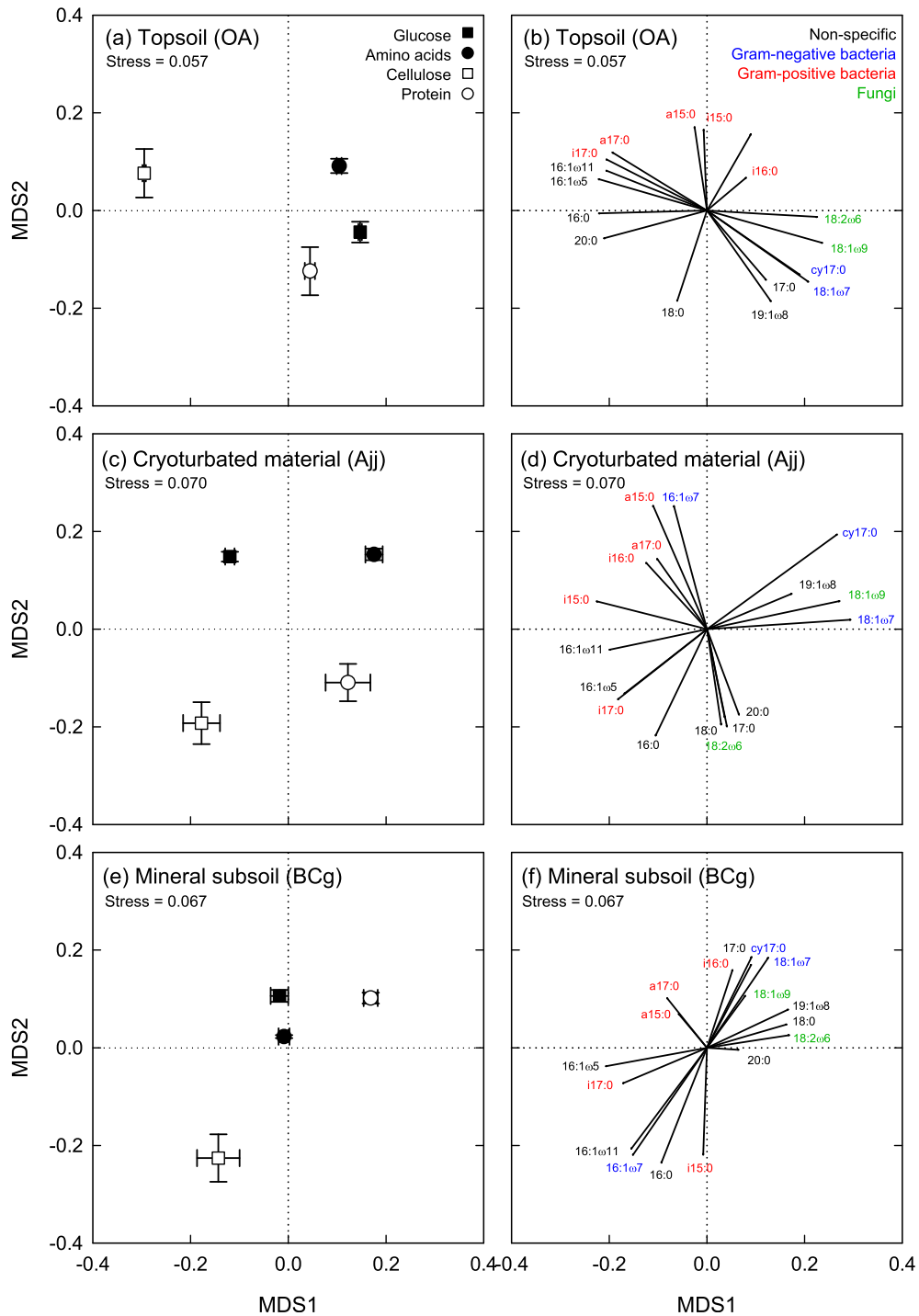


Fig. 5. Incorporation patterns of C from glucose, amino acids, cellulose or protein into phospholipid fatty acids (PLFAs), in topsoil, cryoturbated, and mineral subsoil horizons from a tundra ecosystem in the central Siberian Arctic. Patterns are displayed by non-metric multidimensional scaling (NMDS). Points represent means \pm standard errors of five replicates; in all horizons, patterns for all substrates were significantly different from each other. Data on the incorporation of substrate-derived C into PLFAs are presented in [Supplementary Table 4](#).

Acknowledgments

This study was funded by the Austrian Science Fund (FWF) as part of the International Program CryoCARB (Long-term Carbon Storage in Cryoturbated Arctic Soils; FWF – I370-B17).

Appendix A. Supplementary data

Supplementary data related to this article can be found at <http://dx.doi.org/10.1016/j.soilbio.2014.04.014>.



References

- Allison, S.D., LeBauer, D.S., Ofrecio, M.R., Reyes, R., Ta, A., Tran, T.M., 2009. Low levels of nitrogen addition stimulate decomposition by boreal forest fungi. *Soil Biology & Biochemistry* 41, 293–302.
- Bhatt, U.S., Walker, D.A., Raynolds, M.K., Comiso, J.C., Epstein, H.E., Jia, G., Gens, R., Pinzon, J.E., Tucker, C.J., Tweedie, C.E., Webber, P.J., 2010. Circumpolar Arctic tundra vegetation change is linked to sea ice decline. *Earth Interactions* 14, 1–20.
- Bingeman, C.W., Varner, J.E., Martin, W.P., 1953. The effect of the addition of organic materials on the decomposition of an organic soil. *Soil Science Society of America Journal* 17, 34–38.
- Blagodatskaya, E., Kuzyakov, Y., 2008. Mechanisms of real and apparent priming effects and their dependence on soil microbial biomass and community structure: critical review. *Biology and Fertility of Soils* 45, 115–131.
- Bockheim, J.G., 2007. Importance of cryoturbation in redistributing organic carbon in permafrost-affected soils. *Soil Science Society of America Journal* 71, 1335.
- CAVM Team, 2003. Circumpolar Arctic Vegetation Map. (1:7,500,000 scale), Conservation of Arctic Flora and Fauna (CAFF) Map No. 1. U.S. Fish and Wildlife Service, Anchorage, Alaska.
- Conant, R.T., Ryan, M.G., Ågren, G.I., Birge, H.E., Davidson, E.A., Eliasson, P.E., Evans, S.E., Frey, S.D., Giardina, C.P., Hopkins, F.M., Hyvönen, R., Kirschbaum, M.U., Lavelle, J.M., Leifeld, J., Parton, W.J., Steinweg, J.M., Wallenstein, M.D., Wetterstedt, J.A., Bradford, M.A., 2011. Temperature and soil organic matter decomposition rates – synthesis of current knowledge and a way forward. *Global Change Biology* 17, 3392–3404.
- Craine, J., Morrow, C., Fierer, N., 2007. Microbial nitrogen limitation increases decomposition. *Ecology* 88, 2105–2113.
- de Boer, W., Folman, L.B., Summerbell, R.C., Boddy, L., 2005. Living in a fungal world: impact of fungi on soil bacterial niche development. *FEMS Microbiology Reviews* 29, 795–811.
- Dijkstra, F.A., Carrillo, Y., Pendall, E., Morgan, J.A., 2013. Rhizosphere priming: a nutrient perspective. *Frontiers in Microbiology* 4, 1–8.
- Fontaine, S., Barot, S., Barré, P., Bdioui, N., Mary, B., Rumpel, C., 2007. Stability of organic carbon in deep soil layers controlled by fresh carbon supply. *Nature* 450, 277–280.
- Fontaine, S., Mariotti, A., Abbadie, L., 2003. The priming effect of organic matter: a question of microbial competition? *Soil Biology & Biochemistry* 35, 837–843.
- Frostegård, Å., Tunlid, A., Bååth, E., 1991. Microbial biomass measured as total lipid phosphate in soils of different organic content. *Journal of Microbiological Methods* 14, 151–163.
- Gittel, A., Bárta, J., Kohoutová, I., Mikutta, R., Owens, S., Gilbert, J., Schneckler, J., Wild, B., Hannisdal, B., Maerz, J., Lashchinskiy, N., Capek, P., Santrúcková, H., Gentsch, N., Shibistova, O., Guggenberger, G., Richter, A., Torsvik, V.L., Schleper, C., Ulrich, T., 2014. Distinct microbial communities associated with buried soils in the Siberian tundra. *The ISME Journal* 8, 841–853.
- Goslee, S.C., Urban, D.L., 2007. The ecodist package for dissimilarity-based analysis of ecological data. *Journal of Statistical Software* 22, 1–19.
- Grman, E., Robinson, T.M., 2013. Resource availability and imbalance affect plant-mycorrhizal interactions: a field test of three hypotheses. *Ecology* 94, 62–67.
- Harden, J.W., Koven, C.D., Ping, C., Hugelius, G., McGuire, A.D., Camill, P., Jorgenson, T., Kuhry, P., Michaelson, G.J., O'Donnell, J.A., Schuur, E.A.G., Tarnocai, C., Johnson, K., Grosse, G., 2012. Field information links permafrost carbon to physical vulnerabilities of thawing. *Geophysical Research Letters* 39, L15704.
- Hartley, I.P., Garnett, M.H., Sommerkorn, M., Hopkins, D.W., Fletcher, B.J., Sloan, V.L., Phoenix, G.K., Wookey, P.A., 2012. A potential loss of carbon associated with greater plant growth in the European Arctic. *Nature Climate Change* 2, 875–879.
- Hartley, I.P., Hopkins, D.W., Garnett, M.H., Sommerkorn, M., Wookey, P.A., 2008. Soil microbial respiration in arctic soil does not acclimate to temperature. *Ecology Letters* 11, 1092–1100.
- Hobbie, S.E., 1996. Temperature and plant species control over litter decomposition in Alaskan tundra. *Ecological Monographs* 66, 503–522.
- Hugelius, G., Kuhry, P., Tarnocai, C., Virtanen, T., 2010. Soil organic carbon pools in a periglacial landscape: a case study from the central Canadian Arctic. *Permafrost and Periglacial Processes* 21, 16–29.
- IPCC, 2007. Climate Change 2007: Impacts, Adaptation and Vulnerability. Contribution of Working Group II to the Fourth Assessment Report of the Intergovernmental Panel on Climate Change. Cambridge University Press, Cambridge, UK.
- Inselbacher, E., Ripka, K., Klauauf, S., Fedosoyenko, D., Hackl, E., Gorfer, M., Hood-Novotny, R., von Wirén, N., Sessitsch, A., Zechmeister-Boltenstern, S., Wanek, W., Strauss, J., 2009. A cost-effective high-throughput microcosm system for studying nitrogen dynamics at the plant-microbe-soil interface. *Plant and Soil* 317, 293–307.
- IUSS Working Group WRB, 2007. World Reference Base for Soil Resources 2006, First Update 2007. Rome.
- Kaiser, C., Frank, A., Wild, B., Koranda, M., Richter, A., 2010a. Negligible contribution from roots to soil-borne phospholipid fatty acid fungal biomarkers 18:2 ω 6,9 and 18:1 ω 9. *Soil Biology & Biochemistry* 42, 1650–1652.
- Kaiser, C., Fuchslueger, L., Koranda, M., Gorfer, M., Stange, C.F., Kitzler, B., Rasche, F., Strauss, J., Sessitsch, A., Zechmeister-Boltenstern, S., Richter, A., 2011. Plants control the seasonal dynamics of microbial N cycling in a beech forest soil by belowground C allocation. *Ecology* 92, 1036–1051.
- Kaiser, C., Koranda, M., Kitzler, B., Fuchslueger, L., Schneckler, J., Schweiger, P., Rasche, F., Zechmeister-Boltenstern, S., Sessitsch, A., Richter, A., 2010b. Belowground carbon allocation by trees drives seasonal patterns of extracellular enzyme activities by altering microbial community composition in a beech forest soil. *New Phytologist* 187, 843–858.
- Kaiser, C., Meyer, H., Biasi, C., Rusalimova, O., Barsukov, P., Richter, A., 2007. Conservation of soil organic matter through cryoturbation in arctic soils in Siberia. *Journal of Geophysical Research* 112, G02017.
- Koranda, M., Kaiser, C., Fuchslueger, L., Kitzler, B., Sessitsch, A., Zechmeister-Boltenstern, S., Richter, A., 2014. Fungal and bacterial utilization of organic substrates depends on substrate complexity and N availability. *FEMS Microbiology Ecology* 87, 142–152.
- Nadelhoffer, K.J., Giblin, A.E., Shaver, G.R., Laundre, J.A., 1991. Effects of temperature and substrate quality on element mineralization in six arctic soils. *Ecology* 72, 242–253.
- Oksanen, J., Blanchet, F.G., Kindt, R., Legendre, P., Minchin, P.R., O'Hara, R.B., Simpson, G.L., Solymos, P., Stevens, M.H., Wagner, H., 2012. *vegan: Community Ecology Package*. R Package Version 2.0-3.
- Olk, D.C., Cassman, K.G., Schmidt-Rohr, K., Anders, M.M., Mao, J.D., Deenik, J.L., 2006. Chemical stabilization of soil organic nitrogen by phenolic lignin residues in anaerobic agroecosystems. *Soil Biology & Biochemistry* 38, 3303–3312.
- R Development Core Team, 2012. *R: a Language and Environment for Statistical Computing*. R Foundation for Statistical Computing.
- Rousk, J., Bååth, E., 2007. Fungal and bacterial growth in soil with plant materials of different C/N ratios. *FEMS Microbiology Ecology* 62, 258–267.
- Schaeffer, S.M., Sharp, E., Schimel, J.P., Welker, J.M., 2013. Soil-plant N processes in a High Arctic ecosystem, NW Greenland are altered by longterm experimental warming and higher rainfall. *Global Change Biology* 19, 3529–3539.
- Schimel, J.P., Bilbrough, C., Welker, J.M., 2004. Increased snow depth affects microbial activity and nitrogen mineralization in two Arctic tundra communities. *Soil Biology & Biochemistry* 36, 217–227.
- Schneckler, J., Wild, B., Fuchslueger, L., Richter, A., 2012. A field method to store samples from temperate mountain grassland soils for analysis of phospholipid fatty acids. *Soil Biology & Biochemistry* 51, 81–83.
- Schneckler, J., Wild, B., Hofhansl, F., Alves, R.J.E., Bárta, J., Čapek, P., Fuchslueger, L., Gentsch, N., Gittel, A., Guggenberger, G., Hofer, A., Kienzl, S., Knoltsch, A., Lashchinskiy, N., Mikutta, R., Santrúcková, H., Shibistova, O., Takriti, M., Ulrich, T., Weltin, G., Richter, A., 2014. Effects of soil organic matter properties and microbial community composition on enzyme activities in cryoturbated arctic soils. *PLoS One* 9, e94076.
- Sistla, S.A., Asao, S., Schimel, J.P., 2012. Detecting microbial N-limitation in tussock tundra soil: implications for Arctic soil organic carbon cycling. *Soil Biology & Biochemistry* 55, 78–84.
- Sistla, S.A., Moore, J.C., Simpson, R.T., Gough, L., Shaver, G.R., Schimel, J.P., 2013. Long-term warming restructures Arctic tundra without changing net soil carbon storage. *Nature* 497, 615–618.
- Soil Survey Staff, 1999. *Soil Taxonomy: a Basic System of Soil Classification for Making and Interpreting Soil Surveys*, second ed. U. S. Department of Agriculture Handbook 436.
- Strickland, M.S., Rousk, J., 2010. Considering fungal:bacterial dominance in soils – methods, controls, and ecosystem implications. *Soil Biology & Biochemistry* 42, 1385–1395.
- Tarnocai, C., Canadell, J.G., Schuur, E.A., Kuhry, P., Mazhitova, G., Zimov, S., 2009. Soil organic carbon pools in the northern circumpolar permafrost region. *Global Biogeochemical Cycles* 23, GB2023.
- Weintraub, M.N., Schimel, J.P., 2005. Seasonal protein dynamics in Alaskan arctic tundra soils. *Soil Biology & Biochemistry* 37, 1469–1475.
- Wild, B., Schneckler, J., Bárta, J., Čapek, P., Guggenberger, G., Hofhansl, F., Kaiser, C., Lashchinskiy, N., Mikutta, R., Mooshammer, M., Santrúcková, H., Shibistova, O., Ulrich, T., Zimov, S.A., Richter, A., 2013. Nitrogen dynamics in Turbic Cryosols from Siberia and Greenland. *Soil Biology & Biochemistry* 67, 85–93.
- Wild, B., Wanek, W., Postl, W., Richter, A., 2010. Contribution of carbon fixed by Rubisco and PEPC to phloem export in the Crassulacean acid metabolism plant *Kalanchoë daigremontiana*. *Journal of Experimental Botany* 61, 1375–1383.
- Xu, C., Guo, L., Ping, C., White, D.M., 2009. Chemical and isotopic characterization of size-fractionated organic matter from cryoturbated tundra soils, northern Alaska. *Journal of Geophysical Research* 114, G03002.
- Xu, L., Myneni, R.B., Chapin III, F.S., Callaghan, T.V., Pinzon, J.E., Tucker, C.J., Zhu, Z., Bi, J., Ciais, P., Tømmervik, H., Euskirchen, E.S., Forbes, B.C., Piao, S.L., Anderson, B.T., Ganguly, S., Nemani, R.R., Goetz, S.J., Beck, P.S., Bunn, A.G., Cao, C., Stroeve, J.C., 2013. Temperature and vegetation seasonality diminish over northern lands. *Nature Climate Change* 3, 581–586.

Paper 11

Gentsch N, Wild B, Mikutta R, Capek P, Diakova K, Schrumpf M, Turner S, Minnich C, Schaarschmidt F, Shibistova O, Schnecker J, Urich T, Gittel A, Santruckova H, **Barta J**, Lashchinskiy N, Fuss R, Richter A, Guggenberger G (2018) Temperature response of permafrost soil carbon is attenuated by mineral protection. *GLOBAL CHANGE BIOLOGY* 24:3401-3415.

Temperature response of permafrost soil carbon is attenuated by mineral protection

Norman Gentsch¹  | Birgit Wild^{2,3,4,5} | Robert Mikutta^{1,6} | Petr Čapek⁷ | Katka Diáková⁷ | Marion Schrumpp⁸ | Stephanie Turner⁹ | Cynthia Minnich^{1,10} | Frank Schaarschmidt¹¹ | Olga Shibistova^{1,12} | Jörg Schneckner^{2,3,13}  | Tim Urich^{14,15} | Antje Gittel^{16,17} | Hana Šantrůčková⁷ | Jiří Bárta⁷ | Nikolay Lashchinskiy¹⁸ | Roland Fuß¹⁹ | Andreas Richter^{2,3} | Georg Guggenberger^{1,12}

¹Institute of Soil Science, Leibniz Universität Hannover, Hannover, Germany

²Department of Microbiology and Ecosystem Science, University of Vienna, Vienna, Austria

³Austrian Polar Research Institute, Vienna, Austria

⁴Department of Environmental Science and Analytical Chemistry, Stockholm University, Stockholm, Sweden

⁵Bolin Centre for Climate Research, Stockholm University, Stockholm, Sweden

⁶Soil Science and Soil Protection, Martin-Luther-Universität Halle-Wittenberg, Halle (Saale), Germany

⁷Department of Ecosystems Biology, University of South Bohemia, České Budějovice, Czech Republic

⁸Max Planck Institute for Biogeochemistry, Jena, Germany

⁹Federal Institute for Geosciences and Natural Resources (BGR), Hannover, Germany

¹⁰Soil Ecology, University of Bayreuth, Bayreuth, Germany

¹¹Institute of Biostatistics, Leibniz Universität Hannover, Hannover, Germany

¹²V.N. Sukachev Institute of Forest, Siberian Branch of Russian Academy of Sciences, Krasnoyarsk, Russia

¹³Department of Natural Resources and the Environment, University of New Hampshire, Durham, New Hampshire

¹⁴Department of Ecogenomics and Systems Biology, University of Vienna, Vienna, Austria

¹⁵Institute of Microbiology, Ernst-Moritz-Arndt University, Greifswald, Germany

¹⁶Department of Biology, Centre for Geobiology, University of Bergen, Bergen, Norway

¹⁷Department of Bioscience, Centre for Geomicrobiology, Aarhus, Denmark

¹⁸Central Siberian Botanical Garden, Siberian Branch of Russian Academy of Sciences, Novosibirsk, Russia

¹⁹Thünen Institute of Climate-Smart Agriculture, Braunschweig, Germany

Correspondence

Norman Gentsch, Institute of Soil Science, Leibniz Universität Hannover, Hannover, Germany.

Email: gentsch@ifbk.uni-hannover.de

Funding information

German Federal Ministry of Education and Research, Grant/Award Number: 03F0616A; Russian Ministry of Education and Science, Grant/Award Number: 14.B25.31.0031; Austrian Science Fund, Grant/Award Number: FWF - I370-B17; Czech Science Foundation, Grant/Award Number: n.16-18453S

Abstract

Climate change in Arctic ecosystems fosters permafrost thaw and makes massive amounts of ancient soil organic carbon (OC) available to microbial breakdown. However, fractions of the organic matter (OM) may be protected from rapid decomposition by their association with minerals. Little is known about the effects of mineral-organic associations (MOA) on the microbial accessibility of OM in permafrost soils and it is not clear which factors control its temperature sensitivity. In order to investigate if and how permafrost soil OC turnover is affected by mineral controls, the heavy fraction (HF) representing mostly MOA was obtained by density fractionation from 27 permafrost soil profiles of the Siberian Arctic. In parallel laboratory incubations, the unfractionated soils (bulk) and their HF were comparatively incubated for 175 days at 5 and 15°C. The HF was equivalent to $70 \pm 9\%$ of the bulk CO₂ respiration as compared to a

share of $63 \pm 1\%$ of bulk OC that was stored in the HF. Significant reduction of OC mineralization was found in all treatments with increasing OC content of the HF (HF-OC), clay-size minerals and Fe or Al oxyhydroxides. Temperature sensitivity (Q10) decreased with increasing soil depth from 2.4 to 1.4 in the bulk soil and from 2.9 to 1.5 in the HF. A concurrent increase in the metal-to-HF-OC ratios with soil depth suggests a stronger bonding of OM to minerals in the subsoil. There, the younger ^{14}C signature in CO_2 than that of the OC indicates a preferential decomposition of the more recent OM and the existence of a MOA fraction with limited access of OM to decomposers. These results indicate strong mineral controls on the decomposability of OM after permafrost thaw and on its temperature sensitivity. Thus, we here provide evidence that OM temperature sensitivity can be attenuated by MOA in permafrost soils.

KEYWORDS

carbon mineralization, incubation, mineral-organic association, permafrost soils, radiocarbon, temperature sensitivity

1 | INTRODUCTION

Decomposition of soil organic matter (OM) depends on soil environmental conditions and the accessibility of organic compounds to the decomposer community. In arctic permafrost soils, low temperatures and high moisture lower the biodegradation of OM (Ping, Jastrow, Jorgenson, Michaelson, & Shur, 2015) and lead to the accumulation of large organic carbon (OC) stocks (Hugelius et al., 2014).

Climate change is predicted to increase active layer thickness and deeper drainage in permafrost soils (Harden et al., 2012; Schaefer, Zhang, Bruwiler, & Barette, 2011; Sushama, Laprise, Caya, Verseghy, & Allard, 2007) and ongoing changes have been already observed (Elberling et al., 2013; Im & Kharuk, 2015; Romanovsky et al., 2010). Deepening of the active layer will likely change water and temperature gradients and oxygen availability in permafrost soils, thereby producing changing conditions for a broader microbial community (Gittel et al., 2014) and possibly stimulating OC turnover. The changing climate, however, will also affect physicochemical properties of the soil, such as structure, OM adsorption-desorption processes and nutrient availability. Understanding their effects on OM decomposition and their responses to temperatures is thus imperative for understanding OC dynamics in high-latitude soils in a future climate (Schuur et al., 2015).

The availability of organic molecules and nutrients to the decomposers, determines the decomposability and thus quality of OM (Dungait, Hopkins, Gregory, & Whitmore, 2012). The separation of OM into functional fractions, i.e., particulate OM (plant residues) and mineral-organic associations (MOA), by physical fractionation has provided much insight into the stabilization of OM (Kögel-Knabner et al., 2008). Particulate OM, herein operationally defined as the light fraction (LF; $<1.6 \text{ g/cm}^3$; Crow, Swanston, Lajtha, Brooks, & Keirstead, 2007), is traditionally regarded as a faster-cycling OC fraction. Decomposition of the LF can be slowed down or inhibited only by occlusion in soil aggregates, by compounds that inhibit enzyme activity (e.g.,

tannins), and by a lack of specialized decomposer organisms (Dungait et al., 2012). Longer turnover times and higher ^{14}C -ages have been reported for OM associated with metal ions and pedogenic minerals such as clay minerals or Fe and Al oxides (Herold, Schöning, Michalzik, Trumbore, & Schrumpf, 2014; Kögel-Knabner et al., 2008; Schrumpf et al., 2013). Strong bonds, resulting from the adsorption of OM to mineral surfaces, or precipitation of mineral-organic complexes limit microbial access to these carbon source (Mikutta et al., 2007; Scheel, Dörfler, & Kalbitz, 2007). The percentage of mineral-bound OC with delayed turnover depends on the sorption capacity of the mineral phase, the reactivity of the OM, the mineral surface loading as regulated by the OC input, and the oxygen availability (Hall, McNicol, Natake, & Silver, 2015; Kaiser & Guggenberger, 2003). A recent study highlighted the tight link between Fe oxides, microaggregate structure, and OC stabilization in permafrost soils, similarly as it is known for temperate soils (Mueller et al., 2017).

In temperate environments, the LF is restricted mostly to topsoil O and A horizons, whereas the fraction of mineral-bound OC and the bonding strength increase with soil depth (Kaiser & Guggenberger, 2003; Kögel-Knabner et al., 2008). Vertical transport of dissolved OC (DOC), such as rhizodeposition or products of microbial synthesis are the principle sources of carbon in mineral-organic associations in subsoils (Kaiser & Guggenberger, 2000; Rumpel & Kögel-Knabner, 2011). Permafrost soils, however, are more complex as they are affected by cryoturbation. Cryoturbation is the mass exchange between soil horizons based on frequent freezing-thawing cycles in combination with moisture migration along a thermal gradient (Bockheim & Tarnocai, 1998). Cryoturbation transfers fresh OM such as LF material to the subsoil, where it can even be incorporated into the permafrost and contribute approximately 20% to subsoil OC storage (Gentsch, Mikutta, Alves, et al., 2015). Cryogenic migration also delivers large amounts of DOC to the subsoil, where it is retained in metal-organic precipitates (Gentsch, Mikutta, Alves, et al., 2015; Gundelwein et al., 2007; Ostroumov et al., 2001). The assemblage of pedogenic minerals

in permafrost soils often reflects the current geochemical conditions (low temperature, anaerobiosis) and the low level of soil development (Alekseev, Alekseeva, Ostroumov, Siegert, & Gradusov, 2003; Borden, Ping, McCarthy, & Naidu, 2010). However, changes in redox conditions, soil acidity and composition of the soil solution may have direct consequences for the retention and remobilization of OM in mineral-organic associations (Kleber et al., 2015).

Biochemical reactions in soils are controlled, amongst other factors, by temperature and the response of soil OM to changing climate depends on its temperature sensitivity (Davidson & Janssens, 2006). Temperature sensitivity is commonly expressed as the Q10 factor, which is the factor by which a reaction rate changes as the temperature increases by 10°C. The Q10 of soil OM is controlled by a combination of its chemical composition and its availability, defined as intrinsic and apparent temperature sensitivity (Davidson & Janssens, 2006). Therefore, in soils with variable OM composition and protection mechanisms, the Q10 can be the result of various mechanisms (Gillabel, Cebrian-Lopez, Six, & Merckx, 2010). From laboratory incubation experiments, OM pool sizes and their temperature response can be estimated by applying one or more first-order decay models to CO₂ emission data (Bracho et al., 2016; Conant et al., 2008; Schädel, Luo, David Evans, Fei, & Schaeffer, 2013). Those models provide valuable information on the apparent temperature sensitivity of the substrate. Investigation of the intrinsic temperature sensitivity of laboratory-separated specific OM fractions, however, is complex albeit urgently needed to predict future OC cycling in arctic ecosystems (Karhu et al., 2010; Yang, Wullschleger, Liang, Graham, & Gu, 2016).

The aim of this study was to investigate the temperature sensitivity of OM of all major soil horizons of the active layer and the upper permafrost of cryoturbated permafrost soils across the Siberian Arctic. Mineral-organic associations have been regarded as less important for OM stabilization in permafrost soils than in other soils (Höfle, Rethemeyer, Mueller, & John, 2013; Ping, Jastrow, Jorgenson, Michaelson, & Shur, 2014). Our previous research indicated, however, a certain protective capacity of soil minerals over decomposition (Gentsch, Mikutta, Shibistova, et al., 2015). Additionally, we aimed at understanding the bioavailability of bulk soil and the corresponding MOAs at different temperatures. Towards these aims, we isolated the MOA by density separation and determined the Q10 in laboratory incubations in comparison to the bulk soil. We determined the ¹⁴C activity of MOA fractions and the bulk soil and their respired CO₂. We hypothesized that (i) MOAs in permafrost soils comprise a continuum of organic substances with inherent kinetic properties, ¹⁴C activity and bioaccessibility and that (ii) reduced substrate availability in the subsoil resulted in a greater temperature sensitivity than topsoil horizons.

2 | MATERIALS AND METHODS

2.1 | Field sites and basic soil properties

Soil samples were collected from tundra sites in areas of continuous permafrost in the east, central and west Siberian Arctic (Figure 1; Tazowskiy, TZ; Ari-Mas, AM; Logata, LG; Cherskiy, CH). At each study

site, profiles in different bioclimatic subzones were excavated, which resulted in nine sampling sites, each with three replicated soil profiles (Supporting Information Table S1). For a detailed description of the sampling sites and the sampling design, see Gentsch, Mikutta, Alves, et al. (2015). Briefly, five-metre-wide soil pits were excavated down to the permafrost table, and soil material from all designated horizons within the active layer was sampled across the profile. Permafrost samples were taken from the upper 30–40 cm of the permafrost. Living roots were carefully removed, and the air-dried samples were passed through a 2-mm sieve. Diagnostic soil horizons were identified in accordance with Soil Taxonomy (Soil Survey Staff, 2014) and were clustered into the following five major groups: organic topsoil horizons (O), mineral topsoil horizons (A), cryoturbated OM-rich pockets in the subsoil (A_{jj}, O_{jj}; hereafter referred to as cryoturbated topsoils), mineral subsoil horizons (BC_g, BC_{gjj}, C_{gjj}, C_g; hereafter clustered as B/C) and permafrost horizons (C_{ff}). The term “cryoturbated topsoils” refers only to those horizons that are defined as topsoils, based on their OM content (Soil Survey Staff, 2014), that were buried by cryogenic processes as pockets, involutions or tongues in mineral soil horizons (see Figure 2). Mineral subsoil and permafrost horizons, unless defined otherwise, are subsequently referred to as “subsoil”.

Soil pH was measured in water extracts (soil-to-water ratio of 1:2.5), and soil textures were determined using the sieve-pipette method after OM removal (DIN ISO 11277, 2002). Water-holding capacity (WHC) was measured as described by Schinner, Kandeler, Ohlinger, and Margesin (1993) with modifications of the sample amount (10 g dry weight) and drainage time (24 hr). Iron and Al were extracted from the dry soil samples using selective extraction methods, i.e., sodium dithionite-citrate-bicarbonate, acid-ammonium oxalate (Carter & Gregorich, 2008) and sodium pyrophosphate (modified according to Mikutta, Lorenz, Guggenberger, Haumaier, & Freund, 2014). The extracts yielded estimates of the total amount of pedogenic Fe (Fe_d), poorly crystalline oxyhydroxides (Fe_o, Al_o), and organically complexed Fe and Al (Fe_p, Al_p). For a detailed description of these methods, see Gentsch, Mikutta, Alves, et al. (2015).

Physical fractionation of mineral bulk soil samples by density (method of Golchin, Oades, Skjemstad, & Clarke, 1994; modified by Gentsch, Mikutta, Alves, et al., 2015) yields two OM fractions. The light fraction (LF, <1.6 g/cm³) represents particulate OM such as fine roots, wood, bark, charcoal and litter fragments. The heavy fraction (HF, >1.6 g/cm³) contains mostly MOA (Cerli, Celi, Kalbitz, Guggenberger, & Kaiser, 2012). The HF and the LF were investigated by scanning electron microscopy (FEI Quanta 200 FEG, Oregon, USA) to control the proper separation of the two fractions. The organic matter lost during the fractionation was quantified and is referred to as the “mobilizable fraction” (Gentsch, Mikutta, Alves, et al., 2015). All the bulk soil samples and the physical soil fractions were measured for their OC and TN concentrations and δ¹³C ratios in duplicates using an Elementar IsoPrime 100 IRMS (IsoPrime Ltd., Cheadle Hulme, UK) coupled to an Elementar vario MICRO cube EA C/N analyser (Elementar Analysensysteme GmbH, Hanau, Germany). The isotope ratios are expressed in delta notation relative to the Vienna Pee Dee Belemnite standard (Hut, 1987). Based on the OC concentrations in the HF (HF-

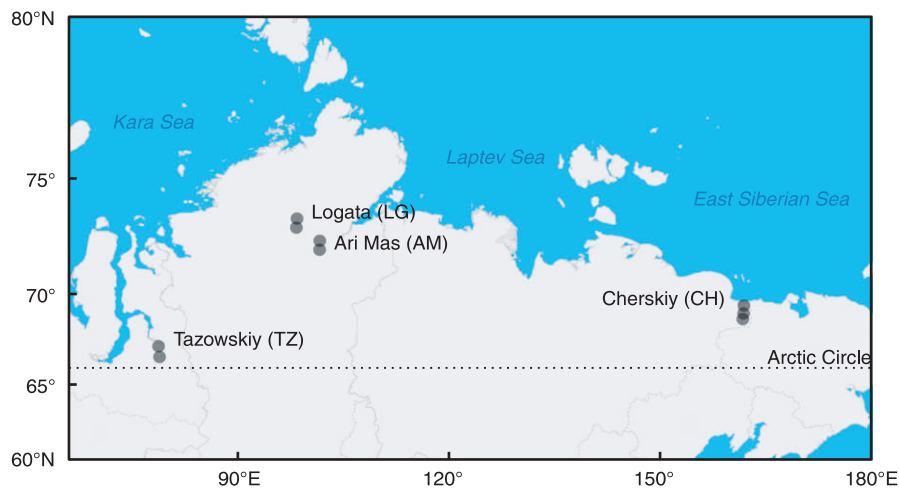


FIGURE 1 Map of sampling sites, with name abbreviations in brackets. Each point represents three replicate soil profiles (27 total soil profiles) [Colour figure can be viewed at wileyonlinelibrary.com]

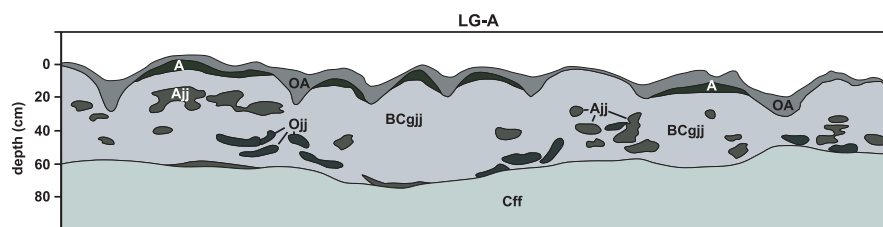


FIGURE 2 Cross-section of a representative Gelisol from Taimyr peninsula (graph adapted from Gentsch, Mikutta, Alves, et al., 2015). Very prominent, the cryoturbated OM-rich pockets in the subsoil (Ajj, Ojj) referred to as cryoturbated topsoils. Horizon designations according to (USDA, 1999) [Colour figure can be viewed at wileyonlinelibrary.com]

OC), the molar ratios of metal to OC ($\text{Fe}_d/\text{HF-OC}$, $(\text{Fe}_o + \text{Al}_o)/\text{HF-OC}$, $(\text{Fe}_p + \text{Al}_p)/\text{HF-OC}$) were calculated.

2.2 | Incubation and assessment of temperature sensitivity

Incubation experiments were performed on the bulk soil samples and their corresponding HFs. Since the HF comprised >80% and the LF only <5% of the total dry weight, we were unable to extract suitable amounts of the LF for incubation. Six profiles and five horizons per pit (O, A, Ajj, B/C, Cff; listed in order of increasing depth categories) were chosen for the bulk soil incubation ($n = 120$) from each site (TZ, AM, LG, CH). For the HF incubation, samples from four mineral horizons (A, Ajj, B/C, Cff) and three profiles per site were chosen ($n = 48$). The bulk and HF samples were incubated aerobically at constant temperatures of 5 and 15°C for 175 days in darkness (total $n = 336$). Below, the term “treatment” refers to a specific fraction (bulk or HF) and temperature (5 or 15°C).

Ten grams of bulk and HF material from the mineral horizons and 5 g of the organic horizons were weighed into 120-ml flasks and were adjusted to 60% water-holding capacity (Howard & Howard, 1993). The flasks were plugged with polyethylene wool to minimize water loss and allow gas exchange. The moisture level was measured gravimetrically, and lost moisture was replaced weekly by adding ultrapure water. A preliminary incubation experiment (14 days at 15°C) was conducted to test the restoration of microbial activity in the bulk soil

and the effect of the density fractionation on microbial diversity in the HF (details Supporting Information, Data S1). Measurement at the start of the preliminary experiment revealed that density fractionation caused a loss of 98.10% rRNA gene copy numbers in the HF. In contrast, the relative abundance of the major groups was only marginally effected (Supporting Information Figures S2 and S3). After 14 days of incubation, the rRNA gene copy numbers of bacteria and fungi showed faster growth rates in the HF as compared to the bulk. Archaea were generally of very low abundance (<0.3% of rRNA gene copy numbers in the bulk samples) and could not be restored after density fractionation. After 14 days, samples were characterized by a strong dominance of fungi in both treatments (bulk 97%, HF 99%). Further, the preincubation had the same respiration pattern between bulk soil and the HF, but 31% lower absolute rates for the latter (Supporting Information Figure S1). Despite the potential loss of the species-level diversity, the respiration pattern suggests substantial functional redundancy (Schimel & Schaeffer, 2012). Therefore, no inoculum was added, and the microbial community was reactivated by preincubating all samples for 14 days starting at 15°C. Residual sodium polytungstate in the HF was negligible and did not affect microbial respiration (Gentsch, Mikutta, Shibistova, et al., 2015). The lower temperature treatment was set to 5°C on day 7 of the preincubation. Gas sampling started after the preincubation (day 0) and was repeated on days 7, 14, 21, 28, 42, 56, 84, 112 and 175. Prior to the gas sampling, the flasks were crimped with hollow stoppers (IVA, Meerbusch, Germany) and flushed with synthetic air (20% O₂, 80%

N₂) until the headspace was replaced a minimum of three times. The headspace samples were taken using rubber-tight syringes 24 hr after closing the flasks and were injected into 20-ml preevacuated exetainers. The proper closing time was tested beforehand to avoid concentrations causing inhibiting effects on microorganisms and concentrations below the detection limit. The CO₂ concentrations were measured using a gas chromatograph equipped with an electron capture detector (Shimadzu GC 2014, Kyoto, Japan modified according to Lofffield, Flessa, Augustin, & Beese, 1997) and were corrected for the dissociated CO₂ in the soil solution in accordance with the method of Sparling and West (1990).

Cumulative OC mineralization during the incubation period was calculated as the sum of the daily CO₂-C evolution. The concentrations on the days between the measurement points were interpolated by applying a cubic spline function to the measured CO₂-C release. The CO₂ evolution was expressed per gram of initial soil OC ($\mu\text{g g}^{-1} \text{OC}^{-1} \text{day}^{-1}$), and the cumulative OC release was fitted to a first-order decay function optimized by a Gauss-Newton algorithm (equation 1).

$$C_{(t)} = C_{(0)} \times e^{-kt}, \quad (1)$$

where $C_{(0)}$ is the preincubation OC concentration of the sample ($\mu\text{g OC}$), k is the decay rate constant, and $C_{(t)}$ is the difference between $C_{(0)}$ and the cumulative amount of respired CO₂-C at time t . The proportion of the HF to the total OC mineralization was expressed as a percentage of the corresponding bulk sample assuming that the decomposition of the HF-OC was independent of the presence of LF-OC and its decay products. Using Eqn. 2, the temperature dependence of the OC mineralization was calculated as the Q10 (Kirschbaum, 1995; Lloyd & Taylor, 1994) based on the decay rate constants (k) at 5°C (T_1) and 15°C (T_2).

$$Q10 = \left(\frac{k_2}{k_1} \right)^{\left(\frac{10}{T_2 - T_1} \right)} \quad (2)$$

The amount of microbial biomass carbon (C_{mic}) was determined using the chloroform fumigation-extraction (CFE) method following the protocols presented by Brookes, Landman, Pruden, and Jenkinson (1985) and Sparling, Feltham, Reynolds, West, and Singleton (1990). Subsets of the postincubation samples were exposed to an ethanol-free chloroform atmosphere in a desiccator for 24 hr in darkness and were subsequently extracted in a 0.5 M K₂SO₄ solution (soil:solution ratio of 1:10), filtered through ash-free filters (Sartorius Stedim, grade 389), and measured for OC and TN (VarioTOCcube, Elementar, Hanau, Germany). The chloroform-labile C is proportional to the microbial biomass, and C_{mic} was calculated as the difference between the fumigated and nonfumigated samples, without a correction factor (Whittinghill & Hobbie, 2012).

2.3 | ¹⁴C analysis

Radiocarbon concentrations (¹⁴C) in the bulk soil and HF as well as in the CO₂ released during the incubation at 15°C were analysed for four profiles at two sites (AM, LG). For the ¹⁴CO₂ analyses, the

headspace CO₂ production was collected at the final stage of incubation between days 144 and 174. To obtain at least 0.4 mg of carbon for the measurements, the flasks were closed, and the headspace production was sampled every 5 days, followed by repeated flushing with synthetic air to prevent elevated CO₂ concentrations. Solid samples (free of inorganic carbon) were combusted in an elemental analyser, and the released CO₂ was purified, measured for ¹³C via IRMS, and reduced to graphite over an iron/silver catalyst. The gas samples were separated from other gasses in a cryogenic CO₂ trap and were treated in the same manner as the CO₂ from the solid samples. The ¹⁴C content was analysed via accelerator mass spectrometry at the Jena Radiocarbon Laboratory (Germany). A more detailed description of the sample preparation was presented by Steinhof, Adamiec, Gleixner, Wagner, and van Klinken (2003). The data were analysed in accordance with the method of Steinhof (2013) and were expressed as percent modern carbon (pMC; 100 pMC = 1950 AD; Stuiver & Polach, 1977). The ages were estimated using OxCal 4.2 (Ramsey & Lee, 2013), and the calibration curves for pMC < 100 and for pMC > 100 were IntCal13 (Reimer et al., 2013) and Bomb13NH2 (Hua, Barbetti, & Rakowski, 2013), respectively.

2.4 | Data analysis

The effects of the incubation treatments on the total OC mineralization (normalized to initial OC content) were analysed using linear mixed-effect models (LMMs) to account for the hierarchical nesting of soil samples within sites and for repeated measurements of a given soil sample (due to the fractionation and temperature treatments). The temperature, OM fraction and soil horizon were treated as fixed effects. We fitted various models (lmer, R package lme4; Bates, Mächler, Bolker, & Walker, 2015) such that the sites, horizons and samples within a site were allowed to interact with temperature and/or OM fraction. Their residuals were checked for normality, and the data were log transformed when needed. The model that fitted the OC mineralization data best was selected based on the Akaike information criterion (AIC). Differences between the treatments within the horizons were tested based on least-squares means obtained from the model fitted to the factor combinations (R package lsmeans; Lenth, 2016), followed by comparisons using approximative t -statistics and calculation of 95% confidence intervals. Differences between C_{mic} in individual treatments were analysed using the approach described above. The effects of the various soil parameters on the OC mineralization and Q10 were analysed by applying individual LMMs on the predictor variables. A detailed description is presented in the Supporting Information (Data S2).

Analysis of variance (ANOVA) was performed on the basic soil parameters, and groups were compared using Tukey's honest significance test (HSD). Below, the term 'significant' indicates that $p < 0.05$. Mean values are presented along with their standard errors (\pm SE) or confidence intervals (<2.5% CI, >97.5% CI). All the statistical analyses were performed using R 3.1.3 (R Core Team, 2015), and the figures were prepared using the ggplot2 package (Wickham, 2009).

3 | RESULTS

3.1 | Basic soil parameters

All the soils were classified as Aquiturbels (Soil Survey Staff, 2014) or Turbic Cryosols (IUSS Working Group WRB, 2014), which display strong evidence of cryoturbation and aquic conditions in the active layer during the thaw period. The soil pH increased from slightly acidic in the topsoil to moderately alkaline in the permafrost (Supporting Information Table S3). The soil texture classes were silty clay loam or silt loam at sites TZ, LG and CH and sandy loam and loam at site AM (Table 1). The total pedogenic Fe contents extracted using dithionite-citrate ranked in the order of AM > TZ > LG > CH but did not vary significantly between horizons (two-way ANOVA, $F_{(3, 79)} = 46$, $p_{\text{site}} < 0.001$; $F_{(3, 79)} = 0.2$, $p_{\text{horizon}} = 0.88$). The Fe liberated from poorly crystalline Fe minerals using acid oxalate represented the largest fraction of pedogenic Fe. The amount of organically complexed Fe and Al present in ultracentrifuged pyrophosphate extracts varied between sites and horizons (two-way ANOVA, $F_{(9, 79)} = 46$, $p_{(\text{site} \times \text{horizon})} < 0.05$), and larger amounts were present in the CH and LG soils than in the AM and TZ soils. The largest amounts of organically complexed Fe and Al were present in the cryoturbated topsoils and exceeded those in the surrounding

mineral horizons on average by a factor of 3. The OC and TN concentrations in the cryoturbated topsoils were up to threefold higher than in the surrounding mineral subsoil (Table 1). The molar ratios of metal (Fe_d , $\text{Fe}_o + \text{Al}_o$, $\text{Fe}_p + \text{Al}_p$) to carbon were significantly smaller in the topsoil and cryoturbated topsoils than in the mineral subsoil and the permafrost (Supporting Information Figure S7). High OC concentrations (>1% on average) were found in the permafrost of CH, AM and LG, except in the TZ soils (<0.2% on average), with their thicker active layers and weaker evidence of cryogenic processes. High proportions of LF-OC were present in the cryoturbated topsoils and permafrost horizons (again, the TZ soils were the exception), but the larger proportion of total OC and TN in all the horizons was still associated with minerals (HF-OC $63 \pm 1\%$; HF-TN $83 \pm 4\%$). Interestingly, the proportion of HF did not differ significantly between sites or horizons, despite the large distances between the sites and differences in soil development. The total soil OC storage within the uppermost metre of soil (calculations from Gentsch, Mikutta, Alves, et al., 2015) varied from 6.5 kg/m^2 at TZ to 36.4 kg/m^2 at LG. Based on an average OC storage of $20.2 \pm 1.5 \text{ kg/m}^2$, 18% of the OC ($2.5 \pm 0.5 \text{ kg/m}^2$) was stored in the cryoturbated topsoils materials and 34% ($8.1 \pm 1.2 \text{ kg/m}^2$) in the permafrost (except at TZ). The organic horizons stored 13% ($2.6 \pm 0.5 \text{ kg/m}^2$) of the total OC in the uppermost metre, whereas

TABLE 1 Properties of the incubated soil samples ($n = 120$, mean \pm SE) according to (Gentsch, Mikutta, Alves, et al., 2015). Note, element contents for the LF and HF are given per g of dry weight bulk soil, while C/N ratios refer to the element concentration of the substrates

Site	Horizon	OC bulk (mg/g)	TN bulk (mg/g)	OC LF (mg/g)	TN LF (mg/g)	OC HF (mg/g)	TN HF (mg/g)	C/N ratio Bulk
TZ	O ($n = 6$)	254.57 ± 20.98	7.46 ± 0.32	n.a.	n.a.	n.a.	n.a.	34.17 ± 2.50
	A ($n = 5$)	26.74 ± 6.84	1.66 ± 0.37	5.55 ± 1.26	0.14 ± 0.04	18.20 ± 4.77	1.35 ± 0.31	15.64 ± 0.78
	Ajj ($n = 6$)	34.95 ± 11.71	2.00 ± 0.49	4.31 ± 1.13	0.11 ± 0.02	19.08 ± 6.86	1.40 ± 0.34	15.09 ± 2.03
	BC ($n = 7$)	3.88 ± 0.94	0.39 ± 0.05	0.91 ± 0.35	0.02 ± 0.01	2.46 ± 0.59	0.34 ± 0.04	9.28 ± 1.20
	Cff ($n = 6$)	1.95 ± 0.27	0.29 ± 0.05	0.20 ± 0.05	0.01 ± 0.00	1.30 ± 0.16	0.26 ± 0.03	6.81 ± 0.48
AM	O ($n = 6$)	211.62 ± 90.25	7.13 ± 2.79	n.a.	n.a.	n.a.	n.a.	29.17 ± 1.25
	A ($n = 5$)	43.05 ± 10.72	2.42 ± 0.51	15.55 ± 7.25	0.58 ± 0.26	18.21 ± 4.13	1.26 ± 0.24	16.70 ± 1.43
	Ajj ($n = 9$)	47.63 ± 15.25	2.35 ± 0.46	26.15 ± 14.97	0.92 ± 0.42	18.54 ± 3.71	1.31 ± 0.27	18.44 ± 2.39
	BC ($n = 5$)	6.16 ± 1.49	0.51 ± 0.10	1.05 ± 0.30	0.04 ± 0.01	4.58 ± 1.24	0.42 ± 0.10	11.77 ± 0.75
	Cff ($n = 5$)	11.9 ± 3.17	0.74 ± 0.15	7.01 ± 5.31	0.34 ± 0.26	12.93 ± 3.31	0.93 ± 0.24	15.12 ± 1.69
LG	O ($n = 4$)	166.07 ± 5.56	8.94 ± 0.07	n.a.	n.a.	n.a.	n.a.	18.58 ± 0.47
	A ($n = 5$)	71.20 ± 8.03	4.58 ± 0.49	18.34 ± 6.34	0.80 ± 0.30	48.38 ± 6.02	3.31 ± 0.36	15.49 ± 0.35
	Ajj ($n = 8$)	80.18 ± 10.16	4.51 ± 0.33	20.27 ± 5.86	0.80 ± 0.19	49.40 ± 4.45	3.19 ± 0.18	17.47 ± 1.29
	BC ($n = 8$)	22.86 ± 2.21	1.59 ± 0.10	4.01 ± 0.63	0.15 ± 0.02	15.91 ± 1.92	1.26 ± 0.09	14.12 ± 0.62
	Cff ($n = 5$)	10.16 ± 0.74	0.89 ± 0.04	2.01 ± 0.22	0.07 ± 0.01	7.14 ± 0.92	0.72 ± 0.05	11.33 ± 0.42
CH	O ($n = 6$)	222.01 ± 8.06	11.00 ± 0.76	n.a.	n.a.	n.a.	n.a.	20.62 ± 1.49
	A ($n = 5$)	36.58 ± 21.89	2.38 ± 1.23	3.13 ± 0.65	0.09 ± 0.01	8.29 ± 1.20	0.85 ± 0.08	13.52 ± 1.14
	Ajj/Ojj ($n = 5$)	128.34 ± 24.32	7.29 ± 1.26	47.94 ± 11.22	1.95 ± 0.43	77.69 ± 15.16	5.64 ± 1.09	17.39 ± 0.43
	BC ($n = 8$)	15.01 ± 2.08	1.22 ± 0.12	1.89 ± 0.29	0.05 ± 0.01	9.99 ± 1.77	0.91 ± 0.10	12.04 ± 0.52
	Cff ($n = 6$)	29.06 ± 12.82	1.64 ± 0.35	3.84 ± 0.78	0.17 ± 0.03	12.45 ± 3.33	1.62 ± 0.48	14.58 ± 3.31
Total $n = 120$								

the LF- and HF-OC contributed 18% ($3.6 \pm 0.4 \text{ kg/m}^2$) and 55% ($11.1 \pm 0.9 \text{ kg/m}^2$) in the mineral horizons, respectively.

3.2 | OC mineralization and temperature response

After 175 days of incubation, the range of cumulative OC mineralization was 1.5 to 178.8 $\text{mg C g}^{-1} \text{ OC}^{-1}$ (Figure 3). The total OC mineralization generally decreased from the O to the B/C and was lowest in the Ajj horizon. However, Cff horizons exhibited high cumulative respiration rates, similar to the O horizon. The total OC mineralization did not differ significantly between sampling sites in the topsoil (O and A horizons) and cryoturbated topsoils (Supporting Information Table S4). Significantly, higher OC mineralization was observed in the B/C samples from TZ and in the permafrost samples from TZ and CH compared to the other sites. A comparison of the different treatments using the LMMs (summarized in Figure 3, right panel) shows significant differences between the bulk and HF samples in the 5°C treatment (except for the permafrost samples) but not in the 15°C treatment (Supporting Information Table S5). The average contribution of the HF to the total OC mineralization was 70.3% (61.3, 79.3), with no significant differences between soil horizons or temperature treatments (Supporting Information Figure S5). This parameter, however, requires a very careful interpretation, as the potential loss of the indigenous microbes during the

fractionation could likely have caused alterations of results. The linear mixed-effect models indicate that mineral stabilization, clay content, poorly crystalline Fe and Al oxyhydroxides and Fe- and Al-organic complexes were important predictors of OC mineralization in the A, B/C and Cff horizons, with higher values associated with 17% to 83% lower OC mineralization (Figure 6, Supporting Information Table S7). Higher temperatures and soil pH stimulated the OC mineralization significantly. Interestingly, higher C/N ratios reduced the OC mineralization in the cryoturbated topsoil and subsoil horizons. The k constant was 20% higher in the HF than in the bulk soil and significantly correlated to the bulk k (5°C: $r^2 = 0.67$, $p < 0.001$, 15°C: $r^2 = 0.57$, $p < 0.001$). Since we cannot rule out a possible effect of a changed microbial diversity on k and the resulting Q10, we treated the bulk soil and the HF independently in the statistical analyses. The average Q10 tended to be higher for the HF than for the bulk soil across all horizons, although this tendency was not statistically significant (Figure 4). For the bulk soil and HF, the Q10 decreased gradually from the topsoil (2.4 ± 0.1 and 2.9 ± 0.5) towards the permafrost (1.4 ± 0.1 and 1.5 ± 0.2). The bulk soil showed strong negative correlations between the Q10 and the molar ratios of metal to HF-OC (Fe_d , $\text{Fe}_o + \text{Al}_o$) and pH (Supporting Information Table S8). Positive relationships were observed between the Q10 and the C/N ratio and $\delta^{13}\text{C}$ content. An increase in the molar ($\text{Fe}_o + \text{Al}_o$)/HF-OC ratio by a factor of 10 in the bulk soil, for exam-

C/N ratio LF	C/N ratio HF	Fe _d (mg/g)	Fe _o (mg/g)	Fe _p (mg/g)	Al _o (mg/g)	Al _p (mg/g)	Clay (wt%)	Silt (wt%)
n.a.	n.a.	n.a.	n.a.	n.a.	n.a.	n.a.	n.a.	n.a.
40.69 ± 1.49	13.02 ± 0.76	5.60 ± 0.34	3.90 ± 0.44	0.81 ± 0.19	1.66 ± 0.25	0.68 ± 0.16	23.9 ± 3.05	68.43 ± 2.72
34.74 ± 3.61	11.75 ± 1.64	6.44 ± 0.28	4.70 ± 0.50	0.96 ± 0.46	1.91 ± 0.51	0.78 ± 0.34	28.53 ± 4.65	65.17 ± 3.52
37.15 ± 3.91	6.65 ± 0.96	4.60 ± 0.29	3.04 ± 0.33	0.25 ± 0.06	0.98 ± 0.11	0.21 ± 0.05	19.61 ± 2.40	70.81 ± 3.66
28.53 ± 1.90	4.88 ± 0.22	4.44 ± 0.79	2.27 ± 0.11	0.15 ± 0.04	0.60 ± 0.05	0.07 ± 0.00	15.16 ± 3.37	63.15 ± 5.96
n.a.	n.a.	n.a.	n.a.	n.a.	n.a.	n.a.	n.a.	n.a.
25.90 ± 1.05	14.19 ± 1.60	2.68 ± 0.18	1.92 ± 0.17	0.46 ± 0.14	0.55 ± 0.08	0.20 ± 0.08	8.46 ± 0.64	22.05 ± 1.22
26.40 ± 2.53	13.83 ± 1.40	3.75 ± 0.50	2.16 ± 0.30	0.57 ± 0.17	0.85 ± 0.13	0.21 ± 0.08	11.55 ± 1.34	32.24 ± 4.10
29.56 ± 2.44	10.41 ± 0.79	4.38 ± 0.43	1.75 ± 0.26	0.16 ± 0.01	0.88 ± 0.10	0.11 ± 0.01	15.31 ± 1.86	40.69 ± 6.93
20.03 ± 0.42	13.97 ± 0.78	5.23 ± 0.99	2.26 ± 0.27	0.31 ± 0.14	0.73 ± 0.12	0.09 ± 0.01	13.04 ± 2.43	34.31 ± 6.41
n.a.	n.a.	n.a.	n.a.	n.a.	n.a.	n.a.	n.a.	n.a.
25.35 ± 1.72	14.57 ± 0.56	5.76 ± 0.73	3.47 ± 0.41	0.94 ± 0.13	0.68 ± 0.09	0.33 ± 0.05	22.80 ± 3.94	53.20 ± 4.07
23.77 ± 1.95	15.49 ± 1.15	6.57 ± 1.08	5.28 ± 1.37	1.81 ± 0.51	0.82 ± 0.10	0.34 ± 0.04	26.57 ± 1.54	61.95 ± 1.99
27.47 ± 0.94	12.33 ± 0.73	8.41 ± 0.38	5.41 ± 0.47	1.11 ± 0.20	0.93 ± 0.08	0.23 ± 0.03	31.49 ± 1.66	64.06 ± 2.29
29.13 ± 1.34	9.95 ± 0.75	6.74 ± 3.32	4.44 ± 0.69	0.57 ± 0.02	0.63 ± 0.01	0.08 ± 0.01	24.83 ± 0.56	74.99 ± 0.58
n.a.	n.a.	n.a.	n.a.	n.a.	n.a.	n.a.	n.a.	n.a.
36.64 ± 6.79	9.62 ± 0.81	11.94 ± 0.92	6.92 ± 0.85	0.55 ± 0.05	1.69 ± 0.35	0.31 ± 0.05	19.80 ± 2.71	73.61 ± 2.44
24.34 ± 0.44	14.02 ± 1.18	11.98 ± 2.78	11.76 ± 3.05	4.82 ± 1.51	2.62 ± 0.36	1.25 ± 0.31	30.83 ± 5.04	66.45 ± 4.80
36.47 ± 2.19	10.54 ± 0.74	10.03 ± 1.03	8.35 ± 1.05	1.13 ± 0.33	1.39 ± 0.09	0.30 ± 0.03	18.91 ± 0.91	75.02 ± 1.33
22.34 ± 2.26	9.65 ± 2.05	9.10 ± 0.81	7.95 ± 0.81	0.90 ± 0.34	1.16 ± 0.11	0.17 ± 0.06	16.47 ± 1.71	79.47 ± 2.88

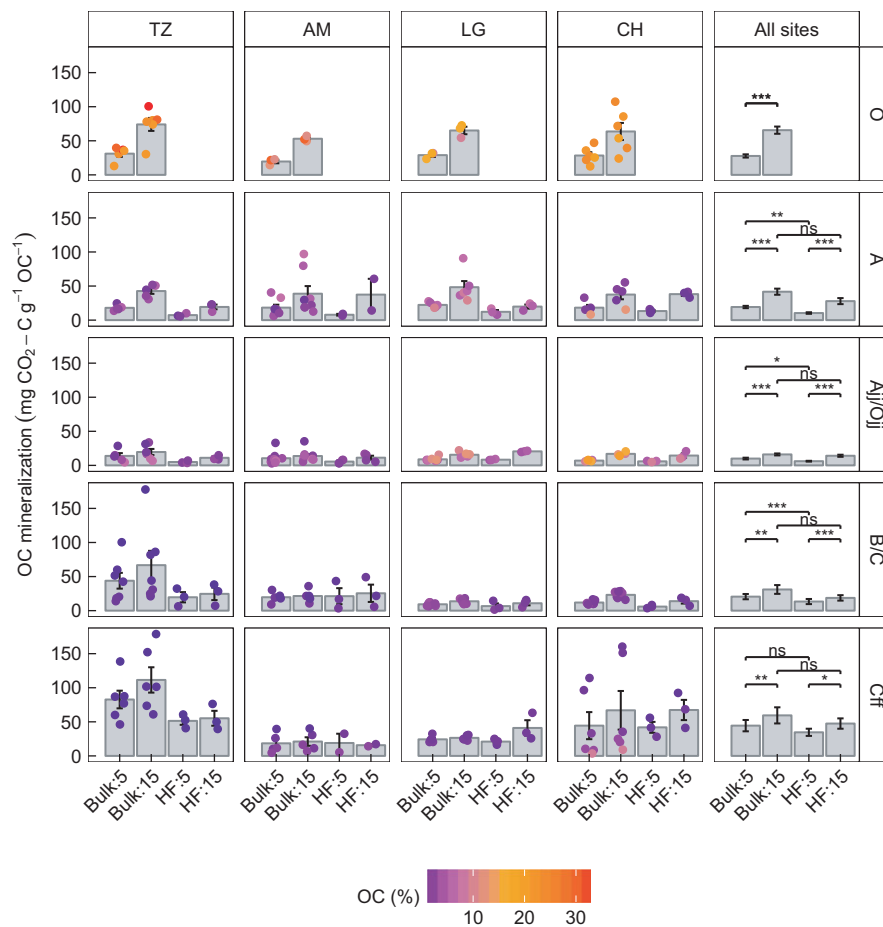


FIGURE 3 Total OC mineralization in the bulk soil and HF during the 175-day incubation period at 5 and 15°C. The panel columns TZ, AM, LG and CH show the mean values \pm SE (as bars and whiskers) of treatments (Bulk 5°C, Bulk 15°C, HF 5°C, HF 15°C) for the individual sampling sites with respect to the individual soil horizon classes (O, A, Ajj/Ojj, B/C, Cff). The positions of the points indicate the OC mineralization of each sample, while the colours show the initial OC concentration (in % dry weight). The right panel column (all sites) summarizes all the sampling sites (mean \pm SE, $n = 336$). Significant differences between the treatments (box brackets) were compared using four linear mixed models (ns, $p > 0.05$; *, $p < 0.05$; **, $p < 0.01$; ***, $p < 0.001$, see Statistics section and Supporting Information Table S4) [Colour figure can be viewed at wileyonlinelibrary.com]

ple, resulted in a significant linear reduction of the Q10 by 11.5%, after taking into account the sampling sites and horizons as random effects (Figure 7 and Supporting Information Table S8). Those effects were observed in the bulk soil and HF but appeared to be significant only in the former.

3.3 | Microbial biomass C

The microbial biomass (C_{mic} per gram of soil) at the end of the incubation was largest in the organic topsoil samples and ranked in order of $O > A = Ajj > B/C = Cff$ (Supporting Information Figure S6). Multiple comparisons indicated significantly larger C_{mic} in the 15°C treatments than in the 5°C treatments across all soil horizons (Supporting Information Table S6). Similarly, C_{mic} was approximately twice as high in the bulk soil samples as in the HF (Supporting Information Table S6). A strong positive linear relationship was evident between C_{mic} and OC concentration in the bulk samples (Supporting Information Figure S6, upper panel). The same trend, although weaker but

still highly significant, was observed for the HF (Supporting Information Figure S6, lower panel). The ratio of the microbial response to the 10°C temperature increase (C_{mic} 15°C divided by C_{mic} 5°C) did not vary between the sites and was constant between all the mineral soil horizons.

3.4 | Radiocarbon signature

The organic topsoil horizons exhibited a modern ^{14}C signature (>115 pMC), suggesting the presence of OM that had accumulated since the mid 1980s (Figure 5 and Supporting Information Table S9 for calibrated ^{14}C ages). The cryoturbated topsoils displayed higher ^{14}C activity (78–96 pMC) than the surrounding soil (21–68 pMC), indicating strong cryogenic activity during the previous 2 kyrs. The lowest ^{14}C activity was observed in the permafrost of the LG samples (5–14 pMC), indicating ^{14}C ages between 19–28 kyrs BP. Except for four samples, lower ^{14}C concentrations were present in the HF than in the bulk soil. These

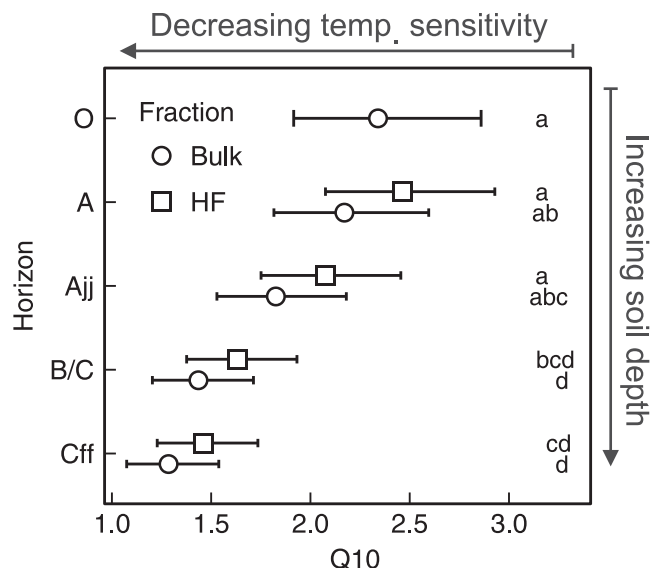


FIGURE 4 Temperature sensitivity of OC mineralization expressed as Q10 (mean \pm 95% CI) in the bulk soil and the corresponding HF. The soil horizons are arranged in order of depth from organic topsoil (O) to permafrost (Cff). Lower case letters denote significant differences between horizons and fractions based on the LMM comparisons ($p < 0.05$)

four samples were characterized by higher proportions of LF-OC (72% in Ajj, 20% in the two B/C samples, and 44% in the Cff samples), with apparently lower ^{14}C activity than in the HF. The ^{14}C in the CO_2 released from the topsoil and cryoturbated topsoil horizons generally followed the pattern of the solid OM but was slightly higher (4–5 pMC) than the latter (Figure 5). Almost equal ^{14}C activities of the bulk OM and their CO_2 response from the O horizons reflect the decomposition of recent OM. Except for one permafrost sample, the ^{14}C activity in the CO_2 from the bulk and HF subsoil samples (B/C, Cff) was 55–77 pMC higher than those of the solid samples. In the A and B/C horizons, the ^{14}C activities in the CO_2 of the HF were higher than that of the bulk soil, whereas those of the Ajj and Cff horizons did not show a clear trend. The ^{14}C activity was significantly negatively related to the molar ratios of metal to HF-OC ($\text{Fe}_d/\text{HF-OC}$: $r^2 = 0.47$, $p < 0.001$; $(\text{Fe}_o + \text{Al}_o)/\text{HF-OC}$: $r^2 = 0.35$, $p < 0.01$; $(\text{Fe}_p + \text{Al}_p)/\text{HF-OC}$: $r^2 = 0.32$, $p < 0.01$).

4 | DISCUSSION

4.1 | Controls on OC turnover in permafrost

Permafrost environments contain unique soils, in which slow degradation of plant residues due to unfavourable abiotic conditions results in the accumulation of large OC stocks (Hugelius et al., 2014; Tarnocai et al., 2009). We compared the potential bioavailability of OM from five major genetic horizons of permafrost-affected soils via laboratory incubation under aerobic conditions. Additionally, we compared the mineralization and temperature response of the MOAs

(i.e., HFs) to that of their bulk OM equivalents. For the bulk OM, our results show that the up-to-28-kyrs-old OM in the permafrost horizons display OC mineralization rates equal to or higher than the recent OM in the organic topsoil horizons (Figure 3). These observations corroborate the results of previous research (e.g., Lee, Schuur, Inglett, Lavoie, & Chanton, 2012; Vonk et al., 2013) and suggest potentially high availability of OM in the permafrost. The permafrost layer within the first soil metre of the investigated soils stored 8.1 kg/m^2 OC on average and 4.4% thereof was readily available within the incubation period, even under the low temperature treatments. The results underpin the vulnerability of ancient permafrost OC to climate change and a substantial fraction of this material can be subject to rapid breakdown upon permafrost thaw (Schuur et al., 2015).

In contrast to the fast turnover in the permafrost, the total bulk OC mineralization in cryoturbated topsoils was up to four orders of magnitude lower than that in our undisturbed topsoils and was quite constant across sampling sites. Despite the very different OC mineralization rates in the mineral topsoils and cryoturbated topsoils, the initial OC content, the C/N ratios, and the microbial biomass at the end of the experiment, did not differ significantly. In addition, the chemical OM compositions in those horizons have been shown to be very similar (Gentsch, Mikutta, Shibistova, et al., 2015). Therefore, microbial biomass and substrate composition can hardly explain all the different OM mineralization patterns among the individual soil horizons. Key factors controlling OM turnover in soils are the properties of the microbial community and the accessibility of organic substrates for extracellular enzyme degradation (Dungait et al., 2012). These key factors appeared to be valid explanations for the retarded decomposition in cryoturbated topsoils, even under the favourable conditions simulated in our experiment. The microbial community composition can be very different between topsoils and cryoturbated topsoils (Gittel et al., 2014) and is closely related to the enzyme activities for OM breakdown in the latter (Schnecker et al., 2015). Further, the decomposition of OM in cryoturbated topsoils has been shown to be constrained by the availability of labile N and C sources (Wild et al., 2016).

Knowledge about the distribution of OC between functionally different OM fractions and their inherent decomposition patterns provides deeper insights into the main controls on total OC mineralization. We found that an average of 63% of the total OC stocks within the mineral soil horizons was present in the HF. The LF accounted for 22% of the subsoil OC stocks, and the rest was mobilized in dissolved form during the density fractionation (Gentsch, Mikutta, Alves, et al., 2015). During the incubation, we discovered that the HF was contributing to about 70% to the bulk soil respiration in all the mineral soil horizons (Supporting Information Figure S4). Consequently, the OC mineralization in the HF followed the pattern of that in the bulk soil: highest in the permafrost and lowest in the cryoturbated topsoils. Also, ^{14}C activity and the corresponding age of the bulk OC were in most cases dominated by the HF. Our results thus indicate that the OC in the HF likely contribute largely to the CO_2 release from mineral horizons. This conclusion is also

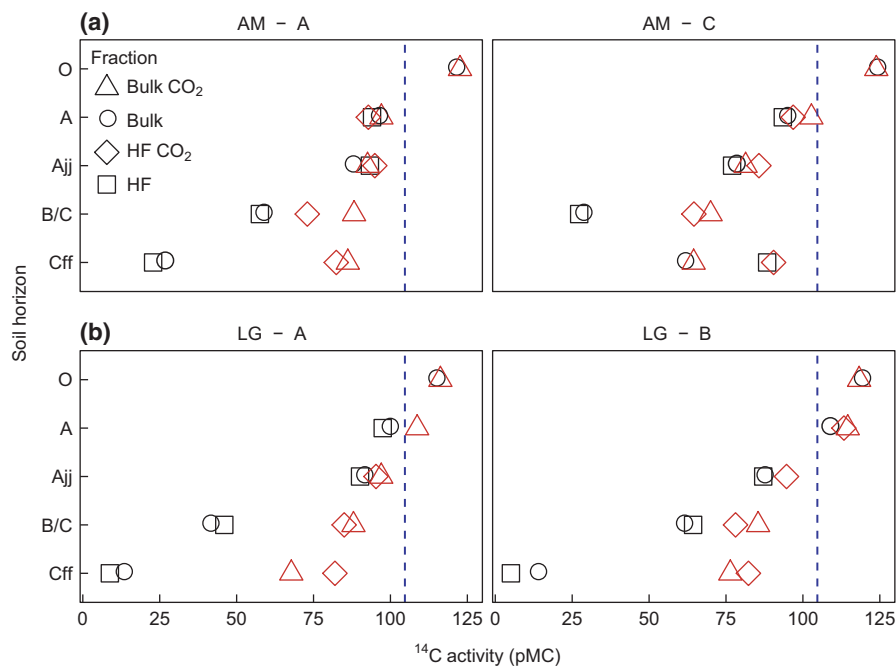


FIGURE 5 Radiocarbon activity (^{14}C in pMC) in soil horizons of four soil profiles from the Taimyr Peninsula (5a: AM, 5b: LG). The soil horizons were arranged in order of depth. The ^{14}C activity of the bulk material (circles) and the corresponding HF (rectangles) are shown in black. Red symbols denote the ^{14}C activity of CO_2 sampled over the last month of incubation at 15°C . The blue dashed line denotes the Northern Hemisphere atmospheric ^{14}C signature during the 2011 sampling campaign (Levin, Kromer, & Hammer, 2013). Uncertainties in the ^{14}C measurements were smaller than the symbols and original data as well as calibrated radiocarbon ages are given in Supporting Information Table S9 [Colour figure can be viewed at wileyonlinelibrary.com]

consistent with a previous short-term incubation experiment showing that the LF in subsoil horizons displayed even lower mineralization rates than the HF (Gentsch, Mikutta, Shibistova, et al., 2015). We further found that the respired HF- CO_2 in the subsoil (Figure 5, B/C and Cff horizons) was between 12 and 26 kyrs younger than the HF-OC source. These large differences demonstrate that MOA is not a homogeneous fraction. The MOA rather is composed of at least two pools: a younger, faster-cycling continuum and an older, more-stable continuum (see also Swanston et al., 2005; Koarashi, Hockaday, Masiello, & Trumbore, 2012; Schrupf et al., 2013). The bioavailable continuum of the HF-OC in the subsoil was <9% of the initial OC and had maximum ages of 0.7 to 3.7 kyrs BP (Figure 5, red symbols). The much older HF-OC continuum was not mineralized within the incubation period. These findings are in agreement with the findings of Mueller et al. (2014) and confirm that the more recently fixed OC was respired first during the incubation.

4.2 | Temperature sensitivity and mineral controls

Temperature was a strong control increasing the OC mineralization during the incubation (Figure 6). According to the principles of kinetic theory, the temperature sensitivity of OM increases with “substrate complexity” (Davidson & Janssens, 2006). In other words, substances requiring low activation energy, such as glucose, display lower temperature sensitivity than molecular complex substances, such as lignin. This so-called ‘carbon-quality-temperature’ (CQT)

hypothesis appears to be valid for topsoil materials in various ecosystems (Conant et al., 2011; Craine, Fierer, & McLauchlan, 2010). By testing the CQT experimentally, those studies indicated that rapidly cycling (high-quality) OM has lower activation energy than slowly decomposing (low-quality) OM. In the permafrost soils in our study, the HF also exhibited a greater sensitivity to temperature than the faster decomposing bulk OM, containing the particulate and leachable OM. However, the CQT concept fails when considering the variation in temperature sensitivity with depth. We observed decreasing temperature sensitivity with depth regardless of the type of OM fraction (Figure 4). At the same time, the Q10 is positively correlated with the C/N ratio and $\delta^{13}\text{C}$ values (Supporting Information Table S8). Following the concept outlined above, such a pattern would suggest greater stability of OM in the upper horizons, which is not supported by the molecular structure. Our previous investigation showed increasing OM transformation with depth. The transformation was indexed by decreasing C/N ratios, increasing $\delta^{13}\text{C}$ values, increasing amounts of aromatic and alkyl-C structures and decreasing O/N-alkyl-C structures such as carbohydrates as well as relative enrichment of lignin-derived phenols and depletion of neutral sugars (Dao et al., 2018; Gentsch, Mikutta, Shibistova, et al., 2015). Therefore, the discrepancy between kinetic theory and the observed temperature sensitivity may be explained by reduced OC availability with increasing depth, and more specifically, by mineral protection of OM (Gillabel et al., 2010).

Most likely, labile substances for cometabolic decomposition of substances that require higher energy input are scarce and are

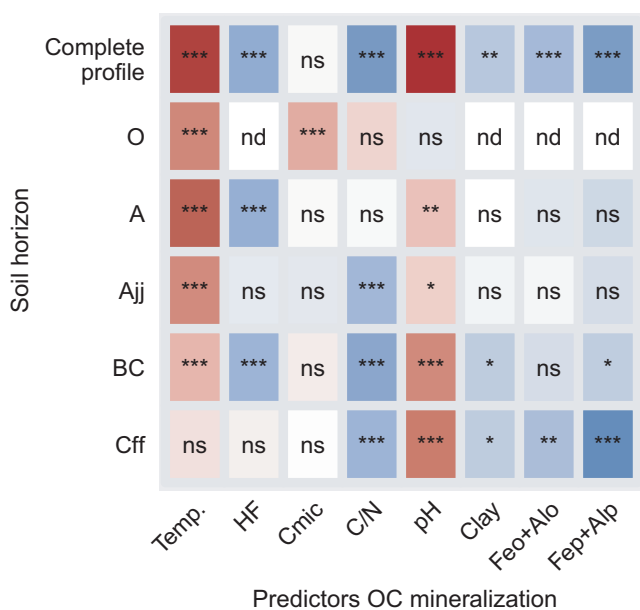


FIGURE 6 Composite plot of LMMs of multiple soil parameters (predictors as fixed factors) on OC mineralization during laboratory incubation. The colours indicate the effect strength (based on *t*-values), with red indicating a positive effect (amplification) and blue indicating a negative effect (attenuation) on OC mineralization. Significance levels of the predictors based on adjusted *p*-values: ns, $p > 0.05$; *, $p < 0.05$; **, $p < 0.01$; ***, $p < 0.001$; nd, not determined. Abbreviations of the predictors from left to right: Temp., Temperature; HF, mineral stabilization; Cmic, microbial biomass; C/N, C/N ratio; pH, soil pH; Clay, clay content; Feo + Alo, poorly crystalline Fe and Al oxyhydroxides and Fe- and Al-organic complexes; Fep + Alp, organically complexed Fe and Al. For all model parameters and detailed description, see Supporting Information Table S7 [Colour figure can be viewed at wileyonlinelibrary.com]

unavailable for potential stimulation of the microbial activity at higher temperatures (Amelung, Flach, & Zech, 1999; Karhu et al., 2010). For example, the OC mineralization in the bulk samples from the cryoturbated topsoils was found to rely on the addition of allochthonous nutrients and solutes from the topsoil (Čapek et al., 2015). Additionally, priming has shown to be specifically pronounced in deeper soil horizons in two studies with cryoturbated permafrost soils (Wild et al., 2014, 2016). These energy constraints affect the apparent temperature sensitivity of the OM, and its intrinsic temperature sensitivity may be attenuated (Lefèvre et al., 2013; Schmidt et al., 2011).

Enzymatic decomposition can be reduced upon sorption of OM to minerals (Mikutta et al., 2007), which can decrease the apparent temperature sensitivity of OM (Davidson & Janssens, 2006). The strong negative link between Q10 and the ratios of metal to HF-OC (Figure 7, Supporting Information Table S8) provide evidence for the attenuation of the Q10 by mineral protection. Higher metal-to-OC ratios result in a greater probability that OM will react with metals or their oxyhydroxides (Kleber et al., 2015). Smaller OC loadings of minerals in the subsoil (operationally mirrored by the increase in the

metal-to-HF-OC-ratios; Supporting Information Figure S7) than in the topsoil may also cause stronger mineral-organic binding (Kaiser & Guggenberger, 2003). Further, the negative correlation between the ^{14}C activity and the metal-to-HF-OC-ratios supports the assumption that samples with a higher organo-mineral reaction capacity showed the longest residence time in the soils. This reasoning is supported by the strong negative effects of clay minerals, HF-OC and Fe and Al forms on the OC mineralization in the subsoil (Figure 6). A recent experiment involving organic Gelisols yielded a similar decrease in the Q10 with increasing mineral content (Bracho et al., 2016).

Finally, in our study, the soil pH appeared to be a highly significant predictor of both the OC mineralization and Q10 (Figure 6, Supporting Information Table S8). Because mineral-OM interactions (i.e., adsorption-desorption, coprecipitation) are strongly controlled by soil pH, weaker binding occurs at neutral and alkaline pH, whereas desorption processes and thus the OM accessibility to decomposers are reduced at low soil pH (see the review by Kleber et al., 2015). Higher OC mineralization with increasing soil pH was observed within the horizons where the mineral predictors significantly reduce OC mineralization (A, B/C, Cff horizons) but not within the organic horizons (Figure 6).

Overall, our results demonstrate that the temperature sensitivity of OC in permafrost soils is not necessarily related to substrate quality but rather to the physicochemical stabilization mechanisms in the soil environment. Mineral protection contributes greatly to the stabilization of OC in permafrost subsoils and apparently has an attenuating effect on temperature sensitivity. We suggest that the Q10 depth gradient in our study is the result of progressive mineral protection counteracting the increasing activation energy of biochemical transformation processes towards more complex substrates in the subsoil OM (see Figure 8 for a schematic representation).

4.3 | Implications for climate change

The findings of this study have important implications for the mechanistic understanding of how permafrost soils may respond to climate change. Despite this, results of the laboratory incubation must be extrapolated to the field with some caution. The experiment was conducted under optimal laboratory conditions and the complexity of large-scale biogeochemical processes in the field cannot be reflected in such experiments. Some limitations in the data interpretation might also derive from the loss of microorganisms during fractionation. However, we analysed bulk soil and HF separately and all trends of the bulk soil were likewise observed for the HF (see discussion in Supporting Information Data S1).

Climate models highlight the sensitivity to hydrologic changes in permafrost environments and project significant soil drainage with further permafrost thawing (Lawrence, Koven, Swenson, Riley, & Slater, 2015; Olefeldt, Turetsky, Crill, & McGuire, 2013; Sushama et al., 2007). Those changes will affect the soil physicochemical conditions and thus the formation of secondary minerals. For example, due to the hydromorphic conditions, most of the soil Fe is currently in a

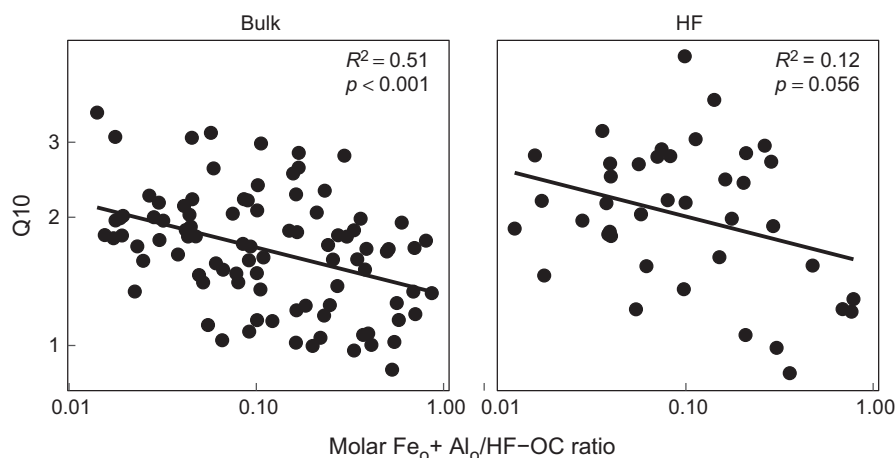


FIGURE 7 Relationship between Q10 and the metal-to-HF-OC ratio of permafrost-affected soils, plotted on logarithmic axes. Note, fitting parameters derived from LMMs with horizon and site as random effects (model details are presented in Supporting Information Table S8). The overall goodness of fit for the two LMMs was obtained according to Nakagawa and Schielzeth (2013)

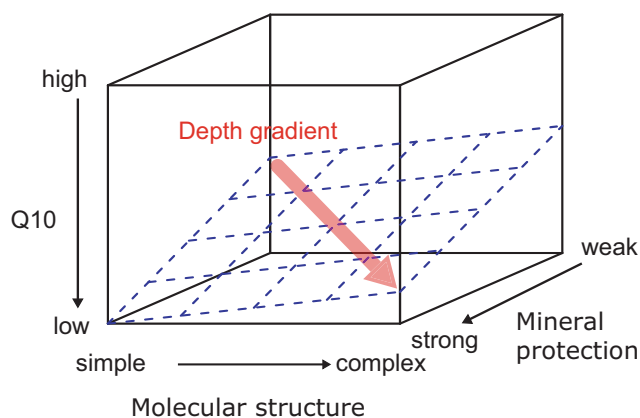


FIGURE 8 Schematic illustration of factors controlling the apparent temperature sensitivity during the incubation experiment (modified according to Davidson & Janssens, 2006). The x-axis refers to the molecular structure of the substrate. Increasing substrate complexity is characterized by increased high molecular weight structures and a slower turnover [Colour figure can be viewed at wileyonlinelibrary.com]

dynamic state in the active layer (Alekseev et al., 2003; Rivkina, Gilichinsky, Wagener, Tiedje, & McGrath, 1998), and the availability of oxygen will rapidly promote the formation of new Fe oxide-organic associations via adsorption or coprecipitation (Kleber et al., 2015). Such physicochemical shifts have been reported by Kawahigashi, Kaiser, Rodionov, and Guggenberger (2006) and suggest higher sorptive capacity and retention of OM with increasing active layer thickness. The latest findings from a subarctic natural warming gradient (despite no permafrost soils) further suggested that soil warming led to a shift in the SOC fraction distribution (Poeplau, Kätterer, Leblans, & Sigurdsson, 2017). The authors found relative enrichment of more stable OC fractions in silt and clay with increasing warming but strong losses and transformation of OC in soil aggregates. Our findings are consistent with those presented by Gillabel et al. (2010) and Poeplau et al. (2017) and demonstrate that factors affecting the

apparent temperature sensitivity such as physicochemical protection need to be understood to gain deeper knowledge of the temperature sensitivity of OM in permafrost soil.

The results of this study highlight the relevance of MOA in permafrost soils to current OC storage. Mineral permafrost soils (such as Turbels and Orthels) store 73% of the soil OC in the northern circumpolar permafrost region (Hugelius et al., 2014), and wherever pedogenic minerals and OM come together, MOA account for approximately 90% of the soil OC, particularly in the subsoil. We conclude that although rising temperatures will promote CO₂ production in mineral permafrost soils, the amount of carbon that is lost can be attenuated by MOA.

ACKNOWLEDGEMENTS

Financial support was provided by the German Federal Ministry of Education and Research (03F0616A) within the ERANET EUROPO-LAR project CryoCARB. N. Gentsch is grateful for financial support from the Evangelisches Studienwerk Villigst. O. Shibistova and G. Guggenberger appreciate funding from the Russian Ministry of Education and Science (No.14.B25.31.0031). A. Richter, B. Wild and J. Schneckner acknowledge the financial support from the Austrian Science Fund (FWF - I370-B17). J. Bárta, H. Šantrůčková, T. Urich and G. Guggenberger were also supported by Czech Science Foundation MiCryoFun project n.16-18453S. We thank all members of the CryoCARB project team for their incredible team spirit and thank C. Borchers for fruitful comments. We are grateful to the technical staff of the Institute of Soil Science in Hannover for laboratory assistance.

ORCID

Norman Gentsch  <http://orcid.org/0000-0003-1166-8973>

Jörg Schneckner  <http://orcid.org/0000-0002-5160-2701>

REFERENCES

- Alekseev, A., Alekseeva, T., Ostroumov, V., Siegert, C., & Gradusov, B. (2003). Mineral transformations in permafrost-affected soils, North Kolyma Lowland, Russia. *Soil Science Society of America Journal*, 67(2), 596–605. <https://doi.org/10.2136/sssaj2003.5960>
- Amelung, W., Flach, K.-W., & Zech, W. (1999). Lignin in particle-size fractions of native grassland soils as influenced by climate. *Soil Science Society of America Journal*, 63(5), 1222–1228. <https://doi.org/10.2136/sssaj1999.6351222x>
- Bates, D., Mächler, M., Bolker, B., & Walker, S. (2015). Fitting linear mixed-effects models using lme4. *Journal of Statistical Software*, 67(1), 1–48. <https://doi.org/10.18637/jss.v067.i01>
- Bockheim, J., & Tarnocai, C. (1998). Recognition of cryoturbation for classifying permafrost-affected soils. *Geoderma*, 81, 281–293. [https://doi.org/10.1016/S0016-7061\(97\)00115-8](https://doi.org/10.1016/S0016-7061(97)00115-8)
- Borden, P. W., Ping, C.-L., McCarthy, P. J., & Naidu, S. (2010). Clay mineralogy in arctic tundra Gelsols, Northern Alaska. *Soil Science Society of America Journal*, 74(2), 580. <https://doi.org/10.2136/sssaj2009.0187>
- Bracho, R., Natali, S., Pegoraro, E., Crummer, K. G., Schädel, C., Celis, G., ... Schuur, E. A. G. (2016). Temperature sensitivity of organic matter decomposition of permafrost-region soils during laboratory incubations. *Soil Biology and Biochemistry*, 97, 1–14. <https://doi.org/10.1016/j.soilbio.2016.02.008>
- Brookes, P. C., Landman, A., Pruden, G., & Jenkinson, D. S. (1985). Chloroform fumigation and the release of soil nitrogen: A rapid direct extraction method to measure microbial biomass nitrogen in soil. *Soil Biology and Biochemistry*, 17(6), 837–842. [https://doi.org/10.1016/0038-0717\(85\)90144-0](https://doi.org/10.1016/0038-0717(85)90144-0)
- Čapek, P., Diáková, K., Dickopp, J.-E., Bárta, J., Wild, B., Schneckner, J., ... Šantrůčková, H. (2015). The effect of warming on the vulnerability of subducted organic carbon in arctic soils. *Soil Biology and Biochemistry*, 90, 19–29. <https://doi.org/10.1016/j.soilbio.2015.07.013>
- Carter, M., & Gregorich, E. (Eds.) (2008). *Soil sampling and methods of analysis*, 2nd ed. Boca Raton, FL: CRC Press.
- Cerli, C., Celi, L., Kalbitz, K., Guggenberger, G., & Kaiser, K. (2012). Separation of light and heavy organic matter fractions in soil - Testing for proper density cut-off and dispersion level. *Geoderma*, 170, 403–416. <https://doi.org/10.1016/j.geoderma.2011.10.009>
- Conant, R. T., Drijber, R. A., Haddix, M. L., Parton, W. J., Paul, E. A., Plante, A. F., ... Steinweg, J. M. (2008). Sensitivity of organic matter decomposition to warming varies with its quality. *Global Change Biology*, 14(4), 868–877. <https://doi.org/10.1111/j.1365-2486.2008.01541.x>
- Conant, R. T., Ryan, M. G., Ågren, G. I., Birge, H. E., Davidson, E. A., Eliasson, P. E., ... Bradford, M. A. (2011). Temperature and soil organic matter decomposition rates - synthesis of current knowledge and a way forward. *Global Change Biology*, 17(11), 3392–3404. <https://doi.org/10.1111/j.1365-2486.2011.02496.x>
- Craine, J. M., Fierer, N., & McLauchlan, K. K. (2010). Widespread coupling between the rate and temperature sensitivity of organic matter decay. *Nature Geoscience*, 3(12), 854–857. <https://doi.org/10.1038/ngeo1009>
- Crow, S. E., Swanston, C. W., Lajtha, K., Brooks, J. R., & Keirstead, H. (2007). Density fractionation of forest soils: Methodological questions and interpretation of incubation results and turnover time in an ecosystem context. *Biogeochemistry*, 85(1), 69–90. <https://doi.org/10.1007/s10533-007-9100-8>
- Dao, T. T., Gentsch, N., Mikutta, R., Sauheitl, L., Shibistova, O., Wild, B., ... Guggenberger, G. (2018). Fate of carbohydrates and lignin in north-east Siberian permafrost soils. *Soil Biology and Biochemistry*, 116, 311–322. <https://doi.org/10.1016/j.soilbio.2017.10.032>
- Davidson, E. A., & Janssens, I. A. (2006). Temperature sensitivity of soil carbon decomposition and feedbacks to climate change. *Nature*, 440(7081), 165–173. <https://doi.org/10.1038/nature04514>
- DIN ISO 11277 (2002). *Soil quality - Determination of particle size distribution in mineral soil material - Method by sieving and sedimentation* (34 pp). Berlin, Germany: Beuth.
- Dungait, J. A. J., Hopkins, D. W., Gregory, A. S., & Whitmore, A. P. (2012). Soil organic matter turnover is governed by accessibility not recalcitrance. *Global Change Biology*, 18(6), 1781–1796. <https://doi.org/10.1111/j.1365-2486.2012.02665.x>
- Elberling, B., Michelsen, A., Schädel, C., Schuur, E. A. G., Christiansen, H. H., Berg, L., ... Sigsgaard, C. (2013). Long-term CO₂ production following permafrost thaw. *Nature Climate Change*, 3(10), 890. <https://doi.org/10.1038/nclimate1955>
- Gentsch, N., Mikutta, R., Alves, R. J. E., Barta, J., Čapek, P., Gittel, A., & Guggenberger, G. (2015). Storage and transformation of organic matter fractions in cryoturbated permafrost soils across the Siberian Arctic. *Biogeosciences*, 12(14), 4525–4542. <https://doi.org/10.5194/bg-12-4525-2015>
- Gentsch, N., Mikutta, R., Shibistova, O., Wild, B., Schneckner, J., Richter, A., ... Guggenberger, G. (2015). Properties and bioavailability of particulate and mineral-associated organic matter in Arctic permafrost soils, Lower Kolyma Region, Russia. *European Journal of Soil Science*, 66, 722–734. <https://doi.org/10.1111/ejss.12269>
- Gillabel, J., Cebrian-Lopez, B., Six, J., & Merckx, R. (2010). Experimental evidence for the attenuating effect of SOM protection on temperature sensitivity of SOM decomposition. *Global Change Biology*, 16(10), 2789–2798. <https://doi.org/10.1111/j.1365-2486.2009.02132.x>
- Gittel, A., Bárta, J., Kohoutová, I., Mikutta, R., Owens, S., Gilbert, J., ... Urich, T. (2014). Distinct microbial communities associated with buried soils in the Siberian tundra. *The ISME Journal*, 8(4), 841–853. <https://doi.org/10.1038/ismej.2013.219>
- Golchin, A., Oades, J., Skjemstad, J., & Clarke, P. (1994). Study of free and occluded particulate organic matter in soils by solid state ¹³C Cp/MAS NMR spectroscopy and scanning electron microscopy. *Soil Research*, 32(2), 285–309. <https://doi.org/10.1071/SR9940285>
- Gundelwein, A., Müller-Lupp, T., Sommerkorn, M., Haupt, E. T. K., Pfeiffer, E.-M., & Wiechmann, H. (2007). Carbon in tundra soils in the Lake Labaz region of arctic Siberia. *European Journal of Soil Science*, 58(5), 1164–1174. <https://doi.org/10.1111/j.1365-2389.2007.00908.x>
- Hall, S. J., McNicol, G., Natake, T., & Silver, W. L. (2015). Large fluxes and rapid turnover of mineral-associated carbon across topographic gradients in a humid tropical forest: Insights from paired ¹⁴C analysis. *Biogeosciences*, 12(8), 2471–2487. <https://doi.org/10.5194/bg-12-2471-2015>
- Harden, J. W., Koven, C. D., Ping, C.-L., Hugelius, G., David Mc Guire, A., Camill, P., ... Grosse, G. (2012). Field information links permafrost carbon to physical vulnerabilities of thawing. *Geophysical Research Letters*, 39(15), L15704. <https://doi.org/10.1029/2012GL051958>
- Herold, N., Schöning, I., Michalzik, B., Trumbore, S., & Schrumpp, M. (2014). Controls on soil carbon storage and turnover in German landscapes. *Biogeochemistry*, 119(1–3), 435–451. <https://doi.org/10.1007/s10533-014-9978-x>
- Höfle, S., Rethemeyer, J., Mueller, C. W., & John, S. (2013). Organic matter composition and stabilization in a polygonal tundra soil of the Lena Delta. *Biogeosciences*, 10(5), 3145–3158. <https://doi.org/10.5194/bg-10-3145-2013>
- Howard, D. M., & Howard, P. J. A. (1993). Relationships between CO₂ evolution, moisture content and temperature for a range of soil types. *Soil Biology and Biochemistry*, 25(11), 1537–1546. [https://doi.org/10.1016/0038-0717\(93\)90008-Y](https://doi.org/10.1016/0038-0717(93)90008-Y)
- Hua, Q., Barbetti, M., & Rakowski, A. Z. (2013). Atmospheric radiocarbon for the period 1950–2010. *Radiocarbon*, 55(4), 2059–2072. https://doi.org/10.2458/azu_js_rc.55.16177
- Hugelius, G., Strauss, J., Zubrzycki, S., Harden, J. W., Schuur, E. A. G., Ping, C.-L., ... Kuhry, P. (2014). Estimated stocks of circumpolar permafrost carbon with quantified uncertainty ranges and identified data

- gaps. *Biogeosciences*, 11(23), 6573–6593. <https://doi.org/10.5194/bg-11-6573-2014>
- Hut, G. (1987). *Consultants' group meeting on stable isotope reference samples for geochemical and hydrological investigations*. Vienna, Austria: International Atomic Energy Agency.
- Im, S. T., & Kharuk, V. I. (2015). Dynamics of water mass in the Central Siberia permafrost zone based on gravity survey from the grace satellites. *Izvestiya, Atmospheric and Oceanic Physics*, 51(8), 806–818. <https://doi.org/10.1134/S0001433815080046>
- IUSS Working Group WRB (2014). *World reference base for soil resources 2014. International soil classification system for naming soils and creating legends for soil maps*. Rome, Italy: Food and Agriculture Organization.
- Kaiser, K., & Guggenberger, G. (2000). The role of DOM sorption to mineral surfaces in the preservation of organic matter in soils. *Organic Geochemistry*, 31(7–8), 711–725. [https://doi.org/10.1016/S0146-6380\(00\)00046-2](https://doi.org/10.1016/S0146-6380(00)00046-2)
- Kaiser, K., & Guggenberger, G. (2003). Mineral surfaces and soil organic matter. *European Journal of Soil Science*, 54(2), 219–236. <https://doi.org/10.1046/j.1365-2389.2003.00544.x>
- Karhu, K., Fritze, H., Hämäläinen, K., Vanhala, P., Jungner, H., Oinonen, M., ... Liski, J. (2010). Temperature sensitivity of soil carbon fractions in boreal forest soil. *Ecology*, 91(2), 370–376. <https://doi.org/10.1890/09-0478.1>
- Kawahigashi, M., Kaiser, K., Rodionov, A., & Guggenberger, G. (2006). Sorption of dissolved organic matter by mineral soils of the Siberian forest tundra. *Global Change Biology*, 12(10), 1868–1877. <https://doi.org/10.1111/j.1365-2486.2006.01203.x>
- Kirschbaum, M. U. F. (1995). The temperature dependence of soil organic matter decomposition, and the effect of global warming on soil organic C storage. *Soil Biology and Biochemistry*, 27(6), 753–760. [https://doi.org/10.1016/0038-0717\(94\)00242-S](https://doi.org/10.1016/0038-0717(94)00242-S)
- Kleber, M., Eusterhues, K., Keiluweit, M., Mikutta, C., Mikutta, R., & Nico, P. S. (2015). Mineral-organic associations: formation, properties, and relevance in soil environments. *Advances in Agronomy*, 130, 1–140.
- Koarashi, J., Hockaday, W. C., Masiello, C. A., & Trumbore, S. E. (2012). Dynamics of decadal cycling carbon in subsurface soils. *Journal of Geophysical Research: Biogeosciences*, 117(G3), 1–13. <https://doi.org/10.1029/2012JG002034>
- Kögel-Knabner, I., Guggenberger, G., Kleber, M., Kandeler, E., Kalbitz, K., Scheu, S., ... Leinweber, P. (2008). Organo-mineral associations in temperate soils: Integrating biology, mineralogy, and organic matter chemistry. *Journal of Plant Nutrition and Soil Science*, 171(1), 61–82. [https://doi.org/10.1002/\(ISSN\)1522-2624](https://doi.org/10.1002/(ISSN)1522-2624)
- Lawrence, D. M., Koven, C. D., Swenson, S. C., Riley, W. J., & Slater, A. G. (2015). Permafrost thaw and resulting soil moisture changes regulate projected high-latitude CO₂ and CH₄ emissions. *Environmental Research Letters*, 10(9), 094011. <https://doi.org/10.1088/1748-9326/10/9/094011>
- Lee, H., Schuur, E. A. G., Inglett, K. S., Lavoie, M., & Chanton, J. P. (2012). The rate of permafrost carbon release under aerobic and anaerobic conditions and its potential effects on climate. *Global Change Biology*, 18(2), 515–527. <https://doi.org/10.1111/j.1365-2486.2011.02519.x>
- Lefèvre, R., Barré, P., Moyano, F. E., Christensen, B. T., Bardoux, G., Eglin, T., ... Chenu, C. (2013). Higher temperature sensitivity for stable than for labile soil organic carbon – Evidence from incubations of long-term bare fallow soils. *Global Change Biology*, 1–8, 185–195. <https://doi.org/10.1111/gcb.12402>
- Lenth, R. V. (2016). Least-squares means: The R Package lsmmeans. *Journal of Statistical Software*, 69(1), 1–33. <https://doi.org/10.18637/jss.v069.i01>
- Levin, I., Kromer, B., & Hammer, S. (2013). Atmospheric $\Delta^{14}\text{CO}_2$ trend in Western European background air from 2000 to 2012. *Tellus Series B*, 65, <https://doi.org/10.3402/tellusb.v65i0.20092>
- Lloyd, J., & Taylor, J. A. (1994). On the temperature dependence of soil respiration. *Functional Ecology*, 8(3), 315–323. <https://doi.org/10.2307/2389824>
- Lofffield, N., Flessa, H., Augustin, J., & Beese, F. (1997). Automated gas chromatographic system for rapid analysis of the atmospheric trace gases methane, carbon dioxide, and nitrous oxide. *Journal of Environmental Quality*, 26(2), 560–564. <https://doi.org/10.2134/jeq1997.00472425002600020030x>
- Mikutta, R., Lorenz, D., Guggenberger, G., Haumaier, L., & Freund, A. (2014). Properties and reactivity of Fe-organic matter associations formed by coprecipitation versus adsorption: Clues from arsenate batch adsorption. *Geochimica et Cosmochimica Acta*, 144, 258–276. <https://doi.org/10.1016/j.gca.2014.08.026>
- Mikutta, R., Mikutta, C., Kalbitz, K., Scheel, T., Kaiser, K., & Jahn, R. (2007). Biodegradation of forest floor organic matter bound to minerals via different binding mechanisms. *Geochimica et Cosmochimica Acta*, 71(10), 2569–2590. <https://doi.org/10.1016/j.gca.2007.03.002>
- Mueller, C. W., Gutsch, M., Kothieringer, K., Leifeld, J., Rethemeyer, J., Brueggemann, N., & Kögel-Knabner, I. (2014). Bioavailability and isotopic composition of CO₂ released from incubated soil organic matter fractions. *Soil Biology and Biochemistry*, 69, 168–178. <https://doi.org/10.1016/j.soilbio.2013.11.006>
- Mueller, C. W., Hoeschen, C., Steffens, M., Buddenbaum, H., Hinkel, K., Bockheim, J. G., & Kao-Kniffin, J. (2017). Microscale soil structures foster organic matter stabilization in permafrost soils. *Geoderma*, 293, 44–53. <https://doi.org/10.1016/j.geoderma.2017.01.028>
- Nakagawa, S., & Schielzeth, H. (2013). A general and simple method for obtaining R² from generalized linear mixed-effects models. *Methods in Ecology and Evolution*, 4(2), 133–142. <https://doi.org/10.1111/j.2041-210x.2012.00261.x>
- Olefeldt, D., Turetsky, M. R., Crill, P. M., & McGuire, A. D. (2013). Environmental and physical controls on northern terrestrial methane emissions across permafrost zones. *Global Change Biology*, 19(2), 589–603. <https://doi.org/10.1111/gcb.12071>
- Ostroumov, V., Hoover, R., Ostroumova, N., Van Vliet-Lanoë, B., Siegert, C., & Sorokovikov, V. (2001). Redistribution of soluble components during ice segregation in freezing ground. *Cold Regions Science and Technology*, 32(2–3), 175–182. [https://doi.org/10.1016/S0165-232X\(01\)00031-3](https://doi.org/10.1016/S0165-232X(01)00031-3)
- Ping, C. L., Jastrow, J. D., Jorgenson, M. T., Michaelson, G. J., & Shur, Y. L. (2014). Permafrost soils and carbon cycling. *SOIL Discussions*, 1(1), 709–756. <https://doi.org/10.5194/soild-1-709-2014>
- Ping, C. L., Jastrow, J. D., Jorgenson, M. T., Michaelson, G. J., & Shur, Y. L. (2015). Permafrost soils and carbon cycling. *SOIL*, 1(1), 147–171. <https://doi.org/10.5194/soil-1-147-2015>
- Poeplau, C., Kätterer, T., Leblans, N. I. W., & Sigurdsson, B. D. (2017). Sensitivity of soil carbon fractions and their specific stabilization mechanisms to extreme soil warming in a subarctic grassland. *Global Change Biology*, 23(3), 1316–1327. <https://doi.org/10.1111/gcb.13491>
- R Core Team (2015). *R: A language and environment for statistical computing*. Vienna, Austria: R Foundation for Statistical Computing.
- Ramsey, C. B., & Lee, S. (2013). Recent and planned developments of the program OxCal. *Radiocarbon*, 55(3–4), 720–730. https://doi.org/10.2458/azu_js_rc.55.16215
- Reimer, P. J., Bard, E., Bayliss, A., Beck, J. W., Blackwell, P. G., Ramsey, C. B., ... van der Plicht, J. (2013). IntCal13 and Marine13 Radiocarbon Age Calibration Curves 0–50,000 Years cal BP. *Radiocarbon*, 55(4), 1869–1887. https://doi.org/10.2458/azu_js_rc.55.16947
- Rivkina, E., Gilichinsky, D., Wagener, S., Tiedje, J., & McGrath, J. (1998). Biogeochemical activity of anaerobic microorganisms from buried permafrost sediments. *Geomicrobiology Journal*, 15(3), 187–193. <https://doi.org/10.1080/01490459809378075>
- Romanovsky, V. E., Drozdov, D. S., Oberman, N. G., Malkova, G. V., Kholodov, A. L., Marchenko, S. S., ... Vasiliev, A. A. (2010). Thermal state

- of permafrost in Russia. *Permafrost and Periglacial Processes*, 21(2), 136–155. <https://doi.org/10.1002/ppp.683>
- Rumpel, C., & Kögel-Knabner, I. (2011). Deep soil organic matter a key but poorly understood component of terrestrial C cycle. *Plant and Soil*, 338(1–2), 143–158. <https://doi.org/10.1007/s11104-010-0391-5>
- Schädel, C., Luo, Y., David Evans, R., Fei, S., & Schaeffer, S. M. (2013). Separating soil CO₂ efflux into C-pool-specific decay rates via inverse analysis of soil incubation data. *Oecologia*, 171(3), 721–732. <https://doi.org/10.1007/s00442-012-2577-4>
- Schaefer, K., Zhang, T., Bruwiler, L., & Barette, A. P. (2011). Amount and timing of permafrost carbon release in response to climate warming. *Tellus Series B*, 63(2), 165–180. <https://doi.org/10.1111/j.1600-0889.2011.00527.x>
- Scheel, T., Dörfler, C., & Kalbitz, K. (2007). Precipitation of dissolved organic matter by aluminum stabilizes carbon in acidic forest soils. *Soil Science Society of America Journal*, 71(1), 64–74.
- Schimel, J. P., & Schaeffer, S. M. (2012). Microbial control over carbon cycling in soil. *Frontiers in Microbiology*, 3, 348. <https://doi.org/10.3389/fmicb.2012.00348>
- Schinner, F., Kandeler, E., Ohlinger, R., & Margesin, R. (eds.) (1993). *Bodenbiologische Arbeitsmethoden* (2nd ed.). Berlin, Germany: Springer Labor. <https://doi.org/10.1007/978-3-642-77936-7>
- Schmidt, M. W. I., Torn, M. S., Abiven, S., Dittmar, T., Guggenberger, G., Janssens, I. A., ... Trumbore, S. E. (2011). Persistence of soil organic matter as an ecosystem property. *Nature*, 478(7367), 49–56. <https://doi.org/10.1038/nature10386>
- Schnecker, J., Wild, B., Takriti, M., Eloy Alves, R. J., Gentsch, N., Gittel, A., ... Richter, A. (2015). Microbial community composition shapes enzyme patterns in topsoil and subsoil horizons along a latitudinal transect in Western Siberia. *Soil Biology and Biochemistry*, 83, 106–115. <https://doi.org/10.1016/j.soilbio.2015.01.016> <https://doi.org/10.1016/j.soilbio.2015.01.016>
- Schrumpf, M., Kaiser, K., Guggenberger, G., Persson, T., Kögel-Knabner, I., & Schulze, E.-D. (2013). Storage and stability of organic carbon in soils as related to depth, occlusion within aggregates, and attachment to minerals. *Biogeosciences*, 10(3), 1675–1691. <https://doi.org/10.5194/bg-10-1675-2013>
- Schuur, E. A. G., McGuire, A. D., Schädel, C., Grosse, G., Harden, J. W., Hayes, D. J., & Vonk, J. E. (2015). Climate change and the permafrost carbon feedback. *Nature*, 520(7546), 171–179. <https://doi.org/10.1038/nature14338> <https://doi.org/10.1038/nature14338>
- Soil Survey Staff (2014). *Keys to soil taxonomy*, Vol. 12. Washington, DC: USDA-Natural Resources Conservation Service.
- Sparling, G. P., Feltham, C. W., Reynolds, J., West, A. W., & Singleton, P. (1990). Estimation of soil microbial C by a fumigation-extraction method: Use on soils of high organic matter content, and a reassessment of the kec-factor. *Soil Biology and Biochemistry*, 22(3), 301–307. [https://doi.org/10.1016/0038-0717\(90\)90104-8](https://doi.org/10.1016/0038-0717(90)90104-8)
- Sparling, G. P., & West, A. W. (1990). A comparison of gas chromatography and differential respirometer methods to measure soil respiration and to estimate the soil microbial biomass. *Pedobiologia*, 34(2), 103–112.
- Steinhof, A. (2013). Data analysis at the Jena ¹⁴C laboratory. *Radiocarbon*, 55(2–3), 282–293. https://doi.org/10.2458/azu_js_rc.55.16350
- Steinhof, A., Adamiec, G., Gleixner, G., Wagner, T., & van Klinken, G. (2003). The new ¹⁴C analysis laboratory in Jena, Germany. *Radiocarbon*, 46(1), 51–58. https://doi.org/10.2458/azu_js_rc.46.4243
- Stuiver, M., & Polach, H. A. (1977). Discussion; reporting of C-14 data. *Radiocarbon*, 19(3), 355–363. https://doi.org/10.2458/azu_js_rc.19.493
- Sushama, L., Laprise, R., Caya, D., Verseghy, D., & Allard, M. (2007). An RCM projection of soil thermal and moisture regimes for North American permafrost zones. *Geophysical Research Letters*, 34(20), L20711. <https://doi.org/10.1029/2007GL031385>
- Swanston, C. W., Torn, M. S., Hanson, P. J., Southon, J. R., Garten, C. T., Hanlon, E. M., & Ganio, L. (2005). Initial characterization of processes of soil carbon stabilization using forest stand-level radiocarbon enrichment. *Geoderma*, 128(1–2), 52–62. <https://doi.org/10.1016/j.geoderma.2004.12.015>
- Tarnocai, C., Canadell, J., Schuur, E., Kuhry, P., Mazhitova, G., & Zimov, S. (2009). Soil organic carbon pools in the northern circumpolar permafrost region. *Global Biogeochemical Cycles*, 23(GB2023), 1–11.
- USDA (1999). *Soil taxonomy. A basic system of classification for making and interpreting soil surveys* (2nd ed., p. 871). Washington, DC: United States Department of Agriculture-Natural Resources Conservation Service.
- Vonk, J. E., Mann, P. J., Davydov, S., Davydova, A., Spencer, R. G. M., Schade, J., ... Holmes, R. M. (2013). High biolability of ancient permafrost carbon upon thaw. *Geophysical Research Letters*, 40(11), 2689–2693. <https://doi.org/10.1002/grl.50348>
- Whittinghill, K., & Hobbie, S. (2012). Effects of pH and calcium on soil organic matter dynamics in Alaskan tundra. *Biogeochemistry*, 111(1–3), 569–581. <https://doi.org/10.1007/s10533-011-9688-6>
- Wickham, H. (2009). *ggplot2: Elegant graphics for data analysis*. New York, NY: Springer. <https://doi.org/10.1007/978-0-387-98141-3>
- Wild, B., Gentsch, N., Čapek, P., Diáková, K., Alves, R. J. E., Bárta, J., ... Richter, A. (2016). Plant-derived compounds stimulate the decomposition of organic matter in arctic permafrost soils. *Scientific Reports*, 6, 25607. <https://doi.org/10.1038/srep25607>
- Wild, B., Schnecker, J., Alves, R. J. E., Barsukov, P., Bárta, J., Čapek, P., ... Richter, A. (2014). Input of easily available organic C and N stimulates microbial decomposition of soil organic matter in arctic permafrost soil. *Soil Biology and Biochemistry*, 75, 143–151. <https://doi.org/10.1016/j.soilbio.2014.04.014>
- Yang, Z., Wullschlegel, S. D., Liang, L., Graham, D. E., & Gu, B. (2016). Effects of warming on the degradation and production of low-molecular-weight labile organic carbon in an Arctic tundra soil. *Soil Biology and Biochemistry*, 95, 202–211. <https://doi.org/10.1016/j.soilbio.2015.12.022>

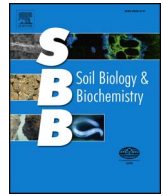
SUPPORTING INFORMATION

Additional supporting information may be found online in the Supporting Information section at the end of the article.

How to cite this article: Gentsch N, Wild B, Mikutta R, et al. Temperature response of permafrost soil carbon is attenuated by mineral protection. *Glob Change Biol*. 2018;24:3401–3415. <https://doi.org/10.1111/gcb.14316>

Paper 12

Santruckova H, Kotas P, **Barta J**, Urich T, Capek P, Palmtag J, Alves Ricardo JE, Biasi C, Diakova K, Gentsch N, Gittel A, Guggenberger G, Hugelius G, Lashchinsky N, Martikainen PJ, Mikutta R, Schleper C, Schnecker J, Schwab C, Shibistova O, Wild B, Richter A (2018) Significance of dark CO₂ fixation in arctic soils. *SOIL BIOLOGY & BIOCHEMISTRY* 119:11-21.



Significance of dark CO₂ fixation in arctic soils

Hana Šantrůčková^{a,*}, Petr Kotas^a, Jiří Bárta^a, Tim Urich^b, Petr Čapek^a, Juri Palmtag^c, Ricardo J. Eloy Alves^{d,j}, Christina Biasi^e, Kateřina Diáková^a, Norman Gentsch^f, Antje Gittel^g, Georg Guggenberger^{f,n}, Gustaf Hugelius^c, Nikolaj Lashchinsky^h, Pertti J. Martikainen^e, Robert Mikuttaⁱ, Christa Schleper^{d,j}, Jörg Schneck^{d,k,l}, Clarissa Schwab^m, Olga Shibistova^{f,n}, Birgit Wild^{k,o,p}, Andreas Richter^{d,k}

^a University of South Bohemia, Department of Ecosystems Biology, České Budějovice, Czech Republic

^b Institute of Microbiology, Ernst-Moritz-Arndt University Greifswald, Greifswald, Germany

^c Department of Physical Geography, Stockholm University, Sweden

^d Austrian Polar Research Institute, Vienna, Austria

^e Department of Environmental Science, University of Eastern Finland, PO Box 1627, FIN/70211 Kuopio, Finland

^f Leibniz Universität Hannover, Institut für Bodenkunde, Hannover, Germany

^g University of Bergen, Centre for Geobiology, Department of Biology, Bergen, Norway

^h Siberian Branch of Russian Academy of Sciences, Central Siberian Botanical Garden, Novosibirsk, Russia

ⁱ Soil Science and Soil Protection, Martin Luther University Halle-Wittenberg, Germany

^j University of Vienna, Department of Ecogenomics and Systems Biology, Division of Archaea Biology and Ecogenomics, Vienna, Austria

^k University of Vienna, Department of Microbiology and Ecosystem Science, Division of Terrestrial Ecosystem Research, Vienna, Austria

^l Department of Natural Resources and the Environment, University of New Hampshire, Durham, NH, USA

^m Laboratory of Food Biotechnology, ETH Zürich, Institute of Food, Nutrition and Health, Schmelzbergstrasse 7, Zürich, Switzerland

ⁿ Siberian Branch of Russian Academy of Sciences, VN Sukachev Institute of Forest, Krasnoyarsk, Russia

^o Department of Environmental Science and Analytical Chemistry, Stockholm University, Stockholm, Sweden

^p Bolin Centre for Climate Research, Stockholm University, Stockholm, Sweden

ARTICLE INFO

Keywords:

Anaplerotic enzymes
Carboxylase genes
Microbial community composition
Permafrost soils
¹³C enrichment of soil profile

ABSTRACT

The occurrence of dark fixation of CO₂ by heterotrophic microorganisms in soil is generally accepted, but its importance for microbial metabolism and soil organic carbon (C) sequestration is unknown, especially under C-limiting conditions. To fill this knowledge gap, we measured dark ¹³CO₂ incorporation into soil organic matter and conducted a ¹³C-labelling experiment to follow the ¹³C incorporation into phospholipid fatty acids as microbial biomass markers across soil profiles of four tundra ecosystems in the northern circumpolar region, where net primary productivity and thus soil C inputs are low. We further determined the abundance of various carboxylase genes and identified their microbial origin with metagenomics. The microbial capacity for heterotrophic CO₂ fixation was determined by measuring the abundance of carboxylase genes and the incorporation of ¹³C into soil C following the augmentation of bioavailable C sources. We demonstrate that dark CO₂ fixation occurred ubiquitously in arctic tundra soils, with increasing importance in deeper soil horizons, presumably due to increasing C limitation with soil depth. Dark CO₂ fixation accounted on average for 0.4, 1.0, 1.1, and 16% of net respiration in the organic, cryoturbated organic, mineral and permafrost horizons, respectively. Genes encoding anaplerotic enzymes of heterotrophic microorganisms comprised the majority of identified carboxylase genes. The genetic potential for dark CO₂ fixation was spread over a broad taxonomic range. The results suggest important regulatory function of CO₂ fixation in C limited conditions. The measurements were corroborated by modeling the long-term impact of dark CO₂ fixation on soil organic matter. Our results suggest that increasing relative CO₂ fixation rates in deeper soil horizons play an important role for soil internal C cycling and can, at least in part, explain the isotopic enrichment with soil depth.

* Corresponding author. University of South Bohemia, Faculty of Science, Department of Ecosystems Biology, Branišovská 1760, České Budějovice 37005, Czech Republic.
E-mail address: hana.santruckova@prf.jcu.cz (H. Šantrůčková).

1. Introduction

Terrestrial ecosystems represent a major sink of CO₂ through fixation by plants but they have been shown to mitigate the rise of atmospheric CO₂ also via microbial CO₂ fixation (Ge et al., 2016; Yuan et al., 2012). Microbial CO₂ fixation has been mostly ascribed to autotrophic microorganisms (Ge et al., 2016), but fundamentally all microorganisms may use inorganic C (IC; i.e. CO₂ or bicarbonate) in their metabolism. All these fixations require energy generated by phototrophic, autotrophic or heterotrophic energy sources. IC is the main or even the only C source for chemoautotrophs and photoautotrophs, while heterotrophs and mixotrophs rely on organic C (OC) but also incorporate IC via a variety of carboxylation reactions that are part of their central or peripheral metabolic pathways (for review see Erb, 2011; Wood and Stjernholm, 1962). The importance of carboxylases in heterotrophic metabolism increases whenever microorganisms experience C limitation through a disproportion between C demand for energy generation and growth and its availability, caused by deficiency or complexity of OC sources, or fast growth (Alonso-Saez et al., 2010; Feisthauer et al., 2008; Merlin et al., 2003). Even though the occurrence of dark and largely heterotrophic CO₂ fixation in soils is generally accepted, very few studies have assessed its relevance for soil microorganisms (Miltner et al., 2004, 2005a,b; Šantrůčková et al., 2005). Estimates of the importance of soil CO₂ fixation for the C balance in certain ecosystems or within an entire soil profile are rare (Ge et al., 2016; Yuan et al., 2012) and analyses of diversity and abundance of carboxylases are missing entirely.

Soil OC becomes progressively enriched in ¹³C with increasing soil depth (Bird et al., 2002; Gentsch et al., 2015; Nadelhoffer and Fry, 1988; Torn et al., 2002). There are several explanations but no one can fully explain the measured isotopic shift. The enrichment of soil OC with depth can be connected with decrease of δ ¹³C of atmospheric CO₂ by 1.3‰ due to Suess effect (McCarroll and Loader, 2004), with preferential decomposition of different organic compounds and microbial fractionation during litter decomposition or mixing of new C input with old soil OC (Buchmann et al., 1997; Ehleringer et al., 2000; Šantrůčková et al., 2000). Another hypothesis that has been discussed but never supported experimentally states that soil microbes should be isotopically heavier as a result of carboxylation reactions (Ehleringer et al., 2000). Whenever carboxylation reactions are involved, CO₂ molecules used in the reactions likely originate from the soil atmosphere, which is isotopically heavier than the organic materials being decomposed (Cerling et al., 1991). The ¹³CO₂ enrichment of bulk soil atmosphere is highest in the uppermost soil horizons, where CO₂ originates mostly from the atmospheric air. In deeper horizons of the soil profile, CO₂ originates from organic matter decomposition and carries the isotopic signal of decomposed material. But still CO₂ remaining in the soil that surrounds microbes is 4.4‰ heavier than organic matter at the location due to slower diffusion of heavier ¹³CO₂ than lighter ¹²CO₂ (Cerling et al., 1991). CO₂ hydrogenation causes further enrichment of ¹³C in HCO₃⁻ by 8–12‰, depending on temperature (Mook et al., 1974). HCO₃⁻ is accepted by many carboxylases operating in a variety of carboxylation reactions, including PEP and biotin carboxylases (Berg et al., 2010; Supplement Appendix B Table SB1), while CO₂ is used as an active species by Rubisco, the most abundant autotrophic carboxylase. Accordingly, incorporation of IC through microbial processes and accumulation of microbial products in soil theoretically might increase the isotopic signal (δ¹³C) of OC.

In arctic permafrost soils, high soil moisture, the presence of a permafrost layer and accumulation of fine particles on the interface between active and permafrost layers (Bockheim and Tarnocai, 1998; Makeev and Kerzhentsev, 1974) restrict air diffusion through the soil profile. Arctic permafrost soils are also a large reservoir of OC whose bioavailability is limited, among other factors, by the OC subduction into subsoil via cryoturbation and the subsequent formation of mineral-organic associations (Gentsch et al., 2015). High moisture content and

the presence of a permafrost horizon restrict air diffusion through the soil profile, which may favor pockets and microsites with elevated CO₂ concentration. Under such conditions, CO₂ fixation might play a more important role than in well-aerated temperate soils. In addition, net primary production and soil carbon input are known to be low in northern ecosystems.

The aim of this study was to elucidate the role of dark CO₂ fixation in arctic soils. We postulated that (i) dark CO₂ fixation is a common attribute of arctic soils and occurs across the whole soil profile. We further hypothesized that (ii) various pathways of CO₂ fixation are operative in soil and distributed among different members of the soil microbial community, including heterotrophs, and (iii) CO₂ incorporation increases ¹³C enrichment of organic carbon with soil age. To test the hypotheses, we measured isotopic signal δ¹³C in OC, IC incorporation into OC, and abundances and taxonomic affiliations of carboxylase genes by shotgun metagenomics in soils across a range of tundra ecosystems from Eastern Siberia to Greenland, covering entire soil profiles. A simple model based on measured data was employed to elucidate a possible effect of IC incorporation on δ¹³C of OC. In addition, ¹³C-labelling experiments with soil from one location were performed under aerobic and anaerobic conditions and the incorporation ¹³CO₂ into OC was addressed by analyzing the ¹³C incorporation into phospholipid fatty acids (PLFA) as microbial biomarkers. To gain supporting evidence of heterotrophic CO₂ fixation, CO₂ incorporation into OC, abundance of carboxylase genes and changes in microbial community composition after augmentation of bioavailable C were measured as well.

2. Material and methods

2.1. Soil sampling

We sampled soils from four different arctic tundra types (heath tundra, tussock tundra, shrub-moss tundra and graminoid tundra) that belong to the bioclimatic subzones E and D (Walker et al., 2005), also called southern tundra and typical tundra subzone in the Russian classification: (i) The heath tundra site was located in eastern Greenland close to the Zackenberg Research Station (ZK; 74° 29' N, 20° 32' W). (ii) The tussock tundra site was located approximately 80 km north of Cherskii (CH; 69° 26' N, 161° 44' E). (iii) The shrubby moss tundra site was on the Taymyr peninsula in the north of central Siberia (Ari Mas, AM; 72° 30' N, 101° 39' E). (iiii) The graminoid (moss) tundra was also on the Taymyr peninsula, a little bit north of AM (Logata, LG; 73° 25' N, 98° 16' E). All areas are in the continuous permafrost zone and thaw depth during sampling reached 65–90 cm (samples were collected in late summer, close to the time of maximum active layer depth). All soils were classified as Turbic Cryosols according to World Reference Base (IUSS Working Group WRB 2007) and as Turbels according to Soil Survey Staff (2010). Two types of soil samples were used in this study, one for the general screening of dark CO₂ fixation and a second one for more detailed microbial and molecular biological analyses.

- (i) Soil samples for measuring natural abundance of bulk soil ¹³C and dark CO₂ fixation (see section 2.2) were obtained on each site from extensive soil sampling for assessment of C storage and distribution (Palmtag et al., 2015). Briefly, soil pits were excavated down to the permafrost and the active layer was sampled using a fixed volume cylinder. Samples from permafrost were collected by coring with a steel pipe (5 cm in diameter) that was hammered into the soil at 5–10 cm depth increments. Samples representative of the uppermost organic, cryoturbated organic (pockets of cryoturbated topsoil material), and adjacent active mineral layers and permafrost horizons were quickly dried in thin layers and kept at 4 °C until analyzed (in total, 149 samples from all sites). For detailed soil characteristics see Palmtag et al. (2015).
- (ii) Soil samples for more detailed microbial and molecular analyses

Table 1

Basic chemical (pH; total soil organic carbon – OC; total soil C/N ratio; extractable C – C_{EX}; natural abundance of soil ¹³C – bulk δ¹³C) and biochemical characteristics (microbial biomass – C_{MB}; microbial C/N – C_{MB}/N_{MB}; net respiration; total microbial phospholipids – PLFA_{tot}) of three different soil horizons from Ari Mas site. Mean values and standard deviations (in brackets) are given (n = 4); different letters in superscript denote significant differences between layers (ANOVA).

soil horizon	pH _{H2O}	OC	C/N	C _{EX}	C _{MB}	C _{MB} /N _{MB}	bulk δ ¹³ C	net respiration	PLFA _{tot}	PLFA _{tot}
		mmol g ⁻¹		μmol g ⁻¹	μmol g ⁻¹		‰	mmol C-CO ₂ mol OC ⁻¹ d ⁻¹	mmol C mol OC ⁻¹	mol C mol C _{MB} ⁻¹
upper organic	6.2	13.4(1.1) ^a	20.4(0.21) ^b	28.2(2.4) ^a	174.1(3.2) ^a	18.7(0.47) ^a	27.5(0.10) ^b	0.796(0.08) ^a	0.339 (0.05) ^a	0.022 ^c
cryoturbated	6.3	3.8(0.23) ^b	26.2(0.32) ^a	3.8(0.76) ^b	10.6(0.05) ^b	16.4(1.9) ^a	27.5(0.17) ^b	0.135 (0.10) ^b	0.284(0.021) ^a	0.085 ^b
mineral	6.7	0.8(0.14) ^c	18.7(0.67) ^b	1.22(0.73) ^c	2.2(0.36) ^c	11.7(4.3) ^b	26.1(0.51) ^a	0.082(0.02) ^c	0.352(0.013) ^a	0.106 ^a

were taken from 5-m long active layer pits on Cherskii, Ari Mas and Logata sites. Soil samples were taken from uppermost organic, mineral and cryoturbated horizons, as well as from the uppermost permafrost layer. One part of the samples was immediately stabilized with RNAlater and kept cold. After transporting the samples to the laboratory within 20 days, RNAlater was washed out with PBS buffer (Gittel et al., 2014) and samples were deep-frozen and later used for DNA extraction and subsequent metagenomics. From the remaining material, living roots were carefully removed and the soil was kept at 4 °C until analyzed for ¹³C. Soils from the AM site were also used for the microbial ¹³C incorporation and C supplementation experiments (see sections 2.3 and 2.4). For basic soil properties we kindly refer to Table 1, while details are given in Gentsch et al. (2015).

2.2. Screening of CO₂-C incorporation into OC across sampling sites

Soil (0.2 g) was moistened to 80% water holding capacity (WHC) in 10 ml vacutainers, which were covered by Parafilm and conditioned for 2 weeks at 12 °C. The vacutainers were then hermetically closed and flushed with CO₂-free air. Thereafter, the headspace was enriched with ¹³CO₂ (99 at% [atomic %] of ¹³C) to a final CO₂ concentration of about 1% v/v, which is realistic for soil pores. In fact, soil CO₂ concentration can fluctuate widely, and values of 1–5% v/v CO₂ are typical, although 10% v/v and higher have also been recorded (Nobel and Palta, 1989). The soil was incubated at 12 °C for 5 days in the dark under the same conditions as in the conditioning phase. At the end of the incubation period, the CO₂ concentration in the headspace was analyzed, the soil was immediately dried at 60 °C and analyzed for total C and N and δ¹³C. All analyses and incubations were run in four replicates.

2.3. CO₂-C incorporation into microbial biomass

Soil taken from pits in the uppermost organic, mineral and cryoturbated horizons of the AM site was used in the ¹³CO₂ incorporation experiment. Soil moisture was adjusted to 80% WHC for incubation under aerobic conditions and to 100% WHC for incubation under anaerobic conditions. Before incubation with ¹³C-labelled CO₂, the soil was conditioned either for 2 weeks (aerobic incubation, four replicates for each horizon, 5 g soil) or 4 weeks (anaerobic conditions, four replicates for each horizon, 5 g soil) in hermetically closed 100 mL bottles at 12 °C in the dark to allow microbial communities to stabilize. After soil conditioning, half of the samples were used for initial soil analyses (controls used for determination of natural abundance of ¹³C in microbial biomass, extractable C and N pools, PLFA and bulk soil). The remaining bottles were flushed with CO₂-free air, and the headspace of each was enriched with ¹³CO₂ (99 at% of ¹³C) to a final CO₂ concentration of about 1% v/v. The soil was incubated for 5 days under the same conditions as used for the conditioning. At the end of the incubation period, respiration was measured and the soil was used for further analyses; one part of the soil sample was immediately dried at 60 °C and used for chemical and isotopic analyses and the other part was deep-frozen and used for PLFA determination.

2.4. Effect of organic C supplement on CO₂ incorporation and carboxylase genes

As in the previous experiment, soil taken from pits in the mineral and cryoturbated horizons of the AM site was used. The soil was incubated only in aerobic conditions and conditioned in the same way as in the previous experiment. After conditioning, soils were amended with either sucrose or lipids extracted from soil (see below) as energy and C sources as follows: sucrose and lipids, respectively, were mixed with C-free silica sand and the mixture was then mixed with soil (sand/soil 1:2, w/w) to get a final concentration of the added C source of approximately 300 μg C per g dry soil. Control soil was mixed with sand only. The final soil mixture was moistened to 80% WHC with Veldkamp nutrient solution containing biotin (Veldkamp, 1970). An aliquot of the soil mixture (of all treatments) was dried to determine the natural abundance of ¹³C before the incubation. The incubation with ¹³CO₂ was carried out in four replicates for each treatment as described above. After 5 days of incubation, soil respiration was measured, 1 g of soil mixture from each replicate was immediately dried (60 °C) for bulk C and ¹³C analyses and the remaining soil was deep-frozen (–80 °C) for DNA extraction and subsequent metagenomics. The lipid mixture used for the soil C supplement had been extracted from soil slurry (equivalent of 450 g of dry soil supplemented by Veldkamp nutrient solution; Veldkamp, 1970) incubated on a shaker for 5 days. The slurry was subsequently centrifuged to remove excess of water and lipids were extracted according to Bligh and Dyer (1959). A part of the resulting extract was fractionated using SPE (Strata SI-1000mg/6 mL, Phenomenex, Torrance, CA, USA) to characterize the extracted lipids. We found that 25, 22 and 23% belonged to neutral-, glyco- and phospholipid fractions, respectively, and 30% was not held by the SPE sorbent and considered as non-lipid fraction.

2.5. Analytical methods

Microbial biomass was estimated by chloroform-fumigation and extraction with 0.5 M K₂SO₄, and calculated as the difference in soluble C between the extracts from fumigated and non-fumigated soils, using K_{EC} = 0.38 (Vance et al., 1987). Extractable organic C was analyzed on a LiqueTOC II (Elementar, Germany). Total CO₂ concentration in the headspace was measured with an HP 5890 gas chromatograph (Hewlett-Packard, East Norwalk, CT, USA), equipped with a thermal conductivity detector, at the beginning and end of the experiment (after the addition of ¹³CO₂ and after the incubation, respectively). The total amount of CO₂ in the bottles (totCO₂, μmol) was calculated as the sum of the amount of CO₂ in the headspace and the amount of CO₂ dissolved in the soil solution (Sparling and West, 1990). Net respiration rate was estimated as the difference between totCO₂ at the beginning and the end of the experiment divided by the number of days of incubation. Analyses of total C and N and ¹³C contents of dried soil material were conducted with an NC Elemental analyzer (ThermoQuest, Bremen, Germany) connected to an isotope ratio mass spectrometer (IR-MS Delta X Plus, Finnigan, Bremen, Germany). Prior to carrying out the analyses, all samples were tested for their carbonate content. No carbonates were detected (data not shown).

A binary mixing model was used to estimate the amount of the pulse-derived ^{13}C immobilized in the various C pools (bulk soil, PLFA):

$$^{13}\text{C} (\mu\text{g g}^{-1}) = [(\text{at}\%_{\text{sample}} - \text{at}\%_{\text{control}}) / (99.90 - 1.10)] \times \text{C pool size} (\mu\text{g C g}^{-1})$$

where $\text{at}\%_{\text{control}}$ is the natural abundance in the control samples, $\text{at}\%_{\text{sample}}$ is the ^{13}C abundance in the samples after labeling, 99.9 is the pulse ^{13}C at% and 1.10 is the at% of the ambient atmosphere. All results were normalized to total C content in order to eliminate differences in C contents of the soils.

PLFA were extracted from subsamples of 0.3–2 g dry soil containing comparable amounts of OC according to Frostegård et al. (1993), with minor modifications. Purification of phospholipids was conducted on silica columns (SPE-SI Supelclean 250mg/3 mL; Supelco, PA, USA) using chloroform, acetone and methanol. Following trans-esterification (Bossio and Scow, 1998), the concentration and isotopic composition of individual PLFAs was determined on a GC-IRMS system consisting of a Trace GC coupled to a Delta V Advantage IRMS via a GC Isolink interface (Thermo Fisher Scientific, Waltham, MA, USA); see Wild et al. (2014) for a detailed description of the instrument setup. Concentration and isotopic composition of each PLFA were corrected for C added during methylation. The microbial community composition was described using PLFAs i14:0, i15:0, a15:0, i16:0, i17:0, a17:0 as markers of Gram-positive bacteria, 16:1 ω 9, 16:1 ω 7, 16:1 ω 5, cy17:0, 18:1 ω 7, cy19:0 as markers of Gram-negative bacteria and 18:1 ω 9, 18:2 ω 6,9 as markers of fungi (Frostegård and Bååth, 1996). Total bacterial biomass was calculated as the sum of general bacterial markers 15:0, 17:0, 18:1 ω 5 and markers for Gram-positive and negative bacteria. The PLFAs 14:0, 16:0, 16:1 ω 11, 18:0, 19:1 ω 8, and 20:0 were considered nonspecific markers (Kaiser et al., 2010).

DNA was extracted from samples of cryoturbated (4 samples), mineral (2) and top soil (4) from Logata, AriMas and Cherskiy sites using bead-beating and the phenol-chloroform method (Gittel et al., 2014; Urich et al., 2008). Total DNA was quantified using SybrGreen (Leininger et al., 2006). In the case of the incubation experiment with added substrates (sucrose or lipids), only the DNA from cryoturbated horizons (9 samples) contained a reasonable amount of DNA of high quality (Table 2). Sequencing of DNA from *in-situ* and incubation experiments was performed on an IonTorrent PGM (Thermo Fisher Scientific, Waltham, MA, USA) sequencer at the Department of Archaea Biology and Ecogenomics (University of Vienna). Barcoded, adapter-ligated DNA libraries were generated and sequenced using 200 bp sequencing chemistry and 318 chips according to the manufacturer's instructions. Sequence reads were quality-trimmed (Phred score > 20) and size-selected (> 100 bp) before further processing. For the identification of carboxylase genes, all metagenome reads were translated into all six frames, with each frame into separate open reading frames (ORFs), avoiding any "*" characters marking stop codons in a resulting ORF. All ORFs equal to 30 amino acids or larger were screened for assignable conserved protein domains using reference hidden Markov

models (HMMs) of the PfamA database (Punta et al., 2012; PfamA release 25, <http://Pfam.janelia.org>) with HMMER tools (<http://hmmer.janelia.org/>). All database hits with *e*-values below a threshold of 10^{-4} were considered significant (Tveit et al., 2015). To obtain taxonomic information of reads with Pfam code, a BLASTX search implemented in diamond software (Buchfink et al., 2015) was performed (-mingscore 50, -maxhits 25) and the resulting hits in sam format were analyzed by MEGAN 5.11.3 (Huson et al., 2007). Taxonomy was assigned using the last common ancestor (LCA) algorithm (LCA parameters: MinScore 50, MaxExpect = 0.01, TopPercent = 10, MinSupport = 1) implemented in MEGAN 5.11.3 software.

The calculations of carboxylase gene abundances per g soil were done by combining relative abundance of SSU rRNA genes of bacteria in the metagenomes with the number of bacterial SSU rRNA genes per g soil as determined by qPCR in the same DNA sample (Table SB2). The absolute number of carboxylase genes per g of soil was used for normalizing their abundance to soil C_{mic} and/or OC contents. The molecular data were processed as follows: metagenome sequences encoding fragments of SSU rRNA genes were extracted with the program SortMeRNA (Kopylova et al., 2012), applying default parameters and the reference databases therein. Extracted reads were compared with BLASTN (Astchul et al., 1990) against the ARB Silva SSUref database v. 119 (Quast et al., 2012) and analyzed in MEGAN 5.11.3. Carboxylase reads were recalculated to absolute number of gene copies per g of soil by combining the absolute quantity of bacterial SSU rRNA genes and the amount of bacterial SSU rRNA reads determined by the MEGAN LCA algorithm in each metagenome, using the following formula:

$$q(\text{carboxylase}) = \frac{\text{seqs}(\text{carboxylase})}{\text{seqs}(\text{bacterial SSU rRNA gene})} \cdot q(\text{bacterial SSU gene})$$

where $\text{seqs}(\text{carboxylase})$ is the amount of metagenome carboxylase gene sequences (assigned by hmmer algorithm using Pfam database), $\text{seqs}(\text{bacterial SSU rRNA gene})$ is the amount of bacterial SSU rRNA gene sequences and $q(\text{bacterial SSU rRNA gene})$ is the quantity of bacterial SSU rRNA genes (gene copies per g soil) determined by qPCR.

2.6. Statistics and modeling

A general linear model, followed by Newman-Keuls post-hoc testing, was used to determine the differences in C incorporation, respiration rate, bulk C content and isotopic signal between sites and horizons at a significance level of $P \leq .05$. To compare total PLFA contents between control and $^{13}\text{C}\text{CO}_2$ -incubated samples in the laboratory experiment, one-way ANOVA and Newman-Keuls post-hoc test was used. Data were log-transformed in all cases except for total PLFA. Statistical evaluation of data was carried out with STATISTICA 13.

The statistical analysis of carboxylase genes was done using the statistical program R (Team, 2016). Because data were not normally distributed, generalized linear models with gamma distribution were

Table 2

DNA concentration, net respiration and inorganic carbon incorporation into soil organic carbon (OC) of cryoturbated and mineral soil horizons from Ari Mas site incubated under aerobic conditions without carbon source addition (control) and with sucrose or mixture of lipids as added carbon source. Mean values and standard deviations are given ($n = 3$). Different letters in superscript denote significant differences between layers (ANOVA).

soil horizon	treatment	DNA concentration	net respiration	^{13}C immobilization	
		ng DNA mol OC $^{-1}$	mmol C mol OC $^{-1}$ d $^{-1}$	$\mu\text{mol } ^{13}\text{C}$ mol OC $^{-1}$ d $^{-1}$	% net respiration
cryoturbated	control	8.61(0.13)	0.168(0.074) ^b	3.06(0.59) ^c	2.08(1.59) ^c
	sucrose	32.8(15.7)	0.541(0.141) ^a	21.7(6.26) ^b	4.32(2.16) ^b
	Lipids	22.8(6.20)	0.106(0.032) ^b	13.0(2.89) ^b	13.2(4.99) ^a
mineral	control	nd	0.144(0.027) ^c	7.37(1.02) ^c	5.16(0.79) ^{ab}
	sucrose	nd	1.254(0.240) ^a	46.8(4.34) ^a	3.82(0.74) ^b
	Lipids	nd	0.333(0.120) ^b	18.3(2.70) ^b	5.81(1.85) ^a

nd – not detected.

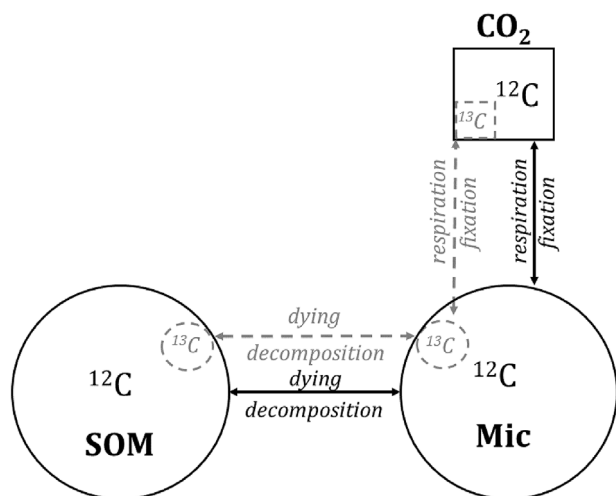


Fig. 1. Scheme of the soil organic matter (SOM) decomposition model that was used to estimate the effect of long-term CO_2 incorporation into SOM on its isotopic signal (for details of the model see Supplementary information, Appendix A).

used to test the significance of the effects of lipids or sucrose addition and soil horizon, respectively, on the abundance of carboxylase genes. Soil horizons had unequal numbers of replicated measurements of carboxylase gene abundance. Therefore, we calculated the type-II F statistic using the package car (Fox and Weisberg, 2011). Post-hoc multiple comparisons were carried out based on least-square means using the package lsmeans (Lenth, 2016).

In order to estimate tentatively the effect of CO_2 fixation on the isotopic signal of OC ($\delta^{13}\text{C}_{\text{OC}}$), we applied a simple model of microbial OC decomposition (Fig. 1; for details see Supplementary Information Appendix A). Briefly, decomposition of OC by heterotrophic soil microorganisms (Mic) is a process with first-order kinetics. Organic C from decomposing organic matter with an initial isotopic signal of -27% is consumed by soil microorganisms and respired or assimilated into microbial biomass. Microbial biomass is dying over time and becomes part of OC. For the sake of simplicity, we assume that no isotopic discrimination occurs during decomposition and microbial dying. Heterotrophic microorganisms largely depend on organic matter as C and energy source but under certain circumstances they use IC as additional C source (see introduction of this article for more details). We assume that microbes are capable of assimilating part of the respired CO_2 back and incorporate it into microbial biomass. Before CO_2 is fixed by soil microorganisms, an isotopic discrimination of 4% occurs because of the faster diffusion of $^{12}\text{CO}_2$ out of the soil. By fixing heavier CO_2 , microbial biomass is becoming more enriched in ^{13}C . When this microbial biomass is dying and becomes part of OC, OC becomes enriched in ^{13}C as well. In the model, CO_2 fixation is set to be proportional to respiration. Four scenarios were modelled, with CO_2 fixation making up 0, 0.1, 1 and 5% of respiration, respectively.

3. Results

3.1. Screening for CO_2 fixation in arctic soils

Sampling site and soil horizon significantly affected soil OC content and respiration rate (Table 3) while natural abundance of ^{13}C in the soil (bulk $\delta^{13}\text{C}$) and CO_2 incorporation were affected only by the type of soil horizon. Consequently, data from the particular horizons were averaged across sampling sites (Table 3). Across all sites, average bulk $\delta^{13}\text{C}$ in the upper organic horizon was -27.3% at the start of incubation. In comparison with the upper organic horizon, the mineral, cryoturbated and permafrost horizons were all ^{13}C -enriched by 1.2, 1.1, and 2.7%, respectively (Table 3). Incorporation of $^{13}\text{CO}_2$ -derived C per unit total

OC was lowest in the upper organic horizon ($4.9 \mu\text{mol } ^{13}\text{C mol C}_{\text{tot}}^{-1} \text{d}^{-1}$) and increased two-to three-fold in cryoturbated and mineral horizons (Table 3). In the permafrost horizon, ^{13}C incorporation was higher by almost two orders of magnitude (Table 3). ^{13}C incorporation reached 0.4, 1.0, 1.1 and 16% of net respiration in the organic, cryoturbated organic, mineral and permafrost horizons, respectively. When ^{13}C incorporation was expressed per mol C of soil OM, it also increased with soil depth, and it rose exponentially with the $\delta^{13}\text{C}$ value of OC ($R^2 = 0.44$, $n = 149$, $P < .001$; $C_{\text{incorp}} = e^{(21.09 + 0.72 \delta^{13}\text{COC})}$).

Carboxylase genes employed in autotrophic as well as heterotrophic metabolism were detected in metagenomes of all horizons and were not affected by site. Their abundances were higher in mineral horizons than in organic and cryoturbated horizons when normalized to microbial biomass ($F = 4.2$, $df = 2$, $P = .02$; Fig. 2a). However, deeper active layer horizons (mineral and cryoturbated) had lower abundances than organic horizons when carboxylase genes were normalized to total C ($F = 4.1$, $df = 2$, $P = .02$; Fig. SB1a). Genes encoding Rubisco contributed about 5% (4.3–5.3%) to the total abundance of carboxylase genes, whilst anaerobic carboxylase genes (pyruvate and PEP carboxylase genes) were the most abundant carboxylase genes and contributed more than 30% (31–42%).

The ^{13}C data of OC within the soil profile corresponds well with the model predictions (Fig. 3). The estimates indicate that dark fixation of C released from decomposed OC could, after 1000 years, cause an increase of the isotopic signal of OC from an initial -27% to -26.7 or -15.2% when IC incorporation represents 0.1 or 5% of net respiration, respectively (Fig. 3). C sequestration via dark CO_2 fixation of 0.1, 1 and 5% of net respiration, respectively, would add 0.1, 1.4 and 7.4 mg C per g soil, respectively, over a time frame of 250 years (Fig. SA4).

3.2. ^{13}C incorporation into microbial biomass at the AM site

Under anaerobic conditions, CO_2 fixation was below the detection limit in the cryoturbated and mineral horizons and negligible in the upper organic horizon ($0.251 \mu\text{mol } ^{13}\text{C mol C}_{\text{tot}}^{-1} \text{day}^{-1}$, corresponding to 0.1% of net respiration). The anaerobic incubation is thus not discussed any further. During aerobic incubation neither microbial functioning (respiration rate) nor microbial biomass (total PLFA) ($P > .3$ for all horizons, $df = 1$, $n = 3$) or PLFA profiles were changed (Table SB3).

Bulk ^{13}C incorporation ranged from $2.4 \mu\text{mol } ^{13}\text{C mol OC}^{-1} \text{day}^{-1}$ (cryoturbated horizon) to $7.6 \mu\text{mol } ^{13}\text{C mol OC}^{-1} \text{day}^{-1}$ (mineral horizon, Table 4), which corresponds well with a range of ^{13}C incorporation observed in the individual horizons during the screening across all study sites (Table 3). It represented less than 2% of net respiration in the organic and cryoturbated horizons but exceeded 13% in the mineral horizons. Of the total amount of ^{13}C incorporated into the soil, generally less than 1% of bulk ^{13}C was found in PLFA biomarkers (^{13}C PLFA to bulk ^{13}C) and less than 0.05% of total PLFA-C was newly incorporated ^{13}C (^{13}C PLFA to PLFA C; Table 4). All detected PLFAs were enriched in ^{13}C , but the distribution of ^{13}C among PLFA markers of individual functional groups showed that more ^{13}C was incorporated into bacterial than fungal PLFA. The ratio of ^{13}C in fungal PLFA to ^{13}C in bacterial PLFA increased from 0.20 in organic and cryoturbated horizons to 0.45 in the mineral horizons. The significantly higher fungal to bacterial PLFA ratio in the organic layers and lower ratio in mineral layers compared to the ^{13}C in fungal to ^{13}C in bacterial PLFA (Table 5) indicate, that bacteria were more active in ^{13}C incorporation per unit of biomass compared to fungi in organic layers, but less active in mineral layers. Within bacteria, Gram-negative bacteria incorporated three to six times more ^{13}C into PLFA than Gram-positive bacteria (Table 5). The ratios of ^{13}C incorporated into PLFAs of Gram-negative to PLFAs of Gram-positive bacteria were on average three times higher compared to ratios of total Gram-negative to Gram-positive PLFA contents. Therefore, the Gram-negative bacteria were not only the overall most active microbial population in the ^{13}C - CO_2 assimilation, but also specifically

Table 3

Soil organic carbon (OC), natural abundance of ^{13}C , soil respiration and CO_2 incorporation into OC pool of four different soil layers from four different arctic tundra localities (upper part of the table). The effects of locality, soil layer, and their interaction were calculated by factorial ANOVA (lower part of the table). Different letters in superscript denote significant differences between soil horizons (Newman-Keuls post-hoc test).

locality	soil horizon	number of samples	OC		net soil respiration		^{13}C -incorporation	
			mmol g^{-1}	‰	$\text{mmol CO}_2 \text{ mol C}_{\text{tot}}^{-1} \text{d}^{-1}$	$\mu\text{mol } ^{13}\text{C mol C}_{\text{tot}}^{-1} \text{d}^{-1}$	‰ of respiration	
Cherskii	upper organic	16	21 ± 9.2	-27.3 ± 0.85	1.3 ± 0.9	7.1 ± 5.1	0.6 ± 0.5	
	cryoturbated	13	4.5 ± 2.5	-25.8 ± 0.36	1.0 ± 0.8	5.2 ± 4.0	0.6 ± 0.2	
	mineral	17	1.9 ± 1.7	-26.1 ± 0.85	2.1 ± 1.5	11.5 ± 6.9	0.9 ± 0.8	
	permafrost	17	1.5 ± 0.9	-24.6 ± 2.58	2.0 ± 1.4	310 ± 496	13.4 ± 20.6	
Ary Mass	upper organic	4	17.8 ± 5.7	-27.8 ± 0.32	2.8 ± 1.7	3.8 ± 1.3	0.2 ± 0.2	
	cryoturbated	4	1.0 ± 0.2	-26.3 ± 0.16	2.2 ± 0.6	8.7 ± 0.6	0.4 ± 0.1	
	mineral	11	0.9 ± 0.4	-25.8 ± 1.02	3.8 ± 1.7	17.2 ± 15.4	1.0 ± 1.3	
	permafrost	15	1.4 ± 1.6	-24.0 ± 1.67	0.9 ± 0.7	81.5 ± 42.3	14.4 ± 13.3	
Logata	upper organic	3	18.6 ± 7.4	-27.3 ± 0.65	3.7 ± 1.1	5.4 ± 4.4	0.1 ± 0.1	
	cryoturbated	6	3.1 ± 2.3	-27.1 ± 0.71	2.9 ± 1.2	21.3 ± 27.2	2.1 ± 4.0	
	mineral	7	2.5 ± 1.4	-27.4 ± 0.18	3.9 ± 1.0	7.1 ± 2.4	0.2 ± 0.1	
	permafrost	9	2.0 ± 0.3	-25.5 ± 1.50	1.3 ± 1.0	102 ± 83.9	20.1 ± 18.9	
Zackenbergl	upper organic	8	16.4 ± 5.8	-27.3 ± 0.75	1.9 ± 1.1	0.8 ± 0.6	0.1 ± 0.1	
	cryoturbated	9	6.4 ± 1.6	-25.2 ± 0.66	0.9 ± 0.5	8.9 ± 17.5	1.3 ± 2.8	
	mineral	8	2.0 ± 1.0	-25.6 ± 1.04	1.2 ± 0.4	15.8 ± 27.2	2.0 ± 4.0	
	permafrost	2	0.9 ± 0.1	-26.0 ± 1.13	0.9 ± 0.6	74.0 ± 69.7	32.1 ± 31.8	
all sites	upper organic	31	19.0 ± 8.18 ^a	-27.3 ± 0.78 ^c	1.88 ± 1.36 ^{ab}	4.86 ± 4.86 ^c	0.37 ± 0.44 ^c	
	cryoturbated	32	4.33 ± 2.72 ^b	-26.2 ± 0.73 ^b	1.47 ± 1.20 ^b	9.71 ± 16.6 ^c	1.08 ± 2.38 ^b	
	mineral	43	1.77 ± 1.44 ^c	-26.1 ± 1.06 ^b	2.62 ± 1.94 ^a	13.1 ± 15.4 ^b	1.00 ± 2.14 ^b	
	permafrost	43	1.55 ± 1.18 ^c	-24.7 ± 2.13 ^a	1.46 ± 1.34 ^b	175.7 ± 338 ^a	16.1 ± 19.5 ^a	
effect of locality			****	n.s.	****	n.s.	n.s.	
effect of layer			****	****	****	****	****	
layer*loc			****	n.s.	****	n.s.	n.s.	

per unit of microbial biomass, which was most apparent in the cryoturbated horizon (Table 5). The proportion of bulk ^{13}C built into PLFA was higher in the organic and cryoturbated horizons than in the mineral horizons. Across all horizons, ^{13}C incorporated into PLFA was closely correlated with net respiration rate RR ($R^2 = 0.89$, $n = 9$; $^{13}\text{C}_{(\text{PLFA}/\text{OC})} = 7.36 + 20.5 \text{ RR}_{(\text{CO}_2/\text{OC})}$).

3.3. Effect of C addition on dark CO_2 fixation

Addition of sucrose significantly increased net respiration rate in the mineral and cryoturbated horizons while addition of lipids had a positive effect only in the mineral soil (Table 2). ^{13}C immobilization ranged from 3.1 $\mu\text{mol } ^{13}\text{C mol OC}^{-1} \text{ day}^{-1}$ (cryoturbated horizon; control) to 46.8 $\mu\text{mol } ^{13}\text{C mol OC}^{-1} \text{ day}^{-1}$ (mineral horizon; sucrose addition) and increased in both the cryoturbated and mineral horizons in the order control < lipids < sucrose. Across all treatments, IC incorporation was closely correlated with respiration rate ($R^2 = 0.91$, $n = 18$; $^{13}\text{C}_{(\text{incorp}/\text{OC})} = 4.86 + 31.9 \text{ RR}_{(\text{CO}_2/\text{OC})}$). Both C substrates induced microbial growth (measured as an increase in DNA amount per gram soil; Table 5, Fig. 4) in the cryoturbated horizon. Unfortunately, the amount of extracted DNA from the mineral soil was too small to be evaluated or used for further analyses. The increase of microbial biomass in the cryoturbated horizon was accompanied by a shift in the composition of the microbial community. Analysis of the SSU rRNA gene fragments in the metagenomes showed that the relative abundance of *Beta-*, *Gammaproteobacteria* and *Saccharibacteria* increased due to substrate addition, whereas the relative abundance of *Alphaproteobacteria*, *Deltaproteobacteria* and *Firmicutes* rather decreased, mainly in the sucrose addition treatment (Fig. 4). The abundance of carboxylase genes normalized to microbial biomass was not affected by C source addition (Fig. 2b) and increased along with microbial biomass growth, thus a significant increase of carboxylase genes per unit of total C was observed with C source addition (Fig. SB1b). Rubisco accounted for 13–18% of total carboxylase and anaplerotic carboxylase genes (pyruvate and PEP carboxylases) accounted for about 40% (37–46%). Annotated PEP carboxylase genes were taxonomically binned (Fig. SB2).

The addition of either sucrose or lipids decreased the proportion of PEP carboxylases affiliated to Alphaproteobacteria, Cyanobacteria and Actinobacteria, but increased those affiliated to Beta-, Gammaproteobacteria, Firmicutes, Chlamydiae/Verrocomicrobia group and Bacteroidetes/Chlorobi group.

4. Discussion

4.1. General relevance of dark CO_2 fixation in arctic soils

The available knowledge about dark CO_2 fixation is still very limited and can be summarized as follows: It is a relevant process in the soil mediated by soil microorganisms, it is correlated with microbial respiration rate, it can be enhanced by addition of bioavailable OC, and it is related to microbial heterotrophic activity (Miltner et al., 2004, 2005a; Šantrůčková et al., 2005). Previous studies estimated that about 2–7% of fixed CO_2 can be incorporated into microbial biomass (Miltner et al., 2004; Šantrůčková et al., 2005). In addition, this study documents that (i) IC incorporation increases with depth in the soil profile and is higher in the permafrost layers by more than one order of magnitude due to higher CO_2 fixation rate, lower OC and higher CO_2 concentrations with depth; (ii) genes encoding Rubisco, the only enzyme operating strictly in autotrophic metabolism, account for a small part of all carboxylase genes only, while anaplerotic carboxylase genes are several times more abundant; (iii) a wide spectrum of soil microorganisms contain genes encoding PEP carboxylases; (iv) IC incorporation may lead to ^{13}C enrichment of soil OC in the long-term and the increase is more pronounced in the deeper soil horizons. Across all study sites, IC incorporation expressed per unit of total C was higher in the mineral than in the organic horizons. The larger C incorporation in mineral horizons was accompanied by the highest abundance of all detected carboxylase genes per unit microbial biomass, suggesting that both the chemoautotrophic and heterotrophic pathways accounted for the larger IC incorporation in the mineral horizons as compared with the top soil. The significant proportion of anaplerotic carboxylase genes (pyruvate and PEP carboxylases) further emphasizes the importance of

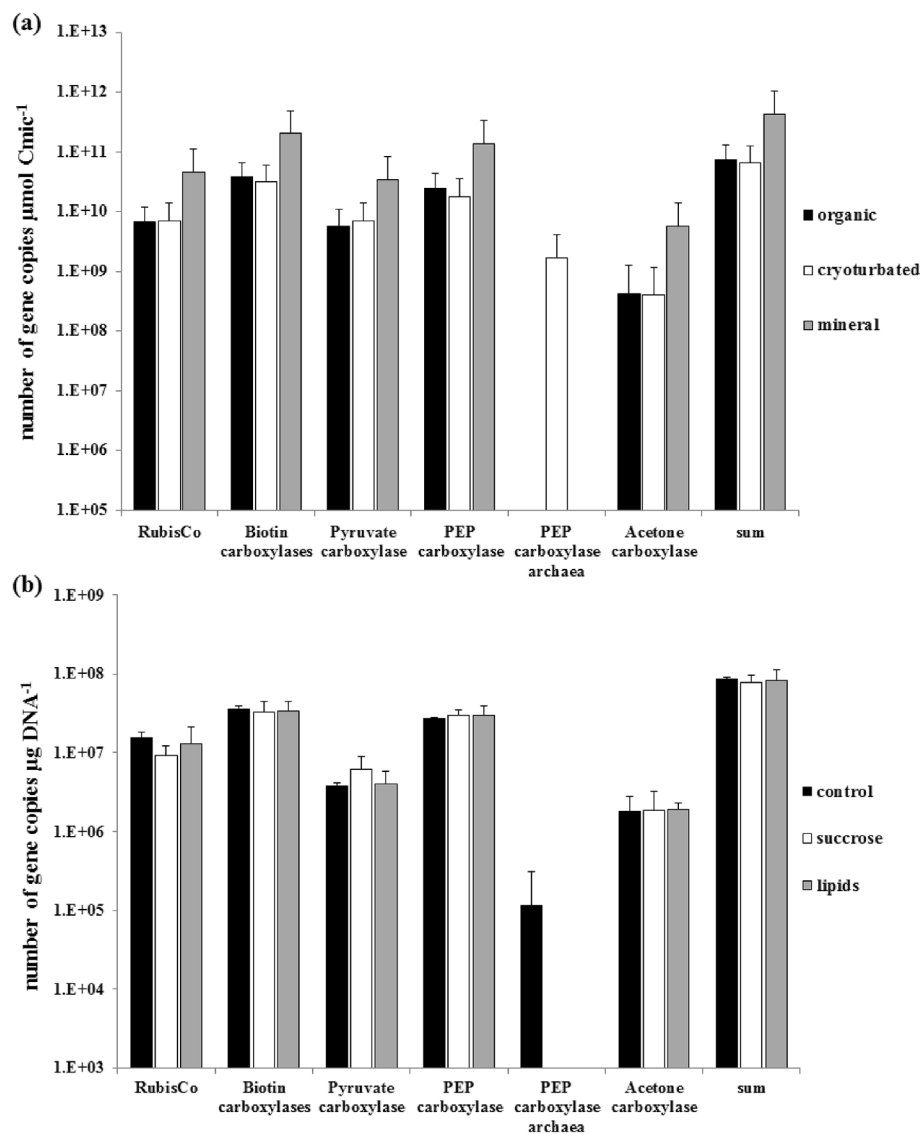


Fig. 2. Abundance of carboxylase genes normalized to microbial biomass in uppermost organic, cryoturbated and mineral soil layers from Cherskii, Ari Mas and Logata sites (a), and in the cryoturbated layer from Ari Mas site, either unamended (control) or amended with organic C sources (b). Note that the scale on y axis is logarithmic. The standard deviations of absolute carboxylase gene counts represent the difference among the localities. They were in some cases larger than average, only positive error bars are thus visualized.

reactions replenishing central metabolic pathways under conditions where microbial C demand exceeds C supply or where microorganisms catabolize complex hydrocarbons, the dominant fractions of OC in mineral horizons (Alonso-Saez et al., 2010; Feisthauer et al., 2008; Merlin et al., 2003). It implies an important regulatory function of CO_2 fixation, which may enable microbes to keep activity in harsh conditions of C limitation.

4.2. Link between dark CO_2 fixation and microbial communities

We found less than 1% of fixed C in PLFA (0.2–0.5%), which is much less than it was found in bulk microbial cells (Miltner et al., 2004; Šantrůčková et al., 2005). The low values can be explained by the fact that membranes constitute only about 4% of cellular material and, therefore, bulk microbial biomass should contain more fixed C. This suggestion is supported by Feisthauer et al. (2008) who found that the amount of fixed C in bulk microbial biomass is higher by one order of magnitude than that of fatty acids, indicating greater incorporation of fixed C into other cell components. Proteins, the most abundant component of cytoplasm, contain four to eight times more fixed C than PLFA (Miltner et al., 2004).

The variety of detected carboxylase genes, the wide spectrum of bacteria linked to PEP carboxylase genes and significant ^{13}C

incorporation into all detected PLFAs including fungal markers imply a general importance of CO_2 incorporation for the microbial community. This matches existing knowledge that, apart from chemoautotrophic bacteria and archaea, which use CO_2 as the only source of C (for review see Berg et al., 2010; Saini et al., 2011) a wide spectrum of heterotrophic bacteria and fungi employ carboxylases to (i) assimilate various organic substrates such as acetone, phenolics, propionate, or leucine, (ii) replenish the citric acid cycle in anaerobic reactions and, finally, (iii) synthesize cellular compounds (e.g. Erb, 2011; Hesselsoe et al., 2005). The significant increase in the amount of genes involved in CO_2 fixation belonging to predominantly heterotrophic genera (*Arthrobacter*, *Nocardioideis* and *Pseudomonas*; Fig. SB3) after addition of sucrose or lipids indicated increased potential of heterotrophic metabolism for additional IC incorporation into the bacterial biomass.

We found a positive effect of bioavailable C addition on IC incorporation, which contradicts our expectation that the importance of heterotrophic carboxylases would increase with any imbalance between C demand and supply (Alonso-Saez et al., 2010; Feisthauer et al., 2008; Merlin et al., 2003). This apparent discrepancy might be partly explained by the increase of chemoautotrophic C fixation because of increasing CO_2 concentration in the system. A more likely explanation is that the added C initiated fast microbial growth as indicated by increased DNA concentration (Table 2), but was exhausted within days,

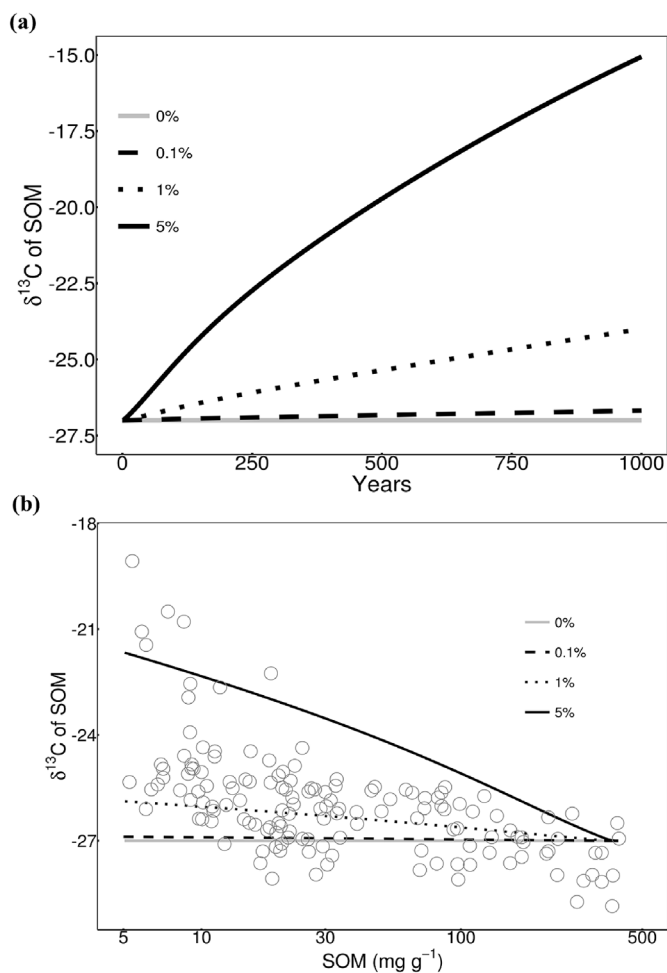


Fig. 3. The modelled shift of SOM isotopic signal over time caused by heterotrophic CO_2 fixation (a), and relationship between the soil SOM concentration and $\delta^{13}\text{C}$ ratio (b) (please note that x-axis is in logarithmic scale). Open circles represent measured data and lines the model predictions. The solid grey line represents control (0% - no fixation), the dashed, dotted and solid black lines represent CO_2 fixation rates equal to 0.1, 1 and 5% of net respiration rate, respectively.

microbes quickly became substrate limited and microbial C demand exceeded C supply at the end of the experiment when the analyses were performed. Therefore, IC had to replenish C for microbial metabolism.

Even though we detected genes for key enzymes in various autotrophic pathways (e.g. Calvin Benson Bassham cycle, reductive citric acid and reductive acetyl-CoA cycles, 3-hydroxypropionate cycle, 4-hydroxybutyrate cycle), we assume a negligible contribution of autotrophs to overall IC incorporation into OC. These chemoautotrophic pathways are, except for the Calvin Benson Bassham cycle and 4-hydroxybutyrate cycle, operated by strictly anaerobic prokaryotes, and in our study the anaerobic CO_2 incorporation was below detection limit. We are aware that the contribution of the chemoautotrophic IC incorporation may be higher under natural conditions, but heterotrophy

should be prevalent. This is supported by the generally lower growth efficiency of chemolithotrophic compared to heterotrophic growth, because the former requires more energy to produce a unit of biomass. In addition, carboxylases have low substrate affinity and need a high concentration of IC for its effective incorporation into organic compounds (Bar-Even et al., 2012). The most kinetically favorable carboxylases are anaplerotic PEP carboxylases, the main carboxylase for replenishing the citric acid cycle, and pyruvate carboxylases (Bar-Even et al., 2012).

4.3. Importance of dark CO_2 fixation for C sequestration

We assessed the importance of dark CO_2 fixation for C sequestration in the soils from two different perspectives: (i) promotion of microbial metabolism and (ii) role in soil C balance. With respect to the promotion of the heterotrophic metabolism, IC may be used as an additional C source to replenish central metabolic cycles (anaplerotic reactions) in situations when organic carbon is limiting and primarily used for energy production. In such a case, microbes may re-fix CO_2 that has been respired for energy production and thus minimize the overall loss of carbon. Carboxylation is also a vital step of fatty acid biosynthesis in general, and it enables the utilization of acetone by nitrate reducing bacteria (Acosta et al., 2014). Inorganic C has a stimulatory effect, which is most apparent under low metabolic activity in resting aerobic and facultative cells (Harris, 1954) and in the metabolism of resource-depleted bacteria (Alonso-Saez et al., 2010). Inorganic C also serves as the only C source for a variety of obligate chemoautotrophs, either bacteria or archaea, which provide many metabolic pathways that are indispensable for soil functioning, such as oxidation of sulphur, ammonia, reduced metal ions, and methane production (Badger and Bek, 2008; Berg et al., 2007; Konneke et al., 2014). With respect to the role in the soil C balance, we consider a mean CO_2 release from tundra soil by soil respiration of about $76 \text{ g m}^{-2} \text{ yr}^{-1}$ (Fahnestock et al., 1999). Our data thus indicate that re-use of 0.1–5% of net respiration may account for dark fixation of $0.08\text{--}3.8 \text{ g C m}^{-2} \text{ yr}^{-1}$. Above-ground net primary production (i.e. IC incorporation into plant material) ranges from 10 to $500 \text{ g C m}^{-2} \text{ yr}^{-1}$ (Gould et al., 2003). Thus microbial CO_2 fixation may correspond in the long term from 0.016 to 38% of plant C fixation.

4.4. Effect of dark CO_2 fixation on isotopic signal of OC

In general, the $\delta^{13}\text{C}$ of organic matter mirrors the $\delta^{13}\text{C}$ of plant input in the uppermost horizons. However it increases with soil depth to values 1–3‰ higher than in the uppermost organic horizon (e.g. Bird et al., 2002; Buchmann et al., 1997). This was also observed for our arctic tundra soils (Tables 1 and 2; Gentsch et al., 2015). The mechanisms behind this enrichment are still unclear and none of the following potential causes can fully explain it: isotopic change of atmospheric CO_2 and microbial processing of OC (Boström et al., 2007), mixing of new C input with old soil organic matter (SOM) and microbial fractionation during litter decomposition (Ehleringer et al., 2000), increase of leaf internal to ambient CO_2 concentration (ci/ca) due to global change during the last 40 years (Betson et al., 2007). Similarly, the causes of the ^{13}C -enrichment of microbial biomass (Dijkstra et al.,

Table 4

Bulk inorganic ^{13}C incorporation into soil organic carbon (OC) and PLFA in three different soil layers from Ari Mas site incubated under aerobic conditions. Mean values and standard deviations (in brackets) are given (n = 3). Different letters in superscript denote significant differences between horizons (Newman-Keuls post-hoc test).

soil layer	bulk ^{13}C incorporation		^{13}C incorporation to PLFA	PLFA ^{13}C to bulk ^{13}C	PLFA ^{13}C to PLFA C
	$\mu\text{mol } ^{13}\text{C mol OC}^{-1} \text{ d}^{-1}$	% respiration rate	$\text{nmol } ^{13}\text{C mol OC}^{-1} \text{ d}^{-1}$	%	%
organic	6.13(0.62) ^b	0.78(0.05) ^c	19.8(2.65) ^a	0.377(0.04) ^a	0.041(0.004) ^a
cryoturbated	2.40(0.21) ^b	1.88(0.25) ^b	11.2(0.75) ^b	0.536(0.11) ^a	0.028(0.002) ^b
mineral	7.61(0.79) ^a	13.57(3.23) ^a	7.26(0.20) ^c	0.153(0.02) ^b	0.015(0.001) ^c

Table 5

The ratios of ^{13}C in fungal PLFA to ^{13}C in bacterial PLFA, ^{13}C in Gram-negative bacterial PLFA to ^{13}C in Gram-positive bacterial PLFA, and ratios of fungi to bacterial and Gram-negative to Gram-positive bacteria C contents together with relative contribution of specific PLFAs to total ^{13}C incorporated in three different soil layers from Ari Mas site incubated under aerobic conditions. Mean values and standard deviations (in brackets) are given ($n = 3$). Different letters in superscript denote significant differences between horizons (Newman-Keuls post-hoc test).

soil layer	^{13}C fungi to ^{13}C bacteria	fungi to bacteria	^{13}C G- to ^{13}C G+	G- to G+	relative contribution of specific PLFAs to total ^{13}C incorporated into PLFA [%]				
					G-	G+	fungi	bacteria	nonspecific
organic	0.21(0.02) ^b	0.44(0.02) ^a	4.42(0.56) ^b	2.42(0.27) ^a	53	12	14	68	18
cryoturbated	0.22(0.004) ^b	0.23(0.01) ^c	6.55(1.27) ^a	1.78(0.06) ^b	57	9	16	67	17
mineral	0.45(0.06) ^a	0.37(0.02) ^b	3.69(0.44) ^b	1.72(0.03) ^b	39	11	24	54	22

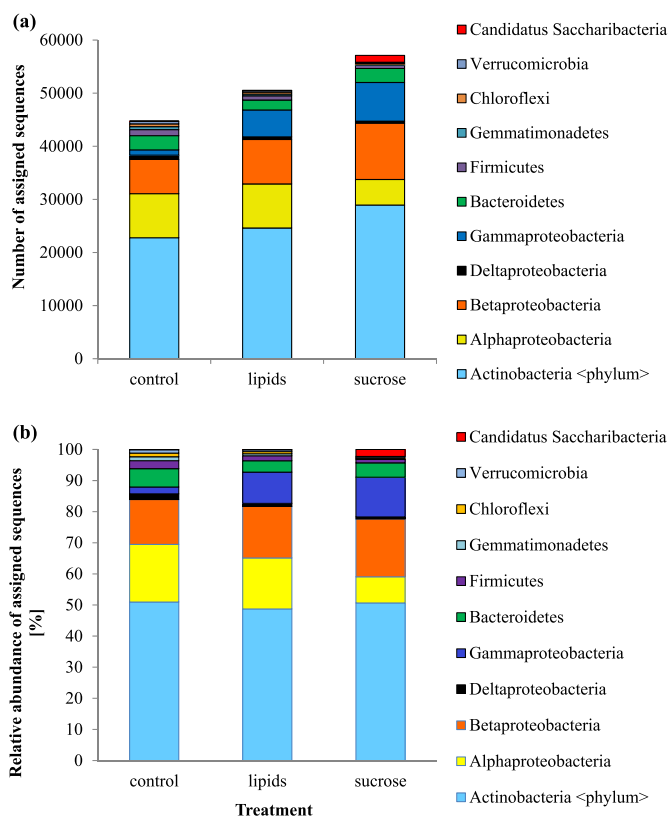


Fig. 4. Composition of the bacterial community (phylum level) based on absolute (a) and relative (b) abundance of assigned sequences in the cryoturbated layer, either unamended (control) or amended with organic C sources from Ari Mas site. Taxonomic assignment is based on LCA classifiers implemented in MEGAN software package.

2006; Šantrůčková et al., 2000) have not been satisfactorily resolved yet. Our results suggest that IC incorporation into microbial biomass and OC can contribute to soil microbial biomass and OC enrichment. Our model of CO_2 fixation, which was parameterized using data from the same locations, indicates that in the long term, IC incorporation into OC can result in similar ^{13}C -fixation as measured for bulk soils in the deep soil. The model assumes CO_2 enrichment in the soil profile corresponding to 0.1–5% of net respiration, which is within the range of measured values. Unfortunately, the uncertainty connected to changes in isotopic signal of various soil pools during decomposition process is high. Our model is therefore largely simplified and the predicted change of SOM isotopic signature is only tentative. We used several assumptions, which may affect model prediction. More specifically, we assumed that there is one pool of well mixed SOM with unique isotopic signal in soil which is decomposed at a constant rate. Including additional, more resistant SOM pool with the same isotopic signal would lead to lesser enrichment of SOM by heterotrophic CO_2 fixation in long-term. It is, however, uncertain whether chemically different pools of SOM have the same isotopic signal. The predicted change of SOM

isotopic signal would largely depend on the signal of the resistant fraction at the start of decomposition process if accounted for. It might be also argued that all initial SOM is in fact decomposable in long-term and the resistant SOM fraction, represented by microbial products, builds up during decomposition. If this was the case, the enrichment of SOM would be similar as predicted but it would take longer. We further assumed that no other processes lead to isotopic discrimination. If any such process would be relevant, our predictions might be affected positively or negatively depending on the particular process, its rate and the connected discrimination.

However, four lines of evidence support our suggestion that IC incorporation can importantly contribute to ^{13}C enrichment of soil OC. **First**, across all sites, inorganic ^{13}C incorporation into OC, expressed on a total C basis, occurred throughout the soil profile and increased with soil depth. The isotopic signal of OC exponentially increased accordingly ($R^2 = 0.44$, $n = 149$). **Second**, IC available in the soil profile is enriched relative to associated SOM and plant material. Soil CO_2 may be more enriched in ^{13}C than SOM by up to 5‰ because of diffusion of lighter $^{12}\text{CO}_2$ out of the soil profile, leaving the heavier $^{13}\text{CO}_2$ behind (Cerling et al., 1991). Carbon dioxide dissolution (CO_2^*) causes only negligible fractionation (around 1‰) and CO_2^* entering carboxylation reactions should be enriched by 4‰ relative to the surrounding OC. Carbon dioxide hydrogenation comes with a huge positive discrimination, and HCO_3^- entering carboxylation reactions is enriched by 9‰ at 25 °C. The discrimination increases with decreasing temperature to 12‰ at 0 °C (equilibrium fractionation factor; Mook et al., 1974). Thus, IC entering carboxylation as HCO_3^- should be enriched relative to the surrounding organic material by 13–16‰ (4‰ plus 9‰–12‰). Methanogenesis in anaerobic microsites and deeper parts of the soil profile can cause further CO_2 enrichment as methanogens strongly discriminate against heavier ^{13}C (difference between CO_2 and CH_4 [$\Delta_{\text{CO}_2/\text{CH}_4}$] from 5‰ to 93‰; Penger et al., 2012), producing relatively light CH_4 and leaving behind much heavier CO_2 (Han et al., 2007). **Third**, genes for anaplerotic, assimilatory and biosynthetic carboxylase enzymes accounted for the major part of detected carboxylase genes. The majority of those enzymes accept HCO_3^- instead of CO_2 (Table SB1). Thus the initial reactant entering the carboxylation reaction is substantially enriched relative to SOM. Although HCO_3^- entering carboxylation can originate from HCO_3^- hydrated in soil solution (see above) or from CO_2^* that is transported from soil solution into the cell, it will always be enriched relative to OC, as intracellular CO_2^* hydration is catalysed by intracellular carbonic anhydrase which prefers ^{13}C . The reaction causes an enrichment of HCO_3^- by 7‰. Carbonic anhydrase is widespread among autotrophs but also among heterotrophic eukaryota and prokaryota (Merlin et al., 2003; Nafi et al., 1990; Smith and Ferry, 2000) and is indispensable for the HCO_3^- concentrating mechanism. If there were no CO_2 leak from cells, every bicarbonate ion pulled into the cell should end up in organic compounds, and the isotopic signal of biomass would be determined by carbonic anhydrase fractionation (Hayes, 1993). Even though there is always a leakage, cells utilizing bicarbonate should be enriched relative to CO_2 (Hayes, 1993). It has been documented in plant cells that initial hydration of CO_2^* to bicarbonate and subsequent PEP carboxylation causes

enrichment of the resulting OC by 5.7‰ at 25 °C relative to gaseous CO₂. The enrichment is dependent on temperature and the amount of carbonic anhydrase present (Cousins et al., 2006; Farquhar, 1983). Finally, while autotrophs mostly discriminate against heavier ¹³C and mean C discrimination of various autotrophic pathways (ΔIC/cell) ranges from zero to 26.7‰ when measured in pure cultures (House et al., 2003 and reference therein), the cells utilizing HCO₃⁻ will not always be depleted relative to CO₂ due to fractionation in the hydration of CO₂ to HCO₃⁻. In addition, the discrimination can be decreased by limited gas diffusion in water and the soil environment (Descolasgros and Fontugne, 1990) and low cell density (House et al., 2003). The autotrophs employing Rubisco, the most common autotrophic carboxylase accepting CO₂* and discriminating against ¹³CO₂ (–11 to –30‰; see Table SB1), should be depleted in ¹³C relative to soil CO₂. The proportion of autotrophs in bulk microbial biomass is, however, generally very low. In our experiment, genes encoding Rubisco represented at most 18% of all carboxylase genes, implying that autotrophic prokaryotes should not determine the isotopic signal of total microbial biomass.

5. Conclusion

Our results demonstrate that dark CO₂ fixation is common in all arctic soils investigated and anaplerotic reactions are mainly responsible for this. Many anaplerotic pathways in heterotrophic CO₂ incorporation do not lead to any net C assimilation and biomass production (Alonso-Saez et al., 2010). Microbial biomass did not increase in soils without addition of bioavailable substrate either, which further suggests that dark IC fixation may only enable microorganisms to maintain metabolic activity even in C poor conditions. Inorganic C incorporation into OC only corresponds to a few percent of net soil respiration, but still it can play an important role in supporting microbial metabolism and organic matter transformation. We further demonstrate a positive impact of bioavailable soil organic compounds on inorganic C incorporation, implying that increases in plant litter decomposition induced by projected warming and input of root-derived compounds may also enhance C incorporation via dark C fixation.

Conflicts of interest

None.

Acknowledgement

This study was supported by the International Program CryoCARB (MSM 7E10073 – CryoCARB, FWF I370-B17), BMBF 03F0616A, MEYS (LM 2015075, cz.02.1.01/0.0/0.0/16_013/0001782) and Grant Agency (16-18453S). TU and CS acknowledge support from NFR – grant 200411. CB acknowledges financial support from the Nessling foundation and the Academy of Finland (project COUP, decision no. 291691; part of the European Union Joint Programming Initiative, JPI Climate) and OS and GG appreciate support from the Russian Ministry of Education and Science (No. 14.B25.31.0031). The authors thank Gerhard Kerstiens for language editing and unknown reviewer for valuable comments.

Appendix A. Supplementary data

Supplementary data related to this article can be found at <http://dx.doi.org/10.1016/j.soilbio.2017.12.021>.

References

Acosta, O.B.G., Schleheck, D., Schink, B., 2014. Acetone utilization by sulfate-reducing bacteria: draft genome sequence of *Desulfococcus biacutus* and a proteomic survey of acetone-inducible proteins. *BMB Genomics* 15.1, 584.

- Alonso-Saez, L., Galand, P.E., Casamayor, E.O., Pedros-Alio, C., Bertilsson, S., 2010. High bicarbonate assimilation in the dark by Arctic bacteria. *The ISME Journal* 4, 1581–1590.
- Atschul, S.F., Gish, W., Miller, W., Myers, E.V., Lipman, D., 1990. Basic local alignment tool. *Journal of Molecular Biology* 215, 403–410.
- Badger, M.R., Bek, E.J., 2008. Multiple Rubisco forms in proteobacteria: their functional significance in relation to CO₂ acquisition by the CBB cycle. *Journal of Experimental Botany* 59, 1525–1541.
- Bar-Even, A., Noor, E., Milo, R., 2012. A survey of carbon fixation pathways through a quantitative lens. *Journal of Experimental Botany* 63, 2325–2342.
- Berg, I.A., Kockelkorn, D., Buckel, W., Fuchs, G., 2007. A 3-hydroxypropionate/4-hydroxybutyrate autotrophic carbon dioxide assimilation pathway in archaea. *Science* 318, 1782–1786.
- Berg, I.A., Kockelkorn, D., Ramos-Vera, W.H., Say, R.F., Zarzycki, J., Hugler, M., Alber, B.E., Fuchs, G., 2010. Autotrophic carbon fixation in archaea. *Nature Reviews Microbiology* 8, 447–460.
- Betson, N.R., Johannisson, C., Lofvenius, M.O., Grip, H., Granstrom, A., Hogberg, P., 2007. Variation in the δ¹³C of foliage of *Pinus sylvestris* L. in relation to climate and additions of nitrogen: analysis of a 32-year chronology. *Global Change Biology* 13, 2317–2328.
- Bird, M.I., Šantrůčková, H., Ameth, A., Grigoriev, S., Gleixner, G., Kalaschnikov, Y.N., Lloyd, J., Schulze, E.D., 2002. Soil carbon inventories and carbon-13 on a latitude transect in Siberia. *Tellus Series B-Chemical and Physical Meteorology* 54, 631–641.
- Bligh, E.G., Dyer, W.J., 1959. A rapid method of total lipid extraction and purification. *Canadian Journal of Biochemistry and Physiology* 37, 911–917.
- Bockheim, J.G., Tarnocai, C., 1998. Recognition of cryoturbation for classifying permafrost-affected soils. *Geoderma* 81, 281–293.
- Bossio, D.A., Scow, K.M., 1998. Impacts of carbon and flooding on soil microbial communities: phospholipid fatty acid profiles and substrate utilization patterns. *Microbial Ecology* 35, 265–278.
- Boström, B., Comstedt, D., Ekblad, A., 2007. Isotope fractionation and ¹³C enrichment in soil profiles during the decomposition of soil organic matter. *Oecologia* 153, 89–98.
- Buchfink, B., Xie, C., Huson, D.H., 2015. Fast and sensitive protein alignment using DIAMOND. *Nature Methods* 12, 59–60.
- Buchmann, N., Kao, W.Y., Ehleringer, J., 1997. Influence of stand structure on carbon-13 of vegetation, soils, and canopy air within deciduous and evergreen forests in Utah, United States. *Oecologia* 110, 109–119.
- Cerling, T.E., Solomon, D.K., Quade, J., Bowman, J.R., 1991. On the isotopic composition of carbon in soil carbon-dioxide. *Geochimica et Cosmochimica Acta* 55, 3403–3405.
- Cousins, A.B., Badger, M.R., Von Caemmerer, S., 2006. Carbonic anhydrase and its influence on carbon isotope discrimination during C-4 photosynthesis. Insights from antisense RNA in *Flaveria bidentis*. *Plant Physiology* 141, 232–242.
- Descolasgros, C., Fontugne, M., 1990. Stable carbon isotope fractionation by marine-phytoplankton during photosynthesis. *Plant, Cell and Environment* 13, 207–218.
- Dijkstra, P., Ishizu, A., Doucet, R., Hart, S.C., Schwartz, E., Menyailo, O.V., Hungate, B.A., 2006. C-13 and N-15 natural abundance of the soil microbial biomass. *Soil Biology and Biochemistry* 38, 3257–3266.
- Ehleringer, J.R., Buchmann, N., Flanagan, L.B., 2000. Carbon isotope ratios in below-ground carbon cycle processes. *Ecological Applications* 10, 412–422.
- Erb, T.J., 2011. Carboxylases in natural and synthetic microbial pathways. *Applied and Environmental Microbiology* 77, 8466–8477.
- Fahnestock, J.T., Jones, M.H., Welker, J.M., 1999. Wintertime CO₂ efflux from arctic soils: implications for annual carbon budgets. *Global Biogeochemical Cycles* 13, 775–779.
- Farquhar, G.D., 1983. On the nature of carbon isotope discrimination in C-4 species. *Australian Journal of Plant Physiology* 10, 205–226.
- Feisthauer, S., Wick, L.Y., Kastner, M., Kaschabek, S.R., Schломann, M., Richnow, H.H., 2008. Differences of heterotrophic ¹³CO₂ assimilation by *Pseudomonas knackmussii* strain B13 and *Rhodococcus opacus* 1CP and potential impact on biomarker stable isotope probing. *Environmental Microbiology* 10, 1641–1651.
- Fox, J., Weisberg, S., 2011. *An (R) Companion to Applied Regression*, second ed. SAGE Publications, London.
- Frostegård, Å., Bååth, E., 1996. The use of phospholipid fatty acid analysis to estimate bacterial and fungal biomass in soil. *Biology and Fertility of Soils* 22, 59–65.
- Frostegård, Å., Bååth, E., Tunlid, A., 1993. Shifts in the structure of soil microbial communities in limed forests as revealed by phospholipid fatty acid analysis. *Soil Biology and Biochemistry* 25, 723–730.
- Ge, T.D., Wu, X.H., Liu, Q., Zhu, Z.K., Yuan, H.Z., Wang, W., Whiteley, A.S., Wu, J.S., 2016. Effect of simulated tillage on microbial autotrophic CO₂ fixation in paddy and upland soils. *Scientific Reports* 6, 19784.
- Gentsch, N., Mikutta, R., Alves, R.J.E., Barta, J., Čapek, P., Gittel, A., Hugelius, G., Kuhry, P., Lashchinskiy, N., Palmtag, J., Richter, A., Šantrůčková, H., Schneckner, J., Shibistova, O., Urich, T., Wild, B., Guggenberger, G., 2015. Storage and transformation of organic matter fractions in cryoturbated permafrost soils across the Siberian Arctic. *Biogeosciences* 12, 4525–4542.
- Gittel, A., Barta, J., Kohoutova, I., Mikutta, R., Owens, S., Gilbert, J., Schneckner, J., Wild, B., Hannisdal, B., Maerz, J., Lashchinskiy, N., Čapek, P., Šantrůčková, H., Gentsch, N., Shibistova, O., Guggenberger, G., Richter, A., Torsvik, V.L., Schleper, C., Urich, T., 2014. Distinct microbial communities associated with buried soils in the Siberian tundra. *The ISME Journal* 8, 841–853.
- Gould, W., Reynolds, M., Walker, D., 2003. Vegetation, plant biomass, and net primary productivity patterns in the Canadian Arctic. *Journal of Geophysical Research: Atmospheres* 108.D2.
- Han, G.H., Yoshikoshi, H., Nagai, H., Yamada, T., Ono, K., Mano, M., Miyata, A., 2007. Isotopic disequilibrium between carbon assimilated and respired in a rice paddy as influenced by methanogenesis from CO₂. *Journal of Geophysical Research*. <http://dx.doi.org/10.1029/2006JG004001>.

- doi.org/10.1029/2006JG000219.
- Harris, J.O., 1954. The influence of carbon dioxide on oxygen uptake by resting cells of bacteria. *Journal of Bacteriology* 67, 476–479.
- Hayes, J.M., 1993. Factors controlling ^{13}C contents of sedimentary organic-compounds - principles and evidence. *Marine Geology* 113, 111–125.
- Hesselsoe, M., Nielsen, J.L., Roslev, P., Nielsen, P.H., 2005. Isotope labeling and microautoradiography of active heterotrophic bacteria on the basis of assimilation of $^{14}\text{CO}_2$. *Applied and Environmental Microbiology* 71, 646–655.
- House, C.H., Schopf, J.W., Stetter, K.O., 2003. Carbon isotopic fractionation by Archaeans and other thermophilic prokaryotes. *Organic Geochemistry* 34, 345–356.
- Huson, D.H., Auch, A.F., Qi, J., Schuster, S.C., 2007. MEGAN analysis of metagenomic data. *Genome Research* 17, 377–386.
- Kaiser, C., Koranda, M., Kitzler, B., Fuchsluger, L., Schnecker, J., Schweiger, P., Rasche, F., Zechmeister-Boltenstern, S., Sessitsch, A., Richter, A., 2010. Belowground carbon allocation by trees drives seasonal patterns of extracellular enzyme activities by altering microbial community composition in a beech forest soil. *New Phytologist* 187, 843–858.
- Konneke, M., Schubert, D.M., Brown, P.C., Hugler, M., Standfest, S., Schwander, T., von Borzyskowski, L.S., Erb, T.J., Stahl, D.A., Berg, I.A., 2014. Ammonia-oxidizing archaea use the most energy-efficient aerobic pathway for CO_2 fixation. *Proceedings of the National Academy of Sciences of the United States of America* 111, 8239–8244.
- Kopylova, E., Noé, L., Touzet, H., 2012. SortMeRNA: fast and accurate filtering of ribosomal RNAs in metatranscriptomic data. *Bioinformatics* 28, 3211–3217.
- Leininger, S., Urich, T., Schloter, M., Schwark, L., Qi, J., Nicol, G.W., Prosser, J.I., Schuster, S.C., Schleper, C., 2006. Archaea predominate among ammonia-oxidizing prokaryotes in soils. *Nature* 442, 806–809.
- Lenth, R.V., 2016. Least-squares means: the R package lsmeans. *Journal of Statistical Software* 69, 1–33.
- Makeev, O.W., Kerzhentsev, A.S., 1974. Cryogenic processes in the soils of northern Asia. *Geoderma* 12, 101–109.
- McCarroll, D., Loader, N.J., 2004. Stable isotopes in tree rings. *Quaternary Science Reviews* 23, 771–801.
- Merlin, C., Masters, M., McAteer, S., Coulson, A., 2003. Why is carbonic anhydrase essential to *Escherichia coli*? *Journal of Bacteriology* 185, 6415–6424.
- Miltner, A., Kopinke, F.D., Kindler, R., Selesi, D.E., Hartmann, A., Kastner, M., 2005a. Non-photosynthetic CO_2 fixation by soil microorganisms. *Plant and Soil* 269, 193–203.
- Miltner, A., Richnow, H.H., Kopinke, F.D., Kastner, M., 2004. Assimilation of CO_2 by soil microorganisms and transformation into soil organic matter. *Organic Geochemistry* 35, 1015–1024.
- Miltner, A., Richnow, H.H., Kopinke, F.D., Kastner, M., 2005b. Incorporation of carbon originating from CO_2 into different compounds of soil microbial biomass and soil organic matter. *Isotopes in Environmental and Health Studies* 41, 135–140.
- Mook, W.G., Bommerson, J.C., Staverman, W.H., 1974. Carbon isotope fractionation between dissolved bicarbonate and gaseous carbon-dioxide. *Earth and Planetary Science Letters* 22, 169–176.
- Nadelhoffer, K.F., Fry, B., 1988. Controls on natural nitrogen-15 and carbon-13 abundances in forest soil organic-matter. *Soil Science Society of America Journal* 52, 1633–1640.
- Nafi, B.M., Miles, R.J., Butler, L.O., Carter, N.D., Kelly, C., Jeffery, S., 1990. Expression of carbonic-anhydrase in *Neisseriae* and other heterotrophic bacteria. *Journal of Medical Microbiology* 32, 1–7.
- Nobel, P.S., Palta, J.A., 1989. Soil O_2 and CO_2 effects on root respiration of cacti. *Plant and Soil* 120, 263–271.
- Palmtag, J., Hugelius, G., Lashchinskiy, N., Tamstorf, M.P., Richter, A., Elberling, B., Kuhry, P., 2015. Storage, landscape distribution, and burial history of soil organic matter in contrasting areas of continuous permafrost. *Arctic Antarctic and Alpine Research* 47, 71–88.
- Penger, J., Conrad, R., Blaser, M., 2012. Stable carbon isotope fractionation by methanotrophic methanogenic archaea. *Applied and Environmental Microbiology* 78, 7596–7602.
- Punta, M., Coghill, P.C., Eberhardt, R.Y., Mistry, J., Tate, J., Bournsnel, Ch., Pang, N., Forslund, K., Ceric, G., Clements, J., Heger, A., Holm, L., Sonnhammer, E.L.L., Eddy, S.R., Bateman, A., Finn, R.D., 2012. The Pfam protein families database. *Nucleic Acids Research* 40 (Database issue), D290–D301.
- Quast, C., Pruesse, E., Yilmaz, P., Gerken, J., Schweer, T., Yarza, P., Peplies, J., Glöckner, F.O., 2012. The SILVA ribosomal RNA gene database project: improved data processing and web-based tools. *Nucleic Acids Research* 41, 590–596.
- Saini, R., Kapoor, R., Kumar, R., Siddiqi, T.O., Kumar, A., 2011. CO_2 utilizing microbes - a comprehensive review. *Biotechnology Advances* 29, 949–960.
- Šantrůčková, H., Bird, M.L., Elhottová, D., Novák, J., Píček, T., Šimek, M., Tykva, R., 2005. Heterotrophic fixation of CO_2 in soil. *Microbial Ecology* 49, 218–225.
- Šantrůčková, H., Bird, M.L., Lloyd, J., 2000. Microbial processes and carbon-isotope fractionation in tropical and temperate grassland soils. *Functional Ecology* 14, 108–114.
- Smith, K.S., Ferry, J.G., 2000. Prokaryotic carbonic anhydrases. *FEMS Microbiology Reviews* 24, 335–366.
- Sparling, G.P., West, A.W., 1990. A comparison of gas chromatography and differential respirometer methods to measure soil respiration and to estimate the soil microbial biomass. *Pedobiologia* 34, 103–112.
- Team, R., 2016. R development core team. R: A Language and Environment Statistical Computing 55, 275–286.
- Torn, M.S., Lapenis, A.G., Timofeev, A., Fischer, M.L., Babikov, B.V., Harden, J.W., 2002. Organic carbon and carbon isotopes in modern and 100-year-old-soil archives of the Russian steppe. *Global Change Biology* 8, 941–953.
- Tveit, A.T., Urich, T., Frenzel, P., Svenning, M.M., 2015. Metabolic and trophic interactions modulate methane production by Arctic peat microbiota in response to warming. *Proceedings of the National Academy of Sciences* 112, E2507–E2516.
- Urich, T., Lanzén, A., Qi, J., Huson, D.H., Schleper, C., Schuster, S.C., 2008. Simultaneous assessment of soil microbial community structure and function through analysis of the meta-transcriptome. *PLoS One* 3, e2527.
- Vance, E.D., Brookes, P.C., Jenkinson, D.S., 1987. An extraction method for measuring soil microbial biomass C. *Soil Biology and Biochemistry* 19, 703–707.
- Veldkamp, H., 1970. Chapter V - enrichment cultures of prokaryotic organisms. *Methods in Microbiology* 3, 305–361.
- Walker, D.A., Reynolds, M.K., Daniëls, F.J.A., Einarsson, E., Elvebakk, A., Gould, W.A., Katenin, A.E., Kholod, S.S., Markon, C.J., Melnikov, E.S., 2005. The circumpolar Arctic vegetation map. *Journal of Vegetation Science* 16, 267–282.
- Wild, B., Bárta, J., Čapek, P., Guggenberger, G., Hofhansl, F., Kaiser, C., Lashinsky, N., Mikutta, R., Mooshammer, P., Šantrůčková, H., Shibistova, O., Urich, T., Zimov, S.A., Richter, A., 2014. Nitrogen dynamics in Turbic Cryosols from Siberia and Greenland. *Soil Biology & Biochemistry* 67, 85–93.
- Wood, H.G., Stjernholm, R.L., 1962. Assimilation of carbon dioxide by heterotrophic organisms. *The Bacteria* 3, 41–117.
- Yuan, H.Z., Ge, T.D., Chen, C.Y., O'Donnell, A.G., Wu, J.S., 2012. Significant role for microbial autotrophy in the sequestration of soil carbon. *Applied and Environmental Microbiology* 78, 2328–2336.